

EMERGING INFECTIOUS DISEASES[®]



Vectorborne Infections

August 2017



Alexander Skachkov (b 1973), Varna, Bulgaria. *Old Mosquito*, 2014. Pencil drawing, continued in Photoshop as greyscale drawing. Colorized with HardLight, Multiply, Overlay, and Color layer color mode, 36 in x 43.5 in/91.44 cm x 110.48 cm.

EMERGING INFECTIOUS DISEASES[®]

EDITOR-IN-CHIEF

D. Peter Drotman

Associate Editors

Paul Arguin, Atlanta, Georgia, USA
 Charles Ben Beard, Ft. Collins, Colorado, USA
 Ermiyas Belay, Atlanta, Georgia, USA
 David Bell, Atlanta, Georgia, USA
 Sharon Bloom, Atlanta, GA, USA
 Mary Brandt, Atlanta, Georgia, USA
 Corrie Brown, Athens, Georgia, USA
 Charles Calisher, Fort Collins, Colorado, USA
 Michel Drancourt, Marseille, France
 Paul V. Effler, Perth, Australia
 Anthony Fiore, Atlanta, Georgia, USA
 David Freedman, Birmingham, Alabama, USA
 Peter Gerner-Smidt, Atlanta, Georgia, USA
 Stephen Hadler, Atlanta, Georgia, USA
 Matthew Kuehnert, Atlanta, Georgia, USA
 Nina Marano, Atlanta, Georgia, USA
 Martin I. Meltzer, Atlanta, Georgia, USA
 David Morens, Bethesda, Maryland, USA
 J. Glenn Morris, Gainesville, Florida, USA
 Patrice Nordmann, Fribourg, Switzerland
 Didier Raoult, Marseille, France
 Pierre Rollin, Atlanta, Georgia, USA
 Frank Sorvillo, Los Angeles, California, USA
 David Walker, Galveston, Texas, USA

Senior Associate Editor, Emeritus

Brian W.J. Mahy, Bury St. Edmunds, Suffolk, UK

Managing Editor

Byron Breedlove, Atlanta, Georgia, USA

Copy Editors

Claudia Chesley, Kristina Clark, Dana Dolan,
 Karen Foster, Thomas Gryczan, Jean Michaels Jones,
 Michelle Moran, Shannon O'Connor, Jude Rutledge,
 P. Lynne Stockton, Deborah Wenger

Production Thomas Ehemann, William Hale, Barbara Segal,
 Reginald Tucker

Editorial Assistants Kristine Phillips, Susan Richardson

Communications/Social Media Sarah Logan Gregory

Founding Editor

Joseph E. McDade, Rome, Georgia, USA

Emerging Infectious Diseases is published monthly by the Centers for Disease Control and Prevention, 1600 Clifton Road, Mailstop D61, Atlanta, GA 30329-4027, USA. Telephone 404-639-1960, fax 404-639-1954, email eideditor@cdc.gov.

The conclusions, findings, and opinions expressed by authors contributing to this journal do not necessarily reflect the official position of the U.S. Department of Health and Human Services, the Public Health Service, the Centers for Disease Control and Prevention, or the authors' affiliated institutions. Use of trade names is for identification only and does not imply endorsement by any of the groups named above.

All material published in Emerging Infectious Diseases is in the public domain and may be used and reprinted without special permission; proper citation, however, is required.

EDITORIAL BOARD

Timothy Barrett, Atlanta, Georgia, USA
 Barry J. Beaty, Ft. Collins, Colorado, USA
 Martin J. Blaser, New York, New York, USA
 Richard Bradbury, Atlanta, Georgia, USA
 Christopher Braden, Atlanta, Georgia, USA
 Arturo Casadevall, New York, New York, USA
 Kenneth C. Castro, Atlanta, Georgia, USA
 Louisa Chapman, Atlanta, Georgia, USA
 Benjamin J. Cowling, Hong Kong, China
 Vincent Deubel, Shanghai, China
 Isaac Chun-Hai Fung, Statesboro, Georgia, USA
 Kathleen Gensheimer, College Park, Maryland, USA
 Duane J. Gubler, Singapore
 Richard L. Guerrant, Charlottesville, Virginia, USA
 Scott Halstead, Arlington, Virginia, USA
 Katrina Hedberg, Portland, Oregon, USA
 David L. Heymann, London, UK
 Keith Klugman, Seattle, Washington, USA
 Takeshi Kurata, Tokyo, Japan
 S.K. Lam, Kuala Lumpur, Malaysia
 Stuart Levy, Boston, Massachusetts, USA
 John S. MacKenzie, Perth, Australia
 John E. McGowan, Jr., Atlanta, Georgia, USA
 Jennifer H. McQuiston, Atlanta, Georgia, USA
 Tom Marrie, Halifax, Nova Scotia, Canada
 Nkuchia M. M'ikanatha, Harrisburg, Pennsylvania, USA
 Frederick A. Murphy, Bethesda, Maryland, USA
 Barbara E. Murray, Houston, Texas, USA
 Stephen M. Ostroff, Silver Spring, Maryland, USA
 Marguerite Pappaioanou, Seattle, Washington, USA
 Johann D. Pitout, Calgary, Alberta, Canada
 Ann Powers, Fort Collins, Colorado, USA
 Mario Raviglione, Geneva, Switzerland
 David Relman, Palo Alto, California, USA
 Guenael R. Rodier, Geneva, Switzerland
 Connie Schmaljohn, Frederick, Maryland, USA
 Tom Schwan, Hamilton, Montana, USA
 Ira Schwartz, Valhalla, New York, USA
 Bonnie Smoak, Bethesda, Maryland, USA
 Rosemary Soave, New York, New York, USA
 P. Frederick Sparling, Chapel Hill, North Carolina, USA
 Robert Swanepoel, Pretoria, South Africa
 Phillip Tarr, St. Louis, Missouri, USA
 John Ward, Atlanta, Georgia, USA
 J. Todd Weber, Atlanta, Georgia, USA
 Jeffrey Scott Weese, Guelph, Ontario, Canada
 Mary E. Wilson, Cambridge, Massachusetts, USA

Use of trade names is for identification only and does not imply endorsement by the Public Health Service or by the U.S. Department of Health and Human Services.

EMERGING INFECTIOUS DISEASES is a registered service mark of the U.S. Department of Health & Human Services (HHS).

∞ Emerging Infectious Diseases is printed on acid-free paper that meets the requirements of ANSI/NISO 239.48-1992 (Permanence of Paper)

EMERGING INFECTIOUS DISEASES®

August 2017



On the Cover

Alexander Skachkov
(b 1973), Varna, Bulgaria.
Old Mosquito, 2014.

Pencil drawing, continued
in Photoshop as greyscale
drawing. Colorized with
HardLight, Multiply, Overlay,
and Color layer color mode,
36 in x 43.5 in/91.44 cm x
110.48 cm.

About the Cover p. 1436

Acute Febrile Illness and
Complications Due to Murine
Typhus, Texas, USA

Z. Afzal et al. 1268

Research

High Infection Rates for Adult
Macaques after Intravaginal or
Intraanal Inoculation with
Zika Virus

A.D. Haddow et al. 1274



Related material available online:
[http://wwwnc.cdc.gov/eid/
article/23/8/17-0036_article](http://wwwnc.cdc.gov/eid/article/23/8/17-0036_article)

Lyme Borreliosis in Finland,
1995–2014

E. Sajanti et al. 1282



Related material available online:
[http://wwwnc.cdc.gov/eid/
article/23/8/16-1273_article](http://wwwnc.cdc.gov/eid/article/23/8/16-1273_article)

Characterization of Fitzroy River
Virus and Serologic Evidence of
Human and Animal Infection

C.A. Johansen et al. 1289



Related material available online:
[http://wwwnc.cdc.gov/eid/
article/23/8/16-1440_article](http://wwwnc.cdc.gov/eid/article/23/8/16-1440_article)

Genomic Characterization of
Recrudescence of *Plasmodium
malariae* after Treatment with
Artemether/Lumefantrine

G.G. Rutledge et al. 1300



Related material available online:
[http://wwwnc.cdc.gov/eid/
article/23/8/16-1582_article](http://wwwnc.cdc.gov/eid/article/23/8/16-1582_article)

1242

Characteristics of Dysphagia
in Infants with Microcephaly
Caused by Congenital Zika Virus
Infection, Brazil, 2015

M.C. Leal et al. 1253



Related material available online:
[http://wwwnc.cdc.gov/eid/
article/23/8/17-0354_article](http://wwwnc.cdc.gov/eid/article/23/8/17-0354_article)

Zika Virus Infection in Patient
with No Known Risk Factors,
Utah, USA, 2016

E.R. Krow-Lucal et al. 1260



Synopses


Added Value of Next-Generation
Sequencing for Multilocus
Sequence Typing Analysis
of a *Pneumocystis jirovecii*
Pneumonia Outbreak

E. Charpentier et al. 1237



Related material available online:
[http://wwwnc.cdc.gov/eid/
article/23/8/16-1295_article](http://wwwnc.cdc.gov/eid/article/23/8/16-1295_article)

Medscape
EDUCATION
ACTIVITY

 *Bartonella quintana*, an
Unrecognized Cause of
Infective Endocarditis
in Children in Ethiopia

D. Tasher et al. 1246

Infection is probably not uncommon in
those with heart defects, and diagnosis
should be considered for patients with
culture-negative endocarditis.

Molecular Characterization of *Corynebacterium diphtheriae* Outbreak Isolates, South Africa, March–June 2015

M. du Plessis et al. 1308

Clinical Laboratory Values as Early Indicators of Ebola Virus Infection in Nonhuman Primates

R.B. Reisler et al. 1316



Related material available online:
http://wwwnc.cdc.gov/eid/article/23/8/17-0029_article

Maguari Virus Associated with Human Disease

A. Groseth et al. 1325



Related material available online:
http://wwwnc.cdc.gov/eid/article/23/8/16-1254_article

Human Infection with Highly Pathogenic Avian Influenza A(H7N9) Virus, China

C. Ke et al. 1332



Related material available online:
http://wwwnc.cdc.gov/eid/article/23/8/17-0600_article

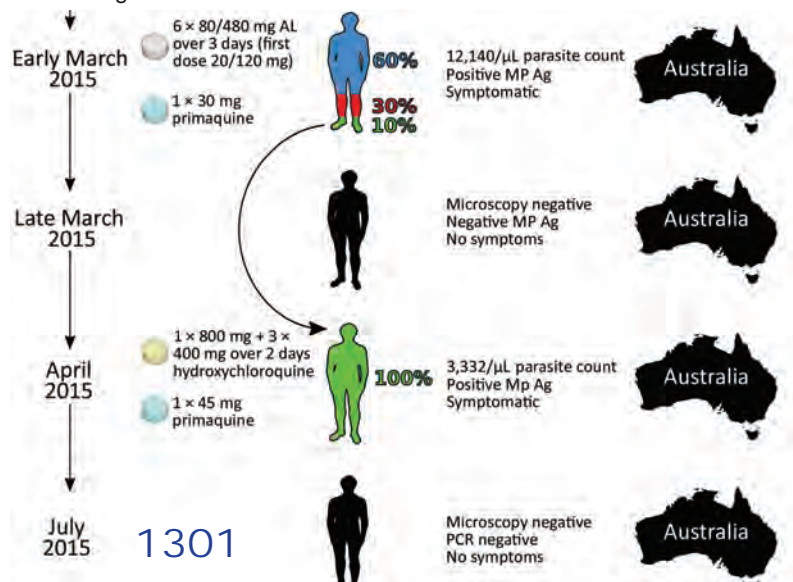
Medscape
EDUCATION
ACTIVITY



Human Metapneumovirus and Other Respiratory Viral Infections during Pregnancy and Birth, Nepal

J.L. Lenahan et al. 1341

Women infected with metapneumovirus during pregnancy had an increased risk of delivering infants who were small for gestational age.



1301

Dispatches

Global Spread of Norovirus GII.17 Kawasaki 308, 2014–2016

M.C.W. Chan et al. 1350



Related material available online:
http://wwwnc.cdc.gov/eid/article/23/8/16-1138_article

Preliminary Epidemiology of Human Infections with Highly Pathogenic Avian Influenza A(H7N9) Virus, China, 2017

L. Zhou et al. 1355

Real-Time Evolution of Zika Virus Disease Outbreak, Roatán, Honduras

T. Brooks et al. 1360

Clonal Expansion of New Penicillin-Resistant Clade of *Neisseria meningitidis* Serogroup W Clonal Complex 11, Australia

S. Mowlaboccus et al. 1364

Genesis of Influenza A(H5N8) Viruses

R. El-Shesheny et al. 1368



Related material available online:
http://wwwnc.cdc.gov/eid/article/23/8/17-0143_article

West Nile Virus Outbreak in Houston and Harris County, Texas, USA, 2014

D. Martinez et al. 1372



Related material available online:
http://wwwnc.cdc.gov/eid/article/23/8/17-0384_article

Density-Dependent Prevalence of *Francisella tularensis* in Fluctuating Vole Populations, Northwestern Spain

R. Rodriguez-Pastor et al. 1377

Occupational Exposures to Ebola Virus in Ebola Treatment Center, Conakry, Guinea

H. Savini et al. 1380

Serologic Evidence of Powassan Virus Infection in Patients with Suspected Lyme Disease

H.M. Frost et al. 1384



Related material available online:
http://wwwnc.cdc.gov/eid/article/23/8/16-1971_article

Serologic Evidence of Scrub Typhus in the Peruvian Amazon

C. Kocher et al. 1389

Influenza D Virus in Animal Species in Guangdong Province, Southern China

S.-L. Zhai et al. 1392

Related material available online:
http://wwwnc.cdc.gov/eid/article/23/8/17-0059_article

Seroprevalence of *Baylisascaris procyonis* Infection among Humans, Santa Barbara County, California, USA, 2014–2016

S.B. Weinstein et al. 1397



Related material available online:
http://wwwnc.cdc.gov/eid/article/23/8/17-0222_article

Opiate Injection–Associated Skin, Soft Tissue, and Vascular Infections, England, UK, 1997–2016

D. Lewer et al. 1400



Related material available online:
http://wwwnc.cdc.gov/eid/article/23/8/17-0439_article

Risk for Death among Children with Pneumonia, Afghanistan

R. Zabihullah et al. 1404



Related material available online:
http://wwwnc.cdc.gov/eid/article/23/8/15-1550_article

Research Letters

Detection of *Elizabethkingia* spp. in *Culicoides* Biting Midges, Australia

P.T. Mee et al. 1409

Early Evidence for Zika Virus Circulation among *Aedes aegypti* Mosquitoes, Rio de Janeiro, Brazil

T. Ayllón et al. 1411



Related material available online:
http://wwwnc.cdc.gov/eid/article/23/8/16-2007_article

Scrub Typhus Outbreak in a Remote Primary School, Bhutan, 2014

T. Tshokey et al. 1412



Related material available online:
http://wwwnc.cdc.gov/eid/article/23/8/16-2021_article

Scrub Typhus as a Cause of Acute Encephalitis Syndrome, Gorakhpur, Uttar Pradesh, India

M. Mittal et al. 1414



Related material available online:
http://wwwnc.cdc.gov/eid/article/23/8/17-0025_article

Human Infection with *Burkholderia thailandensis*, China, 2013

K. Chang et al. 1416



Related material available online:
http://wwwnc.cdc.gov/eid/article/23/8/17-0048_article

mcr-1 and *bla*_{KPC-3} in *Escherichia coli* Sequence Type 744 after Meropenem and Colistin Therapy, Portugal

M. Tacão et al. 1419

Outcomes for 2 Children after Peripartum Acquisition of Zika Virus Infection, French Polynesia, 2013–2014

M. Besnard et al. 1421

Related material available online:



http://wwwnc.cdc.gov/eid/article/23/8/17-0198_article

California Serogroup Virus Infection Associated with Encephalitis and Cognitive Decline, Canada, 2015

D. Webster et al. 1423

Effects of Influenza Strain Label on Worry and Behavioral Intentionist

A.M. Scherer et al. 1425



Related material available online:
http://wwwnc.cdc.gov/eid/article/23/8/17-0364_article

Zika Virus Screening among Spanish Team Members after 2016 Rio de Janeiro, Brazil, Olympic Games

N. Rodriguez-Valero et al. 1426

Candidatus *Dirofilaria hongkongensis* as Causative Agent of Human Ocular Filariosis after Travel to India

S. Winkler et al. 1428



Related material available online:
http://wwwnc.cdc.gov/eid/article/23/8/17-0423_article

Mucus-Activatable Shiga Toxin Genotype *stx2d* in *Escherichia coli* O157:H7

S. Sánchez et al. 1431

Letter

Acute Encephalitis Syndrome and Scrub Typhus in India

M.V. Murhekar 1434



Related material available online:
http://wwwnc.cdc.gov/eid/article/23/8/17-0570_article

Books and Media

Mosquito: A Discovery Channel Documentary 1435

About the Cover

Hematophagous Endeavors, Fact and Fancy

B. Breedlove, P.M. Arguin 1436

Etymologia

Pneumocystis jirovecii

R. Henry 1245

Corrections

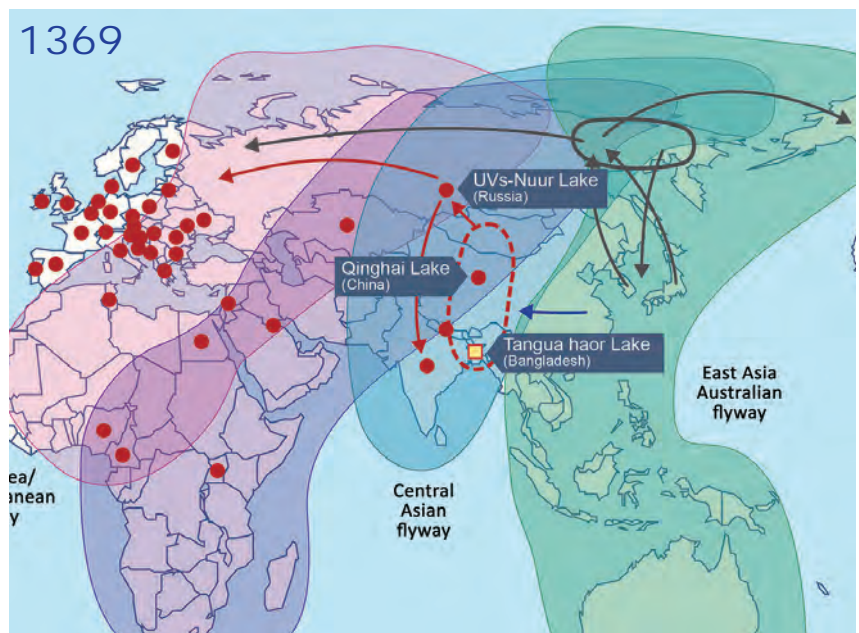
Vol. 22, No. 10, October 2016 1435

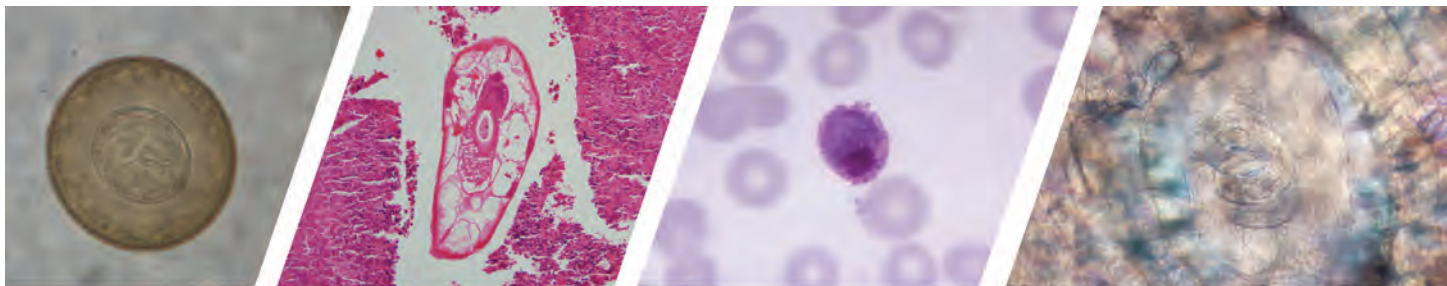
Streptococcus suis was incorrectly described in the text of *Streptococcus suis* Serotype 2 Capsule In Vivo

Vol. 23, No. 6, June 2017 1435

A subhead was missing and layout was incorrect in the Table for *Brucella neotomae* Infection in Humans, Costa Rica

Use of trade names is for identification only and does not imply endorsement by the Public Health Service or by the US Department of Health and Human Services.





Diagnostic Assistance and Training in Laboratory Identification of Parasites

A free service of CDC available to laboratorians, pathologists, and other health professionals in the United States and abroad



Diagnosis from photographs of worms, histological sections, fecal, blood, and other specimen types



Expert diagnostic review



Formal diagnostic laboratory report



Submission of samples via secure file share

Visit the DPDx website for information on laboratory diagnosis, geographic distribution, clinical features, parasite life cycles, and training via Monthly Case Studies of parasitic diseases.

www.cdc.gov/dpdx
dpdx@cdc.gov



U.S. Department of
Health and Human Services
Centers for Disease
Control and Prevention

Added Value of Next-Generation Sequencing for Multilocus Sequence Typing Analysis of a *Pneumocystis jirovecii* Pneumonia Outbreak¹

Elena Charpentier, Cécile Garnaud, Claire Wintenberger, Sébastien Bailly, Jean-Benjamin Murat,² John Rendu, Patricia Pavese, Thibault Drouet, Caroline Augier, Paolo Malvezzi, Anne Thiébaud-Bertrand, Marie-Reine Mallaret, Olivier Epaulard, Muriel Cornet, Sylvie Larrat, Danièle Maubon

Pneumocystis jirovecii is a major threat for immunocompromised patients, and clusters of pneumocystis pneumonia (PCP) have been increasingly described in transplant units during the past decade. Exploring an outbreak transmission network requires complementary spatiotemporal and strain-typing approaches. We analyzed a PCP outbreak and demonstrated the added value of next-generation sequencing (NGS) for the multilocus sequence typing (MLST) study of *P. jirovecii* strains. Thirty-two PCP patients were included. Among the 12 solid organ transplant patients, 5 shared a major and unique genotype that was also found as a minor strain in a sixth patient. A transmission map analysis strengthened the suspicion of nosocomial acquisition of this strain for the 6 patients. NGS-MLST enables accurate determination of subpopulation, which allowed excluding other patients from the transmission network. NGS-MLST genotyping approach was essential to deciphering this outbreak. This innovative approach brings new insights for future epidemiologic studies on this uncultivable opportunistic fungus.

Pneumocystis jirovecii pneumonia (PCP) is a life-threatening opportunistic disease that poses a particular threat in healthcare units that manage patients with oncematologic conditions, patients having received solid organ

transplants (SOTs), and HIV-infected patients. The incidence of PCP among SOT recipients has increased markedly since the early 2000s, concomitant with the development of more intensive immunosuppressive therapy and increasing organ transplant procedures (1). During 2001–2010, the incidence of PCP among HIV-positive/AIDS patients in France dropped from 2.4 to 0.7 cases/10⁵/year (–14.2%/year), whereas incidence increased from 0.13 to 0.35 cases/10⁵/year (+13.3%/year) among patients without HIV infection (2). For SOT patients in France, the incidence of PCP increased by 13% during 2004–2010 (2). Moreover, multiple outbreak clusters in this specific population have been reported (3–5). Patients receiving renal transplants are particularly at risk; most reported PCP clusters have occurred in kidney transplant units (6). These outbreaks support the hypothesis of a de novo person-to-person transmission of *P. jirovecii* and its potential for nosocomial spread (7).

Exploring an outbreak transmission network requires spatiotemporal and strain-typing approaches. Various genotyping approaches to the study of *P. jirovecii* epidemiology have been described (8–12). Genotyping based on multilocus sequence typing (MLST) is standard for strain characterization, especially for organisms that are not easily cultivable, because it provides excellent discriminatory power and reproducibility (3,4,13,14). Multiple *P. jirovecii* strains isolated from a unique respiratory sample have frequently been reported (6–8,10). The proportions of these mixed strains in samples varied substantially according to the genotyping method (6–8). MLST has been

Author affiliations: Centre Hospitalier Universitaire Grenoble Alpes, Grenoble, France (E. Charpentier, C. Garnaud, C. Wintenberger, J.-B. Murat, J. Rendu, P. Pavese, T. Drouet, C. Augier, P. Malvezzi, A. Thiébaud-Bertrand, M.-R. Mallaret, O. Epaulard, M. Cornet, S. Larrat, D. Maubon); Université Grenoble Alpes, Grenoble (E. Charpentier, C. Garnaud, M.-R. Mallaret, O. Epaulard, M. Cornet, S. Larrat, D. Maubon), Institut National de la Santé et de la Recherche Médicale Université Paris Diderot, Paris, France (S. Bailly)

DOI: <https://doi.org/10.3201/eid2308.161295>

¹Preliminary results from this study were presented at the American Society for Microbiology Microbe 2016 Conference, June 16–20, 2016, Boston, Massachusetts, USA.

²Current affiliation: Centre Hospitalier Universitaire Limoges, Limoges, France.

used previously to study PCP outbreaks, but first-generation sequencing technology (i.e., Sanger sequencing) presents limitations for subpopulations characterization. In the use of Sanger sequencing technology, minor variant detection is generally restricted to strains with a relative abundance of DNA (>20% of the total amount) and requires an amplicon cloning step and the sequencing of ≥ 5 clones (6,15–17).

Next-generation sequencing (NGS) technologies yield improved performance. Because of clonal amplification before sequence acquisition, these technologies enable in-depth sequencing and the detection of major, minor, and ultra-minor populations within the same sample (18,19).

During 2009–2014, the incidence of PCP in all SOT patients in our institution was <1 case/year. In 2014, six cases of PCP were diagnosed among SOT patients over a 3-month period (May–July) and 6 more through August 2015. These grouped cases involved recipients of various organs, 5 heart recipients, 4 kidney recipients, 1 lung recipient, 1 liver recipient, and 1 recipient of both a heart and a kidney. This atypical distribution and the substantial increase of incidence triggered the exploration of this outbreak. In this study, we evaluated the added value of an NGS-MLST strategy in the specific context of a PCP cluster among SOT patients, taking advantage of the specific characteristics of NGS in terms of subpopulation detection.

Materials and Methods

Patient Selection and Samples

The Grenoble Alpes University Hospital has a total of 2,200 beds and performs 150 SOTs each year. In 2014, we followed a total of 1,899 SOT patients in our institution (1,380 kidney, 339 liver, 90 heart, and 90 lung recipients). We included 32 PCP patients in the study (Table 1): 12 SOT recipients (mean age 61.6 years, range 34–75 years) and 20 control patients (mean age 57 years, range 7 months–82 years). Control patients were those with sporadic PCP cases diagnosed in the previous 4 years who had diverse underlying conditions and no obvious epidemiologic link. PCP biologic diagnosis was confirmed by quantitative PCR in respiratory samples (bronchoalveolar lavage fluids, bronchoaspiration, or sputum) as described previously (20).

Clinical Epidemiologic Survey

According to the incubation periods described in the literature (median 53 days, range 1–88 days) (21,22), we collected data concerning patients' interactions within the institution from 6 months preceding the date of symptom onset in the first patient until the date of diagnosis of PCP in the last patient. Because colonized patients are potential infectious sources of *P. jirovecii* (23,24), we considered patients to be possibly contagious throughout the whole incubation period, even in the absence of symptoms and for 3 days

after initiating treatment with trimethoprim/sulfamethoxazole. We defined transmission as probable when all of the following criteria were present: 1) the 2 patients were present in the same floor and in the same corridor on the same day, 2) the source patient was in the contagious phase, and 3) the duration from the probable date of transmission to the appearance of the first symptoms was compatible with the incubation period for PCP. If 1 of these criteria was missing, transmission was defined as possible. We defined the incubation period for PCP as the time elapsed from the strain transmission to the onset of symptoms.

MLST Strategy

We used an MLST strategy to genotype *P. jirovecii* strains, as recently recommended (25). We chose a combination of 3 loci belonging to the superoxide dismutase (*SOD*), the mitochondrial large subunit of ribosomal RNA (*mtLSU*), and the cytochrome b (*CYTB*) genes. This scheme displays a high level of strain discrimination and is adapted for accurate *P. jirovecii* strain typing (14). We designed new primers for each locus to obtain ≈ 750 bp amplicons depending on the chosen NGS procedure, which was performed by using GS Junior + (Roche Diagnostics, Meylan, France). Because we used extended sequences to characterize our strains, we could not refer to any previously used sequence type labeling. Thus, we arbitrarily named haplotypes with a capital letter (A), a number (1), and a lowercase letter (a) corresponding to *mtLSU*, *CYTB*, and *SOD* loci. We then labeled final genotypes by the association of the 3 different haplotypes (e.g., A1a). Primers, PCR conditions, and haplotype sequences are summarized in online Technical Appendix Tables 1, 2 (<https://wwwnc.cdc.gov/EID/article/23/8/16-1295-Techapp1.pdf>).

Amplicon Library Preparation and Emulsion PCR

We extracted total DNA by using the QIAmp DNA Mini Kit (QIAGEN, Hilden, Germany), according to the manufacturer's instructions and as previously described (20), and stored extracts at -20°C until library preparation. We prepared the amplicon library by using the universal tailed amplicon sequencing design. We first amplified each region of interest by using specific oligonucleotides coupled to M13 universal primers (PCR1) and then targeted these universal sequences in a second PCR (PCR2) to add a multiplex identifier and the sequencing primers as described in the Guidelines for Amplicon Experimental Design—454 Sequencing System (Roche Diagnostics). We purified PCR products with magnetic beads from an AMPureXP Kit (Beckmann Coulter, Beverly, MA, USA). After qualitative and quantitative analysis, we diluted purified PCR2 products to 1×10^9 molecules/mL and pooled an equal volume of each dilution to generate the amplicon library. We performed emulsion PCR as recommended in the GS Junior + library preparation procedure.

Table 1. Main clinical and biologic characteristics of the 12 patients who had received solid organ transplants and 20 control patients in a study of a *Pneumocystis jirovecii* pneumonia outbreak at a university hospital in France, 2014–2015*

Patient	Age, y/sex	Date of diagnosis	Underlying condition	Time since transplant, mo	Sample type	Fungal load, MSG copies/mL	Outcome
T1	34/F	2014 May 20	Pulmonary transplant	60	BAL	1.1 × 10 ⁹	Died
T2	59/F	2014 May 27	Heart and kidney transplant	300 (H) – 2 (K)	BAL	3.9 × 10 ⁸	Survived
T3	57/F	2014 Jun 19	Heart transplant	137	BAL	2.7 × 10 ⁸	Died
T4	65/M	2014 Jul 7	Heart transplant	37	BAL	1.5 × 10 ⁸	Died
T5	66/M	2014 Aug 19	Kidney transplant	4	Sputum	6.6 × 10 ¹⁰	Survived
T6	48/M	2014 Aug 29	Heart transplant	78	BAL	1 × 10 ⁶	Survived
T7	74/F	2014 Oct 29	Kidney transplant	128	BAL	2 × 10 ⁷	Died
T8	69/F	2014 Nov 24	Kidney transplant	23	BAL	8.8 × 10 ⁶	Survived
T9	63/M	2015 Jan 7	Liver transplant	5	BAL	1.1 × 10 ⁴	Survived
T10	69/M	2015 Jan 10	Kidney transplant	228	Sputum	1.2 × 10 ⁵	Survived
T11	61/F	2015 Mar 3	Heart transplant	122	BAL	3.1 × 10 ³	Survived
T12	75/F	2015 Aug 26	Heart transplant	95	BAL	2 × 10 ⁵	Survived
C1	56/M	2012 Aug 25	Liver transplant	6	BA	6 × 10 ⁶	Died (HCV relapse)
C2	52/M	2013 May 17	Pulmonary transplant	21	BAL	1.7 × 10 ⁵	Survived
C3	82/F	2012 Mar 9	Rheumatoid polyarthritis	–	BAL	5.6 × 10 ³	Survived
C4	62/M	2013 Aug 29	NHL	–	BAL	4.3 × 10 ⁸	Survived
C5	66/M	2013 Sep 10	NHL	–	BAL	1.2 × 10 ⁶	Survived
C6	25/M	2014 Feb 27	HIV	–	BAL	4.2 × 10 ⁸	Survived
C7	1/F	2014 Apr 9	Primary immunodeficiency	–	BAL	5.2 × 10 ⁹	Survived
C8	56/M	2014 Apr 19	HIV	–	BAL	4.3 × 10 ⁹	Survived
C9	47/F	2014 Apr 24	Allografted AML with GVHD	–	BAL	1.4 × 10 ⁶	Survived
C10	74/M	2014 Jul 1	NHL	–	BAL	6.1 × 10 ⁸	Survived
C11	77/M	2014 Sep 4	MPN and NHL	–	BAL	1.2 × 10 ⁵	Survived
C12	82/M	2014 Sep 5	NHL	–	BAL	5.8 × 10 ⁴	Survived
C13	68/M	2014 Oct 10	Glioblastoma	–	BAL	3.4 × 10 ¹⁰	Survived
C14	7 mo/F	2014 Oct 15	Primary immunodeficiency	–	Sputum	4.7 × 10 ⁶	Survived
C15	75/F	2014 Oct 23	B-chronic lymphoid leukemia	–	BAL	3.4 × 10 ⁵	Survived
C16	82/F	2014 Dec 5	B-chronic lymphoid leukemia	–	BAL	1.1 × 10 ⁴	Survived
C17	32/F	2015 Feb 27	Hodgkin's disease	–	BAL	1.2 × 10 ⁴	Survived
C18	50/M	2015 Feb 28	Hodgkin's disease	–	BAL	6.4 × 10 ³	Survived
C19	78/M	2015 Mar 18	B-chronic lymphoid leukemia	–	BAL	5.9 × 10 ⁶	Survived
C20	75/M	2015 Mar 22	NHL	–	BA	3.9 × 10 ⁴	Died

*T1–T12 indicate the 12 solid organ transplant patients from the cluster; C1–C20 indicate the 20 control patients. AML, acute myeloid leukemia; BA, bronchoaspiration; BAL, bronchoalveolar lavage fluids; GVHD, graft-versus-host disease; H, heart; K, kidney; MPN, myeloproliferative neoplasm; MSG, major surface glycoprotein; NA, not applicable; ND, not done; NHL, non-Hodgkin lymphoma; –, nonexistent or unspecified.

NGS and Limit of Detection

We performed NGS to sequence 700–800 bp fragments, according to the manufacturer's instructions, using a forward and reverse sequencing strategy for better coverage. Ninety-six PCR products were distributed in 2 comparably filled runs. We added a control sample to assess the limit of detection of subpopulations under our experimental conditions. This control consisted of 3 purified *mtLSU* amplicons belonging to 3 unique haplotypes, based on the results of the first run at 3 different ratios: 98.9%, 1.0%, and 0.1%.

Bioinformatic Analysis

We analyzed NGS results by using Amplicon Variant Analyzer and GS Reference Mapper software (Roche Diagnostics) and compared sequences to their respective reference sequences; GenBank accession nos. were NC_020331.1 (*mtLSU*), AF146753.1 (*SOD*), and AF320344.1 (*CYTb*). Each polymorphism position was verified and visually validated. We applied a 1% threshold for minor variant consideration based on the result of our artificial mix sample. We

calculated haplotype frequency by using Amplicon Variant Analyzer software (dividing number of reads corresponding to the haplotype by the total number of reads for 1 locus).

Statistical Analysis and Hunter Index

We compared co-infection proportions between cluster and control populations by using the Fisher exact test, calculated a *p* value, and defined statistical significance as *p*<0.05. The Hunter index (D) was calculated to evaluate the discriminatory power of the 3 loci and their association, as previously described (26). Only single strains or strains with an easy extrapolation of the major genotype (variants in only 1 locus or presence of ultra-major variants in all loci) were taken into account for the D calculation. Related samples sharing the outbreak genotype were also excluded, except 1.

Results

NGS Performance

The mean sequencing depths for NGS of *P. jirovecii* strains were 810× (5×–1,998×, median 739×) and 265×

SYNOPSIS

(8×–1,268×, median 233×) for the first and second runs, respectively. Sequence quality was assessed using FastQC software (<http://www.bioinformatics.babraham.ac.uk>). For the first run, the median Phred score (or Qscore) per base, up to a 750 bp read length, was >24 (corresponding to a probability of error <0.4%); for the second run, the median Phred score was >20 until 400 bp read length (corresponding to a probability of error <1%).

Limit of Detection

In the artificial control sample consisting of 3 *mtLSU* haplotypes at defined concentrations (C, 98.9%; B, 1%; and F, 0.1%), the C and B haplotypes were correctly detected with NGS at 99% (C) and 1% (B). The ultra-minor F genotype was not detected, a finding consistent with the limited analysis depth obtained for this sequence (220×).

Nucleotide Polymorphisms, Haplotypes, and Genotypes Determination

We genotyped 12 *P. jirovecii* samples from the SOT patient cluster and 20 samples from unrelated control patients by

using the 3 loci NGS-MLST strategy. Analysis of extended 732 bp *mtLSU* sequences revealed 4 new polymorphisms located both upstream and downstream of the amplicons classically used for genotyping (online Technical Appendix Figure). These polymorphisms correspond to 3 single-nucleotide polymorphisms at positions 13002, 13505, and 13543 in the mitochondrial genome (GenBank accession no. NC_020331.1) and 1 multinucleotide polymorphism between 13554 and 13560. By contrast, extended *CYTB* and *SOD* amplicons did not show new polymorphisms.

Among the 32 samples, we identified 22 different haplotypes for *mtLSU*, 14 for *CYTB*, and 4 for *SOD*, with major and minor variants being considered (Table 2). We identified C2a as the major genotype in 5 SOT patients from the cluster: 1 double (heart and kidney) recipient (T2), 1 heart recipient (T4), and 3 renal transplant recipients (T5, T8, and T10). We also detected this C2a genotype as a minor variant (2%) in 1 other SOT patient belonging to the 2014–2015 outbreak cluster (T7). With major and minor genotypes being considered, 6/12 SOT patients were carrying the C2a genotype. We did not detect this unusual

Table 2. Results of next-generation multilocus sequence typing for the 3 targeted loci of *Pneumocystis jirovecii* strains in a study of a *P. jirovecii* pneumonia outbreak at a university hospital in France, 2014–2015*

Patient	<i>mtLSU</i>			<i>CYTB</i>			<i>SOD</i>			Final major genotype
	No. reads	No. haplotypes	Major haplotype	No. reads	No. haplotypes	Major haplotype	No. reads	No. haplotypes	Major haplotype	
T1	1,413	1	B	531	1	1	946	1	A	<u>B1a</u>
T2	1,062	1	C	1,361	1	2	2,506	1	A	<u>C2a</u>
T3	638	4	N	84	1	3	491	1	B	<u>N3b</u>
T4	87	1	C	215	1	2	204	1	A	C2a
T5	460	1	C	1,030	1	2	337	1	A	C2a
T6	42	1	E	237	1	2	171	1	A	<u>E2a</u>
T7	546	1	C	1,088	1	2	303	4	B	<u>C2bt</u>
T8	606	2	C	1,136	2	2	808	1	A	C2a
T9	194	1	C	160	1	2	8	1	B	C2b
T10	415	1	C	1,360	1	2	898	1	A	C2a
T11	420	3	O	370	2	1	298	3	B	<u>O1b</u>
T12	658	9	F	809	4	3	781	1	A	<u>F3a</u>
C1	318	3	P	1,046	1	3	1,268	1	A	<u>P3a</u>
C2	422	8	B	339	4	3	364	2	A	ND
C3	350	1	I	564	1	3	1,268	1	B	<u>I3b</u>
C4	292	2	N	492	1	3	427	1	B	<u>N3b</u>
C5	71	1	B	651	1	2	880	1	B	<u>B2b</u>
C6	368	12	P	473	3	3	575	4	B	ND
C7	153	2	F	103	2	3	54	4	A	F3a
C8	383	5	I	697	2	3	653	4	B	ND
C9	148	2	F	104	4	2	154	1	a	F2a
C10	934	2	F	1,146	5	2	550	3	a	F2a
C11	229	4	B	750	3	3	119	2	b	<u>B3b</u>
C12	580	2	G	398	1	1	509	1	a	<u>G1a</u>
C13	869	1	F	1,998	1	3	663	1	a	<u>F3a</u>
C14	901	9	B	1,403	1	2	411	1	b	<u>B2b</u>
C15	653	1	N	1,664	2	3	5	1	a	<u>N3a</u>
C16	1,275	1	F	1,052	1	11	591	1	a	<u>F11a</u>
C17	372	10	P	434	3	2	361	1	b	ND
C18	296	1	F	271	1	3	15	3	b	<u>F3b</u>
C19	948	2	F	795	4	1	494	1	a	ND
C20	243	5	A	284	9	2	240	2	b	ND

*T1–T12 indicate the 12 solid organ transplant patients from the cluster; C1–C20 indicate the 20 control patients. Underlined genotypes were included for Hunter Index calculation. *CYTB*, cytochrome b; *mtLSU*, mitochondrial large subunit of ribosomal RNA; ND, undetermined genotypes when haplotypes could not be cross-linked (multiple variants in >1 locus without any clear predominance); *SOD*, superoxide dismutase.

†Patient carrying the C2a genotype as a minor strain.

genotype in any control patient, either as a major or minor strain (Table 2).

Epidemiologic Investigation

We noted the transmission networks between the 6 SOT patients infected with the C2a strain, the time to diagnosis, and the incubation for PCP (Table 3). The transmission map (Figure 1) pointed out potential nosocomial transmission of the C2a strain involving both heart and kidney transplant units, with the index patient being patient T2, who was a long-standing heart recipient who received a kidney transplant 2 months before PCP diagnosis. Transmission was probable in the following patients: between T2 and T5, within the nephrology department; between T2 and T4, within the heart surgery outpatient clinic; between T5 and T8, in the nephrology department; and between T8 and T10, in the transplant outpatient clinic. Transmission between T5 and T7 was considered only possible because the patients were on the same floor the same day but in perpendicular corridors, and the incubation time for patient T5 was relatively short (4 days). Of note, 4 of the 5 suspected nosocomial transmissions of this strain occurred in outpatient clinic areas (T2/T4, T5/T7, T5/T8, and T8/T10), and 1 occurred in the transplant unit (T2/T5). According to the transmission map, PCP incubation intervals (time elapsed between strain acquisition and symptom onset) were 48 (T10), 49 (T4), 99 (T8), 109 (T5), and 170 (T7) days.

Variants Analysis and Mixed Infections

Among the 32 respiratory samples, 11 (34.4%) contained a single and unique *P. jirovecii* strain with no minor variants detected. Thus, 21/32 (65.6%) respiratory samples consisted of multiple *P. jirovecii* strains, and 17/32 (53.1%) had >2 different *P. jirovecii* strains. Co-infection proportions were significantly different between the cluster group (5/12 [41.7%] mixed infections) and the control group (17/20 [85.0%] mixed infections; $p < 0.05$). The exact number of strains within each sample was sometimes difficult to determine because minor haplotypes could not always be

associated. However, we observed an average minimum of 5 strains per sample (corresponding to the highest number of alleles in 1 locus), ranging from 2 to 12, in these co-infected patients. In more than half of the patients, we detected minor variants with a proportion <10%; 18/32 patients (56.2%) had ≥ 1 subpopulation <10%, and 9/32 (28.1%) had only minor variants <10%. The *mtLSU*, *CYTB*, and *SOD* loci enabled detection of 62.5% (20/32), 43.75% (14/32), and 31.25% (10/32) mixed strain infections, respectively. We plotted heatmaps representing strain distribution patterns for each locus (Figure 2). The co-infection proportions were comparable between the 2 sequencing runs (61% and 65%).

Discriminatory Index of the Extended Amplicons

We calculated the Hunter index (D) for each locus of 19 strains (online Technical Appendix Table 3), excluding the clonal C2a strains and uninterpretable genotypes (26). The discriminatory index of the *mtLSU* locus D was 0.754 when considering only known polymorphisms and 0.883 when considering both known and newly described polymorphisms. Similarly, in terms of *CYTB* and *mtLSU* loci association, D increased from 0.918 with only known polymorphisms to 0.953 when adding the newly described polymorphisms. When the 3 loci were considered, D further increased from 0.971 to 0.982.

Discussion

An outbreak of 12 diagnosed PCP cases occurred among SOT recipients in our institute during 2014–2015. This cluster consisted of patients carrying different transplanted organs who were followed up in different organ specialty units. We used an exhaustive NGS-MLST approach to accurately characterize the major and minor strains implicated.

To our knowledge, PCP outbreaks among SOT patients have been commonly described in renal transplant patients, reported more rarely in hepatic transplant recipients, and never reported in cardiac transplant patients (although sporadic cases exist in this population). Also, most reported grouped cases of PCP in SOT recipients

Table 3. Epidemiologic information on patients found to be carrying the C2a genotype as a major or a minor strain in a study of a *Pneumocystis jirovecii* pneumonia outbreak at a university hospital in France, 2014–2015*

Patient	Transmission			Date of symptom onset	Date of diagnosis	Time to diagnosis, d	Incubation, d
	Source	Date	Place				
T2	Index patient	ND	ND	2014 May 25	2014 May 30	5	ND
T4	T2	12 May 2014	Surgical cardiology outpatient unit	2014 Jul 01	2014 Jul 06	5	49
T5	T2	2014 Apr 18	Kidney transplant unit	2014 Aug 05	2014 Aug 19	14	109
T7†	T5	2014 Apr 22	Cardiac echography unit	2014 Oct 09	2014 Oct 29	20	170
T8	T5	2014 Aug 07	Transplant consultation unit	2014 Nov 14	2014 Nov 24	11	99
T10	T8	2014 Nov 23	Transplant consultation unit	2015 Jan 05	2015 Jan 10	5	48

*Date of transmission based on transmission map and previously defined criteria of transmission. ND, not determined.

†Patient carrying the C2a genotype as a minor strain.

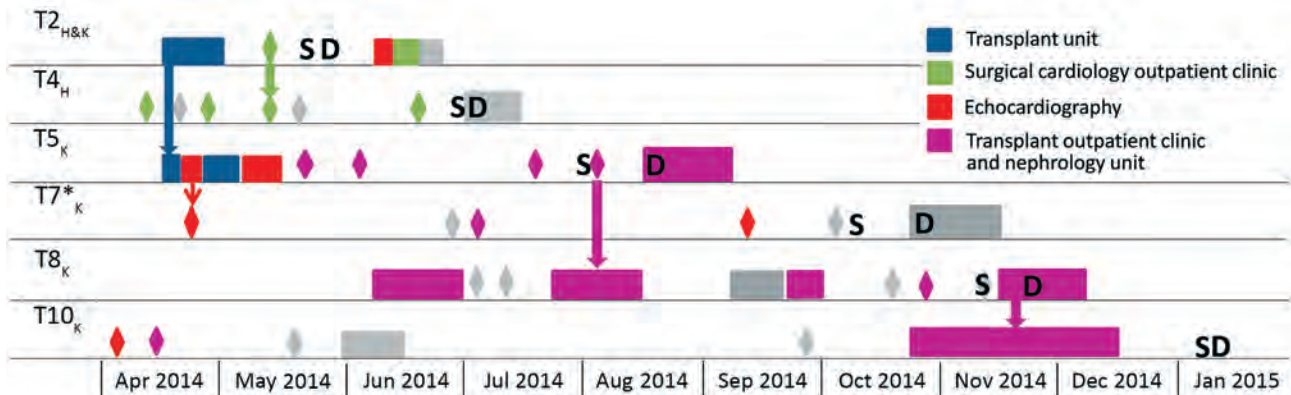


Figure 1. Transmission map illustrating space and time events for cluster patients sharing the clonal C2a genotype identified in a study of a *Pneumocystis jirovecii* pneumonia outbreak at a university hospital in France, 2014–2015. Rectangles indicate hospitalization periods of >1 day; diamonds indicate 1-day presence in the institution (e.g., emergency services, imaging, laboratory, outpatient clinics). Places involved in the transmission network are shown in color, whereas units not involved are shown in gray. Thick arrow refers to probable nosocomial transmission of *P. jirovecii* between 2 patients who were present in the same place (same floor and same corridor) on the same day. Thin arrow represents possible nosocomial transmission of *P. jirovecii* between T5 and T7 (patients were in perpendicular corridors). Subscript letters on patient labels indicate type of transplant (H, heart; K, kidney). D, date of diagnosis and treatment initiation; S, date of symptoms onset. Asterisk indicates that patient was carrying the C2a genotype as a minor strain.

described cases occurring in patients grafted with the same organ; grouped cases in patients transplanted with different organs rarely have been described (4,5). In our study, even though the SOT cluster patients were followed up by different units, they belonged to the same epidemic event according to genotyping results. Five SOT cluster patients shared a common major genotype, and the transmission map (Figure 1) pointed out potential nosocomial transmission of this strain, which might have been present in both the cardiology and nephrology transplant units. This genotype was not detected in the control group, confirming that this *P. jirovecii* strain is not commonly present within our institute.

The epidemiologic survey, guided by the genotyping results, identified potential dates and places of transmission between the patients infected with the same *P. jirovecii* strain. Five probable and 1 possible transmission events between SOT patients were revealed. Of note, 4/5 suspected transmission events occurred in outpatient areas. Waiting rooms and day hospital corridors have been thought to promote person-to-person contact and increase the risk for *P. jirovecii* transmission (7). The wearing of masks in waiting rooms frequently visited by immunocompromised patients was recently suggested for patients with respiratory symptoms but should also be recommended to any patient, given that asymptomatic carrier state or patients in incubation state might also be at risk for transmission (7,27). Also, patients could have met in certain common areas of the hospital (e.g., cafeteria and corridors), encounters that are usually not in the medical records. Recent studies confirmed the high probability of *P. jirovecii* airborne transmission or transmission between patients and healthcare

workers (23,28). In the affected units, it would have been of interest to screen healthcare workers or air samples to identify asymptomatic carriers of the C2a *P. jirovecii* strain or its presence in the environment.

In our study, we used a 1% threshold for minor variant detection according to our artificial mix control. By using this threshold, we detected 21/32 (66%) cases with mixed-strain infections and 17/32 (53%) cases with >2 strains. Previous genotyping studies described *P. jirovecii* multiple infections with diverse proportions of different strains (from 20% to 75%) (29–31). Hauser et al. (29) and Gits-Muselli et al. (12) described mixed populations in 70% of cases with the use of PCR-single-strand-conformation polymorphism or micro-satellite analysis. Our proportion of mixed strains was even higher (85%) when we considered only the control patients, which might more accurately reflect the reality of *P. jirovecii* strain diversity in a nonoutbreak environment. Ultra-deep sequencing of *P. jirovecii* strains outside an outbreak context has indicated a 92% proportion of coinfections (32). The proportion we observed with infections involving >2 strains is higher than previously described (30) because of the more accurate variant detection <10% provided by NGS. We noted a difference in the proportion of co-infections between the cluster group (42%) and control group (85%) ($p < 0.01$) despite identical mean sequencing depth. We can hypothesize that the C2a strain has a particular intrinsic virulence or that this cluster has some specific characteristic, but further study would be required.

By using NGS, we found 1 confirmed C2a genotype as the minor strain in patients belonging to the cluster. The ratio among the different *P. jirovecii* strains can vary over time in a given patient (33). Thus, a previous minor

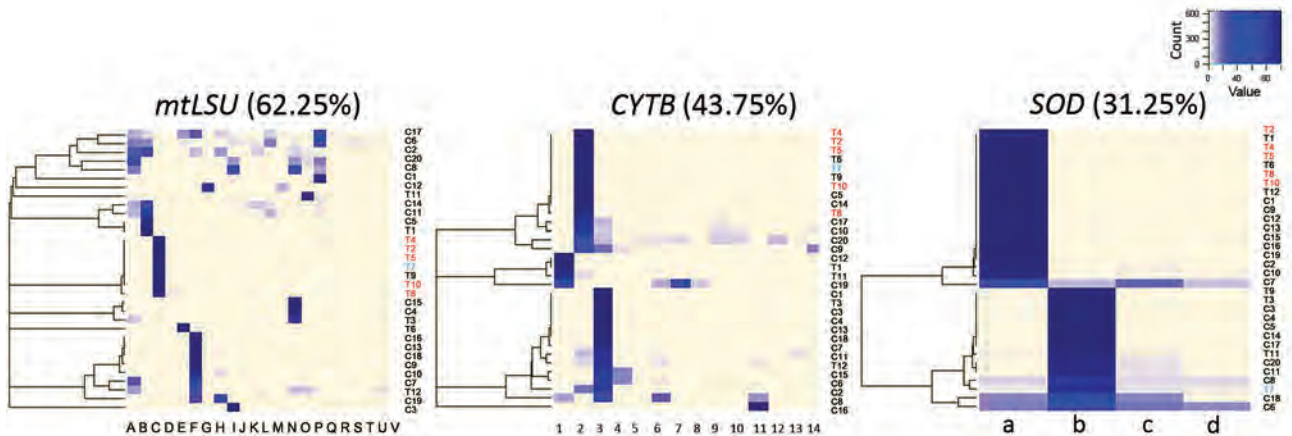


Figure 2. Heatmaps representing distribution for *mtLSU*, *CYTB*, and *SOD* variants among patients infected during a *Pneumocystis jirovecii* pneumonia outbreak at a university hospital in France, 2014–2015. Patients shown in red correspond to cluster patients sharing the common C2a genotype. Patient shown in blue is the patient having the C2a genotype as minor variant (2%). Percentages shown indicate the level of mixed-strain infections for each locus.

strain can theoretically become a major strain over time. The patient with a minor C2a strain (T7) was thus added to the transmission map. NGS also enabled us to exclude other SOT and control patients from the transmission map with a higher degree of certainty compared with first-generation sequencing (Sanger sequencing), which is not accurate for minor strain detection <20%. Therefore, NGS-MLST appears to have a higher accuracy for describing an outbreak event and for specifying the transmission network.

For experimental purposes, we designed new primers to generate longer amplicons. We discovered 4 new mutations within the 732 bp *mtLSU* amplicon but no new polymorphism for the *SOD* or *CYTB* loci. Currently, no established MLST scheme for PCP typing exists; the 3-loci (*mtLSU*, *CYTB*, and *SOD*) scheme has been proposed and previously used in the context of a PCP outbreak (3,14). The 5th European Conference on Infections in Leukemia also recommended this MLST scheme for *P. jirovecii* typing (25). The internal transcribed spacer regions have been used but are difficult to amplify and are at risk for in vitro recombination (14,34). Extended 732 bp *mtLSU* and *CYTB* sequence polymorphisms conferred a high discriminatory power ($D > 0.95$), considered to be sufficient for strain discrimination (35). In addition, *mtLSU* and *CYTB* amplification is facilitated because of their mitochondrial origin (multicopy genes). Hence, the lengthened 732 bp *mtLSU* PCR product could be of interest in light of the previously described 300 or 370 bp amplicons (14). The sequencing of 732 bp *mtLSU* and *CYTB* could be proposed as a rapid screening method to evaluate strain convergence, whereas *SOD* or internal transcribed spacer regions could be sequenced in a second step. Further studies will be needed to assess the added value of these newly described polymorphisms.

Although our study revealed new features in *P. jirovecii* typing, it did not provide evidence for or against features such as diploidy or mitochondrial heteroplasmy of *P. jirovecii* during PCP (32,36). None of our 32 samples exhibited a clear 50/50 allele repartition, which would have suggested heterozygosity, but the presence of heterozygote stages among the described genotypes cannot be entirely ruled out. The mitochondrial genes *mtLSU* and to a lesser extent *CYTB* displayed higher diversity than the nuclear locus *SOD*. However, this finding is not sufficient to confirm mitochondrial heteroplasmy because these differences might also have been attributable to the higher rate of polymorphism in the mitochondrial loci. One third of the samples displayed a unique genotype, suggesting that mitochondrial heteroplasmy was not present during these PCP infections.

This study demonstrated the clear added value of NGS-MLST to analyze major and minor strains in epidemiologic *P. jirovecii* studies. NGS is increasingly attractive because of the rapid development of bioinformatics and the reduced cost of this approach (37). We believe that NGS-MLST represents the next generation of MLST and that this method will become the new standard for strain typing in the next decade, especially for microorganisms that are not cultivable in vitro.

Acknowledgments

We are grateful to François Collyn, Carole Donne-Gousse, and the Roche sequencing service platform for their technical assistance, Katia Fusillier for sharing her experience and skills on the GS Junior, and Joelle Leral for her assistance with Sanger sequencing. We thank Hervé Pelloux for giving us the opportunity to work on this subject and Julien Fauré for granting us access to the Sanger sequencing platform.

This work was supported by Merck Sharp & Dohme.

Ms. Charpentier is an assistant professor at Toulouse University Hospital, France, and previously completed her master's degree on this topic in Grenoble Alpes University Hospital, France. Her primary research interests include medical biology with an emphasis on medical mycology and parasitology.

References

- Roux A, Canet E, Valade S, Gangneux-Robert F, Hamane S, Lafabrie A, et al. *Pneumocystis jirovecii* pneumonia in patients with or without AIDS, France. *Emerg Infect Dis*. 2014;20:1490–7. <http://dx.doi.org/10.3201/eid2009.131668>
- Bitar D, Lortholary O, Dromer F, Coignard B, Che D. Bulletin épidémiologique hebdomadaire—BEH n°12–13/2013 [cited 2016 Jul 19]. <http://www.invs.sante.fr/Publications-et-outils/BEH-Bulletin-epidemiologique-hebdomadaire/Archives/2013/BEH-n-12-13-2013>
- Desoubeaux G, Dominique M, Morio F, Thepault R-A, Franck-Martel C, Tellier A-C, et al. Epidemiological outbreaks of *Pneumocystis jirovecii* pneumonia are not limited to kidney transplant recipients: genotyping confirms common source of transmission in a liver transplantation unit. *J Clin Microbiol*. 2016;54:1314–20. <http://dx.doi.org/10.1128/JCM.00133-16>
- Nankivell BJ, Firacative C, Kable K, Chen SC-A, Meyer W. Molecular epidemiology linking multihospital clusters of opportunistic *Pneumocystis jirovecii* pneumonia. *Clin Infect Dis*. 2013;57:1058–9. <http://dx.doi.org/10.1093/cid/cit413>
- Rostved AA, Sassi M, Kurtzhals JAL, Sørensen SS, Rasmussen A, Ross C, et al. Outbreak of *pneumocystis* pneumonia in renal and liver transplant patients caused by genotypically distinct strains of *Pneumocystis jirovecii*. *Transplantation*. 2013;96:834–42. <http://dx.doi.org/10.1097/TP.0b013e3182a1618c>
- Le Gal S, Damiani C, Rouillé A, Grall A, Tréguer L, Virmaux M, et al. A cluster of *Pneumocystis* infections among renal transplant recipients: molecular evidence of colonized patients as potential infectious sources of *Pneumocystis jirovecii*. *Clin Infect Dis*. 2012;54:e62–71. <http://dx.doi.org/10.1093/cid/cir996>
- Yiannakis EP, Boswell TC. Systematic review of outbreaks of *Pneumocystis jirovecii* pneumonia: evidence that *P. jirovecii* is a transmissible organism and the implications for healthcare infection control. *J Hosp Infect*. 2016;93:1–8. <http://dx.doi.org/10.1016/j.jhin.2016.01.018>
- Esteves F, de Sousa B, Calderón EJ, Huang L, Badura R, Maltez F, et al. Multicentre study highlighting clinical relevance of new high-throughput methodologies in molecular epidemiology of *Pneumocystis jirovecii* pneumonia. *Clin Microbiol Infect*. 2016;22:566.e9–19. <http://dx.doi.org/10.1016/j.cmi.2016.03.013>
- Alanio A, Olivi M, Cabaret O, Foulet F, Bellanger A-P, Millon L, et al. Correlation between *Pneumocystis jirovecii* mitochondrial genotypes and high and low fungal loads assessed by single nucleotide primer extension assay and quantitative real-time PCR. *J Eukaryot Microbiol*. 2015;62:650–6. <http://dx.doi.org/10.1111/jeu.12222>
- Hauser PM. The development of a typing method for an uncultivable microorganism: the example of *Pneumocystis jirovecii*. *Infect Genet Evol*. 2004;4:199–203. <http://dx.doi.org/10.1016/j.meegid.2004.01.011>
- Ripamonti C, Orenstein A, Kutty G, Huang L, Schuegger R, Sing A, et al. Restriction fragment length polymorphism typing demonstrates substantial diversity among *Pneumocystis jirovecii* isolates. *J Infect Dis*. 2009;200:1616–22. <http://dx.doi.org/10.1086/644643>
- Gits-Muselli M, Peraldi M-N, de Castro N, Delcey V, Menotti J, Guigue N, et al. New short tandem repeat-based molecular typing method for *Pneumocystis jirovecii* reveals intrahospital transmission between patients from different wards. *PLoS One*. 2015;10:e0125763. <http://dx.doi.org/10.1371/journal.pone.0125763>
- Schmoldt S, Schuegger R, Wendler T, Huber I, Söllner H, Hogardt M, et al. Molecular evidence of nosocomial *Pneumocystis jirovecii* transmission among 16 patients after kidney transplantation. *J Clin Microbiol*. 2008;46:966–71. <http://dx.doi.org/10.1128/JCM.02016-07>
- Maitte C, Leterrier M, Le Pape P, Miegerville M, Morio F. Multilocus sequence typing of *Pneumocystis jirovecii* from clinical samples: how many and which loci should be used? *J Clin Microbiol*. 2013;51:2843–9. <http://dx.doi.org/10.1128/JCM.01073-13>
- Chen X, Zou X, He J, Zheng J, Chiarella J, Kozal MJ. HIV drug resistance mutations (DRMs) detected by deep sequencing in virologic failure subjects on therapy from Hunan Province, China. *PLoS One*. 2016;11:e0149215. <http://dx.doi.org/10.1371/journal.pone.0149215>
- Liang B, Luo M, Scott-Herridge J, Semeniuk C, Mendoza M, Capina R, et al. A comparison of parallel pyrosequencing and sanger clone-based sequencing and its impact on the characterization of the genetic diversity of HIV-1. *PLoS One*. 2011;6:e26745. <http://dx.doi.org/10.1371/journal.pone.0026745>
- Mello FCA, Lago BV, Lewis-Ximenez LL, Fernandes CA, Gomes SA. Detection of mixed populations of wild-type and YMDD hepatitis B variants by pyrosequencing in acutely and chronically infected patients. *BMC Microbiol*. 2012;12:96. <http://dx.doi.org/10.1186/1471-2180-12-96>
- Wang C, Mitsuya Y, Gharizadeh B, Ronaghi M, Shafer RW. Characterization of mutation spectra with ultra-deep pyrosequencing: application to HIV-1 drug resistance. *Genome Res*. 2007;17:1195–201. <http://dx.doi.org/10.1101/gr.6468307>
- Quiñones-Mateu ME, Avila S, Reyes-Teran G, Martinez MA. Deep sequencing: becoming a critical tool in clinical virology. *J Clin Virol*. 2014;61:9–19. <http://dx.doi.org/10.1016/j.jcv.2014.06.013>
- Chumpitazi BFF, Flori P, Kern J-B, Brenier-Pinchart M-P, Hincky-Vitrat V, Brion JP, et al. Characteristics and clinical relevance of the quantitative touch-down major surface glycoprotein polymerase chain reaction in the diagnosis of *Pneumocystis* pneumonia. *Med Mycol*. 2011;49:704–13.
- Goto N, Oka S. *Pneumocystis jirovecii* pneumonia in kidney transplantation. *Transpl Infect Dis*. 2011;13:551–8. <http://dx.doi.org/10.1111/j.1399-3062.2011.00691.x>
- Yazaki H, Goto N, Uchida K, Kobayashi T, Gatanaga H, Oka S. Outbreak of *Pneumocystis jirovecii* pneumonia in renal transplant recipients: *P. jirovecii* is contagious to the susceptible host. *Transplantation*. 2009;88:380–5. <http://dx.doi.org/10.1097/TP.0b013e3181aed389>
- Le Gal S, Pougnet L, Damiani C, Fréalle E, Guéguen P, Virmaux M, et al. *Pneumocystis jirovecii* in the air surrounding patients with *Pneumocystis* pulmonary colonization. *Diagn Microbiol Infect Dis*. 2015;82:137–42. <http://dx.doi.org/10.1016/j.diagmicrobio.2015.01.004>
- Damiani C, Choukri F, Le Gal S, Menotti J, Sarfati C, Nevez G, et al. Possible nosocomial transmission of *Pneumocystis jirovecii*. *Emerg Infect Dis*. 2012;18:877–8. <http://dx.doi.org/10.3201/eid1805.111432>
- Alanio A, Hauser PM, Lagrou K, Melchers WJG, Helweg-Larsen J, Matos O, et al.; 5th European Conference on Infections in Leukemia (ECIL-5), a joint venture of The European Group for Blood and Marrow Transplantation (EBMT), The European Organization for Research and Treatment of Cancer (EORTC), the Immunocompromised Host Society (ICHS) and The European LeukemiaNet (ELN). ECIL guidelines for the diagnosis of *Pneumocystis jirovecii* pneumonia in patients with haematological

- malignancies and stem cell transplant recipients. *J Antimicrob Chemother.* 2016;71:2386–96. <http://dx.doi.org/10.1093/jac/dkw156>
26. Hunter PR. Reproducibility and indices of discriminatory power of microbial typing methods. *J Clin Microbiol.* 1990;28:1903–5.
 27. Wynckel A, Toubas D, Noël N, Toupance O, Rieu P. Outbreak of *pneumocystis* pneumonia occurring in late post-transplantation period. *Nephrol Dial Transplant.* 2011;26:2417–8, author reply 2418. <http://dx.doi.org/10.1093/ndt/gfr159>
 28. Valade S, Azoulay E, Damiani C, Derouin F, Totet A, Menotti J. *Pneumocystis jirovecii* airborne transmission between critically ill patients and health care workers. *Intensive Care Med.* 2015;41:1716–8. <http://dx.doi.org/10.1007/s00134-015-3835-9>
 29. Hauser PM, Blanc DS, Sudre P, Sengen Manoloff E, Nahimana A, Bille J, et al. Genetic diversity of *Pneumocystis carinii* in HIV-positive and -negative patients as revealed by PCR-SSCP typing. *AIDS.* 2001;15:461–6. <http://dx.doi.org/10.1097/00002030-200103090-00004>
 30. Rabodonirina M, Vanhems P, Couray-Targe S, Gillibert R-P, Ganne C, Nizard N, et al. Molecular evidence of interhuman transmission of *Pneumocystis* pneumonia among renal transplant recipients hospitalized with HIV-infected patients. *Emerg Infect Dis.* 2004;10:1766–73. <http://dx.doi.org/10.3201/eid1010.040453>
 31. Le Gal S, Damiani C, Rouillé A, Grall A, Tréguer L, Virmaux M, et al. A cluster of *Pneumocystis* infections among renal transplant recipients: molecular evidence of colonized patients as potential infectious sources of *Pneumocystis jirovecii*. *Clin Infect Dis.* 2012;54:e62–71. <http://dx.doi.org/10.1093/cid/cir996>
 32. Alanio A, Gits-Muselli M, Mercier-Delarue S, Dromer F, Bretagne S. Diversity of *Pneumocystis jirovecii* during infection revealed by ultra-deep pyrosequencing. *Front Microbiol.* 2016;7:733. <http://dx.doi.org/10.3389/fmicb.2016.00733>
 33. Le Gal S, Blanchet D, Damiani C, Guéguen P, Virmaux M, Abboud P, et al. AIDS-related *Pneumocystis jirovecii* genotypes in French Guiana. *Infect Genet Evol.* 2015;29:60–7. <http://dx.doi.org/10.1016/j.meegid.2014.10.021>
 34. Beser J, Hagblom P, Fernandez V. Frequent in vitro recombination in internal transcribed spacers 1 and 2 during genotyping of *Pneumocystis jirovecii*. *J Clin Microbiol.* 2007;45:881–6. <http://dx.doi.org/10.1128/JCM.02245-06>
 35. Struelens MJ. Consensus guidelines for appropriate use and evaluation of microbial epidemiologic typing systems. *Clin Microbiol Infect.* 1996;2:2–11. <http://dx.doi.org/10.1111/j.1469-0691.1996.tb00193.x>
 36. Urabe N, Ishii Y, Hyodo Y, Aoki K, Yoshizawa S, Saga T, et al. Molecular epidemiologic analysis of a *Pneumocystis* pneumonia outbreak among renal transplant patients. *Clin Microbiol Infect.* 2016;22:365–71. <http://dx.doi.org/10.1016/j.cmi.2015.12.017>
 37. Chen Y, Frazzitta AE, Litvintseva AP, Fang C, Mitchell TG, Springer DJ, et al. Next generation multilocus sequence typing (NGMLST) and the analytical software program MLST-EZ enable efficient, cost-effective, high-throughput, multilocus sequencing typing. *Fungal Genet Biol.* 2015;75:64–71. <http://dx.doi.org/10.1016/j.fgb.2015.01.005>

Address for correspondence: Danièle Maubon, Laboratoire de Parasitologie-Mycologie, Institut de Biologie et Pathologie, CHU Grenoble Alpes, 38048 Grenoble CEDEX 9, France; email: dmaubon@chu-grenoble.fr

etymologia

Pneumocystis jirovecii [noo"mo-sis'tis ye"ro-vet'ze]

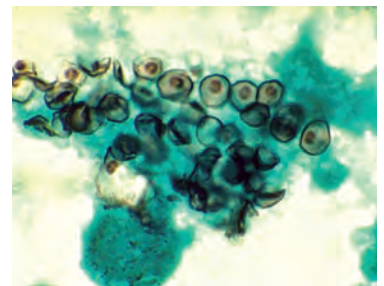
Ronnie Henry

A genus of unicellular fungi, *Pneumocystis* was likely originally described by Carlos Chagas in 1909 in guinea pigs, although he confused it with a trypanosome and placed it in a new genus, *Schizotrypanum*. In 1912, Delanoë and Delanoë at the Pasteur Institute published the first description of the new organism as unrelated to trypanosomes and proposed the species name *P. carinii* in honor of Antonio Carini.

Human *Pneumocystis* infections were first reported in 1942 by van der Meer and Brug, but not until 1976 did Frenkel report different morphologic and physiologic characteristics of human and rat *Pneumocystis* isolates. He proposed the name *P. jirovecii* in honor of Czech parasitologist Otto Jírovec, who reported *Pneumocystis* as a cause of interstitial pneumonia in infants, although this name change was not accepted by researchers at the time. When *Pneumocystis* was reclassified from a protozoan to a fungus, the naming convention shifted from the International Code of Zoological Nomenclature to the International Code of Botanical Nomenclature, and the species epithet was modified from *jiroveci* to *jirovecii*.

Sources

1. Frenkel JK. *Pneumocystis jirovecii* n. sp. from man: morphology, physiology, and immunology in relation to pathology. *Natl Cancer Inst Monogr.* 1976;43:13–30.
2. Hawksworth DL. Responsibility in naming pathogens: the case of *Pneumocystis jirovecii*, the causal agent of pneumocystis pneumonia. *Lancet Infect Dis.* 2007;7:3–5, discussion 5. [http://dx.doi.org/10.1016/S1473-3099\(06\)70663-6](http://dx.doi.org/10.1016/S1473-3099(06)70663-6)
3. Stringer JR, Beard CB, Miller RF, Wakefield AE. A new name (*Pneumocystis jirovecii*) for *Pneumocystis* from humans and new perspectives on the host-pathogen relationship. *Emerg Infect Dis.* 2002;8:891–6. <http://dx.doi.org/10.3201/eid0809.020096>
4. Stringer JR, Beard CB, Miller RF. Spelling *Pneumocystis jirovecii*. *Emerg Infect Dis.* 2009;15:506. <http://dx.doi.org/10.3201/eid1503.081060>
5. Walzer PD, Smulian AG. *Pneumocystis* species. In: Mandell GL, Bennett, JE, Dolin R, editors. *Mandell, Douglas, and Bennett's Principles and Practice of Infectious Disease.* 7th edition. Philadelphia: Elsevier; 2010. p. 3377–90.



Cysts of *Pneumocystis jirovecii* in smear from bronchoalveolar lavage. Methenamine silver stain. CDC/Dr. Russell K. Brynes

Address for correspondence: Ronnie Henry, Centers for Disease Control and Prevention, 1600 Clifton Rd NE, Mailstop E03, Atlanta, GA 30329-4027, USA; email: boq3@cdc.gov

DOI: <https://doi.org/10.3201.eid2308.ET2308>

Bartonella quintana, an Unrecognized Cause of Infective Endocarditis in Children in Ethiopia

Diana Tasher, Alona Raucher-Sternfeld, Akiva Tamir, Michael Giladi, Eli Somekh



JOINTLY ACCREDITED PROVIDER™
INTERPROFESSIONAL CONTINUING EDUCATION

Medscape EDUCATION ACTIVITY

In support of improving patient care, this activity has been planned and implemented by Medscape, LLC and Emerging Infectious Diseases. Medscape, LLC is jointly accredited by the Accreditation Council for Continuing Medical Education (ACCME), the Accreditation Council for Pharmacy Education (ACPE), and the American Nurses Credentialing Center (ANCC), to provide continuing education for the healthcare team.

Medscape, LLC designates this Journal-based CME activity for a maximum of 1.00 **AMA PRA Category 1 Credit(s)**™. Physicians should claim only the credit commensurate with the extent of their participation in the activity.

All other clinicians completing this activity will be issued a certificate of participation. To participate in this journal CME activity: (1) review the learning objectives and author disclosures; (2) study the education content; (3) take the post-test with a 75% minimum passing score and complete the evaluation at <http://www.medscape.org/journal/eid>; and (4) view/print certificate. For CME questions, see page 1439.

Release date: July 14, 2017; Expiration date: July 14, 2018

Learning Objectives

Upon completion of this activity, participants will be able to:

- Distinguish features of infection with *Bartonella quintana*.
- Identify the country of origin of children in the current case series of *Bartonella* endocarditis.
- Assess presenting symptoms of *Bartonella* endocarditis among children.
- Analyze clinical findings associated with *Bartonella* endocarditis among children.

CME Editor

Claudia Chesley, BA, Technical Writer/Editor, Emerging Infectious Diseases. *Disclosure: Claudia Chesley, BA, has disclosed no relevant financial relationships.*

CME Author

Charles P. Vega, MD, Health Sciences Clinical Professor, UC Irvine Department of Family Medicine; Associate Dean for Diversity and Inclusion, UC Irvine School of Medicine, Irvine, California, USA. *Disclosure: Charles P. Vega, MD, has disclosed the following financial relationships: served as an advisor or consultant for McNeil Consumer Healthcare; served as a speaker or a member of a speakers bureau for Shire Pharmaceuticals.*

Authors

Disclosures: Diana Tasher, MD; Alona Raucher-Sternfeld, MD; Akiva Tamir, MD; Michael Giladi, MD; and Eli Somekh, MD, have disclosed no relevant financial relationships.

Bartonella quintana endocarditis, a common cause of culture-negative endocarditis in adults, has rarely been reported in children. We describe 5 patients 7–16 years of age from Ethiopia with heart defects and endocarditis; 4 cases were caused by

infection with *B. quintana* and 1 by *Bartonella* of undetermined species. All 5 patients were afebrile and oligosymptomatic, although 3 had heart failure. C-reactive protein was normal or slightly elevated, and erythrocyte sedimentation rate was high. The diagnosis was confirmed by echocardiographic demonstration of vegetations, the presence of high *Bartonella* IgG titers, and identification of *B. quintana* DNA in excised vegetations. Embolic events were diagnosed in 2 patients. Our data suggest that *B. quintana* is not an uncommon cause of native valve endocarditis in children in Ethiopia with heart defects and that possible *B. quintana* infection should be suspected and pursued among residents of and immigrants from East Africa, including Ethiopia, with culture-negative endocarditis.

Author affiliations: Tel Aviv University Sackler School of Medicine, Tel Aviv, Israel (D. Tasher, A. Raucher-Sternfeld, A. Tamir, M. Giladi, E. Somekh); Wolfson Medical Center, Holon, Israel (D. Tasher, A. Raucher-Sternfeld, A. Tamir, E. Somekh); Tel Aviv Sourasky Medical Center, Tel Aviv (M. Giladi); European Paediatric Association–Union of National European Paediatric Societies and Associations, Berlin, Germany (E. Somekh)

DOI: <https://doi.org/10.3201/eid2308.161037>

Blood culture–negative endocarditis accounts for 2.5%–31% of all cases of endocarditis (1). *Bartonella* spp. (most commonly *B. henselae* and *B. quintana*) are among the most common causes of blood culture–negative endocarditis, being responsible for 9.5%–28.4% of all cases (2,3). The literature regarding *Bartonella* endocarditis among children describes 1 microbiologically confirmed case caused by *B. quintana* (4) and 8 cases caused by *B. henselae* (5–12). In this case series, we describe 5 patients, 7–16 years of age, from Ethiopia who were referred to our center in Israel for heart surgery and diagnosed with endocarditis caused by *B. quintana* (4 cases) or *Bartonella* of an undetermined species (1 case).

Materials and Methods

Wolfson Medical Center in Holon, Israel, provides cardiothoracic care to children from developing regions, such as Africa, Palestinian Authority, and South America, who are referred for care through the Save a Child's Heart fund activity (13). Each year, doctors in the Center perform heart surgery on ≈200 children from developing countries. After the unexpected diagnosis of *B. quintana* endocarditis in this group of children, we reviewed the presurgical cases of infective endocarditis in children referred for heart surgery during 2006–2015.

Before surgery, we conducted a thorough work-up on all patients with endocarditis, including several blood cultures and serologic testing for *Bartonella*, *Legionella*, and *Brucella* spp. and for Q fever (*Coxiella burnetii* infection). In addition, for most patients, we performed microbiologic studies of specimens obtained during cardiac surgery. We performed and interpreted enzyme immunoassays that have been shown to be 98% specific for detection of *B. henselae* IgM and IgG (14,15). We also performed serial dilutions to determine final serum titers.

Similar to other serologic assays used for the diagnosis of *Bartonella* infections (16,17), the enzyme immunoassay used in this study demonstrated high cross-reactivity between *B. quintana* and *B. henselae* (M. Giladi, unpub. data). Thus, we presented serologic results as *Bartonella* sp. IgG and IgM, without species identification. We also performed a genus-specific amplification assay of a 588-bp fragment of the *Bartonella* riboflavin synthase gene as previously reported (18). For species identification, we sequenced the PCR product and submitted it to a BLAST search (<https://blast.ncbi.nlm.nih.gov/Blast.cgi>). We considered patients to have endocarditis only after they were determined to fulfill the Duke criteria (19).

Results

From January 1, 2006, through December 31, 2015, a total of 574 children from Africa underwent cardiac surgery, catheterization, or both at Wolfson Medical Center.

During this time, 7 (1.2%) of the 574 children were diagnosed with infective endocarditis before surgery. The most frequent cause of endocarditis was *B. quintana* infection, which was diagnosed in 4/7 children. The 3 other endocarditis cases were caused by undetermined *Bartonella* spp. infection in an 11-year-old boy from Ethiopia, *Streptococcus viridans* infection in a 2-year-old boy from Zanzibar, and Q fever in a 7-year-old girl from Kenya. All patients with *Bartonella* endocarditis were from Ethiopia, where they lived in poor, crowded conditions. The clinical details of the children with *Bartonella* endocarditis follow.

Cases

Patient A

An asymptomatic 7-year-old girl from Jimma, Ethiopia, with patent ductus arteriosus was referred to the Wolfson Medical Center. At admission, she was afebrile and in good general condition. Her physical examination revealed a grade 2/6 continuous cardiac murmur and splenomegaly but no stigmata of infective endocarditis. Transthoracic echocardiogram (TTE) revealed thickening of the pulmonary valve and the presence of a large (1.1 cm in diameter) mobile mass attached to the middle of the main pulmonary artery and several small masses attached to the pulmonic valve cusps, consistent with vegetations. The main laboratory results were a high erythrocyte sedimentation rate (ESR) and an only slightly elevated CRP (Table).

We obtained blood samples for cultures and then initiated empirical therapy with doxycycline and ceftriaxone for presumed common and culture-negative endocarditis pathogens. The serologic test result for *Bartonella* spp. was positive (IgG titer of 1:1,600), but the test result for IgM was negative (Table). Thus, we initiated treatment with intravenous gentamicin (3 mg/kg bodyweight 1×/d) and oral doxycycline (2 mg/kg bodyweight every 12 h) for *Bartonella* endocarditis (20,21). After 2 weeks of treatment, the patient underwent surgical repair of her heart defect. The vegetations were excised from the main pulmonary artery and the pulmonic valve cusps, a perforation that was revealed in the right pulmonary valve cusp was repaired, and the patent ductus arteriosus was closed. The child had an uneventful postoperative course. PCR testing confirmed the presence of *B. quintana* DNA in the excised vegetation. The child completed a 2-week course of gentamicin and a 5-week course of oral doxycycline and returned to Ethiopia in good condition.

Patient B

A 12-year-old girl from Jimma was admitted for the correction of mitral regurgitation due to rheumatic heart

SYNOPSIS

Table. Features for children from Ethiopia with *Bartonella quintana* endocarditis*

Patient, age, y/sex	Echo finding	Underlying condition	Phenomena		Microbiologic evidence	CRP, mg/dL	ESR, mm/h	Leuk/mm ³	Hb, g/dL	Platelets/mm ³ †
			Vascular	Immunologic						
A, 7/F	Several vegetations (11 mm) on pulmonary valve	CHD	No	RF Ab, 189 IU/mL	<i>Bartonella</i> IgG titer 1:1,600, IgM neg; excised vegetation PCR-neg for <i>Coxiella burnetii</i> , PCR-pos for <i>B. quintana</i> ‡	1.7	128	3,500	8.5	150,000
B, 12/F	Vegetation (7 mm) on mitral valve	RHD	No	RF Ab, <10 IU/mL	<i>Bartonella</i> IgG titer 1:100, IgM neg; excised vegetation PCR-neg for <i>C. burnetii</i> , PCR-pos for <i>B. quintana</i> ‡	0.7	50	5,700	10.3	310,000
C, 16/F	Two vegetations (5 mm) on aortic valve	RHD	Emboli to spleen	GN; 16 Osler nodes	<i>Bartonella</i> IgG titer 1:12,800 (10 wks after surgery: 1:6,400); excised vegetation PCR-neg for <i>C. burnetii</i> , PCR-pos for <i>B. quintana</i> ‡	4.2	150	6,900	7.8	334,000
D, 9/F	Several vegetations (10 mm and 20 mm) on aortic valve	CHD	CVA	RF Ab, 25 IU/mL	<i>Bartonella</i> IgG titer 1:6,400 (5 wks after surgery: 1:1,600); excised vegetation PCR-neg for <i>C. burnetii</i> , PCR-pos for <i>B. quintana</i> ‡	1.5	44	6,100	11.7	189,000
E, 11/M	Vegetation (14 mm) on aortic valve	CHD	No	RF Ab, 2,560 IU/mL	<i>Bartonella</i> IgG titer 1:6,400; <i>C. burnetii</i> IgM neg	2.0	110	9,100	11.8	264,000

*HIV serologic testing and blood culture results were negative for all patients, and no patients had fever. Ab, antibody; CHD, congenital heart disease; CRP, C-reactive protein (reference range 0–10 mg/dL); CVA, cerebral vascular accident; Echo, echocardiogram; ESR, erythrocyte sedimentation rate (reference range 0–20 mm); GN, glomerulonephritis; Hb, hemoglobin (reference range 9.5–13.0 g/dL); Leuk, leukocytes (reference range 6,000–17,500 cells/mm³); neg, negative; pos, positive; RF, rheumatoid factor; RHD, rheumatic heart disease.

†Reference range 150–400 × 10⁹ platelets/L.

‡Sequence comparison analysis demonstrated a 100% identity to *B. quintana*.

disease, which had been diagnosed 4 months earlier due to symptoms of congestive heart failure. On physical examination, she was afebrile and exhibited tachypnea and orthopnea. Cardiac examination revealed a grade 4/6 harsh systolic ejection murmur and a grade 2/4 diastolic rumble at the apex. Physical findings were otherwise unremarkable and showed no stigmata of infective endocarditis. TTE revealed the presence of a 7-mm mobile mass, consistent with vegetation, attached to the mitral chordae. Main laboratory results were high erythrocyte sedimentation rate (ESR) and an only slightly elevated CRP (Table).

We initiated empirical therapy with doxycycline and ceftriaxone, and after serologic results were received, we initiated treatment with gentamicin and oral doxycycline for *Bartonella* endocarditis. After 2 weeks of treatment with doxycycline, the child underwent mitral valvuloplasty; she had an uneventful postoperative course. PCR testing confirmed the presence of *B. quintana* DNA in the excised vegetations. The child completed a 6-week course of oral doxycycline and a 1-week course of gentamicin (during the first week of doxycycline treatment) and returned to Ethiopia in good condition.

Patient C

A 16-year-old girl from Jimma was admitted for surgical repair of mitral and aortic valve disease due to rheumatic

heart disease that had been diagnosed when she was 12 years of age. During the previous year, she had had several heart failure–related hospitalizations. At admission, she was afebrile and exhibited orthopnea and dyspnea. Cardiac examination revealed a grade 3/4 diastolic murmur, and abdominal examination showed liver enlargement. Physical findings were otherwise unremarkable, with no stigmata of infective endocarditis. TTE revealed 2 vegetations (5-mm diameter) attached to the noncoronary aortic valve cusp. As with the previous patients, her laboratory results showed high ESR and only slightly elevated CRP (Table).

After receiving the serologic test results, we initiated treatment with gentamicin and doxycycline. After 2 weeks of treatment, painful reddish lesions suggestive of Osler nodes developed on the patient’s palms, and her spleen was enlarged 4 cm below the costal margin. Repeated TTE revealed a single vegetation. Abdominal ultrasonography showed enlarged spleen (14.5 cm in length) with infarcts compatible with emboli. The patient underwent surgical repair of her mitral and aortic valves. PCR testing confirmed the presence of *B. quintana* DNA in the excised vegetation. The patient completed a 12-week course of oral doxycycline and a 2-week course of gentamicin (during the first 2 weeks of doxycycline treatment). Six months after surgery she was asymptomatic.

Patient D

A 9-year-old girl from Addis Ababa, Ethiopia, was referred for surgical repair of a congenital heart defect. One year before admission, she had a history of febrile illness accompanied by left-sided weakness. The patient was diagnosed in Ethiopia with a large patent ductus arteriosus and severe aortic regurgitation and was suspected to have infective endocarditis. At admission, she was afebrile but had systolic and diastolic murmurs and hepatosplenomegaly. Neurologic examination revealed left hemiparesis. She had no other stigmata of infective endocarditis. TTE revealed several calcified vegetations (10 mm and 20 mm in diameter) attached to the cusps of the aortic valve.

We initiated treatment with gentamicin and oral doxycycline. After receiving treatment for a week, the patient underwent aortic valve replacement, mitral valve repair, and patent ductus arteriosus closure. PCR of the excised aortic valve revealed *B. quintana* DNA. The child had an uneventful postoperative course. She completed a 2-week course of gentamicin and a 10-week course of oral doxycycline.

Patient E

An 11-year-old boy from Addis Ababa was referred for repair of a large coronary artery fistula. He complained mainly of weakness on exertion and chest pain. Physical examination revealed unremarkable vital signs and temperature, continuous machinery murmur, and splenomegaly but no rash or endocarditis stigmata. An echocardiograph revealed a 14-mm vegetation on the aortic valve. Serologic studies revealed a high IgG titer (1:6,400) to *Bartonella* sp.; IgM results were negative. The results of other serologic studies and multiple blood cultures were negative (Table).

We initiated treatment with gentamicin (for 2 weeks) and oral doxycycline (for 3 months). The heart defect was corrected by catheterization without surgery, so we did not have tissue for molecular studies and could not determine the *Bartonella* species. We followed the child for 5 months in our center; he was asymptomatic, and repeated echocardiography showed gradual regression of the vegetation size until its actual disappearance.

Discussion

This case series provides detailed information regarding the clinical presentation, course, and outcome of *Bartonella* endocarditis caused by *B. quintana* infection in 4 children and by *Bartonella* of undetermined species in 1 child. Of interest, all 5 children were natives of Ethiopia. When admitted to our medical center, all of the children were afebrile and had nonspecific symptoms, except for heart failure, which was attributed to their previously known

heart disease. In 4 of the 5 patients, endocarditis was not suspected on clinical grounds, but we pursued the diagnosis after echocardiographs revealed vegetations. The diagnosis of *B. quintana* endocarditis was confirmed in 4 patients (patients A–D) by identification of *B. quintana* DNA in excised vegetations or endocardial tissue. The diagnosis was further supported by the presence of *Bartonella* IgG in these 4 patients, 3 of whom had high titers (1:1,600–1:12,800). The fifth patient had *Bartonella* endocarditis caused by an undetermined species; the diagnosis was based only on serologic test results (IgG titer of 1:6,400) because cardiac tissue was not available for molecular diagnosis. Western blot with cross-absorption studies, a method described by Houpiikian and Raoult (22), could have discriminated between *B. quintana* and *B. henselae* if it had been applied.

Bartonella spp. are small, gram-negative bacilli whose natural cycle includes a reservoir host, in which *Bartonella* causes chronic intraerythrocytic bacteremia. In 1993, *Bartonella* spp. were described as a cause of endocarditis in 2 separate reports and subsequently has become appreciated as a substantial cause of culture-negative endocarditis (3,23,24). Raoult and colleagues have generated several reports on endocarditis caused by *Bartonella* spp., including several multicenter international studies that involved patients from France, England, and Canada (17,25). Seven *Bartonella* spp. have been reported to cause infective endocarditis in humans; >95 percent of the cases involved *B. quintana* or *B. henselae* (17).

This case series of *Bartonella* endocarditis in children reveals several common characteristics. All cases occurred in preadolescent and adolescent patients; all patients were afebrile, and the main pathophysiologic dysfunction was congestive heart failure. All patients had markedly elevated ESRs but normal or only mildly elevated CRP levels. Echocardiography revealed large and even giant vegetations in most of the patients, and 2 (40%) of the patients had embolic phenomena. Medical treatment consisted of a prolonged course of doxycycline combined with gentamicin during the initial period, as was recommended for adults with *Bartonella* endocarditis (21). Even though prolonged administration of doxycycline is relatively contraindicated in children <8 years of age, we suggested a 5-week course for the 7-year-old patient (patient A), as recently recommended (20), because of the extent of her valvular disease.

B. quintana is historically known to cause trench fever, a recurrent febrile disease with acute onset characterized by fever and headache. Trench fever was epidemic among troops during World War I, causing millions of casualties. However, after the introduction of louse control measures, the disease was no longer considered a threat.

Recently, however, trench fever has reemerged, causing bacteremia in homeless persons and persons affected with alcoholism in Europe and North America, where it has now been designated urban trench fever (26). *B. quintana* is mostly associated with human body lice but has also been found in fleas (27,28). The predisposing factors for *B. quintana* endocarditis are homelessness, alcoholism, and exposure to body lice (29). None of these risk factors for *B. quintana* infection were known to exist in the patients in this study.

Patients in this study denied having had lice infestation in the past, and we did not identify body lice, pruritus, or excoriations during the initial physical examinations. However, we believe that detailed and accurate histories regarding lice infestation were lacking, particularly because patients with *B. quintana* endocarditis have probably been infected with *B. quintana* for months or years before hospital admission for endocarditis. We speculate that residence in a developing country with presumably poor hygiene and low socioeconomic status might have exposed the patients in this study to ectoparasite infestations, including body lice, which could have served as a transmitting vector for *B. quintana*.

In contrast to our report of afebrile patients with sizable vegetations, previous reports of *Bartonella* endocarditis have described that fever is usually present (83% of cases) and that valve destruction is characterized by large calcifications but small vegetations (25). Description of *B. quintana* endocarditis in children is currently confined to a case in a 13-year-old girl from Senegal with underlying rheumatic heart disease, an insidious afebrile clinical course, and prominent vegetations of the left side of the heart (4). Another 2 children with endocarditis and *B. quintana*-positive serologic test results were included in a series from India, but no clinical or laboratory details were provided (30).

Of the 5 children in our study with *Bartonella* endocarditis, 4 had involvement of the aortic valve. The predilection for *Bartonella* spp. to infect the aortic valve has been described (25), but the reason is unknown. Before surgery, 4 of the 5 children fulfilled the Duke criteria for definite infective endocarditis, and the fifth child (patient E) fulfilled criteria for possible endocarditis (Table).

The Duke criteria do not address *Bartonella* endocarditis specifically, and a definitive diagnosis of *Bartonella* infection requires positive, high-titer serologic test results; PCR identification of *Bartonella* sp. DNA in affected tissue or blood; or, on rare occasions, isolation of *Bartonella* sp. from blood or tissue culture. Recent studies have shown that direct immunofluorescence antibody assays can reliably detect *Bartonella* IgG, and an IgG titer of >1:800 has a high positive predictive value (95.5%) for *Bartonella* infection

among patients with endocarditis (31,32). However, in 2015, Edouard et al. (32) reported that an IgG titer of <800 does not exclude the diagnosis of *Bartonella* endocarditis in patients with valvulopathy and that a serologic diagnosis can be confirmed by a positive Western blot result, which they showed exhibited a sensitivity of 100%. Similarly, we showed that high *Bartonella* IgG titers can be detected by enzyme immunoassay; only 1 patient in our series had IgG titers <1:800. Thus, the enzyme immunoassay has a meaningful role in the diagnosis of *Bartonella* sp. endocarditis.

Epidemiologic data suggest a north-south gradient distribution in the prevalence of *Bartonella* endocarditis, from 0% in Sweden to 3% in France and Germany and reaching 15.6% in Algeria and 9.8% in Tunisia (32). Lice are a well-recognized reservoir of *B. quintana*. Using reverse transcription PCR testing of lice from residents of 9 African countries, Sangaré et al. (33) showed *B. quintana* DNA was present in 54% of body and 2% of head lice, and they found a clear correlation between the presence of *B. quintana* in head and body lice and the degree of country poverty, as determined by the gross domestic product. *Bartonella* spp. were found among 6 (9.2%) of 65 head lice pools and 1 (3.0%) of 33 clothing lice pools from Jimma (34). These data indicate that *B. quintana* may be quite abundant in East Africa. However, due to the lack of serologic surveys for *Bartonella* species in this region, its extent is unknown.

In our series, *B. quintana* was the most frequent causative organism of native valve endocarditis among children from Africa referred to our center for heart surgery. These cases by no means represent the whole spectrum of infective endocarditis in children in Africa, or even Ethiopia, because a selection bias might exist toward cases of nonacute, indolent, infective endocarditis in patients referred for complicated surgeries. However, the predominance of *B. quintana* infection, even in this specific, small subgroup of patients, is quite impressive and may imply a broader role of this microorganism in infective endocarditis cases in children in Ethiopia or Africa as a whole.

In conclusion, *B. quintana* is a substantial cause of endocarditis in children in Ethiopia with heart disease. Diagnosis may easily be missed because of the afebrile, insidious nature of this disease and the apparent lack of traditional risk factors for *Bartonella* infections.

Acknowledgment

We thank Roger Hertz for reviewing the manuscript.

Dr. Tasher is an attending physician in the Pediatric Infectious Diseases Unit, Wolfson Medical Center, in Holon, Israel. Her primary research interests include vaccines and

vaccine-preventable diseases, periodic fever adenitis pharyngitis aphthous ulcer syndrome; neonatal herpes; and zoonotic infections, including Q fever and infections caused by *Bartonella* spp.

References

- Brouqui P, Raoult D. Endocarditis due to rare and fastidious bacteria. *Clin Microbiol Rev.* 2001;14:177–207. <http://dx.doi.org/10.1128/CMR.14.1.177-207.2001>
- Brouqui P, Raoult D. New insight into the diagnosis of fastidious bacterial endocarditis. *FEMS Immunol Med Microbiol.* 2006;47:1–13. <http://dx.doi.org/10.1111/j.1574-695X.2006.00054.x>
- Fournier PE, Thuny F, Richet H, Lepidi H, Casalta JP, Arzouni JP, et al. Comprehensive diagnostic strategy for blood culture–negative endocarditis: a prospective study of 819 new cases. *Clin Infect Dis.* 2010;51:131–40. <http://dx.doi.org/10.1086/653675>
- Pósfay Barbe K, Jaeggi E, Ninet B, Liassine N, Donatiello C, Gervaix A, et al. *Bartonella quintana* endocarditis in a child. *N Engl J Med.* 2000;342:1841–2. <http://dx.doi.org/10.1056/NEJM200006153422418>
- Baorto E, Payne RM, Slater LN, Lopez F, Relman DA, Min KW, et al. Culture-negative endocarditis caused by *Bartonella henselae*. *J Pediatr.* 1998;132:1051–4. [http://dx.doi.org/10.1016/S0022-3476\(98\)70410-X](http://dx.doi.org/10.1016/S0022-3476(98)70410-X)
- Pitchford CW, Creech CB II, Peters TR, Vnencak-Jones CL. *Bartonella henselae* endocarditis in a child. *Pediatr Cardiol.* 2006;27:769–71. <http://dx.doi.org/10.1007/s00246-006-1383-3>
- Ghidoni JJ. Role of *Bartonella henselae* endocarditis in the nucleation of aortic valvular calcification. *Ann Thorac Surg.* 2004;77:704–6. <http://dx.doi.org/10.1016/j.athoracsur.2003.06.002>
- Walls T, Moshal K, Trounce J, Hartley J, Harris K, Davies G. Broad-range polymerase chain reaction for the diagnosis of *Bartonella henselae* endocarditis. *J Paediatr Child Health.* 2006;42:469–71. <http://dx.doi.org/10.1111/j.1440-1754.2006.00900.x>
- Das BB, Wasser E, Bryant KA, Woods CR, Yang SG, Zahn M. Culture-negative endocarditis caused by *Bartonella henselae* in a child with congenital heart disease. *Pediatr Infect Dis J.* 2009;28:922–5. <http://dx.doi.org/10.1097/INF.0b013e3181a39e0e>
- Atamanyuk I, Raja SG, Kostolny M. *Bartonella henselae* endocarditis of percutaneously implanted pulmonary valve. *J Heart Valve Dis.* 2012;21:682–5.
- Itoh M, Kann DC, Schwenk HT, Gans HA. Fever and renal failure in a child with DiGeorge syndrome and tetralogy of Fallot. *J Pediatric Infect Dis Soc.* 2015;4:373–5. <http://dx.doi.org/10.1093/jpids/piv029>
- Sosa T, Goldstein B, Cnota J, Bryant R, Frenck R, Washam M, et al. Melody valve *Bartonella henselae* endocarditis in an afebrile teen: a case report. *Pediatrics.* 2016;137:e20151548. <http://dx.doi.org/10.1542/peds.2015-1548>
- Ezri T, Sasson L, Houri S, Berlovitz Y, Tamir A. Save a Child's Heart project in Israel. *Lancet.* 2014;384:1575–6. [http://dx.doi.org/10.1016/S0140-6736\(14\)61984-X](http://dx.doi.org/10.1016/S0140-6736(14)61984-X)
- Giladi M, Kletter Y, Avidor B, Metzkor-Cotter E, Varon M, Golan Y, et al. Enzyme immunoassay for the diagnosis of cat-scratch disease defined by polymerase chain reaction. *Clin Infect Dis.* 2001;33:1852–8. <http://dx.doi.org/10.1086/324162>
- Metzkor-Cotter E, Kletter Y, Avidor B, Varon M, Golan Y, Ephros M, et al. Long-term serological analysis and clinical follow-up of patients with cat scratch disease. *Clin Infect Dis.* 2003;37:1149–54. <http://dx.doi.org/10.1086/378738>
- La Scola B, Raoult D. Serological cross-reactions between *Bartonella quintana*, *Bartonella henselae*, and *Coxiella burnetii*. *J Clin Microbiol.* 1996;34:2270–4.
- Raoult D, Fournier PE, Drancourt M, Marrie TJ, Etienne J, Cosserrat J, et al. Diagnosis of 22 new cases of *Bartonella* endocarditis. *Ann Intern Med.* 1996;125:646–52. <http://dx.doi.org/10.7326/0003-4819-125-8-199610150-00004>
- Johnson G, Ayers M, McClure SCC, Richardson SE, Tellier R. Detection and identification of *Bartonella* species pathogenic for humans by PCR amplification targeting the riboflavin synthase gene (ribC). *J Clin Microbiol.* 2003;41:1069–72. <http://dx.doi.org/10.1128/JCM.41.3.1069-1072.2003>
- Baddour LM, Wilson WR, Bayer AS, Fowler VG Jr, Tleyjeh IM, Rybak MJ, et al.; American Heart Association Committee on Rheumatic Fever, Endocarditis, and Kawasaki Disease of the Council on Cardiovascular Disease in the Young, Council on Clinical Cardiology, Council on Cardiovascular Surgery and Anesthesia, and Stroke Council. Infective endocarditis in adults: diagnosis, antimicrobial therapy, and management of complication. A scientific statement for healthcare professionals from the American Heart Association. *Circulation.* 2015;132:1435–86. <http://dx.doi.org/10.1161/CIR.0000000000000296>
- Baltimore RS, Gewitz M, Baddour LM, Beerman LB, Jackson MA, Lockhart PB, et al.; American Heart Association Rheumatic Fever, Endocarditis, and Kawasaki Disease Committee of the Council on Cardiovascular Disease in the Young and the Council on Cardiovascular and Stroke Nursing. Infective endocarditis in childhood: 2015 update. A scientific statement from the American Heart Association. *Circulation.* 2015;132:1487–515. <http://dx.doi.org/10.1161/CIR.0000000000000298>
- Rolain JM, Brouqui P, Koehler JE, Maguina C, Dolan MJ, Raoult D. Recommendations for treatment of human infections caused by *Bartonella* species. *Antimicrob Agents Chemother.* 2004;48:1921–33. <http://dx.doi.org/10.1128/AAC.48.6.1921-1933.2004>
- Houpikian P, Raoult D. Western immunoblotting for *Bartonella* endocarditis. *Clin Diagn Lab Immunol.* 2003;10:95–102.
- Spach DH, Callis KP, Paaup DS, Houze YB, Schoenkecht FD, Welch DF, et al. Endocarditis caused by *Rochalimaea quintana* in a patient infected with human immunodeficiency virus. *J Clin Microbiol.* 1993;31:692–4.
- Daly JS, Worthington MG, Brenner DJ, Moss CW, Hollis DG, Weyant RS, et al. *Rochalimaea elizabethae* sp. nov. isolated from a patient with endocarditis. *J Clin Microbiol.* 1993;31:872–81.
- Raoult D, Fournier PE, Vandenesch F, Mainardi JL, Eykyn SJ, Nash J, et al. Outcome and treatment of *Bartonella* endocarditis. *Arch Intern Med.* 2003;163:226–30. <http://dx.doi.org/10.1001/archinte.163.2.226>
- Ohl ME, Spach DH. *Bartonella quintana* and urban trench fever. *Clin Infect Dis.* 2000;31:131–5. <http://dx.doi.org/10.1086/313890>
- Marié JL, Fournier PE, Rolain JM, Briolant S, Davoust B, Raoult D. Molecular detection of *Bartonella quintana*, *B. elizabethae*, *B. koehlerae*, *B. doshiae*, *B. Taylorii*, and *Rickettsia felis* in rodent fleas collected in Kabul, Afghanistan. *Am J Trop Med Hyg.* 2006;74:436–9.
- Kernif T, Leulmi H, Socolovschi C, Berenger JM, Lepidi H, Bitam I, et al. Acquisition and excretion of *Bartonella quintana* by the cat flea, *Ctenocephalides felis*. *Mol Ecol.* 2014;23:1204–12. <http://dx.doi.org/10.1111/mec.12663>
- Fournier PE, Lelievre H, Eykyn SJ, Mainardi JL, Marrie TJ, Bruneel F, et al. Epidemiologic and clinical characteristics of *Bartonella quintana* and *Bartonella henselae* endocarditis: a study of 48 patients. *Medicine (Baltimore).* 2001;80:245–51. <http://dx.doi.org/10.1097/00005792-200107000-00003>
- Balakrishnan N, Menon T, Fournier PE, Raoult D. *Bartonella quintana* and *Coxiella burnetii* as causes of endocarditis, India.

SYNOPSIS

- Emerg Infect Dis. 2008;14:1168–9. <http://dx.doi.org/10.3201/eid1407.071374>
31. Fournier PE, Mainardi JL, Raoult D. Value of microimmunofluorescence for diagnosis and follow-up of *Bartonella* endocarditis. Clin Diagn Lab Immunol. 2002;9:795–801.
32. Edouard S, Nabet C, Lepidi H, Fournier PE, Raoult D. *Bartonella*, a common cause of endocarditis: a report on 106 cases and review. J Clin Microbiol. 2015;53:824–9. <http://dx.doi.org/10.1128/JCM.02827-14>
33. Sangaré AK, Boutellis A, Drali R, Socolovschi C, Barker SC, Diatta G, et al. Detection of *Bartonella quintana* in African body and head lice. Am J Trop Med Hyg. 2014;91:294–301. <http://dx.doi.org/10.4269/ajtmh.13-0707>
34. Cutler S, Abdissa A, Adamu H, Tolosa T, Gashaw A. *Bartonella quintana* in Ethiopian lice. Comp Immunol Microbiol Infect Dis. 2012;35:17–21. <http://dx.doi.org/10.1016/j.cimid.2011.09.007>

Address for correspondence: Diana Tasher, Pediatric Infectious Diseases Unit, Wolfson Medical Center, Holon, Israel 58100; email: dtasher@gmail.com

May 2016: Vectorborne Diseases



- An Operational Framework for Insecticide Resistance Management Planning
- *Rickettsia parkeri* Rickettsiosis, Arizona, USA
- *Plasmodium falciparum* K76T *pfcr* Gene Mutations and Parasite Population Structure, Haiti,
- Outbreak of Middle East Respiratory Syndrome at Tertiary Care Hospital, Jeddah, Saudi Arabia, 2014
- Expansion of Shiga Toxin–Producing *Escherichia coli* by Use of Bovine Antibiotic Growth Promoters
- Acute Human Inkoo and Chatanga Virus Infections, Finland
- Differences in Genotype, Clinical Features, and Inflammatory Potential of *Borrelia burgdorferi* sensu stricto Strains from Europe and the United States
- Projecting Month of Birth for At-Risk Infants after Zika Virus Disease Outbreaks

- Genetic Characterization of Archived Bunyaviruses and Their Potential for Emergence in Australia potential.

- *Plasmodium falciparum* In Vitro Resistance to Monodesethylamodiaquine, Dakar, Senegal, 2014

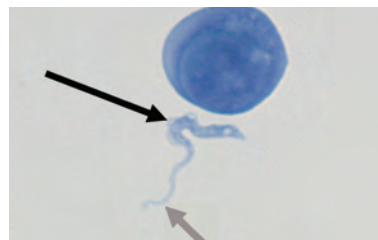
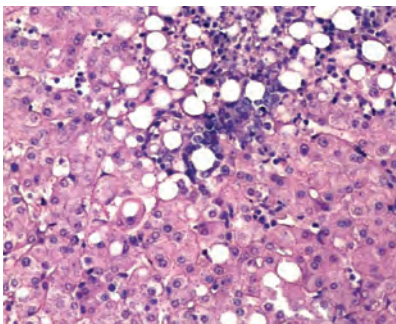
- Astrovirus MLB2, a New Gastroenteric Virus Associated with Meningitis and Disseminated Infection

- Spectrum of Viral Pathogens in Blood of Malaria-Free Ill Travelers Returning to Canada

- Expanded Geographic Distribution and Clinical Characteristics of *Ehrlichia ewingii* Infections, United States

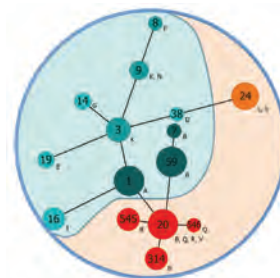
- Molecular Characterization of Canine Rabies Virus, Mali, 2006–2013

- Fatal Monocytic Ehrlichiosis in Woman, Mexico, 2013



- Increased Rotavirus Prevalence in Diarrheal Outbreak Precipitated by Localized Flooding, Solomon Islands, 2014

- *Rickettsia sibirica mongolitimonae* Infection, France, 2010–2014



- Q Fever, Scrub Typhus, and Rickettsial Diseases in Children, Kenya, 2011–2012

- Molecular Characterization of Chikungunya Virus, Philippines, 2011–2013

- Severe Sepsis and Septic Shock Associated with Chikungunya Virus Infection, Guadeloupe, 2014

- Cutaneous Leishmaniasis and Conflict in Syria

**EMERGING
INFECTIOUS DISEASES**

[https://wwwnc.cdc.gov/eid/articles/
issue/22/5/table-of-contents](https://wwwnc.cdc.gov/eid/articles/issue/22/5/table-of-contents)

Characteristics of Dysphagia in Infants with Microcephaly Caused by Congenital Zika Virus Infection, Brazil, 2015

Mariana C. Leal, Vanessa van der Linden, Thiago P. Bezerra, Luciana de Valois, Adriana C.G. Borges, Margarida M.C. Antunes, Kátia G. Brandt, Catharina X. Moura, Laura C. Rodrigues, Coeli R. Ximenes

We summarize the characteristics of dysphagia in 9 infants in Brazil with microcephaly caused by congenital Zika virus infection. The Schedule for Oral Motor Assessment, fiberoptic endoscopic evaluation of swallowing, and the videofluoroscopic swallowing study were used as noninstrumental and instrumental assessments. All infants had a degree of neurologic damage and showed abnormalities in the oral phase. Of the 9 infants, 8 lacked oral and upper respiratory tract sensitivity, leading to delays in initiation of the pharyngeal phase of swallowing. Those delays, combined with marked oral dysfunction, increased the risk for aspiration of food, particularly liquid foods. Dysphagia resulting from congenital Zika virus syndrome microcephaly can develop in infants >3 months of age and is severe.

The identification of a congenital Zika syndrome (CZS) during the November 2015 microcephaly epidemic in Brazil raised many questions (1). So far, the main phenotypic indicator of CZS is microcephaly, but the full spectrum of CZS has not been described and will probably include other systemic abnormalities, and it may be shown that microcephaly is not present in all cases (2,3). Early research indicated that Zika virus has tropism for glial cells and neurons, a finding consistent with the severity of abnormalities seen in the fetal brain (4).

Swallowing is a complex sensorimotor process that depends on information from multiple levels of the central

and peripheral nervous system. Swallowing occurs when descending excitatory and inhibitory signals from the cortex and subcortex and ascending signals from the oropharyngeal area trigger the central pattern generator in the bulbar reticular formation (5). The execution of the sensorimotor aspects associated with swallowing relies on functionally connected pathways between extrapyramidal cortical motor planning regions, centers controlling the brainstem and cranial nerves, and lower motor neurons. The swallowing process has 3 phases: oral, pharyngeal, and esophageal. Dysphagia can result from problems in any 1 of the 3 phases or in more than 1 phase (6). The oral phase and the initiation of the pharyngeal phase are under voluntary neural control, whereas the completion of the pharyngeal phase and the entire esophageal phase are under involuntary neural control (7).

There were a few early initial reports of onset of clinically diagnosed dysphagia in the first months of life of children with CZS; the most relevant are a case series about CZS with arthrogryposis in 7 infants (8) and another about CZS without microcephaly at birth in 13 infants (2). In the latter case series, 76% (10/13) of the infants had dysphagia, which was present in children with neurologic manifestations that were not very severe (2). Feeding problems in persons with neurologic diseases are mainly explained by brain damage leading to lack of swallowing coordination; abnormalities of posture; and abnormalities of digestive tract motility, such as gastroparesis and gastroesophageal reflux (9). Although these problems may be the cause of dysphagia seen in infants with CZS, we suggest that CZS-associated dysphagia might also be caused by anomalies of orofacial anatomy, oral and upper respiratory tract sensitivity, and changes in the motor function of the upper digestive tube caused primarily or secondarily by direct action of the virus. We undertook instrumental evaluation of dysphagia in children with CZS with the objective of describing the characteristics of this condition.

Author affiliations: Hospital Agamenon Magalhães, Recife, Brazil (M.C. Leal); Universidade Federal de Pernambuco, Recife (M.C. Leal, T.P. Bezerra, M.M.C. Antunes, K.G. Brandt, C.R. Ximenes); Hospital Barão de Lucena, Recife (V. van der Linden); Association for Assistance of Disabled Children, Recife (V. van der Linden, L. de Valois); Prived Clinic, Recife (A.C.G. Borges); Real Hospital Português, Recife (C.X. Moura); London School of Hygiene and Tropical Medicine, London, UK (L.C. Rodrigues)

DOI: <https://doi.org/10.3201/eid2308.170354>

Methods

Study Design and Population

We conducted a descriptive, retrospective, case series study by reviewing the medical records of 9 children in Brazil with dysphagia and CZS microcephaly diagnosed during the 2015 epidemic of microcephaly. The study was conducted in 3 tertiary care institutions in Recife, Pernambuco State, Brazil: 1) Associação de Assistência à Criança Deficiente, the reference center for disabled children, where the infants with dysphagia were followed up by a neurologist and speech pathologist; 2) the Pediatric Otolaryngology and Pediatric Gastroenterology Outpatient Unit at the Hospital das Clínicas da Universidade Federal de Pernambuco, where infants received a complete dysphagia assessment, including fiberoptic endoscopic evaluation of swallowing (FEES); and 3) the Division of Radiology at Real Hospital Português, where infants underwent the videofluoroscopic swallowing study (VFSS).

The 9 infants were referred for dysphagia evaluation at 1 of the 3 study sites, where they underwent a complete instrumental evaluation. All infants met the following 3 criteria: 1) they had been diagnosed with microcephaly and had brain imaging results suggestive of congenital Zika virus infection; 2) other causes of infectious congenital microcephaly (toxoplasmosis, cytomegalovirus, rubella, syphilis, and HIV) had been excluded; and 3) their cerebrospinal fluid was Zika virus IgM–positive by capture ELISA (10). Microcephaly was defined as head circumference 2 SDs below the median for newborn gestational age and sex (11). Clinical neurologic evaluation included brain imaging, without contrast, by computed tomography scanning.

Assessment of Dysphagia

Noninstrumental Assessment

We used the Schedule for Oral Motor Assessment (SOMA) to evaluate motor oral dysfunction (12). SOMA is a standardized discriminative assessment that quantifies oropharyngeal dysphagia in children 8–24 months of age. It is used to evaluate oral motor dysfunction and is considered one of the strongest measures for oropharyngeal dysphagia in children with neurologic disabilities (13). The tool categorizes children as having oral motor dysfunction or normal function on the basis of specified thresholds for each of 2 oral motor challenge categories: pureed and semisolid foods. A speech pathologist conducted an assessment using the adapted SOMA protocol (12).

Instrumental Assessment

We used 2 instrumental methods, FEES and VFSS, to evaluate all 3 phases of dysphagia; these methods are considered the reference standards for instrumental evaluation of all phases of dysphagia. FEES and VFSS are graded on

an 8-point scale (the Rosenbek scale) (14) to assess and grade aspiration and penetration. (Aspiration is defined as passage of materials through the vocal folds, and laryngeal penetration is defined as passage of materials into the larynx, but not through the vocal folds [into the airway].)

FEES

FEES was performed on the infants after they underwent physical examination and clinical consultation with an otolaryngologist. FEES was performed according to the Langmore protocol (15) by using a 3.2-mm fiberoptic nasopharyngolaryngoscope (Machida Endoscope Co., Ltd., Tokyo, Japan). The captured images were recorded (Innova Micro-Camera MFX 10G and Halogen Light FX 180R; Innova Technik, São Paulo, Brazil) and transferred to an Inter Core i3-2348M N3 laptop computer (Intel, Recife, Brazil). The otolaryngologist assessed the anatomy and deglutition of the infants with the help of a speech pathologist and recorded the findings for further evaluation.

During the assessment, we gave each infant the following directly in their mouth via a metered syringe: liquids (without thickener); 1 spoon thickened liquid (50 mL of liquid with 3 g of thickener); and 2 spoons food paste or puree, each with 3 g of thickener in 50 mL of liquid. We sequentially administered 1 mL, 3 mL, and 5 mL of each mixture. We used Sustap (Prolev, Abreu e Lima, Brazil) as thickener and added liquid indigo blue food dye to the preparations to obtain better visualization of the food bolus during swallowing. To minimize the risk of aspiration, we varied the sequence of administered mixtures (i.e., paste first, followed by thickened liquid and liquid) and the amount of food given, according to each infant's clinical evaluation and information obtained from otolaryngologist's consultation. Foods were given by a speech pathologist using a 5-mL syringe; maneuvers to facilitate swallowing were performed when needed.

VFSS

The digital fluoroscopy examinations were performed using a Precision GE RXi fluoroscopic radiography system (GE Healthcare, Waukesha, WI, USA). Digital images were transmitted by using a picture archiving and communication system; the images were uploaded in a computerized system and recorded in a standard DVD. The dynamic recording minimum was 3 video frames/s. Oral, pharyngeal, and cervical esophagus swallowing phases were studied with infants positioned in the lateral position. For some infants, the examination was extended on the medium and distal esophagus with infants positioned in an orthostatic laterolateral position. For this study, we added barium sulfate (Bariogel; Cristália, São Paulo, Brazil) to the testing liquids and foods to obtain better visualization during swallowing. Liquids were administered by bottle and cup, and

food paste or puree (prepared as in the FEES study) was administered by spoon.

Assessment of FEES and VFSS

We assessed 6 parameters for the diagnosis of dysphagia by FEES and VFSS: 1) premature spillage; 2) delay in initiation of swallowing; 3) residue of the bolus in the oropharynx after swallowing; 4) residue of the bolus in the hypopharynx after at least 3 swallows (i.e., saliva, secretions, or swallowed materials [contrast-enhanced in VFSS] accumulated in the valleculae, on the lateral or posterior pharyngeal walls, or in the piriform sinuses after deglutition); 5) laryngeal penetration (i.e., presence of contrast [VFSS] or food residues encroached in the airway, above the vocal folds with or without coughing [FEES]); and 6) laryngotracheal aspiration (i.e., presence of contrast-enhanced or noncontrast-enhanced materials below the vocal folds) (16,17). To quantify the severity of the last 2 parameters, laryngeal penetration and laryngotracheal aspiration, we used the 8-point Rosenbek scale (14), in which a score of 1 indicates absence of aspiration or penetration material in the airways; scores of 2–5 indicate degrees of penetration into the airway; and scores of 6–8 indicate degrees of aspiration. Penetration is scored as 2 or 3 if material remains above the vocal folds and as 4 or 5 if material contacts the vocal folds. Each successive score on the scale indicates a more severe sign of dysphagia than the score preceding it. Thus, a score of 8 indicates the most severe condition: aspiration of material without a reflexive or conscious attempt to expel it, which is referred to clinically as silent aspiration.

Other Collected Data

We used a standard form to abstract individual demographic and clinical data from records, including reports by mothers of rash during pregnancy. All described investigations were conducted as part of the clinical protocol or for a clinical indication; none was conducted for research reasons alone. The study was approved by the Ethics Committee on Research (CAAE: 52803316.8.0000.5192).

Results

Nine infants of various ages and with different characteristics at assessment (online Technical Appendix Table 1, <https://wwwnc.cdc.gov/EID/article/23/8/17-0354-Techapp1.pdf>) were referred for dysphagia investigation and received complete instrumental assessment. All infants had a degree of neurologic damage, with global developmental delays, hypertonia of the limbs, and pyramidal and extrapyramidal signs; most infants had abnormal movement of the tongue, contributing to dysphagia. The hypertonia caused abnormal posture with hyperextension of the neck in some infants. Neck hyperextension was associated with irritability, a frequent symptom in children with CZS (6/9 children in this

series), and was a contributing factor to dysphagia. Only 2 of the 9 infants (patients 2 and 6) made any degree of visual contact, and only patient 6 interacted well with the environment. Patient 6 was the only infant who showed any motor development (good neck control and palmar grasping with the right hand) (online Technical Appendix Table 1). Results of brain imaging for the infants were consistent with those described elsewhere for infants with CSZ microcephaly (18): all showed calcifications, predominantly in the cortical and subcortical region, and particularly in the border between white matter and cortex; malformations of the cortical development were present in 8 of the 9 infants (Figure 1). Only 3 of the infants had cerebellum or brainstem hypoplasia (online Technical Appendix Table 2).

Onset of dysphagia was after the third month of life in 8 of the 9 infants. According to their mothers, the first symptoms of dysphagia for most of the infants were choking, cough, regurgitation, respiratory infections, and extended feeding time. All children were being fed by mouth with thickened liquids; 2 infants (patients 2 and 9) needed a nasogastric tube after 6 months of age (Table).

Anatomic Assessment

Our FEES assessment of each infant's respiratory tract showed no malformations or anatomic or functional anomalies. In each infant, the larynx was symmetrical, and mobility of the vocal cords was preserved. A common finding was an omega-shaped epiglottis, but this is common in infants and not considered pathologic.

Abnormal Oral Phase

According to the SOMA and FEES assessments, the oral phase of swallowing was abnormal in all 9 infants. Abnormalities were characterized by premature spillage, presence of bolus residue in the oral cavity and oropharynx (except in patient 6), and marked loss of voluntary activity during the oral phase of swallowing, which is directed by the brain cortex (online Technical Appendix Table 3).

All 9 infants had oral motor dysfunction for pureed food, as demonstrated in the SOMA assessment. Eight infants had significant lack of function in the labial sphincter; only 1 (patient 6) was able to achieve complete labial closure. There were predominant dysfunctions during upper and lower lip activities and, at the same time, an ungraded jaw opening (ability to judge how far the mouth needs to open) while introducing the spoon into the oral cavity. Tongue protrusion beyond incisors was observed in all infants. These findings are evidence of a major impairment of the oral phase of swallowing, which leads to difficulties in oral control and premature spillage of bolus, increasing oral transit time for the bolus preparation.

One of the infants refused semisolid food, so we assessed only 8 infants. All but 1 (patient 6) of the assessed

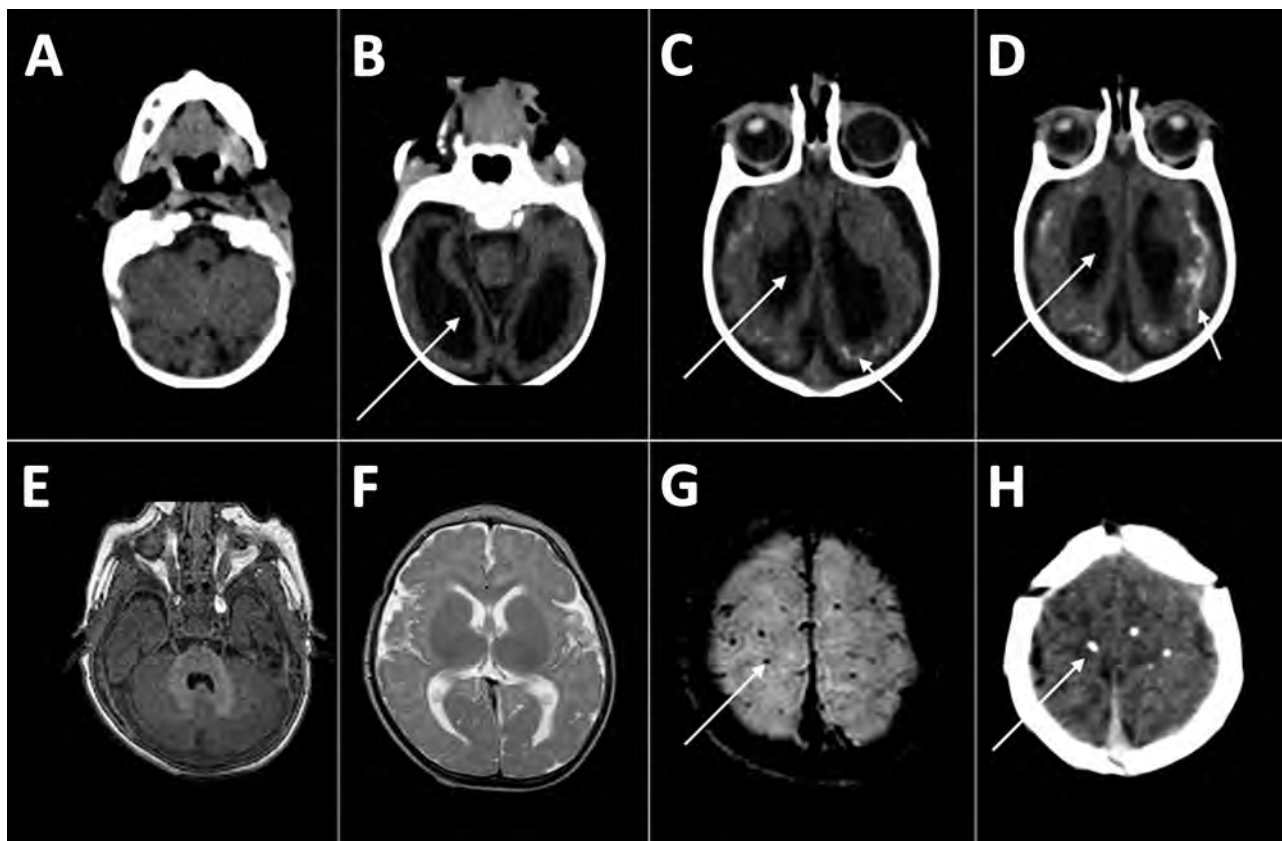


Figure 1. Computed tomography radiographs of the brains of 2 infants with dysphagia and microcephaly caused by congenital Zika virus infection, Brazil, 2015. A–D) Images for patient 4 show malformation of cortical development, ventriculomegaly (long arrows), and calcifications in cortical and subcortical white matter in transition between cortex and white matter (short arrows). E–H) Images for patient 6 show no malformation of cortical development or ventriculomegaly, but calcifications are visible in the cortical area (arrows).

infants had oral motor dysfunction for semisolid food. Changes associated with graded jaw opening while a spoon was introduced into the oral cavity were observed in all infants, pointing to dysfunctions of jaw grading.

Increased Risk of Aspiration in Pharyngeal Phase

Eight of the 9 infants had loss of pharyngeal and laryngeal sensitivity leading to delays in initiation of the pharyngeal (or semiautomatic) swallowing phase and evidence that the swallowing reflex was triggered only when the bolus arrived on pyriform sinuses or the retrocricoid region, a delay that is associated with increased risk of aspiration before swallowing (Figure 2). FEES results showed penetration, aspiration, or both in all 9 infants; VFSS results showed these effects in 4 of the 9. FEES showed no cough reflex, characterizing silent aspiration, in 3 infants (online Technical Appendix Table 3); this finding was more evident with liquid than with pureed food. After the swallowing reflex was completed, 5 of 9 infants had complete pharyngeal clearance. Those with incomplete clearance benefited from digital stimulation of swallowing, a maneuver that efficiently triggered the swallowing reflex.

Insufficient Volume to Assess Esophageal Phase

Because of their clinical condition, 7 of the 9 infants could not swallow a sufficient volume of contrast to enable analysis of esophageal transit time. The 2 infants who could be assessed had delays in emptying the distal esophagus of test material with contrast medium.

Discussion

Dysphagia with onset from the third month of age appears to be a common feature of CZS-associated microcephaly. In this case series, dysphagia appears to have resulted from cortical and extrapyramidal neurologic damage that led to disorganization of voluntary swallowing activity, including oral phase dysfunction with alterations in food capitation and labial closure, loss of food from the mouth, wrong positioning of the bolus, and bolus ejection. This dysfunction leads to premature spillage of bolus and increased risk of airway penetration or aspiration before the swallowing reflex is triggered, which are compatible with sensorial alterations in the oral cavity, pharynx, and larynx, leading to delays in the start of the pharyngeal phase. Liquid foods were more likely than pureed food to lead to penetration, aspiration, or both.

Table. Clinical features in 9 infants with dysphagia due to congenital Zika syndrome microcephaly, Brazil, 2015

Patient no.	Age, mo, at onset of dysphagia	Main symptoms*	Respiratory infection (no.)/hospitalization (no.)	Feeding intervention	Oral feeding time >30 min†
1	4	Irritability, coughing or choking when eating or drinking, breast-feeding difficulties	No	Food thickening	No
2	4	Breast-feeding difficulties, regurgitation, weight loss	No	Nasoenteral tube (at age 6 mo)	Yes
3	3	Breast-feeding difficulties, choking when drinking	No	Food thickening	Yes
4	6	Regurgitation, coughing or choking when eating or drinking, respiratory infections	Yes (1)/Yes (>3)	Food thickening	Yes
5	2	Coughing or choking when eating or drinking	No	Food thickening	No
6	6	Regurgitation	No	Food thickening	No
7	7	Respiratory infections	Yes (2)/Yes (1)	Food thickening	Yes
8	2	Coughing or choking when eating or drinking, regurgitation, respiratory infections, weight loss	Yes (1)/Yes (1)	Food thickening	Yes
9	5	Regurgitation, coughing or choking when eating or drinking, respiratory infection	Yes (1)/Yes (1)	Nasoenteral tube (at age 11 mo)	Yes

*Reported by parent or guardian.
†Before feeding interventions.

Few articles have been published on dysphagia in children with severe disability and nonprogressive, chronic encephalopathy; most published articles refer to dysphagia in persons with cerebral palsy. Gise et al. (19) described oral motor dysfunction in up to 90% of persons with cerebral palsy. Calis et al. (20), Fung et al. (21), and Santoro et al. (22) suggested that the severity and prevalence of dysphagia in children with cerebral palsy are strongly associated with gross motor functional capacity. van den Engel-Hoek et al. (23) showed the influence that dysfunction in any of the different levels of central and peripheral nervous system functions involved in initiating, coordinating, and modulating the swallowing process might have in causing dysphagia in 1 or all 3 phases of swallowing.

Dysphagia in children with different neurologic etiologies is characterized by considerable variability. Cameron et al. (24) described 23 patients with symptomatic congenital cytomegalovirus infections and showed that symptomatic infections often cause a generalized encephalopathy with global functional deficits (including severe swallowing and cognitive impairments) and correlate with severity as determined

by the Gross Motor Function Classification System (<https://www.canchild.ca/en/resources/42-gross-motor-function-classification-system-expanded-revised-gmfcs-e-r>).

The severe form of CZS with microcephaly usually causes severe encephalopathy with cerebral palsy secondary to brain injury, including involvement of cortical and subcortical areas, the basal ganglia, and, in some cases, the brainstem. Some patients with CZS may also have arthrogryposis with involvement of the lower motor neuron. All of these patterns of injuries can cause interference in any phase of swallowing.

As of this writing, children with microcephaly resulting from CZS have only been followed for up to a maximum of 18 months after onset, but it is known that they have multiple disabilities affecting motor function, cognition, sight, and hearing. CZS is a new syndrome, and so far, there are no adequate standardized instruments for the rigorous, integrated, complete evaluation of all the deficits involved.

The discordance between results from FEES and VFSS is well described in the literature (25). The discordant results in this series probably resulted from the infants'

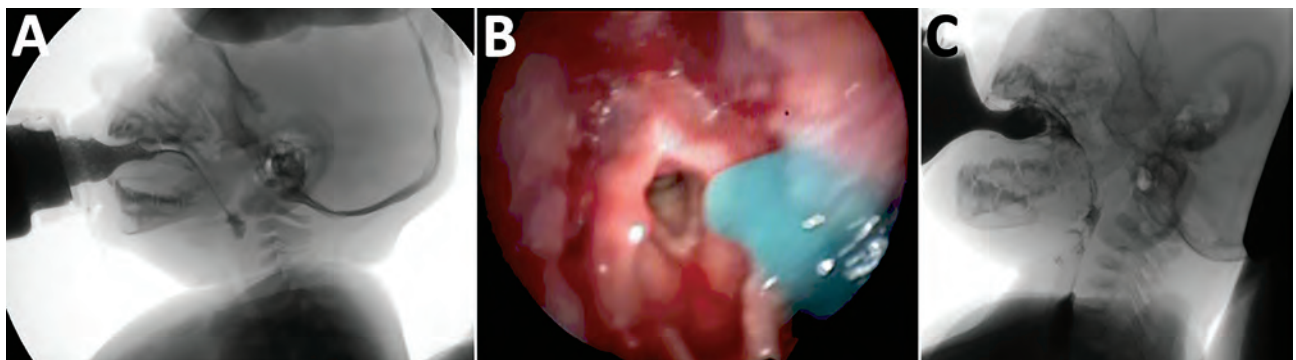


Figure 2. Instrumental evaluation of an infant with dysphagia and microcephaly caused by congenital Zika virus infection, Brazil, 2015. A) Videofluoroscopic swallowing study image showing a lateral view of the infant with premature spillage of liquid food (with added contrast) in the pharynx before triggering of the swallowing reflex. B) Image of the fiberoptic endoscopic evaluation of a delay in initiation of swallowing; thickened, dyed liquid is visible on the supraglottis. C) Silent aspiration, as indicated by a Rosenbek score of 8.

intolerance to FEES, which led to crying and irritability that, in turn, could have facilitated penetration, aspiration, or both. Although VFSS scores agreed more closely with the clinical evaluation, FEES allows a better evaluation of the pharyngeal phase of swallowing and usually can assess laryngeal sensitivity, which cannot be assessed by VFSS. In addition, FEES can be conducted as a bedside examination and is less costly than VFSS (26). However, information from VFSS and FEES is complementary.

To characterize dysphagia among infants in this study, we used the 2 most widely used instrumental methods: VFSS and FEES. The American Speech-Language-Hearing Association (<http://www.asha.org/>) considers these tests the reference standards for diagnosing dysphagia and assessing its management in order to decrease ill health and prevent death.

FEES is a dynamic test conducted in real time that provides direct visualization of the pharyngeal phase of swallowing and investigation of anatomic structures and their sensitivity. One limitation of FEES is that it requires use of nasofibroscope, which often causes discomfort and crying in breast-feeding babies. Children with CZS microcephaly are extremely irritable, possibly because of spasms, epilepsy, or both. This was the case in 6 of the 9 infants in this series; thus, we did not feel that we could consider evaluating pharyngeal and laryngeal sensitivity in the infants.

All instrumental dysphagia evaluations require that the patients have adequate posture for testing and that, to a degree, they cooperate with the testing. Infants with CZS and microcephaly are irritable, are hyperexcited to external stimuli, and retain some primitive reflexes, so they will always be a difficult population to evaluate, in particular using FEES, which can trigger irritability and crying and interfere with the evaluation of penetration, aspiration, or both, especially in the first few months of life. There were no severe complications concerning the endoscopic procedure, suggesting that this examination is safe in this population.

The challenge with VFSS was the small volume ingested and the need to minimize exposure time to x-rays, factors that limited the usefulness of the analysis of transit. This study was based on only 9 cases; however, we expect that knowledge about dysphagia in infants with CZS and microcephaly will increase as more affected children with a wider range of disabilities are studied by instrumental assessment.

In the first few months of life, swallowing is a reflex activity, as the child feeds essentially through suction. The oral or preparatory phase, usually established at that age, is a voluntary activity that requires intact cortical function, which is absent in many children with CZS. In the infants in this series, the transfer of swallowing from a reflex activity to a complex voluntary sensorimotor process led to abnormal oral phase movements that disrupted normal swallowing after 3 months of age. The severity of the

abnormal findings in the infants' brain images is consistent with the infants' symptoms. Compared with the other infants, patient 6, who had no congenital malformation of the cortex, had the least severe dysphagia; the only normal SOMA results; better coordination between suction, swallowing, and breath in VFSS; and clearance of food during the oral and pharyngeal phases. These findings suggest that cortical damage causes the dysfunction in the voluntary phase of swallowing.

This preliminary case report is not intended to be a full evaluation of all cases, or even a representative sample, of CZS-associated or CZS microcephaly-associated dysphagia; such an evaluation will result from the follow-up of representative cohorts. Our results are intended to inform ongoing studies and clinical management of dysphagia in children with CZS or CZS microcephaly.

In conclusion, dysphagia resulting from CZS microcephaly is severe and has onset after 3 months of age. Affected children have marked oral dysfunction, with dystonic movements of the tongue, and lack pharyngeal sensitivity, leading to risk of aspiration, in particular of liquid foods. Infants in this study were better able to swallow pureed than liquid foods; thus, we recommend that pureed or thickened food be fed to children with dysphagia caused by CZS and microcephaly. We also advise that care be taken during feeding to avoid the overextended posture characteristic of many children with CZS, a posture that facilitates aspiration. Furthermore, we recommend that, when feasible, the clinical follow-up of children with CZS should be conducted by a comprehensive and multidisciplinary team of childhood specialists in neurology, gastroenterology, speech pathology, nutrition, and otorhinolaryngology, using clinical and instrumental swallowing assessments (with FEES and VFSS) to identify different aspects of dysphagia. For clinical management, the clinical evaluation remains key.

CZS is a new syndrome, and its definition and progression are still being defined. In addition to continued research into all manifestations of CZS and the overall clinical development of affected children, we also advocate for research into whether all children born to mothers with Zika virus infection during pregnancy, regardless of the presence of microcephaly, have swallowing dysfunction when evaluated by using standardized protocols. Such a study is ongoing in Recife and will establish the prevalence, characteristics, and evolution of dysphagia as well as the possibility of onset of any abnormalities of the intestinal tract.

Acknowledgments

We thank Luís André Silva da Costa, the VFSS technician; and Waldênio Florêncio Porto Filho, the radiologist. We also thank the Real Hospital Português de Pernambuco for performing digital fluoroscopy examinations.

L.C.R. is partially funded by European Union's Horizon 2020 research and innovation program under Zika-PLAN grant agreement No. 734584.

Dr. Leal is a professor of otolaryngology at the Universidade Federal de Pernambuco, and Chief of Otolaryngology division in Hospital Agamenon Magalhães. Her primary research interests are to better understand the clinical manifestations of congenital Zika syndrome and its implications.

References

- Pan American Health Organization, World Health Organization. Epidemiological update: neurological syndrome, congenital anomalies, and Zika virus infection. Washington: The Organizations; 2016 Jan 17.
- van der Linden V, Pessoa A, Dobyns W, Barkovich AJ, Júnior HV, Filho EL, et al. Description of 13 infants born during October 2015–January 2016 with congenital Zika virus infection without microcephaly at birth—Brazil. *MMWR Morb Mortal Wkly Rep*. 2016;65:1343–8. <http://dx.doi.org/10.15585/mmwr.mm6547e2>
- França GV, Schuler-Faccini L, Oliveira WK, Henriques CM, Carmo EH, Pedi VD, et al. Congenital Zika virus syndrome in Brazil: a case series of the first 1501 livebirths with complete investigation. *Lancet*. 2016;388:891–7. [http://dx.doi.org/10.1016/S0140-6736\(16\)30902-3](http://dx.doi.org/10.1016/S0140-6736(16)30902-3)
- Martines RB, Bhatnagar J, de Oliveira Ramos AM, Davi HP, Iglezias SD, Kanamura CT, et al. Pathology of congenital Zika syndrome in Brazil: a case series. *Lancet*. 2016;388:898–904. [http://dx.doi.org/10.1016/S0140-6736\(16\)30883-2](http://dx.doi.org/10.1016/S0140-6736(16)30883-2)
- Leopold NA, Daniels SK. Supranuclear control of swallowing. *Dysphagia*. 2010;25:250–7. <http://dx.doi.org/10.1007/s00455-009-9249-5>
- Arvedson JC. Assessment of pediatric dysphagia and feeding disorders: clinical and instrumental approaches. *Dev Disabil Res Rev*. 2008;14:118–27. <http://dx.doi.org/10.1002/ddr.17>
- Miller AJ. The neurobiology of swallowing and dysphagia. *Dev Disabil Res Rev*. 2008;14:77–86. <http://dx.doi.org/10.1002/ddr.12>
- van der Linden V, Filho EL, Lins OG, van der Linden A, Aragão MF, Brainer-Lima AM, et al. Congenital Zika syndrome with arthrogryposis: retrospective case series study. *BMJ*. 2016;354:i3899. <http://dx.doi.org/10.1136/bmj.i3899>
- Andrew MJ, Parr JR, Sullivan PB. Feeding difficulties in children with cerebral palsy. *Arch Dis Child Educ Pract Ed*. 2012;97:222–9. <http://dx.doi.org/10.1136/archdischild-2011-300914>
- Cordeiro MT, Pena LJ, Brito CA, Gil LH, Marques ET. Positive IgM for Zika virus in the cerebrospinal fluid of 30 neonates with microcephaly in Brazil. *Lancet*. 2016;387:1811–2. [http://dx.doi.org/10.1016/S0140-6736\(16\)30253-7](http://dx.doi.org/10.1016/S0140-6736(16)30253-7)
- Villar J, Cheikh Ismail L, Victora CG, Ohuma EO, Bertino E, Altman DG, et al.; International Fetal and Newborn Growth Consortium for the 21st Century (INTERGROWTH-21st). International standards for newborn weight, length, and head circumference by gestational age and sex: the Newborn Cross-Sectional Study of the INTERGROWTH-21st Project. *Lancet*. 2014;384:857–68. [http://dx.doi.org/10.1016/S0140-6736\(14\)60932-6](http://dx.doi.org/10.1016/S0140-6736(14)60932-6)
- Reilly S, Skuse D, Wolke D. Schedule for oral motor assessment: administration manual. London: Whurr Publishers Ltd; 2000.
- Benfer KA, Weir KA, Boyd RN. Clinimetrics of measures of oropharyngeal dysphagia for preschool children with cerebral palsy and neurodevelopmental disabilities: a systematic review. *Dev Med Child Neurol*. 2012;54:784–95. <http://dx.doi.org/10.1111/j.1469-8749.2012.04302.x>
- Rosenbek JC, Robbins JA, Roecker EB, Coyle JL, Wood JL. A penetration–aspiration scale. *Dysphagia*. 1996;11:93–8. <http://dx.doi.org/10.1007/BF00417897>
- Langmore SE, Schatz K, Olsen N. Fiberoptic endoscopic examination of swallowing safety: a new procedure. *Dysphagia*. 1988;2:216–9. <http://dx.doi.org/10.1007/BF02414429>
- Bastian RW. The videoendoscopic swallowing study: an alternative and partner to the videofluoroscopic swallowing study. *Dysphagia*. 1993;8:359–67. <http://dx.doi.org/10.1007/BF01321780>
- Logeman JA. Evaluation and treatment of swallowing disorders. San Diego (CA): College-Hill Press; 1983.
- de Fatima Vasco Aragao M, van der Linden V, Brainer-Lima AM, Coeli RR, Rocha MA, Sobral da Silva P, et al. Clinical features and neuroimaging (CT and MRI) findings in presumed Zika virus related congenital infection and microcephaly: retrospective case series study. *BMJ*. 2016;353:i1901. <http://dx.doi.org/10.1136/bmj.i1901>
- Gise EG, Applegate-Ferrante T, Benson JE, Bosma JF. Effect of oral sensorimotor treatment on measures of growth, eating efficiency and aspiration in the dysphagic child with cerebral palsy. *Dev Med Child Neurol*. 1995;37:528–43. <http://dx.doi.org/10.1111/j.1469-8749.1995.tb12040.x>
- Calis EA, Veugelers R, Sheppard JJ, Tibboel D, Evenhuis HM, Penning C. Dysphagia in children with severe generalized cerebral palsy and intellectual disability. *Dev Med Child Neurol*. 2008;50:625–30. <http://dx.doi.org/10.1111/j.1469-8749.2008.03047.x>
- Fung EB, Samson-Fang L, Stallings VA, Conaway M, Liptak G, Henderson RC, et al. Feeding dysfunction is associated with poor growth and health status in children with cerebral palsy. *J Am Diet Assoc*. 2002;102:361–73. [http://dx.doi.org/10.1016/S0002-8223\(02\)90084-2](http://dx.doi.org/10.1016/S0002-8223(02)90084-2)
- Santoro A, Lang MB, Moretti E, Sellari-Franceschini S, Orazini L, Cipriani P, et al. A proposed multidisciplinary approach for identifying feeding abnormalities in children with cerebral palsy. *J Child Neurol*. 2012;27:708–12. <http://dx.doi.org/10.1177/0883073811424083>
- van den Engel-Hoek L, Erasmus CE, van Hulst KCM, Arvedson JC, de Groot IJ, de Swart BJ. Children with central and peripheral neurologic disorders have distinguishable patterns of dysphagia on videofluoroscopic swallow study. *J Child Neurol*. 2014;29:646–53. <http://dx.doi.org/10.1177/0883073813501871>
- Cameron NA, Gormley ME Jr, Deshpande S. Severity of disability in patients with cerebral palsy secondary to symptomatic congenital cytomegalovirus encephalopathy. *J Pediatr Rehabil Med*. 2013;6:239–42.
- Kelly AM, Drinnan MJ, Leslie P. Assessing penetration and aspiration: how do videofluoroscopy and fiberoptic endoscopic evaluation of swallowing compare? *Laryngoscope*. 2007;117:1723–7. <http://dx.doi.org/10.1097/MLG.0b013e318123ee6a>
- Aviv JE, Kaplan ST, Thomson JE, Spitzer J, Diamond B, Close LG. The safety of flexible endoscopic evaluation of swallowing with sensory testing (FEESST): an analysis of 500 consecutive evaluations. *Dysphagia*. 2000;15:39–44. <http://dx.doi.org/10.1007/s004559910008>

Address for correspondence: Mariana C. Leal, General Abreu e Lima, 65, apto 901, Tamarineira, Recife, PE, 52041-040, Brazil; email: marianacleal@hotmail.com

Zika Virus Infection in Patient with No Known Risk Factors, Utah, USA, 2016

Elisabeth R. Krow-Lucal, Shannon A. Novosad, Angela C. Dunn, Carolyn R. Brent, Harry M. Savage, Ary Faraji, Dallin Peterson, Andrew Dibbs, Brook Vietor, Kimberly Christensen, Janeen J. Laven, Marvin S. Godsey Jr., Bryan Christensen, Brigette Beyer, Margaret M. Cortese, Nina C. Johnson, Amanda J. Panella, Brad J. Biggerstaff, Michael Rubin, Scott K. Fridkin, J. Erin Staples, Allyn K. Nakashima

In 2016, Zika virus disease developed in a man (patient A) who had no known risk factors beyond caring for a relative who died of this disease (index patient). We investigated the source of infection for patient A by surveying other family contacts, healthcare personnel, and community members, and testing samples for Zika virus. We identified 19 family contacts who had similar exposures to the index patient; 86 healthcare personnel had contact with the index patient, including 57 (66%) who had contact with body fluids. Of 218 community members interviewed, 28 (13%) reported signs/symptoms and 132 (61%) provided a sample. Except for patient A, no other persons tested had laboratory evidence of recent Zika virus infection. Of 5,875 mosquitoes collected, none were known vectors of Zika virus and all were negative for Zika virus. The mechanism of transmission to patient A remains unknown but was likely person-to-person contact with the index patient.

Zika virus is an emerging mosquito-borne flavivirus transmitted primarily through the bite of infected *Aedes (Stegomyia)* mosquitoes. Other modes of transmission, including intrauterine, perinatal, sexual, blood transfusions, and laboratory exposure, have been described (1–6).

In June 2016, a 73-year-old man (index patient) died in a hospital in Salt Lake City, Utah, USA (7) (Figure 1). He

had returned from Mexico 11 days previously and began feeling ill 3 days after his arrival in the United States. He sought care 2 days after illness onset and was hospitalized 3 days later. After admission, his health rapidly declined, and he died 3 days later of suspected dengue hemorrhagic shock syndrome. Postmortem testing identified Zika virus RNA in a blood sample obtained during hospitalization; the level of viremia in his serum sample was uncharacteristically high (7,8).

Six days after the death of the index patient, subjective fever, rash, and conjunctivitis developed in a 38-year-old man who was a family contact (patient A) (7). Patient A had not traveled to an area with ongoing Zika virus transmission, had not had sexual contact with a person who recently traveled to such an area, and had not received a blood transfusion or organ transplant. However, patient A had contact with the index patient during his period of viremia. Patient A also visited the 2 residences of the index patient after his death, suggesting possible vectorborne transmission from *Ae. aegypti* mosquitoes, which have been previously identified in Utah (9). Urine obtained from patient A 7 days after illness onset was positive for Zika virus RNA, and a day 11 serum sample was positive for Zika virus IgM and Zika virus and dengue virus neutralizing antibodies (8). Given the lack of travel or other risk factors for acquiring Zika virus for patient A, a public health investigation was launched to better define his exposures and determine a probable source of infection.

Methods

For this investigation, we defined a contact as a person who resided in the same household with the index patient or who had direct contact with the index patient or his blood or other body fluids, such as conjunctival discharge, respiratory secretions, vomit, stool, or urine, when he was potentially viremic (defined as the date the index patient returned to the United States until his death). Evidence of recent infection was defined as a person with Zika virus RNA in serum or urine or Zika virus IgM and

Author affiliations: Centers for Disease Control and Prevention, Atlanta, Georgia, USA (E.R. Krow-Lucal, S.A. Novosad, C.R. Brent, B. Christensen, M.M. Cortese, N.C. Johnson, S.K. Fridkin); Centers for Disease Control and Prevention, Fort Collins, Colorado, USA (E.R. Krow-Lucal, H.M. Savage, J.J. Laven, M.S. Godsey Jr., A.J. Panella, B.J. Biggerstaff, J.E. Staples); Utah Department of Health, Salt Lake City, Utah, USA (A.C. Dunn, D. Peterson, K. Christensen, A.K. Nakashima); Salt Lake County Health Department, Salt Lake City (C.R. Brent, A. Dibbs); Salt Lake City Mosquito Abatement District, Salt Lake City (A. Faraji); University of Utah, Salt Lake City (B. Vietor, B. Beyer, M. Rubin)

DOI: <https://doi.org/10.3201/eid2308.170479>

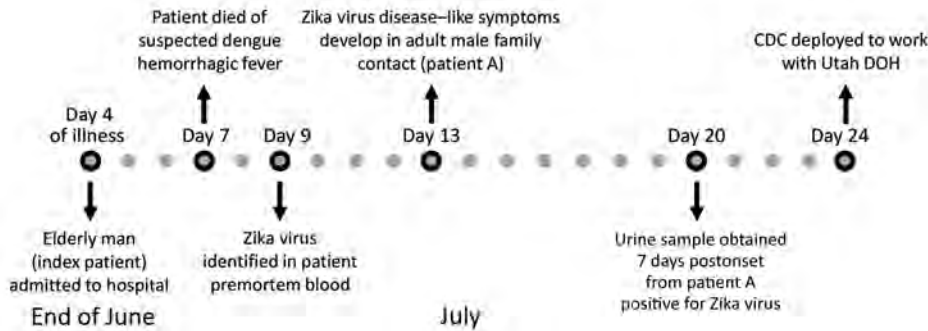


Figure 1. Timeline of events for investigation of Zika virus infection in patient with no known risk factors, Utah, USA, 2016. CDC, Centers for Disease Control and Prevention; DOH, Department of Health.

neutralizing antibodies in serum samples that were negative for neutralizing antibodies against dengue virus (10). We obtained consent for all persons who provided a sample or participated.

Assessment of Person-to-Person Transmission

Evaluation of Family Contacts and Mortuary Workers

State and local health department staff interviewed all family members and friends identified as potential contacts of the index patient from the date when he was found to be positive for Zika virus through when patient A showed a positive test result. Interviewers asked about exposures to the index patient and any recent travel or vaccination that might affect Zika virus test results. All contacts were asked to provide a blood or urine sample to test for recent Zika virus infection. All community funeral and mortuary workers who had contact with the body of the index patient met the definition of a contact and were asked about their exposures and to provide a blood sample.

Assessment of Healthcare Personnel

Hospital medical records of the index patient were reviewed to characterize and quantify clinical conditions and procedures that generated blood or body fluid. A list of all healthcare personnel who potentially interacted with the index patient was generated on the basis of employee assignments. Healthcare personnel with possible contact were called and an interview was scheduled. If after 2 attempts they could not be reached, they were categorized as not reachable. Healthcare personnel were interviewed to determine the level of interaction (e.g., type of contact, type of care provided, exposure to blood or body fluids, use of personal protective equipment [PPE]); recent travel; and vaccinations. Healthcare personnel were defined as having other concerning factors if they reported being pregnant, were attempting to become pregnant, or had ≥ 2 signs/symptoms consistent with Zika virus infection (i.e., fever, rash, arthralgia, or conjunctivitis) in the previous 30 days. All employees with direct contact or other

concerning factors were asked to provide blood or urine samples for Zika virus testing (11).

Assessment of Potential Vectorborne Transmission

Vector Assessment

Local mosquito abatement districts worked in collaboration with the Centers for Disease Control (CDC, Fort Collins, CO, USA) to conduct larval and adult mosquito surveillance in the 3 areas where the index patient (2 residences) and patient A resided. Door-to-door household surveys were conducted, and light traps, CO₂ traps, gravid traps, and BioGents traps (BioGents, Regensburg, Germany) were deployed to collect different species at sites around residences of patient A and the index patient. During mid-July, mosquito abatement district adult mosquito collection was performed for 2 days. Five days after the first trapping, CDC and local mosquito abatement districts collected mosquitoes at 12 sites in each of the 3 areas described. Specifically, 18 BioGents-2, 6 gravid, and 6 CDC light traps with CO₂ were used for 30 traps/day. Ovicups were set at 9 sites to detect container-inhabiting *Aedes* mosquitoes. Adult mosquitoes were shipped on dry ice to CDC in Fort Collins for processing and testing.

Potential larval and pupal habitats were inspected at the 3 residences of interest and nearby homes. Aquatic stages were collected and transported to mosquito control district facilities for rearing and identification.

Community Assessment

All households within a 200-m radius of the 2 properties where the index patient stayed while potentially viremic were surveyed. We determined this radius on the basis of a compromise between the likely movement of *Aedes* mosquitos (estimated as ≈ 30 –450 m/d) and the number of households that could be surveyed (12). A household was eligible for inclusion if ≥ 1 resident of the house had resided in the household for the month before illness onset of patient A. A person who slept in the house ≥ 2 days/week was considered a household member.

Teams visited households in late July for 4 days, provided information about the investigation, and obtained verbal consent. If the person did not wish to participate, they were considered refusing. If no residents or heads of household were available at the initial visit, they were revisited 2 more times at a different time and day. If after 3 visits no one answered, the household was considered not available. For participating households, verbal consent or assent to participate was obtained from all household members ≥ 12 years of age. For children < 18 years of age, permission was obtained from parents or legal guardians.

We surveyed all consenting household members by using a questionnaire that captured information on demographics, signs/symptoms of possible Zika virus infection, recent travel or sexual contact with a traveler, receipt of flavivirus vaccines, pregnancy status, exposures to mosquitoes, and personal and household protective measures. We defined signs/symptoms of possible Zika virus infection as fever, rash, conjunctivitis, or arthralgia with onset after the date of return of the index patient to the United States. Persons whose signs/symptoms began before the return of the index patient or were explained by an alternate etiology (e.g., culture-proven bacterial infection) were not included among those with reported signs/symptoms. After completion of the survey, we asked each household member ≥ 6 months of age to provide a blood sample; for participants symptomatic within the previous 2 weeks, a urine sample was also collected. We did not collect samples from infants < 6 months of age because interpretation of results would be complicated by maternally derived antibodies. However, parents did respond to the questionnaire for those infants.

Laboratory Testing

Serum samples were tested by using a Zika virus IgM capture ELISA at CDC (Fort Collins) or the Utah Public Health Laboratory (Salt Lake City, UT, USA) per standard protocol (13,14). Samples positive for Zika virus IgM were confirmed by using a 90% plaque reduction neutralization test at CDC (Fort Collins) (15). Urine samples were tested by using a reverse transcription PCR (RT-PCR) (Triplex assay) for Zika virus at the Utah Public Health Laboratory (14). If a person reported signs/symptoms in the past week, then their serum sample was also tested by RT-PCR for Zika virus RNA per testing guidelines (13). Mosquito pools were tested for Zika virus and West Nile virus RNA by using described methods (16).

Data Collection and Analysis

We entered survey data with unique identification numbers for participants into either REDCap ([\[project-redcap.org/\]\(https://www.project-redcap.org/\)\) or Epi Info \(CDC\) databases for analysis. We summarized continuous variables as medians and ranges and dichotomous variables as frequencies and proportions. For the community assessment, we first estimated the number of persons residing in the areas around residences of the index patient on the basis of average household size values at the ZIP code level obtained from the 2010 US Census \(17\). We then used the hypergeometric distribution to calculate the probability that a nonparticipant residing in the areas near the residences of the index patient could have been infected with Zika virus.](https://www.</p></div><div data-bbox=)

Procedures and data collection tools for healthcare personnel and community assessments were reviewed by human subject advisors at the Utah Department of Health and CDC. These procedures and tools were determined to be part of a nonresearch public health response.

Results

Evaluation of Family Contacts and Mortuary Worker

A total of 22 family members or friends potentially interacted with the index patient from his return to the United States until after his death; 19 (86%) met the definition of a contact. Of the 19 family contacts, 15 resided with or visited the index patient at his residences, and 13 visited him at the hospital. The most common interactions with the index patient included kissing, primarily on the cheek ($n = 6$), and assisting in care (e.g., cleaning up vomit, stool, or urine, or wiping tears) ($n = 6$). These activities were performed without PPE. Twelve community mortuary workers also interacted with the index patient in the hospital or mortuary, and all met the definition of a contact. Other than patient A, no other contact reported a Zika-like illness after their interaction with the index patient.

Of the 19 family or friend contacts, 18 were negative for Zika virus IgM in serum ($n = 14$) or Zika virus RNA by PCR in urine ($n = 17$). Only patient A had recent evidence of Zika virus infection. All 12 mortuary workers were negative for Zika virus IgM in serum.

The most recent travel of patient A was to Mexico > 1 year earlier. He had not had sexual contact with someone who had recently traveled to an area where Zika virus was known to be circulating and had not received any blood transfusions or organ transplants. He did not have any serious underlying conditions and was not immunosuppressed. Similar to other family members, patient A visited the residences where the index patient was staying before the index patient was hospitalized and after his death. Before hospitalization of the index patient, patient A had only casual contact (e.g., hugging and kissing) with the index patient.

During hospitalization of the index patient, patient A reported staying for 2 days and nights (>48 hours) in his room in the intensive care unit (ICU) and reported hugging, kissing, and touching him frequently. He assisted hospital staff in moving the index patient after a bowel movement, but did not come into contact with fecal matter or any other body fluid. Patient A had no breaks in his skin, including no chronic skin conditions, oral lesions, recent dental work, or needle exposures. Interactions of patient A with the index patient were similar to those reported by other family members. The wife of the index patient reported more frequent and direct contact (assisted with bodily functions, patient cleaning, and in-home care) with the index patient than patient A.

Assessment of Healthcare Workers

The index patient was evaluated in the emergency department twice before being admitted and transferred to an ICU for the duration of his hospitalization. He required intensive clinical care, including mechanical ventilation, hemodialysis (continuous renal replacement therapy), and multiple procedures, including central and arterial line placement and endotracheal intubation (Figure 2). These procedures provided opportunities for contact of healthcare personnel with blood or other body fluids.

A total of 132 healthcare personnel were identified as having potential contact with the index patient, or his immediate environment, waste, or medical equipment. Twenty denied any interaction with the index patient and

14 were not reachable, resulting in 98 (74%) available for a complete interview. Of these personnel, 86 (88%) reported contact with the index patient or his immediate environment or had other concerning factors.

Of the 86 workers, 54 (63%) had contact with the index patient in the ICU and 26 (31%) had contact with the index patient in the emergency department. Most (72, 84%) workers provided direct patient care, and 57 (66%) reported contact with blood or other body fluids (Table 1). These 57 healthcare workers reported 128 separate exposures to blood or body fluids, including 39 (30%) exposures to blood, 35 (27%) to sweat, 18 (14%) to respiratory secretions, 15 (12%) to urine, 10 (8%) to stool, 8 (6%) to tears, and 3 (2%) to vomit. The most common PPE ensemble worn during these encounters was gloves only (81 workers, 63%) followed by gloves and gown (23, 18%); 10 (8%) encounters occurred without any PPE being used, including 8 encounters with sweat and 2 with tears (Table 1). No healthcare workers reported blood or body fluid contact with nonintact skin or mucous membranes, and there were no percutaneous exposures. Two healthcare workers reported having blood-soaked scrubs after postmortem cleaning of the body.

Eighty (93%) of 86 healthcare workers provided blood samples for testing, and 1 person with recent signs (rash and conjunctivitis) provided a urine sample for testing. All 80 (100%) serum samples were negative for Zika virus IgM, and the 1 urine sample was negative for Zika virus by RT-PCR.

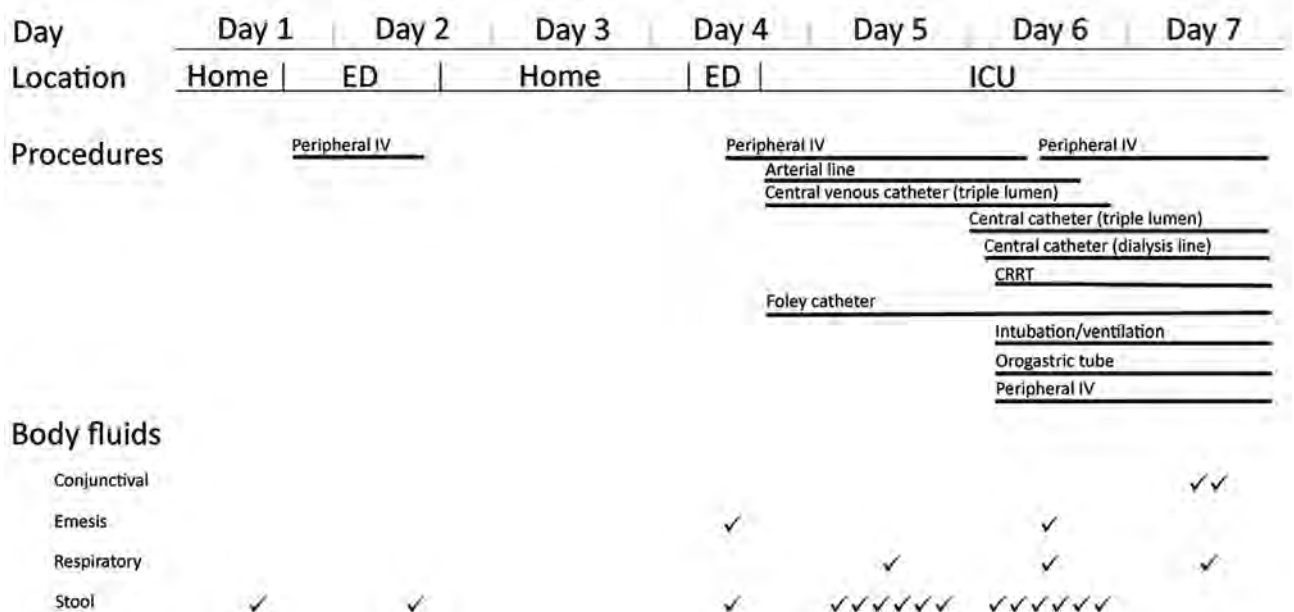


Figure 2. Characteristics of clinical course investigation of Zika virus infection in patient with no known risk factors, Utah, USA, 2016. Patient location, procedures, and body fluid output are as documented in medical records by day of treatment or observation of index patient. Body fluid output is separate from potential exposures generated by procedures. CRRT, continuous renal replacement therapy; ED, emergency department; ICU, intensive care unit; IV, intravenous line; ✓, recorded output (frequency).

Table 1. Characteristics of 128 encounters by 57 healthcare personnel with index patient by type of PPE used during investigation of Zika virus infection in patient with no known risk factors, Utah, USA, 2016*

PPE	Blood, n = 39	Respiratory/GI/GU, n = 46	Sweat, n = 35	Conjunctival, n = 8	Total, n = 128
None	0 (0)	0 (0)	8 (23)	2 (25)	10 (8)
Gloves only	29 (74)	27 (59)	21 (60)	4 (50)	81 (63)
Gloves and gown	8 (21)	11 (24)	3 (9)	1 (13)	23 (18)
Other	2 (5)	6 (13)	0 (0)	0 (0)	8 (6)
Unknown	0 (0)	2 (4)	3 (9)	1 (13)	6 (5)

*Values are no. (%) persons. GI, gastrointestinal; GU, genitourinary; PPE, personal protective equipment.

Assessment of Vectorborne Transmission

Vector Surveillance

Larvae and pupae collected at the 3 residences and nearby areas included only *Culex* and *Culiseta* species (*Cx. pipiens*, *Cx. tarsalis*, *Cs. incidens*, and *Cs. inornata*). Inspection of egg papers from ovicups failed to detect viable mosquito eggs. Mosquito collections from all traps failed to detect the invasive species *Aedes aegypti* or *Ae. albopictus*. A total of 5,875 adult mosquitoes representing 7 species (4,765 *Cx. pipiens*, 658 *Cx. tarsalis*, 4 *Culex* spp., 299 *Cs. incidens*, 138 *Cs. inornata*, 7 *Ae. dorsalis*, 1 *Ae. vexans*, 2 *Aedes* spp., and 1 *Anopheles freeborni*) were collected and tested for virus in 501 pools. All mosquito pools were negative for Zika virus by RT-PCR. However, 2 pools containing female *Cx. pipiens* mosquitoes were positive for West Nile virus RNA by RT-PCR with screening and confirmatory primers.

Community Survey

There were 226 occupied households within a 200-m radius of the residences where the index patient stayed. Of these households, 89 (39%) had ≥1 resident who completed a survey; 72 (32%) were not available, 62 (27%) refused participation, and 3 (1%) were excluded because residents were unable to be interviewed in their native language.

From the 89 participating households, 218 persons completed a questionnaire (for themselves or family members ≤12 years of age). Of the 218 participants, 119 (55%) were female; median age was 35 years (range 4 months–80 years) (Table 2). Most (150, 69%) participants spent an average of ≥1 hours/day outdoors during the preceding month. However, most (172, 79%) reported never wearing insect repellent. Less than half (87, 40%) reported being bitten by mosquitoes in the preceding month. Only 22 (10%) participants reported traveling in the preceding year, but most of them (20, 91%) reported traveling to a country where Zika virus was known to be circulating. Twenty-eight (13%) participants reported having ≥1 of the 4 Zika virus–associated signs/ symptoms in the month before their interview; 15 (7%) reported having ≥2 signs/symptoms.

Of the 218 participants, 132 (61%) also provided ≥1 sample, including 124 who provided only a blood sample, 6 who provided blood and urine samples, and 2 who provided only a urine sample. Of the 130 blood samples, 2

were positive for Zika virus IgM. However, these results for the 2 samples were not confirmed by plaque reduction neutralization test (these samples were negative for Zika virus and dengue virus neutralizing antibodies). Because these 2 samples were obtained from asymptomatic persons, urine samples were not obtained. All other serum samples were negative for Zika virus IgM. All 8 urine samples were negative for Zika virus RNA.

Given the number of persons estimated to live in households in the survey area and who provided a specimen, and that no positive samples were observed, we found that the exact upper 95% confidence limit for the proportion of Zika virus–positive persons in the (untested) population of nearby residents was 2.0% when we used sampling without replacement and the finite population. Thus, it is highly likely that <2.0% of unsampled persons would have been infected with Zika virus.

Discussion

Our investigation of patient A did not identify the probable source of his infection and did not identify any additional persons recently infected with Zika virus among family contacts, healthcare workers, or community members. The index patient was unique when compared with other persons with Zika virus disease because his illness was fatal and his relative viral load was estimated to be ≈100,000 times higher than the average level reported (8). These characteristics, combined with a lack of additional exposure for patient A, make it likely that the index patient was the source of infection for patient A, although inability to sequence virus obtained from patient A prevented a definitive confirmation (7). None of the other family members became infected, despite similar or more frequent and direct contact with the index patient during his viremic period. No healthcare personnel became infected despite the index patient having substantial invasive procedures and moderate production of body fluids. Overall, our findings suggest the infection of patient A represents a rare transmission event through unknown, but likely, person-to-person mechanisms.

On the basis of reported contact of patient A with the index patient, patient A might have been exposed to saliva or tears of the index patient, although patient A had no skin lesions or noted mucous membrane exposures that would have increased his likelihood of becoming infected,

Table 2. Characteristics of 218 community survey questionnaire respondents during investigation of Zika virus infection in patient with no known risk factors, Utah, USA, 2016

Characteristic	No. (%)
Demographic	
Age, y	
<20	65 (30)
20–39	57 (26)
40–59	53 (24)
≥60	31 (14)
Unknown	12 (6)
Sex	
F	119 (55)
M	99 (45)
Pregnant	2 (1)
Born outside United States	63 (29)
Exposures in 30 d before survey	
Average time outdoors/d, h	
<1	55 (25)
1–4	108 (50)
5–10	24 (11)
>10	18 (8)
Unknown	13 (6)
Repellent use while outdoors	
Always	8 (4)
Most of the time	3 (1)
Sometimes	21 (10)
Never	172 (79)
Unknown	14 (6)
Recent mosquito bites	87 (40)
Screens on windows	
All	72 (33)
Most	33 (15)
Some	28 (13)
None	13 (6)
Never leave windows or doors open	52 (24)
Unknown	20 (9)
Travel out of country in previous year	
Traveled internationally	22 (10)
Travel location	
South America	19 (9)
Central America	1 (0)
Caribbean	3 (1)
Europe	1 (0)
Asia	3 (1)
Zika virus–like signs/symptoms in month before survey	
No. reported signs/symptoms	
0	181 (83)
1	13 (6)
2	14 (6)
3	1 (<1)
4	0 (0)
Unknown	9 (4)
Type of signs/symptoms reported	
Fever	16 (7)
Rash	9 (4)
Conjunctivitis	5 (2)
Joint pain	14 (6)

particularly when compared with other family members. To date, Zika virus has been detected by viral culture in several body fluids, including blood, urine, amniotic fluid, a conjunctival swab specimen, breast milk, semen, and saliva (18–22). Zika virus RNA also has been detected in cerebrospinal fluid, aqueous humor, cervical mucous, and nasopharyngeal, vaginal, and endocervical swab specimens

(23–26). However, our knowledge about the timing and amount of Zika virus in blood or body fluids of the index patient was limited. Thus, we are unable to definitively state how patient A was infected.

Although the index patient had a high level of viremia, no healthcare personnel showed evidence of recent Zika virus infection. There were >100 reported encounters with blood and other body fluids with a variety of PPE reflecting standard precautions, which is probably representative of care given to patients in an ICU (27). This finding suggests that healthcare workers caring for severely ill patients with Zika virus disease should continue to use standard precautions with correct PPE when handling body fluids to prevent infection (28).

Although *Ae. aegypti* mosquitoes were previously identified in southwestern Utah in 2013 (9), our vector investigations did not identify *Ae. aegypti* or *Ae. albopictus* mosquitoes. None of the other mosquitoes collected were positive for Zika virus, but 2 pools were positive for West Nile virus, a finding that supports the efficacy of entomologic surveillance. In addition, no persons tested in the 200-m radius around the households in which the index patient stayed had evidence of a recent Zika virus infection. Although low-level transmission could not be definitively ruled out, results of the vector and community investigations do not support the suggestion that patient A was infected by a mosquito that had fed on the index patient before his hospitalization.

Our investigation had several limitations. First, although family contacts and healthcare workers were interviewed several times by professionals trained in interview techniques, recall bias regarding specific exposures they might have had with the index patient was likely. Second, we probably did not identify all healthcare workers who had contact with the index patient because information was obtained retrospectively from the chart for the patient and staffing schedule. Third, documentation in the medical records regarding type and amounts of body fluids might have been incomplete, leading to underestimation of healthcare personnel exposure. Fourth, because of incomplete participation in the community survey, we might have missed persons who were infected by Zika virus in the community, an event we estimated to be low. These limitations might have prohibited identification of an alternate source of infection for patient A. We did not explore potential differences in susceptibility between patient A and other contacts of the index patient but focused on exposure. Thus, other factors, such as history of flavivirus infection in contacts of the index patient, might have contributed to a difference in susceptibility to infection between patient A and other persons.

Currently, Zika virus is known to be transmitted by the bite of an infected mosquito, congenitally from an infected

mother to her fetus, sexually, through blood transfusion, and by laboratory exposure (1–6). Healthcare providers and public health officials should be aware that person-to-person transmission beyond sexual transmission might occur, albeit rarely, and should be investigated to determine the potential source of infection by obtaining various body fluids from persons suspected of transmitting the virus to another person through an undetermined route. Additional investigation is needed to determine the infectious risk various body fluids represent for person-to-person transmission and to determine host factors that might increase susceptibility for infection.

Acknowledgments

We thank Ilene Risk, Mary Hill, Tara Brunatti, Andrea Price, Jeanmarie Meyer, Sankar Swaminathan, Susan Hills, Amy Lambert, Marc Fischer, Dominic Rose, Nicholas Panella, Kristen Burkhalter, Kristen Nordlund, Ryan Lusty, Brian Hougaard, Eric Gardner, Gary Hatch, and Greg White for assistance and input during this study.

Dr. Krow-Lucal is an Epidemic Intelligence Service Officer in the Arboviral Diseases Branch, Division of Vector-Borne Diseases, National Center for Zoonotic and Emerging Infectious Diseases, Centers for Disease Control and Prevention, Fort Collins, CO. Her primary research interests are immunology and infectious diseases.

References

- Besnard M, Lastère S, Teissier A, Cao-Lormeau V, Musso D. Evidence of perinatal transmission of Zika virus, French Polynesia, December 2013 and February 2014. *Euro Surveill.* 2014;19:20751. <http://dx.doi.org/10.2807/1560-7917.ES2014.19.13.20751>
- Foy BD, Kobylinski KC, Chilson Foy JL, Blitvich BJ, Travassos da Rosa A, Haddow AD, et al. Probable non-vector-borne transmission of Zika virus, Colorado, USA. *Emerg Infect Dis.* 2011;17:880–2. <http://dx.doi.org/10.3201/eid1705.101939>
- Hills SL, Russell K, Hennessey M, Williams C, Oster AM, Fischer M, et al. Transmission of Zika virus through sexual contact with travelers to areas of ongoing transmission—continental United States, 2016. *MMWR Morb Mortal Wkly Rep.* 2016;65:215–6. <http://dx.doi.org/10.15585/mmwr.mm6508e2>
- The Subcommittee on Arbovirus Laboratory Safety of the American Committee on Arthropod-Borne Viruses. Laboratory safety for arboviruses and certain other viruses of vertebrates. *Am J Trop Med Hyg.* 1980;29:1359–81.
- Oliveira Melo AS, Malinger G, Ximenes R, Szejnfeld PO, Alves Sampaio S, Bispo de Filippis AM. Zika virus intrauterine infection causes fetal brain abnormality and microcephaly: tip of the iceberg? *Ultrasound Obstet Gynecol.* 2016;47:6–7. <http://dx.doi.org/10.1002/uog.15831>
- Motta IJ, Spencer BR, Cordeiro da Silva SG, Arruda MB, Dobbin JA, Gonzaga YB, et al. Evidence for transmission of Zika virus by platelet transfusion. *N Engl J Med.* 2016;375:1101–3. <http://dx.doi.org/10.1056/NEJMc1607262>
- Swaminathan S, Schlager R, Lewis J, Hanson KE, Couturier MR. Fatal Zika virus infection with secondary nonsexual transmission. *N Engl J Med.* 2016;375:1907–9. <http://dx.doi.org/10.1056/NEJMc1610613>
- Brent C, Dunn A, Savage H, Faraji A, Rubin M, Risk I, et al. Preliminary findings from an investigation of Zika virus infection in a patient with no known risk factors—Utah, 2016. *MMWR Morb Mortal Wkly Rep.* 2016;65:981–2. <http://dx.doi.org/10.15585/mmwr.mm6536e4>
- Hahn MB, Eisen RJ, Eisen L, Boegler KA, Moore CG, McAllister J, et al. Reported distribution of *Aedes (Stegomyia) aegypti* and *Aedes (Stegomyia) albopictus* in the United States, 1995–2016 (Diptera: Culicidae). *J Med Entomol.* 2016;53:1169–75. <http://dx.doi.org/10.1093/jme/tjw072>
- Rabe IB, Staples JE, Villanueva J, Hummel KB, Johnson JA, Rose L, et al. Interim guidance for interpretation of Zika virus antibody test results. *MMWR Morb Mortal Wkly Rep.* 2016;65:543–6. <http://dx.doi.org/10.15585/mmwr.mm6521e1>
- Centers for Disease Control and Prevention. Diagnostic tests for Zika virus, 2016 [cited 2016 Dec 24]. <https://www.cdc.gov/zika/hc-providers/types-of-tests.html>
- Harrington LC, Scott TW, Lerdthusnee K, Coleman RC, Costero A, Clark GG, et al. Dispersal of the dengue vector *Aedes aegypti* within and between rural communities. *Am J Trop Med Hyg.* 2005;72:209–20.
- Centers for Disease Control and Prevention. Guidance for U.S. laboratories testing for Zika virus infection, 2016 [cited 2016 Dec 24]. Available from: <https://www.cdc.gov/zika/laboratories/lab-guidance.html>
- Determination and declaration regarding emergency use of in vitro diagnostic tests for detection of Zika virus and/or diagnosis of Zika virus infection. Federal Register, 2016 [cited 2016 Dec 24] <https://www.federalregister.gov/documents/2016/03/02/2016-04624/determination-and-declaration-regarding-emergency-use-of-in-vitro-diagnostic-tests-for-detection-of>
- Lennette EH, Lennette DA, Lennette ET. Diagnostic procedures for viral, rickettsial, and chlamydial infections. Washington (DC): American Public Health Association; 1995.
- Lanciotti RS, Kosoy OL, Laven JJ, Velez JO, Lambert AJ, Johnson AJ, et al. Genetic and serologic properties of Zika virus associated with an epidemic, Yap State, Micronesia, 2007. *Emerg Infect Dis.* 2008;14:1232–9. <http://dx.doi.org/10.3201/eid1408.080287>
- United States Census Bureau. American fact finder: community facts [cited 2016 Dec 24]. <https://factfinder.census.gov/faces/nav/jsf/pages/index.xhtml#>
- Bonaldo MC, Ribeiro IP, Lima NS, Dos Santos AA, Menezes LS, da Cruz SO, et al. Isolation of infective Zika virus from urine and saliva of patients in Brazil. *PLoS Negl Trop Dis.* 2016;10:e0004816. <http://dx.doi.org/10.1371/journal.pntd.0004816>
- Calvet G, Aguiar RS, Melo ASO, Sampaio SA, de Filippis I, Fabri A, et al. Detection and sequencing of Zika virus from amniotic fluid of fetuses with microcephaly in Brazil: a case study. *Lancet Infect Dis.* 2016;16:653–60. [http://dx.doi.org/10.1016/S1473-3099\(16\)00095-5](http://dx.doi.org/10.1016/S1473-3099(16)00095-5)
- Sun J, Wu D, Zhong H, Guan D, Zhang H, Tan Q, et al. Presence of Zika virus in conjunctival fluid. *JAMA Ophthalmol.* 2016;134:1330–2. <http://dx.doi.org/10.1001/jamaophthalmol.2016.3417>
- Dupont-Rouzeyrol M, Biron A, O'Connor O, Huguon E, Descloux E. Infectious Zika viral particles in breastmilk. *Lancet.* 2016;387:1051. [http://dx.doi.org/10.1016/S0140-6736\(16\)00624-3](http://dx.doi.org/10.1016/S0140-6736(16)00624-3)
- Musso D, Roche C, Robin E, Nhan T, Teissier A, Cao-Lormeau V-M. Potential sexual transmission of Zika virus. *Emerg Infect Dis.* 2015;21:359–61. <http://dx.doi.org/10.3201/eid2102.141363>
- Rozé B, Najioullah F, Fergé J-L, Apetse K, Brouste Y, Cesaire R, et al.; GBS Zika Working Group. Zika virus detection in urine from patients with Guillain-Barré syndrome on Martinique, January 2016. *Euro Surveill.* 2016;21:30154. <http://dx.doi.org/10.2807/1560-7917.ES.2016.21.9.30154>

24. Furtado JM, Espósito DL, Klein TM, Teixeira-Pinto T, da Fonseca BA. Uveitis associated with Zika virus infection. *N Engl J Med*. 2016;375:394–6. <http://dx.doi.org/10.1056/NEJMc1603618>

25. Prisant N, Bujan L, Benichou H, Hayot P-H, Pavili L, Lurel S, et al. Zika virus in the female genital tract. *Lancet Infect Dis*. 2016;16:1000–1. [http://dx.doi.org/10.1016/S1473-3099\(16\)30193-1](http://dx.doi.org/10.1016/S1473-3099(16)30193-1)

26. Fonseca K, Meatherall B, Zarra D, Drebot M, MacDonald J, Pabbaraju K, et al. First case of Zika virus infection in a returning Canadian traveler. *Am J Trop Med Hyg*. 2014;91:1035–8. <http://dx.doi.org/10.4269/ajtmh.14-0151>

27. Siegel JD, Rhinehart E, Jackson M, Chiarello L; Healthcare Infection Control Practices Advisory Committee. 2007 Guideline for isolation precautions: preventing transmission of infectious agents in healthcare settings, 2007 [cited 2017 Jan 9]. <http://www.cdc.gov/ncidod/dhqp/pdf/isolation2007.pdf>

28. Centers for Disease Control and Prevention. Healthcare exposure to Zika and infection control, 2016 [cited 2016 Dec 24]. <https://www.cdc.gov/zika/hc-providers/infection-control.html>

Address for correspondence: J. Erin Staples, Centers for Disease Control and Prevention, 3156 Rampart Rd, Mailstop P02, Fort Collins, CO 80521, USA; email: estaples@cdc.gov

October 2014: Vectorborne Diseases

- Resurgence of Cutaneous Leishmaniasis in Israel, 2001–2012
- Rapidly Growing Mycobacteria Associated with Laparoscopic Gastric Banding, Australia, 2005–2011
- Distinct Characteristics and Complex Evolution of PEDV Strains, North America, May 2013–February 2014
- Person-to-Person Household and Nosocomial Transmission of Andes Hantavirus, Southern Chile, 2011
- Effects of Mefloquine Use on *Plasmodium vivax* Multidrug Resistance
- Risk Factors for Human Lice and Bartonellosis among the Homeless, San Francisco, California, USA
- Influenza-Associated Hospitalizations, Singapore, 2004–2008 and 2010–2012
- Lyme Disease, Virginia, USA, 2000–2011
- Clinical Isolates of Shiga Toxin 1 α -Producing *Shigella flexneri* with an Epidemiological Link to Recent Travel to Hispaniola



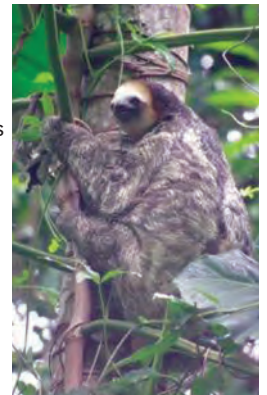
- Prevalence of *Borrelia miyamotoi* in *Ixodes* Ticks in Europe and the United States
- Biomarker Correlates of Survival in Pediatric Patients with Ebola Virus Disease

- Increased Pyrethroid Resistance in Malaria Vectors and Decreased Bed Net Effectiveness, Burkina Faso
- Malaria Control and Elimination, Venezuela, 1800s–1970s



- *Haemophilus ducreyi* Associated with Skin Ulcers among Children, Solomon Islands
- Autochthonous Melioidosis in Humans, Madagascar, 2012 and 2013
- Human Granulocytic Anaplasmosis, South Korea, 2013
- Ongoing Epidemic of Cutaneous Leishmaniasis among Syrian Refugees, Lebanon
- Knemidocoptic Mange in Wild Golden Eagles, California, USA
- Novel Influenza A(H7N2) Virus in Chickens, Jilin Province, China, 2014
- Differences in Influenza Seasonality by Latitude, Northern India
- Human Babesiosis, Maine, USA, 1995–2011

- Prevalence of *Arcobacter* Species among Humans, Belgium, 2008–2013
- Evidence of Recombinant Strains of Porcine Epidemic Diarrhea Virus, United States, 2013
- Treatment of Giardiasis after Nonresponse to Nitroimidazole
- Human Infection with Highly Pathogenic A(H7N7) Avian Influenza Virus, Italy, 2013



**EMERGING
INFECTIOUS DISEASES**

<https://wwwnc.cdc.gov/eid/articles/issue/20/11/table-of-contents>

Acute Febrile Illness and Complications Due to Murine Typhus, Texas, USA^{1,2}

Zeeshan Afzal, Sunand Kallumadanda, Feng Wang, Vagish Hemmige, Daniel Musher

Murine typhus occurs relatively commonly in southern Texas, as well as in California. We reviewed records of 90 adults and children in whom murine typhus was diagnosed during a 3-year period in 2 hospitals in southern Texas, USA. Most patients lacked notable comorbidities; all were immunocompetent. Initial signs and symptoms included fever (99%), malaise (82%), headache (77%), fatigue (70%), myalgias (68%), and rash (39%). Complications, often severe, in 28% of patients included bronchiolitis, pneumonia, meningitis, septic shock, cholecystitis, pancreatitis, myositis, and rhabdomyolysis; the last 3 are previously unreported in murine typhus. Low serum albumin and elevated procalcitonin, consistent with bacterial sepsis, were observed in >70% of cases. Rash was more common in children; thrombocytopenia, hyponatremia, elevated hepatic transaminases, and complications were more frequent in adults. Murine typhus should be considered as a diagnostic possibility in cases of acute febrile illness in southern and even in more northern US states.

Murine (endemic) typhus is most frequently recognized as an acute febrile illness, although the clinical manifestations of this infection cover the full spectrum of disease, from asymptomatic infection to fulminant disease and death (1–5). The causative organism, *Rickettsia typhi*, is a small, gram-negative, obligate intracellular bacterium. Worldwide, especially in tropical and subtropical areas, the roof rat (*Rattus rattus*) and Norway rat (*Rattus norvegicus*) have been the principal reservoirs, with the rat flea, *Xenopsylla cheopis*, as the principal vector (2,6).

In the United States, individual murine typhus cases and outbreaks have been reported from suburban areas; in these instances, opossums (*Didelphis virginiana*) and *Rattus* spp. have been implicated as the reservoirs, with the cat flea, *Ctenocephalides felis*, as the principal vector (2). The incidence of murine typhus declined sharply in the United States after the institution of DDT for control

of rat fleas in 1945 (5), but it now appears to be on the rise, especially in southern Texas and California (2,7,8). We describe 90 murine typhus infections that were diagnosed in 2 hospitals in Hidalgo County, Texas, USA, during a 3-year period, with a comparison of clinical manifestations in adults and children.

Methods

Patient Identification

We searched microbiology laboratory records at McAllen Medical Center (McAllen, TX, USA) and Edinburg Regional Medical Center (Edinburg, TX, USA) for July 1, 2013–June 30, 2016, to identify patients who had typhus group rickettsiae IgM or IgG at a titer $\geq 1:128$ (9) (Focus Diagnostics Rickettsia, Indirect Immunofluorescence Antibody for IgM and IgG; Labcorp, Houston, TX, USA). A total of 101 patients were identified; all had been hospitalized. We carefully reviewed their medical records to be certain that their clinical syndrome was suggestive of murine typhus.

Eleven of the 101 patients were excluded: 5 had incomplete medical records sufficient to make a clinical diagnosis and 6 had another condition that might have caused a fever (otitis media, active hepatitis C, Epstein-Barr virus infection, untreated HIV infection, lymphoma, or tuberculosis). IgG titers had been measured in every case. Of the remaining 90 patients, 41 (45.6%) had been evaluated by an infectious disease consultant, who either concurred with or suggested the diagnosis of murine typhus in every case.

Case Definitions

For case identification, we used the Flea-borne Typhus Epi Case Criteria 2016 Case Definition/Case Classification of the Texas State Department of Health (9). We also used the case classification scheme described by the

Author affiliations: University of Texas Rio Grande Valley, McAllen, Texas, USA (Z. Afzal, S. Kallumadanda, F. Wang); Baylor College of Medicine, Houston, Texas, USA (V. Hemmige, D. Musher); M.E. DeBakey VA Medical Center, Houston (D. Musher)

DOI: <https://doi.org/10.3201/eid2308.161861>

¹A poster form of this study was presented at the Annual Session and Primary Care Summit of Texas Academy of Family Physicians, November 4–6, 2016, Dallas, TX, USA.

²An abstract has been accepted for ID Week 2017, October 4–8, 2017, San Diego, CA, USA, for an oral presentation.

Centers for Disease Control and Prevention for spotted fever rickettsiosis 2010 to categorize our patients with suspected murine typhus, probable murine typhus, or confirmed murine typhus (10). Patients with suspected murine typhus were those with laboratory evidence of past or present infection but without a clinically compatible illness. Patients with probable murine typhus were those in whom the clinical disease was compatible with murine typhus (meets clinical evidence criteria) and with supportive laboratory results. Patients with confirmed murine typhus had a clinically compatible illness and laboratory confirmation. Illnesses that are clinically compatible with murine typhus are characterized by acute onset of fever and ≥ 1 : headache, myalgia, anorexia, nausea/vomiting, thrombocytopenia, or elevated hepatic aminotransferases. Supportive laboratory evidence is defined by indirect immunofluorescence assay (IgM or IgG) serologic titer ≥ 1 :128. Laboratory-confirmed cases are required to have serologic evidence of a 4-fold increase in IgG-specific antibody titer reactive with typhus group rickettsiae antigen by indirect immunofluorescence assay in paired serum specimens (1 taken in the first week of illness and a second 2–4 weeks later).

Data Gathering

We reviewed electronic medical records to obtain data on demography and epidemiology; comorbid conditions; symptoms and their duration before hospitalization; physical findings; laboratory results (hematology, chemistry, and microbiology); imaging; requirements for intensive care; hospital course; antimicrobial drug treatment; response to treatment; and duration of hospital stay. This study was approved by the institutional review board of the University of Texas Rio Grande Valley Medical School.

Data Analysis

Basic descriptive statistics were calculated, and comparisons between the proportion of adult and pediatric patients with different signs and symptoms of murine typhus were calculated with a χ^2 or Fisher exact test, as appropriate. All analyses were performed in Stata 12 (Statacorp LLC, College Station, TX, USA).

Results

On the basis of the definitions we described, 90 patients were given a diagnosis of murine typhus. One patient had a clinical syndrome consistent with murine typhus but the presence of fever was not documented; this illness was characterized as suspected murine typhus. Eighty-six patients met criteria for probable murine typhus, and 3 had confirmed murine typhus. Overall, the initial IgM titer was ≥ 1 :128 in 86 (96%) cases, and the IgG titer was ≥ 1 :128 in 63 (70%) cases. Five patients had a second blood

sample submitted for typhus group rickettsiae IgG; 3 of these exhibited a 4-fold increase in IgG titer (rising from < 1 :64 to 1:512) and were determined to be confirmed murine typhus. One patient had a 2-fold increase in IgG titer; in the other patient, IgG titer remained unchanged but IgM titer doubled from 1:128 to 1:256, thus meeting the criteria for probable murine typhus.

Of the 90 patients, 36 (40%) were < 18 years of age, and 45 (50%) were female. All patients included in the final analysis had a clinical syndrome suggestive of murine typhus (Table 1), including fever in 99%, malaise in 82%, headache in 77%, fatigue in 70%, myalgias in 68%, and rash in 39%. Other causes of the syndrome were sought by bacteriologic and serologic studies in a varying proportion of these cases; no other cause was found.

Complications of murine typhus occurred in 25 (28%) cases. Among documented complications were bronchiolitis in 2 cases, pneumonia in 8, pancreatitis in 3, cholecystitis in 1, myositis (creatinine phosphokinase $> 1,500$ U/L) in 1, rhabdomyolysis (creatinine phosphokinase $> 4,000$ U/L) in 2, meningitis in 2, sepsis with acute kidney injury in 1, and septic shock in 4. In 1 patient, pneumonia and septic shock occurred together. There were no deaths.

Laboratory findings consistent with murine typhus included leukocytes $< 6,000$ cells/mm³ in 21 (23%) patients, platelets $< 120,000$ /mm³ in 49 (54%), aspartate aminotransferase > 50 IU/L in 76 (84%), alanine aminotransferase > 50 IU/L in 67 (74%), and serum sodium ≤ 133 mmol/L in 40 (44%). In no case was the leukocyte count as low as 3,000 cells/mm³. Serum albumin was < 3.5 g/dL in 73 (81%) of 90 cases, and serum procalcitonin was ≥ 0.5 ng/mL in 10 (71%) of 14 cases, both findings consistent with bacterial sepsis. Newly recognized complications of murine typhus in this case series included pancreatitis, myositis, and rhabdomyolysis. Thirteen patients (14%) required care in the intensive care unit.

We found notable differences between adult and pediatric patients (Table 1) in the frequency of diarrhea, platelet count $< 120,000$ /mm³, serum sodium ≤ 133 mmol/L, and aspartate aminotransferase and alanine aminotransferase > 50 IU/L, all of which were more common in adults. Complications occurred in 18 (33%) of 54 adults and 7 (19%) of 36 children ($p = 0.15$).

The median duration from onset of illness to hospitalization was 7 days (range 1–21 days). Many patients saw a physician before coming to the hospital. We determined that the median time between the initial clinical encounter and institution of effective antimicrobial drug therapy was 5 days (range 0–15 days). A wide array of antimicrobial drugs was prescribed. Eight patients never received an antimicrobial drug appropriate to treat murine typhus, but the disease resolved spontaneously.

Table 1. Characteristics of 90 patients with murine typhus, Hidalgo County, Texas, USA, July 1, 2013–June 30, 2016*

Characteristic	No. (%) patients			p value
	Age ≥18 y	Age <18 y	Total	
Symptoms				
Subjective fever/chills	53/54 (98)	36/36 (100)	89/90 (99)	1
Malaise	21/24 (88)	15/20 (75)	36/44 (82)	0.44
Headache	37/46 (80)	23/32 (72)	60/78 (77)	0.38
Fatigue	22/29 (76)	10/17 (59)	32/46 (70)	0.22
Myalgias	29/39 (74)	13/23 (57)	42/62 (68)	0.15
Nausea and/or vomiting	31/52 (60)	21/35 (60)	52/87 (60)	0.97
Cough	21/52 (40)	18/36 (50)	39/88 (44)	0.37
Abdominal pain	17/47(36)	10/33 (30)	27/80 (34)	0.58
Arthralgia	9/34 (26)	4/24 (17)	13/58 (22)	0.53
Diarrhea	9/50 (18)	1/35 (3)	10/85 (12)	0.04
Confusion	6/42 (14)	2/30 (7)	8/72 (11)	0.45
Signs				
Temperature ≥100.4°F	48/54 (89)	34/36 (94)	82/90 (91)	0.47
Rash	16/51 (31)	18/36 (50)	34/87 (39)	0.12
Enlarged liver	1/44 (2)	1/32 (3)	2/76 (3)	1
Enlarged spleen	0/44 (0)	1/32 (3)	1/76 (1)	0.42
Laboratory findings				
Leukocytes <6,000 cells/mm ³	10/54 (19)	11/36 (31)	21/90 (23)	0.19
Leukocytes <3,000 cells/mm ³	0	0	0	1
Platelets <120,000/mm ³	37/54 (69)	12/36 (33)	49/90 (54)	<0.01
Bilirubin ≥1.5 mg/dL	14/54 (26)	3/36 (8)	17/90 (19)	0.05
AST >50 IU/L	51/54 (94)	25/36 (69)	76/90 (84)	<0.01
ALT >50 IU/L	45/54 (83)	22/36 (61)	67/90 (74)	0.02
Serum sodium ≤133 mmol/L	34/54 (63)	6/36 (17)	40/90 (44)	<0.01
Serum albumin <3.5 g/dL	46/54 (85)	27/36 (75)	73/90 (81)	0.23
Serum procalcitonin >0.5 ng/mL	9/13 (69)	1/1 (100)	10/14 (71)	1
IgM ≥1:128	50/54 (93)	36/36 (100)	86/90 (96)	0.15
IgG ≥1:128	41/54 (76)	22/36 (61)	63/90 (70)	0.13
Complications	18/54 (33)	7/36 (19)	25/90 (28)	0.15

*ALT, alanine aminotransferase; AST, aspartate aminotransferase.

Discussion

Murine typhus causes a syndrome characterized by nonspecific manifestations, including fever, headache, myalgias, malaise, nausea, and vomiting in more than half of cases. This syndrome has previously been described throughout the world, including the southwestern United States (1,4,5,11–13) and California (2,14), as well as Europe (3,15–17).

Twenty-three of the 90 patients in this study were first seen in a primary care physician's office. Diagnoses made at the time of that initial encounter, whether in children or adults, included viral syndrome, influenza, and streptococcal pharyngitis; murine typhus was not considered in any of them. Once patients were hospitalized, this nonspecific clinical syndrome, together with characteristic laboratory abnormalities (low leukocyte and platelet counts and elevated levels of liver enzymes) and knowledge of the occurrence of murine typhus in this area, enabled the correct diagnosis to be considered. Serum samples were submitted for supportive laboratory testing, and appropriate therapy was instituted promptly, in most cases before results of serologic tests were known. It is still worth noting that, for 8 patients, the diagnosis of murine typhus was never made during their illness, but only when serologic results were returned. Illness resolved spontaneously in these 8 patients.

Serum procalcitonin, not previously reported in murine typhus, was elevated in 10 (71.4%) of the 14 cases in which it was studied; this test might help distinguish murine typhus from a viral syndrome in an endemic area. The low serum albumin is also consistent with bacterial sepsis (18).

Although the usual symptoms were those of a nonspecific illness suggestive of influenza, another viral syndrome, or streptococcal pharyngitis, many of our patients were, at some point, quite ill. Thirteen (14%) of 90 were hospitalized in an intensive care unit. Six met criteria for sepsis; serum albumin fell to <3.5 g/dL, consistent with serious bacterial infection, in 73 (81%) of the 90 patients. Complications of murine typhus, defined as symptoms, signs, or both beyond nonspecific ones, were seen in 25 (28%) patients and appeared more frequently in adults than in children (Table 2). The most common complications were pulmonary complications, such as bronchiolitis and pneumonia; aseptic meningitis; and sepsis with shock. These complications have been described previously, either in case reports or in case series (1,2,12,16,17,19). Only 2 previous studies have specifically tabulated complications (3,20), with the frequency of complications in 1 prospective series being similar to that in this study (20).

No previous investigation has reported on serum procalcitonin, which was elevated in 10 (71.4%) of 14 patients in the study in which it was measured. Newly described

Table 2. Complications in 90 patients with murine typhus, Hidalgo County, Texas, USA, July 1, 2013–June 30, 2016

Complication	Age ≥18 y, n = 54	Age <18 y, n = 36	Total, n = 90
Bronchiolitis	0	2	2
Pneumonia	7	1	8
Pancreatitis	3	0	3
Cholecystitis	0	1	1
Myositis	0	1	1
Rhabdomyolysis	0	2	2
Meningitis	2	0	2
Septic shock	4	0	4
Sepsis with acute kidney injury	1	0	1
Pneumonia plus septic shock	1	0	1
Total	18	7	25

complications in this series included pancreatitis, myositis, and rhabdomyolysis. Unusual cutaneous manifestations (21), iritis (20), lymphadenopathy (20), splenic rupture (22,23), disseminated intravascular coagulation (3,12), cholecystitis (24), and endocarditis (25,26) have previously been reported; except for 1 patient with cholecystitis, we had no examples of these other unusual complications in our series.

Earlier series of cases have not compared findings in adults and children. Differences between children and adults in this study included greater frequency of rash in children, whereas statistically significant differences were greater incidence of diarrhea, thrombocytopenia, hyponatremia, and elevated hepatic aminotransferases in adults. Complicated illness was more common in older than in younger subjects, as has been suggested in separate reports from a group of investigators in Greece (16,17).

Murine typhus has been increasingly recognized in Texas (8). Two counties in Texas have reported >50 cases of murine typhus per year (1,11), and in 1 of these, a high prevalence of antibodies to *R. typhi* has been described in healthy children (13). To our knowledge, such a study has not been reported in adults in southern Texas, the area of greatest endemicity in the United States. Our finding of 90 recognized cases of murine typhus in 2 hospitals in a 3-year period attests to the frequency of murine typhus in the southwestern United States.

Rats and opossums that coexist in urban and suburban settings appear to be reservoirs for the organism. The vector has traditionally been thought to be *Xenopsylla cheopis*, the rat flea (6). However, recent studies (27,28) have shown that the cat flea, *Ctenocephalides felis*, which also infests opossums, plays a role in transmission. Blanton et al. (27) found rickettsial DNA in pools of fleas obtained from opossums in Galveston, Texas, and documented the emergence of antibodies to *Rickettsia* sp. in these animals. A major outbreak of murine typhus in Austin, Texas, was traced to contact with opossums (11). Because *R. felis* may also be present in fleas living on these same reservoirs (29,30) and

the clinical spectrum of infection due to this organism remains undefined, it is possible that some cases attributed to *R. typhi* and identified as murine typhus may actually be due to *R. felis*.

The natural habitat of the American opossum includes northeastern and northwestern states, suggesting the possibility that murine typhus may not be confined to areas that are currently recognized as endemic, such as southern Texas or California. In Virginia and the Carolinas, illnesses of patients with fever, rash, and nonspecific symptoms are regularly diagnosed as Rocky Mountain spotted fever and treated with doxycycline; however, it is possible that some of these infections may be due to *R. typhi*. PCR (24,31,32) can distinguish among these organisms, but it is not readily available and has uncertain clinical value. *R. felis* may also cause human infection and requires PCR to distinguish it from *R. typhi* (29,30,33). In fact, as suggested by Eremeva et al. (29), murine typhus as we now know it may be a single clinical syndrome that can be caused by either *R. typhi* or *R. felis*.

The principal limitation of our study is that diagnoses were suspected clinically but were supported by detection of serum antibodies reactive with typhus group rickettsial antigen. Cross-reacting IgM may also appear after infection with other organisms in the typhus group (*R. prowazekii*) and the spotted fever group (*R. rickettsii*, the cause of Rocky Mountain spotted fever), as well as *R. felis*; we cannot exclude the possibility that some of our cases may have been caused by these organisms. Other cases of *R. typhi* infection may have been missed because physicians suspected the disease very early and instituted treatment with doxycycline. The principal strengths of this study are that the medical records were reviewed in every case by the principal investigator and that many of the patients had been seen by an infectious disease consultant who concurred with the final diagnosis, usually before serologic results were available.

In conclusion, murine typhus is a multifaceted disease that is common in southern Texas and California and that might be identified more frequently in other areas of the United States if the diagnosis were sought. A major description of this disease, especially with newly proposed case definitions, has not appeared in an American journal for 15 years; pediatric and adult cases have not been compared, and the range of complications in the United States has not been described recently. The population of the American opossum has increased in northern states. In Texas and California, their fleas are known to carry *R. typhi* (27,34) but, to our knowledge, a search for *Rickettsia* spp. in opossums has not been conducted in other parts of the United States. We suggest that, in cases of acute febrile conditions, the diagnosis of murine typhus needs to be considered elsewhere in the southern United

States and, perhaps, farther north as well. Because of the high prevalence of murine typhus in areas of recognized endemicity, medical centers might consider on-site testing for antibodies to typhus group rickettsiae to support a clinical decision and early treatment. A reactive serology might then trigger a reflex request to obtain convalescent titers to provide confirmatory data.

Dr. Afzal is a third-year family medicine resident and serves as assistant chief resident at the McAllen family medicine residency program, University of Texas Rio Grande Valley, McAllen, Texas. He is interested in clinical research and rural health.

Dr. Musher is a distinguished service professor of medicine and professor of molecular virology and microbiology at Baylor College of Medicine in Houston, Texas.

References

- Whiteford SF, Taylor JP, Dumler JS. Clinical, laboratory, and epidemiologic features of murine typhus in 97 Texas children. *Arch Pediatr Adolesc Med.* 2001;155:396–400. <http://dx.doi.org/10.1001/archpedi.155.3.396>
- Civen R, Ngo V. Murine typhus: an unrecognized suburban vectorborne disease. *Clin Infect Dis.* 2008;46:913–8. <http://dx.doi.org/10.1086/527443>
- Chaliotis G, Kritsotakis EI, Psaroulaki A, Tselentis Y, Gikas A. Murine typhus in central Greece: epidemiological, clinical, laboratory, and therapeutic-response features of 90 cases. *Int J Infect Dis.* 2012;16:e591–6. <http://dx.doi.org/10.1016/j.ijid.2012.03.010>
- Taylor JP, Betz TG, Rawlings JA. Epidemiology of murine typhus in Texas, 1980 through 1984. *JAMA.* 1986;255:2173–6. <http://dx.doi.org/10.1001/jama.1986.03370160071029>
- Older JJ. The epidemiology of murine typhus in Texas, 1969. *JAMA.* 1970;214:2011–7. <http://dx.doi.org/10.1001/jama.1970.03180110021004>
- Azad AF. Epidemiology of murine typhus. *Annu Rev Entomol.* 1990;35:553–69. <http://dx.doi.org/10.1146/annurev.en.35.010190.003005>
- Texas Department of State Health Services. Murine typhus [cited 2016 Aug 15]. http://www.dshs.texas.gov/idcu/disease/murine_typhus/
- Blanton LS, Vohra RF, Bouyer DH, Walker DH. Reemergence of murine typhus in Galveston, Texas, USA, 2013. *Emerg Infect Dis.* 2015;21:484–6. <http://dx.doi.org/10.3201/eid2103.140716>
- Mayes B. Rickettsial disease diagnostics and epidemiology [cited 2017 Mar 14]. <https://dshs.texas.gov/WorkArea/linkit.aspx?LinkIdentifier=id&ItemID=8590006123>
- Centers for Disease Control and Prevention. Spotted fever rickettsiosis, case definition 2010 [cited 2017 Mar 14]. <https://www.cdc.gov/nndss/conditions/spotted-fever-rickettsiosis/case-definition/2010/>
- Adjemian J, Parks S, McElroy K, Campbell J, Eremeeva ME, Nicholson WL, et al. Murine typhus in Austin, Texas, USA, 2008. *Emerg Infect Dis.* 2010;16:412–7. <http://dx.doi.org/10.3201/eid1603.091028>
- Dumler JS, Taylor JP, Walker DH. Clinical and laboratory features of murine typhus in south Texas, 1980 through 1987. *JAMA.* 1991;266:1365–70. <http://dx.doi.org/10.1001/jama.1991.03470100057033>
- Purcell K, Fergie J, Richman K, Rocha L. Murine typhus in children, south Texas. *Emerg Infect Dis.* 2007;13:926–7. <http://dx.doi.org/10.3201/eid1306.061566>
- Green JS, Singh J, Cheung M, Adler-Shohet FC, Ashouri N. A cluster of pediatric endemic typhus cases in Orange County, California. *Pediatr Infect Dis J.* 2011;30:163–5. <http://dx.doi.org/10.1097/INF.0b013e3181f4cc25>
- Bernabeu-Wittel M, Pachón J, Alarcón A, López-Cortés LF, Viciano P, Jiménez-Mejías ME, et al. Murine typhus as a common cause of fever of intermediate duration: a 17-year study in the south of Spain. *Arch Intern Med.* 1999;159:872–6. <http://dx.doi.org/10.1001/archinte.159.8.872>
- Gikas A, Kokkini S, Tsioutis C, Athenessopoulos D, Balomenaki E, Blasak S, et al. Murine typhus in children: clinical and laboratory features from 41 cases in Crete, Greece. *Clin Microbiol Infect.* 2009;15(Suppl 2):211–2. <http://dx.doi.org/10.1111/j.1469-0691.2008.02133.x>
- Tsioutis C, Chaliotis G, Kokkini S, Doukakis S, Tselentis Y, Psaroulaki A, et al. Murine typhus in elderly patients: a prospective study of 49 patients. *Scand J Infect Dis.* 2014;46:779–82. <http://dx.doi.org/10.3109/00365548.2014.943283>
- Fleck A, Hawker F, Wallace PI, Raines G, Trotter J, Ledingham IM, et al. Increased vascular permeability: a major cause of hypoalbuminaemia in disease and injury. *Lancet.* 1985;325:781–4. [http://dx.doi.org/10.1016/S0140-6736\(85\)91447-3](http://dx.doi.org/10.1016/S0140-6736(85)91447-3)
- Bernabeu-Wittel M, Villanueva-Marcos JL, Alarcón-González A, Pachón J. Septic shock and multiorgan failure in murine typhus. *Eur J Clin Microbiol Infect Dis.* 1998;17:131–2. <http://dx.doi.org/10.1007/BF01682172>
- Gikas A, Doukakis S, Padiaditis J, Kastanakis S, Psaroulaki A, Tselentis Y. Murine typhus in Greece: epidemiological, clinical, and therapeutic data from 83 cases. *Trans R Soc Trop Med Hyg.* 2002;96:250–3. [http://dx.doi.org/10.1016/S0035-9203\(02\)90090-8](http://dx.doi.org/10.1016/S0035-9203(02)90090-8)
- Blanton LS, Lea AS, Kelly BC, Walker DH. An unusual cutaneous manifestation in a patient with murine typhus. *Am J Trop Med Hyg.* 2015;93:1164–7. <http://dx.doi.org/10.4269/ajtmh.15-0380>
- Fergie J, Purcell K. Spontaneous splenic rupture in a child with murine typhus. *Pediatr Infect Dis J.* 2004;23:1171–2.
- McKelvey SD, Braidey PC, Stansby GP, Weir WRC. Spontaneous splenic rupture associated with murine typhus. *J Infect.* 1991;22:296–7. [http://dx.doi.org/10.1016/S0163-4453\(05\)80017-9](http://dx.doi.org/10.1016/S0163-4453(05)80017-9)
- Schriefer ME, Sacci JB Jr, Dumler JS, Bullen MG, Azad AF. Identification of a novel rickettsial infection in a patient diagnosed with murine typhus. *J Clin Microbiol.* 1994;32:949–54.
- Austin SM, Smith SM, Co B, Coppel IG, Johnson JE. Serologic evidence of acute murine typhus infection in a patient with culture-negative endocarditis. *Am J Med Sci.* 1987;293:320–3. <http://dx.doi.org/10.1097/00000441-198705000-00007>
- Buchs AE, Zimlichman R, Sikuler E, Goldfarb B. Murine typhus endocarditis. *South Med J.* 1992;85:751–3. <http://dx.doi.org/10.1097/00007611-199207000-00019>
- Blanton LS, Idowu BM, Tatsch TN, Henderson JM, Bouyer DH, Walker DH. Opossums and cat fleas: new insights in the ecology of murine typhus in Galveston, Texas. *Am J Trop Med Hyg.* 2016;95:457–61. <http://dx.doi.org/10.4269/ajtmh.16-0197>
- Karpathy SE, Hayes EK, Williams AM, Hu R, Krueger L, Bennett S, et al. Detection of *Rickettsia felis* and *Rickettsia typhi* in an area of California endemic for murine typhus. *Clin Microbiol Infect.* 2009;15(Suppl 2):218–9. <http://dx.doi.org/10.1111/j.1469-0691.2008.02140.x>
- Eremeeva ME, Karpathy SE, Krueger L, Hayes EK, Williams AM, Zaldivar Y, et al. Two pathogens and one disease: detection and identification of flea-borne Rickettsiae in areas endemic for murine typhus in California. *J Med Entomol.* 2012;49:1485–94. <http://dx.doi.org/10.1603/ME11291>
- Abramowicz KF, Rood MP, Krueger L, Eremeeva ME. Urban focus of *Rickettsia typhi* and *Rickettsia felis* in Los Angeles, California. *Vector Borne Zoonotic Dis.* 2011;11:979–84. <http://dx.doi.org/10.1089/vbz.2010.0117>

31. Henry KM, Jiang J, Rozmajzl PJ, Azad AF, Macaluso KR, Richards AL. Development of quantitative real-time PCR assays to detect *Rickettsia typhi* and *Rickettsia felis*, the causative agents of murine typhus and flea-borne spotted fever. *Mol Cell Probes*. 2007;21:17–23. <http://dx.doi.org/10.1016/j.mcp.2006.06.002>

32. Carl M, Tibbs CW, Dobson ME, Paparello S, Dasch GA. Diagnosis of acute typhus infection using the polymerase chain reaction. *J Infect Dis*. 1990;161:791–3. <http://dx.doi.org/10.1093/infdis/161.4.791>

33. Bouyer DH, Stenos J, Crocquet-Valdes P, Moron CG, Popov VL, Zavala-Velazquez JE, et al. *Rickettsia felis*: molecular characterization of a new member of the spotted fever group. *Int J Syst Evol Microbiol*. 2001;51:339–47. <http://dx.doi.org/10.1099/00207713-51-2-339>

34. Maina AN, Fogarty C, Krueger L, Macaluso KR, Odhiambo A, Nguyen K, et al. Rickettsial infections among *Ctenocephalides felis* and host animals during a flea-borne rickettsioses outbreak in Orange County, California. *PLoS One*. 2016;11:e0160604. <http://dx.doi.org/10.1371/journal.pone.0160604>

Address for correspondence: Zeeshan Afzal, McAllen Family Medicine Residency Program, University of Texas Rio Grande Valley, Family and Preventive Medicine, 205 East Toronto Ave, McAllen, TX 78503, USA; email: drzeeshanafzal@gmail.com

July 2013: Vectorborne Infections

- Transmission of *Streptococcus equi* Subspecies *zooepidemicus* Infection from Horses to Humans
- Travel-associated Illness Trends and Clusters, 2000–2010
- Quantifying Effect of Geographic Location on Epidemiology of *Plasmodium vivax* Malaria
- Mutation in Spike Protein Cleavage Site and Pathogenesis of Feline Coronavirus

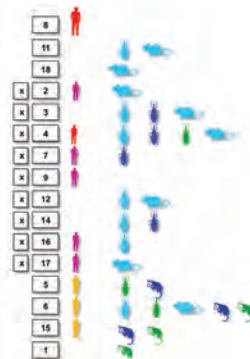


- Pneumococcal Serotypes before and after Introduction of Conjugate Vaccines, United States, 1999–2011
- Influence of Pneumococcal Vaccines and Respiratory Syncytial Virus on Alveolar Pneumonia, Israel
- Avian Metapneumovirus Subgroup C Infection in Chickens, China
- Human Alveolar Echinococcosis in Kyrgyzstan
- Molecular Epidemiologic Source Tracking of Orally Transmitted Chagas Disease, Venezuela
- Unique Clone of *Coxiella burnetii* Causing Severe Q Fever, French Guiana
- *Babesia microti* Infection, Eastern Pennsylvania, USA
- Reemergence of Chikungunya Virus in Bo, Sierra Leone
- Novel *Bartonella* Agent as Cause of Verruga Peruana
- Schmallenberg Virus among Female Lambs, Belgium, 2012
- *Psychrobacter arenosus* Bacteremia after Blood Transfusion, France

- Ciprofloxacin-Resistant *Campylobacter* spp. in Retail Chicken, Western Canada
- Asynchronous Onset of Clinical Disease in BSE-Infected Macaques
- Prevalence of Nontuberculous Mycobacteria in Cystic Fibrosis Clinics, United Kingdom, 2009
- Reducing Visceral Leishmaniasis by Insecticide Impregnation of Bed-Nets, Bangladesh



- Genetic Variants of *Orientia tsutsugamushi* in Domestic Rodents, Northern China
- Undetected Multidrug-Resistant Tuberculosis Amplified by First-line Therapy in Mixed Infection
- Clinical Findings for Early Human Cases of Influenza A(H7N9) Virus Infection, Shanghai, China
- Multidrug-Resistant Atypical Variants of *Shigella flexneri* in China
- MDR TB Transmission, Singapore
- Human Infection with Marten Tapeworm
- *Campylobacter jejuni* in Hospitalized Patients with Diarrhea, Kolkata, India



- Novel Bat-borne Hantavirus, Vietnam
- Neutralizing Antibodies to Severe Fever with Thrombocytopenia Syndrome Virus 4 Years after Hospitalization, China
- Increased Community-Associated Infections Caused by Panton-Valentine Leukocidin–Negative MRSA, Shanghai, 2005–2014

**EMERGING
INFECTIOUS DISEASES**

<https://wwwnc.cdc.gov/eid/articles/issue/19/7/table-of-contents>

High Infection Rates for Adult Macaques after Intravaginal or Intrarectal Inoculation with Zika Virus

Andrew D. Haddow, Aysegul Nalca, Franco D. Rossi, Lynn J. Miller, Michael R. Wiley, Unai Perez-Sautu, Samuel C. Washington, Sarah L. Norris, Suzanne E. Wollen-Roberts, Joshua D. Shamblin, Adrienne E. Kimmel, Holly A. Bloomfield, Stephanie M. Valdez, Thomas R. Sprague, Lucia M. Principe, Stephanie A. Bellanca, Stephanie S. Cinkovich, Luis Lugo-Roman, Lisa H. Cazares, William D. Pratt, Gustavo F. Palacios, Sina Bavari, M. Louise Pitt, Farooq Nasar

Unprotected sexual intercourse between persons residing in or traveling from regions with Zika virus transmission is a risk factor for infection. To model risk for infection after sexual intercourse, we inoculated rhesus and cynomolgus macaques with Zika virus by intravaginal or intrarectal routes. In macaques inoculated intravaginally, we detected viremia and virus RNA in 50% of macaques, followed by seroconversion. In macaques inoculated intrarectally, we detected viremia, virus RNA, or both, in 100% of both species, followed by seroconversion. The magnitude and duration of infectious virus in the blood of macaques suggest humans infected with Zika virus through sexual transmission will likely generate viremias sufficient to infect competent mosquito vectors. Our results indicate that transmission of Zika virus by sexual intercourse might serve as a virus maintenance mechanism in the absence of mosquito-to-human transmission and could increase the probability of establishment and spread of Zika virus in regions where this virus is not present.

Zika virus is a member of the Spondweni serogroup, family *Flaviviridae*, genus *Flavivirus* (1,2). Since the initial isolation of the virus in 1947 (3), intermittent reports of Zika virus infection have been described throughout sub-Saharan Africa and Southeast Asia (4). Recently Zika virus extended its geographic distribution into virus-naïve regions, resulting in large outbreaks in tropical regions (5–7). Most Zika virus infections are asymptomatic, and infections that are symptomatic typically cause a mild febrile illness (2,5–7). However, severe clinical outcomes, including congenital birth defects and Guillian-Barré syndrome, have been reported in a subset of infections (2,5–8).

Author affiliation: United States Army Medical Research Institute of Infectious Diseases, Frederick, Maryland, USA

DOI: <https://doi.org/10.3201/eid2308.170036>

Although the primary mechanism of Zika virus transmission is through the bite of an infective mosquito (3,9,10), sexual transmission involving virus strains originating from African and Asian Zika virus phylogenetic lineages has been reported (11–18). This route of transmission has been identified in nontraveling sexual partners of men who were infected with Zika virus during travel to virus-endemic regions (11–15,17–19).

Recent evidence suggests that sexual transmission of Zika virus is responsible for a substantial number of infections (17–19) and could be a virus maintenance mechanism in the absence of mosquito-to-human transmission, as well as a mechanism by which Zika virus is introduced to virus-naïve regions. Viral persistence studies have demonstrated isolation of infectious Zika virus from ejaculate of a vasectomized patient 69 days postillness (20), detected Zika virus RNA in spermatozoa of another patient 56 days postillness (21), and detected Zika virus in semen specimens for ≥ 6 months after illness (22,23).

Although the titer of infectious Zika virus in semen is unknown, RNA levels of up to 7.5–8.6 \log_{10} copies/mL have been reported (13,21,24,25). These data suggest that male-to-female vaginal, male-to-female anal, and male-to-male anal transmission might occur more often than previously recognized and that persons might be exposed to a higher dose of Zika virus from sexual intercourse with an infectious man than through the bite of an infective mosquito (26,27).

To model risk of Zika virus infection after sexual intercourse, we nontraumatically administered 7.0 \log_{10} PFU (8.7 \log_{10} copies) of the ArD 41525 Zika virus isolate into the vaginal canal or rectum of 16 adult rhesus or cynomolgus macaques and monitored them for evidence of infection through 28 days postinoculation (DPI). This dose was selected to correspond to high Zika virus RNA load(s) reported in human semen (13,21,24,25).

Materials and Methods

Study Design and Data Analyses

This pilot study was designed to determine if nonhuman primates (NHPs) are susceptible to Zika virus infection by the intravaginal and intrarectal routes. We based sample size estimates for the 2 study groups (rhesus and cynomolgus macaques) on historic reports of experimental infections of Zika virus involving NHPs (3,10,28,29). Power analysis with a type I error rate set to 0.05 indicated that a group size of 4 animals had an 80% probability to detect Zika virus infection after intravaginal or intrarectal inoculation with the virus. This study was not designed to have the statistical power to perform analyses of chemical, hematologic, or temperature data. Investigators were not blinded during the course of the study.

Nonhuman Primates

Research was conducted under an Institutional Animal Care and Use Committee–approved protocol at the United States Army Medical Research Institute for Infectious Diseases (Frederick, MD, USA). This protocol complied with the Animal Welfare Act, Public Health Service Policy, and other federal statutes and regulations relating to animals and experiments involving animals. The Institute is accredited by the Association for Assessment and Accreditation of Laboratory Animal Care International and adheres to principles stated in the 2011 Guide for the Care and Use of Laboratory Animals, National Research Council (<https://grants.nih.gov/grants/olaw/guide-for-the-care-and-use-of-laboratory-animals.pdf>).

Four female rhesus macaques from China (R1, R2, R3, and R4) and 4 female cynomolgus macaques from Cambodia (C1, C2, C3, and C4), age range 8.5–9.3 years, were individually housed during the intravaginal inoculation experiment. For the intrarectal inoculation experiment, an additional 4 rhesus macaques from China (R5, male; R6, female; R7, male; and R8, female); and 4 cynomolgus macaques from Cambodia (C5, female; C6, female; C7, male; and C8, male), age range 8.2–11.4 years, were individually housed. All macaques were prescreened and determined to be negative for Zika virus, herpes B virus, simian T-lymphotropic virus 1, simian immunodeficiency virus, simian retrovirus 1/2/3 antibodies, tuberculosis, *Salmonella* spp., *Campylobacter* spp., hypermucoviscous *Klebsiella* spp., and *Shigella* spp.

Virus Isolate

The ArD 41525 Zika virus isolate used in this study was made from a pool of *Aedes africanus* mosquitoes collected in eastern Senegal in 1984 (passage history: AP61 cells 1, C6/36 cells 1, Vero cells 3) and has been sequenced (GenBank accession no. KU955591). We selected the ArD

41525 isolate because of its low passage history and the ancestral nature of the African phylogenetic lineage (4,30). In addition, genetic analyses of the open reading frame (ORF) of the ArD 41525 isolate from Senegal and the PRVABC59 isolate from Puerto Rico showed 88.2% nt identity and 97.3% aa identity (F. Nasar, unpub. data). Although Zika virus sequences are composed of ≥ 2 phylogenetic lineages (African and Asian), these lineages constitute a single virus serotype (1,4,31–33). Furthermore, male-to-female sexual transmission of Zika virus has involved virus strains originating from both Zika virus phylogenetic lineages (11–18). Before initiation of this study, virus challenge stocks were confirmed to be free of mycoplasma and passage-associated mutations (4).

Intravaginal Virus Inoculation

For intravaginal inoculation, anesthetized macaques were placed in dorsal recumbency with their hips elevated above their torso at a 30° angle, and a 3–5-cm lubricated, size 7FR, infant feeding tube (Mallinckrodt Pharmaceuticals, St. Louis, MO, USA) was inserted into the vaginal opening. A 3-mL syringe containing 7.0 log₁₀ PFU (8.7 log₁₀ copies) of cell-free Zika virus suspended in 2 mL of phosphate-buffered saline (PBS) was connected to the end of the infant feeding tube and slowly administered (34). A 500- μ L flush of 0.9% NaCl (Becton Dickinson, Franklin Lakes, NJ, USA) was then used to insure that all Zika virus inoculum was administered. Macaques stayed in dorsal recumbency with hip elevation for ≥ 20 min: R1, 26 min; R2, 23 min; R3, 21 min; R4, 20 min; C1, 21 min; C2, 30 min; C3, 28 min; and C4, 24 min.

Intrarectal Virus Inoculation

For intrarectal inoculation, anesthetized macaques were placed in an inverted Trendelenburg position (25°–30° down angle), and a 3–5-cm lubricated, size 7FR, infant feeding tube was inserted into the rectum. A 10-mL 0.9% NaCl flush was slowly administered to soften impacted fecal material lining the rectum. After the flush, 7.0 log₁₀ PFU (8.7 log₁₀ copies) of cell-free Zika virus suspended in 3 mL of PBS was slowly administered (34), followed by a 500- μ L flush of 0.9% NaCl to ensure that all Zika virus inoculum was administered. Macaques stayed in an inverted Trendelenburg position for ≥ 15 min: R5, 15 min; R6, 15 min; R7, 23 min; R8, 17 min; C5, 20 min; C6, 21 min; C7, 20 min; and C8, 20 min.

Observations and Blood Collections

After exposure to virus, we evaluated macaques daily for signs of illness. The following clinical observations were made daily: presence or absence of rash, appearance of joints, ocular evaluation, presence or absence of

blood and source, motor function, presence or absence of cough, urine output, condition of stool, and food consumption. Blood collections and physical examinations, including weight and rectal temperature, were conducted under anesthesia at -7, 1-7, 9, 12, 15, 21, and 28 DPI. Physical examinations included presence or absence of rash, capillary refill time, dehydration skin test time, joint evaluation, ocular evaluation, oral evaluation, presence or absence of blood and source, severity of bleeding if present, presence or absence of exudate and source, severity of exudate if present, presence or absence of lymphadenopathy, and lymph node size. Menstruation patterns were not recorded before inoculation. Menstruation was noted during the daily observations (0-28 DPI), but may have occurred on additional days (e.g., light or transient events).

Chemical and Hematologic Analysis of Serum

We used comprehensive metabolic panels to test serum samples collected in 2.5-mL Z Serum Separator Clot Activator VACUETTE Tubes (Greiner Bio-One, Monroe, NC, USA) by using a Piccolo Xpress Chemistry Analyzer and Piccolo General Chemistry 13 Panel (Abbott Point of Care, Princeton, NJ, USA). Complete blood counts were performed on whole blood collected in 1.2-mL S-Monovette K3 EDTA Tubes (Sarstedt, Nümbrecht, Germany) by using a CELL-DYN 3700 system (Abbott Point of Care).

Telemetry Devices and Monitoring

Before the study, macaques were surgically implanted with T27F-1B radio telemetry devices (Konigsberg Instruments, Pasadena, CA, USA; the telemetry unit in macaque C4 failed). The Notocord-hem Evolution Software Platform version 4.3.0.47 (Notocord Inc., Newark, NJ, USA) was used to capture and analyze data. Temperature data points were averaged and statistically filtered to remove noise and signal artifacts to generate a single data point every 30 s.

Quantification of Infectious Virus

We performed virus titration on confluent Vero cell (CCL-81; American Type Culture Collection, Manassas, VA, USA) monolayers in 6-well plates by plaque assay. Duplicate wells were infected with 0.1-mL aliquots of serial 10-fold diluted virus in growth medium composed of Dulbecco's modified Eagle medium (Corning Life Sciences, Tewksbury, MA, USA), supplemented with 50 µg/mL gentamicin (GIBCO, Carlsbad, CA, USA), 1.0 mmol/L sodium pyruvate, 1% vol/vol non-essential amino acids (Sigma Aldrich, St. Louis, MO, USA), and 0.4 mL of growth medium. Virus was absorbed for 1 h at 37°C and was then removed before overlaying the cell monolayers with 3 mL of 1% wt/vol Sea-Plaque agarose (Cambrex Bio Science, East

Rutherford, NJ, USA) in growth medium. Cells were incubated at 37°C in an atmosphere of 5% CO₂ for 4-5 days and then fixed with 4% formaldehyde (Fisher Scientific, Waltham, MA, USA) in PBS for 24 h. After removal of the overlay, cell monolayers were stained with 2% crystal violet (Sigma Aldrich) in 70% methanol (Sigma Aldrich) for 5-10 min at ambient temperature, and excess stain was removed with running water. Plaques were counted, and results were reported as number of PFU/mL. The lower limit of detection was 1.0 log₁₀ PFU/mL.

Extraction and Quantification of Virus RNA

To extract RNA, a serum sample (50 µL) was added to 200 µL of diethylpyrocarbonate-treated water (Ambion, Carlsbad, CA, USA), which was then added to 750 µL of TRIzol LS Reagent (Ambion). Samples were incubated for 20 min at ambient temperature. After incubation, 200 µL of chloroform (Sigma Aldrich) was added, mixed thoroughly, and incubated for 10 min at ambient temperature. After incubation, samples were centrifuged at 12,000 × *g* for 15 min at 4°C. A total of 400 µL of the aqueous phase was collected, and the RNA was precipitated by adding 1 µL of GlycoBlue (15 µg/µL) (Ambion) and 400 µL of isopropanol (Sigma Aldrich). Samples were incubated at ambient temperature for 10 min and centrifuged at 12,000 × *g* for 10 min at 4°C. The resulting pellet was then washed in 1 mL of 75% ethanol (Sigma Aldrich) and centrifuged at 12,000 × *g* for 5 min at 4°C, after which the pellet was air-dried for 10 min at ambient temperature and resuspended in 50 µL of diethylpyrocarbonate-treated water. Virus RNA was quantified by using a CFX96 Touch Real-Time PCR Detection System (Bio-Rad Laboratories, Hercules, CA, USA) and primers and a probe specific for the envelope gene (bases 1188-1316) (35). A standard curve was generated against a synthetic oligonucleotide, and genome copies were expressed as copies per milliliter. The lower limit of detection was 3.0 log₁₀ copies/mL.

Serologic Analysis

We performed plaque reduction neutralization tests (PRNTs), considered the standard for clinical diagnosis of past infection, to determine preexposure and postexposure immune responses (36,37). Serum samples were heat-inactivated at 56°C for 30 min. Samples were serially diluted 2-fold in PBS, mixed with an equal volume of 3.3 log₁₀ PFU/mL of Zika virus, and incubated for 1 h at 37°C in an atmosphere of 5% CO₂. Confluent Vero cell monolayers in 6-well plates were inoculated with 100 µL of serum/virus mixture in triplicate. Plates were incubated for 5 days at 37°C in an atmosphere of 5% CO₂, fixed, and stained with crystal violet as described above. PRNT₈₀ titers were calculated and expressed as the reciprocal of serum dilution yielding a >80% reduction in the

number of plaques. Preexposure serum samples collected from rhesus macaques at -28 DPI and from cynomolgus macaques at -20 DPI showed no neutralization activity for Zika virus, indicating that these animals were not previously exposed to the virus. Postexposure serum samples were screened on 7, 15, 21 and 28 DPI.

Results

Intravaginally Inoculated Macaque Viremias and Antibody Responses

After intravaginal inoculation of Zika virus, 50% (2/4) of rhesus macaques and 50% (2/4) cynomolgus macaques had detectable viremias; mean peak titers were $3.8 \log_{10}$ PFU/mL ($7.2 \log_{10}$ copies/mL) for rhesus macaques and $3.5 \log_{10}$ PFU/mL ($6.8 \log_{10}$ copies/mL) for cynomolgus macaques (Figure 1). We detected viremia at 4–6 DPI (mean duration 3.0 d) for rhesus macaques and 3–7 DPI (mean duration 4.0 d) for cynomolgus macaques and virus RNA in serum at 3–7 DPI for rhesus macaques and 3–9 DPI for cynomolgus macaques. By 15 DPI, only those rhesus and cynomolgus macaques that showed viremia or virus RNA in serum seroconverted (R1, R4, C3, and C4), as shown by PRNT₈₀ titers ranging from 1:640 to 1:1,280 (Table 1). We observed no virus neutralization for macaques R2, R3, C1, and C2 (Table 1). Menstruation was observed in all female macaques during the course of the study, but menstruation was not observed in any of the female macaques at the time of virus inoculation.

Intrarectally Inoculated Macaque Viremias and Antibody Responses

After intrarectal inoculation of Zika virus, 75% (3/4) of rhesus macaques and 100% (4/4) of cynomolgus macaques had detectable viremias; mean peak titers were $4.8 \log_{10}$ PFU/mL ($8.0 \log_{10}$ copies/mL) for rhesus macaques and $4.8 \log_{10}$ PFU/mL ($8.6 \log_{10}$ copies/mL) for cynomolgus macaques (Figure 2). Although we did not detect viremia in 1 rhesus macaque (R6), we detected virus RNA in serum samples from this macaque at 6 DPI ($5.2 \log_{10}$ copies/mL) and 7 DPI ($6.1 \log_{10}$ copies/mL). Two cynomolgus macaques (C5, C8) had viremia levels $\geq 5.0 \log_{10}$ PFU/mL for 2 days. We detected viremia at 3–7 DPI (mean duration 3.0 d) for rhesus macaques and at 2–6 DPI (mean duration 2.8 d) for cynomolgus macaques and virus RNA in serum at 2–7 DPI for rhesus macaques and 1–12 DPI for cynomolgus macaques. By 15 DPI, all rhesus and cynomolgus macaques had seroconverted (R5, R6, R7, R8, C5, C6, C7, C8), as shown by PRNT₈₀ titers ranging from 1:320 to 1:1,280 (Table 2).

Clinical Signs and Laboratory Results

We observed no overt clinical signs, including pyrexia, joint swelling, weight loss, or decreased appetite, for any of the infected macaques. The telemetry unit in macaque C6 failed during the study. Therefore, we also used rectal temperatures to determine the absence of pyrexia (online Technical Appendix Figure 1, <https://wwwnc.cdc.gov/EID/article/23/8/17-0034-Techapp1.pdf>). No macaque

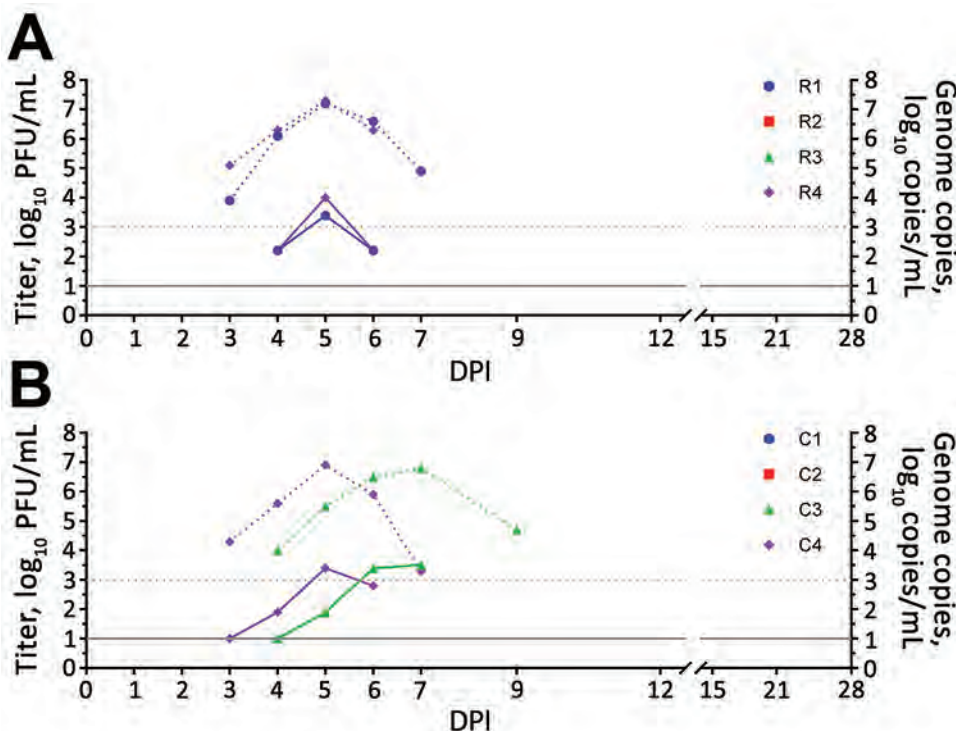


Figure 1. Viremia and virus RNA detected in serum of rhesus and cynomolgus macaques after intravaginal inoculation with Zika virus. A) Rhesus macaques (animals R2 and R3 showed negative results); B) cynomolgus macaques (animals C1 and C2 showed negative results). Solid lines indicate virus titers in \log_{10} PFU/mL. Dotted lines indicate genome copies in \log_{10} copies/mL. The lower limit of detection was $1.0 \log_{10}$ PFU/mL for virus titers and $3.0 \log_{10}$ copies/mL for genome copies. C, cynomolgus; DPI, days postinoculation; R, rhesus.

Table 1. Serologic responses of 8 female rhesus and cynomolgus macaques after intravaginal inoculation of Zika virus*

Macaque	Serologic response, PRNT ₈₀ , by DPI			
	7	15	21	28
Rhesus 1	–	1:640	1:640	1:640
Rhesus 2	–	–	–	–
Rhesus 3	–	–	–	–
Rhesus 4	–	1:640	1:640	1:640
Cynomolgus 1	–	–	–	–
Cynomolgus 2	–	–	–	–
Cynomolgus 3	–	1:640	1:640	1:640
Cynomolgus 4	–	1:1,280	1:1,280	1:1,280

*Values are titers. Limit of detection was a titer of 1:20. DPI, day postinoculation; PRNT₈₀, 80% plaque reduction neutralization test; –, no detectable serologic response.

showed an increase in temperature >1.5°C from its mean rectal temperature (from readings taken at –7 and 0 DPI). Any deviations in temperature obtained by telemetry units were directly correlated with the anesthesia times or the presence of personnel in the macaque room making daily observations (e.g., physical examinations and room entry times were noted). Weights of all macaques remained relatively stable throughout the study, and no macaque showed marked weight loss (online Technical Appendix Figure 2).

Potential marked increases or decreases in clinical laboratory values lasting >1 day in infected macaques were those for glucose (R1, R4, R6); blood urea nitrogen (R4, R8, C5, C6, C8); total protein (R7); alanine aminotransferase (R6, C3, C4, C5, C6, C7, C8); aspartate aminotransferase (R4, R6, C3, C4, C5, C7, C8); alkaline phosphatase

(C6); total bilirubin (R8); γ -glutamyl transferase (C8); amylase (R1, R4, C3); leukocytes (R5); erythrocytes (C3, C4, C6); platelets (R1, R6, R7, R8); neutrophils (R1, R4, R6); lymphocytes (R1, R4, R6); monocytes (R1, R4, R5, R8, C3, C4, C5, C6); basophils (R1, R4, R6); and eosinophils (R1, R5, R8, C3, C4) (online Technical Appendix Figures 3, 4). Macaques observed to menstruate during the study were R1 (days 4–6); R2 (days 1, 2); R3 (day 2); R4 (day 9); C1 (days 8–10); C2 (day 15); C3 (days 14, 15); and C4 (day 7).

Discussion

Sexual transmission of Zika virus is underestimated, and its detection is confounded in regions with active mosquito-to-human virus transmission (17–19). In an effort to gauge the likelihood of infection after exposure by vaginal or anal intercourse, we inoculated the vaginal canal or rectum of rhesus and cynomolgus macaques with Zika virus. Intravaginal and intrarectal exposure resulted in infection in the absence of clinical disease, followed by seroconversion, in both species. The magnitude and duration of detectable viremia after intravaginal and intrarectal inoculation indicates that NHPs, as well as humans, could infect primary mosquito vector species.

Although the infectious dose required for primary urban and sylvatic mosquito Zika virus vectors to become infected and transmit infectious virus remains unknown, other flavivirus–vector host systems have demonstrated mosquito transmission after low-dose experimental exposure

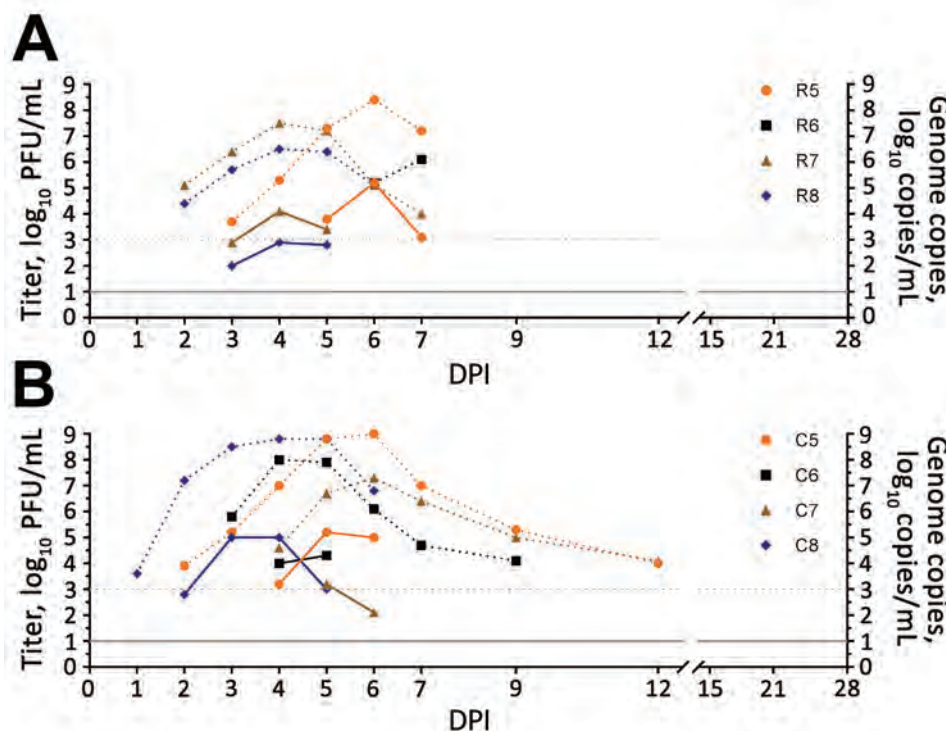


Figure 2. Viremia and virus RNA detected in serum of rhesus and cynomolgus macaques after intrarectal inoculation of Zika virus. A) Rhesus macaques (animal R6 showed negative results); B) cynomolgus macaques. Solid lines indicate virus titers in log₁₀ PFU/mL. Dotted lines indicate genome copies in log₁₀ copies/mL. The lower limit of detection was 1.0 log₁₀ PFU/mL for virus titers and 3.0 log₁₀ copies/mL for genome copies. C, cynomolgus; DPI, days postinoculation; R, rhesus.

Table 2. Serologic responses of 8 rhesus and cynomolgus macaques after intrarectal inoculation of Zika virus*

Macaque	Sex	Serologic response, PRNT ₈₀ , by DPI			
		7	15	21	28
Rhesus 5	M	–	1:1,280	1:1,280	1:1,280
Rhesus 6	F	–	1:320	1:640	1:1,280
Rhesus 7	M	–	1:1,280	1:1,280	1:1,280
Rhesus 8	F	–	1:640	1:640	1:640
Cynomolgus 5	F	–	1:640	1:640	1:1,280
Cynomolgus 6	F	–	1:640	1:640	1:1,280
Cynomolgus 7	M	–	1:640	1:1,280	1:1,280
Cynomolgus 8	M	–	1:640	1:1,280	1:1,280

*Values are titers. Limit of detection was a titer of 1:20. DPI, day postinoculation; PRNT₈₀, 80% plaque reduction neutralization test; –, no detectable serologic response.

(undetectable to $<3.0 \log_{10}$ PFU/mL) (26,38,39). Therefore, the magnitude of viremia in some of the infected macaques was likely 10–100-fold higher than that needed to infect principal mosquito vectors. Moreover, our results suggest that sexual transmission might extend the duration of the current Zika virus epidemic and increase the probability of introduction and establishment of this virus in virus-naïve regions. Likewise, sexual transmission among NHPs might be a secondary mechanism by which Zika virus is maintained in an enzootic cycle.

Despite the presence of viremia in intravaginally and intrarectally exposed macaques, overt clinical signs, such as pyrexia, rash, conjunctivitis, joint swelling, weight loss, or decreased appetite, that have been reported for some Zika virus infections in humans, were not observed in our study. Duration of viremia and clinical signs in NHPs after Zika virus infection resulting from a mosquito bite or intracranial or subcutaneous inoculation of African or Asian Zika virus isolates varies (3,10,28,29,40–46). In comparison to studies in which Zika virus was subcutaneously inoculated into NHPs (3,10,28,29,40–42), we observed a delay in detectable viremia in macaques intravaginally or intrarectally inoculated with this virus. This delay is probably the result of the virus having to infect tissues of the vaginal or rectal mucosa, replicate within these sites, and then disseminate to initiate a systemic infection. Although sentinel NHPs or those experimentally infected with Zika virus show fever or an increased temperature (3,28,42,46) or decreased appetite and weight loss (40), other experimental NHPs with Zika virus infection showed no overt clinical illness (3,10,28,29,41), which is consistent with our study results and findings for most Zika virus infections in humans (2,5–7).

In our study, the only clinical laboratory values that showed marked increases or decreases lasting >1 day in both species of infected macaques were alanine aminotransferase, amylase, aspartate aminotransferase, blood urea nitrogen, monocytes, and eosinophils. Analogous to our observations, recent studies have also reported increased levels of aspartate aminotransferase (40,42,46),

alanine aminotransferase (40,42,46), and monocytes (42) in Zika virus–infected macaques. Although increases in some laboratory values might be the result of repeated daily anesthesia (47), studies with increased numbers of animals are needed to resolve which clinical laboratory parameters are associated with Zika virus infection in NHP models. Ultimately, further studies are needed to determine whether differences in the magnitude/duration of viremia and clinical signs are the result of animal genotype, virus isolate phenotype, inoculum dose, or inoculum route.

Unlike Zika virus, whose primary transmission mechanism is by mosquito bite, the primary transmission mechanism of HIV-1 is by sexual intercourse. The efficiency of HIV-1 transmission by vaginal or anal intercourse depends on a variety of factors, such as seminal viral load, number of sex acts, or co-infection (48,49). These factors also likely contribute to transmission of Zika virus. Similar to findings for other sexually transmitted viruses, such as HIV-1 (48), our model had a higher number of transmission events from intrarectal inoculation than intravaginal inoculation. Although the per act risk for acquiring HIV-1 infection by vaginal or anal intercourse is low (0.08%–1.7%) (48), risk increases proportionally with the cumulative number of sexual acts (49). This trend might be similar for Zika virus, for which the cumulative number of sexual acts (e.g., repeated low or moderate dose exposures) could increase risk over time.

Our experiments were conducted in a controlled research setting in which the vagina and rectum of adult macaques were nontraumatically exposed to Zika virus. Microtears induced during sexual intercourse could further enhance susceptibility to Zika virus infection in human or sylvatic NHP populations. Furthermore, pre-existing sexually transmitted infections are known risk factors for increased susceptibility to secondary viral infections by vaginal or anal intercourse (50). Consequently, sexually transmitted infections might increase the likelihood of acquiring Zika virus through vaginal or anal intercourse.

In summary, our results indicate that sexual intercourse is a mechanism for virus transmission in the absence of mosquito-to-human transmission (i.e., effective mosquito control), as well as a mechanism by which Zika virus could be introduced to virus-naïve regions and initiate human-to-mosquito transmission. Our findings highlight the need for men living in or traveling from areas to which Zika virus is endemic or epidemic to avoid unprotected sexual intercourse.

Acknowledgments

We thank Robert Tesh and Scott Weaver for providing the ArD 41525 isolate of Zika virus.

This study was supported by a grant from the Defense Advanced Research Projects Agency.

The views expressed in this article are those of the authors and do not reflect the official policy of the US Department of Defense or the US Army.

Dr. Haddow is a medical entomologist at the United States Army Medical Research Institute of Infectious Diseases, Frederick, MD. His primary interests are emerging vectorborne and zoonotic pathogens.

References

- Haddow AD, Nasar F, Guzman H, Ponlawat A, Jarman RG, Tesh RB, et al. Genetic characterization of Spondweni and Zika viruses and susceptibility of geographically distinct strains of *Aedes aegypti*, *Aedes albopictus* and *Culex quinquefasciatus* (Diptera: Culicidae) to Spondweni virus. *PLoS Negl Trop Dis*. 2016;10:e0005083. <http://dx.doi.org/10.1371/journal.pntd.0005083>
- Haddow AD, Woodall JP. Distinguishing between Zika and Spondweni viruses. *Bull World Health Organ*. 2016;94:711–711A. <http://dx.doi.org/10.2471/BLT.16.181503>
- Dick GW, Kitchen SF, Haddow AJ. Zika virus. I. Isolations and serological specificity. *Trans R Soc Trop Med Hyg*. 1952;46:509–20. [http://dx.doi.org/10.1016/0035-9203\(52\)90042-4](http://dx.doi.org/10.1016/0035-9203(52)90042-4)
- Haddow AD, Schuh AJ, Yasuda CY, Kasper MR, Heang V, Huy R, et al. Genetic characterization of Zika virus strains: geographic expansion of the Asian lineage. *PLoS Negl Trop Dis*. 2012;6:e1477. <http://dx.doi.org/10.1371/journal.pntd.0001477>
- Musso D, Gubler DJ. Zika virus. *Clin Microbiol Rev*. 2016;29:487–524. <http://dx.doi.org/10.1128/CMR.00072-15>
- Plourde AR, Bloch EM. A literature review of Zika virus. *Emerg Infect Dis*. 2016;22:1185–92. <http://dx.doi.org/10.3201/eid2207.151990>
- Petersen LR, Jamieson DJ, Powers AM, Honein MA. Zika virus. *N Engl J Med*. 2016;374:1552–63. <http://dx.doi.org/10.1056/NEJMr1602113>
- de Araújo TV, Rodrigues LC, de Alencar Ximenes RA, de Barros Miranda-Filho D, Montarroyos UR, de Melo AP, et al.; investigators from the Microcephaly Epidemic Research Group; Brazilian Ministry of Health; Pan American Health Organization; Instituto de Medicina Integral Professor Fernando Figueira; State Health Department of Pernambuco. Association between Zika virus infection and microcephaly in Brazil, January to May, 2016: preliminary report of a case-control study. *Lancet Infect Dis*. 2016;16:1356–63. [http://dx.doi.org/10.1016/S1473-3099\(16\)30318-8](http://dx.doi.org/10.1016/S1473-3099(16)30318-8)
- Haddow AJ, Williams MC, Woodall JP, Simpson DI, Goma LK. Twelve isolations of Zika virus from *Aedes* (*Stegomyia*) *africanus* (Theobald) taken in and above a Uganda forest. *Bull World Health Organ*. 1964;31:57–69.
- Boorman JP, Porterfield JS. A simple technique for infection of mosquitoes with viruses; transmission of Zika virus. *Trans R Soc Trop Med Hyg*. 1956;50:238–42. [http://dx.doi.org/10.1016/0035-9203\(56\)90029-3](http://dx.doi.org/10.1016/0035-9203(56)90029-3)
- Foy BD, Kobylinski KC, Chilson Foy JL, Blitvich BJ, Travassos da Rosa A, Haddow AD, et al. Probable non-vectorborne transmission of Zika virus, Colorado, USA. *Emerg Infect Dis*. 2011;17:880–2. <http://dx.doi.org/10.3201/eid1705.101939>
- Hills SL, Russell K, Hennessey M, Williams C, Oster AM, Fischer M, et al. Transmission of Zika virus through sexual contact with travelers to areas of ongoing transmission—continental United States, 2016. *MMWR Morb Mortal Wkly Rep*. 2016;65:215–6. <http://dx.doi.org/10.15585/mmwr.mm6508e2>
- D'Ortenzio E, Matheron S, Yazdanpanah Y, de Lamballerie X, Hubert B, Piorkowski G, et al. Evidence of sexual transmission of Zika virus. *N Engl J Med*. 2016;374:2195–8. <http://dx.doi.org/10.1056/NEJMc1604449>
- Brooks RB, Carlos MP, Myers RA, White MG, Bobo-Lenoci T, Aplan D, et al. Likely sexual transmission of Zika virus from a man with no symptoms of infection—Maryland, 2016. *MMWR Morb Mortal Wkly Rep*. 2016;65:915–6. <http://dx.doi.org/10.15585/mmwr.mm6534e2>
- Frank C, Cadar D, Schlaphof A, Neddersen N, Günther S, Schmidt-Chanasit J, et al. Sexual transmission of Zika virus in Germany, April 2016. *Euro Surveill*. 2016;21:30252. <http://dx.doi.org/10.2807/1560-7917.ES.2016.21.23.30252>
- Deckard DT, Chung WM, Brooks JT, Smith JC, Woldai S, Hennessey M, et al. Male-to-male sexual transmission of Zika virus—Texas, January 2016. *MMWR Morb Mortal Wkly Rep*. 2016;65:372–4. <http://dx.doi.org/10.15585/mmwr.mm6514a3>
- Moreira J, Peixoto TM, Siqueira AM, Lamas CC. Sexually acquired Zika virus: a systematic review. *Clin Microbiol Infect*. 2017;23:296–305. <http://dx.doi.org/10.1016/j.cmi.2016.12.027>
- Grischott F, Puhan M, Hatz C, Schlagenhauf P. Non-vectorborne transmission of Zika virus: a systematic review. *Travel Med Infect Dis*. 2016;14:313–30. <http://dx.doi.org/10.1016/j.tmaid.2016.07.002>
- Coelho FC, Durovni B, Saraceni V, Lemos C, Codeco CT, Camargo S, et al. Higher incidence of Zika in adult women than adult men in Rio de Janeiro suggests a significant contribution of sexual transmission from men to women. *Int J Infect Dis*. 2016;51:128–32. <http://dx.doi.org/10.1016/j.ijid.2016.08.023>
- Arzuaga M, Bujalance SG, Díaz-Menéndez M, Vázquez A, Arribas JR. Probable sexual transmission of Zika virus from a vasectomised man. *Lancet Infect Dis*. 2016;16:1107. [http://dx.doi.org/10.1016/S1473-3099\(16\)30320-6](http://dx.doi.org/10.1016/S1473-3099(16)30320-6)
- Mansuy JM, Suberbielle E, Chapuy-Regaud S, Mengelle C, Bujan L, Marchou B, et al. Zika virus in semen and spermatozoa. *Lancet Infect Dis*. 2016;16:1106–7. [http://dx.doi.org/10.1016/S1473-3099\(16\)30336-X](http://dx.doi.org/10.1016/S1473-3099(16)30336-X)
- Barzon L, Pacenti M, Franchin E, Lavezzo E, Trevisan M, Sgarabotto D, et al. Infection dynamics in a traveller with persistent shedding of Zika virus RNA in semen for six months after returning from Haiti to Italy, January 2016. *Euro Surveill*. 2016;21:21.
- Nicastri E, Castilletti C, Liuzzi G, Iannetta M, Capobianchi MR, Ippolito G. Persistent detection of Zika virus RNA in semen for six months after symptom onset in a traveller returning from Haiti to Italy, February 2016. *Euro Surveill*. 2016;21:21. <http://dx.doi.org/10.2807/1560-7917.ES.2016.21.32.30314>
- Mansuy JM, Dutertre M, Mengelle C, Fourcade C, Marchou B, Delobel P, et al. Zika virus: high infectious viral load in semen, a new sexually transmitted pathogen? *Lancet Infect Dis*. 2016;16:405. [http://dx.doi.org/10.1016/S1473-3099\(16\)00138-9](http://dx.doi.org/10.1016/S1473-3099(16)00138-9)
- Musso D, Roche C, Robin E, Nhan T, Teissier A, Cao-Lormeau VM. Potential sexual transmission of Zika virus. *Emerg Infect Dis*. 2015;21:359–61. <http://dx.doi.org/10.3201/eid2102.141363>
- Clements AN. *Mosquito biology*. Vol. 3. Transmission of viruses and interactions with bacteria. Cambridge (MA): CABI Publishing; 2012.
- Di Luca M, Severini F, Toma L, Boccolini D, Romi R, Remoli ME, et al. Experimental studies of susceptibility of Italian *Aedes albopictus* to Zika virus. *Euro Surveill*. 2016;21:30223. <http://dx.doi.org/10.2807/1560-7917.ES.2016.21.18.30223>
- Dick GW. Zika virus. II. Pathogenicity and physical properties. *Trans R Soc Trop Med Hyg*. 1952;46:521–34. [http://dx.doi.org/10.1016/0035-9203\(52\)90043-6](http://dx.doi.org/10.1016/0035-9203(52)90043-6)
- Henderson BE, Cheshire PP, Kirya GB, Lule M. Immunologic studies with yellow fever and selected African group B arboviruses in rhesus and vervet monkeys. *Am J Trop Med Hyg*. 1970;19:110–8. <http://dx.doi.org/10.4269/ajtmh.1970.19.110>
- Faye O, Freire CC, Iamarino A, Faye O, de Oliveira JV, Diallo M, et al. Molecular evolution of Zika virus during its emergence in the

- 20th century. *PLoS Negl Trop Dis*. 2014;8:e2636. <http://dx.doi.org/10.1371/journal.pntd.0002636>
31. Dowd KA, DeMaso CR, Pelc RS, Speer SD, Smith AR, Goo L, et al. Broadly neutralizing activity of Zika virus-immune sera identifies a single viral serotype. *Cell Reports*. 2016;16:1485–91. <http://dx.doi.org/10.1016/j.celrep.2016.07.049>
 32. Marchette NJ, Garcia R, Rudnick A. Isolation of Zika virus from *Aedes aegypti* mosquitoes in Malaysia. *Am J Trop Med Hyg*. 1969;18:411–5. <http://dx.doi.org/10.4269/ajtmh.1969.18.411>
 33. Aliota MT, Dudley DM, Newman CM, Mohr EL, Gellerup DD, Breitbach ME, et al. Heterologous protection against Asian Zika virus challenge in rhesus macaques. *PLoS Negl Trop Dis*. 2016;10:e0005168. <http://dx.doi.org/10.1371/journal.pntd.0005168>
 34. Smedley J, Turkbey B, Bernardo ML, Del Prete GQ, Estes JD, Griffiths GL, et al. Tracking the luminal exposure and lymphatic drainage pathways of intravaginal and intrarectal inocula used in nonhuman primate models of HIV transmission. *PLoS One*. 2014;9:e92830. <http://dx.doi.org/10.1371/journal.pone.0092830>
 35. Corman VM, Rasche A, Baronti C, Aldabbagh S, Cadar D, Reusken CB, et al. Assay optimization for molecular detection of Zika virus. *Bull World Health Organ*. 2016;94:880–92. <http://dx.doi.org/10.2471/BLT.16.175950>
 36. De Madrid AT, Porterfield JS. The flaviviruses (group B arboviruses): a cross-neutralization study. *J Gen Virol*. 1974;23:91–6. <http://dx.doi.org/10.1099/0022-1317-23-1-91>
 37. Calisher CH, Karabatsos N, Dalrymple JM, Shope RE, Porterfield JS, Westaway EG, et al. Antigenic relationships between flaviviruses as determined by cross-neutralization tests with polyclonal antisera. *J Gen Virol*. 1989;70:37–43. <http://dx.doi.org/10.1099/0022-1317-70-1-37>
 38. Jupp PG. Laboratory studies on the transmission of West Nile virus by *Culex (Culex) univittatus* Theobald; factors influencing the transmission rate. *J Med Entomol*. 1974;11:455–8. <http://dx.doi.org/10.1093/jmedent/11.4.455>
 39. van den Hurk AF, Smith CS, Field HE, Smith IL, Northill JA, Taylor CT, et al. Transmission of Japanese encephalitis virus from the black flying fox, *Pteropus alecto*, to *Culex annulirostris* mosquitoes, despite the absence of detectable viremia. *Am J Trop Med Hyg*. 2009;81:457–62.
 40. Dudley DM, Aliota MT, Mohr EL, Weiler AM, Lehrer-Brey G, Weisgrau KL, et al. A rhesus macaque model of Asian-lineage Zika virus infection. *Nat Commun*. 2016;7:12204. <http://dx.doi.org/10.1038/ncomms12204>
 41. Adams Waldorf KM, Stencel-Baerenwald JE, Kapur RP, Studholme C, Boldenow E, Vornhagen J, et al. Fetal brain lesions after subcutaneous inoculation of Zika virus in a pregnant nonhuman primate. *Nat Med*. 2016;22:1256–9. <http://dx.doi.org/10.1038/nm.4193>
 42. Osuna CE, Lim SY, Deleage C, Griffin BD, Stein D, Schroeder LT, et al. Zika viral dynamics and shedding in rhesus and cynomolgus macaques. *Nat Med*. 2016;22:1448–55. <http://dx.doi.org/10.1038/nm.4206>
 43. Abbink P, Larocca RA, De La Barrera RA, Bricault CA, Moseley ET, Boyd M, et al. Protective efficacy of multiple vaccine platforms against Zika virus challenge in rhesus monkeys. *Science*. 2016;353:1129–32. <http://dx.doi.org/10.1126/science.aah6157>
 44. Larocca RA, Abbink P, Peron JP, Zanotto PM, Iampietro MJ, Badamchi-Zadeh A, et al. Vaccine protection against Zika virus from Brazil. *Nature*. 2016;536:474–8. <http://dx.doi.org/10.1038/nature18952>
 45. Dowd KA, Ko SY, Morabito KM, Yang ES, Pelc RS, DeMaso CR, et al. Rapid development of a DNA vaccine for Zika virus. *Science*. 2016;354:237–40. <http://dx.doi.org/10.1126/science.aai9137>
 46. Li XF, Dong HL, Huang XY, Qiu YF, Wang HJ, Deng YQ, et al. Characterization of a 2016 clinical isolate of Zika virus in non-human primates. *EBioMedicine*. 2016;12:170–7. <http://dx.doi.org/10.1016/j.ebiom.2016.09.022>
 47. Lugo-Roman LA, Rico PJ, Sturdivant R, Burks R, Settle TL. Effects of serial anesthesia using ketamine or ketamine/medetomidine on hematology and serum biochemistry values in rhesus macaques (*Macaca mulatta*). *J Med Primatol*. 2010;39:41–9. <http://dx.doi.org/10.1111/j.1600-0684.2009.00394.x>
 48. Boily MC, Baggaley RF, Wang L, Masse B, White RG, Hayes RJ, et al. Heterosexual risk of HIV-1 infection per sexual act: systematic review and meta-analysis of observational studies. *Lancet Infect Dis*. 2009;9:118–29. [http://dx.doi.org/10.1016/S1473-3099\(09\)70021-0](http://dx.doi.org/10.1016/S1473-3099(09)70021-0)
 49. Morris MR, Byrreddy SN, Villinger F, Henning TC, Butler K, Ansari AA, et al. Relationship of menstrual cycle and vaginal infection in female rhesus macaques challenged with repeated, low doses of SIVmac251. *J Med Primatol*. 2015;44:301–5. <http://dx.doi.org/10.1111/jmp.12177>
 50. Ward H, Ronn M. The contribution of STIs to the sexual transmission of HIV. *Curr Opin HIV AIDS*. 2010;5:305–10. <http://dx.doi.org/10.1097/COH.0b013e32833a8844>

Address for correspondence: Andrew D. Haddow, Virology Division, United States Army Medical Research Institute of Infectious Diseases, 1425 Porter St, Fort Detrick, Frederick, MD 21702, USA; email: andrew.d.haddow.ctr@mail.mil

World Rabies Day, September 28

September 28 is World Rabies Day, a global health observance started in 2007 to raise awareness about the burden of rabies and bring together partners to enhance prevention and control efforts worldwide. World Rabies Day is observed in many countries, including the United States.

Although rabies is a 100% preventable disease, thousands of people around the world die from the disease each day. World Rabies Day is an opportunity to reflect on our efforts to control this deadly disease and remind ourselves that the fight is not yet over.

**EMERGING
INFECTIOUS DISEASES**

<http://wwwnc.cdc.gov/eid/page/world-rabies-day>



Lyme Borreliosis in Finland, 1995–2014

Eeva Sajanti, Mikko Virtanen, Otto Helve, Markku Kuusi, Outi Lyytikäinen, Jukka Hytönen,¹ Jussi Sane¹

We investigated the epidemiology of Lyme borreliosis (LB) in Finland for the period 1995–2014 by using data from 3 different healthcare registers. We reviewed data on disseminated LB cases from the National Infectious Diseases Register (21,051 cases) and the National Hospital Discharge Register (10,402 cases) and data on primary LB (erythema migrans) cases from the Register for Primary Health Care Visits (11,793 cases). Incidence of microbiologically confirmed disseminated LB cases increased from 7/100,000 population in 1995 to 31/100,000 in 2014. Incidence of primary LB cases increased from 44/100,000 in 2011 to 61/100,000 in 2014. Overall, cases occurred predominantly in women, and we observed a bimodal age distribution in all 3 registers. Our results clearly demonstrate that the geographic distribution of LB has expanded in Finland and underscore the importance of LB as an increasing public health concern in Finland and in northern Europe in general.

Lyme borreliosis (LB) is an infectious disease caused by the spirochete *Borrelia burgdorferi* sensu lato and transmitted by the *Ixodes* spp. ticks. It is characterized by multiple signs and symptoms, varying from the early phase erythema migrans (EM) to neurologic manifestations, arthritis, and acrodermatitis chronica atrophicans and less often to cardiac conduction disorders (1). In the United States, ≈30,000 new LB cases are reported annually to the Centers for Disease Control and Prevention, although current estimates suggest the total number of cases to be 10-fold higher (2–4). In Europe, the annual number of LB cases exceeds 85,000, according to estimates by the World Health Organization (4), and high incidences have been reported from several countries and regions (5–10). The incidence of LB has increased over the past decades in several countries in Europe, the United States, and Canada (4,5,8,11–14). This change might reflect the increased abundance and expanded geographic distribution of *Ixodes* ticks to new habitats (15–17) but also increased awareness of the infection among healthcare providers and the general population.

LB is a notifiable infectious disease in only some countries in Europe, and the reporting practices and surveillance methods and definitions vary widely. Because of

absent or inadequate national surveillance systems for LB observations (8), most epidemiologic data are derived from studies performed on populations with increased risk or in LB-endemic regions (6,18,19). In Finland, the epidemiology of LB was previously investigated in 1988 (20), but increased abundance and northward distribution of *Ixodes* spp. ticks in northern Europe (including Finland) have been more recently reported (15,21,22).

Finland has well-established health registers in place, maintained by the National Institute for Health and Welfare (NIHW), facilitating population-based epidemiologic analyses of infectious diseases. Research results based on the register data of Finland are likely to reflect the epidemiologic situation of LB in northern Europe. In this study, we investigated the incidence and geographic distribution of clinically diagnosed LB (i.e., erythema migrans [EM]) for the period 2011–2014 and those of microbiologically confirmed LB for the period 1995–2014, covering the whole of Finland.

Methods

Study Population

In Finland (population 5.5 million), the national healthcare system is organized into 20 geographically and administratively defined hospital districts (HDs) (online Technical Appendix Figure 1, <https://wwwnc.cdc.gov/EID/article/23/8/16-1273-Techapp1.pdf>). The autonomous region of the Åland Islands is considered a 21st HD. The estimated population in HDs ranges from 28,700 to 1.6 million. Sixteen HDs have primary- and secondary-care hospitals, and 5 HDs also provide tertiary-care services.

Data Sources

To analyze the demographic characteristics, seasonality, and geographic distribution of LB, we reviewed data from the National Infectious Diseases Register (NIDR), National Hospital Discharge Register (Hilmo), and the Register for Primary Health Care Visits (Avohilmo). All 3 registers are maintained by NIHW.

NIDR for Microbiologically Confirmed LB Cases

Routine surveillance of LB in Finland is laboratory based. Since 1995, microbiologic laboratories performing LB diagnostics in Finland notify NIDR electronically of any

Author affiliations: University of Turku, Turku, Finland (E. Sajanti, J. Hytönen); National Institute for Health and Welfare, Helsinki, Finland (M. Virtanen, O. Helve, M. Kuusi, O. Lyytikäinen, J. Sane)

DOI: <https://doi.org/10.3201/eid2308.161273>

¹These authors contributed equally to this article.

positive findings (i.e., serologic or molecular confirmation). Each notification includes the following information: specimen date, each patient's unique national identity code, date of birth, sex, and place of residence. For this study, we extracted all microbiologically confirmed LB cases primarily representing disseminated LB infections from NIDR that were reported during 1995–2014. Multiple notifications for the same LB case received within a 3-month period were combined as 1 case.

Avohilmo and Hilmo Registers for Outpatient and Inpatient Healthcare Visits

According to national guidelines in Finland, when a typical EM is observed after a possible tick exposure, it is diagnosed clinically without any laboratory testing by general practitioners in the primary healthcare setting. Since 2011, these outpatient healthcare visits from the primary healthcare units (municipal health centers and health center wards) have been registered under Avohilmo. These cases are not reported to NIDR because the laboratory diagnosis is missing. Notifications in Avohilmo include the patient's national identity code, age, sex, place of healthcare service, information concerning healthcare admission, investigations, treatment, and discharge diagnoses according to the International Classification of Diseases, 10th Revision (ICD-10). LB cases in Avohilmo were defined as illnesses diagnosed with the ICD-10 code A69.2 ("Lyme borreliosis"). Only the first discharge of each patient was included to avoid recurrent visits with the same diagnosis code being analyzed multiple times in the study. We used Avohilmo data to estimate the number of clinically diagnosed LB cases and simultaneously improve the estimate of the total number of LB cases in Finland during 2011–2014.

Another register, Hilmo, contains nationwide linkable data on all inpatient hospital discharges during 1996–2014 and is comparable to Avohilmo by the notification information; however, LB cases registered under Hilmo for the most part represent disseminated disease. We used Hilmo data to determine the proportions of different clinical manifestations of disseminated LB cases. We have provided detailed descriptions of LB case definitions, diagnostic practices, and laboratory methods used in routine diagnostics (online Technical Appendix Methods).

Statistical Methods

We calculated the crude estimation of the total number and incidence of LB in Finland by summing clinically diagnosed (Avohilmo) and microbiologically confirmed cases (NIDR) together on the basis of 2 assumptions. First, the number of cases of EM diagnosed clinically in the primary healthcare setting does not substantially overlap with the microbiologically confirmed cases representing disseminated LB cases, as validated by individual-level register-linkage studies

(J. Sane, unpub. data). Second, on average, 70% of all LB diagnoses are appropriately coded with the ICD-10 code A69.2 in Avohilmo by the general practitioners (M. Virtanen, unpub. data).

In the time trend analysis by HDs, we considered microbiologically confirmed LB cases in NIDR and outpatient LB cases in Avohilmo. We used Poisson regression for the trend analyses, and statistical significance was defined as $p < 0.01$. We performed the analyses with Stata version 14.0 (StataCorp LLP, College Station, TX, USA). We calculated the average annual incidences of the microbiologically confirmed LB cases over 4 different periods: 1995–1999, 2000–2004, 2005–2009, and 2010–2014. We used data from the National Population Information System as denominators to calculate annual incidence rates and to calculate age- and sex-specific average annualized incidence rates.

Results

Demographic Characteristics of LB Case-Patients

We identified a total of 21,051 microbiologically confirmed LB cases in NIDR (Figure 1). The number of LB cases increased ≈ 5 -fold, from 345 (7/100,000 population) in 1995 to 1,679 (31/100,000) in 2014. On average, $\approx 3,000$ clinically diagnosed LB cases were identified annually in Avohilmo, yielding a total of 11,793 cases. The annual incidence increased from 44/100,000 population in 2011 to 61/100,000 in 2014 (Figure 1). We estimated the total number of annual LB cases to be 5,011 cases in 2011 (incidence of 93/100,000 population) and 6,440 cases in 2014 (118/100,000 population).

Most (54.0%) microbiologically confirmed cases occurred in women ($n = 11,373$). We observed a bimodal age distribution, with high incidence rates occurring in the age group of 5–9 years in both sexes, after which incidence again increased from the age of 40 years, peaking in the age group of 60–69 years among women and >70 years in men (Figure 2, panel A). We did not observe any other significant sex-specific differences in incidences across age groups.

Out of the clinically diagnosed cases, 59.7% occurred in women ($n = 7,042$). Again the age distribution was bimodal, but the second peak occurring in the age groups 60–79 years was notably discernible (Figure 2, panel B). In these age groups, LB incidence was distinctively higher among women than among men (on average 142/100,000 among women and 111/100,000 among men). Case-patients were predominantly female across the age groups except in children 5–14 years of age and persons >80 years of age.

Regarding hospital discharges, we identified a total of 10,402 cases with an LB diagnosis (56.2% of case-patients

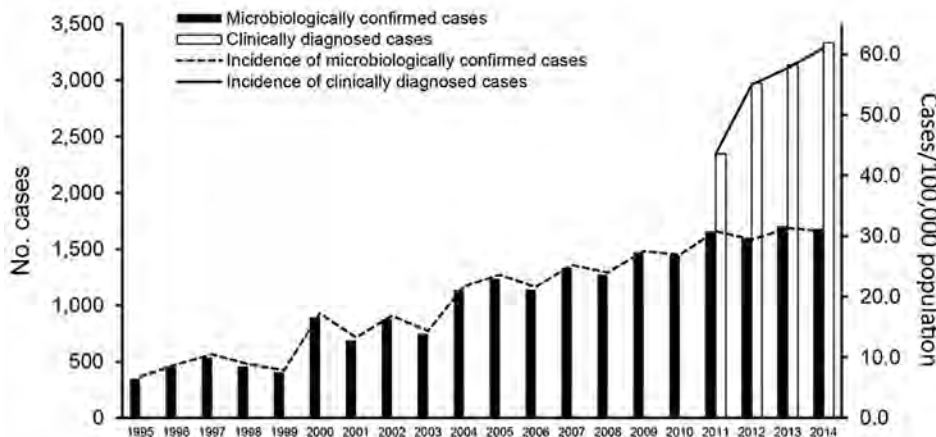


Figure 1. Number and incidence of microbiologically confirmed Lyme borreliosis cases reported in the National Infectious Diseases Register during 1995–2014 and clinically diagnosed cases reported in the Register for Primary Health Care Visits during 2011–2014, Finland.

were female); incidence increased from 0.4/100,000 population in 1996 to 19/100,000 in 2014. We have provided a detailed description of characteristics of case-patients and the different clinical manifestations of disseminated LB (online Technical Appendix Results).

Geographic Distribution and Time Trend

In most of the HDs (15/21 [71.4%]), incidence of microbiologically confirmed LB cases increased significantly over time (Figure 3). We observed the most notable increasing trend in western, southern, and southeastern Finland. The highest average annual incidences in the past 5 years (2010–2014) were reported in southeastern Finland, with HD-specific rates of 49–57 cases/100,000 population (online Technical Appendix Table 1, Figure 1). The lowest incidences of LB were reported in northern and northeastern Finland, with 1–4 cases/100,000 population. The Åland Islands is a hyperendemic region for LB with the average annual incidence of 1,597/100,000 population during 2010–2014, with an increasing trend ($p < 0.01$). The average annual incidence of the whole country (average of all HDs) during 2010–2014 was 30/100,000 population.

We observed the highest average annual incidences of clinically diagnosed LB during 2011–2014 in eastern and southeastern Finland, with HD-specific rates of 143–162 cases/100,000 population, and in southwestern Finland (83/100,000 population). The average annual incidence in the Åland Islands was 885/100,000 population. The countrywide average annual incidence during 2011–2014 was 54/100,000 population. Even during the period of 4 years, incidence increased significantly ($p < 0.05$) in 8 HDs, most notably in eastern and southern Finland (online Technical Appendix Table 2, Figure 1).

Seasonality

Microbiologically confirmed LB cases were reported throughout each year, although we observed a pronounced peak in seasonality in September (14.4% of all LB cases

during 1995–2014) (Figure 4). More than 50% of LB cases were reported during August–November. For clinically diagnosed LB cases, seasonality was even more pronounced, and only a few cases were reported during the wintertime in Finland (November–April). Most cases ($\approx 75\%$) occurred during June–September, with the peak in July (22.1% of all LB cases) and August (21.0%). Year-to-year variation in seasonality was minor among microbiologically confirmed and clinically diagnosed cases (data not shown).

Discussion

By using 3 nationwide registers, we examined the changes in the incidence and geographic distribution of LB in Finland during a ≈ 20 -year period. Our data allowed us to analyze the incidence of microbiologically confirmed disseminated LB cases and clinically diagnosed LB infections (reflecting EM). The incidence of LB in Finland increased significantly from 1995 to 2014, reflecting the epidemiologic situation of LB in northern Europe. As of 2014, $\approx 1,700$ microbiologically confirmed LB cases are diagnosed yearly, compared with a few hundred cases just 15–20 years ago. When clinically diagnosed EM cases are also considered, the crude estimate of the total LB incidence reached 120/100,000 population in 2014. In 2015, after our study period, $\approx 1,900$ microbiologically confirmed LB cases and 3,514 clinically diagnosed cases were recorded, further confirming the increasing trend (https://sampo.thl.fi/pivot/prod/fi/ttr/shp/fact_shp?row=area-12260&column=time-12059&filter=reportgroup-12465).

The increasing trend in LB incidence has been reported in several countries in Europe, various US states, and Canada in the past decade (4). Multiple studies suggest that milder winter temperatures, humid summers, and extended spring and autumn seasons attributable to climate change might enable the tick vectors to spread to higher altitudes and latitudes and thereby increase the risk for tickborne infections in northern Europe, including Finland (5,16,17). As a part of our study, a questionnaire concerning the

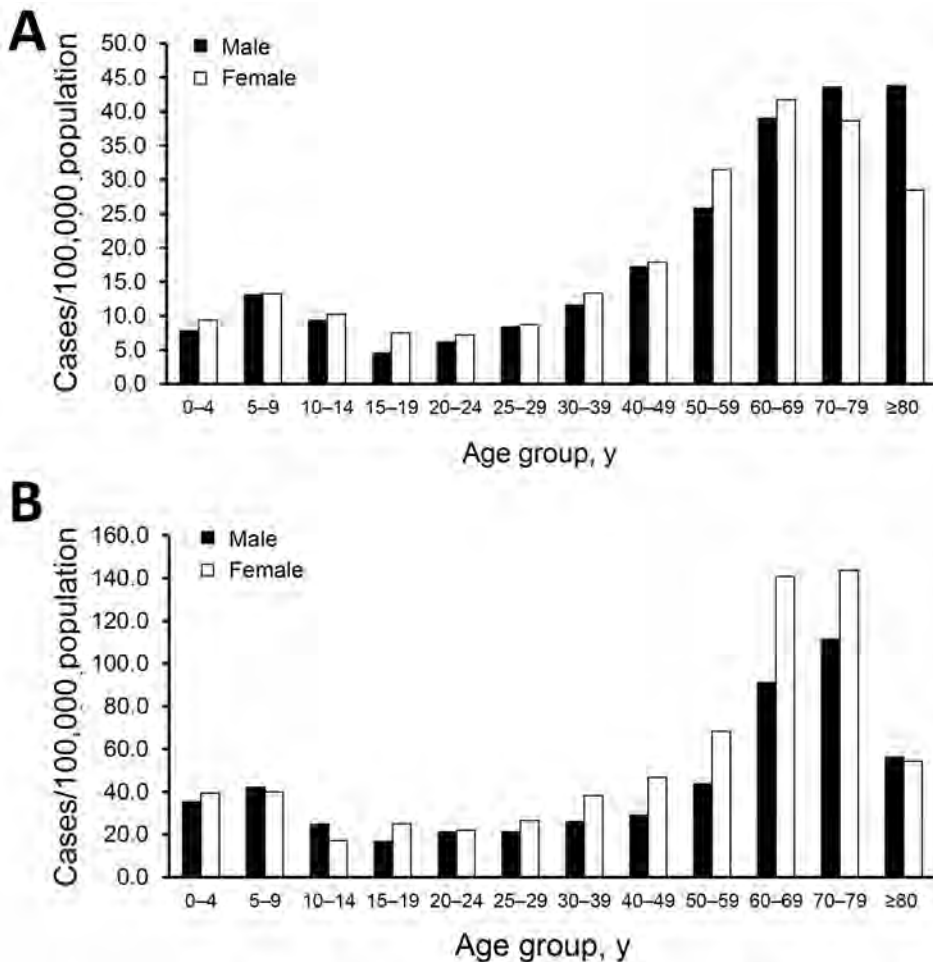


Figure 2. Incidence rates of microbiologically confirmed Lyme borreliosis cases reported in the National Infectious Diseases Register during 1995–2014 (A) and clinically diagnosed cases reported in the Register for Primary Health Care Visits during 2011–2014 (B), by age and sex of case-patients, Finland.

current and previous laboratory methodology was sent to all 8 microbiological laboratories performing LB diagnostics in Finland to assess whether changes in the diagnostic methods could explain the increased incidence of microbiologically confirmed LB cases. The results indicated that no such changes can be identified. If anything, the methods have become more specific through the adoption of a 2-tier approach to *Borrelia* serologic testing.

Substantial variation exists in the regional incidences of LB throughout Finland. The Åland Islands, which is a hyperendemic region both for ticks and LB, stands out from the other HDs. Outside the Åland Islands, the highest incidences are concentrated in the coastal areas of Finland, especially along the coastline of the Baltic Sea and the southwestern archipelago. Southwestern Finland, including the archipelago, has long been well-known as a region with high tick abundance (10). During 1995–2000, the LB incidence was highest in southwestern Finland, but ≈15 years later, the southeastern areas of Finland have surpassed the southwestern areas in terms of LB incidence. In general, in almost all HDs in the southern half of Finland, LB incidence increased during 1995–2014. Central-western parts

of Finland remain low-incidence regions. The same regions can be identified as areas of low tick density on a map of the geographic distribution of ticks in Finland in 2015 (23).

We observed a bimodal age-specific distribution in microbiologically confirmed LB cases and clinically diagnosed LB cases. The similar 2-peaked age distribution has been noted in other studies of LB in the United States and in Europe, but unlike in the previous studies, the second peak in our study occurred in older age groups in both sexes (6,11,19,24,25). One explanation for the peak in older age groups could be increased levels of leisure activity; in Finland, certain outdoor activities, such as berry picking and gardening, might be more popular among older persons, which might increase their exposure to tick bites. Furthermore, because of the aging immune system, the elderly might be at an increased risk for disseminated LB, which is observed as an increased number of LB cases, especially in NIDR (26).

The preponderance of women and girls with cases of EM has been reported in various other epidemiologic studies in Europe, and our data on clinically diagnosed LB cases (59.7% of which occurred in women and girls)

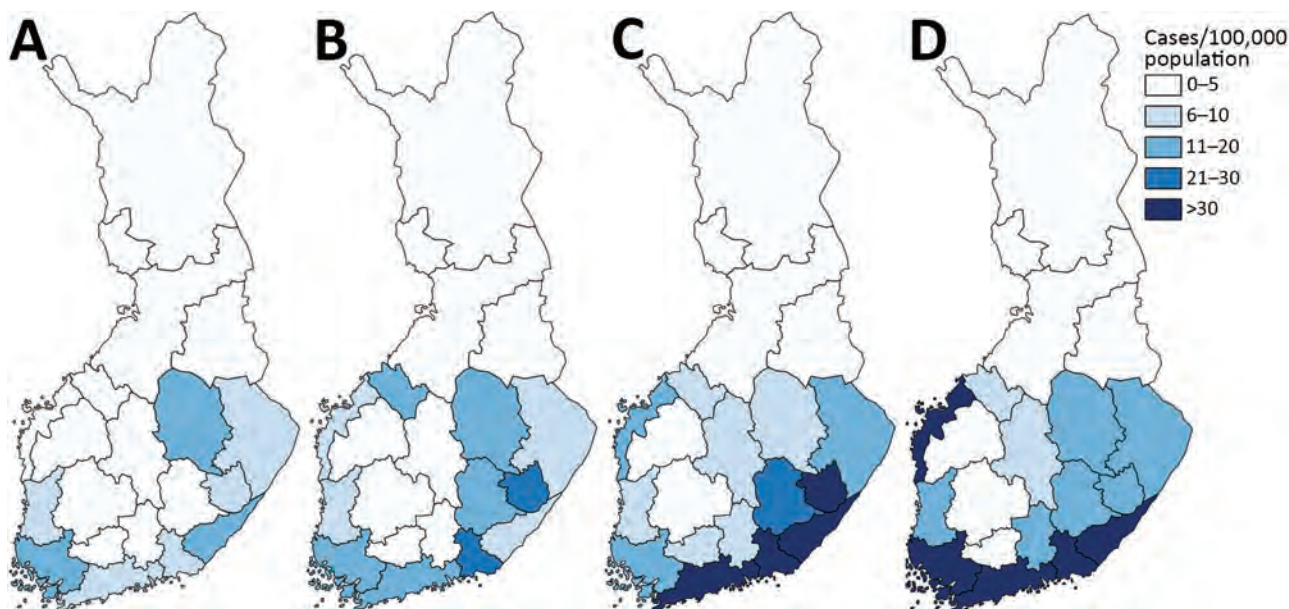


Figure 3. Incidence rates of microbiologically confirmed Lyme borreliosis cases, by hospital district and period, Finland, 1995–2014. A) 1995–1999; B) 2000–2004; C) 2005–2009; D) 2010–2014. The Åland Islands are not shown; only the hospital districts on the mainland are shown.

are in accordance with those previous reports (7,27–30). Incidence of clinically diagnosed LB was higher only among boys 5–14 years of age and men >80 years of age. In adults, especially in the 50–79-year age group, incidence was distinctively higher among women. In terms of microbiologically confirmed LB, differences in LB incidence between men and women were not as large, but women were still slightly predominant across all age groups. However, in the >70-year age group, men were clearly overrepresented. In France, the proportion of men that were hospitalized because of LB during 2004–2012 was substantially higher than the proportion of women (57.8% vs. 42.2%), whereas women represented 52% of the LB cases reported by general practitioners (19). The immunologic or biologic mechanisms that might explain why older men would be more likely to have disseminated LB than women are unknown (30). Women might tend to notice EM more often or they might seek the healthcare services more actively while still in the EM phase of the infection. Either way, in our study, a preponderance of men with microbiologically confirmed LB cases was only observed in the older age groups.

The seasonal distribution of clinically diagnosed LB cases peaked in July and August, followed by a 1–2-month incubation period, before disseminated LB peaked in September. Both the host-seeking tick activity and the human exposure to ticks attributable to summertime outdoor activities affect the seasonality of LB. According to our data, the EM stage infections are observed during the warm summer months during June–September, and few EM cases

are registered in Avohilmo during November–April. The incubation period for disseminated LB ranges from weeks to months, which results in microbiologically confirmed LB cases being reported to NIDR throughout the year, although to a lesser extent during the winter season in Finland (November–April), when only chronic manifestations of LB typically are reported.

The proportions of Lyme neuroborreliosis (9.3%) and Lyme arthritis (4.3%) cases identified were surprisingly low compared with the total number of case-patients discharged from the hospitals during the study period. A reasonable explanation might involve the reporting accuracy; most LB cases are likely registered only under the ICD-10 code A69.2 (“Lyme borreliosis”) instead of the more specific codes referring to Lyme neuroborreliosis and Lyme arthritis. However, the completeness and accuracy of Hilmo data in general have been found to be on a high level (31).

We acknowledge some limitations in this study. First, Avohilmo does not yet cover occupational and private healthcare visits. Thus, the number of clinically diagnosed cases is underestimated in this study, particularly among working-age persons. Second, the reliability of correctly diagnosed EM cases is highly dependent on the healthcare professionals reporting the cases to Avohilmo. However, EM is well-recognized among healthcare workers in Finland, and every healthcare visit must be registered with an ICD-10 code. We have adjusted our total estimate on the number of clinically diagnosed LB cases with a correction factor reflecting the known inaccuracies in reporting.

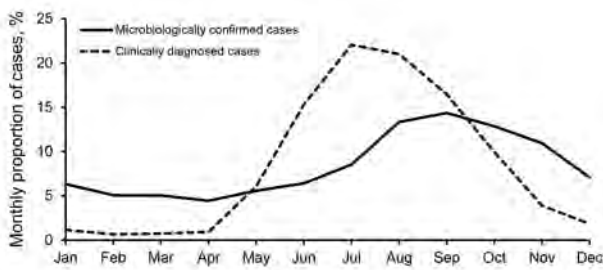


Figure 4. Monthly distribution of microbiologically confirmed Lyme borreliosis cases reported in the National Infectious Diseases Register during 1995–2014 and clinically diagnosed cases reported in the Register for Primary Health Care Visits during 2011–2014, Finland.

However, the trend in LB incidence in Avohilmo is similar to that of microbiologically confirmed LB in NIDR during the past few years. Third, the awareness of LB among healthcare professionals and the public might differ geographically and seasonally, which might cause differences in diagnostic activity. Also, the location where the infection occurred might be different than the place of residence, and the fact that NIDR does not contain any clinical information is a limitation. To further evaluate the register data and to refine our incidence estimates, register-linkage studies on an individual level are needed and ongoing, including the assessment of personalized disease and antibiotic prescription patterns. Risk factors for LB should also be comprehensively assessed. We plan to expand routine surveillance of LB to also include clinically diagnosed cases and will further validate the use of primary healthcare visits for surveillance purposes.

In this study, we showed an increase in the incidence of LB in Finland during a ≈ 20 -year period and described the changes that have taken place in the geographic distribution of LB. The epidemiologic data of LB are useful for healthcare professionals, the general public, and the media to highlight the areas and seasons of the highest infection risk. Furthermore, the results of this study stress the importance of LB as an increasing public health concern and are valuable to the public health decision-makers in guiding surveillance and intervention strategies (e.g., vaccine development), as well as increasing the awareness of the disease among the public.

This work was supported by the University of Turku, NIHW, and the Academy of Finland. The funders of the study had no role in study design, analysis, or writing of the report.

Ms. Sajanti is a physician and a PhD student in the Department of Medical Microbiology and Immunology at the University of Turku, Turku, Finland. Her research interests are Lyme borreliosis and other tickborne diseases.

References

1. Stanek G, Wormser GP, Gray J, Strle F. Lyme borreliosis. *Lancet*. 2012;379:461–73. [http://dx.doi.org/10.1016/S0140-6736\(11\)60103-7](http://dx.doi.org/10.1016/S0140-6736(11)60103-7)
2. Kuehn BM. CDC estimates 300,000 US cases of Lyme disease annually. *JAMA*. 2013;310:1110. <http://dx.doi.org/10.1001/jama.2013.278331>
3. Mead PS. Epidemiology of Lyme disease. *Infect Dis Clin North Am*. 2015;29:187–210. <http://dx.doi.org/10.1016/j.idc.2015.02.010>
4. Theel ES. Tickborne borrelia infections: beyond just Lyme disease. *Clin Lab Med*. 2015;35:ix–x. <http://dx.doi.org/10.1016/j.cll.2015.09.001>
5. Bennet L, Halling A, Berglund J. Increased incidence of Lyme borreliosis in southern Sweden following mild winters and during warm, humid summers. *Eur J Clin Microbiol Infect Dis*. 2006;25:426–32. <http://dx.doi.org/10.1007/s10096-006-0167-2>
6. Wilking H, Stark K. Trends in surveillance data of human Lyme borreliosis from six federal states in eastern Germany, 2009–2012. *Ticks Tick Borne Dis*. 2014;5:219–24. <http://dx.doi.org/10.1016/j.ttbdis.2013.10.010>
7. Strle F, Videcnik J, Zorman P, Cimperman J, Lotric-Furlan S, Maraspin V. Clinical and epidemiological findings for patients with erythema migrans. Comparison of cohorts from the years 1993 and 2000. *Wien Klin Wochenschr*. 2002;114:493–7.
8. Smith R, Takkinen J. Lyme borreliosis: Europe-wide coordinated surveillance and action needed? *Euro Surveill*. 2006;11:E060622.1.
9. Hofhuis A, Harms M, van den Wijngaard C, Sprong H, van Pelt W. Continuing increase of tick bites and Lyme disease between 1994 and 2009. *Ticks Tick Borne Dis*. 2015;6:69–74. <http://dx.doi.org/10.1016/j.ttbdis.2014.09.006>
10. Junttila J, Peltomaa M, Soini H, Marjamäki M, Viljanen MK. Prevalence of *Borrelia burgdorferi* in *Ixodes ricinus* ticks in urban recreational areas of Helsinki. *J Clin Microbiol*. 1999;37:1361–5.
11. Bacon RM, Kugeler KJ, Mead PS; Centers for Disease Control and Prevention (CDC). Surveillance for Lyme disease—United States, 1992–2006. *MMWR Surveill Summ*. 2008;57:1–9.
12. Hofhuis A, van der Giessen JW, Borgsteede FH, Wielinga PR, Notermans DW, van Pelt W. Lyme borreliosis in the Netherlands: strong increase in GP consultations and hospital admissions in past 10 years. *Euro Surveill*. 2006;11:E060622.2.
13. Sykes RA, Makiello P. An estimate of Lyme borreliosis incidence in Western Europe. *J Public Health (Oxf)*. 2017;39:74–81.
14. Hubálek Z. Epidemiology of Lyme borreliosis. *Curr Probl Dermatol*. 2009;37:31–50. <http://dx.doi.org/10.1159/000213069>
15. Jaenson TG, Jaenson DG, Eisen L, Petersson E, Lindgren E. Changes in the geographical distribution and abundance of the tick *Ixodes ricinus* during the past 30 years in Sweden. *Parasit Vectors*. 2012;5:8. <http://dx.doi.org/10.1186/1756-3305-5-8>
16. Lindgren E, Tälleklint L, Polfeldt T. Impact of climatic change on the northern latitude limit and population density of the disease-transmitting European tick *Ixodes ricinus*. *Environ Health Perspect*. 2000;108:119–23. <http://dx.doi.org/10.1289/ehp.00108119>
17. Ogden NH, Maarouf A, Barker IK, Bigras-Poulin M, Lindsay LR, Morshed MG, et al. Climate change and the potential for range expansion of the Lyme disease vector *Ixodes scapularis* in Canada. *Int J Parasitol*. 2006;36:63–70. <http://dx.doi.org/10.1016/j.ijpara.2005.08.016>
18. Chmielewska-Badora J, Moniuszko A, Żukiewicz-Sobczak W, Zwoliński J, Piątek J, Pancewicz S. Serological survey in persons occupationally exposed to tick-borne pathogens in cases of co-infections with *Borrelia burgdorferi*, *Anaplasma phagocytophilum*, *Bartonella* spp. and *Babesia microti*. *Ann Agric Environ Med*. 2012;19:271–4.
19. Vandenesch A, Turbelin C, Couturier E, Arena C, Jaulhac B, Ferquel E, et al. Incidence and hospitalisation rates of Lyme borreliosis, France, 2004 to 2012. *Euro Surveill*. 2014;19:20883. <http://dx.doi.org/10.2807/1560-7917.ES2014.19.34.20883>

RESEARCH

20. Schauman K, Kovanen J, Seppälä I. Lyme borreliosis in Finland in 1986–1988. *Biomed Pharmacother*. 1989;43:427–30. [http://dx.doi.org/10.1016/0753-3322\(89\)90241-2](http://dx.doi.org/10.1016/0753-3322(89)90241-2)
21. Sormunen JJ, Klemola T, Vesterinen EJ, Vuorinen I, Hytönen J, Hänninen J, et al. Assessing the abundance, seasonal questing activity, and Borrelia and tick-borne encephalitis virus (TBEV) prevalence of *Ixodes ricinus* ticks in a Lyme borreliosis endemic area in southwest Finland. *Ticks Tick Borne Dis*. 2016;7:208–15. <http://dx.doi.org/10.1016/j.ttbdis.2015.10.011>
22. Sormunen JJ, Penttinen R, Klemola T, Hänninen J, Vuorinen I, Laaksonen M, et al. Tick-borne bacterial pathogens in southwestern Finland. *Parasit Vectors*. 2016;9:168. <http://dx.doi.org/10.1186/s13071-016-1449-x>
23. Laaksonen M, Sajanti E, Sormunen JJ, Penttinen R, Hänninen J, Ruohomäki K, et al. Crowdsourcing-based nationwide tick collection reveals the distribution of *Ixodes ricinus* and *I. persulcatus* and associated pathogens in Finland. *Emerg Microbes Infect*. 2017;6:e31. <http://dx.doi.org/10.1038/emi.2017.17>
24. Nelson CA, Saha S, Kugeler KJ, Delorey MJ, Shankar MB, Hinckley AF, et al. Incidence of clinician-diagnosed Lyme disease, United States, 2005–2010. *Emerg Infect Dis*. 2015;21:1625–31. <http://dx.doi.org/10.3201/eid2109.150417>
25. Dessau RB, Espenhain L, Mølbak K, Krause TG, Voldstedlund M. Improving national surveillance of Lyme neuroborreliosis in Denmark through electronic reporting of specific antibody index testing from 2010 to 2012. *Euro Surveill*. 2015;20:21184. <http://dx.doi.org/10.2807/1560-7917.ES2015.20.28.21184>
26. Kline KA, Bowdish DM. Infection in an aging population. *Curr Opin Microbiol*. 2016;29:63–7. <http://dx.doi.org/10.1016/j.mib.2015.11.003>
27. Mehnert WH, Krause G. Surveillance of Lyme borreliosis in Germany, 2002 and 2003. *Euro Surveill*. 2005;10:83–5.
28. Stanek G, Flamm H, Groh V, Hirschl A, Kristoferitsch W, Neumann R, et al. Epidemiology of borrelia infections in Austria. *Zentralbl Bakteriol Mikrobiol Hyg [A]*. 1987;263:442–9. [http://dx.doi.org/10.1016/S0176-6724\(87\)80106-2](http://dx.doi.org/10.1016/S0176-6724(87)80106-2)
29. Åsbrink E, Olsson I, Hovmark A. Erythema chronicum migrans Afzelius in Sweden. A study on 231 patients. *Zentralbl Bakteriol Mikrobiol Hyg [A]*. 1986;263:229–36. [http://dx.doi.org/10.1016/S0176-6724\(86\)80126-2](http://dx.doi.org/10.1016/S0176-6724(86)80126-2)
30. Bennet L, Stjernberg L, Berglund J. Effect of gender on clinical and epidemiologic features of Lyme borreliosis. *Vector Borne Zoonotic Dis*. 2007;7:34–41. <http://dx.doi.org/10.1089/vbz.2006.0533>
31. Sund R. Quality of the Finnish Hospital Discharge Register: a systematic review. *Scand J Public Health*. 2012;40:505–15. <http://dx.doi.org/10.1177/1403494812456637>

Address for correspondence: Eeva Sajanti, Department of Medical Microbiology and Immunology, University of Turku, Kiinamyllynkatu 13, Turku FI-20520, Finland; email: eeva.sajanti@utu.fi



Recognize the signs of tickborne disease

Understand diagnostic testing and lab findings

Quickly find treatment recommendations

Order or download at www.cdc.gov/pubs

Characterization of Fitzroy River Virus and Serologic Evidence of Human and Animal Infection

Cheryl A. Johansen,¹ Simon H. Williams,¹ Lorna F. Melville, Jay Nicholson, Roy A. Hall, Helle Bielefeldt-Ohmann, Natalie A. Prow, Glenys R. Chidlow, Shani Wong, Rohini Sinha, David T. Williams, W. Ian Lipkin, David W. Smith

In northern Western Australia in 2011 and 2012, surveillance detected a novel arbovirus in mosquitoes. Genetic and phenotypic analyses confirmed that the new flavivirus, named Fitzroy River virus, is related to Sepik virus and Wesselsbron virus, in the yellow fever virus group. Most (81%) isolates came from *Aedes normanensis* mosquitoes, providing circumstantial evidence of the probable vector. In cell culture, Fitzroy River virus replicated in mosquito (C6/36), mammalian (Vero, PSEK, and BSR), and avian (DF-1) cells. It also infected intraperitoneally inoculated weanling mice and caused mild clinical disease in 3 intracranially inoculated mice. Specific neutralizing antibodies were detected in sentinel horses (12.6%), cattle (6.6%), and chickens (0.5%) in the Northern Territory of Australia and in a subset of humans (0.8%) from northern Western Australia.

In the state of Western Australia, Australia, active surveillance is conducted for mosquito-borne viruses of major human health significance: alphaviruses Ross River virus (RRV) and Barmah Forest virus (BFV) and flaviviruses Murray Valley encephalitis virus (MVEV) and West Nile virus (subtype Kunjin virus; KUNV). These flaviviruses are endemic and epidemic to the northern and central areas of Australia, where surveillance involves year-round testing for seroconversions in sentinel chickens (1) and virus isolation from mosquito pools collected annually (2,3). More frequent mosquito collection is prevented by the

logistical difficulties of accessing remote areas. Commonly isolated arboviruses include the flaviviruses MVEV (and subtype Alfuy virus), KUNV, Kokobera virus (KOKV), and Edge Hill virus (EHV) and the alphaviruses RRV, BFV, and Sindbis virus (4,5). This system occasionally detects viruses that cannot be identified as known viruses, such as Stretch Lagoon virus, an orbivirus isolated in 2002 (6). We describe the detection and characterization of a novel flavivirus named Fitzroy River virus (FRV), isolated from mosquitoes collected in northern Western Australia, and seroepidemiologic evidence of human or animal infection.

Methods

Adult Mosquito Collections

Adult mosquitoes were collected during March and April 2010–2015, at the end of the summer wet season across the Kimberley region of Australia (2) (Figure 1). Mosquitoes were collected in encephalitis vector surveillance traps (7) baited with carbon dioxide and were separated by species and pooled (8–10); blood-fed mosquitoes were excluded from analysis.

Virus Isolation and Identification

Virus isolation from all mosquito pools was performed as previously described (10). In brief, mosquito pools were homogenized and serially passaged from C6/36 (*Aedes albopictus* mosquito) cells onto Vero (African green monkey kidney) and PSEK (porcine squamous equine kidney) cells. PSEK cells were later replaced by BSR (baby hamster kidney) cells. Viruses were detected and identified by use of microscopy and monoclonal antibody (mAb) binding patterns in ELISA. For flavivirus-reactive samples, a flavivirus group-reactive 1-step reverse transcription PCR assay (Invitrogen, Carlsbad, CA, USA) (11) was used to amplify a 0.6-kb fragment of the nonstructural protein 5 (NS5) and 3' untranslated region (3' UTR) for PCR and sequence confirmation.

Author affiliations: The University of Western Australia, Nedlands, Western Australia, Australia (C.A. Johansen, J. Nicholson, S. Wong, D.W. Smith); PathWest Laboratory Medicine Western Australia, Nedlands (C.A. Johansen, G.R. Chidlow, D.W. Smith); Columbia University, New York, New York, USA (S.H. Williams, R. Sinha, W.I. Lipkin); The Northern Territory Government, Darwin, Northern Territory, Australia (L.F. Melville); The University of Queensland, St. Lucia, Queensland, Australia (R.A. Hall, H. Bielefeldt-Ohmann, N.A. Prow); The University of Queensland, Gatton, Queensland, Australia (H. Bielefeldt-Ohmann); CSIRO Australian Animal Health Laboratory, Geelong, Victoria, Australia (D.T. Williams)

DOI: <https://doi.org/10.3201/eid2308.161440>

¹These authors contributed equally to this article.

Whole-Genome Sequencing

RNA from viral stock (the prototype isolate K73884) was extracted with TRI Reagent (Molecular Research Center, Inc., Cincinnati, OH, USA) and sequenced on a HiSeq ultra high-throughput sequencing platform (Illumina, San Diego, CA, USA). Trimmed reads were assessed for quality by using PRINSEQ version 0.20.2 (12) before host (metazoan and mosquito) genome subtraction (Bowtie 2) (13) and assembly (MIRA version 4.0) (14). Resulting contiguous sequences and unique singletons were subjected to homology search by using MegaBLAST and blastx (<https://blast.ncbi.nlm.nih.gov/Blast.cgi>) against the GenBank database. Sequences that were similar to viruses from the yellow fever virus (YFV) group, a monophyletic branch that previously included 3 viruses (Wesselsbron virus [WESSV], Sepik virus [SEPV], and YFV) (15) were manually edited and reassembled by using Geneious version 7.1.5 (16). The complete genome was resequenced by using overlapping PCR and confirmed by bidirectional Sanger sequencing.

The sequences for the 5' and 3' UTRs were acquired by using the SMARTer RACE cDNA amplification kit (Takara Bio USA, Mountain View, CA, USA).

Phylogenetic and Recombination Analyses

Nucleotide sequences for the complete polyproteins representing 44 mosquito-borne and tick-borne flaviviruses, as well as those that are insect specific or have no known vector, were retrieved from GenBank. Alignments with FRV were performed by using MUSCLE in Geneious version 7.1.5, and a maximum-likelihood phylogenetic tree was constructed by using the general time reversible plus gamma distribution site model of nucleotide substitution with 500 bootstrap replicates (MEGA version 7.0.16) (17). Tamana bat virus was used as the outgroup. For alignments of cleavage recognition sequences from members of the YFV group, previously established sites were identified and aligned (18,19). To assess whether FRV was a recombinant virus, we analyzed polyprotein sequence alignments (as described above) by using default parameters for RDP, GENECONV, BootScan, MaxChi, Chimaera, SisScan, 3SEQ, and PhyPro methods available in the RDP4 program suite (20).

Virus Growth Kinetics in Vitro

Virus replication was assessed in mosquito (C6/36), mammalian (Vero and BSR), and avian (DF-1) cells (21) by using a multiplicity of infection of 0.1 in 2% fetal bovine serum in M199 (C6/36 cells) or DMEM (Vero, BSR, and DF-1 cells). After 1 hour of incubation at 28°C (C6/36 cells) or 37°C (Vero, BSR, and DF-1 cells), the inoculum was removed and monolayers were washed before addition of 1 mL of media. Plates were incubated; monolayers examined for cytopathic effect (CPE); and samples removed in triplicate at 0, 1, 2, 3, 4, and 7 days postinoculation (dpi) and stored at -80°C. The 50% tissue culture infectious dose in each sample was determined by serial dilutions and titration in BSR cells in 96-well tissue culture plates, and titers were calculated (22).

Determination of Virulence in Mice

All procedures using animals were approved by The University of Queensland Animal Ethics Committee. Groups of 10 mice (18–19-day weanling CD1 mice, equal numbers of each sex) were challenged by intraperitoneal injection of 50 μ L or intracranial injection of 20 μ L of either 100 or 1,000 50% tissue culture dose infectious units (IU) of FRV. Groups of 3 mice were mock challenged intraperitoneally or intracranially. Veterinarians monitored the mice twice daily for 19 days and then daily through 21 dpi (23,24). At 21 dpi, all mice were deeply anesthetized, bled by cardiac puncture, and killed by cervical dislocation. No animals required euthanasia during the experiment. FRV-specific

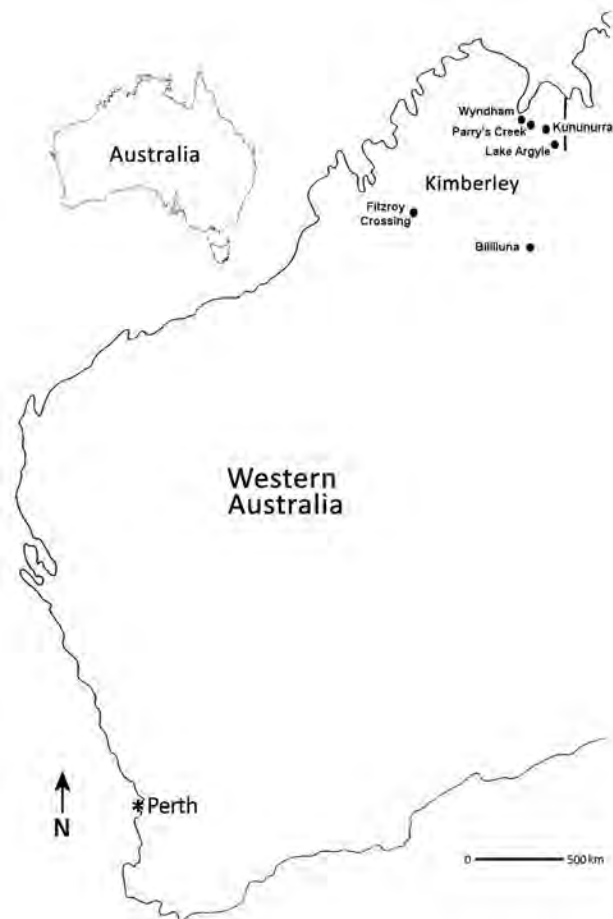


Figure 1. Locations where Fitzroy River virus–positive mosquitoes were collected (black dots), Western Australia, Australia, 2011 and 2012. Perth (asterisk), the capital city and most densely populated area of Western Australia, is shown to indicate its distance from the Kimberley region.

antibodies were detected by fixed-cell ELISA (25), and the brains of mice with mild clinical signs were fixed in 10% neutral-buffered formaldehyde and processed for histopathologic and immunohistochemical examination (23,24).

Serologic Surveys

Human serologic studies were performed with approval from The University of Western Australia Human Ethics Committee. We used human serum samples that were submitted to PathWest Laboratory Medicine WA (Nedlands, Western Australia, Australia) for arbovirus serologic testing and that were positive by flavivirus hemagglutination inhibition assay. We also used serum samples that were submitted for alphavirus testing only (RRV and BFV) and that were serologically negative. Deidentified information about patient age, sex, ZIP code, and test results were provided. Samples from residents of regions in northern Western Australia where FRV had been detected in mosquitoes or where *Aedes normanensis* mosquitoes are abundant were targeted for this survey. Samples were tested in a flavivirus epitope blocking ELISA that used mAb 3H6 (26). Serum containing flavivirus antibodies in ELISA were subsequently tested by serum cross-neutralization assay for antibodies to FRV, MVEV, KUNV, Alfuy virus, KOKV, Stratford virus, and EHV as described previously (27). As controls, we used polyclonal rabbit or mouse serum previously raised to these viruses.

Animal serologic studies were approved by The Charles Darwin University Animal Ethics Committee. Animal serum (sentinel cattle, horses, chickens, and wallabies) from the Northern Territory of Australia was tested for antibodies to FRV by neutralization tests (28) without prior testing by flavivirus epitope blocking ELISA. Cross-neutralizations with SEPV were conducted on a subset of positive samples to confirm antibody specificity.

Results

Viruses and mAb Binding Patterns

We saw little or no visual evidence of infection of C6/36 cell monolayers during the isolation of FRV, and it grew slowly in Vero cells. Cytopathic evidence of infection was most marked in PSEK and BSR cells. Isolates were initially typed by their mAb binding profile against a panel of flavivirus- and alphavirus-reactive mAbs in fixed-cell ELISA.

All isolates of FRV reacted with the flavivirus-reactive mAb 4G2 but failed to react with other flavivirus- and alphavirus-reactive mAbs (data not shown). Preliminary analyses of the nucleotide sequence of the NS5–3' UTR showed 75%–80% identity to SEPV and WESSV, the viruses most closely related to YFV (15,19,29,30). Identity between all FRV isolates in the NS5–3' UTR was 98.9%–100%. The mAb binding profile differed from EHV and SEPV, and positive reactions to FRV were detected with mAbs 4G2 and 4G4 only (Table 1).

Whole-Genome Sequences and Phylogeny

Unbiased high-throughput sequencing results provided >99% of the FRV genome with only partial UTRs not obtained. The completed full-genome length of FRV was 10,807 nt with a single 10,218-nt open reading frame flanked by a 117-nt 5' UTR and a 472-nt 3' UTR (Table 2; online Technical Appendix Figure, panel A, <https://wwwnc.cdc.gov/EID/article/23/8/16-1440-Techapp1.pdf>) and has been deposited in GenBank under accession no. KM361634. At the amino acid level, FRV was more similar to SEPV than to WESSV in most regions, with the exception of the short 2k peptide (70% vs. 91% aa homology), NS4a (87% vs. 92% aa homology), and NS5 (88% vs. 89% aa homology). Because there was a sharp change in amino acid homology between FRV and SEPV across the 2k peptide (70%) and NS4b (94%), we assessed aligned polyprotein sequences for recombination breakpoints by using 8 algorithms in the RDP4 suite, but we found no evidence suggesting that recombination had occurred (data not shown).

FRV was highly similar to SEPV across the structural viral proteins, including the membrane (96%) and envelope (96%) proteins. Over the full genome, FRV displayed the highest nucleotide identity to SEPV (79%), WESSV (77%), and YFV (62%). These lower nucleotide identities are in contrast to the polyprotein amino acid homologies (SEPV 91%, WESSV 89%, YFV 61%), indicating that a large proportion of nucleotide differences between FRV and SEPV or WESSV were synonymous. The level of nucleotide identity was higher in the 5' and 3' UTRs (94% and 86%, respectively) than in structural proteins (up to 81%) for FRV and SEPV, reflecting the functional importance of the UTRs for virus replication. Closer analysis of several conserved features of flavivirus UTRs is shown in the online Technical Appendix

Table 1. Monoclonal antibody binding pattern of FRV isolates from Western Australia*

Virus	Monoclonal antibody†										
	4G2	4G4	6F7	7C6	8G2	6A9	3D11	3B11	3G1	5D3	7C3
FRV‡	+	+	-	-	-	-	-	-	-	-	-
SEPV	+	+	+	-	-	-	-	-	-	-	-
YFV	+	+	-	-	-	-	-	-	-	-	-
EHV	+	-	+	+	+	+	+	+	+	+	+

*EHV, Edge Hill virus; FRV, Fitzroy River virus; SEPV, Sepik virus; YFV, yellow fever virus; +, positive (optical density of ≥0.2 and at least 2 times the mean of negative control wells); -, negative.

†Original descriptions of monoclonal antibody from (31) (4G2), (32) (4G4), (33) (6F7), and (34) (7C6, 8G2, 6A9, 3D11, 3B11, 3G1, 5D3, and 7C3).

‡Monoclonal antibody binding patterns of all FRV isolates were identical to those of the prototype isolate K73884.

Table 2. Comparison of genomic region lengths and similarities between members of the YFV group and FRV*

Genomic region	Virus							
	FRV		SEPV		WESSV		YFV	
	nt	aa	nt	aa	nt	aa	nt	aa
5' UTR	117	NA	116 (94)	NA	118 (92)	NA	118 (52)	NA
Capsid	348	116	348 (77)	116 (84)	348 (74)	116 (78)	363 (54)	121 (39)
Premembrane	267	89	267 (78)	89 (94)	267 (73)	89 (87)	267 (59)	89 (59)
Membrane	225	75	225 (80)	75 (96)	225 (74)	75 (87)	225 (58)	75 (47)
Envelope	1,470	490	1,470 (81)	490 (96)	1,470 (79)	490 (93)	1,479 (63)	493 (54)
NS1	1,059	353	1,059 (79)	353 (93)	1,059 (76)	353 (87)	1,056 (63)	352 (64)
NS2a	678	226	678 (78)	226 (88)	678 (77)	226 (85)	672 (54)	224 (40)
NS2b	390	130	390 (78)	130 (88)	390 (76)	130 (88)	390 (56)	130 (50)
NS3	1,869	623	1,869 (79)	623 (93)	1,869 (77)	623 (92)	1,869 (67)	623 (71)
NS4a	378	126	378 (75)	126 (87)	378 (75)	126 (92)	378 (61)	126 (57)
2k	69	23	69 (71)	23 (70)	69 (74)	23 (91)	69 (61)	23 (57)
NS4b	744	248	744 (79)	248 (94)	744 (77)	248 (91)	750 (66)	250 (64)
NS5	2,721	906	2,721 (78)	906 (88)	2,721 (76)	906 (89)	2,718 (66)	905 (68)
3' UTR	472	NA	459 (86)	NA	478 (84)	NA	508 (65)	NA
Polyprotein	10,218	3,405	10,218 (79)	3,405 (91)	10,218 (77)	3,405 (89)	10,236 (63)	3,411 (61)
Full genome	10,807	NA	10,793 (79)	NA	10,814 (77)	NA	10,862 (62)	NA

*Values are sequence length (% identity with FRV). FRV, Fitzroy River virus (GenBank accession no. KM631634); NS, nonstructural; SEPV, Sepik virus (GenBank accession no. NC008719); UTR, untranslated region; WESSV, Wesselsbron virus (accession no. JN226796); YFV, yellow fever virus (X03700); NA, not applicable.

Figure. Although comparisons of the cyclization sequences (online Technical Appendix Figure, panel C) indicate a high level of conservation among all members of the YFV group, alignments of the upstream AUG region (online Technical Appendix Figure, panel D) highlight a clear separation of FRV, SEPV, and WESSV from YFV. When we assessed the string of tandem repeats in the 3' UTR, some differences between FRV, SEPV, and WESSV emerged. We identified 3 highly conserved repeats in the 3' UTR of FRV (RFR1, RFR2, and RFR3; online Technical Appendix Figure, panel B), which are most similar to the previously described sequences identified in YFV (RYF1, RYF2, and RYF3). Strikingly, WESSV (69.7%–90.6%) and FRV (72.7%–90.6%) retained homologous sequences to RYF1, RYF2, and RYF3, and SEPV retained only a vestigial repeat sequence (RSEP3) that is highly divergent from all other members of the YFV group, including FRV.

FRV shares a common ancestor with SEPV (with 100% bootstrap support) (Figure 2) and is located in the distinct YFV group according to International Committee on Taxonomy of Viruses classification (15). Analysis of the 12 cleavage sites located within the polyprotein open reading frame, following the scheme described by Kuno and Chang (19), supported the phylogenetic structure of the YFV group; YFV displayed marked divergence from FRV, SEPV, and WESSV in several cleavage sites, including Ci/PrM, NS1/NS2a, NS2a/NS2b, and NS2b/NS3 (online Technical Appendix Figure, panel E).

Viruses Isolated from Mosquitoes

Mosquitoes yielding isolates of FRV were collected at Fitzroy Crossing in the West Kimberley region in 2011 (Table 3); FRV was isolated from 2 pools of *Ae. normanensis* and 1 pool of *Anopheles amictus* mosquitoes. In 2012, a similar

level of sampling in the same geographic area (data not shown) showed a shift of activity away from Fitzroy Crossing to a broader area in the eastern and southern Kimberley region, encompassing Billiluna, Kununurra, and Wyndham (Table 3). Sixteen isolates were obtained, most (81.2%) from *Ae. normanensis* mosquitoes (Table 3) and all from female mosquitoes. Additional virus was isolated from *An. amictus*, *Culex annulirostris*, and a pool of damaged and unidentifiable *Aedes* spp. mosquitoes. The minimum infection rate was greatest at Billiluna (2.5 FRV-infected mosquitoes/1,000 mosquitoes; Table 4). Other arboviruses detected during these seasons included MVEV, KUNV, KOKV, RRV, and Sindbis virus (Table 3).

In Vitro Virus Replication

FRV replicated in all 4 cell lines tested. At all time points, the FRV titer grew higher in BSR than in other cell lines, with the exception of Vero cells on day 7; the difference was usually significant (Table 5). Mild CPE was not apparent until day 4 in BSR cells and day 7 in Vero and DF-1 cells; no CPE was evident in C6/36 cells.

Virus Virulence in Mice

Two female mice in the 1,000 IU intracerebrally inoculated group and 1 female mouse in the 100 IU intracerebrally inoculated group had hind limb weakness, intermittent photophobia, and/or mild retrobulbar swelling between 5 and 12–13 dpi; however, only 1 female mouse in each intracerebrally inoculated group received a score of 1 on 1–2 days (days 5 and 9). By 13–14 dpi, all mice appeared to be clinically healthy. The only abnormality in intraperitoneally inoculated mice was mild photophobia in 1 mouse in the 1,000 IU group at 6 dpi. Mock-challenged animals showed no clinical

abnormalities throughout the study period. All intracerebrally inoculated mice seroconverted; antibody titers were ≥ 160 . In the intraperitoneally inoculated group, 6 mice in the 100 IU group seroconverted and 8 mice in the 1,000 IU group seroconverted (titers 40 to ≥ 160), indicating successful FRV replication.

For the 3 mice in which subtle clinical signs developed, we processed the heads for histopathology. We found histopathologic signs of meningoencephalitis in all 3 (Figure 3, panels A–D). The lesions were most notable in the 1,000 IU intracerebrally inoculated group, corroborating

the mild clinical signs observed. The least severe lesions were seen in the mouse from the 100 IU intracerebrally inoculated group; however, the lesions were unilateral in the hemisphere not inoculated. In the other 2 mice, the trend was toward greater severity in the inoculated hemisphere; however, in the other hemisphere and distant from the inoculation site, we found leukocyte infiltration, gliosis, and neuronal degeneration. No viral antigen was detected in the affected brains by immunohistochemistry, suggesting that FRV was cleared at the time of euthanasia (21 dpi).

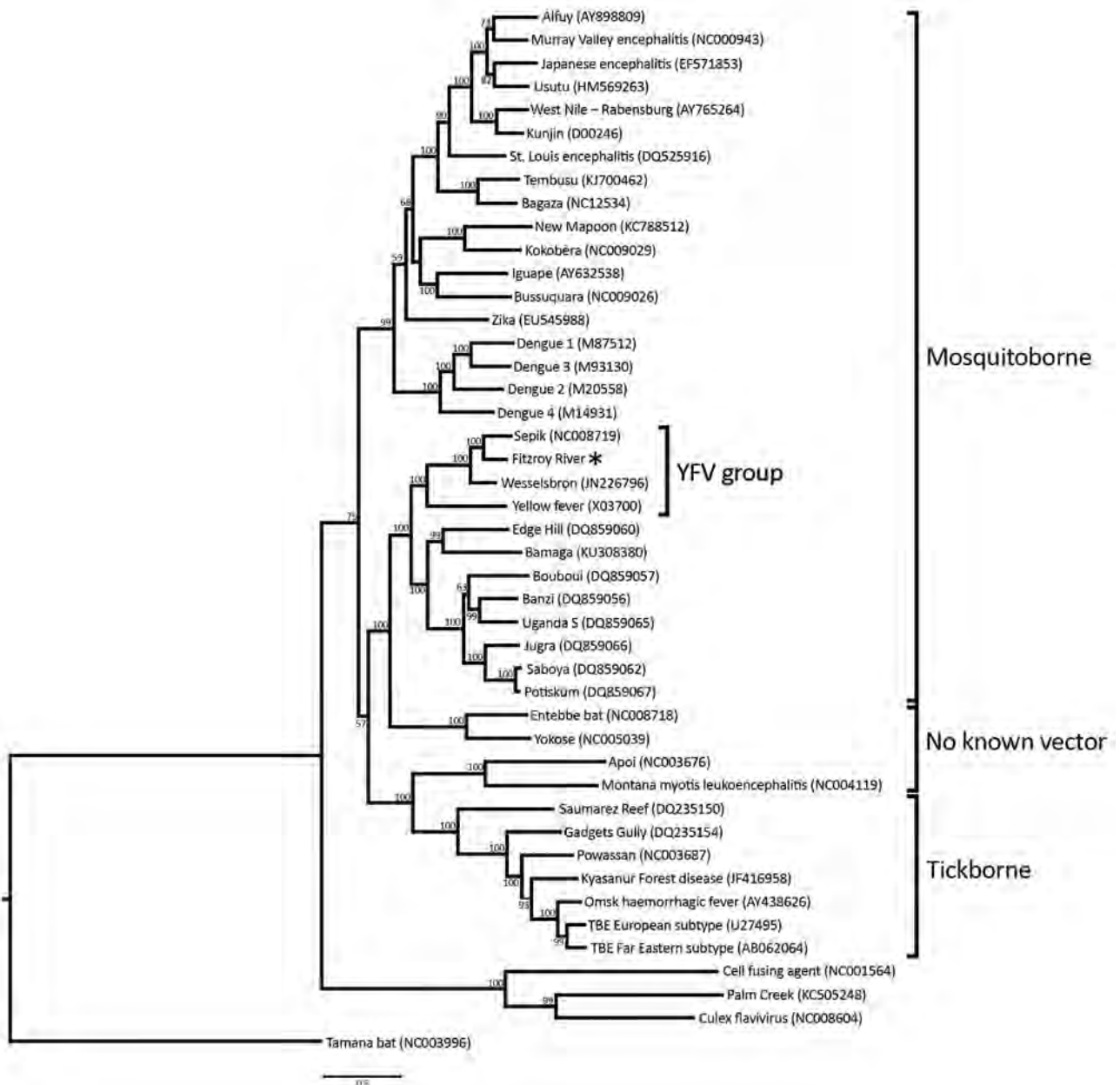


Figure 2. Phylogenetic tree of the genus *Flavivirus*, based on full polyprotein nucleotide sequences. Asterisk (*) indicates Fitzroy River virus. Scale bar indicates nucleotide substitutions per site. YFV, yellow fever virus.

Table 3. Mosquito species collected and arboviruses isolated from the Kimberley region of Western Australia, Australia, 2011 and 2012*

Year, location, mosquito species	No. (%) collected	No. processed	No. pools processed	No. virus isolates
2011				
Fitzroy Crossing				
<i>Ae. (Ochlerotatus) normanensis</i>	4,657 (38.4)	2,497	110	2 FRV, 3 non A/F
<i>An. (Cellia) amictus</i>	750 (6.2)	504	29	1 FRV, 4 non A/F
<i>An. (Cellia) annulipes</i> s.l.	2,879 (23.7)	1,898	84	6 non A/F
<i>Cx. (Culex) annulirostris</i>	3,202 (26.4)	1,773	79	2 MVEV, 1 KUNV, 1 KUNV+SINV, 6 non A/F
Other	635 (5.2)	482	100	1 non A/F†
Subtotal	12,123 (100)	7,154	402	
2012				
Billiluna				
<i>Ae. (Macleaya) tremulus</i>	252 (2.0)	135	14	
<i>Ae. (Ochlerotatus) normanensis</i>	1,679 (13.4)	1,244	58	3 FRV
<i>An. (Cellia) amictus</i>	650 (5.2)	508	42	
<i>An. (Cellia) annulipes</i> s.l.	3,456 (27.5)	1,555	74	
<i>An. (Cellia) novaguinensis</i>	247 (2.0)	152	18	
<i>Cx. (Culex) annulirostris</i>	5,608 (44.6)	3,424	148	2 MVEV
Damaged <i>Anopheles</i> spp.	131 (1.0)	83	14	
Damaged <i>Culex</i> spp.	218 (1.7)	111	15	
Other	326 (2.6)	199	84	
Subtotal	12,567 (100)	7,411	467	
Kununurra				
<i>Ae. (Finlaya) notoscriptus</i>	455 (1.3)	381	31	
<i>Ae. (Neomellanoconion) lineatopennis</i>	3,457 (9.9)	1540	80	
<i>Ae. (Ochlerotatus) normanensis</i>	12,632 (36.2)	4917	219	7 FRV, 2 RRV
<i>An. (Anopheles) bancroftii</i>	2,428 (7.0)	723	52	
<i>An. (Cellia) annulipes</i> s.l.	1,758 (5.0)	1025	67	
<i>An. (Cellia) meraukensis</i>	2,717 (7.8)	863	60	
<i>Cq. (Coquillettidia) xanthogaster</i>	931 (2.7)	796	55	
<i>Cx. (Culex) annulirostris</i>	7,600 (21.8)	4195	193	1 RRV
<i>Ve. (Verrallina) reesi</i>	468 (1.3)	287	33	
Damaged <i>Culex</i> spp.	350 (1.0)	253	30	1 RRV
Other	2,111 (6.0)	1528	369	4 RRV‡
Subtotal	34,907 (100)	16508	1189	
Wyndham				
<i>Ae. (Ochlerotatus) normanensis</i>	1,661 (5.4)	551	30	1 FRV, 1 RRV
<i>An. (Anopheles) bancroftii</i>	532 (1.7)	122	14	
<i>An. (Cellia) amictus</i>	1,589 (5.1)	380	26	
<i>An. (Cellia) annulipes</i> s.l.	982 (3.2)	262	20	
<i>An. (Cellia) meraukensis</i>	1,677 (5.4)	450	27	
<i>Cx. (Culex) annulirostris</i>	21,388 (69.1)	5,357	224	1 FRV, 2 KOKV, 4 RRV
<i>Cx. (Culex) crinicauda</i>	330 (1.1)	62	14	
Damaged <i>Culex</i> spp.	907 (2.9)	247	17	1 RRV
Other	1,881 (6.1)	898	206	1 FRV, 1 RRV§
Subtotal	30,947 (100)	8329	578	
Total	90,544	39,402	2,636	

*Only mosquito collection locations that yielded isolates of FRV are shown; species collected at abundance of <1.0% are grouped as "other"; named species are female mosquitoes only. Results from male mosquitoes are included in "other." *Ae.*, *Aedes*; *An.*, *Anopheles*; *Cq.*, *Coquillettidia*; *Cx.*, *Culex*; FRV, Fitzroy River virus; KOKV, Kokobera virus; KUNV, West Nile (Kunjin) virus; non A/F, not an alphavirus or flavivirus and identity is yet to be determined; MVEV, Murray Valley encephalitis virus; RRV, Ross River virus; SINV, Sindbis virus; *Ve.*, *Verrallina*.

†Isolated from female *Ae. lineatopennis* mosquito.

‡Isolated from female *Aedeomyia catasticta* (1), *Anopheles amictus* (1), and *Mansonia uniformis* (2) mosquitoes.

§FRV isolated from a pool of damaged female *Aedes* spp. mosquitoes, RRV isolated from female *An. bancroftii* mosquitoes.

Antibodies in Humans and Animals

A total of 366 serum samples from humans from northern Western Australia, submitted to PathWest Laboratory Medicine WA for alphavirus or flavivirus serologic testing from March through May in 2014 and 2015, were tested for antibodies to FRV (online Technical Appendix Table). Overall, the prevalence of antibodies to flaviviruses in the ELISA was 33.6%, of which initial screening showed an FRV neutralization titer ≥ 10 in 9 samples. For 3 of these samples, cross-

neutralization titers showed FRV antibody titers ≥ 40 and at least a 4-fold difference between antibody titer to FRV and other flaviviruses from Australia (Table 6), yielding an FRV positivity rate of 0.8% (3/336) of all samples tested and 2.4% (3/123) of samples with evidence of a flavivirus infection by ELISA. All 3 FRV antibody-positive samples were from the West Kimberley (Broome) region.

Serum from 227 sentinel cattle, 87 horses, and 178 sentinel chickens from the Northern Territory sampled

Table 4. Minimum infection rates of mosquitoes infected with FRV, Western Australia, Australia, 2011 and 2012*

Year, location, mosquito species	No. isolates	Minimum infection rate†
2011		
Fitzroy Crossing		
<i>Ae. (Ochlerotatus) normanensis</i>	2	0.8
<i>An. (Cellia) amictus</i>	1	2.0
2012		
Billiluna		
<i>Ae. (Ochlerotatus) normanensis</i>	3	2.5
Kununurra		
<i>Ae. (Ochlerotatus) normanensis</i>	7	1.4
Wyndham		
<i>Ae. (Ochlerotatus) normanensis</i>	1	1.8
<i>Cx. (Culex) annulirostris</i>	1	0.2
Damaged <i>Aedes</i> spp.	1	1.1

**Ae.*, *Aedes*; *An.*, *Anopheles*; *Cx.*, *Culex*; FRV, Fitzroy River virus.

†No. FRV-infected mosquitoes/1,000 mosquitoes; calculated according to (35).

from 2009/10 through 2014/15 were tested for antibodies to FRV. Neutralizing antibodies to FRV were detected in horses (12.6%) and cattle (6.6%). FRV and SEPV cross-neutralization tests on a subsample of FRV antibody-positive serum samples indicated that the FRV infections were not the result of serologic cross-infection with closely related SEPV (data not shown), which occurs in neighboring Papua New Guinea. One sentinel chicken had a low FRV antibody titer. Most FRV infections in domestic animals ($n = 24$; 77%) were from 2012/13. We also tested serum from 25 wallabies, 1 wallaroo, and 1 bandicoot from the Northern Territory, collected from 2006/07 through 2013/14. Low levels of FRV antibodies were found in 1 wallaby from the Darwin region in January 2007. We found no association between infection and clinical disease in any cattle, horses, chickens, or marsupials tested.

Discussion

The new flavivirus from northern Australia, for which we proposed the name Fitzroy River virus, was first isolated from *Ae. normanensis* mosquitoes collected near the Fitzroy River. Phylogenetic analysis of isolate K73884 demonstrates that FRV belongs to the YFV group (15). Cleavage recognition sequence analysis groups FRV together with WESSV and SEPV, but distinct from YFV, reflecting the pattern of amino acid homology of members of the YFV group across the polyprotein. When homology of individual viral proteins is assessed, FRV is

most closely related to SEPV in all regions excluding some nonstructural components that have a required role in replication (36,37), notably NS4a and 2k, where homology to WESSV was higher. We found no evidence of recombination breakpoints occurring along the FRV genome, and the low (70%) amino acid homology observed in the 2k peptide is most likely the result of a collection of nonsynonymous mutations. However, this recombination analysis was limited to 44 reference flavivirus sequences; a larger collection that includes more YFV group isolates from the Southeast Asia region may reveal further insights into the evolutionary history of FRV.

The phylogenetic placement of FRV in the YFV group is further supported by analysis of features in the flavivirus UTRs (cyclization sequence, upstream AUG region, and tandem repeats), sequences that are functionally necessary for enhancing replication through formation of secondary RNA structures (38). Although we observed near complete consensus in the cyclization sequence at each terminus between these 4 viruses, FRV had higher levels of identity to SEPV and WESSV than YFV across the respective upstream AUG regions. Conversely, the tandem repeats found in the 3' UTR showed consistently high nucleotide identities (>80% across all 3 sites) with YFV rather than WESSV and SEPV. Together, these data indicate that FRV possesses a unique collection of sequence signatures that distinguish it from other members of the YFV group.

Table 5. Fitzroy River virus replication in 4 cell lines

Day	Mean Fitzroy River virus titer*			
	C6/36	Vero	BSR	DF-1
1	0 ^a	0 ^a	3.07 ± 0.06 ^b	0 ^a
2	4.68 ± 0.21 ^a	3.78 ± 0.05 ^b	5.13 ± 0.06 ^c	3.81 ± 0.3 ^{ab}
3	5.58 ± 0.05 ^a	4.72 ± 0.02 ^b	6.67 ± 0.08 ^c	5.5 ± 0.08 ^a
4	6.66 ± 0.09 ^a	5.02 ± 0.07 ^b	6.72 ± 0.05 ^a	6.26 ± 0.15 ^a
7	4.41 ± 0.14 ^a	7.01 ± 0.01 ^b	6.6 ± 0.21 ^b	4.25 ± 0.23 ^a

*Statistical significance of log transformed arithmetic means was determined with 2-way analysis of variance with correction for multiple comparisons and using the Tukey method for pairwise multiple comparisons (GraphPad Prism version 6.0; GraphPad Software Inc, San Diego, CA, USA). Means ± SE in the same row followed by the same superscript letter did not differ significantly ($p > 0.05$). Results at day 0 were excluded because virus detected at this time point represented residual inoculum.

The origin of FRV is unknown. Although increased surveillance in neighboring countries is needed, arbovirus and mosquito monitoring has been pursued in northern Western Australia since the early 1970s (39,40) with only minor changes in strategy. FRV was not detected by virus culture from earlier mosquito collections, a finding consistent with recent introduction into Western Australia and possibly elsewhere in Australia, thus highlighting the value of ongoing surveillance activities. We cannot exclude the possibility that FRV was circulating in mosquitoes of species (or other insect vectors) not commonly collected in traps routinely used for surveillance of adult mosquitoes in Western Australia and that genetic changes enabled the virus to adapt to a new host species, as has been seen with chikungunya virus (41).

Phylogenetic analysis indicated that FRV is most closely related to SEPV in the YFV group, which is currently found only in Papua New Guinea, and WESSV, which occurs in Africa and Thailand. Recent experience with introduction of likely or suspected arbovirus and arbovirus vectors into northern Australia suggests that FRV was probably introduced from Southeast Asia. Included are introductions by mosquitoes such as *Aedes aegypti* (L.), *Aedes vexans*, and *Culex gelidus* (42,43) and introductions of viruses including Japanese encephalitis virus from Papua New Guinea (44), bluetongue viruses from Southeast Asia (45,46), and epizootic hemorrhagic disease virus 1 from Indonesia (47).

Most (81%) FRV has been isolated from *Ae. normanensis* mosquitoes, providing circumstantial evidence that this species may be the dominant vector. Mosquito collections at each locality were conducted ≈ 2 –3 weeks after a period of high rainfall following a relatively dry period. These conditions favor an abundance of *Ae. normanensis* mosquitoes because these mosquitoes rapidly hatch from desiccation-resistant eggs (48). The detection of antibodies to FRV in sentinel animals from the Northern Territory is consistent with the range and feeding behavior of *Ae. normanensis* mosquitoes and indicates a wide distribution of FRV in northern Australia.

Our finding of serologic evidence of human infection by FRV, despite low prevalence and apparent confinement to the West Kimberley region, is noteworthy. We detected FRV more extensively across northern Western Australia, so further human infections are likely. Because these samples had been sent for routine diagnostic arbovirus testing, it is presumed that most persons had a clinical illness of concern; however, we did not have access to detailed clinical information. Also, because the samples were single rather than paired acute- and convalescent-phase samples, we could not determine whether the FRV antibodies are the result of acute or previous infections. The antibody titers to FRV in humans were low, and although the cross-neutralizations included all known Australian flaviviruses that replicate in the cell lines we used, these persons may have been infected with an unrecognized flavivirus.

The close relationship of FRV with WESSV and SEPV may indicate potential for FRV to affect domestic animals such as cattle, goats, and sheep. Cattle stations are a dominant agricultural feature of northern Australia. Given that most FRV was isolated from *Ae. normanensis* mosquitoes, that mosquitoes of this species readily feed on cattle and horses, and that the FRV antibody prevalence in sentinel cattle and horses in the Northern Territory was high, we believe that the enzootic transmission cycle for FRV probably involves *Ae. normanensis* mosquitoes and domestic animals such as cattle and horses. Infection with FRV was not associated with clinical disease in animals but could potentially be disguised by other arbovirus infections, such as bovine ephemeral fever (49).

The finding of mild clinical signs in FRV-infected weanling mice, more often in those that were intracerebrally infected, indicates that severe clinical disease may be unlikely unless the health of the animal host is compromised. Further research is required to determine if FRV causes clinical disease in humans or domestic animals. The outcomes of this study demonstrate the value of surveillance for mosquito-borne viruses in the detection, characterization, and impact assessment of novel and known arboviruses.

Table 6. Serologic test results for 9 serum samples from humans from northern Western Australia, which contained FRV neutralizing antibodies at initial testing*

Sample	ELISA, % block	FRV initial neutralization titer	Cross-neutralization titers						Infecting virus	
			FRV	MVEV	KUNV	ALFV	KOKV	STRV		EHV
2014–1	79	10	<10	<10	<10	<10	<10	<10	<10	UD
2014–2	87	20	<10	10	10	<10	10	10	40	EHV
2014–3	86	40	<10	<10	<10	<10	<10	20	80	EHV
2014–4	84	160	40	<10	10	<10	<10	10	<10	FRV
2015–1	90	80	<10	<10	160	<10	<10	<10	<10	KUNV
2015–2	92	20	<10	<10	80	<10	<10	<10	<10	KUNV
2015–3	98	40	80	<10	10	<10	<10	<10	<10	FRV
2015–4	95	80	80	10	20	<10	10	10	20	FRV
2015–5	98	10	<10	<10	10	<10	<10	<10	<10	UD

*ALFV, Alfuy virus (K74157); EHV, Edge Hill virus (K74003); FRV, Fitzroy River virus (K73884); KOKV, Kokobera virus (K69949); KUNV, West Nile (Kunjin) virus (K81136); MVEV, Murray Valley encephalitis virus (K68150); STRV, Stratford virus (C338); UD, undetermined.

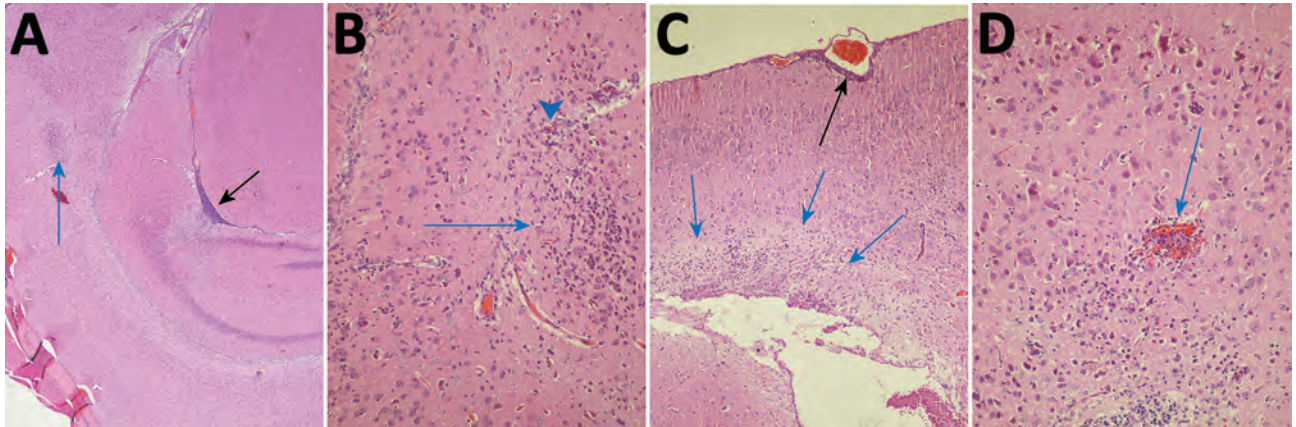


Figure 3. Photomicrographs of Fitzroy River virus (FRV)-induced meningoencephalitis in weanling mice inoculated with 1,000 infectious units of FRV. Panels show multifocal mild to severe perivascular and neuropil infiltration of lymphocytes and monocytes (blue arrows in A–C); meningitis in a sulcus (black arrow in A); glial cell activation with notable astrocytosis, neuron degeneration, and neuronophagia (arrowhead in B); occasional hemorrhage (blue arrow in D); mild periventricular spongiosis (blue arrows in C); and meningitis (black arrow in C). Hematoxylin and eosin staining. Original magnifications: A) $\times 40$, B) $\times 400$, C) $\times 100$, D) $\times 400$.

Acknowledgments

We thank Michael Lindsay, Peter Neville, and Susan Harrington for assistance with mosquito collections. The assistance of Sarah Power, Margaret Wallace, and Michael Burley with mosquito identification and virus detection is gratefully acknowledged. Technical staff at PathWest provided assistance with PCR and sequencing, and Stephen Davis kindly performed the neutralization assays on animal serum from the Northern Territory. Willy Suen, Caitlin O'Brien, and Agathe Colmant assisted with animal experiments. We also thank John Mackenzie for helpful discussion and the Medical Entomology Branch of the WA Department of Health for funding.

Additional financial support was provided by the Department of Health through the Funding Initiative for Mosquito Management in Western Australia. S.H.W. and W.L.L. were supported by the National Institutes of Health (grant no. AI109761, Center for Research and Diagnostics and Discovery, Center for Excellence in Translational Research). D.T.W. was funded by the Australian Government Department of Agriculture and Water Resources.

Dr. Johansen is a senior medical scientist at PathWest Laboratory Medicine WA and adjunct senior research fellow at The University of Western Australia; her research interests include mosquito and arbovirus surveillance and ecology of arboviruses and vectors. Mr. Williams is a staff associate at the Center for Infection and Immunity, Columbia University, New York, USA; his research interests include rodent and arthropodborne viruses and disease transmission.

References

- Broom AK, Lindsay MDA, Harrington SA, Smith DW. Investigation of the southern limits of Murray Valley encephalitis activity in Western Australia during the 2000 wet season. *Vector Borne Zoonotic Dis.* 2002;2:87–95. <http://dx.doi.org/10.1089/153036602321131887>
- Broom AK, Lindsay MDA, Johansen CA, Wright AET, Mackenzie JS. Two possible mechanisms for survival and initiation of Murray Valley encephalitis virus activity in the Kimberley region of Western Australia. *Am J Trop Med Hyg.* 1995;53:95–9. <http://dx.doi.org/10.4269/ajtmh.1995.53.95>
- Johansen CA, Susai V, Hall RA, Mackenzie JS, Clark DC, May FJ, et al. Genetic and phenotypic differences between isolates of Murray Valley encephalitis virus in Western Australia, 1972–2003. *Virus Genes.* 2007;35:147–54. <http://dx.doi.org/10.1007/s11262-007-0091-2>
- Russell RC. Arboviruses and their vectors in Australia: an update on the ecology and epidemiology of some mosquito-borne arboviruses. *Review of Medical and Veterinary Entomology.* 1995;83:141–58.
- Johansen C, Broom A, Lindsay M, Avery V, Power S, Dixon G, et al. Arbovirus and vector surveillance in Western Australia, 2004/05 to 2007/08. *Arbovirus Research in Australia.* 2009;10:76–81.
- Cowled C, Palacios G, Melville L, Weir R, Walsh S, Davis S, et al. Genetic and epidemiological characterization of Stretch Lagoon orbivirus, a novel orbivirus isolated from *Culex* and *Aedes* mosquitoes in northern Australia. *J Gen Virol.* 2009;90:1433–9. <http://dx.doi.org/10.1099/vir.0.010074-0>
- Rohe D, Fall RP. A miniature battery powered CO₂ baited light trap for mosquito borne encephalitis surveillance. *Bulletin of the Society of Vector Ecology.* 1979;4:24–7.
- Broom AK, Wright AE, MacKenzie JS, Lindsay MD, Robinson D. Isolation of Murray Valley encephalitis and Ross River viruses from *Aedes normanensis* (Diptera: Culicidae) in Western Australia. *J Med Entomol.* 1989;26:100–3. <http://dx.doi.org/10.1093/jmedent/26.2.100>
- Lindsay MDA, Broom AK, Wright AE, Johansen CA, Mackenzie JS. Ross River virus isolations from mosquitoes in arid regions of Western Australia: implication of vertical transmission as a means of persistence of the virus. *Am J Trop Med Hyg.* 1993;49:686–96. <http://dx.doi.org/10.4269/ajtmh.1993.49.686>
- Quan PL, Williams DT, Johansen CA, Jain K, Petrosov A, Diviney SM, et al. Genetic characterization of K13965, a strain of Oak Vale virus from Western Australia. *Virus Res.* 2011;160:206–13. <http://dx.doi.org/10.1016/j.virusres.2011.06.021>
- Pierre V, Drouet MT, Deubel V. Identification of mosquito-borne flavivirus sequences using universal primers and reverse transcription/polymerase chain reaction. *Res Virol.* 1994;145:93–104. [http://dx.doi.org/10.1016/S0923-2516\(07\)80011-2](http://dx.doi.org/10.1016/S0923-2516(07)80011-2)

12. Schmieder R, Edwards R. Quality control and preprocessing of metagenomic datasets. *Bioinformatics*. 2011;27:863–4. <http://dx.doi.org/10.1093/bioinformatics/btr026>
13. Langmead B, Salzberg SL. Fast gapped-read alignment with Bowtie 2. *Nat Methods*. 2012;9:357–9. <http://dx.doi.org/10.1038/nmeth.1923>
14. Chevreur B, Wetter T, Suhai S. Genome sequence assembly using trace signals and additional sequence information. *Computer Science and Biology: Proceedings of the German Conference on Bioinformatics*. 1999;99:45–56.
15. King AMQ, Adams MJ, Carstens EB, Lefkowitz EJ. *Virus Taxonomy: Ninth Report of the International Committee of Taxonomy of Viruses*. London: Elsevier Academic Press; 2012.
16. Kearse M, Moir R, Wilson A, Stones-Havas S, Cheung M, Sturrock S, et al. Geneious Basic: an integrated and extendable desktop software platform for the organization and analysis of sequence data. *Bioinformatics*. 2012;28:1647–9. <http://dx.doi.org/10.1093/bioinformatics/bts199>
17. Kumar S, Stecher G, Tamura K. MEGA7: Molecular Evolutionary Genetics Analysis version 7.0 for bigger datasets. *Mol Biol Evol*. 2016;33:1870–4. <http://dx.doi.org/10.1093/molbev/msw054>
18. Rice CM, Lenches EM, Eddy SR, Shin SJ, Sheets RL, Strauss JH. Nucleotide sequence of yellow fever virus: implications for flavivirus gene expression and evolution. *Science*. 1985;229:726–33. <http://dx.doi.org/10.1126/science.4023707>
19. Kuno G, Chang GJ. Characterization of Sepik and Entebbe bat viruses closely related to yellow fever virus. *Am J Trop Med Hyg*. 2006;75:1165–70.
20. Martin DP, Murrell B, Golden M, Khoosal A, Muhire B. RDP4: detection and analysis of recombination patterns in virus genomes. *Virus Evol*. 2015;1:vev003. <http://dx.doi.org/10.1093/ve/vev003>
21. Prow NA, May FJ, Westlake DJ, Hurrellbrink RJ, Biron RM, Leung JY, et al. Determinants of attenuation in the envelope protein of the flavivirus Alfuy. *J Gen Virol*. 2011;92:2286–96. <http://dx.doi.org/10.1099/vir.0.034793-0>
22. Reed LJ, Muench H. A simple method for estimating fifty percent end points. *Am J Hyg*. 1938;27:493–7.
23. Prow NA, Setoh YX, Biron RM, Sester DP, Kim KS, Hobson-Peters J, et al. The West Nile virus–like flavivirus Koutango is highly virulent in mice due to delayed viral clearance and the induction of a poor neutralizing antibody response. *J Virol*. 2014;88:9947–62. <http://dx.doi.org/10.1128/JVI.01304-14>
24. Suen WW, Prow NA, Setoh YX, Hall RA, Bielefeldt-Ohmann H. End-point disease investigation for virus strains of intermediate virulence as illustrated by flavivirus infections. *J Gen Virol*. 2016;97:366–77. <http://dx.doi.org/10.1099/jgv.0.000356>
25. Roby JA, Bielefeldt-Ohmann H, Prow NA, Chang DC, Hall RA, Khromykh AA. Increased expression of capsid protein in trans enhances production of single-round infectious particles by West Nile virus DNA vaccine candidate. *J Gen Virol*. 2014;95:2176–91. <http://dx.doi.org/10.1099/vir.0.064121-0>
26. Hall RA, Broom AK, Hartnett AC, Howard MJ, Mackenzie JS. Immunodominant epitopes on the NS1 protein of MVE and KUN viruses serve as targets for a blocking ELISA to detect virus-specific antibodies in sentinel animal serum. *J Virol Methods*. 1995;51:201–10. [http://dx.doi.org/10.1016/0166-0934\(94\)00105-P](http://dx.doi.org/10.1016/0166-0934(94)00105-P)
27. Johansen CA, Mackenzie JS, Smith DW, Lindsay MD. Prevalence of neutralising antibodies to Barmah Forest, Sindbis and Trubanaman viruses in animals and humans in the south-west of Western Australia. *Aust J Zool*. 2005;53:51–8. <http://dx.doi.org/10.1071/ZO03042>
28. Uren MF. Bovine ephemeral fever virus. In: Corner L, Bagust T, editors. *Australian Standard Diagnostic Techniques for Animal Disease*. Melbourne (Australia): The Commonwealth Scientific and Industrial Research Organisation; 1993.
29. Grard G, Moureau G, Charrel RN, Holmes EC, Gould EA, de Lamballerie X. Genomics and evolution of *Aedes*-borne flaviviruses. *J Gen Virol*. 2010;91:87–94. <http://dx.doi.org/10.1099/vir.0.014506-0>
30. Kuno G, Chang G-JJ, Tsuchiya KR, Karabatsos N, Cropp CB. Phylogeny of the genus *Flavivirus*. *J Virol*. 1998;72:73–83.
31. Henchal EA, Gentry MK, McCown JM, Brandt WE. Dengue virus-specific and flavivirus group determinants identified with monoclonal antibodies by indirect immunofluorescence. *Am J Trop Med Hyg*. 1982;31:830–6. <http://dx.doi.org/10.4269/ajtmh.1982.31.830>
32. Clark DC, Lobigs M, Lee E, Howard MJ, Clark K, Blitvich BJ, et al. In situ reactions of monoclonal antibodies with a viable mutant of Murray Valley encephalitis virus reveal an absence of dimeric NS1 protein. *J Gen Virol*. 2007;88:1175–83. <http://dx.doi.org/10.1099/vir.0.82609-0>
33. Broom AK, Hall RA, Johansen CA, Oliveira N, Howard MA, Lindsay MD, et al. Identification of Australian arboviruses in inoculated cell cultures using monoclonal antibodies in ELISA. *Pathology*. 1998;30:286–8. <http://dx.doi.org/10.1080/00313029800169456>
34. Macdonald J, Poidinger M, Mackenzie JS, Russell RC, Doggett S, Broom AK, et al. Molecular phylogeny of Edge Hill virus supports its position in the yellow fever virus group and identifies a new genetic variant. *Evol Bioinform Online*. 2010;6:91–6.
35. Chiang CL, Reeves WC. Statistical estimation of virus infection rates in mosquito vector populations. *Am J Hyg*. 1962;75:377–91.
36. Campbell CL, Smith DR, Sanchez-Vargas I, Zhang B, Shi PY, Ebel GD. A positively selected mutation in the WNV 2K peptide confers resistance to superinfection exclusion *in vivo*. *Virology*. 2014;464-465:228–32. <http://dx.doi.org/10.1016/j.virol.2014.07.009>
37. Miller S, Kastner S, Krijnse-Locker J, Bühler S, Bartenschlager R. The non-structural protein 4A of dengue virus is an integral membrane protein inducing membrane alterations in a 2K-regulated manner. *J Biol Chem*. 2007;282:8873–82. <http://dx.doi.org/10.1074/jbc.M609919200>
38. Gritsun TS, Gould EA. Origin and evolution of 3'UTR of flaviviruses: long direct repeats as a basis for the formation of secondary structures and their significance for virus transmission. *Adv Virus Res*. 2007;69:203–48. [http://dx.doi.org/10.1016/S0065-3527\(06\)69005-2](http://dx.doi.org/10.1016/S0065-3527(06)69005-2)
39. Liehne CG, Leivers S, Stanley NF, Alpers MP, Paul S, Liehne PFS, et al. Ord River arboviruses—isolations from mosquitoes. *Aust J Exp Biol Med Sci*. 1976;54:499–504. <http://dx.doi.org/10.1038/icb.1976.50>
40. Liehne PFS, Stanley NF, Alpers MP, Liehne CG. Ord River arboviruses—the study site and mosquitoes. *Aust J Exp Biol Med Sci*. 1976;54:487–97. <http://dx.doi.org/10.1038/icb.1976.49>
41. Tsetsarkin KA, Vanlandingham DL, McGee CE, Higgs S. A single mutation in chikungunya virus affects vector specificity and epidemic potential. *PLoS Pathog*. 2007;3:e201. <http://dx.doi.org/10.1371/journal.ppat.0030201>
42. Whelan P, Hayes G, Tucker G, Carter J, Wilson A, Haigh B. The detection of exotic mosquitoes in the Northern Territory of Australia. *Arbovirus Research in Australia*. 2001;8:395–404.
43. Johansen CA, Lindsay MDA, Harrington SA, Whelan PI, Russell RC, Broom AK. First record of *Aedes* (*Aedimorphus*) *vexans vexans* (Meigen) (Diptera: Culicidae) in Australia. *J Am Mosq Control Assoc*. 2005;21:222–4. [http://dx.doi.org/10.2987/8756-971X\(2005\)21\[222:FROAAV\]2.0.CO;2](http://dx.doi.org/10.2987/8756-971X(2005)21[222:FROAAV]2.0.CO;2)
44. Johansen CA, van den Hurk AF, Ritchie SA, Zborowski P, Nisbet DJ, Paru R, et al. Isolation of Japanese encephalitis virus from mosquitoes (Diptera: Culicidae) collected in the Western Province of Papua New Guinea, 1997–1998. *Am J Trop Med Hyg*. 2000;62:631–8. <http://dx.doi.org/10.4269/ajtmh.2000.62.631>

45. Pritchard LI, Sendow I, Lunt R, Hassan SH, Kattenbelt J, Gould AR, et al. Genetic diversity of bluetongue viruses in south east Asia. *Virus Res.* 2004;101:193–201. <http://dx.doi.org/10.1016/j.virusres.2004.01.004>

46. Melville LF, Pritchard LI, Hunt NT, Daniels PW, Eaton B. Genotypic evidence of incursions of new strains of bluetongue viruses in the Northern Territory. *Arbovirus Research in Australia.* 1997;7:181–6.

47. Weir RP, Harmsen MB, Hunt NT, Blacksell SD, Lunt RA, Pritchard LI, et al. EHDV-1, a new Australian serotype of epizootic haemorrhagic disease virus isolated from sentinel cattle in the Northern Territory. *Vet Microbiol.* 1997;58:135–43. [http://dx.doi.org/10.1016/S0378-1135\(97\)00155-7](http://dx.doi.org/10.1016/S0378-1135(97)00155-7)

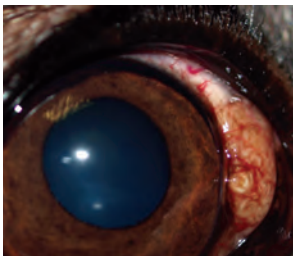
48. Webb C, Doggett S, Russell R. A guide to mosquitoes of Australia. Melbourne (Australia): CSIRO Publishing; 2016.

49. Geoghegan JL, Walker PJ, Duchemin JB, Jeanne I, Holmes EC. Seasonal drivers of the epidemiology of arthropod-borne viruses in Australia. *PLoS Negl Trop Dis.* 2014;8:e3325. <http://dx.doi.org/10.1371/journal.pntd.0003325>

Address for correspondence: Cheryl A. Johansen, PathWest Laboratory Medicine Western Australia–Microbiology, PP Block, QEII Medical Centre, Nedlands, WA 6909, Australia; email: cheryl.johansen@uwa.edu.au

May 2015: Vectorborne Infections

- Detecting Spread of Avian Influenza A(H7N9) Virus Beyond China
- Recent US Case of Variant Creutzfeldt-Jakob Disease—Global Implications
- Novel Thogotovirus Associated with Febrile Illness and Death, United States, 2014
- Transmission of Hepatitis C Virus among Prisoners, Australia, 2005–2012

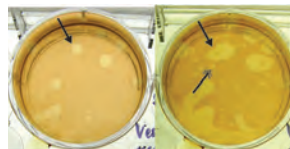


- Pathologic Changes in Wild Birds Infected with Highly Pathogenic Avian Influenza A(H5N8) Viruses, South Korea, 2014
- Itaya virus, a Novel Orthobunyavirus Associated with Human Febrile Illness, Peru
- Isolation of *Onchocerca lupi* in Dogs and Black Flies, California, USA

- Molecular Epidemiology of *Plasmodium falciparum* Malaria Outbreak, Tumbes, Peru, 2010–2012
- Delayed-Onset Hemolytic Anemia in Patients with Travel-Associated Severe Malaria Treated with Artesunate, France, 2011–2013
- Protective Antibodies against Placental Malaria and Poor Outcomes during Pregnancy, Benin
- Canine Distemper in Endangered Ethiopian Wolves
- Comparative Sequence Analyses of La Crosse Virus Strain Isolated from Patient with Fatal Encephalitis, Tennessee, USA
- Low-level Circulation of Enterovirus D68—Associated Acute Respiratory Infections, Germany, 2014
- Transmission Potential of Influenza A(H7N9)

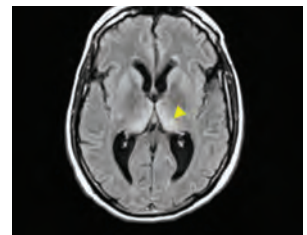


- Virus, China, 2013–2014
- Rapid Emergence of Highly Pathogenic Avian Influenza Subtypes from a Subtype H5N1 Hemagglutinin Variant
- Antimicrobial Drug Resistance of *Vibrio cholerae*, Democratic Republic of the Congo
- Postmortem Stability of Ebola Virus



- Influenza A(H5N8) Virus Similar to Strain in Korea Causing Highly Pathogenic Avian Influenza in Germany
- Malaria Imported from Ghana by Returning Gold Miners, China, 2013
- Canine Infections with *Onchocerca lupi* Nematodes, United States, 2011–2014
- Full-Genome Sequence of Influenza A(H5N8) Virus in Poultry Linked to Sequences of Strains from Asia, the Netherlands, 2014

- Novel Eurasian Highly Pathogenic Influenza A H5 Viruses in Wild Birds, Washington, USA, 2014
- *Culex torrentium* Mosquito Role as Major Enzootic Vector Defined by Rate of Sindbis Virus Infection, Sweden, 2009
- Getah Virus Infection among Racehorses, Japan, 2014
- Characterization of *Shigella sonnei* Isolate Carrying Shiga Toxin 2—Producing Gene
- Outbreak of *Leishmania braziliensis* Cutaneous Leishmaniasis, Saül, French Guiana
- Ciprofloxacin-Resistant *Shigella sonnei* Associated with Travel to India
- Fatal *Balamuthia mandrillaris* Meningoencephalitis in the Netherlands after Travel to The Gambia



**EMERGING
INFECTIOUS DISEASES**

<https://wwwnc.cdc.gov/eid/articles/issue/21/5/table-of-contents>

Genomic Characterization of Recrudescent *Plasmodium malariae* after Treatment with Artemether/Lumefantrine

Gavin G. Rutledge,¹ Ian Marr,¹ G. Khai Lin Huang, Sarah Auburn, Jutta Marfurt, Mandy Sanders, Nicholas J. White, Matthew Berriman, Chris I. Newbold, Nicholas M. Anstey, Thomas D. Otto, Ric N. Price

Plasmodium malariae is the only human malaria parasite species with a 72-hour intraerythrocytic cycle and the ability to persist in the host for life. We present a case of a *P. malariae* infection with clinical recrudescence after directly observed administration of artemether/lumefantrine. By using whole-genome sequencing, we show that the initial infection was polyclonal and the recrudescence isolate was a single clone present at low density in the initial infection. Haplotypic analysis of the clones in the initial infection revealed that they were all closely related and were presumably recombinant progeny originating from the same infective mosquito bite. We review possible explanations for the *P. malariae* treatment failure and conclude that a 3-day artemether/lumefantrine regimen is suboptimal for this species because of its long asexual life cycle.

During the past decade, intensification of malaria control efforts has substantially reduced the global burden of malaria from *Plasmodium falciparum*. This trend has often been associated with increased recognition of the burden of malarial disease caused by the other *Plasmodium* species (1). *P. malariae*, 1 of the 6 *Plasmodium* species that commonly infect humans, is endemic throughout parts of

Africa (2,3), South America (4), Asia, and the western Pacific (5). *P. malariae* is unique among the human-infective *Plasmodium* species in having a 72-hour intraerythrocytic life cycle with variable but often prolonged pre-erythrocytic intrahepatic development (6). *P. malariae* can persist in the human host for years and possibly an entire lifetime. Although it is often asymptomatic, chronic parasitemia in endemic areas is associated with substantial rates of illness, including anemia and nephrotic syndrome (7–9).

A key strategy for malaria elimination is strengthening of health systems to deliver early diagnosis and highly effective therapy. Artemisinin-based combination therapy (ACT) has been central to this approach, with proven efficacy against multidrug-resistant *P. falciparum*, multidrug-resistant *P. vivax*, and *P. knowlesi* (10–13). In recent years, there have been increasing calls for a universal policy of ACT for all species of malaria (10–13). However, the efficacy of ACT against *P. malariae* is poorly documented.

Although chronic infection with *P. malariae* is well-recognized (14), little is known regarding how the parasites manage to evade host immunity and the intrahost dynamics of the underlying parasite population. Recent advances in molecular genetics have produced the first descriptive analyses of the whole genome sequence of *P. malariae* (15,16). The *P. malariae* reference genome is 33.6 Mb in size, has 6,540 genes, and has an average guanine plus cytosine content of 24% (15).

We report a case of a *P. malariae* infection in a patient residing in a non-malaria-endemic environment that resulted in recrudescence months after treatment with artemether/lumefantrine (AL). By using whole-genome sequencing of isolates from the initial and the recrudescence infections, we show that the 2 major *P. malariae* haplotypes, constituting ≈90% of the parasite load in the initial infection, were cleared successfully by AL, whereas a third haplotype, constituting a minority subpopulation in the initial infection, survived and recrudescence.

¹These authors contributed equally to this article.

Author affiliations: Wellcome Trust Sanger Institute, Hinxton, Cambridge, United Kingdom (G.G. Rutledge, M. Sanders, M. Berriman, C.I. Newbold, T.D. Otto); Royal Darwin Hospital, Casuarina, Northern Territory, Australia (I. Marr, G.K.L. Huang, N.M. Anstey, R.N. Price); Menzies School of Health Research and Charles Darwin University, Darwin, Northern Territory, Australia (S. Auburn, J. Marfurt, N.M. Anstey, R.N. Price); Mahidol University Faculty of Tropical Medicine, Mahidol-Oxford Tropical Medicine Research Unit, Bangkok, Thailand (N.J. White); University of Oxford Centre for Tropical Medicine and Global Health, Oxford, United Kingdom (N.J. White, R.N. Price); University of Oxford Weatherall Institute of Molecular Medicine, Oxford (C.I. Newbold)

DOI: <https://doi.org/10.3201/eid2308.161582>

Results

The Patient

A 31-year-old Uganda-born man, weighing ≈77 kg (≈170 lbs), who had been a resident in Australia for 5 years sought care at Royal Darwin Hospital (Darwin, Northern Territory, Australia) on March 1, 2015, with a 4-day history of fevers and headaches. He had returned to Australia 56 days previously after a 2-week trip to Uganda visiting friends and relatives (Figure 1, panels A, E). He had spent 14 days in a rural malaria-endemic area in eastern Uganda. Although he had not taken regular malaria prophylaxis, he had self-medicated with a locally acquired oral course of AL on the second and third days of his trip, despite being clinically well (Figure 1, panels B, D). He returned to Australia (now a malaria-free country) in January 2015 until seeking care after a short febrile illness in

late February. On examination, he had a tympanic temperature of 37.5°C and a heart rate of 110 beats/min but no manifestations of severe malaria. Rapid diagnostic testing with BinaxNOW (Binax, Inc. Inverness Medical Professional Diagnostics, Scarborough, ME, USA) for malaria was positive for aldolase but negative for histidine-rich protein 2. Species-specific PCR was positive for *P. malariae* and negative for all other *Plasmodium* species (online Technical Appendix, <https://wwwnc.cdc.gov/EID/article/23/8/16-1582-Techapp1.pdf>). Thick and thin blood film examination confirmed *P. malariae* parasitemia (12,140 parasites/μL) with all stages of asexual development visible on the blood film (online Technical Appendix Figure 1, panels A, B). The blood film was otherwise unremarkable; in particular, no evidence for hyposplenism was found. The patient was not immunosuppressed, and an HIV serologic test was negative. A hepatitis C

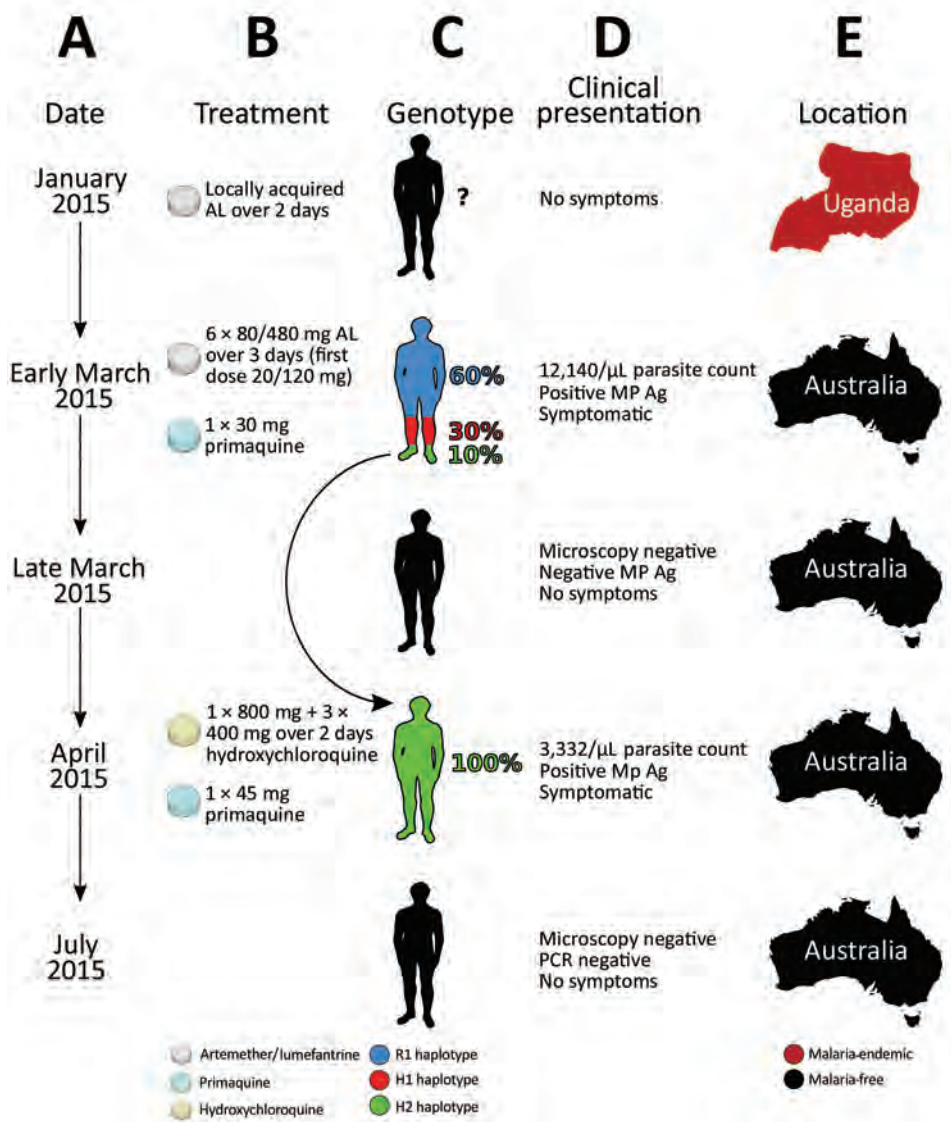


Figure 1. Timeline of the clinical case of a patient with *Plasmodium malariae* infection diagnosed and treated at Royal Darwin Hospital, Darwin, Northern Territory, Australia, March–April 2015, showing the timing (A), treatment (B), parasite’s genotype as inferred from whole-genome sequencing (C), clinical presentation (D), and location (E). The rounded arrow indicates the recrudescence of the minor haplotype 2 in the initial infection to dominate monoclally in the second infection. AL, artemether/lumefantrine; H1, haplotype 1; H2, haplotype 2; MP Ag, pan-malarial antigen; R1, reference haplotype.

serologic test was positive but with a viral load that was below the limit of quantification (<12 IU/mL).

The patient was administered a single 20/120 mg tablet of AL on the first day because of a prescribing error but subsequently continued with a supervised standard regimen of 80/480 mg every 12 hours taken with fatty food to complete a full course of 6 doses over 3 days, equivalent to a total dosage of 6.2 mg/kg of artemether and 37.4 mg/kg of lumefantrine. Glucose 6-phosphate dehydrogenase function was normal, and a single 30-mg dose of primaquine was administered on day 2. His hemoglobin was 126 g/dL and he received no blood transfusion. After treatment, his parasitemia declined to 1,269/ μ L at 32 hours, 488/ μ L at 41 hours, and 55/ μ L at 56 hours. He was afebrile and symptom-free within 36 hours of admission. However, before discharge on day 6, thick blood film examination was still positive (192/ μ L), but by day 11, his repeat blood film examination and his aldolase rapid diagnostic test results were negative.

The patient remained in urban Darwin but returned to the hospital 52 days later, on April 22, 2015, with a 2-week history of fevers, fatigue, and headache. Microscopy again identified *P. malariae* with a parasite count of 3,332/ μ L (online Technical Appendix Figure 1, panels C, D). Chloroquine was unavailable, so the patient was re-treated with oral hydroxychloroquine with an 800-mg loading dose, followed by 400 mg at 6 hours, 400 mg at 24 hours, 400 mg at 48 hours, and a single 45-mg dose of oral primaquine. The parasite count declined rapidly to 37/ μ L at 28 hours, 191/ μ L at 49 hours, and 76/ μ L at 88 hours of treatment. His symptoms resolved rapidly. Thick and thin blood films were negative on day 4 and remained negative on retesting at days 8, 35, 41, and 84, and the patient remained free of symptoms throughout. A PCR on blood collected at 12 weeks was also negative.

Whole-Genome Sequencing

Extensive sequencing was performed from blood samples obtained from the initial (PmUG01) and recrudescence (PmUG02) infection (online Technical Appendix Table 1), covering >99% of the genome at >20 \times for both infections. By using additional *P. malariae* samples published previously (15), we identified single-nucleotide polymorphisms (SNPs) using GATK's UnifiedGenotyper (Broad Institute, Cambridge, MA, USA) (17) and filtered them based on several parameters (online Technical Appendix Table 2). A multidimensional scaling plot of the samples based on their SNP allele frequency-spectra revealed that PmUG01 and PmUG02 were more closely related to each other than to any of the other samples (online Technical Appendix Figure 2), as expected if they were related recombinants derived from the same original infection.

Searching solely for SNPs that distinguish PmUG01 and PmUG02, we identified 2,631 variants after filtering (online Technical Appendix Table 2). PmUG01 was the sample from which the reference genome (R1) was constructed (15), and only 1 SNP in PmUG01 suggested a nucleotide base different from the reference strain, probably because it was in a repetitive region (online Technical Appendix Table 4). PmUG01 appeared to be a polyclonal infection with a bimodal distribution of alternate (i.e., nonreference) alleles at frequencies of 0.15 and 0.35 (online Technical Appendix Figure 3, panel A). Conversely, PmUG02 appeared to be a monoclonal infection with \approx 85% of sites being either fixed for the reference allele or for an alternative allele (online Technical Appendix Figure 3, panel B). Comparison of the initial and recrudescence infections revealed that heterozygous sites in the initial infection had become either homozygous alternate (\approx 40%) or homozygous reference (\approx 45%) (online Technical Appendix Table 4). Analysis of the genotype calls across the genome (online Technical Appendix Figure 4) revealed that, whereas the heterozygous sites from the initial infection were spread evenly across the 14 chromosomes, the homozygous alternate sites in the recrudescence infection were present in distinct clusters, implying that the initial infection was polyclonal and that the recrudescence was attributable to a single clone that was closely related to the reference clone.

Comparison of the distribution of the alternate allele frequencies throughout the genome of the initial and recrudescence strains (Figure 2) revealed bands of alleles at frequencies of \approx 0.15 and \approx 0.35 in the initial infection spatially clustered throughout the genome. The alleles that increased in relative frequency in PmUG02 were mostly at frequencies of \approx 0.15, whereas the alleles at frequencies of \approx 0.35 decreased in frequency and the positions became homozygous reference in PmUG02 (Figure 2). These data strongly suggested that, in addition to R1, 2 minor clones (minor haplotypes) were also present. Of these 2, the clone with the haplotype comprising alternate alleles at frequencies of \approx 0.35 (H1) appeared to have been eliminated during the drug treatment because no alleles specific to H1 were present in the recrudescence infection. The other minor clone comprised a haplotype with alternate alleles at frequencies of \approx 0.15 (H2) in the initial infection; this clone appeared to have caused the recrudescence (Figure 1, panel C). Based on the relative alternate allele frequencies of the 3 haplotypes in the initial infection, \approx 60% of the parasites were of the R1 haplotype, 30% of H1, and 10% of H2. These estimates were broadly consistent with the ratio of alleles in tri-allelic sites (0.69:0.22:0.09) (online Technical Appendix Table 5). The ratio of alleles in these tri-allelic sites changes markedly in PmUG02 (0.13:0.06:0.81), with over half of sites becoming homozygous for H2 but with some heterogeneity in the other sites (online Technical Appendix

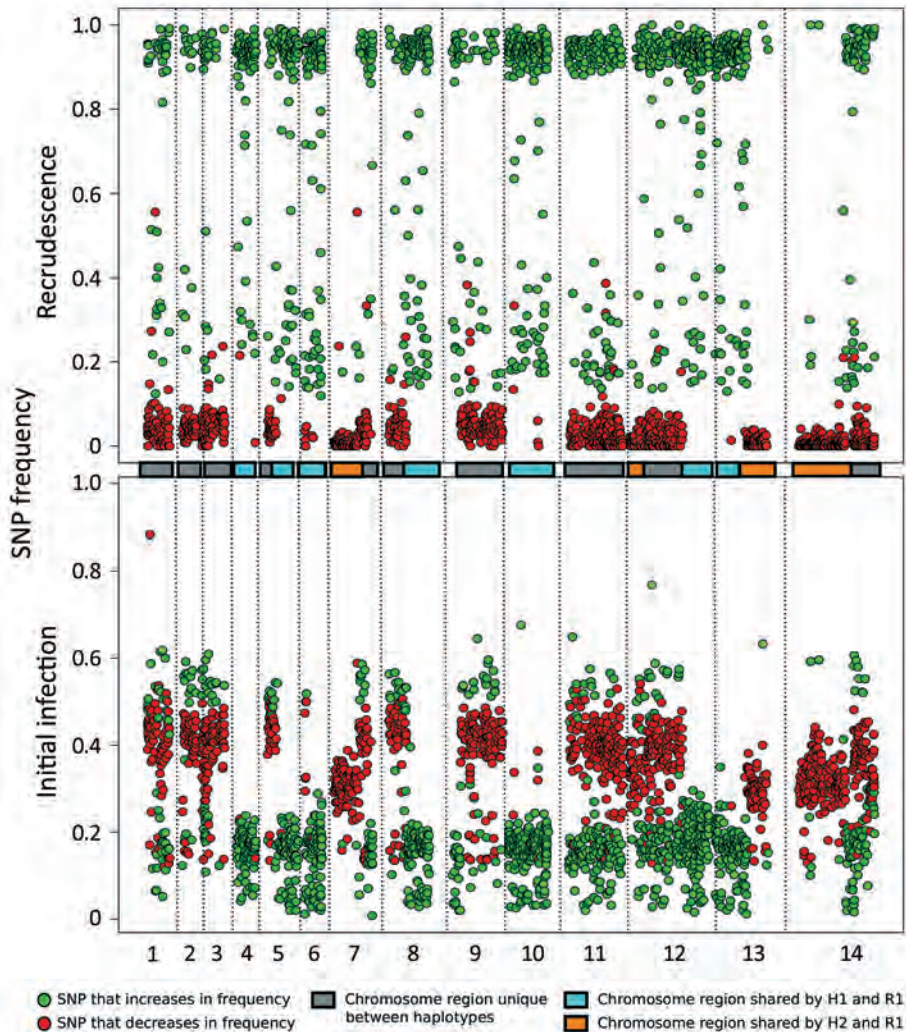


Figure 2. Analysis of the minor haplotype (H2) that caused recrudescence of *Plasmodium malariae* infection in a patient at Royal Darwin Hospital, Darwin, Northern Territory, Australia, March–April 2015, showing distribution of SNP alternative (nonreference) allele frequencies across the 14 chromosomes (boxes in the middle and dotted vertical lines) in the initial infection (bottom plot) and the recrudescence (top plot). The SNP colors (green, increasing in frequency; red, decreasing in frequency) form 2 clear bands, corresponding to H1 (yellow box) and H2 (pink box). H2 probably caused the recrudescence given that all of its alleles increase considerably in frequency. Colored boxes in center of chart indicate chromosome sharing. H1, haplotype 1; H2; haplotype 2; R1, reference genome; SNP, single-nucleotide polymorphism.

Table 6), probably because of the low coverage depth and because they were in repetitive regions.

Unexpectedly, several SNPs at high allele frequencies (>0.4) also increased in frequency in the recrudescence strain. Testing by using additional *P. malariae* samples (15) showed that $\approx 80\%$ of these SNPs were homozygous for the alternate allele in ≥ 1 other *P. malariae* samples, whereas $\approx 30\%$ were homozygous in all other *P. malariae* samples (online Technical Appendix Figure 5). This observation indicated that of these unusual SNPs, $\approx 50\%$ were highly polymorphic, whereas $\approx 30\%$ were probably low-frequency SNPs with rare variants present in the reference strain. This would explain the observation of SNPs with high reference allele frequency in the initial infection that became homozygous alternate in the recrudescence, given that they were probably SNPs with alternate alleles shared by H1 and H2.

To clarify the relationships of the different haplotypes with each other, we classified every genome region by whether any of the 3 haplotypes were identical to each other

(Figure 2; online Technical Appendix). Approximately 25% of the genome is shared between H1 and R1 and between H2 and R1. No regions were shared between H1 and H2, which suggested that both H1 and H2 were half-siblings of R1, although they did not share any parent between themselves (online Technical Appendix Figure 6). The finding that all haplotypes were related to each other through R1 further suggested that all strains were transmitted from the same mosquito bite and that the mosquito ingested at least 4 different parental haplotypes (online Technical Appendix Figure 6).

Analysis of SNPs in orthologs of known drug-resistance genes identified 3 nonsynonymous SNPs in the multidrug resistance protein 2 (*mdr2*) gene, 1 of which was in the ABC transporter domain, and 2 in the ABC transporter domain of ABC transporter C family member 2, present in the recrudescence strain (H2) but not the other strains (online Technical Appendix Table 7). No evidence was found for copy number variation in any gene compared with the reference strain, and the reference strain did not appear to

have an amplification of the multidrug resistance protein 1 gene compared with any of the other *P. malariae* samples.

Discussion

This report of a case of recurrent *P. malariae* malaria is unusual in that it describes the molecular characterization and confirmation of a treatment failure after directly observed, appropriately administered, quality-assured AL dosing in a nonendemic environment where reinfection was not possible. Whole-genome sequencing demonstrated that the recrudescence was attributable to a minor clone present in the initial polyclonal infection. The case raises 2 important questions: first, what was the cause of treatment failure; and second, why did recrudescence arise from the minor clone rather than a dominant reference clone?

Although the efficacy of AL for *P. malariae* infection is assumed in many national guidelines (18), *P. malariae*

monoinfections are relatively unusual and often of low density. To our knowledge, there have been no published efficacy series of AL with the long follow-up necessary to assess efficacy against a parasite with a 72-hour life cycle. In a nonrandomized efficacy study of 4 PCR-confirmed *P. malariae* infections treated with AL in Gabon (1 *P. malariae* monoinfection and 3 mixed *P. malariae/P. falciparum* infections), all 4 were microscopy negative at day 28, with no follow-up beyond this time (19). Among 80 PCR-confirmed *P. malariae/P. falciparum* mixed species infections in Uganda, 12% were still PCR-positive for *P. malariae* at day 7 and 6% were still PCR-positive on day 17 (20). An additional 3 reports have documented *P. malariae* infections occurring at 38 days, 47 days, and 4 months after AL treatment of an initial microscopy-diagnosed *P. falciparum* infection in returned travelers with no further possible malaria exposure (21–23).

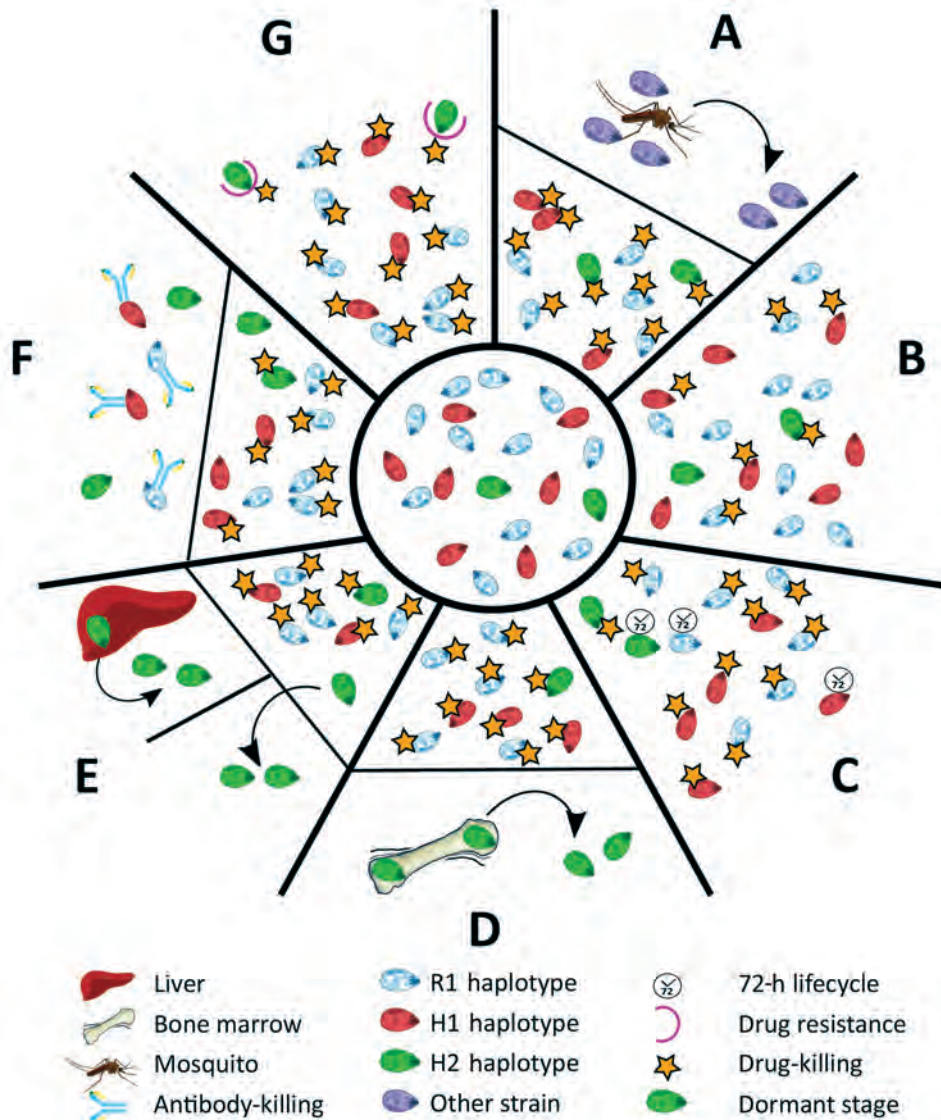


Figure 3. The different scenarios under which a second *Plasmodium malariae* infection could have occurred from the initial infection diagnosed in a patient at Royal Darwin Hospital, Darwin, Northern Territory, Australia, March–April 2015. Initial infection is shown in the inner circle. A) A completely new infection might have caused the second malaria onset. B) The drug might not have been absorbed at sufficient levels to kill all the parasites in the blood (pharmacokinetic cause). C) The longer intraerythrocytic life cycle of *P. malariae* (72 hours) might have enabled some parasites to survive the drug action until lumefantrine concentrations became subtherapeutic (pharmacokinetic cause). D) H2 parasites might have differentially sequestered with a biomass out of proportion with the peripheral parasitemia. E) Some parasites might have formed dormant stages in the liver, blood, or elsewhere (pharmacodynamic cause). F) An immune response might have been differentially primed against haplotypes at higher biomass. G) A haplotype within the initial infection might have been relatively drug resistant (fitness advantage). H1, haplotype 1; H2, haplotype 2; R1, reference genome.

Several plausible explanations might account for a recurrence of *P. malariae* parasitemia after treatment with AL (Figure 3). The last indigenous case of malaria in the Northern Territory was in 1962, with no subsequent cases of introduced malaria or autochthonous transmission (24); hence, the possibility of reinfection can be excluded (Figure 3, panel A). Additionally, the presence of the H2 haplotype in the initial infection and recrudescence infection confirms treatment failure.

Inadequate drug absorption resulting in suboptimal serum drug concentrations can cause treatment failure (Figure 3, panel B). Artemether is rapidly absorbed and eliminated (half-life of a few hours), whereas lumefantrine is variably absorbed and more slowly eliminated (half-life ≈ 3.2 days) (25). Lumefantrine is a lipophilic compound with erratic bioavailability unless administered with a small fatty meal (26), and for this reason, guidelines recommend administration of AL with a fatty meal such as milk or a small biscuit. In the case of our patient, we were unable to confirm adequate serum concentrations of lumefantrine; however, the patient took a complete course of treatment, and all doses were supervised in the hospital and administered with a milk biscuit to ensure good absorption. None of the treatment doses were vomited. In this scenario, one would expect $>98\%$ efficacy against *P. falciparum* (27). In addition, the clones associated with the R1 and H1 haplotypes, accounting for $\approx 90\%$ of the parasite load, were cleared, suggesting that the plasma drug concentrations were sufficient to eliminate both infections. Nevertheless, considerable inter-individual variation exists in lumefantrine exposure, and this patient may have had relatively low concentrations.

Cure of malaria in a nonimmune patient requires that antimalarial blood concentrations are sustained above the parasites' MIC until the entire parasite biomass has been eliminated. In the presence of antimalarial drugs, the parasite biomass generally decreases over time in an exponential manner, with drug concentrations needing to be sustained above the MIC for ≥ 4 life cycles (28). In the case of our patient, the baseline parasitemia at initial presentation was $12,000/\mu\text{L}$, which is relatively high compared with most *P. malariae* clinical infections (6). Thus, the combination of the long parasite life cycle such that 1 rather than 2 asexual cycles were exposed to artemether, and the short period (≈ 16 days) for which lumefantrine was at concentrations sufficient to kill the parasite may have resulted in parasites surviving the initial treatment and reestablishing a chronic parasitemia that was then sustained for 50 days before recrudescing (Figure 3, panel C).

Another possibility is that some parasites could have sequestered (Figure 3, panel D) or become dormant (Figure 3, panel E). Whereas dormancy would allow a proportion of the parasites to evade blood-stage schizontocidal

activity, plausible sites for sequestration of *P. malariae*-infected erythrocytes would still be exposed to therapeutic concentrations of blood-stage antimalarials, making this possibility an unlikely explanation for this patient's recrudescence infection. *P. malariae* is well-recognized as having a prolonged preerythrocytic phase and a prepatent period of 16–59 days (6). The initial treatment course of AL was administered 56 days after the patient left Uganda, so any preerythrocytic stages were probably not present at the time of initial AL treatment.

Although the ability to form hypnozoites (dormant exoerythrocytic stages) occurs in 3 human malaria parasite species (*P. vivax*, *P. ovale curtisi*, and *P. o. wallikeri*), the evidence that latent exoerythrocytic stages do not occur in *P. malariae* is limited (6). Case reports have documented *P. malariae* producing symptomatic disease many years after exposure to infection, as noted in the case of a 74-year-old woman in Greece with *P. malariae* reactivation after ≥ 40 years (29). Such latency suggests that low-level parasitemia could persist for many years after infection, and indeed may be lifelong. In the case of our patient, parasite recrudescence occurred >100 days after he had left a malaria-endemic area.

Although inadequate drug absorption (Figure 3, panel B), duration of treatment (Figure 3, panel C), or dormancy (Figure 3, panel E) all may have contributed to parasite recrudescence, these indiscriminate explanations would be expected to occur primarily in the dominant strain during the initial infection (28) (online Technical Appendix Figure 7). One could speculate that the H2 minor parasite population might have emerged from a hepatic schizont that ruptured days after those giving rise to the majority haplotypes and, despite genetic similarity, had substantial differences in surface antigenicity. The antibody response to the primary infection, which would have reached a maximum ≈ 3 weeks after the illness began, would have been directed against the majority haplotypes and might not have recognized the minor population (Figure 3, panel F). Alternatively, more of the minor population might have been in the dormant state compared with the dominant circulating clones with R1 or H1 haplotypes, or more might have been at a higher biomass in erythrocytes sequestered elsewhere, enabling a proportion to evade antimalarial drug action and recrudescence.

Finally, the minority clone with H2 haplotype might have recrudescence because of a fitness advantage over the other clones/haplotypes (online Technical Appendix Figure 7, panels B, C), possibly including relative resistance to either artemether or lumefantrine (Figure 3, panel G). In *P. falciparum*, resistance to artemether is acquired through mutations in the propeller domain of *K13* (30), whereas *P. falciparum* resistance to lumefantrine is associated with mutations and copy number

variation in the *Pfmdr1* gene (31,32). Although neither of these genes had nonsynonymous mutations in H2, 1 nonsynonymous mutation was noted in the ABC transporter domain of *mdr2*, potentially involved in artemisinin resistance (33,34), and 2 nonsynonymous mutations were noted in the multidrug resistance-associated protein 2 gene, which has been implicated in reduced ex vivo susceptibility to lumefantrine in *P. falciparum* (35). We also identified 2 nonsynonymous SNPs in the dihydrofolate reductase homologue. Low serum concentrations, a modest reduction in lumefantrine efficacy, the prolonged life cycle of *P. malariae*, and rapid elimination of lumefantrine all might have contributed to the observed treatment failure in our patient.

In conclusion, we have described a case of *P. malariae* recrudescence occurring in a non-malaria-endemic country after adequately administered AL. Whole-genome sequencing data revealed that the monoclonal recrudescence consisted of a minor haplotype that accounted for ≈10% of the initial infection and that all the haplotypes in the initial infection were related to each other and therefore probably originated from the same infective mosquito bite. Although the haplotypes were closely related, the genomic data suggest that ≥4 parental haplotypes were ingested by the mosquito, indicating considerable diversity and transmission of *P. malariae*. This case raises concerns about the adequacy of ACTs with a short half-life partner drug, such as AL, in treating *P. malariae* infections and suggests that optimal ACTs to treat *P. malariae* should include a slowly eliminated partner drug. Our findings reinforce the importance of a longer duration of follow-up monitoring of patients infected with *P. malariae* for late recrudescence.

The sequencing data generated in this study are provided in the European Nucleotide Archive under accession codes ERS1110316 and ERS1110319.

This work was supported by the Medical Research Council (grant no. MR/J004111/1) and the Wellcome Trust (grant no. 098051 and Senior Fellowship in Clinical Science to R.N.P., 200909). R.N.P., C.I.N., and N.J.W. are funded by the Wellcome Trust. N.M.A. is supported by the National Health and Medical Research Council (practitioner fellowship no. 1042072).

Author contributions: I.M., G.K.L.H., N.M.A., and R.P. oversaw the clinical presentation and management of the patient; S.A., and J.M. coordinated laboratory processing and collection of isolates; T.D.O. and R.N.P. designed the study; M.S. coordinated sequencing; G.G.R. performed the data analysis and with I.M. wrote the manuscript; and N.M.A., M.B., C.I.N., N.J.W., S.A., J.M., N.M.A., T.D.O., and R.N.P. critically revised the manuscript. All authors read and approved the manuscript. The authors declare that they have no conflicts of interest.

Mr. Rutledge is a doctoral student in the Parasite Genomics and the Natural Genetic Variation groups at the Wellcome Trust Sanger Institute, Hinxton, United Kingdom. His primary research interest is the application of computational tools and methods to improve our understanding of human malaria. Dr. Marr is an infectious disease and microbiology physician at the Royal Darwin Hospital, Darwin, Northern Territory, Australia.

References

- Abeyasinghe RR, Galappaththy GN, Smith Gueye C, Kahn JG, Feachem RG. Malaria control and elimination in Sri Lanka: documenting progress and success factors in a conflict setting. *PLoS One*. 2012;7:e43162. <http://dx.doi.org/10.1371/journal.pone.0043162>
- Boudin C, Robert V, Verhave JP, Carnevale P, Ambroise-Thomas P. *Plasmodium falciparum* and *P. malariae* epidemiology in a West African village. *Bull World Health Organ*. 1991;69:199–205.
- Molineaux L, Storey J, Cohen JE, Thomas A. A longitudinal study of human malaria in the West African Savanna in the absence of control measures: relationships between different *Plasmodium* species, in particular *P. falciparum* and *P. malariae*. *Am J Trop Med Hyg*. 1980;29:725–37.
- Scopel KK, Fontes CJ, Nunes AC, Horta MF, Braga EM. High prevalence of *Plasmodium malariae* infections in a Brazilian Amazon endemic area (Apiacás-Mato Grosso State) as detected by polymerase chain reaction. *Acta Trop*. 2004;90:61–4. <http://dx.doi.org/10.1016/j.actatropica.2003.11.002>
- Kaneko A, Taleo G, Kalkoa M, Yaviong J, Reeve PA, Ganczakowski M, et al. Malaria epidemiology, glucose 6-phosphate dehydrogenase deficiency and human settlement in the Vanuatu Archipelago. *Acta Trop*. 1998;70:285–302. [http://dx.doi.org/10.1016/S0001-706X\(98\)00035-7](http://dx.doi.org/10.1016/S0001-706X(98)00035-7)
- Collins WE, Jeffery GM. *Plasmodium malariae*: parasite and disease. *Clin Microbiol Rev*. 2007;20:579–92. <http://dx.doi.org/10.1128/CMR.00027-07>
- Gilles HM, Hendrickse RG. Nephrosis in Nigerian children. Role of *Plasmodium malariae*, and effect of antimalarial treatment. *BMJ*. 1963;2:27–31. <http://dx.doi.org/10.1136/bmj.2.5348.27>
- Langford S, Douglas NM, Lampah DA, Simpson JA, Kenangalem E, Sugiarto P, et al. *Plasmodium malariae* infection associated with a high burden of anemia: a hospital-based surveillance study. *PLoS Negl Trop Dis*. 2015;9:e0004195. <http://dx.doi.org/10.1371/journal.pntd.0004195>
- Douglas NM, Lampah DA, Kenangalem E, Simpson JA, Poespoprodjo JR, Sugiarto P, et al. Major burden of severe anemia from non-falciparum malaria species in Southern Papua: a hospital-based surveillance study. *PLoS Med*. 2013;10:e1001575, discussion e1001575. <https://doi.org/10.1371/journal.pmed.1001575>
- Douglas NM, Anstey NM, Angus BJ, Nosten F, Price RN. Artemisinin combination therapy for vivax malaria. *Lancet Infect Dis*. 2010;10:405–16. [http://dx.doi.org/10.1016/S1473-3099\(10\)70079-7](http://dx.doi.org/10.1016/S1473-3099(10)70079-7)
- Ratcliff A, Siswanto H, Kenangalem E, Maristela R, Wuwung RM, Laihah F, et al. Two fixed-dose artemisinin combinations for drug-resistant falciparum and vivax malaria in Papua, Indonesia: an open-label randomised comparison. *Lancet*. 2007;369:757–65. [http://dx.doi.org/10.1016/S0140-6736\(07\)60160-3](http://dx.doi.org/10.1016/S0140-6736(07)60160-3)
- Grigg MJ, William T, Menon J, Dhanaraj P, Barber BE, Wilkes CS, et al. Artesunate-mefloquine versus chloroquine for treatment of uncomplicated *Plasmodium knowlesi* malaria in Malaysia (ACT KNOW): an open-label, randomised controlled trial. *Lancet Infect Dis*. 2016;16:180–8. [http://dx.doi.org/10.1016/S1473-3099\(15\)00415-6](http://dx.doi.org/10.1016/S1473-3099(15)00415-6)

13. Nosten F, van Vugt M, Price R, Luxemburger C, Thway KL, Brockman A, et al. Effects of artesunate-mefloquine combination on incidence of *Plasmodium falciparum* malaria and mefloquine resistance in western Thailand: a prospective study. *Lancet*. 2000; 356:297–302. [http://dx.doi.org/10.1016/S0140-6736\(00\)02505-8](http://dx.doi.org/10.1016/S0140-6736(00)02505-8)
14. Assenato SM, Berzuini A, Foglieni B, Spreafico M, Allain JP, Prati D. *Plasmodium* genome in blood donors at risk for malaria after several years of residence in Italy. *Transfusion*. 2014; 54:2419–24. <http://dx.doi.org/10.1111/trf.12650>
15. Rutledge GG, Böhme U, Sanders M, Reid AJ, Cotton JA, Maiga-Ascofare O, et al. *Plasmodium malariae* and *P. ovale* genomes provide insights into malaria parasite evolution. *Nature*. 2017;542:101–4. <http://dx.doi.org/10.1038/nature21038>
16. Ansari HR, Templeton TJ, Subudhi AK, Ramaprasad A, Tang J, Lu F, et al. Genome-scale comparison of expanded gene families in *Plasmodium ovale wallikeri* and *Plasmodium ovale curtisi* with *Plasmodium malariae* and with other *Plasmodium* species. *Int J Parasitol*. 2016;46:685–96. <http://dx.doi.org/10.1016/j.ijpara.2016.05.009>
17. McKenna A, Hanna M, Banks E, Sivachenko A, Cibulskis K, Kernytsky A, et al. The Genome Analysis Toolkit: a MapReduce framework for analyzing next-generation DNA sequencing data. *Genome Res*. 2010;20:1297–303. <http://dx.doi.org/10.1101/gr.107524.110>
18. Lalloo DG, Shingadia D, Bell DJ, Beeching NJ, Whitty CJ, Chiodini PL; PHE Advisory Committee on Malaria Prevention in UK Travellers. UK malaria treatment guidelines 2016. *J Infect*. 2016;72:635–49. <http://dx.doi.org/10.1016/j.jinf.2016.02.001>
19. Mombo-Ngoma G, Kleine C, Basra A, Würbel H, Diop DA, Capan M, et al. Prospective evaluation of artemether-lumefantrine for the treatment of non-falciparum and mixed-species malaria in Gabon. *Malar J*. 2012;11:120. <http://dx.doi.org/10.1186/1475-2875-11-120>
20. Betson M, Sousa-Figueiredo JC, Atuhaire A, Arinaitwe M, Adriko M, Mwesigwa G, et al. Detection of persistent *Plasmodium* spp. infections in Ugandan children after artemether-lumefantrine treatment. *Parasitology*. 2014;141:1880–90. <http://dx.doi.org/10.1017/S003118201400033X>
21. Calleri G, Balbiano R, Caramello P. Are artemisinin-based combination therapies effective against *Plasmodium malariae*? *J Antimicrob Chemother*. 2013;68:1447–8. <http://dx.doi.org/10.1093/jac/dkt005>
22. Franken G, Müller-Stöver I, Holtfreter MC, Walter S, Mehlhorn H, Labisch A, et al. Why do *Plasmodium malariae* infections sometimes occur in spite of previous antimalarial medication? *Parasitol Res*. 2012;111:943–6. <http://dx.doi.org/10.1007/s00436-012-2851-8>
23. Smith A, Denholm J, Shortt J, Spelman D. *Plasmodium* species co-infection as a cause of treatment failure. *Travel Med Infect Dis*. 2011;9:306–9. <http://dx.doi.org/10.1016/j.tmaid.2011.09.006>
24. Knope K, Whelan P, Smith D, Johansen C, Moran R, Doggett S, et al.; National Arbovirus and Malaria Advisory Committee. Arboviral diseases and malaria in Australia, 2010–11: annual report of the National Arbovirus and Malaria Advisory Committee. *Commun Dis Intell Q Rep*. 2013;37:E1–20.
25. Ezzet F, van Vugt M, Nosten F, Looareesuwan S, White NJ. Pharmacokinetics and pharmacodynamics of lumefantrine (benflumetol) in acute falciparum malaria. *Antimicrob Agents Chemother*. 2000;44:697–704. <http://dx.doi.org/10.1128/AAC.44.3.697-704.2000>
26. Ashley EA, Stepniewska K, Lindegårdh N, Annerberg A, Kham A, Brockman A, et al. How much fat is necessary to optimize lumefantrine oral bioavailability? *Trop Med Int Health*. 2007; 12:195–200. <http://dx.doi.org/10.1111/j.1365-3156.2006.01784.x>
27. Worldwide Antimalarial Resistance Network (WWARN) AL Dose Impact Study Group. The effect of dose on the antimalarial efficacy of artemether-lumefantrine: a systematic review and pooled analysis of individual patient data. *Lancet Infect Dis*. 2015;15:692–702. [http://dx.doi.org/10.1016/S1473-3099\(15\)70024-1](http://dx.doi.org/10.1016/S1473-3099(15)70024-1)
28. White NJ. The assessment of antimalarial drug efficacy. *Trends Parasitol*. 2002;18:458–64. [http://dx.doi.org/10.1016/S1471-4922\(02\)02373-5](http://dx.doi.org/10.1016/S1471-4922(02)02373-5)
29. Vinetz JM, Li J, McCutchan TF, Kaslow DC. *Plasmodium malariae* infection in an asymptomatic 74-year-old Greek woman with splenomegaly. *N Engl J Med*. 1998;338:367–71. <http://dx.doi.org/10.1056/NEJM199802053380605>
30. Straimer J, Gnädig NF, Witkowski B, Amaratunga C, Duru V, Ramadani AP, et al. Drug resistance. K13-propeller mutations confer artemisinin resistance in *Plasmodium falciparum* clinical isolates. *Science*. 2015;347:428–31. <http://dx.doi.org/10.1126/science.1260867>
31. Price RN, Uhlemann AC, van Vugt M, Brockman A, Hutagalung R, Nair S, et al. Molecular and pharmacological determinants of the therapeutic response to artemether-lumefantrine in multidrug-resistant *Plasmodium falciparum* malaria. *Clin Infect Dis*. 2006;42:1570–7. <http://dx.doi.org/10.1086/503423>
32. Venkatesan M, Gadalla NB, Stepniewska K, Dahal P, Nsanabana C, Moriera C, et al.; ASAQ Molecular Marker Study Group; WWARN AL. Polymorphisms in *Plasmodium falciparum* chloroquine resistance transporter and multidrug resistance 1 genes: parasite risk factors that affect treatment outcomes for *P. falciparum* malaria after artemether-lumefantrine and artesunate-amodiaquine. *Am J Trop Med Hyg*. 2014;91:833–43. <http://dx.doi.org/10.4269/ajtmh.14-0031>
33. MalariaGEN *Plasmodium falciparum* Community Project. Genomic epidemiology of artemisinin resistant malaria. *Elife*. 2016;5:pii:e08714. <https://doi.org/10.7554/eLife.08714>
34. Miotto O, Amato R, Ashley EA, MacInnis B, Almagro-Garcia J, Amaratunga C, et al. Genetic architecture of artemisinin-resistant *Plasmodium falciparum*. *Nat Genet*. 2015;47:226–34. <http://dx.doi.org/10.1038/ng.3189>
35. Okombo J, Abdi AI, Kiara SM, Mwai L, Pole L, Sutherland CJ, et al. Repeat polymorphisms in the low-complexity regions of *Plasmodium falciparum* ABC transporters and associations with in vitro antimalarial responses. *Antimicrob Agents Chemother*. 2013;57:6196–204. <http://dx.doi.org/10.1128/AAC.01465-13>

Address for correspondence: Ric N. Price, Menzies School of Health Research, GPO Box 41096, Darwin, Northern Territory 0811, Australia; email: rprice@menzies.edu.au; or Thomas D. Otto, Wellcome Trust Sanger Institute, Wellcome Genome Campus, Hinxton, CB10 1SA, UK; email: tdo@sanger.ac.uk.

Molecular Characterization of *Corynebacterium diphtheriae* Outbreak Isolates, South Africa, March–June 2015

Mignon du Plessis, Nicole Wolter, Mushal Allam, Linda de Gouveia, Fahima Moosa, Genevieve Ntshoe, Lucille Blumberg, Cheryl Cohen, Marshagne Smith, Portia Mutevedzi, Juno Thomas, Valentino Horne, Prashini Moodley, Moherndran Archary, Yesholata Mahabeer, Saajida Mahomed, Warren Kuhn, Koleka Mlisana, Kerrigan McCarthy, Anne von Gottberg

In 2015, a cluster of respiratory diphtheria cases was reported from KwaZulu-Natal Province in South Africa. By using whole-genome analysis, we characterized 21 *Corynebacterium diphtheriae* isolates collected from 20 patients and contacts during the outbreak (1 patient was infected with 2 variants of *C. diphtheriae*). In addition, we included 1 cutaneous isolate, 2 endocarditis isolates, and 2 archived clinical isolates (ca. 1980) for comparison. Two novel lineages were identified, namely, toxigenic sequence type (ST) ST-378 (n = 17) and nontoxigenic ST-395 (n = 3). One archived isolate and the cutaneous isolate were ST-395, suggesting ongoing circulation of this lineage for ≥ 30 years. The absence of preexisting molecular sequence data limits drawing conclusions pertaining to the origin of these strains; however, these findings provide baseline genotypic data for future cases and outbreaks. Neither ST has been reported in any other country; this ST appears to be endemic only in South Africa.

Respiratory diphtheria, caused by toxigenic strains of the gram-positive bacillus *Corynebacterium diphtheriae*, is an upper respiratory tract disease characterized by a sore throat; mild fever; and gray-white pseudomembrane

Author affiliations: National Health Laboratory Service, Johannesburg, South Africa (M. du Plessis, N. Wolter, M. Allam, L. de Gouveia, F. Moosa, G. Ntshoe, L. Blumberg, C. Cohen, M. Smith, P. Mutevedzi, J. Thomas, K. McCarthy, A. von Gottberg); University of the Witwatersrand, Johannesburg (M. du Plessis, N. Wolter, C. Cohen, A. von Gottberg); National Health Laboratory Service, Cape Town, South Africa (V. Horne); University of KwaZulu-Natal, Durban, South Africa (P. Moodley, M. Archary, Y. Mahabeer, S. Mahomed, W. Kuhn, K. Mlisana); National Health Laboratory Service, Durban (Y. Mahabeer, K. Mlisana); National Department of Health, KwaZulu-Natal, South Africa (W. Kuhn)

DOI: <https://doi.org/10.3201/eid2308.162039>

on the tonsils, larynx, or pharynx. Introduction of the diphtheria toxoid vaccine in 1923 and widespread mass immunization in the 1940s and 1950s led to the near elimination of the disease in the industrialized world (1). However, diphtheria remains endemic in many developing countries despite implementation of the World Health Organization Expanded Programme on Immunization in 1974. Epidemic diphtheria resurged in Russia and Eastern Europe in the early 1990s, with >150,000 reported cases occurring predominantly in older children and adults (2).

Molecular epidemiology can be used for investigating diphtheria case clusters in the postvaccine era to improve our understanding of patterns of transmission and spread of epidemic clones. At the time of the Russia epidemic, ribotyping was the established gold standard method of strain typing; however, if deviations from the prescribed protocols occurred, reproducibility could have been compromised (3). Subsequently, multilocus sequence typing (MLST) was developed, which is highly reproducible and provides more accurate information regarding the population structure and evolution (4). More recently, core-genome phylogenetic analysis showed a high level of discrimination and was able to provide insight into *C. diphtheriae* genomic diversity and identify factors contributing to virulence (5). In addition, the highly discriminatory, clustered, regularly interspaced short palindromic repeats (CRISPR) spoligotyping was used for a more detailed analysis of the Russia epidemic clone (6).

In South Africa, early studies in the 1940s and 1950s reported rates of respiratory diphtheria significantly higher than those in industrialized countries, ranging 20–35 cases/100,000 population and equating to $\approx 3,000$ case notifications annually (7,8). During 1980–2014, a total of 412 diphtheria cases were reported in South Africa through the World Health Organization–UNICEF joint reporting process with most (>80%) notified before 1990 (9). The last

laboratory-confirmed respiratory diphtheria case reported in South Africa occurred in a 22-year-old woman in February 2010 in Western Cape Province (10).

During March–June 2015, a cluster of 15 respiratory diphtheria patients with a case-fatality ratio of 27% was reported from KwaZulu-Natal Province in South Africa (11). In 2014, before the outbreak, a KwaZulu-Natal official reported that the province had 96% coverage for the primary series of diphtheria vaccinations and 83% coverage for the 18-month booster (N. McKerrow, KwaZulu-Natal Department of Health, pers. comm., 2015 Jun 8). However, the tetanus-diphtheria booster coverage rates were 54% for 6-year-olds and 20% for 12-year-olds. In response to the outbreak of diphtheria, contact tracing was conducted and postexposure prophylaxis was given to family members and school and clinic contacts (11). Educational leaflets about social mobilization and health promotion activities were distributed in affected communities. The KwaZulu-Natal Department of Health embarked on a catch-up vaccination campaign for schoolgoing children 6–15 years of age in the affected districts. National guidelines for the management and public health response to diphtheria were developed (12), and healthcare practitioners countrywide were notified to be on the alert for possible cases. Laboratories in South Africa were requested to include selective media for isolation of *C. diphtheriae* when processing throat swabs and to submit all potential *C. diphtheriae* isolates to the national reference laboratory for confirmation and to establish an isolate repository for molecular surveillance. We conducted a molecular epidemiologic investigation by using whole-genome data to characterize isolates from cases and contacts linked to this KwaZulu-Natal outbreak.

Methods

Definitions

We defined a confirmed case as the occurrence of clinical symptoms consistent with respiratory diphtheria (sore throat; low-grade fever; and an adherent membrane on the pharynx, tonsils, larynx, or nose) in a person who was positive for toxin-producing *C. diphtheriae* and a probable case as the occurrence of mild respiratory symptoms or clinical symptoms of respiratory diphtheria in a *C. diphtheriae* culture-negative person who was epidemiologically linked to a patient or carrier positive for toxin-producing *C. diphtheriae*. For the purposes of this investigation, we defined a carrier as a person with a laboratory-confirmed, toxin-producing or non-toxin-producing *C. diphtheriae* infection with no respiratory symptoms.

Bacterial Strain Collection

During the 2015 KwaZulu-Natal diphtheria outbreak investigation, we received 21 *C. diphtheriae* isolates swabbed from

the throat or nasopharynx (or groin in 1 case). We confirmed identification of cultures by matrix-assisted laser desorption/ionization time-of-flight technology (13) and confirmed the presence of the A and B subunit genes of the *C. diphtheriae* toxin and phenotypic toxin production by 2 different real-time PCR assays (14,15) and Elek testing (16). Isolates were biotyped with the API Coryne kit (BioMérieux, Lyon, France). We included 2 archived clinical isolates of *C. diphtheriae* that were isolated in South Africa during the 1980s (although no clinical or demographic data were available for these isolates) and 2 *C. diphtheriae* isolates from pre-adolescent children with endocarditis obtained in July and August 2015 (Table 1). Positive controls for PCR and Elek testing were *C. diphtheriae* vaccine-type strain PW8 (ATCC 13812; American Type Culture Collection, Manassas, VA, USA); toxin-positive *C. diphtheriae* NCTC 3984 and 10648 (National Collection of Type Cultures, Salisbury, UK); and toxin-negative *C. diphtheriae* NCTC 10356. Negative controls were *C. ulcerans* (NCTC 12077), *C. bovis* (ATCC 7715), and *C. striatum* (ATCC BAA-1293) (Table 1).

Whole-Genome Sequencing

We extracted DNA from overnight broth cultures with the QIAamp DNA Mini Kit (QIAGEN, Hilden, Germany). We prepared multiplexed paired-end libraries (2 × 300 bp) with the Nextera XT DNA sample preparation kit (Illumina, San Diego, CA, USA) and performed sequencing on an Illumina MiSeq instrument with depth of coverage ranging from 95× to 182×. The raw reads were checked for quality, trimmed, and mapped to the reference genome of *C. diphtheriae* NCTC 13129 (17) by using CLC Genomics Workbench version 8.5.1 (CLC Bio-QIAGEN, Aarhus, Denmark), which resulted in an 89.7%–93.8% coverage of the reference genome. We performed de novo assembly for all genomes with CLC Genomics and ordered them relative to NCTC 13129 by using the Mauve genome alignment package version 2.3.1 (18). We annotated all genomes by using PROKKA version 1.11 (<http://www.vicbioinformatics.com/software/prokka.shtml>) and screened the annotated genomes to confirm the presence or absence of the A and B subunits of the *C. diphtheriae* toxin gene and the toxin repressor gene (*dtxR*). *C. diphtheriae* draft genomes for the South Africa isolates have been deposited at DDBJ/European Nucleotide Archive/GenBank (accession nos. MIOA00000000–MIOP00000000, MINX00000000–MINZ00000000, and MIYN00000000–MIYS00000000).

Multilocus Sequence Typing

We retrieved the sequence type (ST) for each isolate from the whole-genome sequence with the Bio-MLST-MLST-Check module (<http://search.cpan.org/dist/Bio-MLST-Check/>) and applied the eBURST version 3 algorithm (<http://eburst.mlst.net/>) to generate a population snapshot

for *C. diphtheriae* (19). We defined a clonal complex as a cluster of related STs linked as single-locus variants to another ST in the group. We used all available *C. diphtheriae* isolates (n = 616) listed in the global MLST database (<https://pubmlst.org/cdiphtheriae/>) at the time of analysis (accessed June 13, 2017), including 25 isolates from South Africa, to provide context for the South Africa isolates.

Whole-Genome Phylogeny and CRISPR Analysis

We constructed the core-genome alignment by using rapid large-scale prokaryote pan genome analysis (Roary) software (20) to determine the genetic relatedness between the outbreak, outbreak-associated, historical, and endemic isolates. We generated a maximum-likelihood phylogenetic tree by using RaxML version 8 (21). To contextualize the South Africa isolates, we included *C. diphtheriae* genomes from ATCC and NCTC control strains (Table 1) together with publicly available genomes from Brazil (n = 3) (5), India (n = 2) (22), and Malaysia (n = 2) (23) (selected from GenBank). We identified CRISPR-Cas systems in silico with the online CRISPRFinder program (24) and determined CRISPR-Cas cassettes by using the classification and nomenclature described by Makarova et al. (25).

Ethics

In South Africa, the National Health Act of 2003 (Act No. 61 of 2003) and the Health Professions Act of 1974 (Act No. 56 of 1974) allow access to patient medical records for those working on investigations directed at ensuring the public health. Further, the Human Research Ethics Committee of the University of the Witwatersrand serves the

interests of the public in the collection, analysis, and interpretation of communicable disease data. This institution, which has oversight over the National Institute of Communicable Diseases and ensures the application of good clinical and laboratory practices, approved this outbreak investigation (ethics certification no. M160667).

Results

Description of Patients and Contacts with *C. diphtheriae*

As of June 13, 2015, a total of 15 illnesses were under investigation: 11 were classified as laboratory-confirmed cases and 2 as probable cases (Table 2). One probable case occurred in a patient who was linked to a carrier of toxigenic *C. diphtheriae* and died; the postmortem throat swab from this patient was culture negative. The second probable case occurred in a patient infected with non-toxin-producing *C. diphtheriae* who was linked to 3 carriers colonized with toxin-producing *C. diphtheriae*. The remaining 2 illnesses under investigation could not be classified as confirmed or probable cases; they occurred in culture-negative patients with respiratory diphtheria symptoms who could not be epidemiologically linked to a patient or carrier with toxin-producing *C. diphtheriae*. Of the 11 patients with laboratory-confirmed cases, 6 patients were not up-to-date with the South African vaccination schedule and 2 had received all scheduled vaccines recommended for their age group. Vaccination status was unknown for 4 patients. With the exception of patient 9, who was white, all other patients and carriers were black.

Among the 292 patients and contacts with throat swab samples taken during the KwaZulu-Natal outbreak investigation, we isolated *C. diphtheriae* from 19 persons (Table 2). *C. diphtheriae* isolates from the 11 laboratory-confirmed cases were a mixture of biotypes *mitis* (n = 8), *gravis* (n = 1), and *intermedius* (n = 2). One patient (no. 3) was infected with both toxigenic (biotype *mitis*) and nontoxigenic (biotype *gravis*) *C. diphtheriae*. The 1 culture-positive probable case (no. 14) was defined as such because the patient had respiratory diphtheria symptoms but was culture-positive for nontoxigenic *C. diphtheriae*. However, this patient had 3 contacts who were carriers (nos. 15, 16, and 17) colonized with toxigenic *C. diphtheriae* and 1 contact (no. 18) who was a carrier colonized with non-toxin-producing *C. diphtheriae*. We isolated toxigenic *C. diphtheriae* from carriers (nos. 7 and 8) who were family members of patients with laboratory-confirmed cases (nos. 5 and 6). One carrier (no. 13) had toxigenic *C. diphtheriae* and was a contact of another patient with probable diphtheria who died.

C. diphtheriae biotype *mitis* was predominant among carriers (5/7, 71%). Cutaneous *C. diphtheriae* biotype *gravis* was isolated from the groin of a patient (no. 4) who had contact with 2 carriers of non-toxin-producing

Table 1. *Corynebacterium* controls and non-outbreak-associated *C. diphtheriae* isolates from South Africa*

Isolate no.	Organism (biotype)	Toxin-producing	ST
ATCC 13812 (PW8)	<i>C. diphtheriae</i> (<i>gravis</i>)	Yes	44
NCTC 10648	<i>C. diphtheriae</i> (<i>gravis</i>)	Yes	25
NCTC 10356	<i>C. diphtheriae</i> (<i>belfanti</i>)	No	106
NCTC 3984	<i>C. diphtheriae</i> (<i>gravis</i>)	Yes	10
NCTC 5011	<i>C. diphtheriae</i> (<i>intermedius</i>)	Yes	143
NCTC 13129†	<i>C. diphtheriae</i> (<i>gravis</i>)	Yes	8
NCTC 12077	<i>C. ulcerans</i>	No	NA
ATCC 7715	<i>C. bovis</i>	No	NA
ATCC BAA-1293	<i>C. striatum</i>	No	NA
6853‡	<i>C. diphtheriae</i>	No	395
2337‡	<i>C. diphtheriae</i>	No	402
46403§	<i>C. diphtheriae</i>	No	391
46337§	<i>C. diphtheriae</i>	No	390

*ATCC, American Type Culture Collection; NA, not applicable; NCTC, National Collection of Type Cultures; ST, sequence type.

†Clinical isolate from a 72-year-old woman in the United Kingdom isolated following her return from a Baltic cruise in 1997. This isolate is representative of the Russia outbreak clone (17).

‡Historical clinical isolates from South Africa ca. 1980s. No clinical information is available for these isolates.

§Clinical isolates from 8-year-old (46403) and 9-year-old (46337) endocarditis patients from the Western Cape Province of South Africa, July–August 2015.

Table 2. Characteristics of patients and carriers who were *Corynebacterium diphtheriae* culture-positive, KwaZulu-Natal Province, South Africa, March–June 2015*

No.	Age, y	Isolate no.	Diagnosis	Vaccination status†	Outcome	Specimen type	Biotype	Elek	tox gene PCR	ST	CRISPR-Cas system (no. spacers)
1	8	45903	Respiratory diphtheria	Incomplete (missed 18 mo and 6 y boosters)	Died	Tonsillar swab	<i>mitis</i>	Pos	Pos	378	I-E-a (33)
2	8	45236	Respiratory diphtheria	Incomplete (missed 18 mo and 6 y boosters)	Survived	Throat swab	<i>mitis</i>	Pos	Pos	378	I-E-a (33)
3‡	9	45237	Respiratory diphtheria	Incomplete (missed 6 y booster)	Survived	Throat and nasal swabs	<i>gravis</i>	Neg	Neg	395	I-E-a (41), I-E-b (22)
		45238					<i>mitis</i>	Pos	Pos	378	I-E-a (37)
4	31	45262	Cutaneous diphtheria	Unknown	Survived	Groin swab	<i>gravis</i>	Neg	Neg	395	I-E-a (28), I-E-b (21)
5	9	45902	Respiratory diphtheria§	Unknown	Survived	Tracheal aspirate	<i>mitis</i>	Pos	Pos	378	I-E-a (37)
6	5	45463	Respiratory diphtheria§	Unknown	Survived	Tracheal aspirate	<i>gravis</i>	Pos	Pos	378	I-E-a (37)
7	8	45461	Carrier§	Unknown	Survived	Throat swab	<i>gravis</i>	Pos	Pos	378	I-E-a (37)
8	1	45462	Carrier§	Unknown	Survived	Throat swab	<i>mitis</i>	Pos	Pos	378	I-E-a (37)
9	41	45464	Respiratory diphtheria	Unknown	Died	Throat swab	<i>mitis</i>	Pos	Pos	378	I-E-a (33)
10	17	45465	Respiratory diphtheria	Incomplete (missed 12 y booster)	Survived	Throat swab	<i>mitis</i>	Pos	Pos	378	I-E-a (37)
11	13	45466	Respiratory diphtheria	Incomplete (missed 18 mo, 6 y, and 12 y boosters)	Died	Tonsillar swab	<i>mitis</i>	Pos	Pos	378	I-E-a (37)
12	21	45785	Respiratory diphtheria	Unknown	Survived	Throat and nasal swabs	<i>mitis</i>	Pos	Pos	378	I-E-a (34)
13	6	45786	Carrier¶	Unknown	Survived	Throat and nasal swabs	<i>mitis</i>	Pos	Pos	378	I-E-a (33)
14	11	45784	Probable diphtheria	Up-to-date	Survived	Throat and nasal swabs	<i>intermedius</i>	Neg	Neg	395	I-E-a (38), I-E-b (21)
15	11	45789	Carrier#	Unknown	Survived	Throat and nasal swabs	<i>mitis</i>	Pos	Pos	378	I-E-a (31)
16	9	45790	Carrier#	Unknown	Survived	Throat and nasal swabs	<i>mitis</i>	Pos	Pos	378	I-E-a (31)
17	11	45791	Carrier#	Unknown	Survived	Throat and nasal swabs	<i>mitis</i>	Pos	Pos	378	I-E-a (31)
18	10	45792	Carrier#	Unknown	Survived	Throat and nasal swabs	<i>gravis</i>	Neg	Neg	395	I-E-a (42), I-E-b (22)
19	13	45787	Respiratory diphtheria**	Incomplete (missed 14 wk, 18 mo, and 6 y boosters)	Survived	Throat swab	<i>intermedius</i>	Pos	Pos	378	I-E-a (35)
20	4	45788	Respiratory diphtheria**	Up-to-date	Survived	Throat swab	<i>intermedius</i>	Pos	Pos	378	I-E-a (35)

*CRISPR, clustered, regularly interspaced, short palindromic repeats; DTaP, diphtheria, tetanus, and pertussis; neg, negative; pos, positive; ST, sequence type.

†The Expanded Programme on Immunization in South Africa recommends DTaP vaccination at 6 weeks, 10 weeks, and 14 weeks with a booster at 18 months, and a tetanus-diphtheria booster at 6 years and 12 years (<https://www.health-e.org.za/wp-content/uploads/2014/02/South-Africa-EPI-vaccines-revised-Oct-2010.pdf>).

‡Two different genotypes were isolated from 1 patient during the same disease episode.

§Members of the same family.

¶Family member of a person who had respiratory diphtheria symptoms and died. The postmortem throat swab from this person was culture negative.

#Contact of patient 14.

**Members of the same family.

C. diphtheriae. Isolates from both these carriers were discarded at the source laboratory, and no further characterization of their isolates was possible.

Tox and *dtxR* Genes

PCR and whole-genome analysis confirmed the results of the phenotypic Elek testing. In addition, all of the South Africa isolates (both toxigenic and nontoxigenic) were found to harbor an intact *dtxR* gene.

MLSTs and Population Structure

At the time of this analysis, the *C. diphtheriae* PubMLST database had records from 32 countries dating from 1948 through 2017, with *C. diphtheriae* isolates from France accounting for 28% of submissions. Overall, the population snapshot revealed a highly diverse population structure for *C. diphtheriae* globally (Figure 1, <https://wwwnc.cdc.gov/EID/article/23/8/16-2039-F1.htm>). The 25 South Africa isolates (21 outbreak-associated and 4 historical) represented

5 novel STs: ST-378 (n = 17), ST-395 (n = 5), ST-390 (n = 1), ST-391 (n = 1), and ST-402 (n = 1). The toxigenic outbreak strain from KwaZulu-Natal was ST-378 and the nontoxigenic strain was unrelated ST-395. The 2 historical isolates from the 1980s (both toxin negative) were ST-395 and unrelated ST-402. The toxin-negative isolates from the endocarditis patients were ST-390 and ST-391 (Table 1), each of which shares 4 of 7 alleles with ST-395.

Core-Genome Phylogeny

Consistent with MLST data, we identified 2 distinct lineages among the KwaZulu-Natal outbreak isolates. The 17 toxigenic isolates (from 11 patients and 6 contacts) clustered closely together on the whole-genome phylogenetic tree (Table 2; Figure 2). The second lineage consisted of 5 toxin-negative ST-395 *C. diphtheriae* isolates: the isolate from the cutaneous diphtheria patient (no. 4), the isolate from the patient with probable diphtheria (no.

14), an isolate from a carrier (no. 18) linked to the patient with probable diphtheria (no. 14), the nontoxigenic isolate from the patient (no. 3) infected with 2 strains of *C. diphtheriae*, and historical isolate 6853 (Table 1). Comparator genomes from Malaysia (n = 2), Brazil (n = 1), and India (n = 2) and the historical isolate 2337 from South Africa were more closely related to the ST-378 lineage. Two genomes from Brazil (from nontoxigenic isolates) and the UK genome (representative of the Russia outbreak strain) were more closely related to the nontoxigenic ST-395 lineage than to ST-378 (Figure 2; Table 1). The nontoxigenic endocarditis isolates were most closely related to the ST-395 lineage.

CRISPR-Cas Diversity

All of the toxigenic ST-378 isolates harbored a type I-E-a CRISPR-Cas system, with 5 different variants determined by numbers of spacers (Table 2). The 2 carriers (nos. 7 and

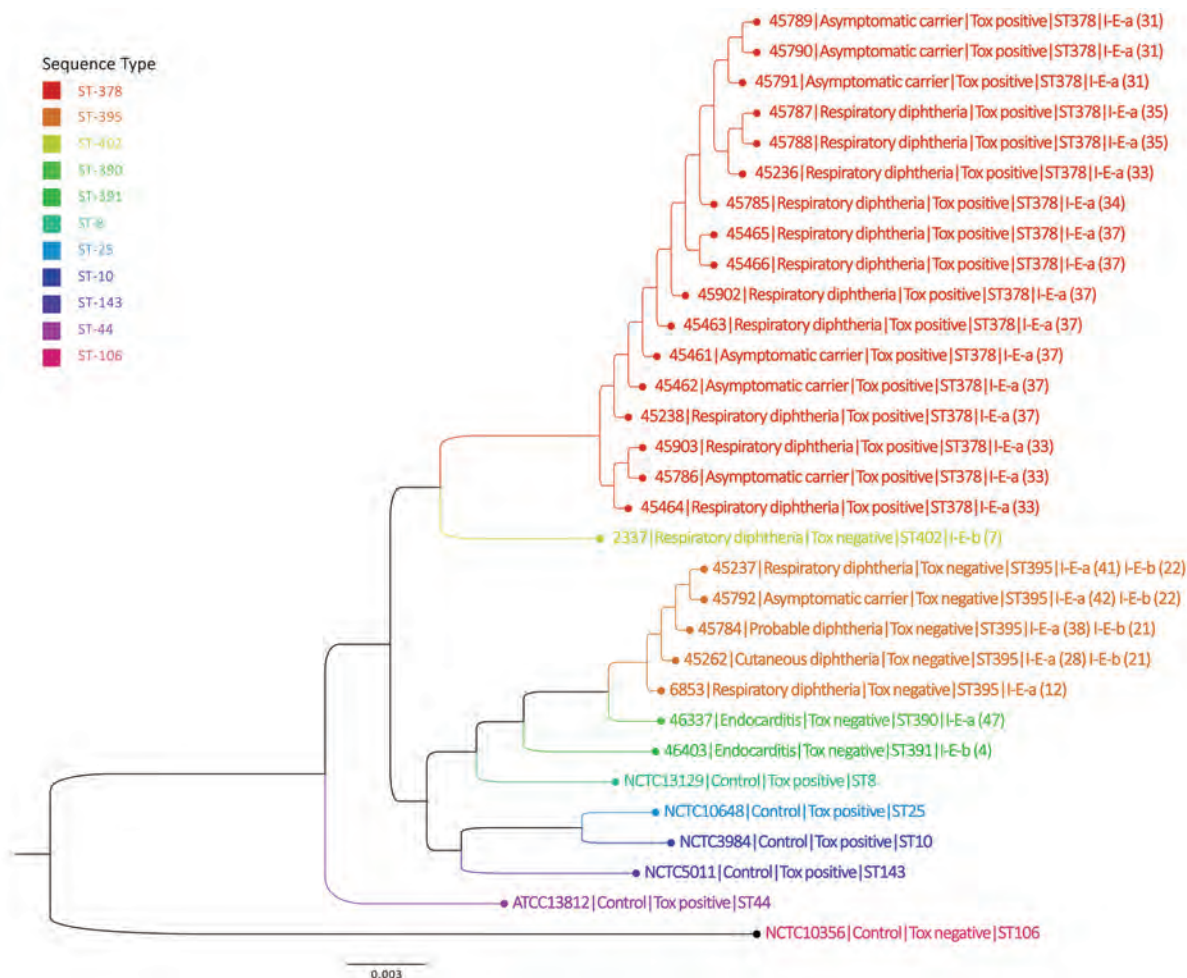


Figure 2. Phylogenetic analysis of *Corynebacterium diphtheriae* isolates based on sequence type, KwaZulu-Natal Province, South Africa, March–June 2015. Maximum likelihood phylogenetic tree demonstrating core-genome phylogeny among isolates from South Africa (n = 25) relative to selected genomes (publicly available from GenBank) from other countries. Scale bar indicates nucleotide substitutions per site. ST, sequence type.

8) and 2 patients (nos. 5 and 6) that were from the same family shared an identical CRISPR-Cas type: I-E-a (37 spacers). This specific variant was present in *C. diphtheriae* from 3 other patients (nos. 3, 10, and 11). The remainder of the ST-378 isolates harbored other type I-E-a variants. Toxigenic *C. diphtheriae* from carriers from the same family (nos. 15, 16, and 17) harbored identical type I-E-a (31 spacers) CRISPRs.

Toxin-negative ST-395 isolates harbored 2 CRISPR-Cas systems, type I-E-a and type I-E-b, and each of the 4 isolates had their own unique combination of variants. Historical isolate 6853 had CRISPR type I-E-a (12 spacers) and historical isolate 2337 had CRISPR type I-E-b (7 spacers), both of which were unrelated to the KwaZulu-Natal isolates. Similarly, *C. diphtheriae* from the 2 endocarditis patients had unique CRISPR types I-E-a (47 spacers) and I-E-b (4 spacers).

Discussion

We describe the molecular epidemiology of *C. diphtheriae* isolated from a cluster of respiratory diphtheria cases in KwaZulu-Natal, South Africa, during the autumn and winter months of 2015 (11). Suboptimal vaccination coverage rates might have contributed to increased vulnerability of older children and adults to *C. diphtheriae* infection, leading to this localized cluster of cases. The KwaZulu-Natal outbreak was caused by a single strain, with a novel ST that does not currently belong to any known clonal complex. This toxigenic strain was unrelated to the nontoxigenic strain isolated during this outbreak investigation from the carrier and patients with respiratory and cutaneous diphtheria. The strain was also not related to the historical and non-outbreak-associated isolates from South Africa or to any other documented *C. diphtheriae* ST from elsewhere in the world.

Biotype does not appear associated with disease severity and is regarded as having limited utility in epidemiologic investigations because of poor discrimination and lack of correlation with genotype (4,26). Nevertheless, a shift in the predominant circulating biotype of *C. diphtheriae* was demonstrated during a Russia outbreak (27,28). However, of the 2 studies on the Russia outbreak, neither had genome data available for comparison. In our investigation, no relationship between biotype and genotype was evident. In addition, no epidemiologic correlation with biotype was apparent, as demonstrated by 4 members of the same family being infected with identical *C. diphtheriae* genotypes but having different biotypes (*mitis* and *gravis*).

MLST was consistent with core-genome phylogeny: isolates of the same ST clustered together. In addition to the MLST and core-genome phylogeny, analysis of the CRISPR systems provided additional resolution between the 2 KwaZulu-Natal lineages and allowed a better understanding of the transmission dynamics. Finding *C. diphtheriae* with identical CRISPR variants among family members

confirmed circulation and transmission of the same strain. Sequence errors might have resulted in misclassification of some variants that were not confirmed by another method or repeat sequencing; nevertheless, a good depth of sequencing coverage together with other parameters validated the quality of the reads and accuracy of base calling.

C. diphtheriae has been shown to exhibit a high degree of genome plasticity (29), which was reflected by the highly diverse global population (consisting of mostly unrelated genotypes) seen with the STs from PubMLST. Individual population snapshots by country reiterate this heterogeneity, and many STs are unique to their respective countries (data not shown). One dominant clone ST-42 and its associated single and double-locus variants, which were predominantly isolated in France, accounted for 7% of *C. diphtheriae* isolates in PubMLST; however, the global database is overrepresented by submissions from France and, thus, might not accurately reflect the true population. The MLST database includes a mixture of unrelated STs from countries of North and West Africa, and Angola (the geographically closest neighbor to South Africa for which data were available) has reported a single ST-316 isolate. None of the isolates from Africa share the same or related STs as those identified in the outbreak we report. MLST data for *C. diphtheriae* isolates collected over ≥ 20 years (1992–2015) in Algeria showed most isolates were ST-116 (unrelated to any other ST in the PubMLST database), the predominant ST circulating during the 1992–1999 epidemic in that country (30). In later years, the population structure of *C. diphtheriae* in Algeria was more heterogeneous.

The South Africa outbreak-associated isolates represented 2 novel STs not previously reported or related to any other PubMLST-listed ST in the global database. The lack of data for *C. diphtheriae* from other countries in Africa makes it difficult to speculate whether these strains were imported from close neighboring countries or farther away, or whether they are endemic to South Africa. Subsequent to the 2015 cluster of cases in South Africa, we also reported 2 additional cases in May 2016 in the same region, and both were ST-378.

During the KwaZulu-Natal outbreak, co-circulation of the toxigenic and nontoxigenic genotypically unrelated strains were noted during laboratory investigations. Both genotypes (ST-378 and ST-395) were detected in patients and carriers. In 1 case, 2 *C. diphtheriae* isolates (1 toxigenic, 1 nontoxigenic) were detected from the same patient. Because CRISPR analysis indicated that the nontoxigenic isolate had a distinctive combination of CRISPR variants not seen in any of the other isolates, the possibility of contamination was excluded. We expect that disease in this patient was caused by the toxigenic strain and not the nontoxigenic strain. In 1 probable case, a person with symptoms clinically suggestive of diphtheria was infected with

the nontoxigenic ST-395 strain but was epidemiologically linked to 3 asymptomatic persons colonized with the ST-378 toxigenic strain. In 1978, a similar phenomenon occurred with a 25-year-old woman in Toronto; 3 different *C. diphtheriae* variants exhibiting 2 different phage types and a mixture of toxigenic and nontoxigenic isolates were isolated from her throat (31). In our study, sampling and testing methods might not have been sensitive enough to detect all *C. diphtheriae* variants present. Laboratory workers should be aware of the possibility of mixed *C. diphtheriae* populations in a single person. Although mixtures might be evident through differences in colony and microscopic morphologies, molecular characterization might be more sensitive in detecting such variants.

Cases of nontoxigenic and cutaneous *C. diphtheriae* might not be clinically as important as toxigenic and respiratory diphtheria and are not notifiable. However, skin lesions can serve as a reservoir of strains that are toxigenic or strains that could potentially become toxigenic if the bacteria possess functional toxin repressor genes and become infected with a *tox* gene-bearing lysogenic coryneophage (32,33). In addition, countries with high vaccination coverage have reported the emergence of invasive disease caused by nontoxigenic *C. diphtheriae*, particularly in high-risk groups such as persons who are homeless, persons who use intravenous drugs or alcohol, persons with diabetes mellitus, and persons with dental caries (34–36). The South Africa isolates from the 2015 KwaZulu-Natal outbreak were not derived from a single lineage; 2 distinct genotypes were identified within the community. The nontoxigenic lineage has been in circulation for ≥ 30 years, verified by sequence typing and close phylogenomic clustering of the archived 1980s isolate (6853) with the ST-395 KwaZulu-Natal outbreak-associated isolates. Because no respiratory or cutaneous diphtheria cases have been reported for several years in South Africa, we have no baseline genotypic data regarding the underlying population diversity, and hence, we are unable to track transmission patterns or changes in genotypes over time. The nontoxigenic South Africa isolates in this study all harbored *dtxR* genes, indicating the potential for toxin production if lysogenized by a bacteriophage.

We identified 2 novel strains of *C. diphtheriae* in a province of South Africa during an outbreak investigation occurring ≥ 30 years after diphtheria ceased to be a public health concern. The absence of preexisting molecular sequence data limits conclusions pertaining to the origin of these strains; however, these findings provide baseline genotypic data for future cases and outbreaks as well as information on transmission dynamics for the 2015 outbreak. A better understanding of the molecular epidemiology of this pathogen might assist in directing and strengthening public health interventions. Active and passive surveillance for diphtheria and *C. diphtheriae*

carriage is required locally and on the subcontinent, particularly in the context of suboptimal vaccination coverage, especially in older children. We are exploring the idea of a serosurvey in South Africa among different age groups, which might provide insight into the epidemiology of diphtheria in this country.

Acknowledgments

We would like to acknowledge the tireless efforts of our public health colleagues in KwaZulu-Natal, who were instrumental in confirming cases and coordinating the public health response during the outbreak: Premi Govender and the KwaZulu-Natal Department of Health (DoH) staff; Vusi Mbuthu, Nokuthula Ndlovu, Ayodeji Olowolagba and team, and the Ethekekwini Metro DoH staff; Nelly Gumede, Sharon Fynn, Zohra Banoo and team, and the Ethekekwini DoH staff; and Siphumelele Mlambo and the Ugu District DoH staff. In addition, we thank all clinicians who were involved in treating patients.

Laboratory testing and molecular characterization was funded by the National Institute for Communicable Diseases.

Dr. du Plessis is a medical laboratory scientist for the Centre for Respiratory Diseases and Meningitis at the National Institute for Communicable Diseases, South Africa, and holds a joint appointment as lecturer at the University of the Witwatersrand, South Africa. Her research interests include the molecular epidemiology of respiratory pathogens and exploring new molecular diagnostic platforms.

References

1. Efstratiou A, George RC. Microbiology and epidemiology of diphtheria. *Rev Med Microbiol.* 1996;7:31–42. <http://dx.doi.org/10.1097/00013542-199601000-00004>
2. Vitek CR, Wharton M. Diphtheria in the former Soviet Union: reemergence of a pandemic disease. *Emerg Infect Dis.* 1998;4:539–50. <http://dx.doi.org/10.3201/eid0404.980404>
3. Dallman T, Neal S, Green J, Efstratiou A. Development of an online database for diphtheria molecular epidemiology under the remit of the DIPNET project. *Euro Surveill.* 2008;13:18865.
4. Bolt F, Cassiday P, Tondella ML, Dezoysa A, Efstratiou A, Sing A, et al. Multilocus sequence typing identifies evidence for recombination and two distinct lineages of *Corynebacterium diphtheriae*. *J Clin Microbiol.* 2010;48:4177–85. <http://dx.doi.org/10.1128/JCM.00274-10>
5. Trost E, Blom J, de Castro Soares S, Huang I-H, Al-Dilaimi A, Schröder J, et al. Pangenomic study of *Corynebacterium diphtheriae* that provides insights into the genomic diversity of pathogenic isolates from cases of classical diphtheria, endocarditis, and pneumonia. *J Bacteriol.* 2012;194:3199–215. <http://dx.doi.org/10.1128/JB.00183-12>
6. Mokrousov I, Narvskaya O, Limeschenko E, Vyazovaya A. Efficient discrimination within a *Corynebacterium diphtheriae* epidemic clonal group by a novel macroarray-based method. *J Clin Microbiol.* 2005;43:1662–8. <http://dx.doi.org/10.1128/JCM.43.4.1662-1668.2005>
7. Bokkenheuser V, Heymann CS. Diphtheria in South Africa. *S Afr Med J.* 1954;28:685–9.

8. Bokkenheuser V. Geographical and racial distribution of diphtheria in South Africa. *S Afr Med J*. 1961;35:711–5.
9. World Health Organization. Diphtheria reported cases [cited 2016 Aug 22]. http://apps.who.int/immunization_monitoring/globalsummary/timeseries/tsincidediphtheria.html
10. National Institute for Communicable Diseases. Diphtheria. National Institute for Communicable Diseases Communiqué. 2010;9(2):4–5 [cited 2016 Jul 25]. http://www.nicd.ac.za/assets/files/NICDCCommFeb10Vol09_02.pdf
11. Mahomed S, Archary M, Mutevedzi P, Mahabeer Y, Govender P, Ntshoe G, et al. An isolated outbreak of diphtheria in South Africa, 2015. *Epidemiol Infect*. 2017;1–9. <http://dx.doi.org/10.1017/S0950268817000851>
12. Cohen C, de Gouveia L, du Plessis M, McCarthy K, Mlisana K, Moodley P, et al. National Institute for Communicable Diseases. Diphtheria: NICD recommendations for diagnosis, management and public health response. Version 2.3. 2016 Mar 22 [cited 25 July 2016]. http://www.nicd.ac.za/assets/files/Guidelines_diphtheria_20160322_v2_3.pdf
13. Konrad R, Berger A, Huber I, Boschert V, Hörmansdorfer S, Busch U, et al. Matrix-assisted laser desorption/ionisation time-of-flight (MALDI-TOF) mass spectrometry as a tool for rapid diagnosis of potentially toxigenic *Corynebacterium* species in the laboratory management of diphtheria-associated bacteria. *Euro Surveill*. 2010;15:19699.
14. Mancini F, Monaco M, Pataracchia M, von Hunolstein C, Pantosti A, Ciervo A. Identification and molecular discrimination of toxigenic and nontoxigenic diphtheria *Corynebacterium* strains by combined real-time polymerase chain reaction assays. *Diagn Microbiol Infect Dis*. 2012;73:111–20. <http://dx.doi.org/10.1016/j.diagmicrobio.2012.02.022>
15. Mothershed EA, Cassiday PK, Pierson K, Mayer LW, Popovic T. Development of a real-time fluorescence PCR assay for rapid detection of the diphtheria toxin gene. *J Clin Microbiol*. 2002;40:4713–9. <http://dx.doi.org/10.1128/JCM.40.12.4713-4719.2002>
16. Efstratiou A, Maple PAC. WHO manual for the laboratory diagnosis of diphtheria. Document ICP-EPI 038 (C). Geneva: World Health Organization; 1994.
17. Cerdeño-Tárraga AM, Efstratiou A, Dover LG, Holden MT, Pallen M, Bentley SD, et al. The complete genome sequence and analysis of *Corynebacterium diphtheriae* NCTC13129. *Nucleic Acids Res*. 2003;31:6516–23. <http://dx.doi.org/10.1093/nar/gkg874>
18. Rissman AI, Mau B, Biehl BS, Darling AE, Glasner JD, Perna NT. Reordering contigs of draft genomes using the Mauve aligner. *Bioinformatics*. 2009;25:2071–3. <http://dx.doi.org/10.1093/bioinformatics/btp356>
19. Feil EJ, Li BC, Aanensen DM, Hanage WP, Spratt BG. eBURST: inferring patterns of evolutionary descent among clusters of related bacterial genotypes from multilocus sequence typing data. *J Bacteriol*. 2004;186:1518–30. <http://dx.doi.org/10.1128/JB.186.5.1518-1530.2004>
20. Page AJ, Cummins CA, Hunt M, Wong VK, Reuter S, Holden MT, et al. Roary: rapid large-scale prokaryote pan genome analysis. *Bioinformatics*. 2015;31:3691–3. <http://dx.doi.org/10.1093/bioinformatics/btv421>
21. Stamatakis A. RAxML version 8: a tool for phylogenetic analysis and post-analysis of large phylogenies. *Bioinformatics*. 2014;30:1312–3. <http://dx.doi.org/10.1093/bioinformatics/btu033>
22. Veeraraghavan B, Anandan S, Rajamani Sekar SK, Gopi R, Devanga Ragupathi NK, Ramesh S, et al. First report on the draft genome sequences of *Corynebacterium diphtheriae* isolates from India. *Genome Announc*. 2016;4:e01316-16. <http://dx.doi.org/10.1128/genomeA.01316-16>
23. Ahmad N, Hii FSY, Mohd Khalid MKN, Abd Wahab MA, Hashim R, Tang SN, et al. First draft genome sequences of Malaysian clinical isolates of *Corynebacterium diphtheriae*. *Genome Announc*. 2017;5:e016701-16. <http://dx.doi.org/10.1128/genomeA.01670-16>
24. Grissa I, Vergnaud G, Pourcel C. CRISPRFinder: a web tool to identify clustered regularly interspaced short palindromic repeats. *Nucleic Acids Res*. 2007;35(Web Server):W52–7. <http://dx.doi.org/10.1093/nar/gkm360>
25. Makarova KS, Haft DH, Barrangou R, Brouns SJ, Charpentier E, Horvath P, et al. Evolution and classification of the CRISPR-Cas systems. *Nat Rev Microbiol*. 2011;9:467–77. <http://dx.doi.org/10.1038/nrmicro2577>
26. Sangal V, Burkovski A, Hunt AC, Edwards B, Blom J, Hoskisson PA. A lack of genetic basis for biovar differentiation in clinically important *Corynebacterium diphtheriae* from whole genome sequencing. *Infect Genet Evol*. 2014;21:54–7. <http://dx.doi.org/10.1016/j.meegid.2013.10.019>
27. Kolodkina V, Titov L, Sharapa T, Grimont PA, Efstratiou A. Molecular epidemiology of *C. diphtheriae* strains during different phases of the diphtheria epidemic in Belarus. *BMC Infect Dis*. 2006;6:129. <http://dx.doi.org/10.1186/1471-2334-6-129>
28. Markina SS, Maksimova NM, Vitek CR, Bogatyreva EY, Monisov AA. Diphtheria in the Russian Federation in the 1990s. *J Infect Dis*. 2000;181(Suppl 1):S27–34. <http://dx.doi.org/10.1086/315535>
29. Iwaki M, Komiya T, Yamamoto A, Ishiwa A, Nagata N, Arakawa Y, et al. Genome organization and pathogenicity of *Corynebacterium diphtheriae* C7(-) and PW8 strains. *Infect Immun*. 2010;78:3791–800. <http://dx.doi.org/10.1128/IAI.00049-10>
30. Benamrouche N, Hasnaoui S, Badell E, Guettou B, Lazri M, Guiso N, et al. Microbiological and molecular characterization of *Corynebacterium diphtheriae* isolated in Algeria between 1992 and 2015. *Clin Microbiol Infect*. 2016;22:1005.e1–7. <http://dx.doi.org/10.1016/j.cmi.2016.08.013>
31. Chang DN, Laughren GS, Chalvardjian NE. Three variants of *Corynebacterium diphtheriae* subsp. *mitis* (Belfanti) isolated from a throat specimen. *J Clin Microbiol*. 1978;8:767–8.
32. Belsey MA, LeBlanc DR. Skin infections and the epidemiology of diphtheria: acquisition and persistence of *C. diphtheriae* infections. *Am J Epidemiol*. 1975;102:179–84. <http://dx.doi.org/10.1093/oxfordjournals.aje.a112145>
33. De Zoysa A, Efstratiou A, Hawkey PM. Molecular characterization of diphtheria toxin repressor (*dtxR*) genes present in nontoxigenic *Corynebacterium diphtheriae* strains isolated in the United Kingdom. *J Clin Microbiol*. 2005;43:223–8. <http://dx.doi.org/10.1128/JCM.43.1.223-228.2005>
34. Farfour E, Badell E, Zasada A, Hotzel H, Tomaso H, Guillot S, et al. Characterization and comparison of invasive *Corynebacterium diphtheriae* isolates from France and Poland. *J Clin Microbiol*. 2012;50:173–5. <http://dx.doi.org/10.1128/JCM.05811-11>
35. Romney MG, Roscoe DL, Bernard K, Lai S, Efstratiou A, Clarke AM. Emergence of an invasive clone of nontoxigenic *Corynebacterium diphtheriae* in the urban poor population of Vancouver, Canada. *J Clin Microbiol*. 2006;44:1625–9. <http://dx.doi.org/10.1128/JCM.44.5.1625-1629.2006>
36. Zasada AA. Nontoxigenic highly pathogenic clone of *Corynebacterium diphtheriae*, Poland, 2004–2012. *Emerg Infect Dis*. 2013;19:1870–2. <http://dx.doi.org/10.3201/eid1911.130297>

Address for correspondence: Mignon du Plessis, Centre for Respiratory Diseases and Meningitis, 1 Modderfontein Rd, Sandringham, Johannesburg 2031 South Africa; email: mignond@nicd.ac.za

Clinical Laboratory Values as Early Indicators of Ebola Virus Infection in Nonhuman Primates

Ronald B. Reisler, Chenggang Yu, Michael J. Donofrio, Travis K. Warren, Jay B. Wells, Kelly S. Stuthman, Nicole L. Garza, Sean A. Vantongeren, Ginger C. Donnelly, Christopher D. Kane, Mark G. Kortepeter, Sina Bavari, Anthony P. Cardile

The Ebola virus (EBOV) outbreak in West Africa during 2013–2016 demonstrated the need to improve Ebola virus disease (EVD) diagnostics and standards of care. This retrospective study compared laboratory values and clinical features of 3 nonhuman primate models of lethal EVD to assess associations with improved survival time. In addition, the study identified laboratory values useful as predictors of survival, surrogates for EBOV viral loads, and triggers for initiation of therapeutic interventions in these nonhuman primate models. Furthermore, the data support that, in nonhuman primates, the Makona strain of EBOV may be less virulent than the Kikwit strain of EBOV. The applicability of these findings as potential diagnostic and management tools for EVD in humans warrants further investigation.

The Ebola virus (EBOV) outbreak in West Africa during 2013–2016 highlighted the need to improve Ebola virus disease (EVD) diagnostics and standards of care (1). With regard to standards of care and EVD outcomes, it is important to explore potential factors associated with improved survival. In previous epidemics, dating back to 1976, EVD case fatality rates ranged from 47% to 90% (2). The Centers for Disease Control and Prevention (CDC) reported a crude death rate of 40% (11,310 deaths/28,616 cases) when including suspected, probable, and confirmed cases from the West Africa outbreak; however, when only confirmed cases were included, the EVD case fatality rate was 74% (11,310 deaths/15,227 cases), consistent with historical rates (1).

Analysis of the most recent EBOV epidemic and previous outbreaks has identified predictors associated with decreased survival: high quantitative viral load (3–7); low PCR cycle threshold (8–12); age (very young and very old) (5,6,10,13–16); male sex (12,17); country of residence (1,17); levels of D-dimer (18), aspartate aminotransferase (AST) (5,10,11), blood urea nitrogen (BUN) (5), and serum creatinine (5,10); and clinical symptoms of diarrhea, pain, myalgia, hemorrhage, and difficulty breathing

(10,12,15,19,20). Of the various EVD animal models that have been developed, those using nonhuman primates (NHPs) appear to most closely reproduce the known features of lethal disease in humans. Herein, we summarize and compare the clinical features and laboratory values of 3 NHP lethal models of EVD and explore features associated with early manifestations of infection and improved survival. Similar to Janvier et al. (11), who recommended the use of high AST levels in humans as a surrogate marker of EBOV viral load and, therefore, disease detection and survival, we explored whether NHP laboratory data would lend support to the use of clinical laboratory values as predictors of survival and surrogates for EBOV viral loads. Further analysis was conducted to determine if clinical laboratory values could be used for indication of infection with the goal of developing a standardized trigger for the initiation of treatment in the NHP model.

Materials and Methods

Animal Use and Viral Challenge

The 30 NHPs described herein served as control animals in larger therapeutic studies conducted in 2014 and 2015. We retrospectively analyzed existing data from those studies. The NHP experiments and tests for this study were performed by the same researchers at the United States Army Medical Research Institute of Infectious Diseases (USAMRIID; Fort Detrick, Frederick, MD, USA), using the same institutional standard operating procedures and processes, the same laboratory instruments, and the same standardized EBOV challenge (1,000 PFU administered intramuscularly [IM]).

We collected blood samples from all 30 NHPs immediately before virus challenge (day 0) and at 3, 5, and 7 days postinoculation (dpi). Methods for EBOV challenge of the NHPs have been described in detail (21). In brief, we first IM inoculated 18 rhesus macaques (*Macaca mulatta*; 3 groups of 6 animals, male and female, weighing 3.71–7.26 kg) with a target titer of 1,000 PFU of the Kikwit strain of EBOV (EBOV Kikwit; back titration titer range 950–1,358 PFU). Next, we IM inoculated 6 cynomolgus macaques

Author affiliation: United States Army Medical Research Institute of Infectious Diseases, Fort Detrick, Frederick, Maryland, USA

DOI: <https://doi.org/10.3201/eid2308.170029>

(*M. fascicularis*; male and female, weighing 3.49–7.33 kg) with a target titer of 1,000 PFU of EBOV Kikwit (back titration titer 1,600 PFU). The EBOV Kikwit strain we used is a USAMRIID stock virus, EBOV H.sapiens-tc/COD/1995/Kikwit-9510621; this virus was primarily the 7U (7 uridylyls) variant at the mRNA editing site. This challenge virus was propagated from a clinical specimen by using cultured cells for a total of 4 passages. Last, we IM inoculated 6 rhesus macaques (male and female, weighing 4.79–5.40 kg) with a target titer of 1,000 PFU (back titration titer 800 PFU) of the USAMRIID stock virus EBOV H.sapiens-tc/LBR/2014/Makona (EBOV Makona); this virus was also primarily the 7U variant at the mRNA editing site. This challenge virus was propagated from a clinical specimen by using cultured cells for a total of 2 passages.

We conducted all studies in Biosafety Level 4 containment. Beginning on day 0 and continuing for the duration of the in-life phase, we recorded clinical observations and closely monitored animals at least 3 times daily for disease progression (22). According to protocol, we provided the NHPs with basic support with regard to pain, oral hydration, and antimicrobial drugs. We administered antimicrobial drugs only if the facility veterinarian diagnosed a secondary bacterial infection. Moribund animals were euthanized on the basis of prespecified criteria (22).

Clinical Laboratory Samples

When possible, we processed and analyzed samples obtained for analyses within 6 h of collection. We used a Vitros 350 Chemistry System (Ortho Clinical Diagnostics, Raritan, NJ, USA) to analyze serum chemistries; an Advia 120 Hematology Analyzer (Siemens, Tarrytown, NY, USA) with multispecies software to analyze hematology parameters; and a Sysmex CA-1500 (Siemens) for coagulation analyses. The samples yielded a panel of 46 routine clinical laboratory values (21).

Viral RNA

We used quantitative real-time PCR (qRT-PCR) to determine viral RNA copy numbers in plasma samples collected at prespecified time points (21). No definition has been established for high viral load in this qRT-PCR assay or in NHP models of EVD. Thus, we used a value of $9 \log_{10}$ RNA copies/mL as a cutoff value for high versus low viral load. The rationale for this cutoff was that the median viremia value for the EBOV Kikwit–infected macaques at 5 dpi and that for the EBOV Makona–infected macaques at 7 dpi was $\approx 9 \log_{10}$ copies/mL.

Statistical Analysis

We performed univariate and multivariate regression modeling of available demographic and laboratory data and used Mann-Whitney U test and Fischer exact test, where

appropriate, for the descriptive analyses. To assess the effect of variables on survival time (measured in hours), we used linear and logistic regression models with Microsoft Excel (Microsoft Corp, Redmond, WA, USA) and Stata 12 (StataCorp LLC, College Station, TX, USA). We used p value thresholds of <0.05 for statistical tests and included an adjusted p value of ≤ 0.001 , based on a simplified Bonferroni correction, for multiple comparisons (online Technical Appendix Table 1, <https://wwwnc.cdc.gov/EID/article/23/8/17-0029-Techapp1.pdf>).

We used the receiver operating characteristic (ROC) curve to illustrate a predictor's performance in 2 metrics, with 1 as a tradeoff of another (e.g., sensitivity and specificity); we obtained the ROC curve by varying the laboratory threshold values of a tested predictor. Using ROC area under the curve (AUC), we evaluated the ability of routine laboratory values (alone or in combination) and \log_{10} plasma viral load RNA concentrations obtained at 3, 5, or 7 dpi to predict infection. The combinations of routine laboratory values analyzed were chosen on the basis of the characteristics of individual laboratory values, clinical relevance, and likely access to the test in a field Ebola treatment unit. Day 0 laboratory values were used as baseline values. Because blood samples for viral RNA assessment and routine laboratory analysis were obtained before virus challenge, day 0 values were used to represent uninfected animals. Values obtained at 3, 5, and 7 dpi were used to represent infected animals because all NHPs were experimentally IM inoculated with EBOV (1,000 PFU target dose), and plasma viral RNA was detected in a sample from at least 1 sampling event for all NHPs included in this analysis. As part of this analysis, we combined the following variables: AST; lactate dehydrogenase (LDH); C-reactive protein (CRP); and the combination of AST, LDH, CRP, and hemoglobin (Hgb). A combined variable C was defined as the mean value of all normalized variables and v_i :

$$C = \frac{1}{m} \sum_{i=1}^m \frac{s_i}{\mu_i + \sigma_i} v_i$$

v_i was normalized by dividing the sum of its mean and standard deviation of baseline values (i.e., values on day 0). s_i is 1 (or -1) for variables whose value increases (or decreases) after infection. m is the number of independent variables to be combined. Values of variable C were calculated for each sample on each day (including day 0) after μ_i , σ_i , and s_i were determined. We denote the 2 combined variables as (AST+LDH+CRP) and (AST+LDH+CRP–Hgb) because AST, LDH, and CRP values increase after infection, whereas Hgb decreases after infection.

Ethics Statement

Animal research at USAMRIID was conducted under an Institutional Animal Care and Use Committee–approved

protocol in compliance with the Animal Welfare Act, US Public Health Service policy, and other federal statutes and regulations relating to animals and experiments involving animals. The facility where this research was conducted is accredited by the Association for Assessment and Accreditation of Laboratory Animal Care, International and adheres to principles stated in the Guide for the Care and Use of Laboratory Animals, National Research Council, 2011.

Results

Similarities and differences in baseline summary characteristics of the 3 groups of NHPs are worth noting (Tables 1, 2) as well as similarities and differences in Kaplan–Meier survival analysis (Figure 1). Median RNA viral loads peaked in all 3 NHP groups at 7 dpi (Figure 2), but RNA viral loads for some EBOV Kikwit–infected NHPs peaked at 5 dpi. At each time point, viremia values ranged widely between the 3 groups. The only significant differences between the NHP groups were at 3 dpi, when the EBOV Kikwit–infected rhesus macaques had higher mean \log_{10} RNA values (4.50 RNA copies/mL [range <3.0 to 6.54]) than the EBOV Makona–infected rhesus macaques, all of whom had \log_{10} RNA values below the limit of detection (<3.00 RNA copies/mL; $p < 0.001$), and at 5 dpi, when the EBOV Kikwit–infected rhesus macaques had higher mean \log_{10} RNA values (8.94 RNA copies/mL [range 5.94 to 10.47]) than the EBOV Makona–infected rhesus macaques (6.57 RNA copies/mL [range <3.0 to 9.33]; $p < 0.049$).

In the EBOV Kikwit–infected rhesus macaques, the median survival time was significantly different between animals with high viral loads (214.6 h) and those with low viral loads (148.0 h) ($p = 0.013$) (Figure 3). In general, viral load correlated with survival time as early as 3 dpi for EBOV Kikwit–infected rhesus macaques ($r = 0.57$; $p = 0.013$); 5 dpi for EBOV Kikwit–infected cynomolgus

macaques ($r = 0.75$; $p = 0.084$); and 7 dpi for EBOV Makona–infected rhesus macaques ($r = 0.90$; $p = 0.016$).

EBOV Kikwit–Infected Rhesus Macaques versus EBOV Makona–Infected Rhesus Macaques

Among rhesus macaques, survival time was longer for those infected with EBOV Makona (337.5 hours) than those infected with EBOV Kikwit (186.9 hours; $p = 0.005$) (Table 1). Clinical assessments showed significant differences between clinical disease progression in EBOV Kikwit–infected and EBOV Makona–infected NHPs at 5 and 7 dpi (Table 1). In addition, we found significant differences in laboratory assessments at 5 and 7 dpi (Table 2). And, at 5 dpi, \log_{10} plasma concentrations of viral RNA were significantly higher among EBOV Kikwit–infected rhesus macaques (8.94 RNA copies/mL) than among EBOV Makona–infected rhesus macaques (6.57 RNA copies/mL; $p = 0.049$).

EBOV Kikwit–Infected Rhesus Macaques versus EBOV Kikwit–Infected Cynomolgus Macaques

We found no significant difference in survival time between EBOV Kikwit–infected rhesus (186.9 hours) and cynomolgus (175.2 hours) macaques. In addition, at 5 and 7 dpi, we found no significant difference in clinical findings between these 2 groups (Table 1). However, there were subtle differences in laboratory values (Table 2). Compared with rhesus macaques, cynomolgus macaques had worsened markers of renal function at 7 dpi, as evidenced by mean laboratory values: BUN levels of 112.6 mg/dL for cynomolgus macaques versus 58.7 mg/dL for rhesus macaques ($p = 0.015$); serum creatinine levels of 24.3 mg/dL for cynomolgus macaques versus 2.3 mg/dL for rhesus macaques ($p = 0.037$); and serum potassium levels of 6.2 mEq/L for cynomolgus macaques versus 4.2 mEq/L for rhesus macaques. Furthermore, at 7 dpi, mean platelet counts tended to be lower for rhesus

Table 1. Baseline characteristics and clinical data for 3 nonhuman primate models of lethal Ebola virus disease*

Variable	Models of infection				
	Rhesus macaque with		p value†	Cynomolgus macaque with Kikwit strain, n = 6	
	Kikwit strain, n = 18	Makona strain, n = 6			
Baseline characteristic					
Weight, kg	4.92	4.79	0.894	4.44	0.526
Age, y	3.94	3.49	0.575	4.92	0.107
Postchallenge clinical data					
Survival time, h	186.9	337.5	0.005	175.2	0.739
Clinical responsiveness score, d§					
3	0	0	None	0	None
5	0.56	0	0.078	0.55	0.729
7	1.64	0.17	0.004	2.60	0.059
Presence of petechial rash, d	5.65	8.17	<0.001	5.17	0.265
Decreased food consumption, d	5.11	8.33	<0.001	4.67	0.178
Presence of anuria, d	6.43	8.20	0.008	6.40	0.500

*Data are means.

†For rhesus macaque model with Ebola virus (EBOV) Kikwit strain vs. Makona strain. Bold indicates $p < 0.05$.

‡For rhesus macaque model with EBOV Kikwit strain vs. cynomolgus macaque model with EBOV Kikwit strain.

§Clinical Responsiveness Score: 0 = active, 1 = decreased activity; 2 = mildly unresponsive (becomes active when approached), occasional prostration; 3 = moderate unresponsiveness (may require prodding to respond), weakness; 4 = moderate to severe unresponsiveness (requires prodding), moderate prostration; 5 = moribund, severe unresponsiveness, pronounced prostration.

Table 2. Results of selected laboratory tests for 3 nonhuman primate models at various days after challenge with EBOV*

Laboratory variable, d	Models of infection			Cynomolgus macaque with Kikwit strain, mean (range), n = 6	
	Rhesus macaque with Kikwit strain, mean (range), n = 18†	Makona strain, mean (range), n = 6	p value‡		p value§
BUN, mg/dL					
0	16.1 (11–22)	15.2 (10–19)	0.544	17.8 (16–23)	0.217
3	15.3 (11–20)	14.3 (8–19)	0.615	17.3 (13–21)	0.215
5	20.0 (10–39)	14.2 (10–17)	0.365	38.5 (15–116)	0.124
7	58.7 (11–108)	17.2 (11–24)	0.050	112.6 (58–135)	0.015
Creatinine, mg/dL					
0	0.6 (0.5–0.8)	0.5 (0.5–0.6)	0.012	0.6 (0.5–0.9)	0.871
3	0.6 (0.5, 0.8)	0.5 (0.4–0.6)	0.030	0.6 (0.4–0.9)	0.662
5	1.1 (0.6–2.6)	0.6 (0.5–0.7)	0.005	1.8 (0.8–5.2)	0.094
7	2.3 (0.7–5.6)	0.8 (0.7–1.0)	0.055	24.3 (1.7 to >56.0)	0.037
AST, U/L					
0	37.9 (22– 62)	35.8 (26– 53)	0.702	64.7 (37– 151)	0.192
3	49.4 (32, 74)	42.0 (31–57)	0.230	95.7 (47–145)	0.002
5	411.6 (46–1,716)	47.0 (33–56)	0.001¶	423.2 (116–743)	0.386
7	991.4 (145–1,585)	244.5 (113–398)	0.009	1,626.6 (752 to >3,400)	0.624
ALT, U/L					
0	32.1 (10–64)	17.5 (7–27)	0.009	53.8 (36–94)	0.078
3	45.2 (10–87)	25.0 (10–38)	0.009	60.2 (51–81)	0.028
5	137.2 (19–554)	29.0 (13–46)	0.008	87.8 (51–138)	0.790
7	299.4 (68–606)	67.2 (21–108)	0.016	610.0 (154–2,087)	0.955
CRP, mg/L					
0	5.6 (0–20)	5.2 (5–6)	0.651	6.8 (4–11)	0.385
3	10.1 (5–31)	5.2 (5–6)	0.013	19.7 (8–59)	0.047
5	71.2 (43–83)	17.2 (6–44)	<0.001¶	73.8 (70–78)	0.764
7	59.5 (44–74)	57.3 (32–71)	0.960	48.2 (13–72)	0.533
LDH, IU/L					
0	510.8 (366–679)	456.0 (390–537)	0.083	964.7 (653–1,267)	0.008
3	641.0 (381–829)	563.3 (454–775)	0.110	1,511.5 (894–2,532)	<0.001¶
5	3,897.2 (670 to >9,000)	700.8 (551–826)	0.001¶	5,799.8 (1,667 to >9,000)	0.229
7	7,965.7 (1,531 to >9,000)	5,524.3 (1,562 to >9,000)	0.042	9,000 (>9,000 to >9,000)	0.353
CPK, U/L					
0#	435.2 (55–915)	214.7 (84–395)	0.006	ND	
3	507.3 (181–874)	557.0 (333–897)	0.594	ND	
5	1,721.3 (183–5157)	494.5 (287–755)	0.014	ND	
7	4,599.1(320 to >6,400)	2,459.3 (700–5,692)	0.065	ND	
Platelets, × 10 ³ /mm ³					
0	347.5 (240–502)	274.3 (220–318)	0.002	312.5 (278–373)	0.102
3	330.4 (223–557)	285.7 (244–330)	0.193	288.2 (237–352)	0.217
5	172.0 (91–303)	253.7 (199–286)	0.006	197.3 (144–312)	0.350
7	89.6 (34–161)	112.3 (26–191)	0.482	142.4 (106–195)	0.047
PT, s					
0	11.2 (10.4–14.9)	11.4 (10.8–12.2)	0.374	10.6 (9.8–11.3)	0.010
3	10.7 (9.8–12.7)	10.9 (10.1–12.0)	0.365	10.4 (9.7–10.9)	0.545
5	13.9 (10.9–18.1)	10.4 (10.0–10.9)	<0.001¶	14.1 (12.6–17.1)	0.739
7	15.7 (12–19.6)	12.4 (11.7–13.8)	0.004	18.0 (14.6–22.8)	0.282
APTT, s					
0	27.0 (24.5–32.0)	27.5 (26.8–29.6)	0.440	25.8 (24.4–27.5)	0.095
3	26.7 (23.8–31.5)	26.1 (25.0–28.5)	0.841	27.1 (25.0–32.9)	0.947
5	43.4 (31.5–62.6)	27.6 (24.7–31.8)	<0.001¶	41.2 (35.2–48.4)	0.571
7	60.4 (42.3–111.1)	41.9 (34.9–47.6)	0.012	62.5 (51.3–67.4)	0.532
AT, %					
0	101.8 (85.8–116.9)	105.7 (90.5–121.6)	0.450	100.5 (92.0–118.6)	0.768
3	104.2 (76.0–127.3)	110.0 (98.8–119.8)	0.286	103.0 (92.8–115.3)	0.689
5	76.9 (55.5–100.9)	113.8 (103.1–129.2)	<0.001¶	73.5 (70.4–83.3)	0.505
7	67.7 (38.5–94.8)	103.1 (95.5–116.0)	<0.001¶	49.4 (34.0–55.9)	0.031

*ALT, alanine aminotransferase; APTT, activated partial thromboplastin time; AST, aspartate aminotransferase; AT, antithrombin; BUN, blood urea nitrogen; CPK, creatine phosphokinase; CRP, C-reactive protein; EBOV, Ebola virus; LDH, lactate dehydrogenase; ND, not done; PT, prothrombin time.

†Results for 6 macaques in the EBOV Kikwit strain group were previously reported as a mean difference from day 7 to day 0 (28).

‡For results for rhesus macaque model of infection with EBOV Kikwit strain vs. Makona strain. Bold indicates p<0.05.

§For rhesus macaque model with EBOV Kikwit strain vs. cynomolgus macaque model with EBOV Kikwit strain. Bold indicates p<0.05.

¶Adjusted p value of ≤0.001, based upon a simplified Bonferroni correction for multiple comparisons.

#In the 24 nonhuman primates infected with EBOV for whom CPK values were analyzed, 16 (67%) had levels >5,000 U/L during the course of disease.

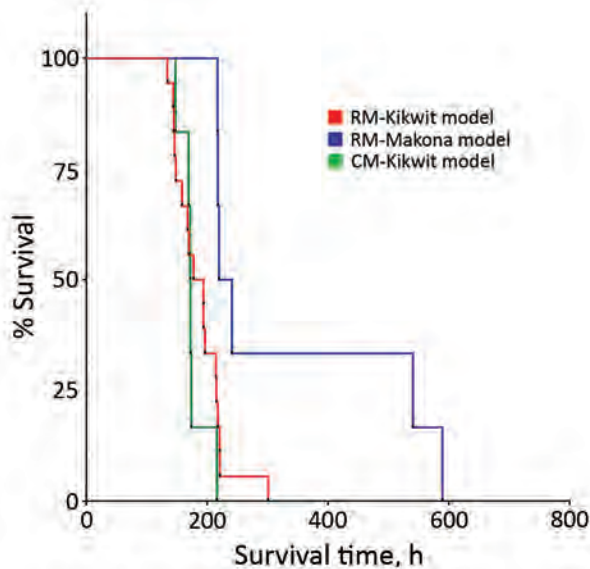


Figure 1. Kaplan–Meier survival analysis for each of 3 nonhuman primate models of Ebola virus disease: rhesus macaque model with EBOV Kikwit strain ($n = 18$ monkeys); rhesus macaque model with EBOV Makona strain ($n = 6$ monkeys); and cynomolgus macaque model with EBOV Kikwit strain ($n = 6$ monkeys). Overall comparison of the 3 Kaplan–Meier survival curves yielded a statistically significant value ($p = 0.007$) using the Mantel–Cox log-rank test. CN-Kikwit, cynomolgus macaque model of EBOV Kikwit strain; EBOV, Ebola virus; RM-Kikwit, rhesus macaque model of EBOV Kikwit strain; RM-Makona, rhesus macaque model of EBOV Makona strain.

($89.6 \times 10^3/\text{mm}^3$) than cynomolgus ($142.4 \times 10^3/\text{mm}^3$; $p = 0.047$) macaques (Table 2).

Regression Analyses for Predicting Viral Load from Routine Laboratory Values

Due to small sample sizes, we limited our presentation of regression analyses to the 18 EBOV Kikwit–infected rhesus macaques. In a univariate regression model, \log_{10} plasma concentrations of viral RNA correlated significantly with survival time at peak viremia (5–7 dpi) and at 3, 5, and 7 dpi (online Technical Appendix). At 5 dpi, the following laboratory values correlated significantly with time to death and with plasma viral load: platelet counts; prothrombin time; and levels of AST; alanine aminotransferase (ALT); LDH; and creatine phosphokinase (CPK) (online Technical Appendix). Similarly, LDH and CPK values at 7 dpi correlated significantly with time to death and with \log_{10} viral RNA (online Technical Appendix).

ROC Curve Analyses for Assessing Clinical Laboratory Values as Early Indicators of EBOV Infection

In the following datasets, ROC curve analysis yielded the best available laboratory predictors as signs of EBOV infection at 3, 5, and 7 dpi: \log_{10} RNA, AST, ALT, CRP,

LDH, CPK, and Hgb (online Technical Appendix Table 2). \log_{10} concentrations of viral RNA outperformed all other individual laboratory values as a predictor of EBOV infection. However, ROC AUC values for \log_{10} RNA were only slightly better than those for LDH, CRP, and AST (online Technical Appendix Table 2). In fact, when the 3 chemistries were combined (AST+LDH+CRP), they performed almost as well as \log_{10} RNA values in all 3 NHP models. When we compared the combined predictor AST+LDH+CRP-Hgb with \log_{10} RNA values at 3 dpi, it outperformed \log_{10} RNA in all 3 NHP models. For example, at 3 dpi in the EBOV Kikwit–infected rhesus macaque model, ROC AUC was 0.83 for \log_{10} RNA and 0.93 for the combined predictor AST+LDH+CRP-Hgb.

Discussion

Unlike some other reports showing abnormal laboratory values in NHP EVD models, we have presented our findings in a systematic format concentrating on laboratory values that we think reflect EVD pathogenesis, are easily translatable to human disease, and are potentially available in the human clinical setting. A better understanding of EBOV NHP models will enhance characterization of the disease and facilitate standardization of the models to support possible future vaccine and therapeutic drug submissions under the Food and Drug Administration Animal Rule (<https://www.fda.gov/downloads/Drugs/GuidanceComplianceRegulatoryInformation/Guidances/UCM399217.pdf>). Similar to what has been reported in human EVD (3–12), our findings demonstrate that a lower plasma concentration of viral RNA predicted increased survival time in the 3 NHP models we assessed.

Marzi et al. (23) observed that disease progression in EBOV Makona–infected cynomolgus macaques was delayed compared with that in cynomolgus macaques infected with the EBOV Mayinga strain. Wong et al. (24) compared infections with EBOV Kikwit with infections with 2 different EBOV Makona strains in rhesus macaques and found that the EBOV Makona strains were either similar in virulence or more virulent than the EBOV Kikwit strain they were using. We observed that disease progression in EBOV Makona–infected rhesus macaques was delayed compared with that in EBOV Kikwit–infected rhesus macaques; the observation was supported by viral load data, clinical assessments, and laboratory values. This finding might suggest that, in NHPs, the EBOV Makona strain we used is somewhat less virulent than the EBOV Kikwit strain we used; although, in rhesus macaques, 1,000 PFU of EBOV Makona still resulted in death among all untreated animals. Data are insufficient to determine the relative pathogenicity of EBOV Makona in comparison with that of other EBOV strains. To make this determination, further

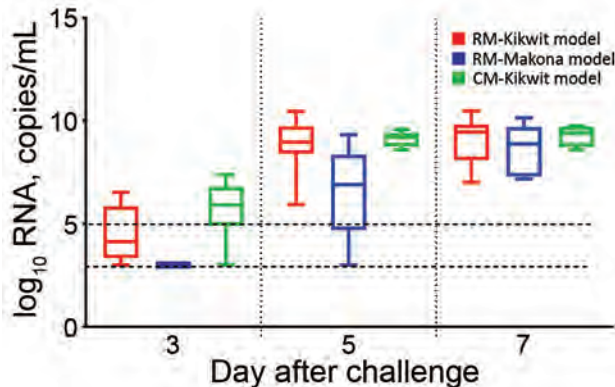


Figure 2. \log_{10} RNA level, by day after EBOV challenge, for each of 3 nonhuman primate models of Ebola virus disease. Box and whisker plots were created by using the available data for each day. Boxes indicate range from 25th (bottom line) to 75th (top line) percentiles; horizontal line within each box indicates median; whiskers indicate entire range of values (maximum to minimum). Dashed lines indicate limit of detection (LOD) (bottom line, $3.0 \log_{10}$ RNA copies/mL) and lower limit of quantification (LLOQ) (top line, $5.0 \log_{10}$ RNA copies/mL) for the assay. Values below the LOD were assigned the value $3.0 \log_{10}$ RNA copies/mL; values between the LLOQ and the LOD were assigned the actual measured value. CM-Kikwit, cynomolgus macaque model of EBOV Kikwit strain; EBOV, Ebola virus; RM-Kikwit, rhesus macaque model of EBOV Kikwit strain; RM-Makona, rhesus macaque model of EBOV Makona strain.

studies are needed, taking into consideration different EBOV strains and quasispecies.

The difference in survival time between EBOV Kikwit-infected rhesus and cynomolgus macaques (11.7 hours) was not significant; rhesus macaques survived longer. Of interest, at 7 dpi, cynomolgus macaques demonstrated increased impairment of renal function (as determined by BUN and creatinine levels) compared with that for rhesus macaques. This finding does not appear to be associated with a significant observable difference in oral fluid consumption between the animals, and the pathogenesis merits further study.

The search for reliable biomarkers for early diagnosis of EBOV infection and predictors of survival has been a high priority (25,26), but reverse transcription PCR (RT-PCR) remains the reference standard for EVD diagnosis (27). ROC analysis demonstrated that, in all 3 NHP models, qRT-PCR outperformed all individual laboratory values with regard to EVD confirmation. It is noteworthy that the combination of AST+LDH+CRP-Hgb values outperformed qRT-PCR as a laboratory sign of Ebola virus infection at 3 dpi in all 3 NHP models. This could be an important finding and potentially serve as a trigger to treat NHPs in therapeutic studies of IM administered EBOV Kikwit.

Currently, there are no standardized triggers for the initiation of treatment of EBOV-infected NHPs in therapeutics

studies. Various time points after virus exposure have been used for therapeutics initiation in NHP models of EBOV infection (28–30). One study used a positive RT-PCR result plus documented fever of $\geq 1.5^{\circ}\text{C}$ above baseline for 1 hour as a prespecified trigger to treat (31). However, it is logistically difficult to obtain timely PCR results in a Biosafety Level 4 laboratory (especially for a large study), and implantation of a telemetry device would be required for optimal fever detection. Thus, standard clinical laboratory values may be a more practical trigger to treat. For example, a calculator (spreadsheet or smartphone application) could be developed to calculate a combined variable value (e.g., AST+LDH+CRP-Hgb) from clinical laboratory values. This approach would be similar to a disease severity smartphone application advocated by Colubri et al. (32) for use with human EBOV patients. Once the threshold laboratory value is reached or exceeded, the therapeutic could be initiated. We intend to conduct a follow-up ROC AUC analysis with a larger sample size to further validate and optimize these preliminary findings.

Our finding that, in lieu of viral load, laboratory values at 5 dpi could potentially predict survival duration is not entirely surprising given that Warren et al. (28) published NHP data that showed the course of EBOV viral load is mirrored by the course of clinical chemistries in the setting of successful EVD treatment using the nucleotide prodrug GS-5734. Although it has been shown that AST levels can predict survival in EBOV-infected humans (5,10,11), we found that LDH may be a better predictor of survival time in NHP models using IM administered EBOV. In all 3 models in our study, LDH and viral load significantly increased at 5 dpi in EBOV Kikwit-infected rhesus and cynomolgus macaques and at 7 dpi in EBOV Makona-infected rhesus macaques. In the EBOV Kikwit-infected rhesus macaque model, LDH values at 5 dpi correlated with viral load and survival time at 5 dpi. Incidentally, LDH has been shown to correlate with survival time in humans with Crimean-Congo hemorrhagic fever, severe fever with thrombocytopenia syndrome, and Dengue virus infection (33–36).

LDH is abundant in the cytoplasm of all human cells and helps catalyze the conversion of pyruvate to lactate, the last step of glycolysis (37). Markedly elevated levels of LDH are often seen in association with cardiogenic shock; hepatic ischemia or necrosis; and intestinal and/or mesenteric ischemia or necrosis (36,38). However, no signs of cardiogenic shock, severe chemical transaminitis corresponding to hepatic ischemia or necrosis, or severe hemolysis were observed at 5 dpi in EBOV Kikwit-infected NHPs or at 7 dpi in EBOV Makona-infected NHPs. One possibility is that the NHPs were experiencing either intestinal and/or mesenteric ischemia or necrosis, conditions that have been seen in other viral infections (39,40) and which may, as postulated by Lynn (41), precipitate late Ebola sepsis-like syndrome.

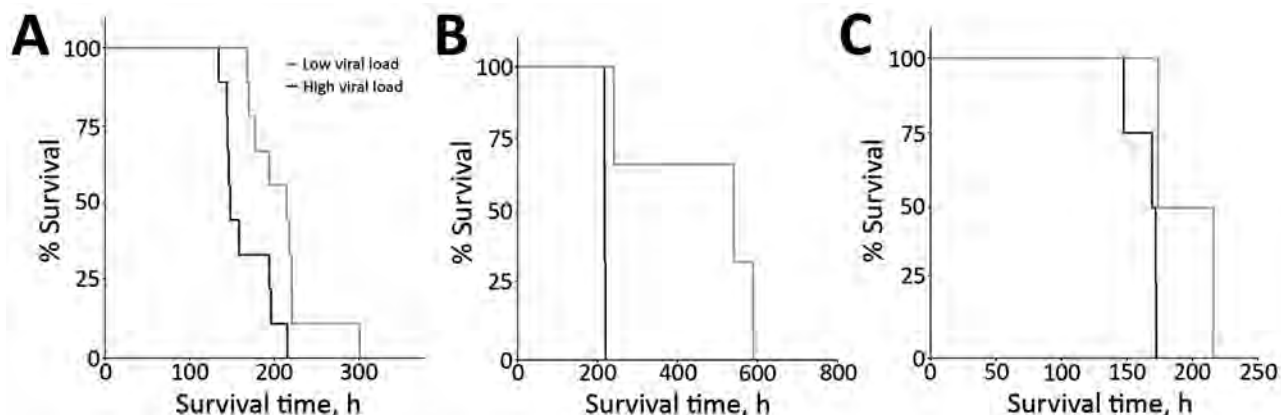


Figure 3. Survival curves, stratified by high ($>9 \log_{10}$ RNA copies/mL) and low ($<9 \log_{10}$ RNA copies/mL) viral loads, for each of 3 nonhuman primate models of Ebola virus disease. A) Comparison of survival on postinoculation day 5 for rhesus macaques infected with the Kikwit strain of Ebola virus (EBOV). Median survival time was 148.0 hours for macaques with high viral loads ($n = 9$) and 214.6 hours for macaques with low viral loads ($n = 9$). Comparison of the 2 survival curves yielded a statistically significant value ($p = 0.010$ by Mantel-Cox log-rank test). B) Comparison of survival on postinoculation day 7 for rhesus macaques infected with the Makona strain of EBOV. Median survival time was 217.7 hours for macaques with high viral loads ($n = 3$) and 540.4 hours for macaques with low viral loads ($n = 3$). Comparison of the 2 survival curves yielded a statistically significant value ($p = 0.025$ by Mantel-Cox log-rank test). C) Comparison of survival on postinoculation day 5 for cynomolgus macaques infected with the Kikwit strain of EBOV. Median survival time was 170.6 hours for macaques with high viral loads ($n = 4$) and 195.0 hours for macaques with low viral loads ($n = 2$). Comparison of the 2 survival curves yielded a nearly statistically significant value ($p = 0.074$ by Gehan–Breslow–Wilcoxon test).

Kortepeter et al. (42) reported that, in a rhesus macaque model, animals lethally challenged with EBOV Kikwit experienced a rapid increase in plasma viral RNA beginning at 4 dpi and a rapid increase in serum lactate beginning at 7 dpi. In humans, serum lactate levels have been shown to correlate with serum LDH levels (43), and both have independently been associated with death (44–47). Thus, further study is needed of lactate and LDH levels in humans and NHPs with EVD.

A key caveat to our analysis is that our data reflect a retrospective analysis of NHPs used as controls in 5 different studies of IM administered EBOV. The trajectory of early increases in clinical laboratory values, especially CPK and LDH, could be affected by the IM route of EBOV administration. However, Johnson et al. (48) reported similar early increases in LDH and CPK in rhesus macaques in an aerosol model of EBOV Zaire infection. In future analyses, we intend to explore how the route of EBOV administration affects changes in clinical laboratory values. Another limitation to this analysis is that survival time was determined to be time to euthanasia. The strict adherence to the USAMRIID euthanasia criteria, in the setting of 3 clinical assessments daily, supports the supposition that time to euthanasia approximates time to death. Another limitation is that, in this dataset, all animals died, so we were only able to look at survival time. Therefore, we were unable to derive odds ratios for individual variables to assess predictors of death. Future analyses of datasets that include NHPs that survived EBOV infection, with or without treatment with a therapeutic product, will be useful to identify such predictors. Although our analysis included a

large number of NHPs ($N = 30$), we also acknowledge that this retrospective analysis was primarily hypothesis-generating and that there were no prespecified hypotheses. We used p value thresholds of <0.05 for our statistical tests and included an adjusted p value of ≤ 0.001 on the basis of a simplified Bonferroni correction for multiple comparisons.

Much can be learned from a critical analysis of EBOV NHP models. Our data support the finding that the virulence of the EBOV Makona strain used in our study may be decreased as compared to that of the EBOV Kikwit strain we used. We did not find a statistically significant difference in survival time when comparing rhesus to cynomolgus macaques in the EBOV Kikwit model, although there were subtle differences in some of the laboratory values. In addition, our data support EBOV studies in humans that indicate basic laboratory values could potentially be used as surrogate markers for viral load and, thus, disease detection and survival. However, validation of this approach in the human clinical setting would also require a comparison with clinical laboratory values associated with endemic diseases present in a given geographic area, such as malaria, rickettsial illnesses, and diseases caused by other hemorrhagic fever viruses. In addition, a combined score of AST, LDH, CRP, and Hgb values could be further evaluated as a trigger to treat NHPs in therapeutics studies of IM administered EBOV. Further work in the NHP model of EVD with regard to clinical and laboratory markers would ideally lead to improvements in predicting survival time in EBOV-infected NHPs and enhancements in the treatment of disease in NHPs, with potential applicability to the management of human EVD.

Dr. Reisler is a lead clinical research contract physician in the Division of Medicine at USAMRIID. His current areas of research interest are biothreat agent research, animal models, vaccine development, and development of therapeutic interventions.

References

- Centers for Disease Control and Prevention. 2014 Ebola outbreak in West Africa—case counts [cited 2016 Dec 5]. <https://www.cdc.gov/vhf/ebola/outbreaks/2014-west-africa/case-counts.html>
- Kortepeter MG, Bausch DG, Bray A. Basic clinical and laboratory features of filoviral hemorrhagic fever. *J Infect Dis.* 2011;204 (Suppl 3):S810–6. <http://dx.doi.org/10.1093/infdis/jir299>
- Faye O, Andronico A, Faye O, Salje H, Boëlle PY, Magassouba N, et al. Use of viremia to evaluate the baseline case fatality ratio of Ebola virus disease and inform treatment studies: a retrospective cohort study. *PLoS Med.* 2015;12:e1001908. <http://dx.doi.org/10.1371/journal.pmed.1001908>
- Towner JS, Rollin PE, Bausch DG, Sanchez A, Cray SM, Vincent M, et al. Rapid diagnosis of Ebola hemorrhagic fever by reverse transcription-PCR in an outbreak setting and assessment of patient viral load as a predictor of outcome. *J Virol.* 2004;78:4330–41. <http://dx.doi.org/10.1128/JVI.78.8.4330-4341.2004>
- Schieffelin JS, Shaffer JG, Goba A, Gbakie M, Gire SK, Colubri A, et al.; KGH Lassa Fever Program; Viral Hemorrhagic Fever Consortium; WHO Clinical Response Team. Clinical illness and outcomes in patients with Ebola in Sierra Leone. *N Engl J Med.* 2014;371:2092–100. <http://dx.doi.org/10.1056/NEJMoa1411680>
- de La Vega M-A, Caleo G, Audet J, Qiu X, Kozak RA, Brooks JJ, et al. Ebola viral load at diagnosis associates with patient outcome and outbreak evolution. *J Clin Invest.* 2015;125:4421–8. <http://dx.doi.org/10.1172/JCI83162>
- Lanini S, Portella G, Vairo F, Kobinger GP, Pesenti A, Langer M, et al.; INMI-EMERGENCY EBOV Sierra Leone Study Group. Blood kinetics of Ebola virus in survivors and nonsurvivors. *J Clin Invest.* 2015;125:4692–8. <http://dx.doi.org/10.1172/JCI83111>
- Crowe SJ, Maenner MJ, Kuah S, Erickson BR, Coffee M, Knust B, et al. Prognostic indicators for Ebola patient survival. *Emerg Infect Dis.* 2016;22:217–23. <http://dx.doi.org/10.3201/eid2202.151250>
- Fitzpatrick G, Vogt F, Moi Gbabai OB, Decroo T, Keane M, De Clerck H, et al. The contribution of Ebola viral load at admission and other patient characteristics to mortality in a Médecins Sans Frontières Ebola case management centre, Kailahun, Sierra Leone, June–October 2014. *J Infect Dis.* 2015;212:1752–8. <http://dx.doi.org/10.1093/infdis/jiv304>
- Hunt L, Gupta-Wright A, Simms V, Tamba F, Knott V, Tamba K, et al. Clinical presentation, biochemical, and haematological parameters and their association with outcome in patients with Ebola virus disease: an observational cohort study. *Lancet Infect Dis.* 2015;15:1292–9. [http://dx.doi.org/10.1016/S1473-3099\(15\)00144-9](http://dx.doi.org/10.1016/S1473-3099(15)00144-9)
- Janvier F, Foissaud V, Cotte J; Healthcare Workers Ebola Treatment Center Medical Team; Aletti M, Savini H, Cordier PY, et al. Monitoring of prognostic laboratory markers in Ebola virus disease. *J Infect Dis.* 2016;213:1049. <http://dx.doi.org/10.1093/infdis/jiv546>
- Haaskjold YL, Bolkan HA, Krogh KØ, Jongopi J, Lundeby KM, Mellesmo S, et al. Clinical features of and risk factors for fatal Ebola virus disease, Moyamba District, Sierra Leone, December 2014–February 2015. *Emerg Infect Dis.* 2016;22:1537–44. <http://dx.doi.org/10.3201/eid2209.151621>
- Xu Z, Jin B, Teng G, Rong Y, Sun L, Zhang J, et al. Epidemiologic characteristics, clinical manifestations, and risk factors of 139 patients with Ebola virus disease in western Sierra Leone. *Am J Infect Control.* 2016;44:1285–90. <http://dx.doi.org/10.1016/j.ajic.2016.04.216>
- Wong JY, Zhang W, Kargbo D, Haque U, Hu W, Wu P, et al. Assessment of the severity of Ebola virus disease in Sierra Leone in 2014–2015. *Epidemiol Infect.* 2016;144:1473–81. <http://dx.doi.org/10.1017/S0950268815003003>
- Qin E, Bi J, Zhao M, Wang Y, Guo T, Yan T, et al. Clinical features of patients with Ebola virus disease in Sierra Leone. *Clin Infect Dis.* 2015;61:491–5. <http://dx.doi.org/10.1093/cid/civ319>
- Sadek RF, Khan AS, Stevens G, Peters CJ, Ksiazek TG. Ebola hemorrhagic fever, Democratic Republic of the Congo, 1995: determinants of survival. *J Infect Dis.* 1999;179(Suppl 1):S24–7. <http://dx.doi.org/10.1086/514311>
- WHO Ebola Response Team; Agua-Agum J, Ariyaratna A, Blake IM, Cori A, Donnelly CA, Dorigatti I, et al. Ebola virus disease among male and female persons in West Africa. *N Engl J Med.* 2016;374:96–8. <http://dx.doi.org/10.1056/NEJMc1510305>
- Rollin PE, Bausch DG, Sanchez A. Blood chemistry measurements and D-dimer levels associated with fatal and nonfatal outcomes in humans infected with Sudan Ebola virus. *J Infect Dis.* 2007;196(Suppl 2):S364–71. <http://dx.doi.org/10.1086/520613>
- Barry M, Touré A, Traoré FA, Sako FB, Sylla D, Kpamy DO, et al. Clinical predictors of mortality in patients with Ebola virus disease. *Clin Infect Dis.* 2015;60:1821–4. <http://dx.doi.org/10.1093/cid/civ202>
- Barry M, Traoré FA, Sako FB, Kpamy DO, Bah EI, Poncin M, et al. Ebola outbreak in Conakry, Guinea: epidemiological, clinical, and outcome features. *Med Mal Infect.* 2014;44:491–4. <http://dx.doi.org/10.1016/j.medmal.2014.09.009>
- Martins K, Cooper C, Warren T, Wells J, Bell T, Raymond J, et al. Characterization of clinical and immunological parameters during Ebola virus infection of rhesus macaques. *Viral Immunol.* 2015;28:32–41. <http://dx.doi.org/10.1089/vim.2014.0085>
- Warren TK, Trefry JC, Marko ST, Chance TB, Wells JB, Pratt WD, et al. Euthanasia assessment in Ebola virus infected nonhuman primates. *Viruses.* 2014;6:4666–82. <http://dx.doi.org/10.3390/v6114666>
- Marzi A, Feldmann F, Hanley PW, Scott DP, Günther S, Feldmann H. Delayed disease progression in cynomolgus macaques infected with Ebola virus Makona strain. *Emerg Infect Dis.* 2015;21:1777–83. <http://dx.doi.org/10.3201/eid2110.150259>
- Wong G, Qiu X, de La Vega MA, Fernando L, Wei H, Bello A, et al. Pathogenicity comparison between the Kikwit and Makona Ebola virus variants in rhesus macaques. *J Infect Dis.* 2016;214 (Suppl 3):S281–9. <http://dx.doi.org/10.1093/infdis/jiw267>
- McElroy AK, Spiropoulou CF. Biomarkers for understanding Ebola virus disease. *Biomarkers Med.* 2014;8:1053–6. <http://dx.doi.org/10.2217/bmm.14.75>
- Villinger F, Rollin PE, Brar SS, Chikkala NF, Winter J, Sundstrom JB, et al. Markedly elevated levels of interferon (IFN)- γ , IFN- α , interleukin (IL)-2, IL-10, and tumor necrosis factor- α associated with fatal Ebola virus infection. *J Infect Dis.* 1999;179(Suppl 1):S188–91. <http://dx.doi.org/10.1086/514283>
- Leroy EM, Baize S, Lu CY, McCormick JB, Georges AJ, Georges-Courbot MC, et al. Diagnosis of Ebola hemorrhagic fever by RT-PCR in an epidemic setting. *J Med Virol.* 2000;60:463–7. [http://dx.doi.org/10.1002\(SICI\)1096-9071\(200004\)60:4<463::AID-JMV15>3.0.CO;2-M](http://dx.doi.org/10.1002(SICI)1096-9071(200004)60:4<463::AID-JMV15>3.0.CO;2-M)
- Warren TK, Jordan R, Lo MK, Ray AS, Mackman RL, Soloveva V, et al. Therapeutic efficacy of the small molecule GS-5734 against Ebola virus in rhesus monkeys. *Nature.* 2016;531:381–5. <http://dx.doi.org/10.1038/nature17180>
- Geisbert TW, Lee AC, Robbins M, Geisbert JB, Honko AN, Sood V, et al. Postexposure protection of non-human primates against a lethal Ebola virus challenge with RNA interference: a proof-of-concept study. *Lancet.* 2010;375:1896–905. [http://dx.doi.org/10.1016/S0140-6736\(10\)60357-1](http://dx.doi.org/10.1016/S0140-6736(10)60357-1)

30. Qiu X, Wong G, Audet J, Bello A, Fernando L, Alimonti JB, et al. Reversion of advanced Ebola virus disease in nonhuman primates with ZMapp. *Nature*. 2014;514:47–53.
31. Pettitt J, Zeitlin L, Kim DH, Working C, Johnson JC, Bohorov O, et al. Therapeutic intervention of Ebola virus infection in rhesus macaques with the MB-003 monoclonal antibody cocktail. *Sci Transl Med*. 2013;5:199ra113. <http://dx.doi.org/10.1126/scitranslmed.3006608>
32. Colubri A, Silver T, Fradet T, Retzepi K, Fry B, Sabeti P. Transforming clinical data into actionable prognosis models: machine-learning framework and field-deployable app to predict outcome of Ebola patients. *PLoS Negl Trop Dis*. 2016;10:e0004549. <http://dx.doi.org/10.1371/journal.pntd.0004549>
33. Hasanoglu I, Guner R, Carhan A, Kocak Tufan Z, Yagci-Caglayik D, Guven T, et al. Crucial parameter of the outcome in Crimean Congo hemorrhagic fever: Viral load. *J Clin Virol*. 2016;75:42–6. <http://dx.doi.org/10.1016/j.jcv.2015.12.006>
34. Ozturk B, Tutuncu E, Kuscu F, Gurbuz Y, Sencan I, Tuzun H. Evaluation of factors predictive of the prognosis in Crimean-Congo hemorrhagic fever: new suggestions. *Int J Infect Dis*. 2012;16:e89–93. <http://dx.doi.org/10.1016/j.ijid.2011.06.005>
35. Gai ZT, Zhang Y, Liang MF, Jin C, Zhang S, Zhu CB, et al. Clinical progress and risk factors for death in severe fever with thrombocytopenia syndrome patients. *J Infect Dis*. 2012;206:1095–102. <http://dx.doi.org/10.1093/infdis/jis472>
36. Sirikutt P, Kalayanaroj S. Serum lactate and lactate dehydrogenase as parameters for the prediction of dengue severity. *J Med Assoc Thai*. 2014;97(Suppl 6):S220–31.
37. Adeva-Andany M, López-Ojén M, Funcasta-Calderón R, Ameneiros-Rodríguez E, Donapetry-García C, Vila-Altesor M, et al. Comprehensive review on lactate metabolism in human health. *Mitochondrion*. 2014;17:76–100. <http://dx.doi.org/10.1016/j.mito.2014.05.007>
38. Guzmán-de la Garza FJ, Ibarra-Hernández JM, Cordero-Pérez P, Villegas-Quintero P, Villarreal-Ovalle CI, Torres-González L, et al. Temporal relationship of serum markers and tissue damage during acute intestinal ischemia/reperfusion. *Clinics (Sao Paulo)*. 2013;68:1034–8. [http://dx.doi.org/10.6061/clinics/2013\(07\)23](http://dx.doi.org/10.6061/clinics/2013(07)23)
39. Yasuda H, Okita Y, Imaoka H, Fujikawa H, Ohi M, Araki T, et al. Intestinal necrosis due to norovirus enteritis. *Clin J Gastroenterol*. 2015;8:10–3. <http://dx.doi.org/10.1007/s12328-014-0540-0>
40. de Villiers FPR, Driessen M. Clinical neonatal rotavirus infection: association with necrotising enterocolitis. *S Afr Med J*. 2012;102:620–4. <http://dx.doi.org/10.7196/SAMJ.5150>
41. Lynn LA. Combined endothelial and epithelial barrier disruption of the colon may be a contributing factor to the Ebola sepsis-like syndrome. *Patient Saf Surg*. 2015;9:1. <http://dx.doi.org/10.1186/s13037-014-0048-z>
42. Kortepeter MG, Lawler JV, Honko A, Bray M, Johnson JC, Purcell BK, et al. Real-time monitoring of cardiovascular function in rhesus macaques infected with *Zaire ebolavirus*. *J Infect Dis*. 2011;204(Suppl 3):S1000–10. <http://dx.doi.org/10.1093/infdis/jir337>
43. Zein JG, Lee GL, Tawk M, Dabaja M, Kinasewitz GT. Prognostic significance of elevated serum lactate dehydrogenase (LDH) in patients with severe sepsis. *Chest*. 2004;126(4_Meeting Abstracts):873S. http://doi.org/10.1378/chest.126.4_MeetingAbstracts.873S
44. Kruse O, Grunnet N, Barfod C. Blood lactate as a predictor for in-hospital mortality in patients admitted acutely to hospital: a systematic review. *Scand J Trauma Resusc Emerg Med*. 2011;19:74. <http://dx.doi.org/10.1186/1757-7241-19-74>
45. Vincent JL, Quintairo E Silva A, Couto L Jr, Taccone FS. The value of blood lactate kinetics in critically ill patients: a systematic review. *Crit Care*. 2016;20:257. <http://dx.doi.org/10.1186/s13054-016-1403-5>
46. Duman A, Akoz A, Kapci M, Ture M, Orun S, Karaman K, et al. Prognostic value of neglected biomarker in sepsis patients with the old and new criteria: predictive role of lactate dehydrogenase. *Am J Emerg Med*. 2016;34:2167–71. <http://dx.doi.org/10.1016/j.ajem.2016.06.012>
47. Erez A, Shental O, Tchebiner JZ, Laufer-Perl M, Wasserman A, Sella T, et al. Diagnostic and prognostic value of very high serum lactate dehydrogenase in admitted medical patients. *Isr Med Assoc J*. 2014;16:439–43.
48. Johnson E, Jaax N, White J, Jahrling P. Lethal experimental infections of rhesus monkeys by aerosolized Ebola virus. *Int J Exp Pathol*. 1995;76:227–36.

Address for correspondence: Anthony P. Cardile, United States Army Medical Research Institute of Infectious Diseases, 1425 Porter St, Rm 529, Fort Detrick, Frederick, MD 21702, USA; email: anthony.p.cardile.mil@mail.mil

EID SPOTLIGHT TOPIC

Ebola, previously known as Ebola hemorrhagic fever, is a rare and deadly disease caused by infection with one of the Ebola virus strains. Ebola can cause disease in humans and nonhuman primates (monkeys, gorillas, and chimpanzees).

Ebola is caused by infection with a virus of the family *Filoviridae*, genus *Ebolavirus*. There are five identified Ebola virus species, four of which are known to cause disease in humans. Ebola viruses are found in several African countries; they were first discovered in 1976 near the Ebola River in what is now the Democratic Republic of the Congo. Before the current outbreak, Ebola had appeared sporadically in Africa.

The natural reservoir host of Ebola virus remains unknown. However, on the basis of evidence and the nature of similar viruses, researchers believe that the virus is animal-borne and that bats are the most likely reservoir. Four of the five virus strains occur in an animal host native to Africa.



**EMERGING
INFECTIOUS DISEASES**

<http://wwwnc.cdc.gov/eid/page/ebola-spotlight>

Maguari Virus Associated with Human Disease

Allison Groseth, Veronica Vine, Carla Weisend, Carolina Guevara, Douglas Watts,¹
Brandy Russell, Robert B. Tesh, Hideki Ebihara

Despite the lack of evidence for symptomatic human infection with Maguari virus (MAGV), its close relation to Cache Valley virus (CVV), which does infect humans, remains a concern. We sequenced the complete genome of a MAGV-like isolate (OBS6657) obtained from a febrile patient in Pucallpa, Ucayali, Peru, in 1998. To facilitate its classification, we generated additional full-length sequences for the MAGV prototype strain, 3 additional MAGV-like isolates, and the closely related CVV (7 strains), Tlacotalpan (1 strain), Playas (3 strains), and Fort Sherman (1 strain) viruses. The OBS6657 isolate is similar to the MAGV prototype, whereas 2 of the other MAGV-like isolates are located on a distinct branch and most likely warrant classification as a separate virus species and 1 is, in fact, a misclassified CVV strain. Our findings provide clear evidence that MAGV can cause human disease.

Maguari virus (MAGV) was first isolated from a mixed pool of mosquitoes collected in Utinga forest in Brazil in 1957 and has since been isolated from a variety of mosquito species (including *Aedes* spp., *Anopheles* spp., *Culex* spp., *Wyeomyia* spp., and *Psorophora* spp.) in Ecuador, Brazil, Trinidad and Tobago, Colombia, Argentina, and French Guiana (1). MAGV also has been isolated from horses in Guyana and Colombia (2,3) and from sentinel mice in Brazil (1), with further serologic evidence for infection with MAGV-like viruses in cattle, water buffalo, sheep, and birds (1). However, there had been no clear evidence of symptomatic human infection with MAGV.

In 2015, an orthobunyavirus isolate from a patient with febrile illness that had been tentatively classified as MAGV on the basis of serologic reactivity by indirect immunofluorescence test was shown instead to be a new Caraparu (Group C) reassortant, for which the name Itaya virus has been proposed (4). However, serologic evidence

of infection with MAGV-like viruses in humans has been reported in Argentina, Brazil, Peru, Colombia, and French Guiana (1,5,6). Furthermore, MAGV is considered a subtype of Cache Valley virus (CVV), which sometimes causes symptomatic human infection (7–9), reinforcing lingering concerns about the possible pathogenicity of MAGV for humans.

Given that cross-reactivity among bunyaviruses when using serologic techniques is not uncommon, their identification has increasingly involved incorporating genetic approaches to characterize these virus isolates. Such serologic cross-reactivity appears particularly to be an issue with MAGV, which was originally reported as CVV, and also shows cross-reactivity to other closely related viruses (1). Therefore, to clarify the genetic relationship between MAGV or MAGV-like viruses and the closely related CVV, as well as their association with acute human disease, we determined the complete genome sequences for all available MAGV isolates and conducted a comprehensive sequencing analysis of several full-length reference sequences for CVV strains and available strains of the closely related Tlacotalpan virus (TLAV), Playas virus (PLAV), and Fort Sherman virus (FSV) to facilitate the reliable classification of these and related virus isolates.

Materials and Methods

Viruses

We obtained 4 isolates identified as MAGV (including the prototype strain BeAr7272), spanning 1957–1998 and originating from 3 of the 7 countries from which the virus has been isolated (Colombia, Brazil, and Argentina) (Figure 1). Isolates were obtained from the World Reference Center for Emerging Viruses and Arboviruses (WRCEVA) or the Division of Vector-Borne Diseases, National Center for Emerging and Zoonotic Infectious Diseases, Centers for Disease Control and Prevention (DVBD-CDC, Atlanta, GA, USA) (online Technical Appendix Table 1, <https://wwwnc.cdc.gov/EID/article/23/8/16-1254-Techapp1.pdf>). In addition, we obtained 7 isolates of CVV spanning 1956–2003 and originating from diverse locations throughout the United States and Mexico, as well as 1 isolate of Tlacotalpan virus (Mexico),

Author affiliations: Friedrich-Loeffler-Institut, Greifswald–Insel Riems, Germany (A. Groseth); National Institutes of Health, Hamilton Montana, USA (A. Groseth, V. Vine, C. Weisend, H. Ebihara); US Naval Medical Research Unit 6, Lima, Peru (C. Guevara, D. Watts); Centers for Disease Control and Prevention, Ft. Collins, Colorado, USA (B. Russell); University of Texas Medical Branch, Galveston, Texas, USA (R.B. Tesh); Mayo Clinic, Rochester, Minnesota, USA (H. Ebihara)

DOI: <https://doi.org/10.3201/eid2308.161254>

¹Current affiliation: University of Texas, El Paso, Texas, USA.

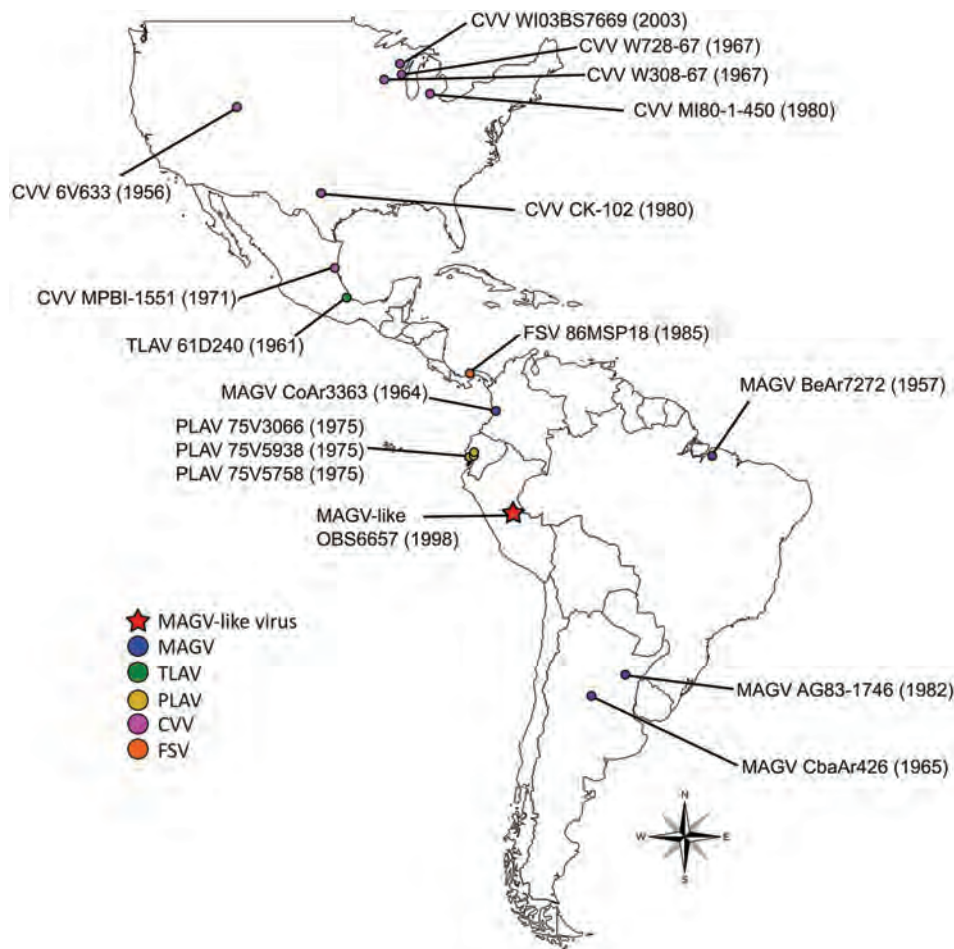


Figure 1. Geographic locations from which virus strains used in study of human infection with MAGV were isolated. Star indicates the location of the MAGV-like isolate OBS6657; circles indicate source locations for other isolates used in this study. CVV, Cache Valley virus; FSV, Fort Sherman virus; MAGV, Maguari virus; PLAV, Playas virus; TLAV, Tlacotalpan virus.

3 isolates of Playas virus (Ecuador), and 1 isolate of FSV (Panama) (Figure 1) from either WRCEVA or DVBD-CDC. An additional MAGV-like virus strain, isolated from a patient exhibiting fever, headache, myalgia, and chills in Pucallpa, Ucayali, Peru, in 1998 (strain OBS6657), was obtained from WRCEVA. This isolate was collected under the terms of a human use protocol (NMRCD.2000.0006), which, along with the consent procedure, were approved by the Naval Medical Research Center Institutional Review Board in compliance with all US and Peruvian federal regulations governing the protection of human subjects.

Sequencing

We extracted viral RNA using the QIAamp viral RNA mini kit (QIAGEN, Hilden, Germany) according to the manufacturer's instructions with reverse transcription PCR (RT-PCR) reactions performed using the Superscript III reverse transcription kit (Life Technologies, Carlsbad, CA, USA) and the iProof High-Fidelity PCR Kit (Bio-Rad Laboratories, Hercules, CA, USA). We obtained preliminary virus genome sequences of the MAGV BeAr7272 and

AG83-1746 strains, as well as PLAV (strain 75V3066), TLAV (strain 61D240), and FSV (strain 86MSP18), using the 454 FLX pyrosequencing technology platform (454 Life Sciences [Roche], Branford, CT, USA). We constructed libraries using previously described methods (10) and assembled and analyzed genomes using various publically available algorithms. Based on the preliminary 454-determined sequences, we designed primer sets to enable confirmation by Sanger sequencing, including analysis of additional strains of MAGV and PLAV. CVV strains were similarly sequenced by using primers based on complete sequences of the MNZ-92011 strain (GenBank accession nos. KC436108 [small (S) segment], KC436107 [medium (M) segment], KC436106 [large (L) segment]). The sequences of the noncoding regions, including the conserved genome termini, were amplified by using 3' and 5' rapid amplification of cDNA ends based on ligation-anchored PCR, as previously described (11-13). We deposited complete genome sequences determined in this study in GenBank (online Technical Appendix Table 1); primer sequences are available on request.

Phylogenetic and Sequence Analyses

Phylogenetic and sequence divergence analyses were conducted on the open reading frames (ORFs) and their corresponding amino acid sequences. These analyses incorporated the sequences for MAGV, CVV, TLAV, PLAV, and FSV determined in this study and additional representative orthobunyavirus sequences available in GenBank (online Technical Appendix Table 2).

Sequences for each ORF or corresponding amino acid sequence were aligned using the MUSCLE algorithm, and the evolutionary history for each tree construction was inferred using the neighbor-joining (14) and maximum-likelihood (15) methods, as implemented in MEGA5 (16). For neighbor-joining analysis of amino acid sequences, we used a Poisson model (17) and uniform rates; for analysis of nucleotides, uniform rates also were specified. We computed evolutionary distances using the maximum composite likelihood method (18). For maximum-likelihood analysis of amino acids the Jones, Taylor, and Thornton model (JTT) (19), gamma-distributed (+ G) was used for all 3 segments. Alternatively, for both the amino acid and nucleotide analyses, we used the best fit model for each segment, based on the calculated Bayesian information criterion, as determined using the Model Selection Tool implemented in MEGA5 (16) (i.e., JTT + G [N amino acid]; Le-Gascuel [LG] model [20] + G plus invariant sites [+ I] [LG + G + I; GPC amino acid], LG + G, + I plus frequencies [LG + G + I + F; L amino acid] or Tamura 3-parameter [21] + G [T92 + G, N nucleotide]; general time reversible [22] + G + I [GTR + G + I; GPC and L nucleotide]). Evaluation of statistical support for the neighbor-joining and maximum-likelihood tree topologies was based on bootstrap resampling (23); values were calculated on the basis of 1,000 replicates, and values >60 are indicated. We conducted an additional analysis based on Bayesian inference using Mr Bayes version 3 (24,25), as implemented in TOPALi version 2 (26) with the best fit model for each segment selected on the basis of the calculated Bayesian information criterion, using the integrated model selection tool in TOPALi (i.e., JTT + G [N amino acid]; JTT + G + I [GPC and L amino acid] or GTR + G [N amino acid]; GTR + G + I [GPC and L amino acid]). Posterior probability values >0.60 were indicated. The use of these different methods and models did not produce substantially different tree topologies with respect to the virus lineages under study (Figure 2; online Technical Appendix Figures 1, 2).

We calculated sequence divergence values on the basis of nucleotide and amino acid alignments constructed with ClustalW as implemented in MegAlign (LaserGene 12; DNASTAR, Madison, WI, USA). Furthermore, an additional recombination analysis was performed on concatenated (S, M, and L) genome sequences of all CVV, MAGV, PLAV, TLAV, and FSV isolates where full-length sequences were available. Initial alignment was performed by using the MUSCLE algorithm, as implemented in

MEGA5 (16), and these data were then further analyzed by using the RDP (27), GENECONV (28), BOOTSCAN/RECSCAN (29), MAXCHI (30), CHIMAERA (31), SISCAN (32), and 3SEQ (33) programs, as implemented in RDP4 Beta 4.83 (34).

Results and Discussion

Analysis of MAGV and MAGV-Like Sequences

In our phylogenetic analysis, the MAGV isolates we examined form 2 distinct clades: 1 contains the prototype strain BeAr7272 and “PLAV” (strain 75V5758), the other comprises the AG83-1746 strain and the CbaAr426 strain (Figure 2). Both of these atypical “MAGV” isolates (AG83-1746 and CbaAr426) were collected in Argentina and were isolated 17 years apart, indicating that this virus most likely continues to stably circulate in that region. MAGV (CoAr3363) was found to be an incorrectly classified isolate of CVV and thus is not considered further in this section. Of particular interest to the aims of this study was the MAGV-like isolate designated OBS6657, which was previously identified by complement fixation as a MAGV-like virus, after isolation from a symptomatic patient in Peru. Phylogenetic analysis indicates that this virus is closely related to the prototype MAGV isolate BeAr7272, with which it shares a clade.

Our divergence analysis comparing the 2 groups formed by the isolates originally identified as MAGV showed 95.7% (N), 84.3%–85.2% (GPC), and 90.1%–90.7% (L) amino acid divergence. The extremely low level of N protein variability seems to be a characteristic of these and related virus groups, and the L protein divergence values are barely above the 10%-aa divergence sometimes suggested as a cutoff for speciation. However, the glycoprotein, which is the most variable of the viral protein products, differs substantially from all other related virus groups and also between these 2 groups. Furthermore, the consistent evidence for separate evolutionary histories inferred by the phylogenies for all 3 proteins indicates that these viruses most likely differ sufficiently to warrant reclassification of the AG83-1746 strain and CbaAr426 strains as a distinct virus species. In accordance with the prevailing naming conventions for bunyaviruses, which dictate naming based on the location of initial isolation, we use “Córdoba virus” (CODV) and “CODV lineage” herein to refer to viruses belonging to this group and to distinguish them from the canonical MAGV strains.

In contrast to these various misidentified viruses, the OBS6657 isolate clearly grouped with the prototype MAGV strain BeAr7272 and showed 100% (N), 97.1% (GPC), and 99.0% (L) amino acid identity, respectively, across each of the three major gene products, despite being isolated >40 years later. Given that this virus was isolated from a patient exhibiting clear evidence of an acute febrile infection, our data provide strong evidence that MAGV infection can

cause clinical disease in humans. In light of this evidence, and particularly when considered together with serologic

data that indicate frequent infection with MAGV-like viruses (2%–64% positive serum samples) (1,5,6) in South America,

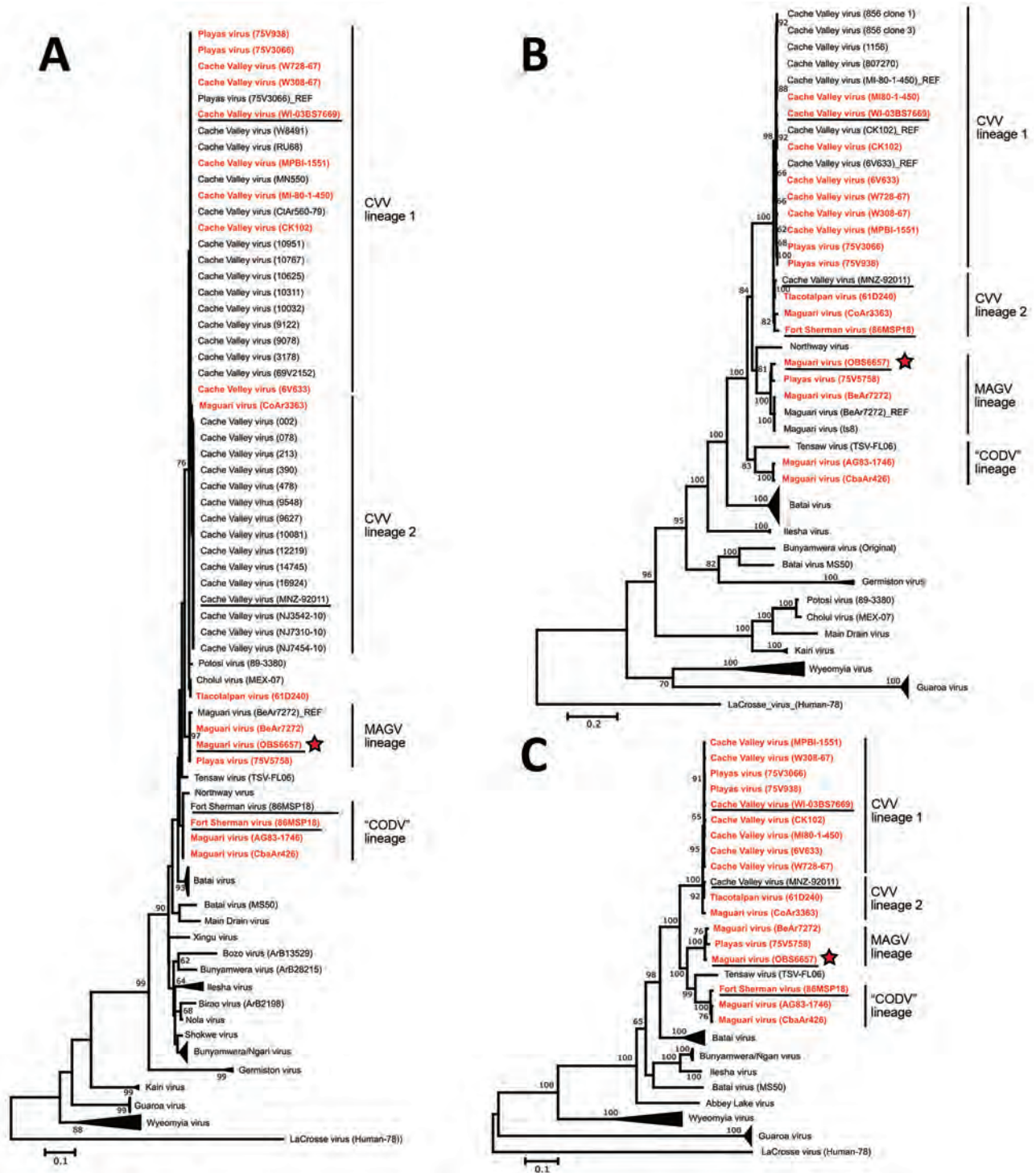


Figure 2. Phylogenetic relationship of MAGV-like isolate OBS6657 to other MAGV and CVV isolates and reference orthobunyaviruses. Maximum-likelihood trees (Jones, Taylor, and Thornton model, gamma-distributed) were constructed on the basis of the amino acid sequences of the nucleoprotein (A), glycoprotein (B), and polymerase (C). Bootstrap values based on 1,000 replicates are indicated for values >60. Sequences generated in this study are shown in red bold. Human isolates within the CVV, MAGV, and Córdoba virus clades are underlined, and the OBS6657 isolate is indicated with a red star. Scale bars indicate nucleotide substitutions per site. CVV, Cache Valley virus; CODV, Córdoba virus; MAGV, Maguari virus.

it appears likely that the failure to recognize MAGV as a causative agent of febrile infection in humans is due to a lack of systematic surveillance and diagnostic testing rather than a lack of pathogenic potential. Furthermore, the inclusion of PLAV (75V5758) in this group suggests that, even if human virulence were restricted to this group, the affected region might cover a large portion of Central and South America, including Brazil (strain BeAr7272), Peru (strain OBS6657), and Ecuador (PLAV strain 75V5758).

Analysis of CVV Sequences

To obtain sufficient data to provide a reliable framework for analyzing the MAGV isolates in this study, and in light of their recently demonstrated potential as human pathogens, we further conducted full-genome sequence analysis for several CVV strains and for the closely related PLAV and TLAV, and for the human pathogenic FSV, which also has been described to be closely related to CVV (35). Of the 7 CVV isolates that we fully sequenced, all appear to belong to the recently described lineage 1 of CVV, consistent with the suggestions that older strains from the United States, such as those used in this study, belong to this lineage and have only recently been supplanted in some areas by lineage 2 viruses (36). In addition, TLAV (strain 61D240) and 2 of the 3 strains of PLAV virus analyzed (strains 75V3066 and 75V5938) clearly grouped within the CVV clade for all 3 segments (Figure 2). The other PLAV strain (strain 75V5758) belonged to the canonical MAGV lineage, as noted earlier. The need to reclassify these virus strains as isolates of CVV is further supported by divergence analysis (online Technical Appendix Figure 3, panels A–C), which shows that each of these viruses shows >90% aa identity to all known CVV isolates for all 3 major proteins, including the highly variable glycoprotein. Given the surprising nature of this result, we further confirmed this finding using multiple virus passages and stocks provided from 2 different collections (WRCEVA and DVBD-CDC); however, the results remained consistent (data not shown). Overall, our data provide unequivocal support, on the basis of full-genome sequencing data for all 3 segments of multiple virus strains, for previous observations from S-segment data from single strains of each of TLAV and PLAV (36) that had suggested these strains might indeed have been misclassified as new virus species upon discovery. Similarly, we also identified 1 isolate previously classified as MAGV (strain CoAr3363) as a misidentified CVV lineage 2 virus (Figure 2; online Technical Appendix Figure 3, panels A–C).

We also included FSV in our analysis. This isolate was collected in 1985 at Fort Sherman, a former US Army base in Panama, from a patient exhibiting fever (101°F), malaise, muscle aches, and sore throat. The isolate cross-reacted very closely with CVV, MAGV, and PLAV virus in complement

fixation but only with CVV and PLAV by plaque-reduction neutralization test (37). During the original isolation, FSV was suggested to be a subtype of CVV (35). However, sequencing of the S segment has shown it to be only moderately related to CVV, although statistical support for the branching arrangement was poor (38). On the basis of our full-length analysis of all 3 gene segments, we can now clarify and reconcile these apparently disparate findings, by identifying FSV as a reassortant between CVV lineage 2 and “CODV” (CODV_S/CVV_M/CODV_L). Taken together, the phylogenetic arrangement (Figure 2) and divergence analysis (online Technical Appendix Figure 3, panels A–C), as well as a recombination/reassortment analysis using concatenated genomes (online Technical Appendix Figure 3, panel D), indicate that CODV (CbaAr426) is the closest relative of the S and L segment donor, and the strain CoAr3363 (previously misclassified as MAGV) from CVV lineage 2 is the closest to the M segment donor. This observation would appear to explain the close antigenic relationship of FSV to both CVV and MAGV by complement fixation but not plaque-reduction neutralization test, as well as the lack of sequence relationship between the S segments of these viruses.

One important consequence of the genetic reassignment of not only TLAV and PLAV, but also of MAGV (CoAr3363) to the CVV group, and identification of FSV as a previously unrecognized CVV reassortant, is to substantially expand the known geographic range of CVV. On the basis of these data, the range of CVV must now be considered to include not only the United States and northern and central Mexico but probably all of Central America and the northern areas of South America. Furthermore, although both PLAV strains appear to belong to CVV lineage 1, TLAV belongs to CVV lineage 2, as does the CVV donor of the FSV M segment. This finding suggests that both lineages exist in Central America and that lineage 2 has been circulating in that region since at least the 1960s, when the first of these viruses were isolated. This supposition is also supported by the assignment of the MAGV CoAr3363 strain, which was isolated in 1964, to lineage 2. Taken together, these findings suggest that although these CVV lineage 2 strains have only recently emerged in the eastern United States, they might in fact have been circulating in South America for decades and have only recently been introduced into the United States from these regions.

Technical Considerations in the Genetic and Serologic Analysis of Nucleoprotein Sequences

Our analysis of the ORF and amino acid data identified several distinct clades representing CVV (lineages 1 and 2) and 2 separate clades of what had been identified as MAGV strains (Figure 2). These clades were all well-supported for the GPC and L ORFs. However, although the members of the identified groups also were suggested to remain consistent

when data for the nucleoprotein were analyzed, suggesting a lack of reassortment in these viruses, the branching was only poorly supported. This observation most likely resulted from an overall low level of total variation between these closely related groups, which is exacerbated when shorter datasets, such as that for N, are used. It is possible (and maybe even likely) that this issue will continue to present a growing problem for orthobunyavirus group analyses based on N as an increasing number of sequences for related virus groups continue to become available.

The extent of this issue is further highlighted by our divergence analysis (online Technical Appendix Figure 3, panels A–C), which shows extremely high sequence identity (93.6%–100% aa) among members of these groups, even when the analysis includes more distantly related and clearly geographically distinct viruses, such as Batai virus. These high levels of conservation may then also suggest a basis for the historical difficulties in serologic virus identification that seem to be increasingly identified during retrospective virus identification efforts, including this one. Surprisingly, a recent report showed that a virus isolate originally reported as MAGV was, in fact, a reassortant of Caraparu, a group C virus (4), which is genetically only distantly related to the Bunyamwera serogroup viruses. This finding suggests that the accurate serologic identification of orthobunyaviruses is difficult. This observed lack of overall variability in the N proteins of these viruses seems to suggest that the serologic identification of Bunyamwera group viruses, and perhaps also other groups, by complement fixation might be particularly difficult, if not impossible, and needs to be approached carefully. Furthermore, given the apparent extent of this problem and the widespread availability and modest costs associated with RT-PCR and Sanger sequencing, it may be prudent to recommend routinely incorporating at least partial genetic characterization as a part of the identification process for all new bunyavirus isolates. Indeed, given the high level of conservation observed within the N gene of related orthobunyavirus groups, it would make an ideal target for the development of broadly cross-reactive RT-PCR primer sets for diagnostic applications.

In summary, we identified MAGV as the causative agent of a human febrile infection in Peru and showed that the virus associated with this infection is highly similar to the prototype MAGV isolate, suggesting that other viruses of this lineage also might have pathogenic potential in humans. In addition, our in-depth analysis of the closely related CVV group and other similar viruses showed that PLAV and TLAV do not exist as distinct virus species but are misclassified strains of other existing groups and that the human pathogenic FSV is a previously unrecognized reassortant between CVV, itself a known human pathogen, and a new lineage whose members had previously been

identified as MAGV but are genetically distinct from the lineage occupied by the prototypical MAGV isolates. On the basis of its location of origin, we suggest the name “Córdoba virus” for this new lineage. Based on the reclassification of these virus isolates, it is clear that the endemic region for CVV is much larger than previously recognized and that CVV and MAGV most likely are responsible for unrecognized febrile infections throughout North, Central, and South America. We hope that a better understanding of the genetic relationships between bunyavirus groups, particularly in relation to their relevance for human infection, coupled with an increased availability of reference genome sequence information, such as provided by this study, will help enable future surveillance and diagnostic efforts and increase awareness of the importance of orthobunyaviruses as human pathogens.

Acknowledgments

We are grateful to WRCEVA, DVBD-CDC, and the US Naval Medical Research Unit 6 for providing us with the virus strains. We especially thank the Peruvian Ministry of Health (Dirección General de Epidemiología and Instituto Nacional de Salud) for giving us access to samples from febrile patients and the febrile surveillance system partners who participated in the collection of isolates from febrile patients. We also thank the members of the Rocky Mountain Laboratory Genomics Unit for their services, Thomas Hoenen for critical reading of the manuscript and assistance with figure preparation, and El-Sayed M. Abd El-Whab for assistance with TOPLAI.

This work was supported by the Intramural Research Program of the National Institutes of Health, National Institute of Allergy and Infectious Diseases. R.B.T. was supported by National Institutes of Health contract HHSN272201000040I/HHSN200004/D04.

Dr. Groseth is the group leader for the Arenavirus Biology Workgroup, Friedrich-Loeffler-Institut. Her research focuses on virus evolution, virulence acquisition, and the identification of virulence determinants.

References

1. Shope RE, Whitman L, Maguari. In: Karabatsos N, editor. International catalogue of arboviruses including certain other viruses of vertebrates. 3rd ed. San Antonio (TX): American Society of Tropical Medicine and Hygiene; 1985. p. 641–2.
2. Spence L, Jonkers AH, Grant LS. Arboviruses in the Caribbean Islands. *Prog Med Virol.* 1968;10:415–86.
3. Sanmartín C, Mackenzie RB, Trapido H, Barreto P, Mullenax CH, Gutiérrez E, et al. Venezuelan equine encephalitis in Colombia, 1967 [in Spanish]. *Bol Oficina Sanit Panam.* 1973;74:108–37.
4. Hontz RD, Guevara C, Halsey ES, Silvas J, Santiago FW, Widen SG, et al. Itaya virus, a novel orthobunyavirus associated with human febrile illness, Peru. *Emerg Infect Dis.* 2015;21:781–8. <http://dx.doi.org/10.3201/eid2105.141368>

5. Mettler NE, Casals J, Parodi AS. Survey for antibodies against arthropod-borne viruses in man in Argentina. *Am J Trop Med Hyg.* 1963;12:653.
6. Sabattini MS, Shope RE, Vanella JM. Serological survey for arboviruses in Córdoba Province, Argentina. *Am J Trop Med Hyg.* 1965;14:1073–8.
7. Sexton DJ, Rollin PE, Breitschwerdt EB, Corey GR, Myers SA, Dumais MR, et al. Life-threatening Cache Valley virus infection. *N Engl J Med.* 1997;336:547–9. <http://dx.doi.org/10.1056/NEJM199702203360804>
8. Campbell GL, Mataczynski JD, Reisdorf ES, Powell JW, Martin DA, Lambert AJ, et al. Second human case of Cache Valley virus disease. *Emerg Infect Dis.* 2006;12:854–6. <http://dx.doi.org/10.3201/eid1205.051625>
9. Nguyen NL, Zhao G, Hull R, Shelly MA, Wong SJ, Wu G, et al. Cache valley virus in a patient diagnosed with aseptic meningitis. *J Clin Microbiol.* 2013;51:1966–9. <http://dx.doi.org/10.1128/JCM.00252-13>
10. Groseth A, Mampilli V, Weisend C, Dahlstrom E, Porcella SF, Russell BJ, et al. Molecular characterization of human pathogenic bunyaviruses of the Nyando and Bwamba/Pongola virus groups leads to the genetic identification of Mojuí dos Campos and Kaeng Khoi virus. *PLoS Negl Trop Dis.* 2014;8:e3147. <http://dx.doi.org/10.1371/journal.pntd.0003147>
11. Li Z, Yu M, Zhang H, Wang HY, Wang LF. Improved rapid amplification of cDNA ends (RACE) for mapping both the 5' and 3' terminal sequences of paramyxovirus genomes. *J Virol Methods.* 2005;130:154–6. <http://dx.doi.org/10.1016/j.jviromet.2005.06.022>
12. Tillett D, Burns BP, Neilan BA. Optimized rapid amplification of cDNA ends (RACE) for mapping bacterial mRNA transcripts. *Biotechniques.* 2000;28:448, 450, 452–3, 456.
13. Troutt AB, McHeyzer-Williams MG, Pulendran B, Nossal GJ. Ligation-anchored PCR: a simple amplification technique with single-sided specificity. *Proc Natl Acad Sci U S A.* 1992;89:9823–5. <http://dx.doi.org/10.1073/pnas.89.20.9823>
14. Saitou N, Nei M. The neighbor-joining method: a new method for reconstructing phylogenetic trees. *Mol Biol Evol.* 1987;4:406–25.
15. Tamura K, Nei M. Estimation of the number of nucleotide substitutions in the control region of mitochondrial DNA in humans and chimpanzees. *Mol Biol Evol.* 1993;10:512–26.
16. Tamura K, Peterson D, Peterson N, Stecher G, Nei M, Kumar S. MEGA5: molecular evolutionary genetics analysis using maximum likelihood, evolutionary distance, and maximum parsimony methods. *Mol Biol Evol.* 2011;28:2731–9. <http://dx.doi.org/10.1093/molbev/msr121>
17. Zuckerkandl, E., Pauling, L. Evolutionary divergence and convergence in proteins. In: Bryson V, Vogel HJ, editors. *Evolving genes and proteins.* 6th ed. New York: Academic Press; 1965. p. 97–166.
18. Tamura K, Nei M, Kumar S. Prospects for inferring very large phylogenies by using the neighbor-joining method. *Proc Natl Acad Sci U S A.* 2004;101:11030–5. <http://dx.doi.org/10.1073/pnas.0404206101>
19. Jones DT, Taylor WR, Thornton JM. The rapid generation of mutation data matrices from protein sequences. *Comput Appl Biosci.* 1992;8:275–82.
20. Le SQ, Gascuel O. An improved general amino acid replacement matrix. *Mol Biol Evol.* 2008;25:1307–20. <http://dx.doi.org/10.1093/molbev/msn067>
21. Tamura K. Estimation of the number of nucleotide substitutions when there are strong transition-transversion and G+C-content biases. *Mol Biol Evol.* 1992;9:678–87.
22. Nei M, Kumar S. *Molecular evolution and phylogenetics.* 6th ed. New York: Oxford University Press; 2000.
23. Felsenstein J. Confidence limits on phylogenies: an approach using the bootstrap. *Evolution.* 1985;39:783–91. <http://dx.doi.org/10.2307/2408678>
24. Huelsenbeck JP, Ronquist F. MRBAYES: Bayesian inference of phylogenetic trees. *Bioinformatics.* 2001;17:754–5. <http://dx.doi.org/10.1093/bioinformatics/17.8.754>
25. Ronquist F, Huelsenbeck JP. MrBayes 3: Bayesian phylogenetic inference under mixed models. *Bioinformatics.* 2003;19:1572–4. <http://dx.doi.org/10.1093/bioinformatics/btg180>
26. Milne I, Wright F, Rowe G, Marshall DF, Husmeier D, McGuire G. TOPALi: software for automatic identification of recombinant sequences within DNA multiple alignments. *Bioinformatics.* 2004;20:1806–7. <http://dx.doi.org/10.1093/bioinformatics/bth155>
27. Martin D, Rybicki E. RDP: detection of recombination amongst aligned sequences. *Bioinformatics.* 2000;16:562–3. <http://dx.doi.org/10.1093/bioinformatics/16.6.562>
28. Padidam M, Sawyer S, Fauquet CM. Possible emergence of new geminiviruses by frequent recombination. *Virology.* 1999; 265:218–25. <http://dx.doi.org/10.1006/viro.1999.0056>
29. Martin DP, Posada D, Crandall KA, Williamson C. A modified bootscan algorithm for automated identification of recombinant sequences and recombination breakpoints. *AIDS Res Hum Retroviruses.* 2005;21:98–102. <http://dx.doi.org/10.1089/aid.2005.21.98>
30. Smith JM. Analyzing the mosaic structure of genes. *J Mol Evol.* 1992;34:126–9. <http://dx.doi.org/10.1007/BF00182389>
31. Posada D, Crandall KA. Evaluation of methods for detecting recombination from DNA sequences: computer simulations. *Proc Natl Acad Sci U S A.* 2001;98:13757–62. <http://dx.doi.org/10.1073/pnas.241370698>
32. Gibbs MJ, Armstrong JS, Gibbs AJ. Sister-scanning: a Monte Carlo procedure for assessing signals in recombinant sequences. *Bioinformatics.* 2000;16:573–82. <http://dx.doi.org/10.1093/bioinformatics/16.7.573>
33. Boni MF, Posada D, Feldman MW. An exact nonparametric method for inferring mosaic structure in sequence triplets. *Genetics.* 2007;176:1035–47. <http://dx.doi.org/10.1534/genetics.106.068874>
34. Martin DP, Murrell B, Golden M, Khoosal A, Muhire B. RDP4: Detection and analysis of recombination patterns in virus genomes. *Virus Evol.* 2015;1:vev003. PMID: 27774277
35. Mangiafico JA, Sanchez JL, Figueiredo LT, LeDuc JW, Peters CJ. Isolation of a newly recognized Bunyamwera serogroup virus from a febrile human in Panama. *Am J Trop Med Hyg.* 1988;39:593–6.
36. Armstrong PM, Andreadis TG, Anderson JF. Emergence of a new lineage of Cache Valley virus (Bunyaviridae: Orthobunyavirus) in the northeastern United States. *Am J Trop Med Hyg.* 2015;93:11–7. <http://dx.doi.org/10.4269/ajtmh.15-0132>
37. Mangiafico JA. Fort Sherman. International catalogue of arboviruses including certain other viruses of vertebrates [cited 2016 Jan 14]. <https://www.cdc.gov/arbovat/VirusDetails.aspx?ID=152>
38. Lambert AJ, Lanciotti RS. Molecular characterization of medically important viruses of the genus Orthobunyavirus. *J Gen Virol.* 2008;89:2580–5. <http://dx.doi.org/10.1099/vir.0.2008/002253-0>

Address for correspondence: Hideki Ebihara, Department of Molecular Medicine, Mayo Clinic, 200 First St SW, Rochester, MN 55905, USA; email: Ebihara.Hideki@mayo.edu

Human Infection with Highly Pathogenic Avian Influenza A(H7N9) Virus, China

Changwen Ke,¹ Chris Ka Pun Mok,¹ Wenfei Zhu,¹ Haibo Zhou,¹ Jianfeng He, Wenda Guan, Jie Wu, Wenjun Song, Dayan Wang, Jiexiong Liu, Qinhan Lin, Daniel Ka Wing Chu, Lei Yang, Nanshan Zhong, Zifeng Yang,² Yuelong Shu,² Joseph Sriyal Malik Peiris²

The recent increase in zoonotic avian influenza A(H7N9) disease in China is a cause of public health concern. Most of the A(H7N9) viruses previously reported have been of low pathogenicity. We report the fatal case of a patient in China who was infected with an A(H7N9) virus having a polybasic amino acid sequence at its hemagglutinin cleavage site (PEVPKRKRRTAR/GL), a sequence suggestive of high pathogenicity in birds. Its neuraminidase also had R292K, an amino acid change known to be associated with neuraminidase inhibitor resistance. Both of these molecular features might have contributed to the patient's adverse clinical outcome. The patient had a history of exposure to sick and dying poultry, and his close contacts had no evidence of A(H7N9) disease, suggesting human-to-human transmission did not occur. Enhanced surveillance is needed to determine whether this highly pathogenic avian influenza A(H7N9) virus will continue to spread.

Avian influenza A(H7N9) viruses with zoonotic potential emerged in East China in early 2013. From February 2013 through February 20, 2017, a total of 1,222 patients with A(H7N9) disease had been reported to the World Health Organization, with 304 of these patients being reported January 19–February 14, 2017 (1,2). The overall case fatality ratio was ≈37%. Most patients with A(H7N9) disease primarily had viral pneumonia, with some progressing to acute respiratory distress syndrome

(ARDS). Unlike patients with influenza A(H5N1) disease, patients with A(H7N9) disease were more likely to be older and have underlying comorbidities (3). In healthy young persons with A(H7N9) infections, symptoms were often mild, and potentially a substantial proportion of these infections was asymptomatic and not recognized (4–6).

The A(H7N9) virus is a low pathogenicity avian influenza (LPAI) virus that typically causes no signs of disease in birds and has become enzootic in poultry. A(H7N9) infections have been reported in poultry and humans from 22 provinces and municipalities in mainland China, with cases acquired in mainland China sometimes being reported in Hong Kong, China; Macao, China; Taiwan; Malaysia; and Canada (2).

Phylogenetic analyses of the A(H7N9) hemagglutinin (HA) genes showed that the viruses that emerged in the Yangtze River Delta region in 2013 rapidly spread to other parts of South and South East China and that distinct virus clades became established in these different geographic regions (7). Genetic analysis of A(H7N9) viruses has revealed some adaptations in the virus HA that allow binding to the sialic acid receptors on the epithelium of the mammalian upper respiratory tract. Upon infection in humans, these viruses rapidly acquire mutations in the viral polymerase basic 2 (PB2) gene (8). Unlike A(H5N1) viruses, A(H7N9) viruses efficiently infect and replicate in *ex vivo* cultures of the human bronchus (9) and are transmitted between ferrets, albeit inefficiently, by the airborne route (10), indicating the substantial potential for efficient human-to-human transmission. Although there have been occasional clusters of cases, some likely caused by limited human-to-human transmission, no evidence of sustained human-to-human transmission has been reported (2).

When transmitting among domestic, terrestrial poultry, LPAI type A viruses of the H5 and H7 subtypes can undergo mutations that lead to multiple basic amino acids being present at the HA cleavage site, a signature associated with increased pathogenicity in chickens. Such viruses can disseminate beyond the respiratory and intestinal tracts to affect the brain, liver, spleen, and pancreas and are

Author affiliations: Guangdong Provincial Center for Disease Control and Prevention, Guangzhou, China (C. Ke, J. He, J. Wu); First Affiliated Hospital of Guangzhou Medical University, State Key Laboratory of Respiratory Disease, Guangzhou (C.K.P. Mok, W. Guan, N. Zhong, Z. Yang, J.S.M. Peiris); The University of Hong Kong, Hong Kong, China (C.K.P. Mok, D.K.W. Chu, J.S.M. Peiris); National Institute for Viral Disease Control and Prevention, China CDC, Beijing, China (W. Zhu, D. Wang, L. Yang, Y. Shu); The Sixth Affiliated Hospital of Guangzhou Medical University, Qingyuan, China (H. Zhou, J. Liu, Q. Lin); Jinan University, Guangzhou (W. Song); Macau University of Science and Technology, Macau, China (N. Zhong, Z. Yang)

DOI: <https://doi.org/10.3201/eid2308.170600>

¹These authors contributed equally to this article.

²These authors contributed equally to this article.

lethal in chicken; these viruses are then designated highly pathogenic avian influenza (HPAI) (11,12). Since their emergence in 2013, the A(H7N9) viruses have remained LPAI viruses in poultry, which has made detection and containment of these viruses more challenging than these activities were for A(H5N1), an HPAI virus that usually caused severe disease in poultry flocks.

We report the investigation of illness in a patient in China infected with an A(H7N9) virus with a novel polybasic amino acid sequence at its HA cleavage site, a change that corresponds with increased pathogenicity in poultry and potentially (although not invariably) increased pathogenicity in humans. Relevant epidemiologic information, such as history of contact with poultry and evidence of transmission of infection to close contacts, is provided.

Methods

The Patient

The patient was a 56-year-old man with diabetes and hypertension who lived in Lianzhou, China, in Guangdong Province. He raised chickens in his backyard and noticed some of them were sick and dying weeks before his illness.

Some of these chickens were slaughtered, cooked, and consumed by the patient and his family members.

On January 7, 2017, day 1 of illness, he had a fever (39.8°C) and cough; shortly thereafter, shortness of breath developed, and on January 10, day 4 of illness, he was admitted to a local hospital (Figure 1). Bilateral pneumonia was diagnosed based on his clinical signs and computed tomography (CT) results. The patient's throat swab from a point-of-care test was negative for influenza A/B. Because he had a history of contact with poultry, oseltamivir treatment (75 mg 2×/d) was commenced. On day 6, his clinical condition deteriorated markedly, with progression to severe respiratory failure, hypoxia (oxygen saturation 78.6%), and coma. He was transferred to the intensive care unit for invasive mechanical ventilation.

RNA extracted from an endotracheal aspirate acquired on day 6 was positive for influenza A(H7N9) virus. On day 7, he had mild gastrointestinal bleeding and a cardiac arrest. No endoscopy was performed, and he was rescued by cardiopulmonary resuscitation and intravenous injection of norepinephrine. The size and shape of his heart were within reference range. Chest radiography showed he had extensive bilateral infiltration of the lungs with prominent hilar shadowing (Figure 2, panel A). The patient had progressed

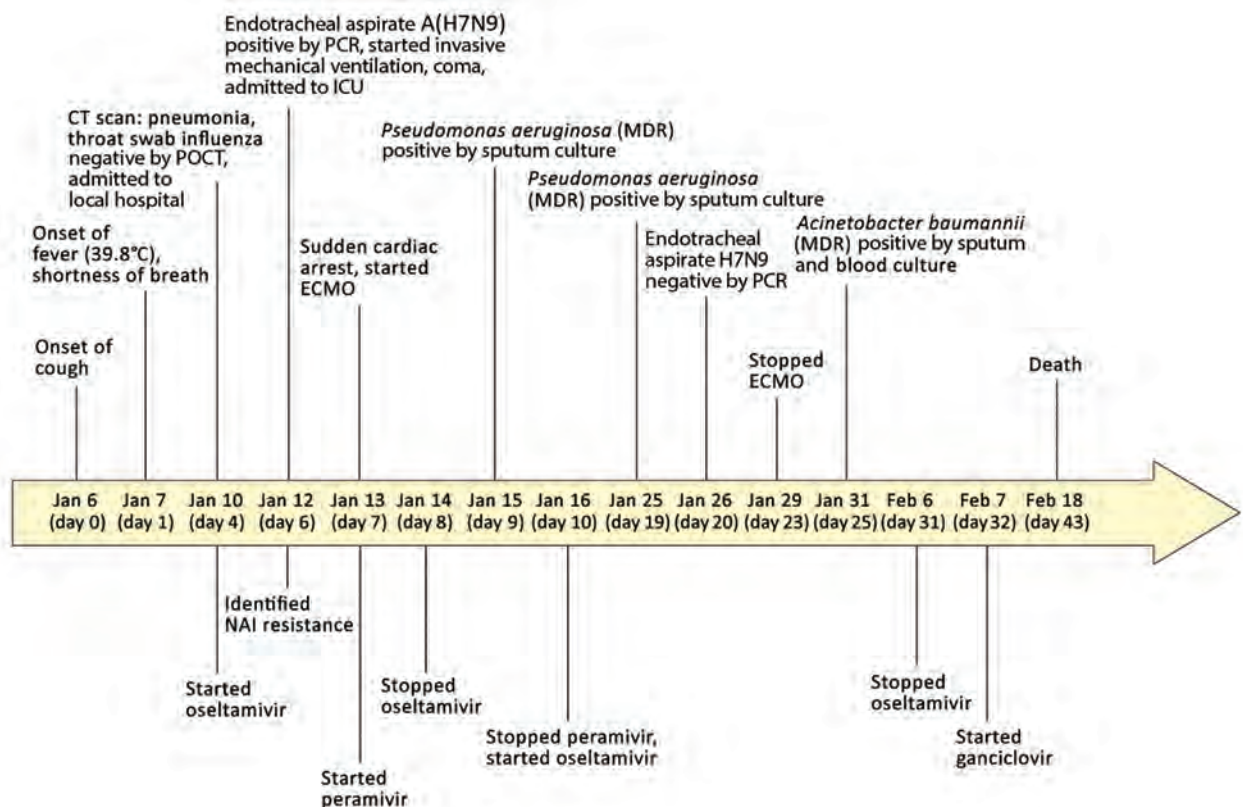


Figure 1. Clinical course of 56-year-old man with diabetes and hypertension infected with highly pathogenic avian influenza A(H7N9) virus, China, 2017. CT, computed tomography; ECMO, extracorporeal membrane oxygenation; ICU, intensive care unit; MDR, multidrug resistant; NAI, neuraminidase inhibitor; POCT, point-of-care test.

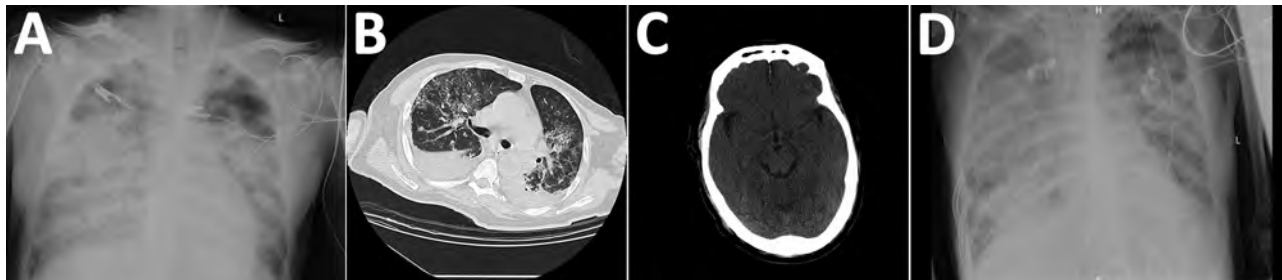


Figure 2. Chest and brain imaging of 56-year-old man infected with highly pathogenic avian influenza A(H7N9) virus, China, 2017: radiograph imaging of chest at day 7 (A) and day 40 (D); computed tomographic scans of the chest (B) and the brain (C) at day 30.

to severe ARDS. Antiviral therapy was changed from oseltamivir to peramivir (0.6 g intravenous 4×/d), and he was given antibiotics (cefoperazone sodium/sulbactam sodium [2:1], 3 g/8 h). Extracorporeal membrane oxygenation (ECMO) was commenced.

Laboratory tests showed high total leukocyte and neutrophil counts and high levels of procalcitonin, aspartate aminotransferase, serum creatinine, lactate dehydrogenase, blood urea nitrogen, and d-dimers throughout the hospitalization (online Technical Appendix Table 1, <https://wwwnc.cdc.gov/EID/article/23/8/17-0600-Techapp1.pdf>). His hemoglobin level remained low. Continuous renal replacement therapy was applied because of increasing renal dysfunction (days 8–14). His oxygenation index was maintained at around 200 mm Hg by the use of ECMO (Figure 3). On day 10, treatment with peramivir was stopped and oseltamivir recommenced. Viral load in the endotracheal aspirate started to decline on day 16 and was undetectable on day 20 (Figure 3). However, his clinical condition continued to deteriorate gradually after removal from ECMO.

Secondary bacterial infections developed with multidrug-resistant *Pseudomonas aeruginosa* (detected in sputum days 9 and 19) and *Acinetobacter baumannii* (detected in blood cultures day 25). Combination antibiotic therapy was used to treat these infections (online Technical Appendix Table 2).

Cytomegalovirus (CMV) DNA was detected in patient serum on day 11 of illness, suggesting CMV reactivation. Because of the lack of clinical response to oseltamivir and antibiotics and the detection of CMV DNA in serum, ganciclovir therapy was initiated on day 32 to suppress possible systemic CMV disease. A CT scan of the lungs on day 30 showed multiple bilateral patchy hyperdense lesions and bilateral pleural effusions (Figure 2, panel B). Repeated electrocardiography tracings did not reveal evidence of myocarditis, and Doppler echocardiography examinations showed effective myocardial contraction. CT scan of the brain on the same day showed patchy hypodense lesions with unclear borders in the left corona radiata and right centrum semiovale (Figure 2, panel C), the largest measuring 8 × 10 mm with a CT value (8 H) indicative of lacunar infarction. The CT scan also showed symmetric, bilateral cerebral hemispheres; preservation of gray-white differentiation; no obvious lesions in the brain parenchyma; no deepening or widening of sulci, fissures, and cisterns; no dilatation or deformity in the ventricular system; and no midline shift. However, intracerebral edema was evident (Figure 2, panel C).

On day 40, extensive bilateral shadowing of the lung fields with blurring of the costophrenic angles continued to be observed on chest radiography (Figure 2, panel D). On day 43, the patient died.

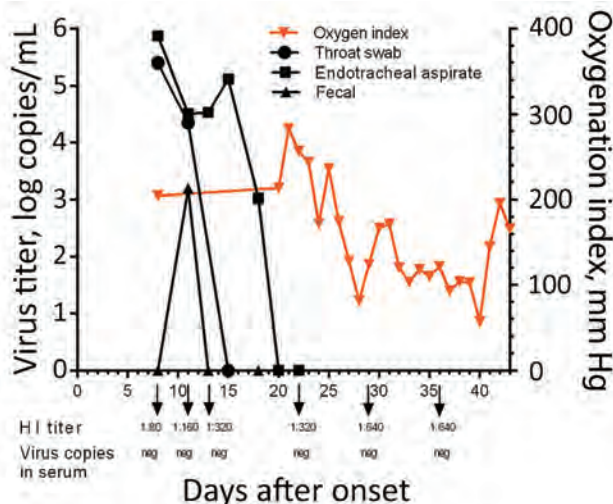


Figure 3. Kinetics of viral load, oxygenation index, and HI antibody titers in 56-year-old man infected with highly pathogenic avian influenza A(H7N9) virus, China, 2017. Arrows indicate the days HI titers and viral titers in serum were acquired. HI, hemagglutination inhibition; neg, negative.

Clinical and Epidemiologic Data Collection

The clinical history and epidemiologic information were obtained from the patient at hospital admission and from relatives during interviews. Progression of clinical symptoms and laboratory and radiologic findings were obtained by retrospective chart review.

Viral Diagnosis

Serially acquired throat swabs, endotracheal aspirates, serum samples, and fecal samples were collected from the patient and stored in viral transport medium. We extracted viral RNA by using QIAamp MinElute Virus Spin kit (QIAGEN, Hilden, Germany) according to the manufacturer's instructions. The extracted RNA was subjected to reverse transcription and amplification with SuperScript III One-Step RT-PCR System (ThermoFisher, Waltham, MA, USA). We synthesized complementary DNA by using uni-12 primers (5'-AGCAAAGCAGG-3'), and conducted real-time PCR with an A(H7N9) detection kit (Shanghai Zj Bio-Tech Co., Ltd, Shanghai, China) to detect avian influenza A(H7N9) virus.

Genome Sequencing and Phylogenetic Analysis

Staff of the Guangdong Provincial Center for Disease Control and Prevention isolated virus from the endotracheal aspirate specimen obtained on day 6 of illness onset. Whole-genome sequencing was implemented on the Ion Torrent S5 platform (ThermoFisher) with a mean read length of ≈ 200 bp. We analyzed data predominantly with CLC Genomics Workbench 7.5.1 software (<https://www.qiagen-bioinformatics.com/products/clc-genomics-workbench/>). Low-quality reads were trimmed by using CLC trimmer with a quality limit set at 0.05. We assembled filtered reads de novo in CLC under default parameters. Contigs with coverage >10 bp were extracted and blasted against the GISAID (Global Initiative on Sharing All Influenza Data) databases (<http://platform.gisaid.org>). Sequences with the highest similarity were selected as references for read mapping (parameters: length fraction = 0.8, similarity fraction = 0.8). We obtained influenza A genome sequences by extracting consensus sequences from the mapping results with a coverage depth of $\geq 30\times$ at each nucleotide site of the 8 gene segments. The viral sequences generated in this study (online Technical Appendix Table 3) were submitted to the GISAID database.

We used the MEGA software version 5.05 (<http://www.megasoftware.net>) to construct phylogenetic trees, and maximum likelihood trees were constructed with PhyML (<http://www.atgc-montpellier.fr/phyml/>) by using the general time reversible plus gamma distribution plus proportion of invariable sites model. We estimated node support by the SH-like aLRT method and report values >0.8 . Bootstrap values from 1,000 replicates were calculated to assess the reliability of the phylogenetic trees.

Serology

A(H7N9)-specific antibody titers were quantified in serially acquired serum samples by hemagglutination inhibition (HI) assay by using horse erythrocytes according to the World Health Organization recommended protocol

(http://www.who.int/influenza/gisrs_laboratory/cnic_serological_diagnosis_hai_a_h7n9_20131220.pdf). A recombinant A/PR/8/34 virus with the HA and neuraminidase (NA) genes of A/Zhejiang/DTID-ZJU01/2013 (H7N9) was used for serologic tests. All bioassays were conducted in a Biosafety Level 3 laboratory. Seropositivity was defined as an HI titer $\geq 1:40$.

Ethical Approval

Guangdong Center for Disease Control and Prevention is legally tasked with data collection on patients in the course of a public health investigation during an emerging infectious disease outbreak. Thus, informed consent was waived.

Results

This patient initially tested negative for influenza A/B, but on day 6, real-time reverse transcription PCR performed using an endotracheal aspirate showed positive results for A(H7N9) virus RNA. Viral RNA was detectable in the patient's endotracheal aspirate at high levels (>4 log RNA copies/mL) until day 17 (Figure 3), was undetectable in serum throughout the course of illness, and was transiently detected in the feces on day 11. Antibody to A(H7N9) virus was first detected in serum collected on day 8 (HI titer 1:80); serum titers increased until day 29 (1:640) (Figure 3).

We performed phylogenetic analyses on the virus (designated A/Guangdong/17SF006/2017 [17SF006/17]) isolated from the patient on day 6. The HA segment of 17SF006/17 was related to A(H7N9) clade W2-C (7) (Figure 4). An insertion that led to the addition of multiple basic amino acid residues (PEVPKRKRRTAR/GL) was found at the HA cleavage site, suggesting that this virus might be highly pathogenic in birds (Table) (13). A similar mutation was found for 2 other cases of A(H7N9) infection identified in Taiwan (A/Taiwan/1/2017) (14) and Guangdong Province (A/Guangdong/17SF003/2016, reported as A/Guangdong/Th008/2017) (15). The HA and matrix sequences of these 3 viruses clustered together in our phylogenetic analysis.

We also sequenced and studied the HA and NA genes of 7 A(H7N9) viruses isolated from environmental samples (from birds at live poultry markets) collected previously in the Guangdong Province. Six of the 7 were mixed with A(H9N2) viruses, and thus, the genes for the internal proteins could not be analyzed. All of the A(H7N9) viruses isolated from the environmental samples had the same HA cleavage site sequence motif as the A(H7N9) human viruses (except for an amino acid change [G] at position -6 from the cleavage site) and clustered with them in the phylogenetic tree, suggesting the emergence of a single subclade of A(H7N9) virus with an HA progressively acquiring HPAI mutations. Similar to other A(H7N9) viruses, the

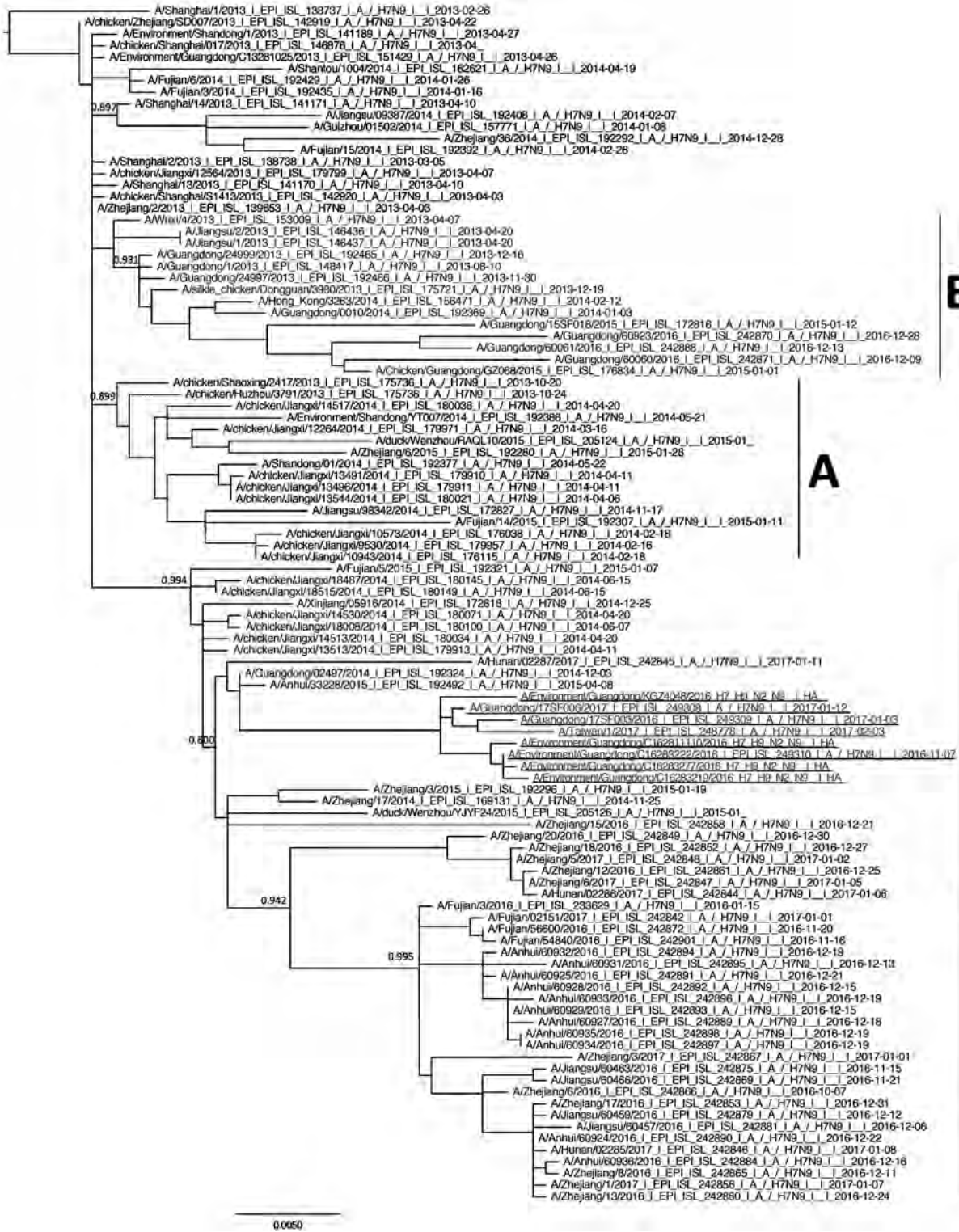


Figure 4. Phylogenetic analysis of the hemagglutinin gene of highly pathogenic avian influenza A(H7N9) viruses in Guangdong Province, China, and reference viruses. Maximum likelihood trees were constructed with PhyML by using the general time reversible plus gamma distribution plus proportion of invariable sites model. Node support was estimated by the SH-like aLRT method, and values >0.8 are shown. Virus clades A, B, and C—previously defined as W2-A, W2-B, and W2-C (5)—are labeled. A/ Guangdong/17SF006/2017 (from a 56-year-old man), A/Guangdong/17SF003/2016, A/Taiwan/1/2017, and environmental isolates are underlined. Scale bar indicates nucleotide substitutions per site.

Table. Key molecular signatures of avian influenza A(H7N9) virus from patient in Guangdong Province, China, compared with other closely related viruses*

Strain	HA			NA	M2	PB2			PA
	321–331†	G186V‡	Q226L‡	R292K§	S31N¶	E627K#	K526R**	K702R††	V100A††
A/Guangdong/17SF006/2017 (H7N9)‡‡	PEVPKRKRTAR/GL	V	Q	K	N	K	K	K	V
A/Guangdong/17SF003/2016 (H7N9)	PEVPKRKRTAR/GL	V	Q	K	N	E	K	R	V
A/Taiwan/1/2017 (H7N9)	PEVPKRKRTAR/GL	V	Q	K	N	K	R	K	A
A/Environment/Guangdong/C16283222/2016 (H7N9)	PEVPKGKRTAR/GL	V	Q	R	N	E	R	K	A
A/Fujian/3/2016 (H7N9)	PEIPKG—R/GL	V	L	R	N	K	R	K	A
A/Zhejiang/3/2017 (H7N9)	PEIPKG—R/GL	V	L	R	N	K	K	K	V
A/Netherlands/219/2003 (H7N7)	PEIPKRRRR/GL	G	Q	R	S	K	R	K	A

*HA, hemagglutinin; NA, neuraminidase; NAI, neuraminidase inhibitor; M2, matrix protein 2; PA, polymerase acidic; PB2, polymerase basic 2.

†Cleavage site.

‡Receptor binding site.

§Associated with NAI drug resistance.

¶Associated with amantadine resistance.

#Associated with increased virulence in mice.

**Associated with enhanced viral replication in mammalian hosts.

††Species-associated signature position.

‡‡Virus from patient in this report.

amino acid substitution G180V in the HA protein, which is known to enhance the binding to mammalian α -2,6-linked sialic acid receptors, was found.

The NA genes of 17SF006/17, A/Guangdong/17SF003/2016, and the environmental isolates grouped together, but A/Taiwan/1/2017 did not cluster, suggesting that the origin of this NA gene was distinct (online Technical Appendix Figure, panel A). A mutation associated with oseltamivir resistance (one leading to R292K substitution in NA) was identified in the NA gene of 17SF006/17 virus. The patient had been on oseltamivir for 2 days before the mutation was detected. Both A/Guangdong/17SF003/2016 and A/Taiwan/1/2017 also had the mutation associated with oseltamivir resistance, but the viruses from the Guangdong environmental samples did not. Similar to other A(H7N9) viruses, 17SF006/17 had a mutation leading to the S31N amino acid substitution in the matrix protein, which is associated with amantadine resistance. A mutation in PB2 that causes substitution E627K, which is a key signature of mammalian adaptation, was also found in this virus. The other viral gene segments of the 3 human viruses are not monophyletic and appear to be derived from reassortment with genetically diverse A(H7N9) viruses (online Technical Appendix Figure, panels A–G).

To investigate the potential for human-to-human transmission of HPAI A(H7N9), an epidemiologic investigation was conducted immediately after virus detection in the patient. Seventy close contacts (5 family members and 65 healthcare workers) were placed under medical

observation for 2 weeks. None of them showed signs of illness.

Discussion

We report the illness and death of a patient in Guangdong Province who was infected with a putative HPAI A(H7N9) virus carrying an HA cleavage site with multiple basic amino acids. Previous A(H7N9) viruses were low pathogenicity, containing only a single arginine residue at the HA cleavage site. Although the HA cleavage site we describe in this report was not a typical HPAI motif for H7 viruses, similar motifs have been reported in H7 viruses in Chile and Canada that were shown to be highly pathogenic in chickens by intravenous pathogenicity tests (13). More studies are needed to determine the pathogenicity of these putative HPAI A(H7N9) viruses (e.g., direct isolation from sick and dying poultry and intravenous pathogenicity index testing in chickens). Viruses isolated from live poultry markets had a sequence motif similar to that of the human isolates (identical except for a glycine at the position –6 from the cleavage site). An additional patient identified in Guangdong Province was infected with an A(H7N9) virus (A/Guangdong/Th005/2017) with HA cleavage site KG-KRIAR/GL (15). This evidence suggests that the polybasic HA cleavage site was acquired progressively through multiple mutations within the avian species in a subclade of the A(H7N9) viruses.

The patient had reported that chickens in his backyard had started dying in the weeks before his disease onset,

indicating the possibility that these chickens were infected with an HPAI and that the patient acquired his infection from them. However, we do not have direct evidence of A(H7N9) infection in these birds, and alternative explanations for their deaths exist.

A(H7N9) viruses having HA cleavage sites with multiple basic amino acids were reported in 2 human cases in the Guangdong Province and Taiwan (Table) (14,15). The HA sequences of these 2 viruses clustered with that of A/Guangdong/17SF006/2017 in our phylogenetic tree. These viruses also clustered with viruses from the environmental samples from Guangdong, which had a similar sequence motif (1 amino acid difference) at the cleavage site as the human isolates, suggesting the progressive emergence of this HPAI motif in a subclade of A(H7N9) viruses in this region. Although the HA gene segments of these viruses are monophyletic, the other gene segments are not and have diverse origins, suggesting that these HPAI viruses continue to reassort their gene segments. Introduction of the polybasic cleavage site into A(H5N1) was associated with increased viral titers in the respiratory tract, increased virus dissemination to distant organs, increased death in mice and ferrets (but not in macaques), and increased virus replication in endothelial cells (16,17).

A question of public health interest is whether acquisition of the polybasic cleavage site in A(H7N9) HA enhances pathogenicity of A(H7N9) viruses in humans. Similar to most patients with A(H7N9) disease (18), the patient in this report had underlying comorbidities (diabetes and hypertension), which probably contributed to the increased disease severity. The clinical progression of the illness to fulminant viral pneumonia and ARDS was relatively rapid, in spite of commencing oseltamivir on day 4 of illness. The patient required mechanical ventilation and became comatose on day 6 of illness and had a sudden cardiac arrest on day 7, necessitating ECMO. Myocarditis and encephalitic illness were not evident by either clinical observation or imaging investigations, and the most likely cause of the coma was respiratory failure. One of the other patients in Guangdong who had a similar HPAI A(H7N9) virus infection had less severe illness, indicating that the HA cleavage sequence did not invariably increase pathogenicity in humans (15).

By day 6 of patient disease onset, 2 days after commencement of oseltamivir, the virus had acquired a mutation leading to an R292K change in the NA protein known to be associated with oseltamivir resistance (19,20). The other 2 viruses with the same HA cleavage site mutation (A/Guangdong/17SF003/2016 and A/Taiwan/1/2017) also had this oseltamivir resistance mutation. It is likely that the viruses from all 3 patients acquired this resistance mutation after commencement of oseltamivir therapy. Although the

emergence of R292K has been reported before in a minority of patients following oseltamivir treatment and treatment failure (19), mutations causing this amino acid substitution have not been found in poultry as of May 30, 2017 (7), and accordingly, the resistance mutation was not observed in the related environmental samples collected from live poultry markets. The frequency with which R292K has been detected in patients with the polybasic HA cleavage site is a cause for concern. Whether acquisition of the polybasic HA cleavage site in the A(H7N9) virus contributes to the enhanced probability of the virus acquiring the NA R292K during oseltamivir treatment is unknown. Studies of HPAI A(H5N1) viruses in vitro and in vivo have demonstrated that viruses with polybasic residues at the HA cleavage site or the PB2 E627K amino acid change enhances replication efficiency, which might increase the likelihood of resistance emerging under the selective pressure of oseltamivir therapy (21–23).

NA R292K confers resistance to both oseltamivir and peramivir, the antiviral drugs used in this patient's therapy (20). Viral load in the endotracheal aspirates remained high for 10 days following commencement of antiviral therapy, probably reflecting lack of efficacy of the antiviral regimens. Viral load only began to decline on day 18 of illness, probably because of increasing antibody titers. Thus, the uncontrolled viral replication and emergence of antiviral resistance in this patient possibly contributed to the adverse clinical outcome. In spite of the prolonged infection and high virus titer within the respiratory tract, virus RNA was not detectable in the serum (Figure 3). Thus, systemic dissemination of the virus was unlikely. This patient was not treated with corticosteroids until day 41, shortly before his demise; thus, corticosteroid therapy did not increase viral load or facilitate the emergence of antiviral resistance, a phenomenon speculated to have occurred in other patients in whom oseltamivir resistance mutations arose (19).

The emergence of antibiotic-resistant *Acinetobacter* and other bacteria might also have contributed to the adverse clinical outcome. Detection of CMV DNA in serum (rather than in leukocytes) is suggestive of clinically significant CMV viremia following CMV reactivation in a seriously ill patient. CMV viremia is an indication for ganciclovir therapy in immunocompromised patients, which was the rationale for initiating ganciclovir therapy. However, the benefit of using ganciclovir in this context remains unknown.

The patient had increasing levels of serum creatinine and blood urea nitrogen, indicating moderate renal dysfunction, and moderately elevated aspartate aminotransferase, indicating moderate liver dysfunction. Similar features have been previously reported in A(H7N9) patients and are not necessarily indicative of systemic virus dissemination (8).

No evidence of human-to-human transmissibility was apparent; family members and healthcare workers who were in contact with the patient did not have evidence of clinical disease. The HA cleavage site mutation that makes avian influenza viruses highly pathogenic in birds does not necessarily affect the transmissibility of the virus between humans. However, unlike LPAI viruses, which are restricted to the chicken respiratory and intestinal tracts, HPAI viruses spread systemically within chickens and are likely to be found at high titer in multiple organs, including muscle. Thus, the risk for zoonotic transmission through handling or butchering infected poultry and consuming undercooked poultry is likely to increase with HPAI viruses.

In summary, we report the clinical disease progression of a patient infected with a mutant A(H7N9) virus that acquired sequence motifs similar to those found in HPAI viruses. The clinical features of human disease with this isolate did not appear to differ from previous infections with low pathogenicity A(H7N9) viruses, and the clinical and virologic evidence suggested that systemic dissemination of the virus did not occur. The emergence of R292K in NA, which is associated with NA inhibitor resistance, probably contributed to the adverse clinical outcome. In China, heightened surveillance of A(H7N9) in humans with severe respiratory disease and poultry is needed to determine how widespread the polybasic HA cleavage sequence has become and to monitor for evidence of oseltamivir resistance.

Acknowledgments

We acknowledge the contributions of Professor Honglin Chen and his colleagues from the Department of Microbiology at the University of Hong Kong and the colleagues from Qingyuan Center for Disease Control and Prevention. We also thank the Global Initiative for Sharing Influenza Data for providing sequences.

This study was financially supported by National Key Research and Development Program of China (2016YFC1200200 to Y.S. and 2016YFD0500208 to D.W.), National Natural Science Foundation of China (grant nos. 81761128014 and 81490534 to N.Z.), Science Research Project of the Guangdong Province (grant nos. 2016A050503047), Municipal Science and Technology Bureau Foundation of Guangzhou (grant no. 2014Y2-00031), the US National Institute of Allergy and Infectious Diseases under Centers of Excellence for Influenza Research and Surveillance (contract no. HHSN272201400006C), and Research Grants Council of Hong Kong, China, through the Theme-based Research Scheme (ref. T11-705/14N).

Mr. Ke works at the Guangdong Provincial Center for Disease Control and Prevention. His research interests include the emerging outbreak of influenza virus.

References

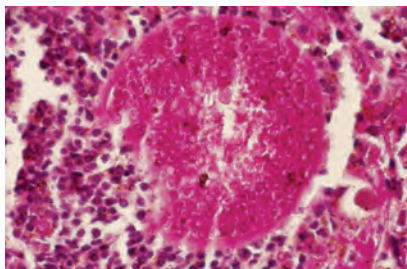
1. World Health Organization. Human infection with avian influenza A(H7N9) virus—China. *Disease outbreak news* 2017 Feb 20 [cited 2017 May 1]. <http://www.who.int/csr/don/20-february-2017-ah7n9-china/en/>
2. World Health Organization. Human infection with avian influenza A(H7N9) virus—China. *Disease outbreak news* 2017 Feb 22 [cited 2017 May 1]. <http://www.who.int/csr/don/22-february-2017-ah7n9-china/en/>
3. Qin Y, Horby PW, Tsang TK, Chen E, Gao L, Ou J, et al. Differences in the epidemiology of human cases of avian influenza A(H7N9) and A(H5N1) viruses infection. *Clin Infect Dis*. 2015;61:563–71. <http://dx.doi.org/10.1093/cid/civ345>
4. Yu H, Cowling BJ, Feng L, Lau EH, Liao Q, Tsang TK, et al. Human infection with avian influenza A H7N9 virus: an assessment of clinical severity. *Lancet*. 2013;382:138–45. [http://dx.doi.org/10.1016/S0140-6736\(13\)61207-6](http://dx.doi.org/10.1016/S0140-6736(13)61207-6)
5. Chen Z, Liu H, Lu J, Luo L, Li K, Liu Y, et al. Asymptomatic, mild, and severe influenza A(H7N9) virus infection in humans, Guangzhou, China. *Emerg Infect Dis*. 2014;20:1535–40. <http://dx.doi.org/10.3201/eid2009.140424>
6. Lin YP, Yang ZF, Liang Y, Li ZT, Bond HS, Chua H, et al. Population seroprevalence of antibody to influenza A(H7N9) virus, Guangzhou, China. *BMC Infect Dis*. 2016;16:632. <http://dx.doi.org/10.1186/s12879-016-1983-3>
7. Lam TT, Zhou B, Wang J, Chai Y, Shen Y, Chen X, et al. Dissemination, divergence and establishment of H7N9 influenza viruses in China. *Nature*. 2015;522:102–5. <http://dx.doi.org/10.1038/nature14348>
8. Gao R, Cao B, Hu Y, Feng Z, Wang D, Hu W, et al. Human infection with a novel avian-origin influenza A (H7N9) virus. *N Engl J Med*. 2013;368:1888–97. <http://dx.doi.org/10.1056/NEJMoa1304459>
9. Chan MC, Chan RW, Chan LL, Mok CK, Hui KP, Fong JH, et al. Tropism and innate host responses of a novel avian influenza A H7N9 virus: an analysis of ex-vivo and in-vitro cultures of the human respiratory tract. *Lancet Respir Med*. 2013;1:534–42. [http://dx.doi.org/10.1016/S2213-2600\(13\)70138-3](http://dx.doi.org/10.1016/S2213-2600(13)70138-3)
10. Zhu H, Wang D, Kelvin DJ, Li L, Zheng Z, Yoon SW, et al. Infectivity, transmission, and pathology of human-isolated H7N9 influenza virus in ferrets and pigs. *Science*. 2013;341:183–6. <http://dx.doi.org/10.1126/science.1239844>
11. Luczo JM, Stambas J, Durr PA, Michalski WP, Bingham J. Molecular pathogenesis of H5 highly pathogenic avian influenza: the role of the haemagglutinin cleavage site motif. *Rev Med Virol*. 2015;25:406–30. <http://dx.doi.org/10.1002/rmv.1846>
12. Schrauwen EJ, Herfst S, Leijten LM, van Run P, Bestebroer TM, Linstre M, et al. The multibasic cleavage site in H5N1 virus is critical for systemic spread along the olfactory and hematogenous routes in ferrets. *J Virol*. 2012;86:3975–84. <http://dx.doi.org/10.1128/JVI.06828-11>
13. World Organisation for Animal Health and Food and Agriculture Organization. Influenza A cleavage sites [cited 2017 Feb 24]. http://www.offlu.net/fileadmin/home/en/resource-centre/pdf/Influenza_A_Cleavage_Sites.pdf
14. Yang JR, Liu MT. Human infection caused by an avian influenza A (H7N9) virus with a polybasic cleavage site in Taiwan, 2017. *J Formos Med Assoc*. 2017;116:210–2. <http://dx.doi.org/10.1016/j.jfma.2017.02.011>
15. Zhang F, Bi Y, Wang J, Wong G, Shi W, Hu F, et al. Human infections with recently-emerging highly pathogenic H7N9 avian influenza virus in China. *J Infect*. 2017;S0163-4453(17)30108-1.
16. Suguitan AL Jr, Matsuoka Y, Lau YF, Santos CP, Vogel L, Cheng LL, et al. The multibasic cleavage site of the hemagglutinin of highly pathogenic A/Vietnam/1203/2004 (H5N1) avian influenza virus acts as a virulence factor in a host-specific

- manner in mammals. *J Virol.* 2012;86:2706–14. <http://dx.doi.org/10.1128/JVI.05546-11>
17. Zeng H, Pappas C, Belser JA, Houser KV, Zhong W, Wadford DA, et al. Human pulmonary microvascular endothelial cells support productive replication of highly pathogenic avian influenza viruses: possible involvement in the pathogenesis of human H5N1 virus infection. *J Virol.* 2012;86:667–78. <http://dx.doi.org/10.1128/JVI.06348-11>
 18. Gao HN, Lu HZ, Cao B, Du B, Shang H, Gan JH, et al. Clinical findings in 111 cases of influenza A (H7N9) virus infection. *N Engl J Med.* 2013;368:2277–85. <http://dx.doi.org/10.1056/NEJMoa1305584>
 19. Hu Y, Lu S, Song Z, Wang W, Hao P, Li J, et al. Association between adverse clinical outcome in human disease caused by novel influenza A H7N9 virus and sustained viral shedding and emergence of antiviral resistance. *Lancet.* 2013;381:2273–9. [http://dx.doi.org/10.1016/S0140-6736\(13\)61125-3](http://dx.doi.org/10.1016/S0140-6736(13)61125-3)
 20. Yen HL, McKimm-Breschkin JL, Choy KT, Wong DD, Cheung PP, Zhou J, et al. Resistance to neuraminidase inhibitors conferred by an R292K mutation in a human influenza virus H7N9 isolate can be masked by a mixed R/K viral population. *MBio.* 2013;4:e00396-13. <http://dx.doi.org/10.1128/mBio.00396-13>
 21. Mok CK, Lee HH, Lestra M, Nicholls JM, Chan MC, Sia SF, et al. Amino acid substitutions in polymerase basic protein 2 gene contribute to the pathogenicity of the novel A/H7N9 influenza virus in mammalian hosts. *J Virol.* 2014;88:3568–76. <http://dx.doi.org/10.1128/JVI.02740-13>
 22. Neumann G, Kawaoka Y. Host range restriction and pathogenicity in the context of influenza pandemic. *Emerg Infect Dis.* 2006;12:881–6. <http://dx.doi.org/10.3201/eid1206.051336>
 23. Yamayoshi S, Fukuyama S, Yamada S, Zhao D, Murakami S, Uraki R, et al. Amino acids substitutions in the PB2 protein of H7N9 influenza A viruses are important for virulence in mammalian hosts. *Sci Rep.* 2015;5:8039. <http://dx.doi.org/10.1038/srep08039>

Address for correspondence: Yuelong Shu, National Institute for Viral Disease Control and Prevention, China CDC, Key Laboratory for Medical Virology, National Health and Family Planning Commission, 155 Changbai Rd, Beijing, 102206, P.R. China; email: yshu@cnic.org.cn; Zifeng Yang, The First Affiliated Hospital of Guangzhou Medical University, No.151, Yanjiangxi Rd, Guangzhou, Guangdong, China; email: jeffyah@163.com

April 2012: Vectorborne Diseases

- Determinants for Autopsy after Unexplained Deaths Possibly Resulting from Infectious Causes, United States



- Influenza-associated Hospitalizations by Industry, 2009–10 Influenza Season, United States
- Geographic Distribution of Hantaviruses Associated with Neotomine and Sigmodontine Rodents, Mexico
- Shiga Toxin-producing *Escherichia coli* Serotype O78:H⁻ in Family, Finland, 2009
- Identification of Intermediate in Evolutionary Model of Enterohemorrhagic *Escherichia coli* O157

- Emergence of Unusual G6P[6] Rotaviruses in Children, Burkina Faso, 2009–2010
- Comparison of *Escherichia coli* ST131 Pulsotypes, by Epidemiologic Traits, 1967–2009
- Lessons Learned during Dengue Outbreaks in the United States, 2001–2011
- Malaria in Highlands of Ecuador since 1900
- Dengue and US Military Operations from Spanish–American War through Today
- *Bartonella* spp. in Rats and Zoonoses, Los Angeles, California, USA
- Detection of *Plasmodium* spp. in Human Feces
- Extraintestinal Infections Caused by *Salmonella enterica* Subspecies II–IV
- Subclinical Infections with Crimean-Congo Hemorrhagic Fever Virus, Turkey
- Crimean-Congo Hemorrhagic Fever, Kazakhstan, 2009–2010



- Vector Blood Meals and Chagas Disease Transmission Potential, United States
- *emm59* Group A Streptococcus Strains, United States
- Characterization of *Mycobacterium orygis* as *M. tuberculosis* Complex Subspecies
- Cosavirus Infection in Persons with and without Gastroenteritis, Brazil
- Drug Susceptibility of *Mycobacterium tuberculosis* Beijing Genotype and Association with MDR TB
- Highly Divergent Novel Lyssavirus in an African Civet
- *Coccidioides posadasii* Infection in Bats, Brazil
- Risk Factors for Chronic Q Fever, the Netherlands

Human Metapneumovirus and Other Respiratory Viral Infections during Pregnancy and Birth, Nepal

Jennifer L. Lenahan, Janet A. Englund, Joanne Katz, Jane Kuypers, Anna Wald, Amalia Magaret, James M. Tielsch, Subarna K. Khatri, Stephen C. LeClerq, Laxman Shrestha, Mark C. Steinhoff, Helen Y. Chu



JOINTLY ACCREDITED PROVIDER™
INTERPROFESSIONAL CONTINUING EDUCATION

Medscape EDUCATION ACTIVITY

In support of improving patient care, this activity has been planned and implemented by Medscape, LLC and Emerging Infectious Diseases. Medscape, LLC is jointly accredited by the Accreditation Council for Continuing Medical Education (ACCME), the Accreditation Council for Pharmacy Education (ACPE), and the American Nurses Credentialing Center (ANCC), to provide continuing education for the healthcare team.

Medscape, LLC designates this Journal-based CME activity for a maximum of 1.00 **AMA PRA Category 1 Credit(s)**™. Physicians should claim only the credit commensurate with the extent of their participation in the activity.

All other clinicians completing this activity will be issued a certificate of participation. To participate in this journal CME activity: (1) review the learning objectives and author disclosures; (2) study the education content; (3) take the post-test with a 75% minimum passing score and complete the evaluation at <http://www.medscape.org/journal/eid>; and (4) view/print certificate. For CME questions, see page 1440.

Release date: July 13, 2017; Expiration date: July 13, 2018

Learning Objectives

Upon completion of this activity, participants will be able to:

- Evaluate incidence of and risk factors for human metapneumovirus (HMPV) infection during pregnancy, based on a surveillance study in Nepal.
- Compare clinical presentation and symptoms of HMPV infection during pregnancy, based on a surveillance study in Nepal.
- Identify birth outcomes associated with HMPV infection during pregnancy, based on a surveillance study in Nepal.

CME Editor

Deborah Wenger, MBA, Copyeditor, Emerging Infectious Diseases. *Disclosure: Deborah Wenger, MBA, has disclosed no relevant financial relationships.*

CME Author

Laurie Barclay, MD, freelance writer and reviewer, Medscape, LLC. *Disclosure: Laurie Barclay, MD, has disclosed the following relevant financial relationships: owns stock, stock options, or bonds from Alnylam; Biogen; Pfizer.*

Authors

Disclosures: Jennifer L. Lenahan, MPH; Joanne Katz, ScD; Jane Kuypers, PhD; James M. Tielsch, PhD; Subarna K. Khatri, MBBS, DOMS, FRCS; Stephen C. LeClerq, MPH; Laxman Shrestha, MD; Mark C. Steinhoff, MD; and Helen Y. Chu, MD, MPH, have disclosed no relevant financial relationships. Janet A. Englund, MD, has disclosed the following relevant financial relationships: served as an advisor or consultant for Gilead; received grants for clinical research from Allos; Gilead; GlaxoSmithKline; Novavax; Pfizer. Anna Wald, MD, MPH, has disclosed the following relevant financial relationships: served as an advisor or consultant for AiCuris; Amgen; GlaxoSmithKline; Merck; received grants for clinical research from Genocoea; Vical. Amalia Magaret, PhD, has disclosed the following relevant financial relationships: served as an advisor or consultant for AiCuris; Immune Design.

Author affiliations: University of Washington, Seattle, Washington, USA (J.L. Lenahan, J.A. Englund, J. Kuypers, A. Wald, A. Magaret, H.Y. Chu); Seattle Children's Hospital, Seattle (J.L. Lenahan, J.A. Englund, H.Y. Chu); Johns Hopkins University Bloomberg School of Public Health, Baltimore, Maryland, USA (J. Katz, S.C. LeClerq); George Washington University,

Washington, DC, USA (J.M. Tielsch); Nepal Nutritional Intervention Project, Kathmandu, Nepal (S.K. Khatri, S.C. LeClerq); Institute of Medicine, Tribhuvan University Teaching Hospital, Kathmandu (L. Shrestha); Cincinnati Children's Hospital Medical Center, Cincinnati, Ohio, USA (M.C. Steinhoff)

DOI: <https://doi.org/10.3201/eid2308.161358>

Human metapneumovirus (HMPV) is a respiratory virus that can cause severe lower respiratory tract disease and even death, primarily in young children. The incidence and characteristics of HMPV have not been well described in pregnant women. As part of a trial of maternal influenza immunization in rural southern Nepal, we conducted prospective, longitudinal, home-based active surveillance for febrile respiratory illness during pregnancy through 6 months postpartum. During 2011–2014, HMPV was detected in 55 of 3,693 women (16.4 cases/1,000 person-years). Twenty-five women were infected with HMPV during pregnancy, compared with 98 pregnant women who contracted rhinovirus and 7 who contracted respiratory syncytial virus. Women with HMPV during pregnancy had an increased risk of giving birth to infants who were small for gestational age. An intervention to reduce HMPV febrile respiratory illness in pregnant women may have the potential to decrease risk of adverse birth outcomes in developing countries.

Human metapneumovirus (HMPV), a paramyxovirus discovered in 2001, is a previously unrecognized cause of respiratory infections in infants, children, and adults (1). HMPV is estimated to cause 5%–25% of respiratory infections among infants and children (2–5) and 1.5%–10.5% of respiratory infections among adults (6–11). In children, HMPV is responsible for 5%–15% of hospitalizations for lower respiratory tract illness (12). In adult populations, HMPV is responsible for up to 11% of hospitalizations for acute respiratory illness, particularly in adults with underlying heart or lung disease (5,10,11).

Illness and death from respiratory viruses among pregnant women have received greater appreciation globally following the pandemic influenza outbreak in 2009. Pregnancy is known to have an immunomodulating effect, and pregnant women are at elevated risk for complications of both seasonal and pandemic influenza (13,14). The epidemiology and clinical presentation of noninfluenza respiratory viral infections, including HMPV, during pregnancy, as well as the consequence of such infections on the fetus, are not well described, despite advances in sensitive and rapid molecular diagnostic methods and increasing surveillance of respiratory viruses in diverse populations.

This study describes the clinical characteristics of infection due to HMPV and other respiratory viruses among pregnant women in a rural population in South Asia. It also examines the effects of HMPV infection during pregnancy on birth outcomes.

Methods

We obtained data for this study during 2 consecutive community-based randomized controlled trials of year-round seasonal influenza vaccination among pregnant women in a rural population in Sarlahi, Nepal. We conducted an active, home-based surveillance with a door-to-door census

to identify married women of reproductive age during April 2011–September 2013 (15). Follow-up occurred every 5 weeks at households where women of reproductive age resided to determine whether a woman had become pregnant. All married women 15–40 years of age identified as pregnant with gestational age of 17–34 weeks during the study period were offered enrollment and randomized into 1 of 2 study arms: vaccination or placebo.

From the time of vaccination with study vaccine or placebo through 180 days postpartum, a field interviewer visited the household weekly to conduct a morbidity interview for each day in the preceding week. If a participant had an influenza-like illness (ILI) episode (defined as reported fever plus ≥ 1 of the following symptoms: cough, myalgia, rhinorrhea, or sore throat), a midnasal swab specimen was collected and tested for respiratory viral infection by real-time reverse transcription PCR (16–19). Viral infection was defined as the molecular detection of the virus concurrent with symptoms of a respiratory illness. Any symptoms separated from the illness episode by at least 7 symptom-free days were considered part of a separate illness episode. This analysis does not include influenza, however, because it is analyzed separately as part of the clinical trial of maternal immunization (20).

We estimated gestational age at time of respiratory virus infection in pregnancy by subtracting the date of last menstrual period from the date of delivery, based on maternal recall. The “mother’s smoking” variable captured whether cigarettes or bidi (a hand-rolled cigarette common in South Asia) were smoked in the previous 30 days. Ethnic group was dichotomized as Pahadi (origins in the hills of Nepal) versus Madheshi (origin in the plains of Nepal). We placed women in the categories of Brahmin (highest caste), Chhetri (higher caste), Vaiysha (working caste), Shudra (lower caste), and Muslim. We defined household size as number of persons sharing a cookstove; we defined household density as the number of persons per room, excluding kitchen and storerooms.

We calculated the incidence of infection by using days of follow-up from enrollment through 180 days postpartum. Among women with HMPV and other respiratory viruses, the duration of illness and the week following the illness period were excluded from time at risk. Descriptive statistics were used to summarize the characteristics of pregnant and postpartum women with and without HMPV and other respiratory viral infections. Bivariate Poisson regression analyses were performed to assess potential risk factors including household density, number of children <5 years of age in the household, caste, ethnic group, maternal education, and smoking.

To assess differential clinical symptoms related to infection comparing pregnant and postpartum women, we assigned a 1-point score to each of the following symptoms:

fever, cough, sore throat, rhinorrhea/nasal congestion, and myalgia (21–23). We used a Wilcoxon rank-sum test to compare severity scores and total days with symptoms among pregnant and postpartum women. We also compared the proportion of women experiencing each individual symptom for pregnant and postpartum women.

Birth outcomes assessed were birthweight and gestational age at birth. We defined low birthweight (LBW) as <2,500 g. We defined small for gestational age (SGA) with INTERGROWTH-21 standards (24). We defined preterm birth (PTB) as birth before 37 weeks completed gestation. We assessed associations between HMPV during pregnancy and birthweight and gestational age with linear regression, whereas we used Poisson regression to assess binary outcomes (LBW, SGA, PTB). As a reference, we also compared birth outcomes between women with and without any febrile respiratory illness during pregnancy. Finally, we calculated the proportion of ILI episodes with respiratory viruses other than HMPV; the symptoms associated with these episodes are reported.

We performed analyses using SAS version 9.4 (SAS Institute, Cary, NC, USA) and Stata version 13.1 (StataCorp LLP, College Station, TX, USA). Institutional review board approval for the randomized controlled trial was given by the Johns Hopkins University Bloomberg School of Public Health, Cincinnati Children's Hospital, the Institute of Medicine at Tribhuvan University, and the Nepal Health Research Council, with deferral from Seattle Children's Hospital. Approval for this analysis was received from the University of Washington institutional review board. The primary trial was registered under ClinicalTrials.gov NCT01034254.

Results

Incidence and Risk Factors

During April 2011–September 2013, we enrolled and vaccinated 3,693 eligible women; weekly surveillance visits continued through May 2014. Median follow-up time was 48 weeks (interquartile range [IQR] 44–53 weeks) among women with HMPV and 49 weeks (IQR 43–55 weeks) among women without HMPV. Overall, we collected 944 nasal swab specimens from enrolled women.

During this 3-year period, 55 (1.5%) women had an HMPV illness episode. The overall incidence of HMPV was 16.4 cases/1,000 person-years (95% CI 8.9–30.3); this represents 25 cases among pregnant women (16.7 cases/1,000 person-years, 95% CI 10.8–25.8) and 30 cases among postpartum women (16.1 cases/1,000 person-years, 95% CI 7.5–30.1). Incidence peaked at 71.9 cases/1,000 person-years for September 2011–January 2012. During May 2013–January 2014, no HMPV infections were observed (Figure 1). Other respiratory viruses detected among pregnant women in this cohort were rhinovirus (n = 98), coronavirus (n = 30), parainfluenza (n = 23), bocavirus (n = 9), respiratory syncytial virus (RSV) (n = 7), and adenovirus (n = 6) (Table 1).

Among the 25 pregnant women with HMPV, median gestational age at time of illness was 32.5 weeks (IQR 22.0–37.0 weeks). Women with and without HMPV had similar body mass indexes at enrollment: a median of 20.1 (IQR 18.4–22.4 weeks) among women with HMPV and 20.7 (IQR 19.1–28.0 weeks) among women without HMPV. Hypertension was uncommon in the cohort, identified in 43 (1.2%) of women without HMPV and in no women with HMPV.

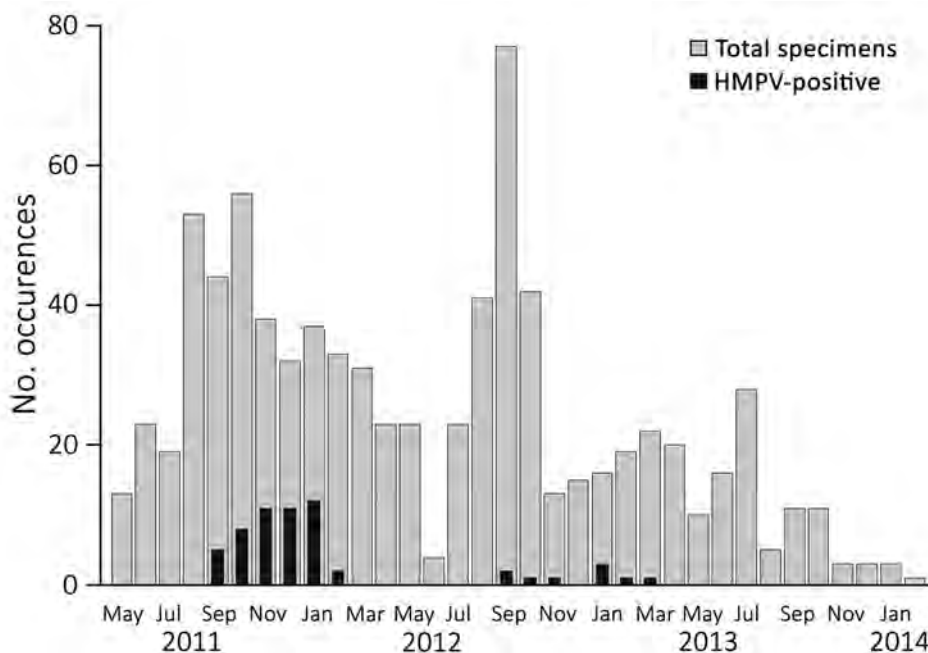


Figure 1. HMPV positivity and seasonality among pregnant women in study of HMPV and pregnancy, Sarlahi, Nepal, April 2011–September 2013. Women were followed until 180 days after birth. HMPV, human metapneumovirus.

Table 1. Etiology of febrile respiratory illness among pregnant women in Sarlahi, Nepal, April 2011–September 2013*

Type	No. infections	No. co-infections	Frequency of symptoms, no. (%) patients				Sought care/MD, no. (%)†	Median duration of symptoms, d (range)			Severity score
			Cough	ST	RN	Myalgia		Fever	Cough	Any	
Adenovirus	6	2	2 (33)	4 (67)	4 (67)	3 (50)	2 (33)/1 (17)	4 (2–6)	0 (0–4)	5 (4–15)	10 (6–22)
Bocavirus	9	5	8 (89)	6 (67)	7 (78)	5 (56)	5 (56)/0	3 (1–7)	5 (0–11)	7 (3–38)	22 (6–50)
Coronavirus	30	7	21 (70)	17 (57)	19 (63)	16 (53)	17 (57)/1 (3)	2 (1–7)	2 (0–11)	5 (1–67)	11 (2–86)
HMPV	25	11	19 (70)	12 (44)	17 (63)	14 (52)	12 (48)/1 (4)	3 (1–7)	3 (0–26)	5 (2–50)	13 (3–61)
PIV1	4	0	2 (50)	2 (50)	3 (75)	2 (50)	1 (25)/0	4 (2–6)	2 (0–7)	5 (3–13)	16 (5–23)
PIV2	9	4	7 (78)	5 (56)	8 (89)	5 (56)	4 (44)/0	2 (1–7)	2 (0–6)	7 (2–18)	16 (5–27)
PIV3	7	2	4 (57)	4 (57)	6 (86)	5 (71)	6 (86)/1 (14)	3 (2–6)	3 (0–6)	7 (2–12)	21 (3–31)
PIV4	3	0	3 (100)	2 (67)	3 (100)	1 (33)	2 (67)/1 (33)	2 (2–3)	6 (4–13)	7 (5–13)	15 (10–21)
Rhinovirus	98	13	71 (72)	63 (64)	66 (67)	45 (46)	39 (40)/8 (8)	2 (1–10)	3 (0–25)	5 (1–50)	9 (1–93)
RSV	7	4	5 (71)	3 (43)	6 (86)	4 (57)	4 (57)/1 (14)	2 (1–7)	2 (0–3)	3 (2–18)	9 (4–24)

*No virus was detected in 137 women; no swab was taken from 452 women. Total febrile respiratory illnesses: 767; because of co-infections, the number of total infections is 789. HMPV, human metapneumovirus; PIV, parainfluenza virus; RSV, respiratory syncytial virus; RN, rhinorrhea/nasal congestion; ST, sore throat.

†Care means seen for care because of illness; MD means seen by a medical doctor.

Median household density was 3 persons/room among women with and without HMPV. Median years of maternal education was 0 (IQR 0–8.0) among women with HMPV and 5 (IQR 0–10.0) among women without HMPV. Three (5.5%) women with HMPV and 108 (3.1%) women without HMPV had smoked in the 30 days before enrollment (Table 2). In Poisson regression analysis, none of the risk factors analyzed, including caste and household density, altered HMPV risk.

Clinical Symptoms

The most common symptom among pregnant and postpartum participants with HMPV infection was cough (67.3%), followed by rhinorrhea/nasal congestion (58.2%) and myalgia (56.4%). All women with HMPV detected had fever, as this symptom was required for a swab to be taken (Table 3). Median symptom duration was 5 days among both pregnant and postpartum women (Table 3; Figure 2). No difference was noted in the presence

or duration of symptoms between pregnant and postpartum women.

In respiratory disease associated with respiratory viruses among pregnant women overall, cough was the most common symptom in all illnesses except parainfluenza and RSV, for which rhinorrhea/nasal congestion was the most common symptom. The longest duration of symptoms was observed among women with bocavirus and parainfluenza 2–4 (7 days). The highest severity score was observed among women with bocavirus, who had a score of 22 (range 6–50) (Table 1).

Twenty-four (43.6%) women with HMPV also experienced viral co-infections, with rhinovirus the most common ($n = 14$; 25.4%), followed by coronavirus ($n = 4$; 7.3%) and parainfluenza ($n = 3$; 5.5%). One pregnant woman had HMPV, rhinovirus, and coronavirus concurrently. Symptom duration and severity were similar between women with and without viral co-infection.

Twelve pregnant women (48.0%) and 18 postpartum women (60.0%) received medical care during the period

Table 2. Demographic characteristics and bivariate RR estimates for HMPV infection among pregnant and postpartum women in Sarlahi, Nepal, April 2011–September 2013*

Characteristic	HMPV-positive, $n = 55$	HMPV-negative, $n = 3,638$	RR (95% CI)	p value
Age at enrollment, y, median (IQR)	22 (20–25)	23 (20–26)	1.0 (0.9–1.1)	0.96
Smoking†	3 (5)	108 (3)	0.6 (0.0–37.9)	0.83
BMI at enrollment, median (IQR)	20 (18–22)	21 (19–28)	1.0 (0.8, 1.2)	0.66
Ethnic group				
Pahadi	30 (56)	1,997 (57)	Ref	
Madhesi	24 (44)	1,503 (43)	1.0 (0.4–3.3)	0.89
Caste				
Brahmin	3 (5)	377 (11)	0.5 (0.0–5.4)	0.56
Chhetri	5 (9)	445 (13)	Ref (combined)	
Vaiysha	30 (56)	1,933 (55)		
Shudra	11 (20)	452 (13)		
Muslim	4 (7)	284 (8)		
Household size, median (IQR)				
Children <5 y of age	1 (0–1)	0 (0–1)	1.3 (0.7–2.4)	0.41
Density‡	3 (2–6)	3 (2–4)	1.1 (0.9–1.3)	0.20
Education, y, median (IQR)	0 (0–8)	5 (0–10)	0.9 (0.8–1.1)	0.22
Literacy	25 (50)	1,991 (60)	0.6 (0.2–2.2)	0.46

*Values are no. (%) patients except as indicated. BMI, body mass index; HMPV, human metapneumovirus; IQR, interquartile range; Ref, referent; RR, relative risk.

†Defined as smoking at enrollment.

‡Defined as persons/room.

Table 3. Proportion of pregnant and postpartum women with HMPV infections who had selected symptoms and illness severity, Sarlahi, Nepal, April 2011–September 2013*

Measure	Total, n = 55	Pregnant, n = 25	Postpartum, n = 30	p value
Symptom, no. (%)				
Fever†	55 (100)	25 (100)	30 (100)	NA
Cough	37 (67)	17 (68)	20 (67)	0.92
Sore throat	23 (42)	11 (44)	12 (40)	0.76
Rhinorrhea/nasal congestion	32 (58)	15 (60)	17 (57)	0.80
Myalgia	31 (56)	12 (48)	19 (63)	0.25
Visit for care	27 (49)	12 (48)	18 (60)	0.49
Severity measure, median (range)				
Severity score	10 (1–61)	13 (3–61)	9 (1–38)	0.70
Fever duration, d	3 (1–8)	3 (1–8)	2 (1–8)	0.15
Cough duration, d	2 (0–27)	3 (0–27)	2 (0–10)	0.78
Symptom duration, d	5 (1–31)	5 (2–31)	5 (1–28)	0.36

*NA, not applicable.

†Subjective fever required for nasal swab specimen collection.

of their HMPV illness episode (Table 3 Figure 3). Six women (10.9%) sought care >1 time during their illness. Of the 38 total visits, 16 (42.1%) women visited a medicine shop or local doctor, 12 (31.6%) visited a health post, and 10 (24.4%) visited a primary health center, a medicine shop or local doctor, or hospital. Only 1 woman’s hospital visit was potentially related to HMPV. This woman was 4 weeks postpartum at the start of symptoms and had rhinovirus concurrently; she reported 11 days of symptoms, and visited the hospital twice and a health post once during her illness. No participant died of respiratory illness potentially related to HMPV.

Effect on Birth Outcomes

All women with HMPV during pregnancy delivered live infants. Two (8.0%) of the 25 women with HMPV during pregnancy gave birth to preterm infants; 5 (25.0%) delivered LBW infants. The median gestational age of infants in both groups was 40 weeks (IQR 38–41 weeks), and the

median birthweight in both groups was 2.8 kg (IQR 2.4–2.9 kg among women with HMPV, 2.5–3.1 kg among women without HMPV). No differences were noted in birthweight or preterm birth between infants born to women with and without HMPV during pregnancy, nor were differences noted between women with and without fever during pregnancy. However, women with HMPV during pregnancy were found to be 1.7 times as likely to deliver an SGA infant compared with women without HMPV during pregnancy (p = 0.031). Non-HMPV fever during pregnancy did not have a notable effect on SGA risk (Table 4).

Women with HMPV during pregnancy who delivered preterm infants experienced the onset of symptoms 25–30 days before delivery (median 27.5 days); women who delivered LBW infants had symptom onset 25–90 days before delivery (median 42 days) (Figure 4). Three women (60.0%) who delivered LBW infants visited a health post during their illness period; 1 woman (50.0%) who delivered a preterm infant visited a medicine shop/local doctor during her illness.

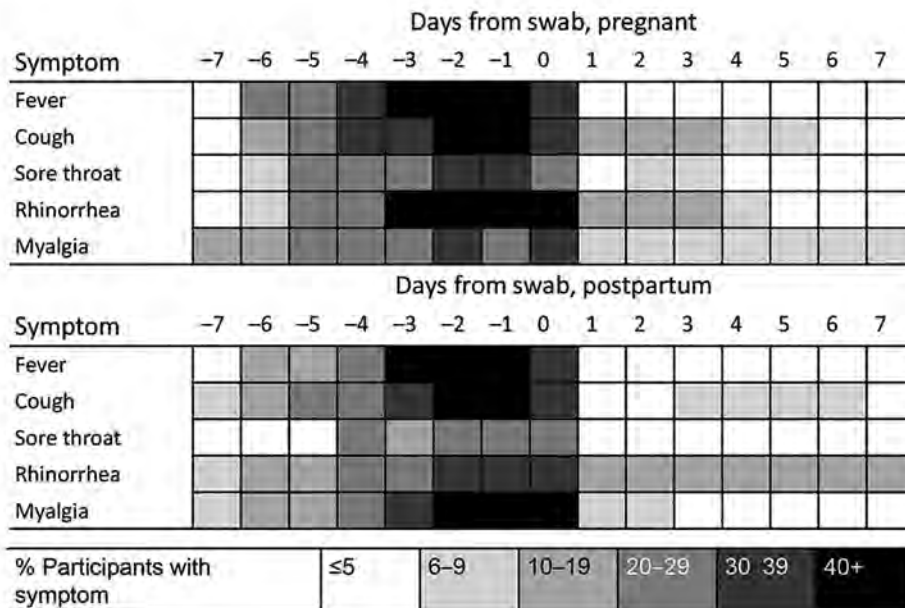


Figure 2. Symptom duration among pregnant and postpartum women in study of human metapneumovirus and pregnancy, Sarlahi, Nepal, April 2011–September 2013.

Table 4. Associations between illness during pregnancy and birth outcomes, Sarlahi, Nepal, April 2011–September 2013 *

Characteristic	No. (%) or median (IQR)			RR (95% CI) or mean difference			
	No fever, n = 3,000	Fever		Any fever	p value	HMPV-positive with fever	p value
		HMPV-negative, n = 668	HMPV-positive, n = 25				
Birthweight, kg	2.8 (2.5–3.1)	2.8 (2.5–3.1)	2.8 (2.4–2.9)	0.0 (–0.1 to 0.1)	0.77	–0.1 (–0.3 to 0.1)	0.23
Low birthweight	542 (25)	132 (26)	5 (26)	1.0 (0.9–1.2)	0.59	1.0 (0.5–2.3)	0.91
Gestational age	40 (38–41)	39 (38–41)	40 (38–41)	–0.2 (–0.3 to 0.1)	0.077	0.2 (–0.7 to –1.1)	0.69
Small for gestational age	830 (38)	198 (39)	12 (63)	1.0 (0.9–1.2)	0.72	1.7 (1.0–2.6)	0.031
Preterm birth	372 (13)	97 (15)	2 (8)	1.2 (0.9–1.4)	0.12	0.5 (0.1–1.9)	0.33

*HMPV, human metapneumovirus; IQR: interquartile range; RR, relative risk.

Among the 30 women with HMPV postpartum, 8 (26.7%) had infants who had HMPV within 1 month of their mother’s illness. Four of these mother–infant pairs had HMPV simultaneously; in 2 pairs, the mother had a positive swab before the infant’s swab, and in 2 pairs the infant had a positive swab before the mother’s swab.

Discussion

In this analysis, we describe the incidence and clinical presentation of HMPV and other respiratory viruses during pregnancy, as well as birth outcomes associated with HMPV infection during pregnancy. HMPV was a relatively common cause of ILI during and after pregnancy and was associated with an increased risk of SGA birth in women with HMPV respiratory illness compared with women without such illness. HMPV exhibited a clear peak during the first of the 3 years of the study. Despite the rural, resource-limited setting, most women with HMPV accessed healthcare, and nearly 20% visited a health center or physician during their illness.

Incidence of HMPV among women during and after pregnancy was 16.5/1,000 person-years, >4 times as high as the RSV incidence in this cohort during the same time period (3.9/1,000 person-years). Pregnant and postpartum women with HMPV also appeared to exhibit longer fever

duration (3 days vs. 2 days) and longer overall symptom duration (5 days vs. 4 days) compared with women in the same cohort with RSV (25). Overall, rhinovirus was the most commonly detected pathogen among pregnant women in this cohort (n = 98); coronavirus was also relatively common (n = 30). This finding is notable because Middle East respiratory syndrome coronavirus and severe acute respiratory syndrome coronavirus during pregnancy have been found to be associated with severe complications and illness in the woman and the infant (26–28).

No notable difference in HMPV severity was noted between pregnant and postpartum women. This finding contrasts with previous literature on influenza and RSV, which demonstrates elevated risk for severe disease among pregnant women (13,14,29–31). However, much previous research on respiratory illness severity in pregnancy focused on hospital-related outcomes, such as admission to an intensive care unit, which we were unable to capture in this study.

Previous estimates of adult HMPV incidence ranged from 15 to 53/1,000 person-years (6–11), but accurate estimates of HMPV incidence are difficult to obtain, particularly in a community setting. Many adults with HMPV infections do not seek medical care, and among those who do, many are not tested for viral infections (11). Walsh et al. followed

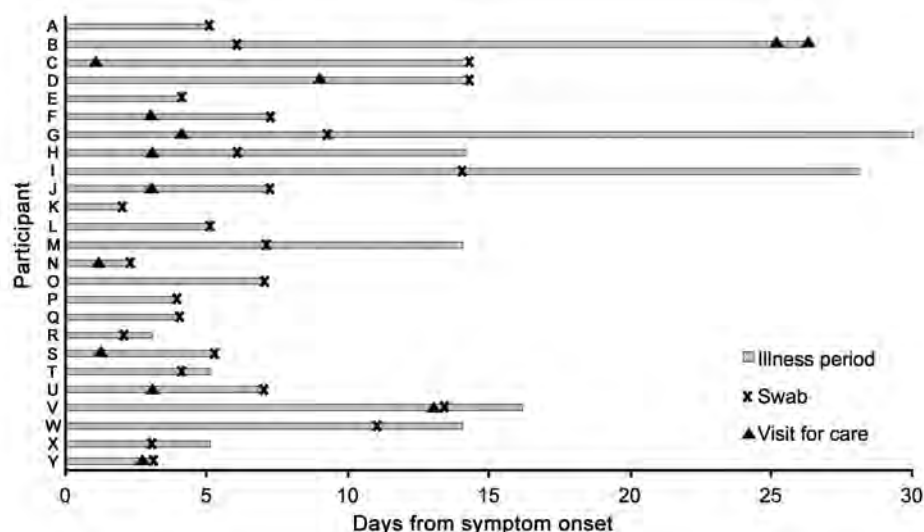


Figure 3. Timing of nasal swab specimen collection and visits for care among 25 pregnant women with human metapneumovirus infection, Sarlahi, Nepal, April 2011–September 2013.

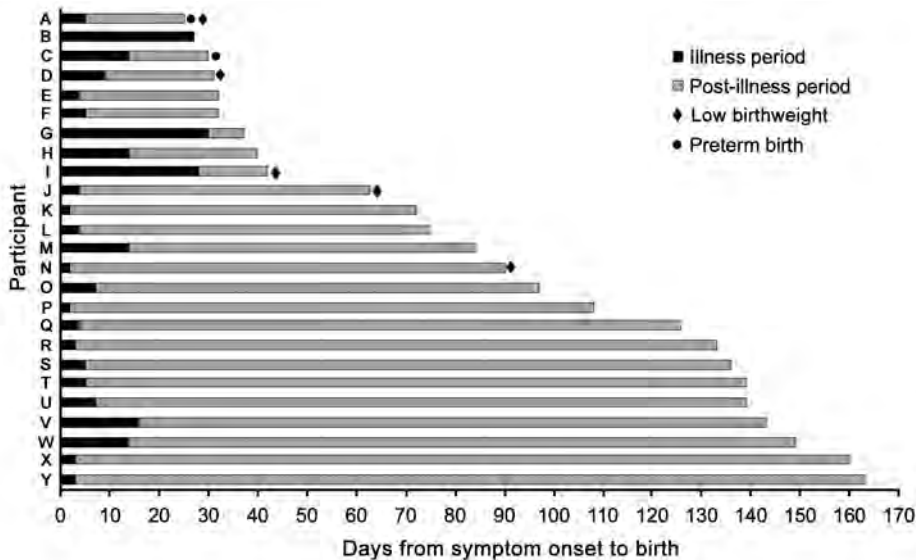


Figure 4. Timing of illness episode and birth outcomes among 25 pregnant women with human metapneumovirus infection, Sarlahi, Nepal, April 2011–September 2013.

prospectively enrolled young adults (18–40 years of age), healthy elderly adults (≥ 65 years of age), and high-risk adults (those with symptomatic lung disease) over 4 consecutive winters (32). That study found that 4.3%–10.6% of young adults experienced HMPV infection in any given year, higher than the proportion noted in the healthy elderly (2.2%–6.4%) or the high-risk cohort (2.9%–8.6%), supporting our finding that HMPV is a major pathogen among young adults. These findings also align with the proportion of maternal respiratory swabs positive for HMPV in our study (6.7%), although only 55% of participants in the Walsh et al. young adult cohort reported fever (32).

The HMPV seasonality demonstrated in this subtropical area is somewhat earlier than the seasonality documented in other settings in the Northern Hemisphere, with most cases typically occurring in January through April (2,4,6,11,32–37). Although most research has been done in temperate climate zones, a study from India demonstrated only 1 HMPV peak over the 3-year study period, which suggests that HMPV may exhibit a nonannual cycle in this setting (37).

Although clinic visits in this area of Nepal can be heavily confounded by factors such as location and socioeconomic status, we found that most women with HMPV were seen by a healthcare provider and one quarter of the visits were to a primary health center or MD/MMBS doctor. Considering the frequency of healthcare visits among women with HMPV in this resource-limited region, future research should investigate lower respiratory complications and longer-term sequelae of HMPV in pregnant and postpartum women.

We found that febrile illness due to HMPV during pregnancy is associated with increased SGA risk (risk ratio 1.7; $p = 0.031$). Infants who are born SGA are at increased

risk for poor growth and early death, particularly in developing countries. Reasons for SGA births include maternal malnutrition, use of drugs or alcohol during pregnancy, intrauterine infection, maternal anemia, or hypertension during pregnancy (38). Rates of hypertension, maternal smoking, and alcohol use are low in this cohort, and we found no difference in body mass index between pregnant women with and without SGA births. It is possible that a systemic inflammatory response due to HMPV febrile respiratory illness may be associated with increased risk of SGA, although it is not clear why this would be due to HMPV alone rather than febrile respiratory illness in general. No difference was noted in LBW or PTB between infants born to women with and without HMPV during pregnancy. Overall, the observed incidences of LBW and PTB in this cohort were slightly lower than previous estimates in the region, reflecting an overall improvement in health in the population. Among all women enrolled, 25% gave birth to an LBW infant, compared with 30.4% in previous studies; 13% gave birth preterm, compared with 18.3% in previous studies (15,39). In the parent trial of maternal influenza immunization, influenza vaccination during pregnancy was effective in prevention of influenza infection in infants and was also associated with increased birthweight (20). This finding suggests that prevention of potential respiratory illness during pregnancy may decrease the risk of adverse birth outcomes.

Limitations of this study included the relatively small number of women with HMPV during pregnancy. We observed most outcomes at rates at 10%–50%, but with only 25 women having HMPV during pregnancy, we had the power only to detect risk ratios of 1.6 to 3.5. A further limitation was the collection of swabs only in cases of febrile respiratory illness; asymptomatic or afebrile infections

would not have been captured. Because previous studies have found that adults with HMPV are often afebrile, with fever reported among 0–55% of adults, we likely underestimated the true incidence of HMPV (6,11,32,34,40). Preceding respiratory viral infections may increase risk for secondary bacterial infections, such as pneumococcus and staphylococcus. Unfortunately, in this study we did not test for bacterial infections and thus cannot assess whether these had an effect on clinical outcomes. The study was confined to a single rural district, which may have limited the variation in risk factors, such as caste and education. However, this region of Nepal (in the plains along the border with Bihar, India) is broadly representative of South Asia, a region with a population density and birth rate among the highest in the world. Few studies of HMPV have been conducted in these types of settings, particularly among pregnant women, which is notable because the presentation and clinical outcomes of disease may differ in regions of the world with high rates of household density, malnutrition, and indoor air pollution.

In summary, in this prospective study involving active, home-based surveillance in a rural South Asia setting, we found that HMPV is a relatively frequent cause of symptomatic febrile illness during pregnancy. These data may help providers to make decisions about therapeutic care, particularly as more inexpensive viral diagnostic tests become available. Finally, as attempts to develop a vaccine or antiviral therapy for HMPV are currently under way, the identification of risk factors for infection and for severe disease is crucial to identify groups that would benefit most from these advances, and to help develop focused prevention strategies.

Acknowledgments

We acknowledge the Nepal Nutrition Intervention Project–Sarlahi staff in Kathmandu and Sarlahi District, Nepal, and the mothers and infants who participated in this study.

This study was supported by National Institutes of Health grants K23-AI103105 (H.Y.C.) and the Bill and Melinda Gates Foundation (grant 50274).

Ms. Lenahan is currently a research manager at Save the Children Federation, Inc., focusing on pneumonia. She previously worked as a senior infectious disease research associate at Seattle Children's Hospital in Seattle, Washington, USA. Her research interests include respiratory illness, viral surveillance, and vaccine-preventable illnesses.

References

- van den Hoogen BG, de Jong JC, Groen J, Kuiken T, de Groot R, Fouchier RA, et al. A newly discovered human pneumovirus isolated from young children with respiratory tract disease. *Nat Med*. 2001;7:719–24. <http://dx.doi.org/10.1038/89098>

- Caracciolo S, Minini C, Colombrita D, Rossi D, Miglietti N, Vettore E, et al. Human metapneumovirus infection in young children hospitalized with acute respiratory tract disease: virologic and clinical features. *Pediatr Infect Dis J*. 2008;27:406–12. <http://dx.doi.org/10.1097/INF.0b013e318162a164>
- Foulongne V, Guyon G, Rodière M, Segondy M. Human metapneumovirus infection in young children hospitalized with respiratory tract disease. *Pediatr Infect Dis J*. 2006;25:354–9. <http://dx.doi.org/10.1097/01.inf.0000207480.55201.f6>
- Williams JV, Harris PA, Tollefson SJ, Halburnt-Rush LL, Pingsterhaus JM, Edwards KM, et al. Human metapneumovirus and lower respiratory tract disease in otherwise healthy infants and children. *N Engl J Med*. 2004;350:443–50. <http://dx.doi.org/10.1056/NEJMoa025472>
- Kahn JS. Epidemiology of human metapneumovirus. *Clin Microbiol Rev*. 2006;19:546–57. <http://dx.doi.org/10.1128/CMR.00014-06>
- Falsey AR, Erdman D, Anderson LJ, Walsh EE. Human metapneumovirus infections in young and elderly adults. *J Infect Dis*. 2003;187:785–90. <http://dx.doi.org/10.1086/367901>
- da Silva RC, da Silva Mendes G, Rojas MA, Amorim AR, Couceiro JN, Lupi O, et al. Frequency of viral etiology in symptomatic adult upper respiratory tract infections. *Braz J Infect Dis*. 2015;19:30–5. <http://dx.doi.org/10.1016/j.bjid.2014.08.005>
- Zimmerman RK, Rinaldo CR, Nowalk MP, Gk B, Thompson MG, Moehling KK, et al. Influenza and other respiratory virus infections in outpatients with medically attended acute respiratory infection during the 2011–12 influenza season. *Influenza Other Respi Viruses*. 2014;8:397–405. <http://dx.doi.org/10.1111/irv.12247>
- Widmer K, Griffin MR, Zhu Y, Williams JV, Talbot HK. Respiratory syncytial virus- and human metapneumovirus-associated emergency department and hospital burden in adults. *Influenza Other Respi Viruses*. 2014;8:347–52. <http://dx.doi.org/10.1111/irv.12234>
- Reiche J, Jacobsen S, Neubauer K, Hafemann S, Nitsche A, Milde J, et al. Human metapneumovirus: insights from a ten-year molecular and epidemiological analysis in Germany. *PLoS One*. 2014;9:e88342. <http://dx.doi.org/10.1371/journal.pone.0088342>
- Haas LE, Thijsen SF, van Elden L, Heemstra KA. Human metapneumovirus in adults. *Viruses*. 2013;5:87–110. <http://dx.doi.org/10.3390/v5010087>
- Feuillet F, Lina B, Rosa-Calatrava M, Boivin G. Ten years of human metapneumovirus research. *J Clin Virol*. 2012;53:97–105. <http://dx.doi.org/10.1016/j.jcv.2011.10.002>
- Memoli MJ, Harvey H, Morens DM, Taubenberger JK. Influenza in pregnancy. *Influenza Other Respi Viruses*. 2013;7:1033–9. <http://dx.doi.org/10.1111/irv.12055>
- Jamieson DJ, Honein MA, Rasmussen SA, Williams JL, Swerdlow DL, Biggerstaff MS, et al.; Novel Influenza A (H1N1) Pregnancy Working Group. H1N1 2009 influenza virus infection during pregnancy in the USA. *Lancet*. 2009;374:451–8. [http://dx.doi.org/10.1016/S0140-6736\(09\)61304-0](http://dx.doi.org/10.1016/S0140-6736(09)61304-0)
- Tielsch JM, Steinhoff M, Katz J, Englund JA, Kuypers J, Khatri SK, et al. Designs of two randomized, community-based trials to assess the impact of influenza immunization during pregnancy on respiratory illness among pregnant women and their infants and reproductive outcomes in rural Nepal. *BMC Pregnancy Childbirth*. 2015;15:40. <http://dx.doi.org/10.1186/s12884-015-0470-y>
- Kuypers J, Wright N, Corey L, Morrow R. Detection and quantification of human metapneumovirus in pediatric specimens by real-time RT-PCR. *J Clin Virol*. 2005;33:299–305. <http://dx.doi.org/10.1016/j.jcv.2004.11.023>
- Martin ET, Taylor J, Kuypers J, Magaret A, Wald A, Zerr D, et al. Detection of bocavirus in saliva of children with and without respiratory illness. *J Clin Microbiol*. 2009;47:4131–2. <http://dx.doi.org/10.1128/JCM.01508-09>

18. Kuypers J, Martin ET, Heugel J, Wright N, Morrow R, Englund JA. Clinical disease in children associated with newly described coronavirus subtypes. *Pediatrics*. 2007;119:e70–6. <http://dx.doi.org/10.1542/peds.2006-1406>
19. Kuypers J, Wright N, Ferrenberg J, Huang ML, Cent A, Corey L, et al. Comparison of real-time PCR assays with fluorescent-antibody assays for diagnosis of respiratory virus infections in children. *J Clin Microbiol*. 2006;44:2382–8. <http://dx.doi.org/10.1128/JCM.00216-06>
20. Steinhoff MC, Katz J, Englund JA, Khatri SK, Shrestha L, Kuypers J, et al. Year-round influenza immunisation during pregnancy in Nepal: a phase 4, randomised, placebo-controlled trial. *Lancet Infect Dis*. 2017;S1473-3099(17)30252-9. [http://dx.doi.org/10.1016/S1473-3099\(17\)30252-9](http://dx.doi.org/10.1016/S1473-3099(17)30252-9)
21. Roussy JF, Carbonneau J, Ouakki M, Papenburg J, Hamelin MÈ, De Serres G, et al. Human metapneumovirus viral load is an important risk factor for disease severity in young children. *J Clin Virol*. 2014;60:133–40. <http://dx.doi.org/10.1016/j.jcv.2014.03.001>
22. Papenburg J, Hamelin MÈ, Ouhoumane N, Carbonneau J, Ouakki M, Raymond F, et al. Comparison of risk factors for human metapneumovirus and respiratory syncytial virus disease severity in young children. *J Infect Dis*. 2012;206:178–89. <http://dx.doi.org/10.1093/infdis/jis333>
23. Hahn A, Wang W, Jaggi P, Dvorchik I, Ramilo O, Koranyi K, et al. Human metapneumovirus infections are associated with severe morbidity in hospitalized children of all ages. *Epidemiol Infect*. 2013;141:2213–23. <http://dx.doi.org/10.1017/S0950268812002920>
24. Papageorgiou AT, Ohuma EO, Altman DG, Todros T, Ismail LC, Lambert A, et al.; International Fetal and Newborn Growth Consortium for the 21st Century (INTERGROWTH-21st). International standards for fetal growth based on serial ultrasound measurements: the Fetal Growth Longitudinal Study of the INTERGROWTH-21st Project. *Lancet*. 2014;384:869–79. [http://dx.doi.org/10.1016/S0140-6736\(14\)61490-2](http://dx.doi.org/10.1016/S0140-6736(14)61490-2)
25. Chu HY, Katz J, Tielsch J, Khatri SK, Shrestha L, LeClerq SC, et al. Clinical presentation and birth outcomes associated with respiratory syncytial virus infection in pregnancy. *PLoS One*. 2016;11:e0152015. <http://dx.doi.org/10.1371/journal.pone.0152015>
26. Malik A, El Masry KM, Ravi M, Sayed F. Middle East Respiratory Syndrome Coronavirus during Pregnancy, Abu Dhabi, United Arab Emirates, 2013. *Emerg Infect Dis*. 2016;22:515–7. <http://dx.doi.org/10.3201/eid2203.151049>
27. Alserahi H, Wali G, Alshukairi A, Alraddadi B. Impact of Middle East respiratory syndrome coronavirus (MERS-CoV) on pregnancy and perinatal outcome. *BMC Infect Dis*. 2016;16:105. <http://dx.doi.org/10.1186/s12879-016-1437-y>
28. Wong SF, Chow KM, Leung TN, Ng WF, Ng TK, Shek CC, et al. Pregnancy and perinatal outcomes of women with severe acute respiratory syndrome. *Am J Obstet Gynecol*. 2004;191:292–7. <http://dx.doi.org/10.1016/j.ajog.2003.11.019>
29. Rasmussen SA, Jamieson DJ. Influenza and pregnancy in the United States. *Clin Obstet Gynecol*. 2012;55:487–97. <http://dx.doi.org/10.1097/GRF.0b013e31824df23e>
30. Bhalerao-Gandhi A, Chhabra P, Arya S, Simmerman JM. Influenza and pregnancy: a review of the literature from India. *Infect Dis Obstet Gynecol*. 2015;2015:867587. <http://dx.doi.org/10.1155/2015/867587>
31. Wheeler SM, Dotters-Katz S, Heine RP, Grotegut CA, Swamy GK. Maternal effects of respiratory syncytial virus infection during pregnancy. *Emerg Infect Dis*. 2015;21:1951–5. <http://dx.doi.org/10.3201/eid2111.150497>
32. Walsh EE, Peterson DR, Falsey AR. Human metapneumovirus infections in adults: another piece of the puzzle. *Arch Intern Med*. 2008;168:2489–96. <http://dx.doi.org/10.1001/archinte.168.22.2489>
33. McAdam AJ, Hasenbein ME, Feldman HA, Cole SE, Offermann JT, Riley AM, et al. Human metapneumovirus in children tested at a tertiary-care hospital. *J Infect Dis*. 2004;190:20–6. <http://dx.doi.org/10.1086/421120>
34. Talaat KR, Karron RA, Thumar B, McMahon BA, Schmidt AC, Collins PL, et al. Experimental infection of adults with recombinant wild-type human metapneumovirus. *J Infect Dis*. 2013;208:1669–78. <http://dx.doi.org/10.1093/infdis/jit356>
35. Wilkesmann A, Schildgen O, Eis-Hübinger AM, Geikowski T, Glatzel T, Lentze MJ, et al. Human metapneumovirus infections cause similar symptoms and clinical severity as respiratory syncytial virus infections. *Eur J Pediatr*. 2006;165:467–75. <http://dx.doi.org/10.1007/s00431-006-0105-4>
36. Aberle SW, Aberle JH, Sandhofer MJ, Pracher E, Popow-Kraupp T. Biennial spring activity of human metapneumovirus in Austria. *Pediatr Infect Dis J*. 2008;27:1065–8. <http://dx.doi.org/10.1097/INF.0b013e31817ef4fd>
37. Banerjee S, Sullender WM, Choudekar A, John C, Tyagi V, Fowler K, et al. Detection and genetic diversity of human metapneumovirus in hospitalized children with acute respiratory infections in India. *J Med Virol*. 2011;83:1799–810. <http://dx.doi.org/10.1002/jmv.22176>
38. Katz J, Lee ACC, Kozuki N, Lawn JE, Cousens S, Blencowe H, et al.; CHERG Small-for-Gestational-Age-Preterm Birth Working Group. Mortality risk in preterm and small-for-gestational-age infants in low-income and middle-income countries: a pooled country analysis. *Lancet*. 2013;382:417–25. [http://dx.doi.org/10.1016/S0140-6736\(13\)60993-9](http://dx.doi.org/10.1016/S0140-6736(13)60993-9)
39. Hughes MM, Katz J, Mullany LC, Khatri SK, LeClerq SC, Darmstadt GL, et al. Seasonality of birth outcomes in rural Sarlahi District, Nepal: a population-based prospective cohort. *BMC Pregnancy Childbirth*. 2014;14:310. <http://dx.doi.org/10.1186/1471-2393-14-310>
40. Widmer K, Zhu Y, Williams JV, Griffin MR, Edwards KM, Talbot HK. Rates of hospitalizations for respiratory syncytial virus, human metapneumovirus, and influenza virus in older adults. *J Infect Dis*. 2012;206:56–62. <http://dx.doi.org/10.1093/infdis/jis309>

Address for correspondence: Helen Y. Chu, University of Washington, 325 9th Ave, MS 359779, Harborview Medical Center, Seattle, WA 98104, USA; email: helenchu@u.washington.edu

Global Spread of Norovirus GII.17 Kawasaki 308, 2014–2016

**Martin C.W. Chan, Yunwen Hu, Haili Chen,
Alexander T. Podkolzin, Ekaterina V. Zaytseva,
Jun Komano, Naomi Sakon, Yong Poovorawan,
Sompong Vongpunsawad,
Thanundorn Thanusuwannasak, Joanne Hewitt,
Dawn Croucher, Nikail Collins, Jan Vinjé,
Xiaoli L. Pang, Bonita E. Lee, Miranda de Graaf,
Janko van Beek, Harry Vennema,
Marion P.G. Koopmans, Sandra Niendorf,
Mateja Poljsak-Prijatelj, Andrej Steyer,
Peter A. White, Jennifer H. Lun, Janet Mans,
Tin-Nok Hung, Kirsty Kwok, Kelton Cheung,
Nelson Lee, Paul K.S. Chan**

Analysis of complete capsid sequences of the emerging norovirus GII.17 Kawasaki 308 from 13 countries demonstrated that they originated from a single haplotype since the initial emergence in China in late 2014. Global spread of a sublineage SL2 was identified. A new sublineage SL3 emerged in China in 2016.

Author affiliations: The Chinese University of Hong Kong, Hong Kong, China (M.C.W. Chan, T.-N. Hung, K. Kwok, K. Cheung, N. Lee, P.K.S. Chan); Fudan University, Shanghai, China (Y. Hu, H. Chen); Central Research Institute of Epidemiology, Moscow, Russia (A.T. Podkolzin, E.V. Zaytseva); Nagoya Medical Center, Nagoya, Japan (J. Komano); Osaka Prefectural Institute of Public Health, Osaka, Japan (N. Sakon); Chulalongkorn University, Bangkok, Thailand (Y. Poovorawan, S. Vongpunsawad, T. Thanusuwannasak); The Institute of Environmental Science and Research, Porirua, New Zealand (J. Hewitt, D. Croucher); Centers for Disease Control and Prevention, Atlanta, Georgia, USA (N. Collins, J. Vinjé); University of Alberta, Edmonton, Alberta, Canada (X.L. Pang, B.E. Lee); Alberta Provincial Laboratory for Public Health, Edmonton, Canada (X.L. Pang); Erasmus MC, Rotterdam, the Netherlands (M. de Graaf, J. van Beek, M.P.G. Koopmans); National Institute for Public Health and the Environment, Bilthoven, the Netherlands (J. van Beek, H. Vennema, M.P.G. Koopmans); Robert Koch-Institute, Berlin, Germany (S. Niendorf); University of Ljubljana, Ljubljana, Slovenia (M. Poljsak-Prijatelj, A. Steyer); University of New South Wales, Sydney, New South Wales, Australia (P.A. White, J.H. Lun); University of Pretoria, Pretoria, South Africa (J. Mans)

DOI: <https://doi.org/10.3201/eid2308.161138>

Norovirus infections are a leading cause of acute gastroenteritis worldwide in persons of all age groups. Despite the broad genetic diversity, norovirus GII.4 has predominated during the past 20 years (1). During winter 2014–15, a new norovirus GII genotype 17 variant, known as Kawasaki 308–like 2014 (GII.17 Kawasaki), emerged and became the predominant genotype in Hong Kong, China (2), several major cities of mainland China (3,4), and Japan (5). This variant also was detected sporadically outside of Asia in countries such as Italy, Romania, and the United States (6–8). This new GII.17 Kawasaki variant is distinct from other GII.17 strains, including the co-circulating Kawasaki 323–like strains; it has 2 characteristic amino acid insertions in the most surface-exposed antigenic region of the major capsid viral protein 1 (VP1) (2). These changes have the potential to alter the antigenic properties or the virus–host cell binding preference, raising concern about the global spread of this variant and its replacement of GII.4 variants (9). To study the phylodynamic transmission pattern of norovirus GII.17 Kawasaki, we analyzed full-length VP1 nucleotide sequences collected worldwide during late 2014 through early 2016.

The Study

We chose the region VP1 to analyze because it contained the most hypervariable protruding domain 2 across the norovirus genome and represented most sequences deposited in the public domain. The entire dataset comprised 254 complete VP1 sequences from 13 countries, and all were obtained from samples collected during September 2014–March 2016 (Table). Among them, 129 sequences from 10 countries were determined for this study (online Technical Appendix, <https://wwwnc.cdc.gov/EID/article/23/8/16-1138-Techapp1.pdf>), and the remaining 125 sequences were retrieved from GenBank. These sequences were collected from diverse settings, including outbreaks in healthcare facilities and food-serving sites, sporadic community cases, and hospitalized patients (online Technical Appendix Table 1).

GII.17 Kawasaki viruses were found in 13 countries across 4 continents: Canada, China, Germany, Hungary, Italy, Japan, the Netherlands, New Zealand, Russia, Slovenia, South Korea, Thailand, and the United States. Australia and South Africa reported no GII.17 Kawasaki as of mid-2015 and early 2016, respectively. Maximum-likelihood phylogenetic inference showed different genetic clusters within GII.17 Kawasaki, indicating rapid genetic diversification

Table. Number of complete viral protein 1 nucleotide sequences of norovirus genogroup II genotype 17 Kawasaki analyzed from September 2014 to March 2016, grouped by country, source of sequence, and time of collection*

Region and country	Source of sequence		Year of collection, quarter							Total
	GenBank	This study	2014		2015				2016	
			Q3	Q4	Q1	Q2	Q3	Q4	Q1	
Asia										
China										
Hong Kong	81	45	1	26	67	12		2	18	126
Shanghai	3	8		2	1	1		2	5	11
Other cities	31			3	28					31
Other countries										
Japan	2	13			8		2		5	15
South Korea	5			2	2	1				5
Thailand		7		1			1	5		7
Oceania: New Zealand		6					2	2	2	6
Europe										
Germany		5				1		3	1	5
Hungary	1							1		1
Italy	1				1					1
The Netherlands		5			1	2		2		5
Russia		25			1	2	8	12	2	25
Slovenia		4				1	2		1	4
North America										
Canada		6					1	2	3	6
United States	1	5		1		1	2		2	6
Total	125	129	1	35	109	21	18	31	39	254

*Blank cells indicate 0.

of viral population during spread (Figure 1; online Technical Appendix Figure). Sequences from the same continent scattered into different genetic clusters, inferring multiple introduction and frequent transmission events. To investigate the virus transmission pattern, we constructed a median-joining haplotype network based on complete VP1 nucleotide sequences (online Technical Appendix). Overall, the 254 VP1 sequences comprised 207 different haplotypes (Figure 2). We identified a highly connected basal haplotype (Figure 2) that consisted of 8 identical VP1 sequences collected in the initial phase of the epidemic during November 2014–March 2015 from 6 cities mostly in Asia (2 from Hong Kong; 1 from Shanghai, China; 1 from Guangzhou, China; 1 from Taiwan; 2 from South Korea; and 1 from Russia). The same basal haplotype was concluded using integer neighbor-joining and tight span walker network models. The central node might represent a competent virus haplotype capable of replicating and spreading efficiently among humans and from which nearly all haplotypes originated. We found only 2 nucleotide differences without amino acid change between the basal haplotype and the first case-patient with GII.17 Kawasaki virus in this study (NS-405; collected in September 2014 from Hong Kong) (Figure 2, black arrow). We determined complete genomes that comprised the basal haplotype for this study for the 2 Hong Kong strains and downloaded data for the 2 South Korea strains. These viruses had 4 unique amino acid substitutions distinct from NS-405: 2 in the nonstructural polyprotein (A187D in N terminal protein and N739S in protease) and 2 in VP2 (K58R and A89S; outside of the VP1-interacting domain) (online Technical Appendix

Table 2). Substitution in the protease might mediate changes in the cleavage efficiency of the polyprotein in norovirus replication (10). Although we noted no substitutions in the RNA-dependent RNA polymerase, N terminal protein and VP2 were previously implicated in modulating polymerase activity, virus tropism, and persistence (11,12). The 4 non-VP1 residues may affect viral fitness of the emergent GII.17 Kawasaki in humans; however, functional characterization is required (13).

We identified 3 important sublineages by topology (Figure 2). Viruses belonging to sublineage SL1 (Figure 2, blue shading) clustered closest to the first GII.17 Kawasaki isolate in this study. SL1 included strains from 6 countries outside of China across 3 continents: Thailand (collected in October 2014), United States (November 2014), Italy and the Netherlands (February 2015), Slovenia (August 2015), and Canada (December 2015–January 2016). The global spread of GII.17 Kawasaki viruses within a few months after the initial emergence in China in late 2014 highlights rapid transmissibility of these viruses. Despite the molecular evidence of early global presence of SL1, the apparent limited circulation of this sublineage is intriguing. SL1 was the only sublineage not originating from the basal haplotype but directly from the earliest NS-405. Sequence analysis of the other 2 SL1 complete genomes available, collected from the United States (Hu/GII.17/Gaithersburg/2014/U.S.; GenBank accession no. KR083017) and Taiwan (Hu/GII.17/CGMH70/2015/TW; GenBank accession no. KR154231), found none of the 4 non-VP1 substitutions observed in the basal haplotype. In this dataset, viruses belonging to sublineage SL2 had the

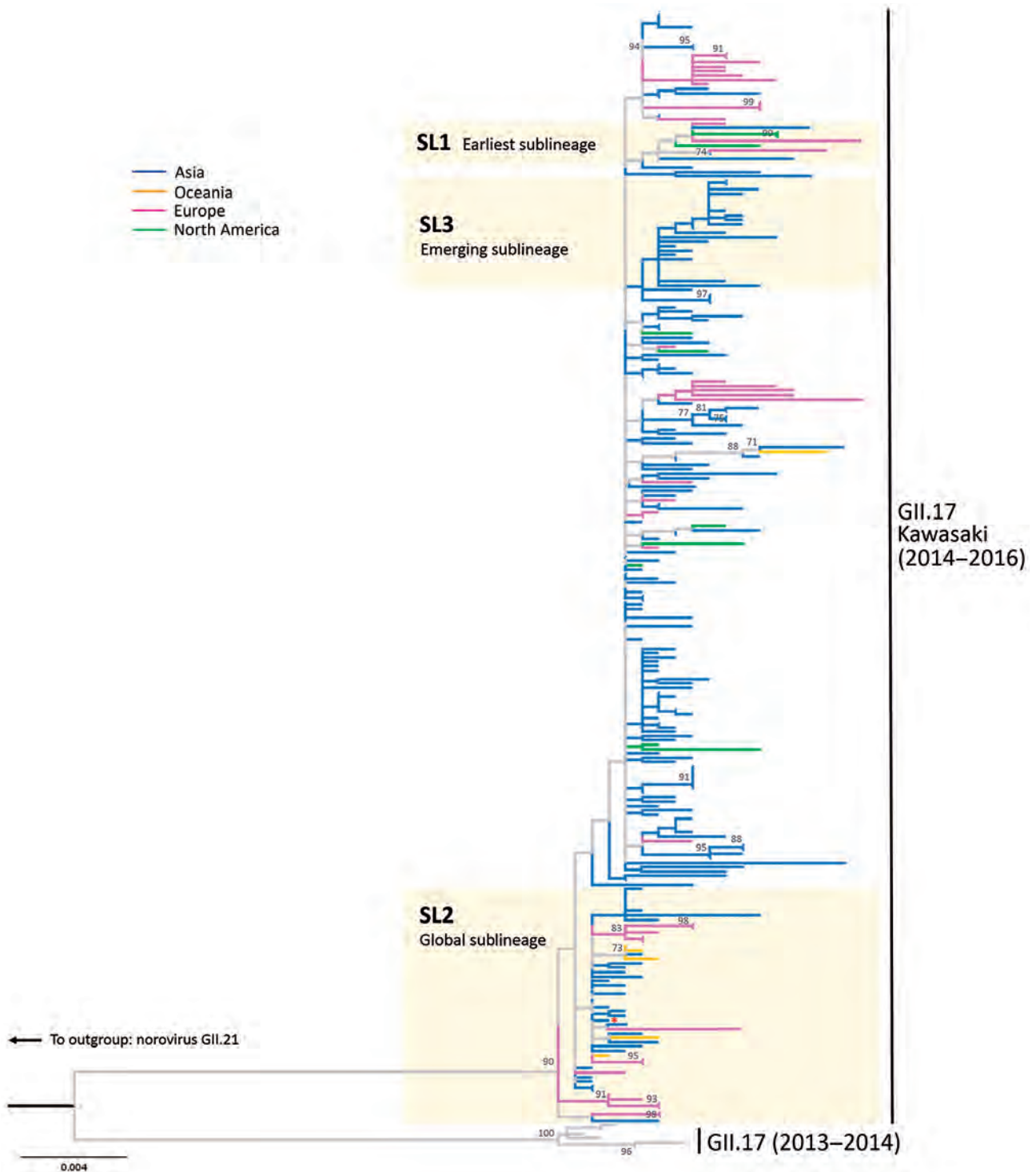


Figure 1. Maximum-likelihood phylogenetic inference of complete viral protein 1 nucleotide sequences of norovirus GII.17 Kawasaki. The tree was constructed using MEGA6 (<http://www.megasoftware.net>) (online Technical Appendix, <https://wwwnc.cdc.gov/EID/article/23/8/16-1138-Techapp1.pdf>). The red asterisk denotes the reference sequence of GII.17 Kawasaki virus (Hu/GII/JP/2015/GII.P17_GII.17/Kawasaki308; GenBank accession no. LC037415). The tree is rooted to genotype GII.21 (not shown for clarity). Bootstrap values ≥ 70 (percentage) are shown at nodes. Sublineages SL1 to SL3 are defined by the topology of haplotype network shown in Figure 2. Branches are colored by the continent of sequence origin. The tree is drawn in scale; scale bar indicates nucleotide substitutions per site.

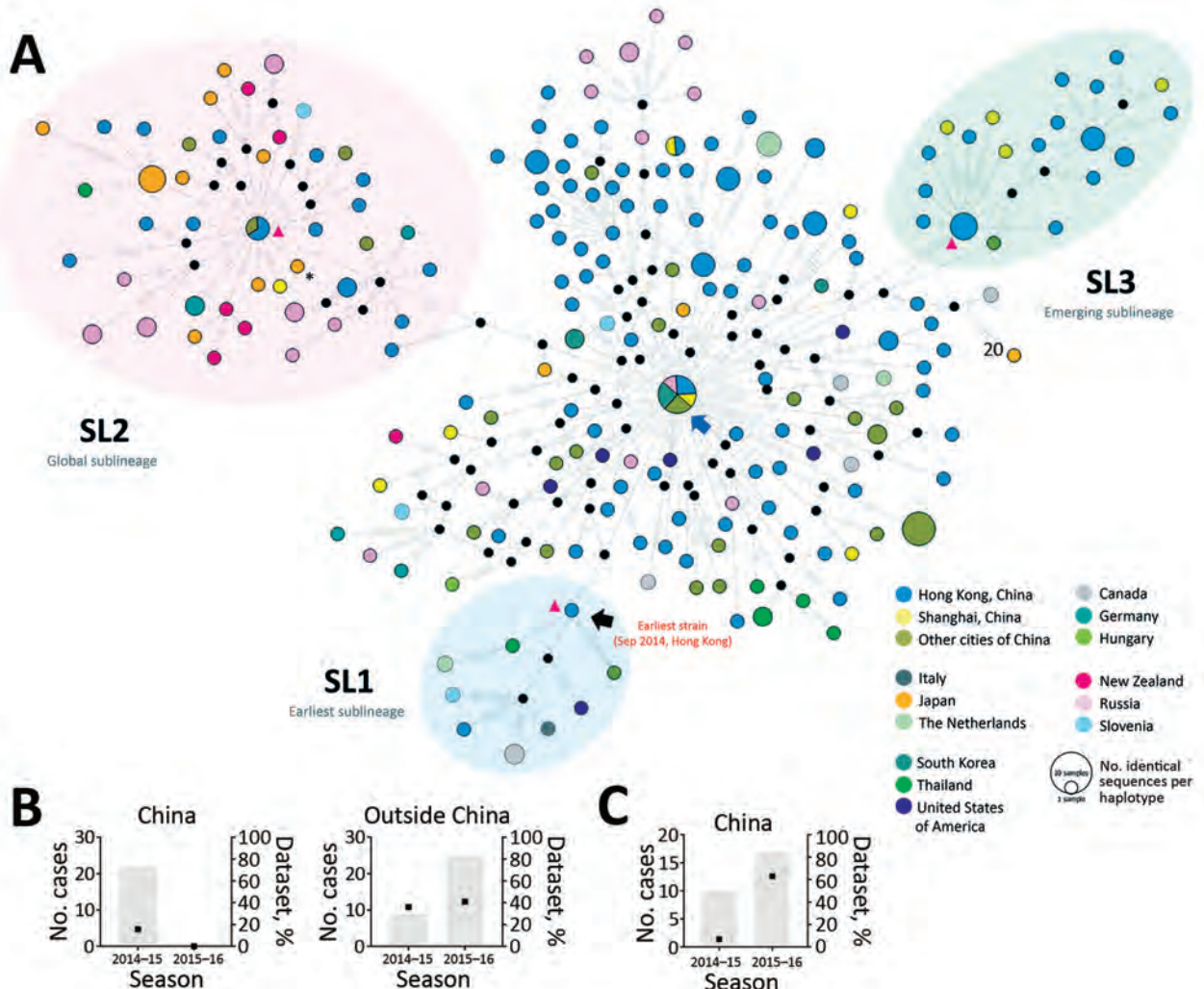


Figure 2. Median-joining haplotype network of 254 complete viral protein 1 nucleotide sequences of norovirus GII.17 Kawasaki. A) Each vertex represents a unique sampled haplotype. Internal black nodes are unsampled intermediate hypothetical haplotypes. Black arrow denotes the first case of norovirus GII.17 Kawasaki in this study (NS-405; collected in September 2014 from Hong Kong). Blue arrow denotes a highly connected basal haplotype from which nearly all haplotypes originated. Vertices are colored by country of collection. Blue shading indicates a sublineage (SL1) genetically closest to the first case of GII.17 Kawasaki virus in this study. Pink shading indicates a sublineage (SL2) with global spread. Green shading indicates an emergent sublineage (SL3) in China in 2016. Vertex size is proportional to the number of sampled sequences sharing the same haplotype. Length of edge is not drawn to scale. Each hatch mark indicates 1 nt difference between connecting haplotypes/nodes. Red triangles represent reference strains of corresponding sublineage (online Technical Appendix Table 1, <https://wwwnc.cdc.gov/EID/article/23/8/16-1138-Techapp1.pdf>). The asterisk denotes the reference sequence of GII.17 Kawasaki virus (Hu/GII/JP/2015/GII.P17_GII.17/Kawasaki308; GenBank accession no. LC037415). Bar charts show the number (gray bars) and percentage (black squares) of cases of sublineages SL2 (B) and SL3 (C) by country in the seasons of 2014–15 (September 2014–June 2015) and 2015–16 (July 2015–March 2016).

most cases and widest geographic breadth (Figure 2, pink shading). SL2 was detected in 6 countries outside of China across 3 continents (Germany, Japan, New Zealand, Russia, Slovenia, and Thailand) and most of the non-China sequences from 2014–15 (36%) and 2015–16 (41%) seasons belonged to this sublineage (Figure 2, inset). The most successful SL2 might have an advantage to global spread, although we cannot rule out sampling bias. During the 2015–16 season, SL2 continued to circulate over

a wide geographic area, although none of the sequences from China belonged to this sublineage. Instead, sublineage SL3, first detected in January 2015 as a minority (7%) in China in the 2014–15 season, became the predominant (63%) circulating GII.17 Kawasaki virus in both southern (Hong Kong) and eastern (Shanghai) parts of China during 2015–16 among sequences analyzed (Figure 2, green shading and inset). No sequences from other countries clustered into SL3. This emerging sublineage highlights that GII.17

Kawasaki viruses were still circulating and, more important, rapidly evolving in various regions of China. Robustness of sublineage topology was confirmed in the phylogenetic tree (Figure 1).

Conclusions

We determined the complete VP1 sequences of 129 GII.17 Kawasaki strains from 10 countries. Our analyses suggest that the new GII.17 Kawasaki originated from a single haplotype from which rapid genetic diversification into multiple sublineages occurred during global spread after the initial emergence in China in late 2014. Norovirus diversification into sublineages provides a preepidemic virus pool from which new pandemic GII.4 variants emerged (14). Although our study is limited by its focus on VP1 sequence analysis and not on virus genomes, it nevertheless is a good demonstration that a global network of norovirus laboratories sharing virus sequence information can delineate virus transmission pattern upon spread.

Acknowledgments

We thank Yuanyuan Qiu and Eloisa Hasing for technical support.

This study was supported in part by the Commissioned Health and Medical Research Fund (Phase 3) of Food and Health Bureau of the Hong Kong Special Administrative Region Government (to M.C.W.C.; reference number CU-15-C2); institutional direct grant for research (to M.C.W.C.; reference number 2015.1.036); Thailand's Research Chair Grant from the National Science and Technology Development Agency (to Y.P.); and European Union H2020 grant COMPARE under grant agreement number 643476. The New Zealand samples were collected for norovirus outbreak surveillance purposes, which is funded by the New Zealand Ministry of Health.

Dr. Martin C.W. Chan is an assistant professor in the Department of Microbiology of the Chinese University of Hong Kong. His research interest focuses on molecular epidemiology and pathogenesis of human noroviruses.

References

1. Pringle K, Lopman B, Vega E, Vinje J, Parashar UD, Hall AJ. Noroviruses: epidemiology, immunity and prospects for prevention. *Future Microbiol.* 2015;10:53–67. <http://dx.doi.org/10.2217/fmb.14.102>
2. Chan MC, Lee N, Hung TN, Kwok K, Cheung K, Tin EK, et al. Rapid emergence and predominance of a broadly recognizing and fast-evolving norovirus GII.17 variant in late 2014. *Nat Commun.* 2015;6:10061. <http://dx.doi.org/10.1038/ncomms10061>
3. Lu J, Sun L, Fang L, Yang F, Mo Y, Lao J, et al. Gastroenteritis outbreaks caused by norovirus GII.17, Guangdong Province, China, 2014–2015. *Emerg Infect Dis.* 2015;21:1240–2. <http://dx.doi.org/10.3201/eid2107.150226>
4. Gao Z, Liu B, Huo D, Yan H, Jia L, Du Y, et al. Increased norovirus activity was associated with a novel norovirus GII.17 variant in Beijing, China during winter 2014–2015. *BMC Infect Dis.* 2015;15:574. <http://dx.doi.org/10.1186/s12879-015-1315-z>
5. Matsushima Y, Ishikawa M, Shimizu T, Komane A, Kasuo S, Shinohara M, et al. Genetic analyses of GII.17 norovirus strains in diarrheal disease outbreaks from December 2014 to March 2015 in Japan reveal a novel polymerase sequence and amino acid substitutions in the capsid region. *Euro Surveill.* 2015;20:21173. <http://dx.doi.org/10.2807/1560-7917.ES2015.20.26.21173>
6. Medici MC, Tummolo F, Calderaro A, Chironna M, Giammanco GM, De Grazia S, et al. Identification of the novel Kawasaki 2014 GII.17 human norovirus strain in Italy, 2015. *Euro Surveill.* 2015;20:30010. <http://dx.doi.org/10.2807/1560-7917.ES.2015.20.35.30010>
7. Dinu S, Nagy M, Negru DG, Popovici ED, Zota L, Opreșan G. Molecular identification of emergent GII.P17–GII.17 norovirus genotype, Romania, 2015. *Euro Surveill.* 2016;21:30141. <http://dx.doi.org/10.2807/1560-7917.ES.2016.21.7.30141>
8. Parra GI, Green KY. Genome of emerging norovirus GII.17, United States, 2014. *Emerg Infect Dis.* 2015;21:1477–9. <http://dx.doi.org/10.3201/eid2108.150652>
9. de Graaf M, van Beek J, Vennema H, Podkolzin AT, Hewitt J, Bucardo F, et al. Emergence of a novel GII.17 norovirus—end of the GII.4 era? *Euro Surveill.* 2015;20:21178. <http://dx.doi.org/10.2807/1560-7917.ES2015.20.26.21178>
10. Hardy ME. Norovirus protein structure and function. *FEMS Microbiol Lett.* 2005;253:1–8. <http://dx.doi.org/10.1016/j.femsle.2005.08.031>
11. Subba-Reddy CV, Goodfellow I, Kao CC. VPg-primed RNA synthesis of norovirus RNA-dependent RNA polymerases by using a novel cell-based assay. *J Virol.* 2011;85:13027–37. <http://dx.doi.org/10.1128/JVI.06191-11>
12. Nice TJ, Strong DW, McCune BT, Pohl CS, Virgin HW. A single-amino-acid change in murine norovirus NS1/2 is sufficient for colonic tropism and persistence. *J Virol.* 2013;87:327–34. <http://dx.doi.org/10.1128/JVI.01864-12>
13. Jones MK, Grau KR, Costantini V, Kolawole AO, de Graaf M, Freiden P, et al. Human norovirus culture in B cells. *Nat Protoc.* 2015;10:1939–47. <http://dx.doi.org/10.1038/nprot.2015.121>
14. Eden JS, Hewitt J, Lim KL, Boni MF, Merif J, Greening G, et al. The emergence and evolution of the novel epidemic norovirus GII.4 variant Sydney 2012. *Virology.* 2014;450–451:106–13. <http://dx.doi.org/10.1016/j.virol.2013.12.005>

Address for correspondence: Paul K.S. Chan, Department of Microbiology, 1/F Lui Che Woo Clinical Sciences Building, Prince of Wales Hospital, Shatin, Hong Kong, China; email: paulkschan@cuhk.edu.hk

Preliminary Epidemiology of Human Infections with Highly Pathogenic Avian Influenza A(H7N9) Virus, China, 2017

Lei Zhou,¹ Yi Tan,¹ Min Kang,¹ Fuqiang Liu,¹ Ruiqi Ren,¹ Yali Wang, Tao Chen, Yiping Yang, Chao Li, Jie Wu, Hengjiao Zhang, Dan Li, Carolyn M. Greene, Suizan Zhou, A. Danielle Iuliano, Fiona Havers, Daxin Ni, Dayan Wang, Zijian Feng, Timothy M. Uyeki, Qun Li

We compared the characteristics of cases of highly pathogenic avian influenza (HPAI) and low pathogenic avian influenza (LPAI) A(H7N9) virus infections in China. HPAI A(H7N9) case-patients were more likely to have had exposure to sick and dead poultry in rural areas and were hospitalized earlier than were LPAI A(H7N9) case-patients.

Since the first human infections with avian influenza A(H7N9) virus were identified in early 2013 (1), mainland China has experienced 5 epidemics of human infections with A(H7N9) virus (2). As of March 31, 2017, a total of 1,336 cases of laboratory-confirmed A(H7N9) virus infections were detected; case-fatality proportion was ≈40%. The fifth epidemic began September 1, 2016, and the number of A(H7N9) virus infection cases has surged since December 2016 (2). Until recently, all human infections were with low pathogenic avian influenza (LPAI) A(H7N9) virus, which causes little or no disease in infected poultry. Risk factors for human infection with LPAI A(H7N9) virus include visiting a live poultry market (LPM) or raising backyard poultry, and mortality is higher among older adults with chronic comorbid conditions (3,4).

On February 18, 2017, the National Health and Family Planning Commission of China reported genetic sequencing results on virus isolates from 2 patients from Guangdong Province who had A(H7N9) virus infection

(initially reported to the Chinese Center for Disease Control and Prevention [China CDC] in January 2017) that were consistent with highly pathogenic avian influenza (HPAI) viruses. Insertions at the hemagglutinin gene cleavage site consistent with HPAI A(H7N9) virus were confirmed by the Chinese National Influenza Center (CNIC) (5). Detection of HPAI A(H7N9) virus in LPMs in Guangdong Province was reported on February 20, 2017 (6). An additional case of HPAI A(H7N9) virus infection was identified in Taiwan in a patient with illness onset in Guangdong Province (5,7,8). To assess whether disease severity in humans has changed with HPAI A(H7N9) compared with LPAI A(H7N9) virus infection, we described the epidemiologic characteristics of cases of HPAI and LPAI A(H7N9) virus infections identified during the current fifth epidemic in mainland China.

The Study

Detection, reporting, and confirmation of HPAI A(H7N9) virus infection was the same as for LPAI A(H7N9) and HPAI A(H5N1) virus infections, as previously described (3,9,10). Since the first case of HPAI A(H7N9) virus infection was identified in 2017, genetic analyses are performed at provincial China CDC laboratories or at CNIC on respiratory specimens collected from all case-patients identified with A(H7N9) virus infection to distinguish between HPAI and LPAI A(H7N9) viruses. Field investigations and data collection protocols for HPAI A(H7N9) cases were the same as for LPAI A(H7N9) cases (3).

We extracted information from field investigation reports and the notifiable infectious surveillance system to describe the demographic, clinical, and epidemiologic characteristics of HPAI A(H7N9) case-patients. We used descriptive statistics to compare HPAI A(H7N9) cases with all LPAI A(H7N9) cases reported throughout mainland China and with LPAI A(H7N9) cases identified in the same provinces as HPAI A(H7N9) cases during the fifth epidemic reported as of March 31, 2017. Collection and analyses of data from human infections with A(H7N9) virus were determined to be part of an ongoing public health investigation of emerging outbreaks and thus were exempt from institutional review board assessment in China (3).

Author affiliations: Chinese Center for Disease Control and Prevention, Beijing, China (L. Zhou, R. Ren, Y. Wang, T. Chen, C. Li, D. Li, D. Ni, D. Wang, Z. Feng, Q. Li); Guangxi Center for Disease Control and Prevention, Nanning, China (Y. Tan, Y. Yang); Guangdong Center for Disease Control and Prevention, Guangzhou, China (M. Kang, J. Wu); Hunan Center for Disease Control and Prevention, Changsha, China (F. Liu, H. Zhang); Centers for Disease Control and Prevention, Atlanta, Georgia, USA (C.M. Greene, S. Zhou, A.D. Iuliano, F. Havers, T.M. Uyeki)

DOI: <https://doi.org/10.3201/eid2308.170640>

¹These authors contributed equally to this article.

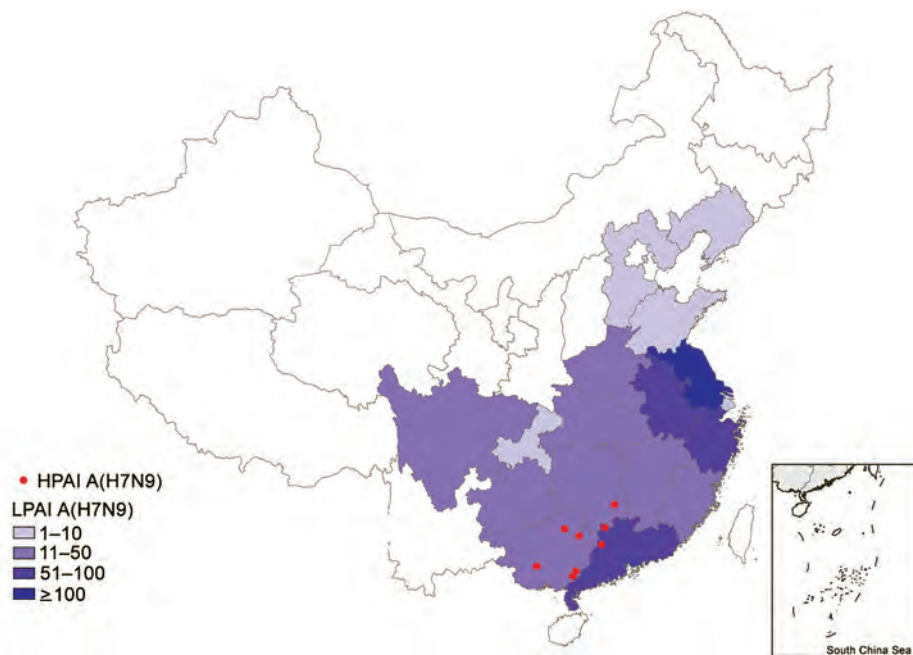


Figure 1. Geographic distribution of human cases of infection with HPAI A(H7N9) virus, China, September 1, 2016–March 31, 2017. The red circles indicate the counties with HPAI A(H7N9) virus infections within Guangxi, Guangdong, and Hunan Provinces during the fifth epidemic. Shading indicates the total numbers of LPAI A(H7N9) virus infections by province during the fifth epidemic. HPAI, highly pathogenic avian influenza; LPAI, low pathogenic avian influenza.

Eight cases of HPAI A(H7N9) virus infection were identified from 3 provinces in southern China (Figure 1). The first 2 case-patients had illness onset on December 30, 2016, and January 5, 2017, in Guangdong Province. Additional case-patients were identified in Hunan and Guangxi Provinces with illness onset during February 2017 (Figure 2). Of the 8 total case-patients, the median age was 57 years (range 28–71 years), and 4 (50%) were male. Most (75%) case-patients lived in rural areas, as defined previously (4), and all were exposed to poultry within 10 days of illness onset. Five case-patients had exposure to backyard poultry, including 4 exposed to sick or dead poultry; 2 had household exposure to poultry purchased from LPMs, including 1 with poultry that were sick and died in the home; and 1 was a poultry worker who sold and slaughtered poultry at an LPM. One cluster of HPAI A(H7N9) cases was identified in 2 adult sisters; 1 sister had household exposure to sick and dead poultry, and the other sister had exposures to sick and dead poultry at her sister's house, to poultry brought inside her home from her sister's house, and to her ill sister while that sister was hospitalized.

All 8 HPAI A(H7N9) case-patients were admitted to hospital a median of 2.5 days (range 0–5 days) after illness onset. All 8 case-patients received oseltamivir treatment a median of 4 days (range 1–8 days) after illness onset; 7 were admitted to an intensive-care unit, and 6 were placed on mechanical ventilation for a median of 5.5 days (range 4–7 days) after illness onset. Four case-patients died a median of 6.5 days (range 5–44 days) after illness onset, and 4 recovered and were discharged home after a median of 29 days (range 21–52 days) (Table).

Compared with all LPAI A(H7N9) case-patients reported during the fifth epidemic, HPAI A(H7N9) case-patients were significantly more likely to live in rural areas (88% vs. 47%; $p = 0.031$), have exposure to sick or dead poultry (50% vs. 16%; $p = 0.037$), and be hospitalized earlier (median 2.5 vs. 5 days; $p = 0.032$) (Table). No significant differences were observed in median age, sex, prevalence of underlying chronic medical conditions, median time from illness onset to starting antiviral treatment, or proportion of patients who received oseltamivir treatment, intensive-care unit admission, or mechanical ventilation (Table). Although the median time from illness onset to death (6.5 vs. 13 days) was shorter and the overall case-fatality proportion (50% vs. 37%) was higher for HPAI A(H7N9) case-patients than for LPAI A(H7N9) case-patients, these differences were not statistically significant (Table). When the analysis was restricted to the 3 provinces with HPAI A(H7N9) cases identified during the fifth epidemic, the only significant difference was a shorter median time from illness onset to death for HPAI A(H7N9) case-patients compared with LPAI A(H7N9) case-patients in Guangxi Province (5 vs. 17 days; $p = 0.0192$).

Conclusions

Our preliminary findings indicate that HPAI A(H7N9) virus infection was associated with exposure to sick and dead backyard poultry in rural areas. In the ongoing fifth epidemic in mainland China, HPAI A(H7N9) case-patients were hospitalized earlier than LPAI A(H7N9) case-patients but otherwise had similar epidemiologic characteristics and disease severity.

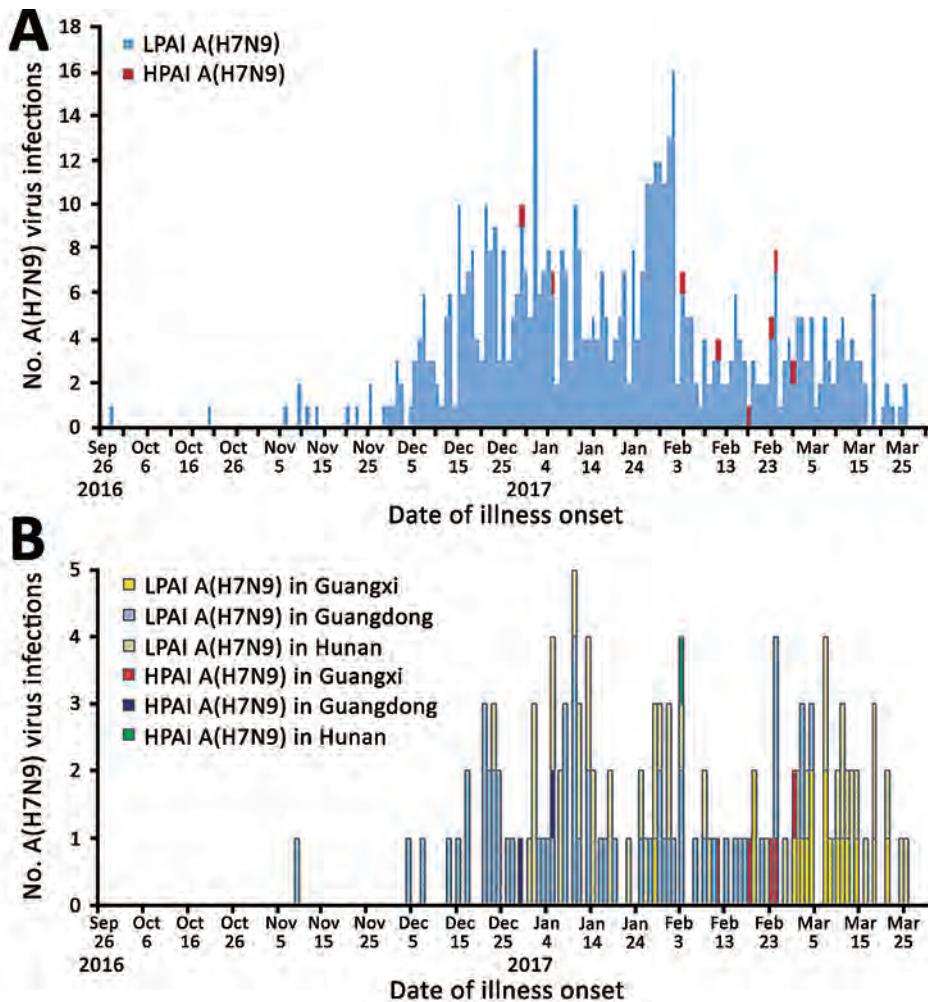


Figure 2. Human infections with HPAI or LPAI A(H7N9) viruses, by illness onset date, China, September 1, 2016–March 31, 2017. A) Dates of illness onset for the 8 HPAI A(H7N9) cases compared with those for all LPAI A(H7N9) cases. B) Dates of illness onset for the 8 HPAI A(H7N9) cases compared with those for LPAI A(H7N9) cases in 3 provinces (Guangxi, Guangdong, and Hunan).

The small number of HPAI A(H7N9) cases limited our statistical power to detect differences in epidemiologic characteristics and disease severity between HPAI and LPAI A(H7N9) case-patients. Data were not available for all variables analyzed, including outcomes for some LPAI A(H7N9) case-patients who remained hospitalized. Our findings might suggest more rapid progression and greater disease severity for HPAI A(H7N9) case-patients, because mortality was higher and the intervals from illness onset to diagnosis and to death were shorter compared with LPAI A(H7N9) case-patients; however, these differences were not significant.

Because A(H7N9) virus circulation among poultry is ongoing in mainland China, extensive efforts are needed to prevent and control the spread of LPAI and HPAI A(H7N9) viruses among poultry, including in rural areas. Avoidance of sick or dead poultry that might be infected with HPAI A(H7N9) virus can reduce transmission of HPAI A(H7N9) virus to humans. Enhanced surveillance of HPAI and LPAI A(H7N9) viruses in poultry and humans, timely virus

characterization, and ongoing assessments of the epidemiology of human infections with A(H7N9) viruses are critical to guide prevention and control efforts and to provide information on the risk of these novel influenza A viruses to public health.

Acknowledgments

We thank staff members in the local and provincial China CDC sites for providing assistance with data collection. We also thank Yuelong Shu and colleagues at CNIC for their contributions to laboratory testing and analyses to confirm HPAI A(H7N9) virus infections.

This work was supported by the Ministry of Science and Technology of China, Emergency Technology Research Issue on Prevention and Control for Human Infection with A(H7N9) Avian Influenza Virus (grant no. KJYJ-2013-01-02), the China–US Collaborative Program on Emerging and Re-emerging Infectious Disease, and National Mega-Projects for Infectious Diseases (grant no. 2014ZX10004002-002-004).

Table. Selected characteristics of case-patients with HPAI and LPAI A(H7N9) virus infections, mainland China, September 1, 2016–March 31, 2017*

Characteristics	Infection type		p value
	HPAI, n = 8	LPAI, n = 553	
Median age (range), y	56.5 (28–71)	57 (3–91)	0.632†
Age group, y			
0–14	0	5/553 (1)	NA
15–59	5 (63)	313/553 (57)	–
≥60	3 (38)	235/553 (42)	–
Sex			
M	4 (50)	400/553 (72)	0.317
F	4 (50)	153/553 (28)	–
Residence area‡			
Urban	1 (13)	193/364 (53)	0.031§
Rural	7 (88)	171/364 (47)	–
Having ≥1 underlying medical conditions¶	5 (63)	234/432 (54)	0.733#
Poultry exposure within 10 d of illness onset			
Any exposure to poultry	8 (100)	442/500 (90)	1.000§
Visited live poultry market	3 (38)	324/442 (73)	NA
Exposure to backyard poultry	4 (50)	98/442 (22)	NA
Occupational exposure to poultry	1 (13)	20/442 (5)	NA
Exposure to sick or dead poultry	4 (50)	43/268 (16)	0.037#
Clinical management			
Hospitalization	8 (100)	478/480 (99)	NA
Antiviral treatment	8 (100)	392/404 (97)	NA
ICU	7 (88)	323/403 (80)	1.000
Mechanical ventilation	6 (75)	221/386 (57)	0.476
Timeline of clinical management (median), d†			
Illness onset to first medical service seeking	0.5 (0–5)	2 (0–34)	0.096
Illness onset to hospitalization	2.5 (0–5)	5 (0–35)	0.032
Illness onset to antiviral treatment	4 (1–8)	6 (0–29)	0.168
Illness onset to diagnosis	6.5 (4–9)	8 (0–31)	0.241
Illness onset to death	6.5 (5–44)	13 (2–62)	0.180
Outcome			
Death	4 (50)	203/376 (54)	1.000
Recovered and discharged	4 (50)	173/376 (46)	–

*Values are no. (%) unless otherwise indicated. The χ^2 test was used to compare the variables between HPAI and LPAI groups. Data were missing for some variables, and data on final outcomes were missing for case-patients with LPAI A(H7N9) virus infection who remained hospitalized as of March 31, 2017. We were not able to perform the statistical analyses to assess differences for some variables because the number of cells with expected frequency of <5 was >20% and some cells had expected frequency of <1. HPAI, highly pathogenic avian influenza; ICU, intensive-care unit; LPAI, low pathogenic avian influenza; NA, not available.

†The z-test was used to compare median age and median days of the timeline of clinical management between HPAI and LPAI groups.

‡Urban was defined as cities, towns, and suburbs; rural was defined as villages and countryside (3).

§Residence area and “any exposure to poultry” were compared between HPAI and LPAI groups by using the Fisher exact test.

¶Three HPAI case-patients had chronic cardiovascular disease, and 2 HPAI case-patients had chronic metabolic disease.

#“Having ≥1 underlying medical conditions” and “exposure to sick or dead poultry” were compared between HPAI and LPAI groups by using the χ^2 test for continuous correction.

L.Z., T.M.U., and Q.L. conceived, designed, and supervised the study; A.D.I. and F.H. helped with study conception and design; Y.T., M.K., F.Q.L., R.Q.R., Y.L.W., Y.P.Y., C.L., J.W., H.J.Z., and D.L. assisted in data collection; T.C. and D.Y.W. assisted in specimens collection and laboratory testing; L.Z. and R.Q.R. analyzed the data; L.Z. and T.M.U. finalized the analysis; L.Z. wrote the draft of the manuscript; T.M.U., C.M.G., S.Z.Z., F.H., A.D.I., D.X.N., Z.J.F., and Q.L. helped interpret the findings; T.M.U., C.M.G., S.Z.Z., F.H., and A.D.I. commented on and helped revise drafts of the manuscript. L.Z. is guarantor.

Dr. Zhou is the Deputy Chief of the Branch for Emerging Infectious Diseases, Public Health Emergency Center, China CDC. Her research interests are prevention and control of emerging infectious diseases as well as pandemic influenza preparedness and response.

References

- Gao R, Cao B, Hu Y, Feng Z, Wang D, Hu W, et al. Human infection with a novel avian-origin influenza A (H7N9) virus. *N Engl J Med.* 2013;368:1888–97. <http://dx.doi.org/10.1056/NEJMoa1304459>
- Iuliano AD, Jang Y, Jones J, Davis CT, Wentworth DE, Uyeki TM, et al. Increase in human infections with avian influenza A(H7N9) virus during the fifth epidemic—China, October 2016–February 2017. *MMWR Morb Mortal Wkly Rep.* 2017;66:254–5. <http://dx.doi.org/10.15585/mmwr.mm6609e2>
- Li Q, Zhou L, Zhou M, Chen Z, Li F, Wu H, et al. Epidemiology of human infections with avian influenza A(H7N9) virus in China. *N Engl J Med.* 2014;370:520–32. <http://dx.doi.org/10.1056/NEJMoa1304617>
- Zhou L, Ren R, Ou J, Kang M, Wang X, Havers F, et al. Risk Factors for influenza A(H7N9) disease in China, a matched case control study, October 2014 to April 2015. *Open Forum Infect Dis.* 2016;3:ofw182. <http://dx.doi.org/10.1093/ofid/ofw182>
- World Health Organization. Human infection with avian influenza A(H7N9) virus—China. *Disease outbreak news*, 27 February 2017

- [cited 2017 May 16]. <http://www.who.int/csr/don/27-february-2017-ah7n9-china/en>
6. World Organisation for Animal Health (OIE). OIE report of HPAI H7N9 virus infection in poultry, Guangdong Province, China, February 20, 2017 [cited 2017 May 16]. http://www.oie.int/wahis_2/temp/reports/en_imm_0000022933_20170221_163854.pdf
 7. World Health Organization. Human infection with avian influenza A(H7N9) virus—China. Disease outbreak news, 22 February 2017 [cited 2017 May 16]. <http://www.who.int/csr/don/22-february-2017-ah7n9-china/en>
 8. Yang JR, Liu MT. Human infection caused by an avian influenza A (H7N9) virus with a polybasic cleavage site in Taiwan, 2017. *J Formos Med Assoc.* 2017;116:210–2. <http://dx.doi.org/10.1016/j.jfma.2017.02.011>
 9. Xu C, Havers F, Wang L, Chen T, Shi J, Wang D, et al. Monitoring avian influenza A(H7N9) virus through national influenza-like illness surveillance, China. *Emerg Infect Dis.* 2013;19:1289–92. <http://dx.doi.org/10.3201/eid1907.130662>
 10. Yu H, Gao Z, Feng Z, Shu Y, Xiang N, Zhou L, et al. Clinical characteristics of 26 human cases of highly pathogenic avian influenza A (H5N1) virus infection in China. *PLoS One.* 2008;3:e2985. <http://dx.doi.org/10.1371/journal.pone.0002985>

Address for correspondence: Qun Li, Public Health Emergency Center, Chinese Center for Disease Control and Prevention, Beijing, 102206, China; email: liqun@chinacdc.cn

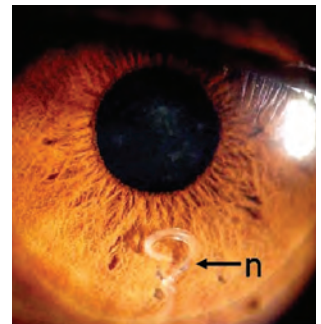
May 2011: Vectorborne Infections

- Intravenous Artesunate for Severe Malaria in Travelers, Europe
- Lessons Learned about Pneumonic Plague Diagnosis, Democratic Republic of the Congo
- Evolution of New Genotype of West Nile Virus in North America

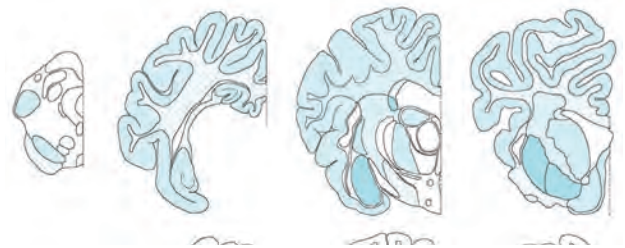


- Transstadial Transmission of *Francisella tularensis holarctica* in Mosquitoes, Sweden
- Molecular Epidemiology of Oropouche Virus, Brazil
- Severe Imported *Plasmodium falciparum* Malaria, France, 1996–2003
- *Plasmodium knowlesi* Malaria in Children, Malaysia
- Travel-related Dengue Virus Infection, the Netherlands, 2006–2007
- Experimental Infection of *Amblyomma aureolatum* Ticks with *Rickettsia rickettsii*
- Genotypic Profile of *Streptococcus suis* Serotype 2 and Clinical Features of Infection in Humans, Thailand
- Babesiosis in Lower Hudson Valley, New York, USA
- Experimental Oral Transmission of Atypical Scrapie to Sheep

- Evidence of Tungiasis in Pre-Hispanic America
- Human Intraocular Filariasis Caused by *Dirofilaria* sp. Nematode, Brazil
- Human Intraocular Filariasis Caused by *Pelecitus* sp. Nematode, Brazil



- *Linguatula serrata* Tongue Worm in Human Eye, Austria
- *Rickettsia rickettsii* Transmission by a Lone Star Tick, North Carolina
- Tick-Borne Encephalitis Virus, Kyrgyzstan
- Probable Non-Vector-borne Transmission of Zika Virus, Colorado, USA
- Tick-Borne Relapsing Fever Borreliosis, Rural Senegal
- Novel Bluetongue Virus Serotype, Kuwait
- Spotted Fever Group Rickettsiae in Ticks, Germany
- *Bartonella* spp. in Feral Pigs, Southeastern United States



**EMERGING
INFECTIOUS DISEASES**

<https://wwwnc.cdc.gov/eid/articles/issue/17/5/table-of-contents>

Real-Time Evolution of Zika Virus Disease Outbreak, Roatán, Honduras

**Trevor Brooks, Arup Roy-Burman,
Cascade Tuholske, Michael P. Busch,
Sonia Bakkour, Mars Stone, Jeffrey M. Linnen,
Kui Gao, Jayleen Coleman, Evan M. Bloch**

A Zika virus disease outbreak occurred in Roatán, Honduras, during September 2015–July 2016. Blood samples and clinical information were obtained from 183 patients given a clinical diagnosis of suspected dengue virus infection. A total of 79 patients were positive for Zika virus, 13 for chikungunya virus, and 6 for dengue virus.

Zika virus is a mosquito-borne flavivirus that is clinically nonspecific and associated with severe congenital injury (1–5). Zika virus is closely related to dengue virus (DENV), which is endemic to Roatán, the largest Honduran Bay island (population ≈46,000 persons), located 50 km north of the Honduras mainland (6). However, most cases of DENV infection are diagnosed clinically because of limited capacity for laboratory confirmation.

We initiated a pilot study in 2015 to correlate clinical (signs and symptoms) and laboratory diagnostic findings for cases of presumptive dengue. As of September 2015, Zika virus had not been identified in Roatán. We report emergence of Zika virus on Roatán.

The Study

We conducted a cross-sectional survey of patients who came to Public Hospital Roatán during September 2015–July 2016 and were given a clinical diagnosis of suspected dengue fever. This hospital, the only public hospital in Roatán, has 58 inpatient beds. Approximately 90% of dengue cases on Roatán are diagnosed at this hospital; most case-patients came to the emergency department, which had 18,578 visits in 2015 (Public Hospital Roatán Internal Statistics, unpub. data).

Author affiliations: University of California School of Medicine, San Francisco, California, USA (T. Brooks, A. Roy-Burman, M.P. Busch); University of California, Santa Barbara, California, USA (C. Tuholske); Blood Systems Research Institute, San Francisco (M.P. Busch, S. Bakkour, M. Stone, E.M. Bloch); Hologic Inc., San Diego, California, USA (J.M. Linnen, K. Gao); Public Hospital Roatán, Coxen Hole, Honduras (J. Coleman); Johns Hopkins School of Medicine, Baltimore, Maryland, USA (E.M. Bloch)

DOI: <https://doi.org/10.3201/eid2308.161944>

We used a convenience sampling approach. All patients >2 years of age given a diagnosis of clinically suspected DENV infection at the hospital during the enrollment period were eligible. Suspected DENV infection was diagnosed by using criteria of the Honduran Ministry of Health, which are fever plus 2 of the following: nausea/vomiting, rash, headache/retroorbital pain, myalgias/arthralgias, petechiae/positive tourniquet test result, leukopenia, and bleeding.

Patients were enrolled after we obtained informed consent; minors were enrolled only after we obtained parental permission. Ethical approval was granted by institutional review boards of the University of California, San Francisco, and Universidad Nacional Autónoma de Honduras. Enrollment of participants and blood collection were restricted to workday hours (8:00 AM–4:00 PM) Monday through Friday. Patients underwent a phlebotomy and completed a clinical questionnaire, administered verbally in English or Spanish that addressed demographics, migration history, employment, medical history, and symptoms and signs of arbovirus infection.

Samples of whole blood (5–9 mL) were collected in EDTA-treated vacutainers (BD Diagnostics, Franklin Lakes, NJ, USA) within 1 h of diagnosis. Samples were centrifuged (35,000 rpm), which yielded sufficient plasma to prepare 5 equal aliquots (minimum 0.5 mL/aliquot). Aliquots were labeled with patient identification numbers and stored frozen at –30°C pending testing.

In July 2016, samples were shipped on dry ice to Blood Systems Research Institute (San Francisco, CA, USA) where initial testing was performed by using the Trioplex Assay (Centers for Disease Control and Prevention, Atlanta, GA, USA) for detection of DENV, chikungunya virus (CHIKV), and Zika virus RNA. RNA was extracted from 140 µL of plasma and eluted in 60 µL of buffer (QIAamp Viral RNA Mini Kit; QIAGEN, Valencia, CA, USA).

Multiplex real-time reverse transcription PCR (RT-PCR) was performed using the SuperScript III Platinum One-Step qRT-PCR Kit (ThermoFisher Scientific, Pittsburgh, PA, USA) with DENV, CHIKV, and Zika virus primers and probes developed at the Centers for Disease Control and Prevention. Each duplicate reaction contained 10 µL of sample RNA in a reaction volume of 25 µL. Samples were tested in a 96-well format in a real-time instrument (LightCycler 480 System; Roche, Basel, Switzerland). Results were considered positive if the cycle threshold was <38.

A more sensitive Zika virus–only test based on transcription-mediated amplification (Aptima Zika Virus Assay; Hologic Inc., San Diego, CA, USA), which processed 0.5-mL plasma into each amplification reaction, was performed in parallel for all samples to confirm Zika virus infections detected by the Trioplex Assay and detect low levels of Zika virus RNA (7). The Aptima Assay was used for further analysis.

At conclusion of study enrollment, addresses of participants were mapped by using a hand-held eTrex 20 (Garmin, Lenexa, KS, USA), which generated global positioning system coordinates for their homes. The survey, laboratory test data, and global positioning system coordinates were uploaded into ArcGIS version 10.3.1 software (Esri, Inc., Redlands, CA, USA). All potential predictors of Zika virus infection were analyzed by using univariate logistic regression models in Stata version 13 (StataCorp LLC, College Station, TX, USA). Characteristics that were significant ($p = 0.10$) by univariate analysis were entered into a multivariable logistic regression model.

A total of 183 patients participated and provided blood samples (Table 1). Most (60%) patients were women. Mean age was 26 (interquartile range 19–37 years). Mean time to seeking treatment after onset of signs or symptoms was 3.2 days. The most commonly reported signs or symptoms were headache (90%), arthralgia (89%), myalgia (87%),

retroorbital pain (71%), and rash (55%). Most patients lived in homes that had a nondirt floor (93%), running water (81%), and electricity (90%). Only 25% reported having mosquito nets over their beds. Six (3%) of 183 patients were positive for DENV RNA, and 13 (75%) were positive for CHIKV RNA. In contrast, Zika virus RNA was detectable in 66 (36%) of 183 patients by the Trioplex assay and in 79 (43%) of 183 patients by the Aptima assay.

The enrollment rate was low through the first part of the study, when ≤ 3 case-patients/wk were enrolled (Figure 1). In the first week of February 2016, eight case-patients were enrolled, followed by 26 case-patients the following week. The first case of laboratory-confirmed Zika virus infection on Roatán occurred on January 27, 2016; Zika virus infection peaked (16 cases) during February 8–14. Timing of accrual of positive case-patients matched expected seasonality of arbovirus infection. Cases decreased steadily through the remainder of the sample collection period.

The Zika virus outbreak was focused in the major population centers in Coxen Hole, Los Fuertes, and French Harbor (Figure 2). Except for West Bay and West End, cases were widely distributed on the island. West Bay and West End are major tourist centers on Roatán; absence of cases might be ascribed to tourists and expatriates who were unlikely to seek medical attention at Public Hospital Roatán.

Table 1. Demographic characteristics of persons with suspected Zika virus infections, Roatán, Honduras, September 2015–July 2016*

Characteristic	Total, n = 183	Zika virus infection, n = 79	No Zika virus infection, n = 104
Age, y	26 (19–37)	27 (21–38)	24 (17–35)
Sex			
M	73 (39.9)	28 (35.4)	45 (43.3)
F	110 (60.1)	51 (64.6)	59 (56.7)
Living conditions			
Dirt floor	12 (6.6)	4 (5.1)	8 (7.7)
Running water	149 (81.4)	71 (89.9)	78 (75.0)
Electricity	165 (90.2)	75 (94.9)	90 (86.5)
Mosquito nets over beds	46 (25.1)	22 (27.8)	24 (23.1)
Rooms	2 (1–2)	2 (1–3)	2 (1–2)
Persons in household	4 (3–5.5)	4 (3–5)	4 (3–6)
Sign or symptoms			
Headache	165 (90.2)	75 (94.9)	90 (86.5)
Muscle aches	159 (86.9)	67 (84.8)	92 (88.5)
Joint ache	162 (88.5)	71 (89.9)	91 (87.5)
Eye pain	131 (71.6)	61 (77.2)	70 (67.3)
Rash	102 (55.7)	73 (92.4)	29 (27.9)
Bleeding	1 (0.5)	0	1 (1.0)
Vomiting	49 (26.8)	11 (13.9)	38 (36.5)
Petechiae	5 (2.7)	2 (2.5)	3 (2.9)
Epistaxis	1 (0.5)	0	1 (1.0)
Gingivitis	3 (1.6)	1 (1.3)	2 (1.9)
Other	123 (67.2)	53 (67.1)	70 (67.3)
Body temperature, °C, mean (SD)	37.8 (1.1)	37.3 (0.9)	38.1 (1.1)
Days between symptom onset and seeking treatment	3 (1–4)	3 (1–4.5)	2 (2–4)
History of infectious diseases			
Dengue	45 (24.6)	21 (26.6)	24 (23.1)
Malaria	33 (18.0)	18 (22.8)	15 (14.4)
Chikungunya	61 (33.3)	28 (35.4)	33 (31.7)

*Values are median (IQR) or no. (%) unless indicated otherwise. IQR, interquartile range.

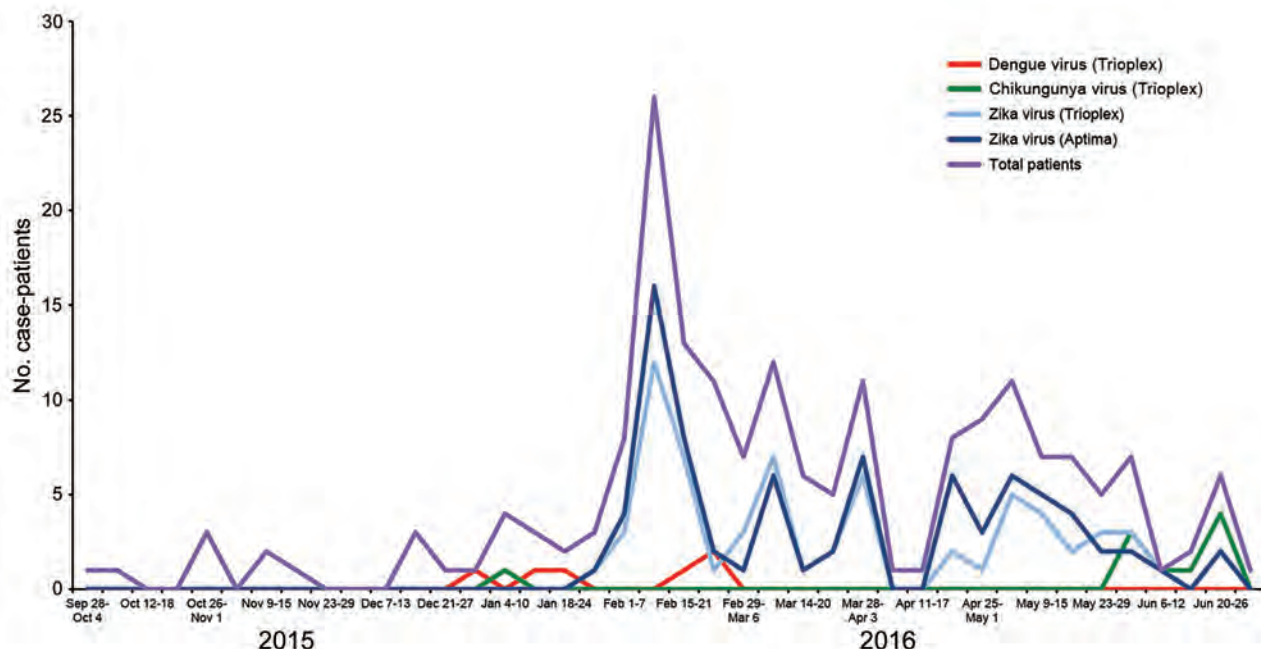


Figure 1. Weekly case occurrence of Zika virus, dengue virus, and chikungunya virus infections, by testing type, Roatán, Honduras, September 2015–July 2016. Aptima, Aptima Zika Virus Assay (Hologic Inc., San Diego, CA, USA); Trioplex, Trioplex Assay (Centers for Disease Control and Prevention, Atlanta, GA, USA).

Multivariable analysis showed that rash (odds ratio [OR] 30.6, 95% CI 10.8–86.9) and headache (OR 11.2, 95% CI 2.7–46.7) were independently associated with Zika virus infection. Fever (OR 0.44, 95% CI 0.26–0.74) and vomiting (OR 0.25, 95% CI 0.08–0.73) were associated with a decreased risk for Zika virus infection (Table 2).

This study had limitations. Our exclusive enrollment of patients who came to Public Hospital Roatán excluded patients who came to other healthcare facilities or outside daytime working hours who were not sufficiently symptomatic to seek care. Alternative body fluids (e.g., saliva, urine, whole blood) were not available for testing, and serologic testing for Zika virus was not performed because of cost constraints and cross-reactivity between Zika virus and DENV antibodies. We did not perform confirmatory testing of CHIKV- and

DENV-positive samples. This study could be biased for detecting Zika virus and not DENV/CHIKV because of use of a more sensitive assay.

Conclusions

We demonstrated the evolution of the Zika virus disease outbreak in Roatán, Honduras, in early 2016. Findings highlight challenges in case ascertainment based only on clinical diagnosis. In the absence of laboratory confirmation, clinical diagnosis has low specificity because of overlap of signs and symptoms between infections with Zika virus, DENV, CHIKV, and a host of other regionally endemic infections. Enrollment was contingent upon a suspected diagnosis of dengue. However, DENV was detected in <5% of case-patients, whereas 43% of case-patients had acute Zika virus infections.

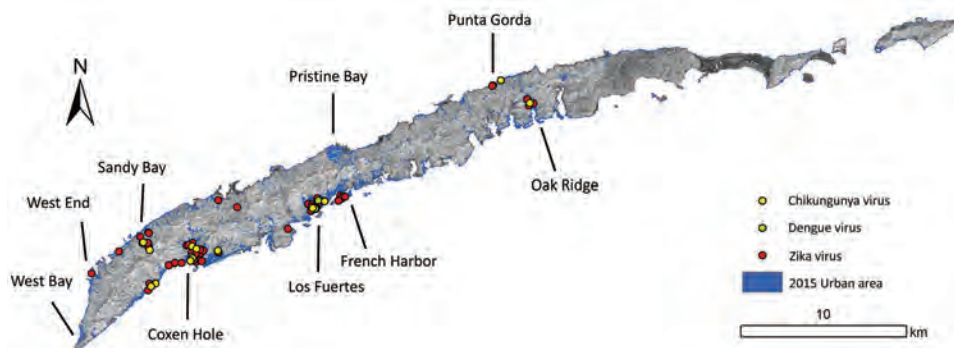


Figure 2. Spatial distribution of confirmed cases of infection with Zika virus, dengue virus, and chikungunya virus, Roatán, Honduras, September 2015–July 2016.

Table 2. Logistic regression analysis of predictors for Zika virus infection, Roatán, Honduras, September 2015–July 2016

Characteristic	Univariate logistic regression		Multivariable logistic regression	
	Odds ratio (95% CI)	p value	Odds ratio (95% CI)	p value
Household				
Running water	2.96 (1.26–6.96)	0.01	2.93 (0.78–11.1)	0.11
Electricity	2.92 (0.92–9.24)	0.07	2.36 (0.39–14.3)	0.35
Sign or symptom				
Headache	2.92 (0.92–9.24)	0.07	11.20 (2.70–46.7)	0.001
Rash	31.5 (12.3–80.2)	<0.0001	30.6 (10.8–86.9)	<0.0001
Vomiting	0.28 (0.13–0.60)	0.001	0.25 (0.08–0.73)	0.01
Fever	0.38 (0.25–0.57)	<0.0001	0.44 (0.26–0.74)	0.002

After a rapid peak in early February 2016, there was a slow decrease in reported cases through July 2016, when enrollment concluded. Access to laboratory testing remains a barrier to surveillance and clinical management in low-resource countries where Zika virus disease outbreaks are predominantly focused, but laboratory infrastructure is lacking (2).

Acknowledgments

We thank Martha Medina and staff at the Public Hospital Roatán for support, Omar Brito and Fermin Lopez for approving and supporting the study, Liz Vinelli for kindly facilitating logistical oversight, Eva Harris for providing mentorship and input on the initial study, and the US Geological Survey for providing Landsat imagery.

This study was supported by a Doris Duke International Clinical Research Fellowship, the Broom Center for Demography, and the National Center for Advancing Translational Sciences, National Institutes of Health (grant UL1 TR000004).

Mr. Brooks is a fourth-year medical student at the University of California School of Medicine, San Francisco, CA. His research interests are global health and infectious diseases.

References

1. World Health Organization. Zika situation report. September, 29, 2016 [cited 2017 Apr 20]. <http://www.who.int/emergencies/zika-virus/situation-report/29-september-2016/en/>
2. Plourde AR, Bloch EM. A literature review of Zika virus. *Emerg Infect Dis.* 2016;22:1185–92. <http://dx.doi.org/10.3201/eid2207.151990>
3. Hayes EB. Zika virus outside Africa. *Emerg Infect Dis.* 2009;15:1347–50. PubMed <http://dx.doi.org/10.3201/eid1509.090442>
4. Duffy MR, Chen TH, Hancock WT, Powers AM, Kool JL, Lanciotti RS, et al. Zika virus outbreak on Yap Island, Federated States of Micronesia. *N Engl J Med.* 2009;360:2536–43. <http://dx.doi.org/10.1056/NEJMoa0805715>
5. Hennessey M, Fischer M, Staples JE. Zika virus spreads to new areas—region of the Americas, May 2015–January 2016. *MMWR Morb Mortal Wkly Rep.* 2016;65:55–8. <http://dx.doi.org/10.15585/mmwr.mm6503e1>
6. National Statistics Institute. Census of population and housing, 2013. October 22, 2015. Tegucigalpa [in Spanish] [cited 2017 Apr 20]. <http://www.ine.gov.hn/index.php/component/content/article?id=102>
7. Stone M, Lanteri MC, Bakkour S, Deng X, Galel SA, Linnen JM, et al. Relative analytical sensitivity of donor nucleic acid amplification technology screening and diagnostic real-time polymerase chain reaction assays for detection of Zika virus RNA. *Transfusion.* 2017;57:734–47. <http://dx.doi.org/10.1111/trf.14031>

Address for correspondence: Trevor Brooks, University of California School of Medicine, 505 Parnassus Ave, San Francisco, CA 94143-0410, USA; email: trevor.brooks@ucsf.edu

EID Adds Advanced Search Features for Articles

Emerging Infectious Diseases now has an advanced search feature that makes it easier to find articles by using keywords, names of authors, and specified date ranges. You can sort and refine search results by manuscript number, volume or issue number, or article type. A quick start guide and expandable help section show you how to optimize your searches.

<https://wwwnc.cdc.gov/eid/AdvancedSearch>

EID's new mapping feature allows you to search for articles from specific countries by using a map or table to locate countries. You can refine search results by article type, volume and issue, and date, and bookmark your search results.

<https://wwwnc.cdc.gov/eid/ArticleMap>



Clonal Expansion of New Penicillin-Resistant Clade of *Neisseria meningitidis* Serogroup W Clonal Complex 11, Australia

Shakeel Mowlaboccus, Keith A. Jolley,
James E. Bray, Stanley Pang, Yung Thin Lee,
Jane D. Bew, David J. Speers, Anthony D. Keil,
Geoffrey W. Coombs, Charlene M. Kahler

In Western Australia, *Neisseria meningitidis* serogroup W clonal complex 11 became the predominant cause of invasive meningococcal disease in 2016. We used core-genome analysis to show emergence of a penicillin-resistant clade that had the *penA_253* allele. This new penicillin-resistant clade might affect treatment regimens for this disease.

Invasive meningococcal disease (IMD) is caused by a meningococcus, *Neisseria meningitidis*. The main manifestations of this disease are septicemia or meningitis. Meningococcal strains can be classified into 12 serogroups phenotypically and into sequence types (STs) by multilocus sequence typing (1). Similar STs are grouped into the same clonal complex (cc). IMD is most commonly caused by isolates expressing a serogroup A, B, C, W, X, or Y polysaccharide capsule. Until recently, serogroup A was the major cause of disease in Africa (2). Serogroups B, C, and Y continue to predominate in the United States, Europe, Asia, and Australia (3,4).

In Australia, after introduction of serogroup C conjugate vaccine in the national immunization program in 2003, incidence of serogroup C has decreased; serogroup B predominated during 2004–2015. However, during 2016, the prevalence of serogroup W disease increased because of *N. meningitidis* strains in the cc11 lineage (MenW:cc11) (5,6), which have also been reported worldwide. Although extensive core-genome analyses of these MenW:cc11 strains have been reported (7,8), antimicrobial drug susceptibility of these clinical isolates has not been generally reported.

Author affiliations: University of Western Australia, Perth, Western Australia, Australia (S. Mowlaboccus, D.J. Speers, C.M. Kahler); University of Oxford, Oxford, UK (K.A. Jolley, J.E. Bray); Murdoch University, Murdoch, Western Australia, Australia (S. Pang, Y.T. Lee, G.W. Coombs); Fiona Stanley Hospital, Perth (S. Pang, G.W. Coombs); Queen Elizabeth II Medical Centre, Perth (J.D. Bew, D.J. Speers); Princess Margaret Hospital for Children, Perth (A.D. Keil); Telethon Kids Institute, Perth (C.M. Kahler)

DOI: <https://doi.org/10.3201/eid2308.170259>

Although penicillin has been used for control of IMD, clinical isolates relatively resistant to this drug have been reported worldwide. For meningococci, a penicillin MIC >2 mg/L is caused by plasmid-mediated β -lactamase production but is extremely rare (9). Conversely, isolates conferring intermediate resistance to penicillin (MIC 0.12–0.25 mg/L) are uncommon but the frequency of these isolates varies geographically. The mechanism of relative resistance in these isolates involves expression of altered forms of 1 of 4 penicillin-binding proteins (PBPs) that are involved in peptidoglycan biosynthesis during bacterial growth and cell division (10).

Although treatment with penicillin is still effective against these penicillin-intermediate strains, low-dose treatment regimens may fail for cases involving penicillin-resistant isolates (MIC ≥ 0.5 mg/L) (11). We report recent emergence and clonal expansion of a phylogenetically related cluster of penicillin-resistant MenW:cc11 isolates in Western Australia.

The Study

Western Australia is the largest state in Australia (land area 1.02 million square miles). However, it has a population of only 2.5 million persons. In concordance with the national trend, there has been a shift in the predominant serogroup in Western Australia; MenW was responsible for most IMD cases in 2016. The first laboratory-confirmed MenW:cc11 case in Western Australia was recorded in April 2013 and was the only MenW case for that year. Since that time, an additional 18 MenW:cc11 laboratory-confirmed cases have been reported, representing 11% ($n = 2$) of all IMD cases in 2014, 27% ($n = 3$) in 2015, and 67% ($n = 13$) in 2016, a significant increase from 2014 through 2016 ($p = 0.0004$, by Fisher exact test). Three deaths were caused by MenW:cc11 infection, 1 in 2015 and 2 in 2016.

The 19 MenW:cc11 strains isolated during January 1, 2013–December 31, 2016, were assessed for susceptibility to penicillin, ciprofloxacin, ceftriaxone, and rifampin. We performed drug susceptibility testing by using the Etest (bioMérieux, Marcy l’Etoile, France). MIC results were interpreted according to Clinical Laboratory Standard Institute (<http://clsi.org>) breakpoints. All isolates were susceptible to ciprofloxacin (MIC ≤ 0.03 mg/L), ceftriaxone (≤ 0.12 mg/L), and rifampin (≤ 0.5 mg/L). However, variation in

penicillin susceptibility was observed: 8 were susceptible (≤ 0.06 mg/L), 2 were less susceptible (0.12–0.25 mg/L), and 9 were resistant (≥ 0.5 mg/L). All isolates less susceptible to or resistant to penicillin were identified in 2016.

We further characterized isolates by using whole-genome sequencing with the Miseq Platform (Illumina, San Diego, CA, USA). Raw reads were assembled, auto-tagged, and curated by using the BIGSdb genomics platform on the PubMLST website (<http://pubmlst.org/neisseria>) (12). Four STs, all belonging to cc11, were identified: ST-11 (n = 11), ST-1287 (n = 2), ST-3298 (n = 1), and ST-12351 (n = 5). All isolates had the same PorA:FetA profile (P1.5,2:F1–1) as that identified in the MenW:cc11 collection responsible for outbreaks in South America and the United Kingdom (8). Furthermore, genomic sequences indicated the isolates from Western Australia were within the same United Kingdom–South America cluster as isolates from the eastern coast of Australia (13).

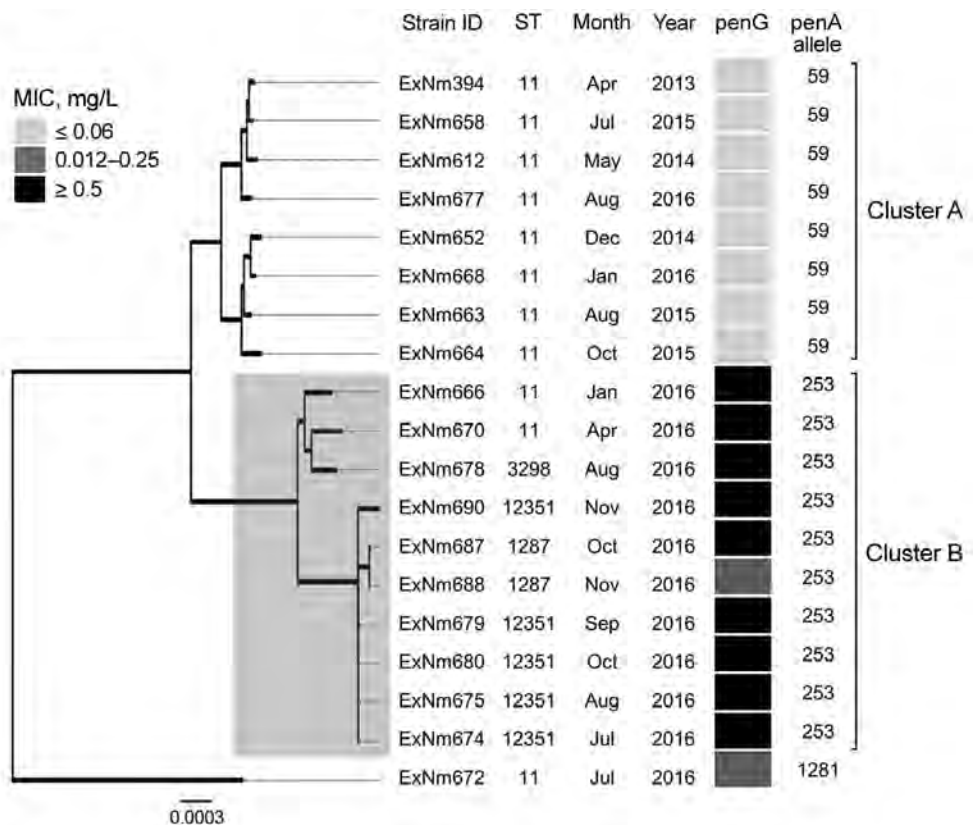
Phylogenetic analysis of the meningococcal core genome (14) identified 2 distinct clusters within the MenW:cc11 population of Western Australia (Figure 1). One isolate (ExNm672) was an outlier and could not be clustered. ExNm672 was isolated from a traveler from

Asia who had recently arrived in Western Australia, which would likely explain the different genealogy of this strain. All isolates less susceptible to or resistant to penicillin were in cluster B. Geocoding analysis showed that the 10 isolates in cluster B were obtained from 7 geographically well-separated regions in Western Australia. This observation suggests successful expansion of a new penicillin-resistant clone in 2016.

For *N. meningitidis*, polymorphisms within the gene encoding PBP2, also known as *penA*, are associated with a reduced affinity, and thus a decrease in susceptibility, to penicillin. All isolates in cluster A had the *penA*₅₉ allele, and isolates in cluster B had the *penA*₂₅₃ allele. These alleles differ by 101 nt, and the encoded peptides differ at 25 aa positions. The different amino acid residues are located in the second half of the protein, which contains the transpeptidase domain for penicillin binding. Six of the amino acid mutations encoded by *penA*₂₅₃ (F504L, A510V, N512Y, I515V, H541N, and I566V) have been reported to be associated with decreased susceptibility to penicillin (15).

The *penA*₂₅₃ allele was identified in MenB isolates of the cc32 lineage in Europe in early 2012. The PubMLST

Figure 1. Neighbor-joining dendrogram (500 bootstrap values) for core genome sequences of clonal complex 11 *Neisseria meningitidis* strains with serogroup W capsules, Western Australia, Australia, January 2013–December 2016. The resistance phenotype for the penicillin G (PenG) gene for each isolate is provided using the following breakpoints: sensitive (MIC ≤ 0.06 mg/L), intermediate (0.12–0.25 mg/L) and resistant (≥ 0.5 mg/L). Two clusters (A and B) were observed, which contain isolates that differ in penicillin resistance profile. Of 1,605 core-genome loci, a minimum of 244 are different between clusters A and B. The more recent cluster B appeared in early 2016 and contains penicillin-resistant isolates. Strain ExNm672 does not belong to either cluster. The dendrogram is drawn to scale, and sum of branch lengths between 2 strains indicates the proportion of nucleotide differences between those core genomes (≈ 1.5 Mb) within the pairwise alignment. Gray shaded box indicates isolates in cluster B. Scale bar indicates nucleotide substitutions per site. ID, identification; ST, sequence type.



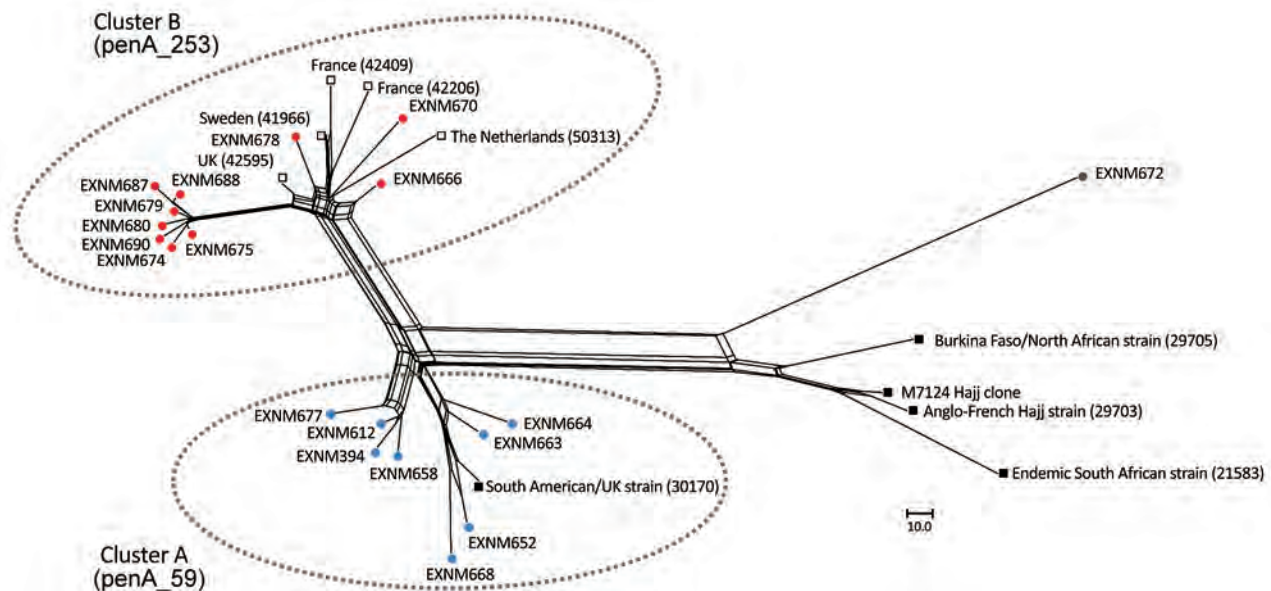


Figure 2. Phylogenetic reconstruction by using an unrooted neighbor-net algorithm of core genomes of clonal complex 11 *Neisseria meningitidis* strains with serogroup W capsules (MenW:cc11), Western Australia, Australia, January 2013–December 2016. Blue circles indicate isolates in cluster A from Western Australia; red circles indicate isolates in cluster B from Western Australia; gray circle indicates ExNm672, a strain isolated from a traveler; open squares indicate the 5 MenW:cc11 isolates in the PubMLST database (<http://pubmlst.org/neisseria>) that contains the *penA_253* allele; and black squares indicate reference MenW:cc11 strains, isolated after 2010, as described by Lucidarme et al. (8). M7124 is the Hajj clone isolated in Saudi Arabia in 2000. Numbers in parentheses indicate PubMLST numbers of reference isolates. Scale bar indicates nucleotide substitutions per site.

database has 5 MenW:cc11 invasive isolates harboring this allele, all of which were obtained in Europe in 2016: 2 from France, 1 from Sweden, 1 from the United Kingdom, and 1 from the Netherlands. Core-genome analysis showed clustering of these isolates from Europe with cluster B isolates from Western Australia. (Figure 2).

To assess whether *penA* was responsible for the difference in penicillin resistance between the 2 clusters, the *penA_253* allele from cluster B was transformed into all 8 penicillin-sensitive isolates in cluster A. We subsequently tested the *penA_253* isogenic mutants obtained for penicillin resistance by using the Etest. All transformants displayed intermediate resistance to penicillin (4-fold increase in MIC to 0.25 mg/L). These results indicate that the *penA_253* allele plays a major role in increased resistance to penicillin among cluster B isolates.

However, exchange of *penA* did not fully account for the level of resistance displayed by drug-resistant clinical isolates. This finding suggests that acquisition of penicillin resistance among cluster B isolates is multifactorial. Because PBP1, PBP3, and PBP4 were identical in all isolates in clusters A and B, there must be additional as yet undetermined factors that play a role in conferring resistance to penicillin in cluster B isolates. A comparison of the core and accessory genomes of isolates in the 2 clusters is required to further elucidate this issue.

Conclusions

MenW is now the predominant serogroup causing IMD in Western Australia. Core-genome analysis identified a new cluster of penicillin-resistant MenW:cc11 clinical isolates that emerged throughout this region during early 2016. We demonstrated that the *penA_253* allele has a major role in increasing penicillin resistance among isolates in this new cluster. Because *penA_253* has been identified in MenW:cc11 isolates in Europe in 2016, jurisdictions are encouraged to monitor emergence of strains harboring this allele by PCR for culture-negative cases.

Acknowledgments

We thank the scientific staff in the microbiology laboratory at PathWest Medicine, Perth, Australia, for serogrouping, storing, and collecting data for the meningococcal isolates.

This study was supported by a grant from the Amanda Young Foundation (<http://www.amandayoungfoundation.org.au/>), a not-for-profit, charitable organization of Western Australia, to C.M.K. C.M.K. is also supported by the National Health and Medical Research Council of Australia (APP1003697). S.M. is supported by an International Postgraduate Research Scholarship from the University of Western Australia. We used the *Neisseria* Multi Locus Sequence Typing website (<http://pubmlst.org/neisseria>), which is supported by grant 104992 from the Wellcome Trust to Martin Maiden and K.A.J.

Mr. Mowlaboccus is a doctoral candidate and a sessional lecturer at the University of Western Australia, Perth, Australia. His primary research interests include evolution and changing epidemiology of *N. meningitidis* and investigating the mechanism of antimicrobial resistance for this microorganism.

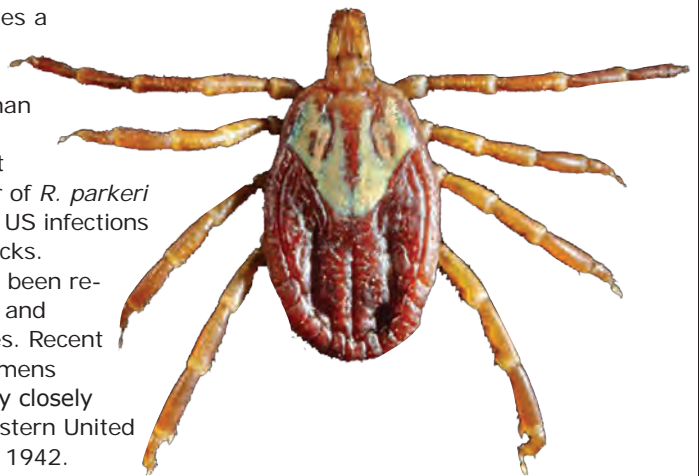
References

- Maiden MC, Bygraves JA, Feil E, Morelli G, Russell JE, Urwin R, et al. Multilocus sequence typing: a portable approach to the identification of clones within populations of pathogenic microorganisms. *Proc Natl Acad Sci U S A*. 1998;95:3140–5. <http://dx.doi.org/10.1073/pnas.95.6.3140>
- Meningitis control in countries of the African meningitis belt, 2015. *Wkly Epidemiol Rec*. 2016;91:209–16.
- Caugant DA, Maiden MC. Meningococcal carriage and disease—population biology and evolution. *Vaccine*. 2009;27(Suppl 2):B64–70. <http://dx.doi.org/10.1016/j.vaccine.2009.04.061>
- Mowlaboccus S, Perkins TT, Smith H, Sloots T, Tozer S, Premph LJ, et al. Temporal changes in BEXSERO® antigen sequence type associated with genetic lineages of *Neisseria meningitidis* over a 15-year period in Western Australia. *PLoS One*. 2016;11:e0158315. <http://dx.doi.org/10.1371/journal.pone.0158315>
- Martin NV, Ong KS, Howden BP, Lahra MM, Lambert SB, Beard FH, et al.; Communicable Diseases Network Australia MenW Working Group. Rise in invasive serogroup W meningococcal disease in Australia 2013–2015. *Commun Dis Intell Q Rep*. 2016;40:E454–9.
- Carville KS, Stevens K, Sohail A, Franklin LJ, Bond KA, Brahma A, et al. Increase in meningococcal serogroup W disease, Victoria, Australia, 2013–2015. *Emerg Infect Dis*. 2016;22:1785–7. <http://dx.doi.org/10.3201/eid2210.151935>
- Ladhani SN, Beebejaun K, Lucidarme J, Campbell H, Gray S, Kaczmarek E, et al. Increase in endemic *Neisseria meningitidis* capsular group W sequence type 11 complex associated with severe invasive disease in England and Wales. *Clin Infect Dis*. 2015;60:578–85. <http://dx.doi.org/10.1093/cid/ciu881>
- Lucidarme J, Hill DM, Bratcher HB, Gray SJ, du Plessis M, Tsang RS, et al. Genomic resolution of an aggressive, widespread, diverse and expanding meningococcal serogroup B, C and W lineage. *J Infect*. 2015;71:544–52. <http://dx.doi.org/10.1016/j.jinf.2015.07.007>
- Oppenheim BA. Antibiotic resistance in *Neisseria meningitidis*. *Clin Infect Dis*. 1997;24(Suppl 1):S98–101. http://dx.doi.org/10.1093/clinids/24.Supplement_1.S98
- Zapun A, Morlot C, Taha MK. Resistance to β -lactams in *Neisseria* spp due to chromosomally encoded penicillin-binding proteins. *Antibiotics (Basel)*. 2016;5:E35. <http://dx.doi.org/10.3390/antibiotics5040035>
- Turner PC, Southern KW, Spencer NJ, Pullen H. Treatment failure in meningococcal meningitis. *Lancet*. 1990;335:732–3. [http://dx.doi.org/10.1016/0140-6736\(90\)90852-V](http://dx.doi.org/10.1016/0140-6736(90)90852-V)
- Jolley KA, Maiden MC. BIGSdb: scalable analysis of bacterial genome variation at the population level. *BMC Bioinformatics*. 2010;11:595. <http://dx.doi.org/10.1186/1471-2105-11-595>
- Bond KA, Stevens K, Bulach D, Carville K, Ong KS, Howden BP. Rising incidence of invasive meningococcal disease caused by *Neisseria meningitidis* serogroup W in Victoria. *Med J Aust*. 2016;204:265–6. <http://dx.doi.org/10.5694/mja15.01222>
- Bratcher HB, Corton C, Jolley KA, Parkhill J, Maiden MC. A gene-by-gene population genomics platform: de novo assembly, annotation and genealogical analysis of 108 representative *Neisseria meningitidis* genomes. *BMC Genomics*. 2014;15:1138. <http://dx.doi.org/10.1186/1471-2164-15-1138>
- Harrison OB, Clemence M, Dillard JP, Tang CM, Trees D, Grad YH, et al. Genomic analyses of *Neisseria gonorrhoeae* reveal an association of the gonococcal genetic island with antimicrobial resistance. *J Infect*. 2016;73:578–87. <http://dx.doi.org/10.1016/j.jinf.2016.08.010>

Address for correspondence: Shakeel Mowlaboccus, School of Biomedical Sciences, University of Western Australia, 35 Stirling Hwy, Crawley, Perth, WA 6009, Australia; email: shakeel.mowlaboccus@uwa.edu.au

EID Podcast: A Tick on the Move?

Rickettsia parkeri, a tickborne bacterium that causes a febrile, eschar-associated illness throughout many countries of the Western Hemisphere, is transmitted by *Amblyomma* ticks. In the United States, more than 40 cases of *R. parkeri* rickettsiosis have been reported since its recognition in 2004. The Gulf Coast tick (*Amblyomma maculatum*) is the principal vector of *R. parkeri* in the United States, and all previously documented US infections arose within the known geographic range of these ticks. Confirmed cases of *R. parkeri* rickettsiosis also have been reported from Uruguay and Argentina, where *A. triste* and *A. tigrinum* ticks serve as the principal vector species. Recent reviews of tick collection records and archived specimens documented and identified the presence of ticks very closely related to *A. triste* in several regions of the southwestern United States and adjacent regions of Mexico since at least 1942.



Visit our website to listen: <http://www2c.cdc.gov/podcasts/player.asp?f=8643021> **EMERGING INFECTIOUS DISEASES**

Genesis of Influenza A(H5N8) Viruses

**Rabeh El-Shesheny, Subrata Barman,
Mohammed M. Feeroz, M. Kamrul Hasan,
Lisa Jones-Engel, John Franks, Jasmine Turner,
Patrick Seiler, David Walker, Kimberly Friedman,
Lisa Kercher, Sajeda Begum, Sharmin Akhtar,
Ashis Kumar Datta, Scott Krauss, Ghazi Kayali,
Pamela McKenzie, Richard J. Webby,
Robert G. Webster**

Highly pathogenic avian influenza A(H5N8) clade 2.3.4.4 virus emerged in 2016 and spread to Russia, Europe, and Africa. Our analysis of viruses from domestic ducks at Tangar haor, Bangladesh, showed genetic similarities with other viruses from wild birds in central Asia, suggesting their potential role in the genesis of A(H5N8).

Highly pathogenic avian influenza (HPAI) viruses of the H5 subtype remain a serious concern for poultry and human health. The Gs/GD lineage of HPAI A(H5N1) viruses continues to circulate and spread, and the hemagglutinin (HA) genes have diversified into multiple genetic clades. H5 clade 2.3.4.4 of the H5N8 subtype was first detected in domestic poultry in China in 2010; by 2014, this virus had caused multiple outbreaks among domestic ducks, chickens, geese, and wild birds in South Korea and subsequent outbreaks in Japan, China, Europe, and North America (1,2). During these outbreaks, 2 distinct clusters of HPAI A(H5N8) viruses were identified: group A viruses were detected in China in early 2014 and later in South Korea, Japan, Taiwan, Canada, the United States, and Europe; group B viruses were detected only in China in 2013 and South Korea in 2014 (3,4). Co-circulation of group A viruses with low pathogenicity avian influenza (LPAI) viruses led to new reassortants, including H5N1, H5N2, and H5N8 (3).

Author affiliations: National Research Centre, Giza, Egypt (R. El-Shesheny); St. Jude Children's Research Hospital, Memphis, Tennessee, USA (R. El-Shesheny, S. Barman, J. Franks, J. Turner, P. Seiler, D. Walker, K. Friedman, L. Kercher, S. Krauss, P. McKenzie, R.J. Webby, R.G. Webster); Jahangirnagar University, Savar, Dhaka, Bangladesh (M.M. Feeroz, M.K. Hasan, S. Begum, S. Akhtar, A.K. Datta); University of Washington, Seattle, Washington, USA (L. Jones-Engel); University of Texas Health Sciences Center, Houston, Texas, USA (G. Kayali); Human Link, Hazmieh, Lebanon (G. Kayali)

DOI: <https://doi.org/10.3201/eid2308.170143>

In late May 2016, a novel reassortant group B HPAI A(H5N8) clade 2.3.4.4 virus was detected in a wild bird in UVs-Nuur Lake in the Republic of Tyva, Siberia (5). As of March 2017, the virus had spread across most European countries, the Middle East, and Africa (6). To better understand the evolution and origin of the novel HPAI A(H5N8) viruses, we sequenced and analyzed the full genomes of LPAI viruses isolated from wild and free-ranging domestic ducks in the Tangar haor area of Bangladesh, located in the central Asian flyway, and compared them with the novel HPAI A(H5N8) viruses.

The Study

Since 2008, we have conducted long-term, active surveillance of influenza viruses in poultry in Bangladesh (7). From February 2015 through February 2016, we collected samples from wild birds and free-ranging domestic ducks in the Tangar haor area, a vast wetland in northeastern Bangladesh, where ≈200 types of migratory birds overwinter. Tangar haor is located in the central Asian flyway and is near the Eastern Asian–Australian and Black Sea–Mediterranean flyways (Figure 1). We collected cloacal swabs from the birds and performed virus isolation and subtyping via reverse transcription PCR (7).

During the surveillance period, we isolated 4 influenza A(H3N6), 4 influenza A(H7N1), 1 influenza A(H7N5), 3 influenza A(H7N9), and 2 influenza A(H15N9) viruses, all from free-ranging domestic ducks except for a single H7N5 virus, which was isolated from a migratory black-tailed godwit (online Technical Appendix Table, <https://wwwnc.cdc.gov/EID/article/23/8/17-0143-Techapp1.pdf>). When analyzed individually, gene segments across viruses of different subtypes seem to have evolved closely with viruses from Eurasia. To determine the genetic relatedness between these viruses and the 2016 novel HPAI A(H5N8) virus, we compared our isolates with available sequences of A(H5N8) viruses in GenBank and the GISAID database (<http://platform.gisaid.org>). We used MEGA6 to generate phylogenetic trees (9).

HA, neuraminidase (NA), and nonstructural protein (NS) genes of novel HPAI A(H5N8) viruses were closely related to those of the group B HPAI A(H5N8) viruses that circulated in China in 2013 and in South Korea in 2014 (5,10). In contrast, the polymerase basic (PB) 2, PB1, polymerase acidic (PA), nucleoprotein (NP), and matrix protein (M) genes of the novel HPAI A(H5N8) viruses were most closely related to those of the LPAI

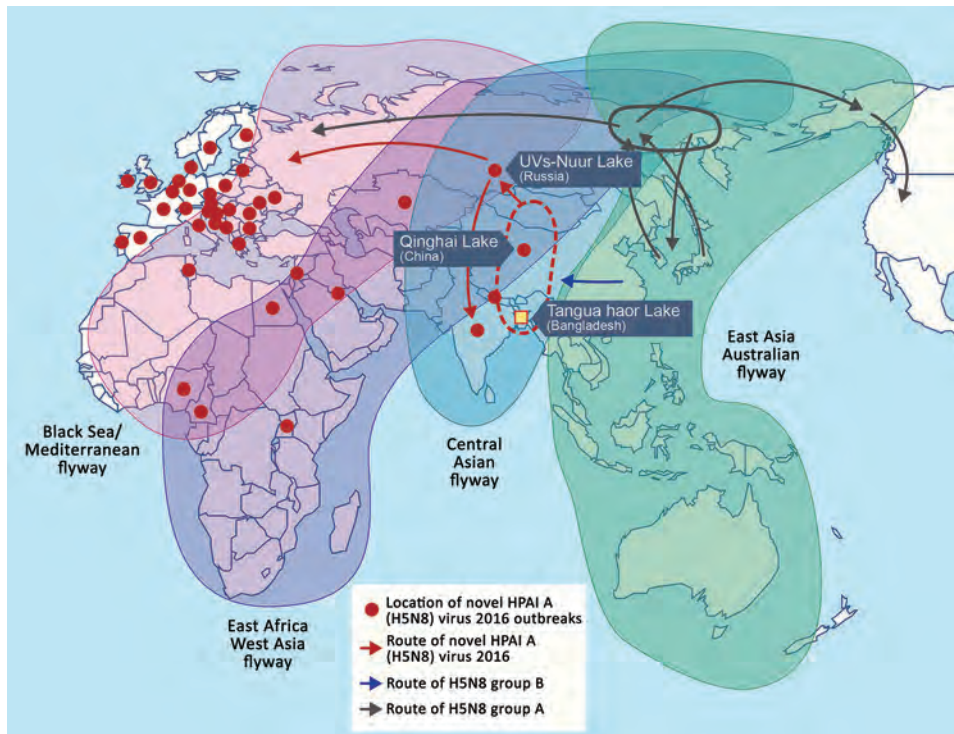


Figure 1. Global movement of wild birds (adapted from [8]) and geographic distribution of novel HPAI A(H5N8) viruses, 2016. Influenza A viruses were isolated from wild birds and free-ranging domestic ducks in the Tangua haor region of Bangladesh (yellow square) during February 2015–February 2016. Dissemination of novel HPAI A(H5N8) clade 2.3.4.4 viruses (red arrows). The solid zone (circle) indicates the location of group A viruses that evolved during the breeding season, and subsequently spread along different flyways. The dashed zone (circle) indicates the location of proposed reassortment between HPAI A(H5N8) group B viruses and low pathogenicity avian influenza viruses circulating along the Central Asian flyway. HPAI, highly pathogenic avian influenza.

viruses isolated from the central Asia flyway (online Technical Appendix Figure).

Sequence analysis of novel HPAI A(H5N8) viruses revealed that sequence similarity of HA, NA, PB1, M, and NS was 99.9%–100%. Sequence homology of PB2, PA, and NP gene segments led to classification of novel HPAI A(H5N8) viruses into 2 genotypes: genotype 1 viruses isolated from Siberia and genotype 2 viruses isolated from Europe (Figure 2).

To explore the possible genetic exchange between LPAI viruses isolated from the Tangua haor area and novel HPAI A(H5N8) viruses, we analyzed the phylogeny and nucleotide identity of the M gene and internal gene sequences (online Technical Appendix). The PB2 genes of HPAI A(H5N8) genotype 1 viruses were closely related to those of the influenza A(H4N6) virus strain from Mongolia and shared identity homology with 3 influenza A(H7N1) viruses; sequence identities ranged from 98.1% to 98.6%. Genotype 2 viruses were related to influenza A(H3N6) viruses; identities were 98.6%–98.9%. The PB1 genes of HPAI A(H5N8) genotype 1 and 2 viruses were related to those of A/duck/Bangladesh/26918/2015(H3N6); identities were 97.3%–98.0% (Table). The PA genes of genotype 1 viruses were more closely related to those of the Mongolia strains of influenza A(H3N8) and A(H4N6) viruses. Genotype 2 viruses were more closely related to those of A/duck/Bangladesh/26918/2015(H3N6); identities were 97.1%–97.3%. The NP genes of genotype 1 viruses were more closely related to those of influenza A(H7N9) viruses;

identities were 98.4%–98.6%. However, the NP genes of genotype 2 viruses were more closely related to those of influenza A(H3N6) and A(H7N1) viruses; identities were 97%–97.2%. The M genes of genotypes 1 and 2 viruses were related to those of influenza A(H15N9) viruses; identities were 98%–98.5% (Table).

We next determined the presence of genetic markers associated with pathogenicity and virulence in mammals or adaptation to new hosts. On the basis of the amino acids at positions 591, 627, and 701 in the PB2 protein, the viruses are likely to exhibit low pathogenicity in mice. However, NS residues P42S and V149A, associated with virulence and pathogenicity in mammals, were in all Tangua haor isolates and HPAI A(H5N8) viruses (11,12).

Conclusions

In 2016, a novel HPAI A(H5N8) virus clade 2.3.4.4 emerged and spread to Russia, Europe, and Africa. We demonstrated that several internal genes from viruses in ducks in Bangladesh have an equivalent or higher consensus identity to those of other viruses of wild birds in central Asia, suggesting that these viruses could be gene donors to the novel reassortant A(H5N8) viruses, which were then disseminated by wild birds. The novel HPAI A(H5N8) viruses diverged along 2 genotypes with independent origins of reassortment for several gene segments. The HA, NA, and NS genes were related to group B of H5N8 clade 2.3.4.4 viruses that circulated in China from 2013. Group B is still circulating in China, and a previous study showed that these viruses had PB2 and NS

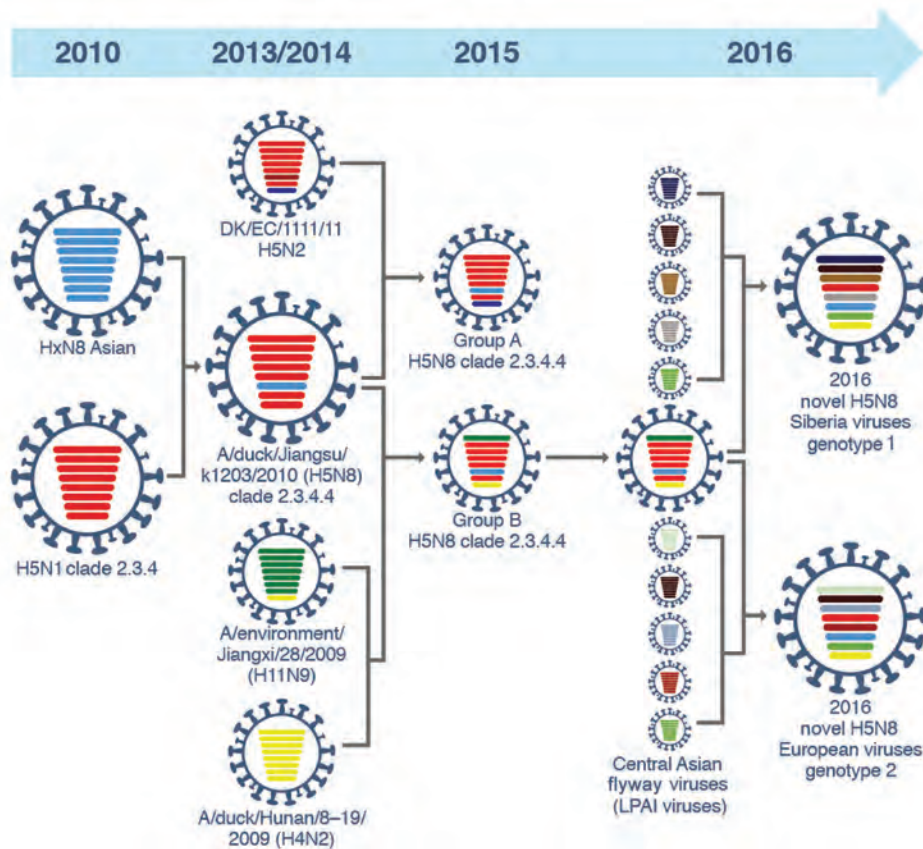


Figure 2. Illustration of original reassortment events of novel highly pathogenic avian influenza (HPAI) A(H5N8) viruses isolated from Siberia and Europe in 2016. The 8 gene segments (from top to bottom) in each virus are polymerase basic 2, polymerase basic 1, polymerase acidic, hemagglutinin, nucleoprotein, neuraminidase, matrix, and nonstructural. Each color indicates a separate virus background. In 2010, HPAI A(H5N1) clade 2.3.4 viruses reassorted with subtype N8 viruses from Eurasia and produced A/duck/Jiangsu/k1203/2010(H5N8). Until late 2013, HPAI viruses with H5N8 subtypes circulated in eastern China and South Korea. In 2014, HPAI A(H5N8) viruses reassorted with A/duck/Hunan/8–19/2009(H4N2) and A/environment/Jiangxi/28/2009(H11N9) to generate group B viruses. The subsequent reassortment between HPAI A(H5N8) group B viruses and low pathogenicity (LPAI) viruses circulating along the central Asian flyway led to generation of the novel HPAI A(H5N8) genotype 1 and 2 viruses.

genes derived from domestic ducks in eastern China (13), indicating further reassortment events.

The route of spread of HPAI A(H5N1) viruses from eastern Asia to Europe, Africa, and the Middle East in 2005 and 2006 most likely occurred by spillover infection from wild birds. HPAI A(H5N1) viruses were detected during an outbreak among migratory birds at Qinghai

Lake in China, which is located in the central Asian flyway (14), suggesting that this flyway is a route for dissemination of HPAI A(H5N1) viruses. A recent study suggested that only the PA and NP segments of 2016 A(H5N8) viruses isolated in Germany differed from those of genotype 1 viruses isolated in Siberia, suggesting that reassortment occurred with viruses circulating in central

Table. Nucleotide identity of novel HPAI A(H5N8) clade 2.3.4.4 virus and viruses isolated from Tanguar haor, Bangladesh*

Gene and genotype, novel HPAI A(H5N8) clade 2.3.4.4, 2016	Viruses from Tanguar haor (Central Asian flyway)†	% Identity
PB2		
Genotype 1‡	A/duck/Bangladesh/24705/2015(H7N1)§	98.4–98.6
Genotype 2‡	A/duck/Bangladesh/26920/2015(H3N6)	98.7–98.9
PB1	A/duck/Bangladesh/26918/2015(H3N6)	97.3–98
PA		
Genotype 1‡	A/duck/Bangladesh/24706/2015(H7N1)	95.3
Genotype 2‡	A/duck/Bangladesh/26918/2015(H3N6)	97.1–97.3
NP		
Genotype 1‡	A/duck/Bangladesh/26992/2015(H7N9)	98.6
Genotype 2‡	A/duck/Bangladesh/24706/2015(H7N1)	97–97.1
M	A/duck/Bangladesh/24704/2015(H15N9)	98–98.5

*HPAI, highly pathogenic avian influenza; NP, nucleoprotein; M, matrix; PA, polymerase acidic; PB, polymerase basic.

†All Eurasian low-pathogenicity avian influenza lineage.

‡Genotype 1 viruses isolated from Siberia; genotype 2 viruses isolated from Europe.

§Selected 1 representative virus isolate from the Tanguar haor region of Bangladesh.

Asia and northwestern Europe (10). However, we show that the PB2, PA, and NP genes of genotype 1 viruses not only differed from those of genotype 2 viruses but clustered with and were more closely related to those of viruses from Bangladesh and central Asia. Active surveillance of influenza viruses among migratory wild birds and molecular studies need to be sustained to monitor the spread of these viruses through wild birds.

Acknowledgments

We thank Mark Zanin for reviewing the manuscript, James Knowles for administrative assistance, Nisha Badders for scientific editing, and Brandon Stelter for generating Figures 1 and 2.

This work was funded, in part, by the National Institute of Allergy and Infectious Diseases, National Institutes of Health (contract nos. HHSN266200700005C and HHSN272201400006C), and by American Lebanese Syrian Associated Charities.

Dr. El-Shesheny is a postdoctoral research associate at St. Jude Children's Research Hospital, Memphis, Tennessee, USA. His research interests include molecular virology, evolution, and emerging viruses at the animal–human interface.

References

1. Lee YJ, Kang HM, Lee EK, Song BM, Jeong J, Kwon YK, et al. Novel reassortant influenza A(H5N8) viruses, South Korea, 2014. *Emerg Infect Dis.* 2014;20:1087–9. <http://dx.doi.org/10.3201/eid2006.140233>
2. Lee DH, Torchetti MK, Winker K, Ip HS, Song CS, Swayne DE. Intercontinental spread of Asian-origin H5N8 to North America through Beringia by migratory birds. *J Virol.* 2015;89:6521–4. <http://dx.doi.org/10.1128/JVI.00728-15>
3. Lee DH, Bahl J, Torchetti MK, Killian ML, Ip HS, DeLiberto TJ, et al. Highly pathogenic avian influenza viruses and generation of novel reassortants, United States, 2014–2015. *Emerg Infect Dis.* 2016;22:1283–5. <http://dx.doi.org/10.3201/eid2207.160048>
4. Hill SC, Lee YJ, Song BM, Kang HM, Lee EK, Hanna A, et al. Wild waterfowl migration and domestic duck density shape the epidemiology of highly pathogenic H5N8 influenza in the Republic of Korea. *Infect Genet Evol.* 2015;34:267–77. <http://dx.doi.org/10.1016/j.meegid.2015.06.014>
5. Lee DH, Sharshov K, Swayne DE, Kurskaya O, Sobolev I, Kabilov M, et al. Novel reassortant clade 2.3.4.4 avian influenza A(H5N8) virus in wild aquatic birds, Russia, 2016. *Emerg Infect Dis.* 2017;23:359–60. <http://dx.doi.org/10.3201/eid2302.161252>
6. World Organisation for Animal Health. Update on highly pathogenic avian influenza in animals (type H5 and H7) [cited 2017 Mar 21]. <http://www.oie.int/animal-health-in-the-world/update-on-avian-influenza/2017/>
7. Marinova-Petkova A, Shanmuganatham K, Feeroz MM, Jones-Engel L, Hasan MK, Akhtar S, et al. The continuing evolution of H5N1 and H9N2 influenza viruses in Bangladesh between 2013 and 2014. *Avian Dis.* 2016;60(Suppl):108–17. <http://dx.doi.org/10.1637/11136-050815-Reg>
8. Olsen B, Munster VJ, Wallensten A, Waldenström J, Osterhaus ADME, Fouchier RAM. Global patterns of influenza A virus in wild birds. *Science.* 2006;312:384–8. <http://dx.doi.org/10.1126/science.1122438>
9. Tamura K, Stecher G, Peterson D, Filipski A, Kumar S. MEGA6: Molecular Evolutionary Genetics Analysis version 6.0. *Mol Biol Evol.* 2013;30:2725–9. <http://dx.doi.org/10.1093/molbev/mst197>
10. Pohlmann A, Starick E, Harder T, Grund C, Höper D, Globig A, et al. Outbreaks among wild birds and domestic poultry caused by reassorted influenza A(H5N8) clade 2.3.4.4 viruses, Germany, 2016. *Emerg Infect Dis.* 2017;23:633–6. <http://dx.doi.org/10.3201/eid2304.161949>
11. Jiao P, Tian G, Li Y, Deng G, Jiang Y, Liu C, et al. A single-amino-acid substitution in the NS1 protein changes the pathogenicity of H5N1 avian influenza viruses in mice. *J Virol.* 2008;82:1146–54. <http://dx.doi.org/10.1128/JVI.01698-07>
12. Seo SH, Hoffmann E, Webster RG. Lethal H5N1 influenza viruses escape host anti-viral cytokine responses. *Nat Med.* 2002;8:950–4. <http://dx.doi.org/10.1038/nm757>
13. Wu H, Peng X, Xu L, Jin C, Cheng L, Lu X, et al. Novel reassortant influenza A(H5N8) viruses in domestic ducks, eastern China. *Emerg Infect Dis.* 2014;20:1315–8. <http://dx.doi.org/10.3201/eid2008.140339>
14. Chen H, Smith GJ, Zhang SY, Qin K, Wang J, Li KS, et al. Avian flu: H5N1 virus outbreak in migratory waterfowl. *Nature.* 2005;436:191–2. <http://dx.doi.org/10.1038/nature03974>

Address for correspondence: Robert G. Webster, Department of Infectious Diseases, MS 330, St. Jude Children's Research Hospital, 262 Danny Thomas Pl, Memphis, TN 38105-3678, USA; email: robert.webster@stjude.org

West Nile Virus Outbreak in Houston and Harris County, Texas, USA, 2014

Diana Martinez, Kristy O. Murray, Martin Reyna, Raouf R. Arafat, Roberto Gorena, Umair A. Shah, Mustapha Debboun

Since 2002, West Nile virus (WNV) has been detected every year in Houston and the surrounding Harris County, Texas. In 2014, the largest WNV outbreak to date occurred, comprising 139 cases and causing 2 deaths. Additionally, 1,286 WNV-positive mosquito pools were confirmed, the most reported in a single mosquito season.

West Nile virus (WNV) emerged in the United States in 1999 and in Texas in 2002 (1). During 2002–2011, Texas reported 2,202 WNV cases and 135 deaths (2). In 2012, the largest statewide WNV outbreak in Texas occurred; 1,868 cases and 89 deaths were reported (3).

Every year since 2002, WNV has been detected in Houston and the surrounding Harris County (Houston/Harris County), the third most populous US county. This area was affected by the statewide outbreak in 2012, and then in 2014, the largest WNV outbreak to date occurred in this area. We examined the epidemiology of WNV in Houston/Harris County in 2014.

The Study

We investigated epidemiologic surveillance data on reported WNV case-patients who had onset of illness during January 1, 2002–December 31, 2014, from the Texas Department of State Health Services and the Houston-area local health departments: Harris County Public Health (HCPH) and the Houston Health Department (HHD). We determined case severity (West Nile neuroinvasive disease [WNND] and West Nile fever [WNF]) by using established criteria (4) and calculated attack rates by demographic characteristics by using population estimates for 2014 (5). We used Stata 14.0 (StataCorp LLP, College Station, TX, USA) to conduct statistical analyses.

During 2002–2014, a total of 650 human WNV cases were reported to HCPH and HHD (online Technical

Appendix Table 1, <https://wwwnc.cdc.gov/EID/article/23/8/17-0384-Techapp1.pdf>), including 35 deaths (case-fatality rate 5.4%). This total represented 14% of all cases reported from Texas during this period. The epidemic curve revealed an increased number of cases in 2002, 2006, 2012, and 2014 (Figure 1), which correlated with the minimum infection rate for mosquitoes (Pearson correlation coefficient $r = 0.74$).

During 2014, Harris County reported its highest number of WNV human cases to date: 139 cases and 2 deaths. This total represented 37% of all cases in Texas. Most (76%) cases were WNND (Table 1). Overall, incidence was 3.26 cases/100,000 population; 69% of case-patients were male. Mean case-patient age was 57 years (range 6–92 years); most (76%) case-patients were ≥ 45 years of age. Attack rates increased with age, from 0.4 cases/100,000 population for those < 18 years of age to 14.5 cases/100,000 population for those ≥ 65 years of age. A higher attack rate was observed among non-Hispanic whites when compared with black, Hispanic white, and Asian populations. We did not detect statistically significant differences between WNND and WNF occurrence related to race/ethnicity, age, or sex (all p values > 0.05). This finding is in contrast to the Texas 2012 statewide outbreak, during which being male, > 65 years of age, and of a minority population were statistically associated with WNND (3). Although results from this study had similar trends, the lack of statistical significance was likely caused by the small sample size of WNF cases ($n = 34$).

In 2014, the HCPH Mosquito and Vector Control Division also identified the largest number of WNV-positive mosquito pools to date: 1,286 positive pools were identified through the Rapid Analyte Measurement Platform (Response Biomedical Corp, Burnaby, British Columbia, Canada) (Table 2). In Harris County, 782,551 mosquitoes were collected, comprising 34 of 56 species recorded (6). We tested 12,608 mosquito pools from 19 species (online Technical Appendix Table 2) and confirmed in 1,285 *Culex quinquefasciatus* (Say) mosquito pools and in 1 *Aedes albopictus* (Skuse) pool. The first WNV-positive mosquito pool was detected during epidemiologic week 23 of 2014 (June 6). Viral detection continued for 20 weeks, ending in week 42 (October 14). The peak of positive pools ($n = 168$) occurred during week 30 (July 20–26). In comparison, dates of symptom onset for human cases occurred during February 5–December 1, 2014, and peaked during week 33 (Figure 1).

Author affiliations: Harris County Public Health, Houston, Texas, USA (D. Martinez, M. Reyna, R. Gorena, U.A. Shah, M. Debboun); Baylor College of Medicine and Texas Children's Hospital, Houston (K.O. Murray); Houston Health Department, Houston (R.R. Arafat)

DOI: <https://doi.org/10.3201/eid2308.170384>

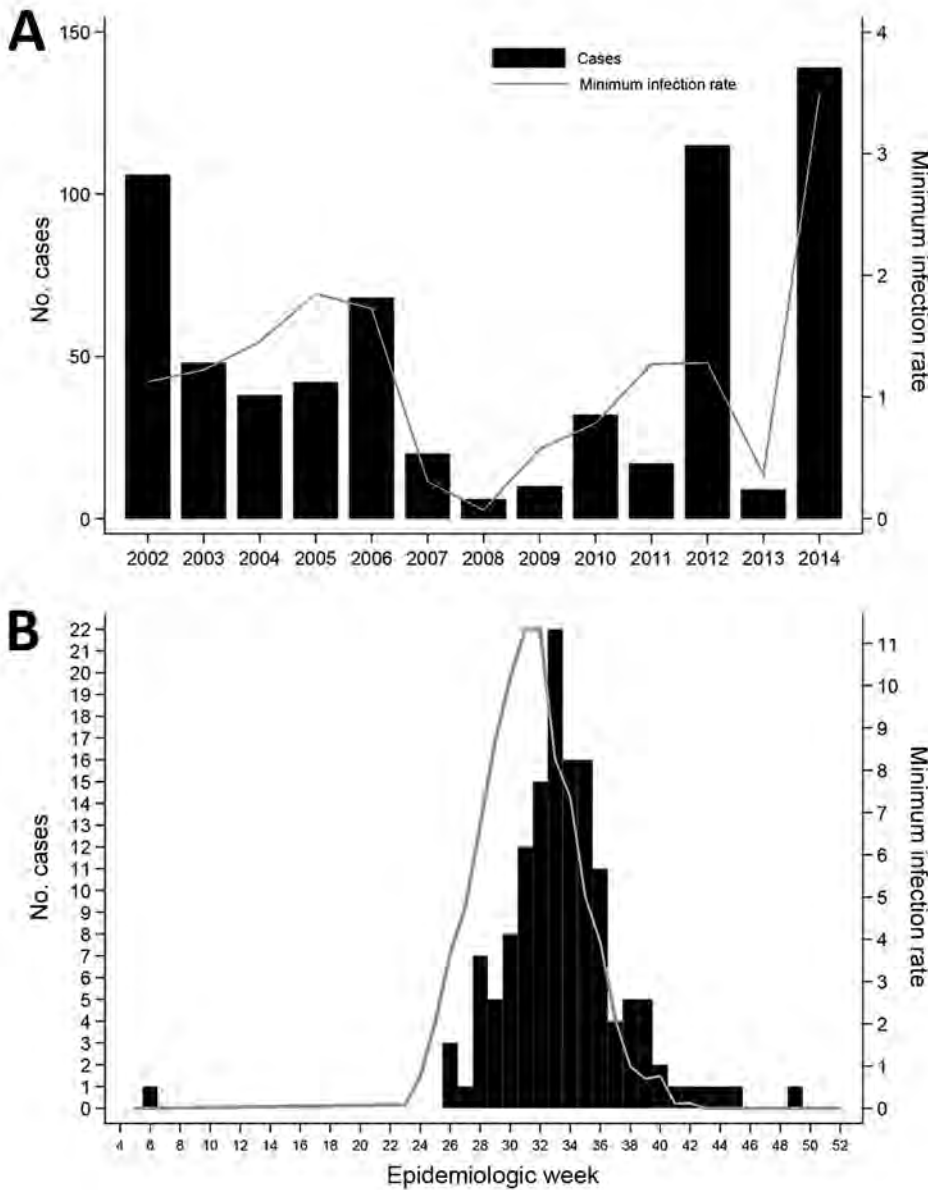


Figure 1. Epidemic curves depicting number of cases of West Nile among humans and minimum infection rate (MIR) of positive mosquito pools by year (A) and by epidemiologic week (B), Houston/Harris County, Texas, 2002–2014. MIR was calculated by the formula (no. positive mosquito pools × 1,000)/no. female mosquitoes pooled).

We used ArcMap 10.2.1 (Environmental Systems Research Institute, Inc. [ESRI], Redlands, CA, USA) to determine the distributions of positive mosquitoes and residences of case-patients where available (n = 128). Throughout the transmission season, WNV was detected in 237 (88%) of the 268 Mosquito Control Districts (MCD) in Harris County. We used the Optimized Hot Spot Analysis Tool (ArcGIS Pro; ESRI, Redlands, CA, USA) to calculate the Getis-Ord Gi statistic, which we used to determine statistically significant clusters (hotspots) of mosquito activity. We then converted data for case-patients to graduated frequency dots to determine spatial patterns. In the hotspot analysis (Figure 2), red shading indicates MCDs with statistically significant

clustering of positive mosquito pools (90%, 95%, and 99% CIs) compared with neighboring MCDs. The dark blue areas show where mosquito-positive pools were statistically less likely to occur. We observed a similar hotspot pattern in prior years (D. Martinez et al., Harris County Public Health, Houston, TX, unpub. data). Hotspots are likely related to ecologic areas with higher vegetation and creeks (7).

The 2014 WNV outbreak in Houston/Harris County was unexpected, particularly because transmission activity across the state was at low levels, and only 379 cases were reported statewide. It is likely that the actual number of WNV cases was considerably higher, particularly considering that 76% of reported case-patients had severe WNND,

Table 1. Demographics and attack rates of West Nile virus cases reported to HCPH and HHD, Houston/Harris County, Texas, USA, 2014*

Case-patient characteristics	All case-patients, no. (%), n = 139	Attack rate†/100,000 population	WNV, no. (%), n = 34	WNND, no. (%), n = 105
Sex				
M	96 (69)	4.5	26 (76)	70 (67)
F	43 (31)	2.0	8 (24)	35 (33)
Age, y				
<18	5 (4)	0.4	1 (3)	4 (4)
18–24	3 (2)	0.7	1 (3)	2 (2)
25–44	25 (18)	1.9	6 (18)	19 (18)
45–64	52 (37)	5.2	11 (32)	41 (39)
≥65	54 (39)	14.5	15 (44)	39 (37)
Race/ethnicity				
White, non-Hispanic	73 (53)	5.3	17 (50)	56 (53)
Black	19 (14)	2.4	6 (18)	13 (12)
White, Hispanic	30 (22)	1.7	4 (12)	26 (25)
Asian	2 (1)	0.7	1 (3)	1 (1)
Other/unknown	15 (11)	NA	6 (18)	9 (9)

*HCPH, Harris County Public Health; HHD, Houston Health Department; WNV, West Nile fever; WNND, West Nile neuroinvasive disease; NA, not applicable.

†Attack rates based on 2014 population estimates from the Texas State Data Center (3), accessed February 10, 2017. Total population of Harris County = 4,269,608.

which indicates a probable diagnostic bias. Prior studies showed that <1% of WNV infections manifest as WNND (8,9). A recent study in Houston showed that WNV testing was ordered for only 37% of viral meningitis/encephalitis case-patients (10), further highlighting concerns for underestimation of the true extent of disease.

We recently reported that WNV activity appears to have a 3-year pattern that showed increases in reported cases observed in 2003, 2006, 2009, and 2012 (2,3). During the years in which we observed increased numbers of cases, we also observed earlier detection of positive mosquito pools, which first appeared in May, compared to June in non-outbreak years. Vector abundance and increased amplitude of transmission are likely driven by ecologic and environmental factors. In 2014, we were unsure why such a large outbreak occurred in this region compared with prior years. Weather patterns during 2012–2014 were different: 2012, after the drought of 2011, had mild winter temperatures. Conversely, 2014 had below-average winter temperatures, above-average rainfall, and no drought conditions. Further research would aid our understanding of factors that drive WNV transmission.

Vector surveillance is vital to disease prevention. The year-round Integrated Mosquito Management Program includes surveillance-guided vector control. It is difficult to estimate the number of WNV cases prevented; however,

considering the high minimum infection rate in 2014 in the densely populated city of Houston, we believe that 139 cases are a much lower number than what could have otherwise occurred if no surveillance/control activities had been implemented. Barber et al. found that vector control is cost-effective if at least 15 cases of WNND are prevented (11).

Continuous WNV disease activity has had a high economic effect on the Houston/Harris County area. By using estimates provided by Barber et al. (11) (adjusted to 2014 US dollar value [12]), we calculated the acute medical care and productivity costs of the 2014 outbreak to be ≈\$6 million (online Technical Appendix Table 3). In addition to high medical costs, costs related to rehabilitation/long-term care, surveillance, and vector control would be considerable.

Conclusions

The 2014 outbreak of WNV in the Houston/Harris County area is a reminder of the continuous effect and the unpredictable nature of disease transmission. With no specific therapeutic options or vaccine available, the costs related to medical care, surveillance, and vector control will continue to mount. Public health authorities should remain vigilant to prevent mosquito-borne infections. We expect endemic levels of transmission and occasional epizootics in the years to come.

Table 2. WNV-confirmed mosquito pools collected from 4 different types of mosquito traps, Houston/Harris County, Texas, USA, 2014*

Trap type†	Species	No. traps	Total no. pools	Females pooled	WNV	SLE	WNV/MIR
CDC Gravid Trap	<i>Culex quinquefasciatus</i>	3,971	5,025	192,441	716	0	3.72
CDC Miniature Light Trap	<i>Cx. quinquefasciatus</i>	3,748	4,617	154,124	566	1	3.67
Biogents Sentinel Trap	<i>Cx. quinquefasciatus</i>	926	54	680	3	0	4.41
CDC Gravid Trap	<i>Aedes albopictus</i>	1,315	359	952	1	0	1.05

*WNV, West Nile virus; SLE, St. Louis encephalitis virus; MIR, minimum infection rate.

†CDC Gravid Trap and CDC Miniature Light Trap, John W. Hock Company, Gainesville, FL; Biogents Sentinel Trap, Biogents AG, Regensburg, Germany.

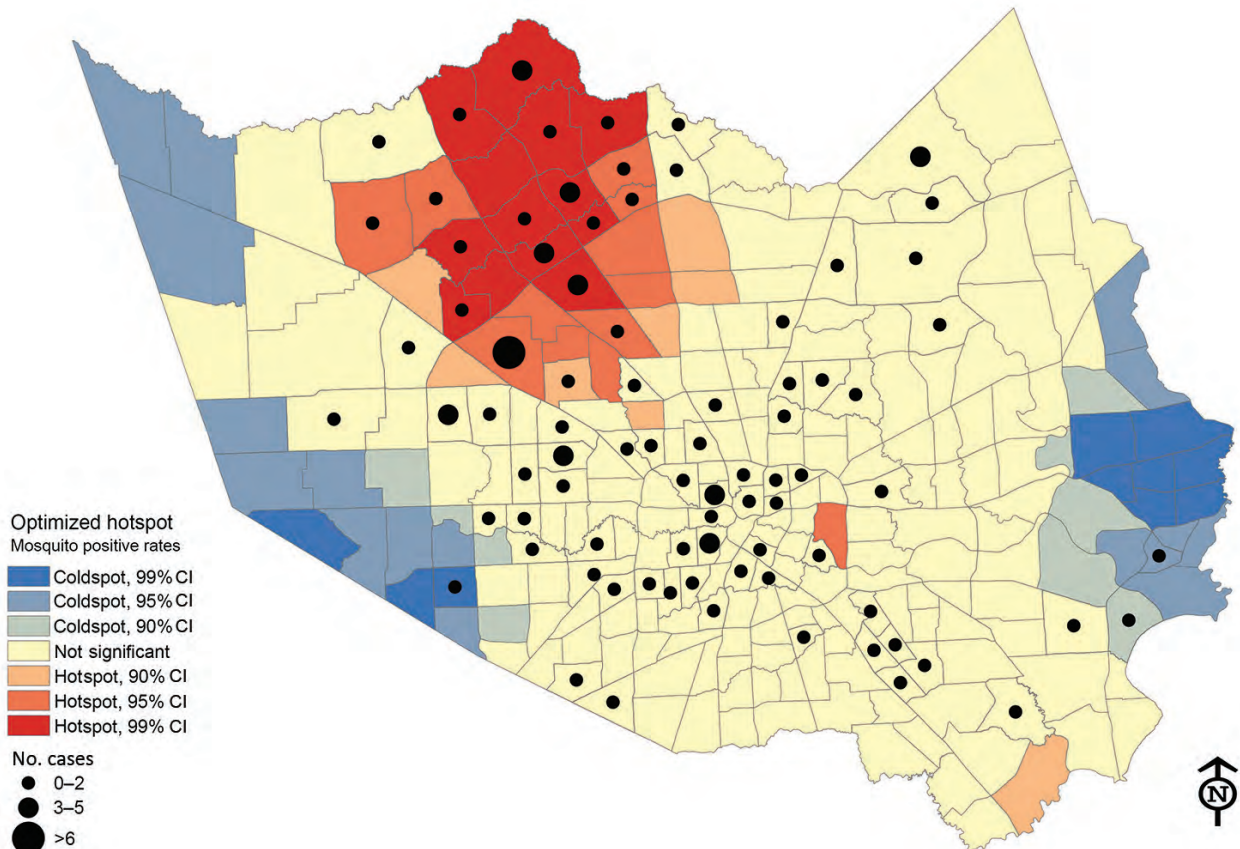


Figure 2. Optimized hotspot analysis results showing residential locations of persons who had West Nile virus and their association with positive mosquito hotspots, Houston/Harris County, Texas, 2002–2014. Red “hot” areas represent statistically significant high-risk virus-positive mosquito activity, compared with blue “cold” areas with low risk for positive mosquitoes.

Acknowledgments

The authors thank all epidemiologists at both health departments and mosquito surveillance technicians at Harris County Public Health Mosquito and Vector Control Division for their assistance with data collection. We also thank Melina Evdemon and Chris Fredregill for their technical assistance during the creation of the figures.

This project was generously funded in part by the National Institutes of Health, National Institute of Allergy and Infectious Diseases (5R01AI091816-01).

Dr. Martinez is the Epidemiology Program Manager/Senior Epidemiologist for Harris County Public Health and serves as liaison for programmatic, quality assurance, and surveillance activities of the Epidemiology Program. Her research interests are emerging and acute infectious disease epidemiology and surveillance.

References

- Lillibridge KM, Parsons R, Randle Y, Travassos da Rosa AP, Guzman H, Siirin M, et al. The 2002 introduction of West Nile virus into Harris County, Texas, an area historically endemic for St. Louis encephalitis. *Am J Trop Med Hyg.* 2004;70:676–81.
- Nolan MS, Schuermann J, Murray KO. West Nile virus infection among humans, Texas, USA, 2002–2011. *Emerg Infect Dis.* 2013;19:137–9. <http://dx.doi.org/10.3201/eid1901.121135>
- Murray KO, Ruktanonchai D, Hesalroad D, Fonken E, Nolan M. West Nile virus, Texas, USA, 2012. *Emerg Infect Dis.* 2013;19:1836–8. <http://dx.doi.org/10.3201/eid1911.130768>
- Centers for Disease Control and Prevention. Arboviral diseases, neuroinvasive and non-neuroinvasive 2014 case definition [cited 2017 Apr 11]. <https://www.cdc.gov/nndss/conditions/arboviral-diseases-neuroinvasive-and-non-neuroinvasive/case-definition/2014/>
- The Texas State Data Center TTSD. Texas population projections program [cited 2017 Apr 11]. <http://txsdc.utsa.edu/Data/TPEPP/Projections/Index.aspx>
- Nava MR, Debboun M. A taxonomic checklist of the mosquitoes of Harris County, Texas. *J Vector Ecol.* 2016;41:190–4. <http://dx.doi.org/10.1111/jvec.12212>
- Nolan MS, Zangeneh A, Khuwaja SA, Martinez D, Rossmann S, Cardenas V, Murray KO. Proximity of residence to bodies of water and risk for West Nile virus infection: a case-control study in Houston, Texas. *J Biomed Biotechnol.* 2012;159578. <http://dx.doi.org/10.1155/2012/159578>
- Mostashari F, Bunning ML, Kitsutani PT, Singer DA, Nash D, Cooper MJ, et al. Epidemic West Nile encephalitis, New York, 1999: results of a household-based seroepidemiological survey.

- Lancet. 2001;358:261–4. [http://dx.doi.org/10.1016/S0140-6736\(01\)05480-0](http://dx.doi.org/10.1016/S0140-6736(01)05480-0)
9. Carson PJ, Borchardt SM, Custer B, Prince HE, Dunn-Williams J, Winkelman V, et al. Neuroinvasive disease and West Nile virus infection, North Dakota, USA, 1999–2008. *Emerg Infect Dis.* 2012;18:684–6. <http://dx.doi.org/10.3201/eid1804.111313>
 10. Vanichanan J, Salazar L, Wootton SH, Aguilera E, Garcia MN, Murray KO, et al. Use of testing for West Nile virus and other arboviruses. *Emerg Infect Dis.* 2016;22:1587–93. <http://dx.doi.org/10.3201/eid2209.152050>
 11. Barber LM, Schleier JJ III, Peterson RK. Economic cost analysis of West Nile virus outbreak, Sacramento County, California, USA, 2005. *Emerg Infect Dis.* 2010;16:480–6. <http://dx.doi.org/10.3201/eid1603.090667>
 12. Bureau of Labor Statistics Consumer Price Index Calculator [cited 2017 Feb 13]. http://www.bls.gov/data/inflation_calculator.htm

Address for correspondence: Kristy O. Murray, Baylor College of Medicine, National School of Tropical Medicine, 1102 Bates Ave, Ste 550, Houston, TX 77030, USA; email: kmurray@bcm.edu

March 2010: Vectorborne Infections



- Preparing a Community Hospital to Manage Work-related Exposures to Infectious Agents
- *Bartonella* spp. Transmission and Ticks
- Potential for Tick-borne Bartonellosis
- Malaria in Areas of Low Endemicity, Somalia, 2008
- West Nile Virus in American White Pelicans, Montana
- Murine Typhus in Austin, Texas
- Chikungunya Virus Infection during Pregnancy, Réunion, France
- Mumps Outbreak in Hospital, Chicago, Illinois
- Reservoir Hosts for *Amblyomma americanum* Ticks
- *Borrelia*, *Ehrlichia*, and *Rickettsia* spp. in Ticks, Texas
- *Legionella pneumophila* Serogroup 1 Clones, Ontario, Canada
- Invasive *Haemophilus influenzae* Disease, Europe, 1996–2006
- Vaccine Preventability of Meningococcal Clone, Germany
- Avian Bornavirus and Proventricular Dilatation Disease

- Climate Warming and Tick-borne Encephalitis, Slovakia
- Cost Analysis of West Nile Virus Outbreak, Sacramento County, California
- *Paenibacillus larvae* Bacteremia in Injection Drug Users
- *Rickettsia helvetica* in Patient with Meningitis, Sweden
- Influenza A (H3N2) Variants with Reduced Sensitivity to Antiviral Drugs
- *Sarcocystis* Species Lethal for Domestic Pigeons, Germany
- *Candidatus* Bartonella mayotimonensis and Endocarditis
- First-wave Pandemic (H1N1) 2009, Northern California
- Experimental Infection of Squirrel Monkeys with Nipah Virus
- Q Fever in Greenland
- Bluetongue Virus Serotypes 1 and 4 in Red Deer, Spain
- Spotted Fever Group Rickettsiosis, Brazil
- Kissing Bugs and *T. cruzi*, Arizona
- Banna Virus, China, 1987–2007



- Parvovirus 4–like Virus in Blood Products
- Terrestrial Rabies and Human Postexposure Prophylaxis, New York
- Skin Infections and *Staphylococcus aureus* Complications in Children, England
- Pandemic (H1N1) 2009 Virus Infection in Domestic Cat
- School Closure and Mitigation of Pandemic (H1N1) 2009, Hong Kong
- Global Origin of *Mycobacterium tuberculosis* in the Midlands, UK
- Quinine-Resistant Malaria in Traveler Returning from Senegal
- Putative New Lineage of West Nile Virus, Spain
- Venezuelan Equine Encephalitis and 2 Human Deaths, Peru
- Extensively Drug-Resistant *Mycobacterium tuberculosis* from Aspirates, South Africa
- Rhabdomyolysis and Pandemic (H1N1) 2009 Pneumonia in Adult
- *Yersinia pseudotuberculosis* and *Y. enterocolitica* Infections
- Measles Outbreak, the Netherlands, 2008
- Neurologic Manifestations of Pandemic (H1N1) 2009 Virus Infection



Density-Dependent Prevalence of *Francisella tularensis* in Fluctuating Vole Populations, Northwestern Spain

Ruth Rodríguez-Pastor, Raquel Escudero,
Dolors Vidal, François Mougeot, Beatriz Arroyo,
Xavier Lambin, Ave Maria Vila-Coro,
Isabel Rodríguez-Moreno, Pedro Anda,
Juan J. Luque-Larena

Tularemia in humans in northwestern Spain is associated with increases in vole populations. Prevalence of infection with *Francisella tularensis* in common voles increased to 33% during a vole population fluctuation. This finding confirms that voles are spillover agents for zoonotic outbreaks. Ecologic interactions associated with tularemia prevention should be considered.

Emerging infectious zoonotic diseases are increasing worldwide, and most zoonoses are linked to wildlife (1,2). Thus, quantifying disease prevalence in potential wildlife hosts is critical to understanding the outbreak dynamics of zoonoses (3). Tularemia, which is caused by *Francisella tularensis*, is a problematic zoonotic disease worldwide, but its ecology remains poorly understood. This pathogen is classified by the US Centers for Disease Control and Prevention as a class A bio-threat agent (*F. tularensis* subsp. *holarctica* in Europe) because only a few bacteria are needed to induce tularemia in humans or susceptible animal species (>250 hosts described) (4). However, the relative epidemiologic roles (i.e., reservoir, spillover, and amplification agents) for different hosts are uncertain.

A major hotspot for tularemia in Europe is northwestern Spain (Castilla and León region), where the largest recent outbreaks of the disease have been recorded (>1,000 officially confirmed human cases during 1997–1998 and 2007–2008) (5). In intensive farmlands in Europe, rodents

and lagomorphs are the main putative mammalian hosts (5,6), but most studies addressing the epidemiologic roles of these species have been correlative or used opportunistic sampling.

A recent study suggests that common voles (*Microtus arvalis*) are a key agent for human tularemia in northwestern Spain because of a spatial and temporal coincidence between human tularemia cases and increases in number of voles (5). Voles periodically fluctuate in density and can reach high numbers during specific periods in farming areas (5). Dead voles infected with *F. tularensis* subsp. *holarctica* have been reported in northwestern Spain during massive decreases in vole populations (7). If, as hypothesized (5), common voles are a key amplifying and spillover agent for tularemia in intensive farming areas in northwestern Spain, we should expect an increased prevalence of tularemia in voles as their numbers increase. Thus, it is crucial to empirically evaluate whether such a density-dependent pattern occurs in natural populations.

We obtained samples from live voles periodically collected during population increases (2013–2015) in northwestern Spain. Our goal was to determine how prevalence of *F. tularensis* in common voles varies with population density.

The Study

We complied with all necessary licenses and permits for conducting this study. During 2013–2015, a common vole population fluctuation, which peaked in 2014, was observed in agricultural areas of Castilla and León, Spain (8). This increase in vole numbers was moderate (in terms of peak density) compared with previous increases when tularemia outbreaks among humans were reported (1997–1998 and 2007–2008) by the National Network of Epidemiologic Surveillance of Spain (5,8). In 2014, no outbreak of tularemia was reported. However, there was a higher-than-average number of identified cases of tularemia ($n = 95$) among humans in the area (the regional average is 3 [range 0–11] cases/y, excluding outbreak years) (5).

To monitor vole abundance during the complete population fluctuation, we sampled 80 km² of farmland in Palencia Province, Spain (42°1'N, 4°42'W), where human tularemia cases have been reported (5,8). We live-trapped voles seasonally (every 4 months) during March 2013–March 2015.

Author affiliations: Universidad de Valladolid, Palencia, Spain (R. Rodríguez-Pastor, J.J. Luque-Larena); Instituto Universitario de Investigación en Gestión Forestal Sostenible, Palencia (R. Rodríguez-Pastor, J.J. Luque-Larena); Instituto de Salud Carlos III, Madrid, Spain (R. Escudero, A.M. Vila-Coro, I. Rodríguez-Moreno, P. Anda); Universidad de Castilla-La Mancha, Ciudad Real, Spain (D. Vidal); Instituto de Investigación en Recursos Cinégeticos del Consejo Superior de Investigaciones Científicas, Ciudad Real (F. Mougeot, B. Arroyo); University of Aberdeen, Aberdeen, Scotland, UK (X. Lambin)

DOI: <https://doi.org/10.3201/eid2308.161194>

Our vole trapping effort was constant (840 traps set for 24 h/seasonal sampling), and our sampling design was spatially stratified (we obtained random samples from 8 alfalfa fields, 8 grain fields, and 8 fallow fields at each seasonal sampling). Vole abundance was estimated as the number of captures/100 traps/24 h in each season. Trapping was extractive, and animals were brought alive to our laboratory in rodent cages provided with food, water, and bedding immediately after their capture. Voles were euthanized by using CO₂. Carcasses were individually frozen at -30°C.

We extracted DNA from a homogenized mixture of liver and spleen (≈25 mg). DNA was extracted by using standard procedures (QIAamp DNA Mini Kit; QIAGEN, Valencia, CA, USA). A phylogenetically informative region of the lipoprotein A (*lpaA*) gene (231 bp) was amplified by conventional PCR and hybridized with specific probes by reverse-line blotting as described (9). We tested positive samples by using a real-time multitarget TaqMan PCR and *tul4* and *ISFtu2* assays (10). Negative controls for PCR and DNA extraction were included in each group of samples processed. We used R 3.2.4 software (<https://stat.ethz.ch/pipermail/r-announce/2016/000597.html>) for statistical analyses.

We tested 243 live voles and found an average prevalence of *F. tularensis* of 20.16%. Prevalence greatly varied between samplings (range 0%–33%) and was strongly related to vole abundance (generalized linear model, $\chi^2 = 21.64$, $df = 1$, $p < 0.001$) with a direct and positive density-dependent association (Figure). The predicted odds of tularemia infection increased by 1.037 (95% CI 1.021–1.056) when vole density increased by +1 captured vole/100 traps/24 h (range during the study 1–60 voles/100 traps/24 h). During the vole population peak in July 2014, a total of 34 (33%) of 102 sampled live voles were infected with *F. tularensis*.

Conclusions

We report a direct and positive density-dependent association between prevalence of *F. tularensis* in common voles and their abundance in agricultural landscapes. These findings are consistent with vole-to-vole transmission and amplification of the bacterium as vole density increases. Voles experimentally infected with *F. tularensis* die within a few days after rapid acute infection and generally show high bacterial loads in organs (11). Thus, transmission between voles might involve direct contact, cannibalism, or contamination of the environment. In our study, all voles tested were alive and free of obvious signs of disease when captured, which implied that prevalence could be higher than what we estimated if moribund voles were less trappable and underrepresented in trapped animals.

The role that exogenous sources (i.e., other animals, environmental sources) might play in modulating infection prevalence among vole populations still needs to be

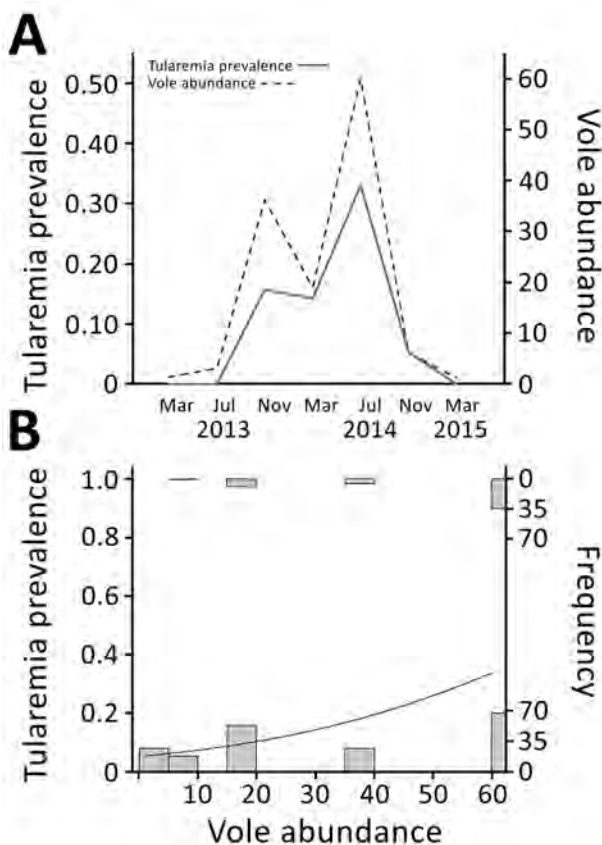


Figure. Vole abundance and tularemia prevalence, northwestern Spain. A) Temporal variations in vole abundance (no. captures/100 traps/24 h) and tularemia prevalence. Four voles were tested in March 2013, 15 in July 2013, 32 in November 2013, 63 in March 2014, 102 in July 2014, 19 in November 2014, and 8 in March 2015. B) Relationship between tularemia prevalence and vole abundance. Histograms show number of positive (top) or negative (bottom) voles sampled at each level of vole density. Curved line indicates a generalized linear model result.

clarified. Notwithstanding and irrespective of the precise mechanism(s) of transmission, our results support the hypothesis that exponential growth of common vole populations is crucial for amplification of tularemia transmission in farmlands, and that increases in vole populations are linked to periodic emergence of human cases of tularemia in Spain (5). Vole density can reach >1,000 voles/hectare (i.e., >300 tularemia-infected voles/hectare) during outbreaks, potentially leading to contamination of the environment and other wildlife, including harvestable species, such as crayfish and hares, which have higher contact rates with humans than voles (5).

Tularemia is probably not completely enzootic in vole populations because we did not detect *F. tularensis* at low densities of voles, which suggests involvement of animal or environmental reservoirs. A key unknown facet of the

ecologic cycle of *F. tularensis* is where does it persist between epizootic periods (5,6). There is no evidence for *F. tularensis* replication in arthropods. However, ticks might be a reservoir of this pathogen because they have life-long infections. Thus, mammalian populations are probably needed to amplify tularemia in the environment (11).

Characteristic spatial and social behaviors of voles, including increased contact rates, aggression, and wounding, during massive population increases readily account for amplification of disease transmission rates and spread (5,12). Although reservoir and vector hosts of *F. tularensis* at variable densities can play major roles in the ecologic cycle of tularemia in different ecosystems, there appears to be a common link between tularemia outbreaks and rodent population fluctuations across Europe (5,6,11,13).

Common voles are useful for surveillance of tularemia, and strategic prevention programs should incorporate their temporal fluctuations in planned preventive actions. Because vole numbers seem to modulate the risk for disease exposure in humans, monitoring vole population dynamics can help anticipate and increase awareness of the risk for tularemia in rural areas of Spain.

J.J.L.L., F.M., and R.R.P. held official licenses for trapping wildlife in Spain. Capture permits were provided by the Dirección General del Medio Natural, Junta de Castilla y León.

This study was supported by projects ECOVOLE (grant CGL2012-35348), ECOTULA (grant CGL2015-66962-C2-1-R), and RESERTULA (grant CLG2015-66962-C2-2-R), which were funded by the Ministerio de Economía y Competitividad MINECO/FEDER, Spain. R.R.P. was supported by a PhD studentship from the University of Valladolid (co-funded by Banco Santander).

Ms. Rodríguez-Pastor is a biologist and doctoral candidate in the Department of Agroforestry Sciences, University of Valladolid, Palencia, Spain. Her primary research interests are ecology of zoonoses and disease dynamics in animal populations.

References

1. Karesh WB, Dobson A, Lloyd-Smith JO, Lubroth J, Dixon MA, Bennett M, et al. Ecology of zoonoses: natural and unnatural histories. *Lancet*. 2012;380:1936–45. [http://dx.doi.org/10.1016/S0140-6736\(12\)61678-X](http://dx.doi.org/10.1016/S0140-6736(12)61678-X)
2. Han BA, Schmidt JP, Bowden SE, Drake JM. Rodent reservoirs of future zoonotic diseases. *Proc Natl Acad Sci U S A*. 2015;112:7039–44. <http://dx.doi.org/10.1073/pnas.1501598112>
3. Walton L, Marion G, Davidson RS, White PCL, Smith LA, Gavier-Widen D, et al. The ecology of wildlife disease surveillance: demographic and prevalence fluctuations undermine surveillance. *J Appl Ecol*. 2016;53:1460–9. <http://dx.doi.org/10.1111/1365-2664.12671>
4. World Health Organization. Guidelines on tularaemia. Geneva: The Organization; 2007 [cited 2017 May 3]. <http://www.who.int/iris/handle/10665/43793>
5. Luque-Larena JJ, Mougeot F, Roig DV, Lambin X, Rodríguez-Pastor R, Rodríguez-Valín E, et al. Tularemia outbreaks and common vole (*Microtus arvalis*) irruptive population dynamics in northwestern Spain, 1997–2014. *Vector Borne Zoonotic Dis*. 2015;15:568–70. <http://dx.doi.org/10.1089/vbz.2015.1770>
6. Gyuranecz M, Reiczigel J, Krisztalovics K, Monse L, Szabóné GK, Szilágyi A, et al. Factors influencing emergence of tularemia, Hungary, 1984–2010. *Emerg Infect Dis*. 2012;18:1379–81. <http://dx.doi.org/10.3201/eid1808.111826>
7. Vidal D, Alzaga V, Luque-Larena JJ, Mateo R, Arroyo L, Viñuela J. Possible interaction between a rodenticide treatment and a pathogen in common vole (*Microtus arvalis*) during a population peak. *Sci Total Environ*. 2009;408:267–71. <http://dx.doi.org/10.1016/j.scitotenv.2009.10.001>
8. Luque-Larena JJ, Mougeot F, Viñuela J, Jareño D, Arroyo L, Lambin X, et al. Recent large-scale range expansion and outbreaks of the common vole (*Microtus arvalis*) in NW Spain. *Basic and Applied Ecology*. 2013;14:432–41. <http://dx.doi.org/10.1016/j.baae.2013.04.006>
9. Escudero R, Toledo A, Gil H, Kováčsová K, Rodríguez-Vargas M, Jado I, et al. Molecular method for discrimination between *Francisella tularensis* and *Francisella*-like endosymbionts. *J Clin Microbiol*. 2008;46:3139–43. <http://dx.doi.org/10.1128/JCM.00275-08>
10. Versage JL, Severin DD, Chu MC, Petersen JM. Development of a multitarget real-time TaqMan PCR assay for enhanced detection of *Francisella tularensis* in complex specimens. *J Clin Microbiol*. 2003;41:5492–9. <http://dx.doi.org/10.1128/JCM.41.12.5492-5499.2003>
11. Rossow H, Forbes KM, Tarkka E, Kinnunen PM, Hemmilä H, Huitu O, et al. Experimental infection of voles with *Francisella tularensis* indicates their amplification role in tularemia outbreaks. *PLoS One*. 2014;9:e108864. <http://dx.doi.org/10.1371/journal.pone.0108864>
12. Ostfeld RS, Mills JN. Social behavior, demography, and rodent-borne pathogens. In: Wolff JO, Sherman PW, editors. *Rodent societies: an ecological and evolutionary perspective*. Chicago: University of Chicago Press; 2007. p. 478–86.
13. Rossow H, Ollgren J, Hytönen J, Rissanen H, Huitu O, Henttonen H, et al. Incidence and seroprevalence of tularaemia in Finland, 1995 to 2013: regional epidemics with cyclic pattern. *Euro Surveill*. 2015;20:21209. <http://dx.doi.org/10.2807/1560-7917.ES2015.20.33.21209>

Address for correspondence: Juan J. Luque-Larena, Departamento de Ciencias Agroforestales, Escuela Técnica Superior de Ingenierías Agrarias, Universidad de Valladolid, Avenida de Madrid 44, Palencia, E-34004, Spain; email: j.luque@agro.uva.es

Occupational Exposures to Ebola Virus in Ebola Treatment Center, Conakry, Guinea

**Hélène Savini, Frédéric Janvier,
Ludovic Karkowski, Magali Billhot, Marc Aletti,
Julien Bordes, Fassou Koulibaly,
Pierre-Yves Cordier, Jean-Marie Cournac,
Nancy Maugey, Nicolas Gagnon, Jean Cotte,
Audrey Cambon, Christine Mac Nab,
Sophie Morage, Claire Rousseau,
Vincent Foissaud, Thierry De Greslan,
Hervé Granier, Gilles Cellarier, Eric Valade,
Philippe Kraemer, Philippe Alla, Audrey Mérens,
Emmanuel Sagui, Thierry Carmoi,
Christophe Rapp**

We report 77 cases of occupational exposures for 57 healthcare workers at the Ebola Treatment Center in Conakry, Guinea, during the Ebola virus disease outbreak in 2014–2015. Despite the high incidence of 3.5 occupational exposures/healthcare worker/year, only 18% of workers were at high risk for transmission, and no infections occurred.

Occupational infections during the West Africa Ebola virus disease (EVD) outbreak in 2014–2015 were a major concern because this outbreak caused 109 deaths among the healthcare workers in Guinea (1). There was also international concern when secondary cases occurred in Spain and the United States (2,3).

The Healthcare Workers Treatment Center in Conakry, Guinea, sought to diagnose and treat healthcare

Author affiliations: French Military Teaching Hospital Laveran, Marseille, France (H. Savini, P.-Y. Cordier, S. Morage, P. Kraemer, E. Sagui); French Military Teaching Hospital Saint Anne, Toulon, France (F. Janvier, J. Bordes, J. Cotte, G. Cellarier, P. Alla); French Military Teaching Hospital Legouest, Metz, France (L. Karkowski, N. Gagnon); French Military Teaching Hospital Val de Grâce, Paris, France (M. Billhot, A. Cambon, T. De Greslan, T. Carmoi); French Military Teaching Hospital Percy, Clamart, France (M. Aletti, J.-M. Cournac, C. Mac Nab, V. Foissaud); Guinean Military Health Services, Conakry, Guinea (F. Koulibaly); Frégate Européenne Multi-Mission Aquitaine, Bordeaux Consortium for Regenerative Medicine, Brest, France (N. Maugey); French Military Teaching Hospital Clermont Tonnerre, Brest, France (C. Rousseau, H. Granier); Institut de Recherche Biomédicale des Armées, Brétigny sur Orge, France (E. Valade); French Military Teaching Hospital Bégin, Saint Mandé, France (A. Mérens, C. Rapp)

DOI: <https://doi.org/10.3201/eid2308.161804>

workers with suspected or proven EVD by offering extensive medical care (e.g., blood or plasma transfusions, central venous catheterization, biologic monitoring). This center had 5 persons with suspected EVD and 9 persons with confirmed EVD.

The first objective of this study was to describe the occupational exposures occurring in the Healthcare Workers Treatment Center. The second objective was to analyze factors associated with the frequency of high-risk exposures.

The Study

A total of 66 volunteers from the French Armed Forces Medical Service worked in the high-risk zone for EVD. These volunteers wore personal protective equipment (PPE): coveralls with hoods, large goggles, waterproof respirator masks that filter $\geq 94\%$ of airborne particles, waterproof overshoes, a double pair of nitrile gloves, and a third pair of latex gloves. They followed preliminary biosafety training on basic rules, prevention of percutaneous injuries, and management of incidents in exposed or infected areas (e.g., skin exposure, body fluid projection, fainting). Because removal of PPE was considered the highest risk for virus transmission (4), we opted for PPE removal by protected persons trained to undress persons without spraying the high-risk zone with bleach.

We conducted a descriptive prospective study during January 23–May 8, 2015, of all occupational exposures in the high-risk zone and reported by a healthcare worker. Occupational exposure was defined as any malfunction of PPE or any noncompliance of biosafety protocols in the high-risk zone. Incidental and demographic data, risk evaluation, and interventions were obtained by using a standardized questionnaire for all reported exposures.

When an exposure occurred, the exposed healthcare worker had to report the exposure to the physician at the Healthcare Workers Treatment Center. This physician used a detailed questionnaire to obtain information on conditions of exposure and evaluated the risk for transmission as low or high, as per French recommendations (Table 1) (5). On the basis of results of this evaluation, clinical monitoring or postexposure prophylaxis (PEP) with favipiravir was prescribed. Correlates of risk exposure were examined by using the χ^2 test for categorical variables and the Mann-Whitney test for continuous variables.

A total of 22 healthcare workers from Guinea with confirmed EVD were treated in the Healthcare Workers

Table 1. Risk levels of transmission factors for Ebola virus disease for healthcare workers, Conakry, Guinea*

Exposure	Risk level	
	EVD with diarrhea, vomiting, and hemorrhaging	EVD without diarrhea, vomiting, and hemorrhaging
Contact (≥ 1 m) with patients not projecting biological fluids	Low	Low
Close contact (< 1 m) with patients not projecting biological fluids	Low	High
Direct contact with biological fluids	High	High
Cumulative incidents during removal of PPE	Low	High
Transcutaneous or mucosal exposure to infected biological fluids	Maximum	Maximum

*Adapted from recommendations of the French High Council on Public Health (5). EVD, Ebola virus disease; PPE, personal protective equipment.

Treatment Center during the study. These workers represented 85% of infected healthcare workers from Guinea during the same period. Six of these workers died (mortality rate 27%). None of them worked in an Ebola Treatment Center but all were infected in their community or in other public/private healthcare facilities when not using PPE. During January 23–May 8, 2015, healthcare workers from France at the Healthcare Workers Treatment Center had 3,081 encounters with the high-risk zone for EVD. A total of 77 cases of occupational exposures in the high-risk zone were reported by 57 healthcare workers (30 nurses) from France, which represented an incidence of 2.5% (3.5 occupational exposures/worker/y) (Table 2). Most (62, 80.6%) workers had a low risk for virus transmission.

The most frequent type of exposure incident ($n = 63$) was exposure of healthy skin on the face because goggles or respirator masks did not stay correctly in place during patient care. Only 4 healthcare workers reported problems during removal of PPE. Only 14 high-risk occupational

exposures were reported; 11 were exposures of healthy skin ≤ 1 m from a patient projecting biologic fluid, 2 were projections of biologic fluids to healthy skin, and 1 was fluid projection to mucous membranes. This final incident occurred during discharge of a cured patient who had an undetectable viral load. Percutaneous exposure did not occur during the study period.

Age, sex, carrying glasses, activity, experience with an activity, duration of the activity in the high-risk zone, exposure time, and time of the study were not associated with a higher frequency of high-risk exposure. The only factor associated with high-risk exposure was obtaining a blood sample ($p = 0.016$). Most (72.7%) occupational exposures occurred during the first month of the study. For all exposures, skin disinfection with 0.05% sodium hypochlorite and monitoring of body temperature were initiated. PEP with favipiravir was not used, and no patients were evacuated to France. EVD did not develop in healthcare workers at the Healthcare Workers

Table 2. Characteristics of 77 occupational exposures for healthcare workers at Ebola Treatment Center, Conakry, Guinea, January–May 2015*

Characteristic	Total, n = 77	Low risk, n = 62	High risk, n = 15
Exposure			
Healthy skin ≥ 1 m from patient†	52 (67.5)	52 (83.9)	0
Healthy skin < 1 m from patient†	11 (14.3)	0	11 (73.3)
Mucous membrane > 1 m from patient	1 (1.3)	1 (1.6)	0
Undressing patient	6 (7.8)	6 (9.7)	0
Fluid projection on healthy skin†	2 (2.6)	0	2 (13.3)
Fluid projection on mucous membrane	1 (1.3)	0	1 (6.7)
Percutaneous exposure	0	0	0
Other	4 (5.2)	3 (4.8)	1 (6.7)
Exposed worker activity†			
Fluid management	26 (33.8)	21 (33.9)	5 (33.3)
Patient care or clinical examination	35 (45.5)	28 (45.2)	7 (46.7)
Blood sampling†	13 (16.9)	7 (11.3)	6 (40.0)
Supervision	6 (7.8)	4 (6.5)	2 (13.3)
Undressing patient	9 (11.7)	9 (14.5)	0
Other	5 (6.5)	4 (6.5)	1 (6.7)
Mean activity duration, min			
	53.5	53.9	52
Exposure time interval			
6:00 AM–10:00 AM	30 (39.0)	24 (38.7)	6 (40.0)
10:01 AM–4:00 PM	16 (20.8)	11 (17.7)	5 (33.3)
4:01 PM–8:00 PM	21 (27.3)	18 (29.0)	3 (20.0)
8:01 PM–5:59 AM	9 (11.7)	8 (12.9)	1 (6.7)
No data	1 (1.3)	1 (1.6)	0
Time of exposure			
First month	56 (72.7)	45 (72.6)	11 (73.3)
Last month	21 (27.3)	17 (27.4)	4 (26.7)

*Values are no. (%). Unless otherwise indicated.

†Associated with high risk of virus transmission ($p < 0.05$).

‡ > 1 activity was possible.

Treatment Center during the study or after they returned from Guinea to France.

Conclusions

To our knowledge, there are few data regarding occupational exposures in a medical facility caring for EVD patients. Limited data are available for potential occupational exposures in an Ebola Treatment Center (6). Rare cases of EVD in healthcare workers have been reported from Africa (7–9) or other areas (2,3,9). However, all healthcare workers from Guinea who we treated were infected in their communities or when providing care in other healthcare facilities (7,8). In the Healthcare Workers Treatment Center, we observed a high incidence of 3.5 occupational exposures/healthcare worker/year, which was much higher than the incidence of 0.077 occupational exposures/nurse/year typically observed in hospitals in France (10). This high incidence was responsible of excessive concern by some of the healthcare workers from France. However, this concern should be balanced by the low risk for Ebola virus transmission for each exposure.

Classification of transmission risk was difficult. The French recommendations (5) were established for exposures in hospitals in France and were not adapted for poorly equipped hospitals (e.g., the Healthcare Workers Treatment Center was composed of tents and direct contact with infected walls was frequent because of lack of space and displacement of goggles or masks). Data show that infection with Ebola virus from environment is possible (11). More than 80% of occupational exposures were at low risk for virus transmission and did not justify prescription of antiviral treatment, such as favipiravir, which has been used to prevent EVD infection despite lack of data concerning its efficiency (12–14). A large part of skin exposure should be avoided by improving PPE and limiting activities could displace goggles or masks.

We observed various circumstances that could affect exposure to Ebola virus. In contrast to what we expected (4), exposure incidents during removal of PPE were rare, probably because healthcare workers are extensively trained for this activity. Thus, an increase in infections was not observed. No demographic, professional, or incidental factors were associated with a higher frequency of risk exposure. Obtaining a blood sample was a high-risk activity because this can be a stressful procedure and because of constraints associated with PPE, such as an increased core body temperature (15).

Technical training for healthcare workers dealing with EVD patients should be increased. A large number of occupational exposures occurred in the first month of the study, which showed that more technical experience could decrease the risk for infection. Despite the high incidence of occupational exposures, no infections occurred

during or after the study, which showed that countermeasures we implemented were efficient in preventing virus transmission. Nosocomial transmission of Ebola virus can be avoided by appropriate materials, reliable biosafety protocols, and training. These suggestions could explain why only a few cases of transmission at the Ebola Treatment Center were observed. However, improvements in PPE components, training of healthcare workers, and PEP strategy are required to face future outbreaks of virus diseases.

Acknowledgments

We thank all healthcare workers at the Healthcare Workers Treatment Center and the Health Supplies Center of the French Military Health Service for support, participation, and assistance.

Dr. Savini is medical practitioner in the unit of infectious and tropical disease, Military Teaching Hospital of Laveran, Marseille, France. Her primary research interest is travel medicine, notably imported malaria.

References

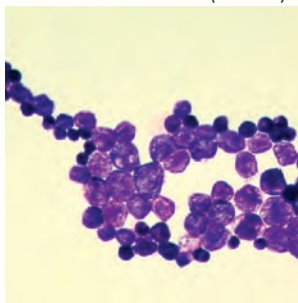
1. World Health Organization. Health workers Ebola infections in Guinea, Liberia, and Sierra Leone. A preliminary report [cited 2015 May 21]. http://apps.who.int/iris/bitstream/10665/171823/1/WHO_EVD_SDS_REPORT_2015.1_eng.pdf
2. Lopaz MA, Amela C, Ordobas M, Dominguez-Berjon MF, Alvarez C, Martinez M, et al. Working group of Ebola outbreak investigation team of Ma=drid. *Euro Surveill.* 2015;20:pii=21003.
3. Liddell AM, Davey RT Jr, Mehta AK, Varkey JB, Kraft CS, Tseggay GK, et al. Characteristics and clinical management of a cluster of 3 patients with Ebola virus disease, including the first domestically acquired cases in the United States. *Ann Intern Med.* 2015;163:81–90. <http://dx.doi.org/10.7326/M15-0530>
4. Zellmer C, Van Hoof S, Safdar N. Variation in health care worker removal of personal protective equipment. *Am J Infect Control.* 2015;43:750–1. <http://dx.doi.org/10.1016/j.ajic.2015.02.005>
5. French High Council on Public Health. Advice relative to the management of an occupational exposure from a patient with suspected of proven Ebola viral disease [in French] [cited 2014 Dec 4]. <http://www.hsep.fr>
6. Mulligan MJ, Siebert PN. Era of global Ebola: risk of exposure in health-care workers. *Lancet Infect Dis.* 2015;15:1248–9. [http://dx.doi.org/10.1016/S1473-3099\(15\)00291-1](http://dx.doi.org/10.1016/S1473-3099(15)00291-1)
7. Grinnell M, Dixon MG, Patton M, Fitter D, Bilivogui P, Johnson C, et al. Ebola virus disease in health care workers—Guinea, 2014. *MMWR Morb Mortal Wkly Rep.* 2015;64:1083–7. <http://dx.doi.org/10.15585/mmwr.mm6438a6>
8. Olu O, Kargbo B, Kamara S, Wurie AH, Amone J, Ganda L, et al. Epidemiology of Ebola virus disease transmission among health care workers in Sierra Leone, May to December 2014: a retrospective descriptive study. *BMC Infect Dis.* 2015;15:416. <http://dx.doi.org/10.1186/s12879-015-1166-7>
9. Forrester JD, Hunter JC, Pillai SK, Arwady MA, Ayscue P, Matanock A, et al. Cluster of Ebola cases among Liberian and U.S. health care workers in an Ebola treatment unit and adjacent hospital—Liberia, 2014. *MMWR Morb Mortal Wkly Rep.* 2014;63:925–9.
10. Tarantola A, Golliot F, Astagneau P, Fleury L, Brücker G, Bouvet E; CCLIN Paris-Nord Blood and Body Fluids (BBF) Exposure Surveillance Taskforce. Occupational blood and body fluids

- exposures in health care workers: four-year surveillance from the northern France network. *Am J Infect Control*. 2003;31:357–63. [http://dx.doi.org/10.1016/S0196-6553\(03\)00040-3](http://dx.doi.org/10.1016/S0196-6553(03)00040-3)
11. Youkee D, Brown CS, Lilburn P, Shetty N, Brooks T, Simpson A, et al. Assessment of environmental contamination and environmental decontamination practices within an Ebola holding unit, Freetown, Sierra Leone. *PLoS One*. 2015;10:e0145167. <http://dx.doi.org/10.1371/journal.pone.0145167>
 12. Smither SJ, Eastaugh LS, Steward JA, Nelson M, Lenk RP, Lever MS. Post-exposure efficacy of oral T-705 (favipiravir) against inhalational Ebola virus infection in a mouse model. *Antiviral Res*. 2014;104:153–5. <http://dx.doi.org/10.1016/j.antiviral.2014.01.012>
 13. Van Herp M, Declercq H, Decroo T. Favipiravir—a prophylactic treatment for Ebola contacts? *Lancet*. 2015;385:2350. [http://dx.doi.org/10.1016/S0140-6736\(15\)61095-9](http://dx.doi.org/10.1016/S0140-6736(15)61095-9)
 14. Jacobs M, Aarons E, Bhagani S, Buchanan R, Cropley I, Hopkins S, et al. Post-exposure prophylaxis against Ebola virus disease with experimental antiviral agents: a case-series of health-care workers. *Lancet Infect Dis*. 2015;15:1300–4. [http://dx.doi.org/10.1016/S1473-3099\(15\)00228-5](http://dx.doi.org/10.1016/S1473-3099(15)00228-5)
 15. Grélot L, Koulibaly F, Maugey N, Janvier F, Foissaud V, Aletti M, et al. Moderate thermal strain in healthcare workers wearing personal protective equipment during treatment and care activities in the context of the 2014 Ebola virus disease outbreak. *J Infect Dis*. 2015.

Address for correspondence: Helene Savini, Department of Infectious and Tropical Disease, French Military Teaching Hospital Laveran, 34 Bd Laveran, 13013 Marseille, France; email: helene.savini13@gmail.com

July 2009: Vectorborne Diseases

- Sylvatic Epidemic Typhus Associated with Flying Squirrels
- Host Species Diversity and Prevalence of Sin Nombre Virus
- Lymphocytic Choriomeningitis Virus in Wild Rodents, Northern Italy
- Tick-borne Relapsing Fever and *Borrelia hermsii*, Los Angeles County, California, USA
- Risk Factors for Human Infection with Puumala Virus, Southwestern Germany
- Invasions by Eurasian Avian Influenza Virus H6 Genes and Replacement of the Virus' North American Clade
- Multiple Origins of Foot-and-Mouth Disease Virus Serotype Asia 1 Outbreaks
- Clusters of Multidrug-Resistant *Mycobacterium tuberculosis* Cases, Europe
- Relapse Associated with Active Disease Caused by Beijing Strain of *Mycobacterium tuberculosis*
- Azole Resistance in *Aspergillus fumigatus* Associated with Treatment Failure
- Co-infections with Chikungunya Virus and Dengue Virus in Delhi, India
- Influenza Virus A (H1N1) in Giant Anteaters



- Lack of Macrolide Resistance in *Chlamydia trachomatis* after Azithromycin Distributions
- Intergenogroup Recombinant Sapovirus in Japan, 2007–2008
- *Arcanobacterium pyogenes* Sepsis in Farmer, Brazil



- Coronaviruses in Wild Bird Populations of Northern England
- WU Polyomavirus in Patients Infected with HIV or Hepatitis C Virus, Connecticut, USA
- Methicillin-Resistant *Staphylococcus aureus* ST398 in Swine Farm Personnel, Belgium
- Eczema Herpeticum and Clinical Criteria for Investigating Smallpox
- *Rickettsia slovaca* and *R. raoultii* in Tick-borne Rickettsioses
- Scrub Typhus, South Korea, 2001–2006
- Latent Tuberculosis and Active Disease Rates among the Homeless, New York, New York, USA
- Chinese-like Strain of Porcine Epidemic Diarrhea Virus, Thailand
- Human T-cell Lymphotropic Virus Type 1 Infection in Blood Donors, Israel
- Recurrent Lymphocytic Meningitis and Herpes Simplex Virus Type 2
- Possible Streptomycin-Resistant *Mycobacterium tuberculosis* Beijing, Benin
- *Rickettsia felis* Infection in Man, France
- Fatal Algaemia and Chronic Lymphocytic Leukemia
- Reactivation of Bovine Tuberculosis in Patient Treated with Infliximab



Serologic Evidence of Powassan Virus Infection in Patients with Suspected Lyme Disease¹

Holly M. Frost, Anna M. Schotthoefer, Angela M. Thomm, Alan P. Dupuis II, Sue C. Kehl, Laura D. Kramer, Thomas R. Fritsche, Yvette A. Harrington, Konstance K. Knox

Powassan virus (POWV) lineage II is an emerging tick-borne flavivirus with an unknown seroprevalence in humans. In a Lyme disease–endemic area, we examined the seroreactivity to POWV in 2 patient cohorts and described the clinical features of the POWV-seroreactive patients. POWV disease might be less neuroinvasive than previously thought.

Powassan virus (POWV) lineage II, also known as deer tick virus, is an emerging tickborne flavivirus (*I*) transmitted by *Ixodes scapularis* ticks, which are also the primary vector for *Borrelia burgdorferi* (Lyme disease pathogen). In POWV-endemic regions, up to 7% of ticks carry the virus, and seroprevalence among small mammalian hosts can exceed 90% (2,3). Because the territory of *I. scapularis* is expanding and the prevalence of POWV in ticks and mammals is increasing, POWV poses an increasing threat (2–5). The seroprevalence of POWV in humans in some regions of North America is known (range 0.5%–3.3%), but because the geographic distribution is quite extensive, the seroprevalence of most at-risk populations is uncertain (6).

POWV is typically detected with an IgM antibody capture ELISA or an IgM immunofluorescence antibody (IFA) assay. Cases are confirmed by $\geq 90\%$ or $\geq 50\%$ plaque reduction neutralization test (PRNT₉₀ or PRNT₅₀), detection of virus-specific nucleic acids, isolation in culture, or a ≥ 4 -fold increase in antibody titers from paired acute and convalescent sera (7–9). Using these assays, investigators have identified ≈ 100 cases of POWV encephalitis; however, the actual incidence is likely higher (1,6).

Although nonneuroinvasive disease has been described for other arboviral illnesses, our knowledge of POWV has been limited to patients with neuroinvasive disease (1,8,10,11). In this study, we evaluated the seroreactivity for POWV in US Midwest patients, many of whom did not have neuroinvasive disease.

The Study

We selected patients with suspected tickborne disease (TBD; $n = 95$) and patients undergoing routine chemical screening ($n = 50$) who sought treatment during July–August 2015 at the Marshfield Clinic in northern Wisconsin, a TBD-endemic area. Patients were considered to have suspected TBD if a serologic test for *B. burgdorferi* was ordered. The chemical screening cohort included patients who had a complete metabolic or lipid panel ordered as part of their clinical care. We evaluated POWV seroreactivity of specimens from these patient cohorts and, of the patients with serologic evidence of POWV infection and available clinical data, described the clinical features of their disease. All human subject research protocols were approved by the Marshfield Clinic Research Institute Institutional Review Board.

We performed screening assays on all specimens for tick-borne encephalitis virus complex (TBEV-C) and *B. burgdorferi* and performed POWV serology on TBEV-C–positive specimens (Figure; detailed methods in online Technical Appendix, <https://wwwnc.cdc.gov/EID/article/23/8/16-1971-Techapp1.pdf>). To evaluate heterologous flavivirus cross-reactivity, we performed the West Nile virus (WNV) enzyme immunoassay (EUROIMMU, Mountain Lakes, NJ, USA) with TBEV-C–positive samples. We also performed the Flavivirus Mosaic Panel (EUROIMMUN), an IgG IFA assay panel including tests for TBEV, WNV, yellow fever virus, dengue viruses 1–4, and Japanese encephalitis virus, on samples positive for POWV IgG by the IFA assay. Patient vaccination status and travel history were also considered.

Clinical data were available for 51 (53.7%) TBD patients and 50 (100%) patients with routine chemistry screening completed. For those with clinical data available, we classified their cases as probable or confirmed by using the Centers for Disease Control and Prevention case

Author affiliations: Marshfield Clinic Research Foundation, Minocqua, Wisconsin, USA (H.M. Frost); Marshfield Clinic Research Foundation, Marshfield, Wisconsin, USA (H.M. Frost, A.M. Schotthoefer, T.R. Fritsche); Coppe Laboratories, Waukesha, Wisconsin, USA (A.M. Thomm, Y.A. Harrington, K.K. Knox); New York State Department of Health, Slingerland, New York, USA (A.P. Dupuis II, L.D. Kramer); Medical College of Wisconsin, Milwaukee, Wisconsin, USA (S.C. Kehl)

DOI: <https://doi.org/10.3201/eid2308.161971>

¹Preliminary results from this study were presented at IDWeek; October 26–30, 2016; New Orleans, Louisiana, USA.

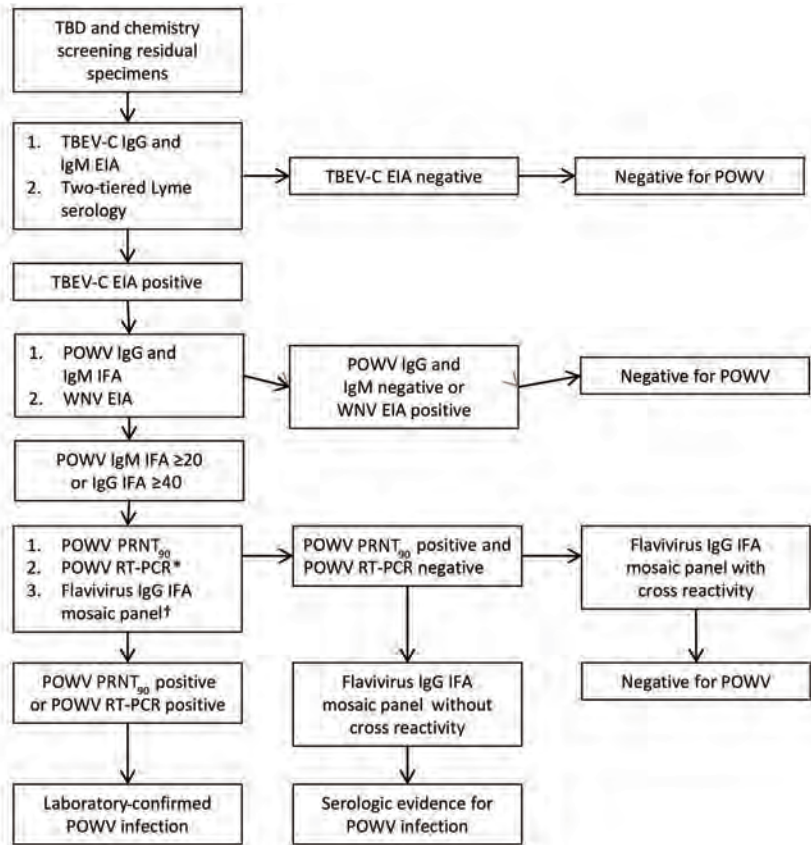


Figure. Flow chart showing series of tests performed on specimens obtained from patients with suspected TBD and patients undergoing routine chemical screening to determine POWV seroreactivity, Wisconsin, July–August 2015. *Performed for TBD samples positive for POWV IgG or IgM and chemical screening samples positive for POWV IgM by IFA assay. †Performed for samples positive for POWV IgG by IFA assay. EIA, enzyme immunoassay; IFA, immunofluorescence antibody assay; POWV, Powassan virus; PRNT₉₀, ≥90% plaque reduction neutralization test; RT-PCR, reverse transcription PCR; TBD, tickborne disease; TBEV-C, tick-borne encephalitis virus complex; WNV, West Nile virus.

definitions (7). We performed statistical analysis with SAS 9.3 (SAS Institute, Inc., Cary NC, USA) and compared categorical variables by using Fisher exact tests. Significance was defined as $p < 0.05$.

Serologic evidence of POWV infection was present in 9 (9.5%) TBD patients and 2 (4.0%) patients with routine chemistry screening completed ($p = 0.33$) (Table 1). POWV infection was confirmed in 3 (3.2%) TBD patients (2 by

Table 1. TBEV-C and *Borrelia burgdorferi* serologic test results and POWV RT-PCR test results of patients with positive POWV IFA assay results, Wisconsin, July–August 2015*

Patient no.	TBEV-C IgM EIA	TBEV-C IgG EIA	POWV IgM IFA assay†	POWV IgG IFA assay‡	POWV PRNT§	POWV RT-PCR¶	<i>B. burgdorferi</i> #
Suspected TBD patients							
1**††	–	+	–	+	–	–	–
2††	–	+	–	+	+	–	IgG and IgM
3††	+	–	+	–	–	–	IgG and IgM
4††	+	–	+	–	–	–	IgG and IgM
5	+	–	+	–	–	+	–
6	+	–	+	–	–	–	IgG and IgM
7	+	–	+	–	–	–	IgM
8	+	+	+	+	+	–	IgG and IgM
9††	+	–	+	–	–	–	IgG and IgM
Patients screened by chemical methods							
1c	+	–	–	+	–	NA	–
2c††	+	+	+	+	–	NA	–

*EIA, enzyme immunoassay; IFA, immunofluorescence antibody; NA, not assayed; POWV, Powassan virus; PRNT, plaque reduction neutralization test; PRNT₉₀, ≥90% plaque reduction neutralization test; RT-PCR, reverse transcription PCR; TBD, tickborne disease; TBEV-C, tick-borne encephalitis virus complex.

†Titers ≥1:20 were considered positive.

‡Titers ≥1:40 were considered positive.

§Positive if sample had a PRNT₉₀ titer.

¶Not performed in specimens with a negative POWV IgM IFA assay result.

#Samples were screened by EIA and followed up by Western blot.

**Cross-reactivity on POWV IgG IFA assay is consistent with a history of West Nile virus infection.

††Clinical data were available.

PRNT₉₀ [titer range 1:160–1:320] and 1 by reverse transcription PCR) and 0 chemical screening patients (p = 0.55). Of the 3 patients with confirmed POWV infection, evidence

of acute infection (IgM positivity) was found in 2 (2.7%). Patients positive only for IgM by IFA assay did not have PRNT₉₀ titers, which was expected because neutralizing

Table 2. Clinical features and histories of patients with positive POWV IFA assay results, Wisconsin, July–August 2015*

Patient no.	POWV test results	<i>Borrelia burgdorferi</i> test results†	Clinical features	Comorbidities	CDC case classification	Travel history	Location of tick exposure‡	Vaccine history§
Suspected TBD patients								
1¶	IgG >1:40	IgG and IgM	56-year-old man with 2-wk history of erythema migrans. Treated with doxycycline for 14 d.	Metabolic syndrome, hypertension, 9 y previous had WNV infection		–	Midwest	–
2	IgG >1:40, PRNT 1:160	IgG and IgM	53-year-old man with 3-d history of urticarial rash, malaise, fever, and fatigue. Patient had chills 3 wks prior that resolved. CBC results: leukocytes $7.3 \times 10^9/L$, Hb 13.6 g/dL, Hct 39.9%, Plt count $322 \times 10^3/\mu L$; CRP 3.9 nmol/L. PCR neg for <i>Anaplasma</i> sp., <i>Babesia</i> sp., and <i>Ehrlichia muris</i> . Treated with doxycycline for 21 d with complete resolution of symptoms. No history of neuroinvasive disease or TBD.	Hyperlipidemia		–	–	–
3	IgM >1:20	IgG and IgM	14-year-old girl with 3-d history of urticarial rash. CBC results: leukocytes $8.8 \times 10^9/L$, Hb 13.0 g/dL, Hct 40.3%, Plt $393 \times 10^3/\mu L$; CRP 3.6 nmol/L. Treated with doxycycline for 14 d.	None		–	–	–
4	IgM >1:20	IgG and IgM	4-year-old girl with 1-wk history of fever (103°F), listless, headache, fatigue, and maculopapular rash. PCR neg for <i>Anaplasma</i> sp., <i>Babesia</i> sp., and <i>Ehrlichia muris</i> . Treated with amoxicillin for 21 d.	None	Probable	–	–	–
9	IgM >1:20	IgG and IgM	3-year-old girl with 1-wk history of intermittent fever, fussiness, and erythema migrans. After development of an urticarial rash, treatment with cefuroxime was changed to amoxicillin for 21 d.	None	Probable	–	Midwest	–
Patients screened by chemical methods								
1c	IgG >1:40	Neg	68-year-old man with no signs or symptoms of acute infectious disease. No history of neuroinvasive disease or TBD. Died from liver cirrhosis.	Coronary artery disease, liver cirrhosis, end stage renal disease		–	–	–
2c	IgM >1:20, IgG >1:40	Neg	76-year-old woman with 2-d history of fever, chills, and MRSA infection of the right hand. Mild abdominal pain and diarrhea occurred later in course. CBC results: leukocytes $13.7 \times 10^9/L$, Hb 9.2 g/dL, Hct 29.7%, Plt $180 \times 10^3/\mu L$; CRP 1.5 nmol/L; Procalcitonin 0.1 $\mu g/L$. Received daptomycin for 16 d with full recovery. Currently deceased, unknown cause of death.	Congestive heart failure, rheumatoid arthritis on immune-suppressive medications	Probable	–	–	–

*CBC, complete blood cell count; CDC, Centers for Disease Control and Prevention; CRP, C-reactive protein; Hb, hemoglobin; Hct, hematocrit; IFA, immunofluorescence antibody; MRSA, multidrug-resistant *Staphylococcus aureus*; neg, negative; Plt, platelet; POWV, Powassan virus; PRNT, plaque reduction neutralization test; WNV, West Nile virus; TBD, tickborne disease; –, no history.

†Samples were screened by EIA and followed up by Western blot.

‡Patient-reported tick exposure.

§Known history of vaccination against yellow fever virus, Japanese encephalitis virus, or tick-borne encephalitis virus.

¶Cross-reactivity on POWV IgG IFA assay is consistent with a history of West Nile virus infection.

antibodies are often not present during early infection (12). The 2 patients screened by chemical methods who were positive for POWV IgG failed to show neutralization by PRNT; however, rather than PRNT₅₀, we used POWV PRNT₉₀, which has greater specificity but lower sensitivity. In addition, our PRNT was based on POWV lineage I; thus, our test was potentially less sensitive at detecting POWV lineage II-specific antibodies and thus less capable of detecting previous POWV lineage II infection.

Similar to other flavivirus serologic assays, considerable cross-reactivity occurred with the Flavivirus Mosaic IgG IFA assay (online Technical Appendix Table) (13). The fluorescence intensity was stronger for TBEV than it was for other flaviviruses in all TBD patients except for 1 patient with prior confirmed WNV infection. Both patients with routine chemistry screening completed who were POWV IgG-positive were TBEV IgM-positive. Neither had a history of yellow fever or dengue virus exposure or vaccination, although the panel showed cross-reactivity with these viruses.

Evidence of current or prior *B. burgdorferi* infection was present in 63 (66.3%) TBD patients and 4 (8%) patients with routine chemistry screening completed ($p < 0.0001$). Of the 41 (43.2%) TBD patients with evidence of *B. burgdorferi* infection, 7 (17.1%) had serologic evidence of acute POWV infection and 3 (7.3%) had laboratory-confirmed POWV infection. When controlling for differences in seroprevalence rates of *B. burgdorferi*, no statistical differences were evident for POWV seroprevalence ($p = 1.0$) or confirmed infections ($p = 1.0$) between patients with routine chemistry screening completed and TBD patients, although the study was underpowered in this regard.

B. burgdorferi IgM was detected in 6 (85.7%) of the 7 patients with serologic evidence of acute POWV infection, suggesting concurrent infection, which is consistent with surveillance data indicating that POWV and *B. burgdorferi* co-infect *I. scapularis* ticks (2,3). The rate of concurrent antibodies we report is higher than that described for regions of Europe endemic for TBE and Lyme disease (14).

Clinical data were available for 7 of the patients with serologic evidence of POWV infection (Table 2). Infection probably occurred in 3 patients. A laboratory-confirmed nonacute infection was found in a patient (patient no. 2) who did not meet Centers for Disease Control and Prevention criteria. Patient symptoms could not be attributed specifically to POWV because all TBD patients with clinical data available were positive for *B. burgdorferi* antibodies, and testing for the possibility of infection with additional endemic tick pathogens was performed for only 2 patients.

Consistent with previous studies showing increased susceptibility of children to arboviral diseases, 3 patients who might have had POWV infection were children

(Table 2) (15). Fever was present in all patients with evidence of POWV acute infection; other common symptoms were fatigue, malaise, fussiness, listlessness, and headache. Complete blood cell count and C-reactive protein did not indicate severe infection. Consistent with other arboviral diseases, urticarial or maculopapular rash was documented in 3 patients (15). No patients had neuroinvasive disease.

This study had limitations. Similar to other serologic studies, cross-reactivity and prior exposure to POWV cannot be completely excluded in serologically positive cases. Analysis for other flaviviruses, prior yellow fever virus vaccination, and history of travel to dengue-endemic regions, as well as PRNT, were completed to address this concern. The study population was limited to persons in the US upper Midwest, although POWV is likely an increasing problem throughout the territory *I. scapularis* ticks occupy. Our study results might not be applicable to these other regions.

Conclusions

In a Lyme disease-endemic area, POWV seroreactivity and confirmed POWV infection were present. The spectrum of disease is broader than previously realized, with most patients having minimally symptomatic infection (1,10,11). Further studies are needed to characterize clinical disease of POWV monoinfection, document POWV seroprevalence in humans, and monitor epidemiologic trends.

Acknowledgments

We thank Marshfield Clinic Research Foundation staff for supporting this study and Marshfield Labs staff for collecting specimens. We also thank Diep Johnson for assisting with this study.

Dr. Frost is a pediatrician and physician scientist at Marshfield Clinic in Minocqua, Wisconsin. Her research interests include tickborne pathogens, blastomycosis, and antimicrobial stewardship.

References

1. Piantadosi A, Rubin DB, McQuillen DP, Hsu L, Lederer PA, Ashbaugh CD, et al. Emerging cases of Powassan virus encephalitis in New England: clinical presentation, imaging, and review of the literature. *Clin Infect Dis*. 2016;62:707–13. <http://dx.doi.org/10.1093/cid/civ1005>
2. Dupuis AP II, Peters RJ, Prusinski MA, Falco RC, Ostfeld RS, Kramer LD. Isolation of deer tick virus (Powassan virus, lineage II) from *Ixodes scapularis* and detection of antibody in vertebrate hosts sampled in the Hudson Valley, New York state. *Parasit Vectors*. 2013;6:185. <http://dx.doi.org/10.1186/1756-3305-6-185>
3. Knox K, Thomm A, Harrington Y, Baewer D, Carrigan D. Arbovirus co-infections in Wisconsin tick populations. Poster presentation at: IDWeek; October 7–11, 2015; San Diego, CA, USA.

4. Eisen RJ, Eisen L, Beard CB. County-scale distribution of *Ixodes scapularis* and *Ixodes pacificus* (Acari: Ixodidae) in the continental United States. *J Med Entomol*. 2016;53:349–86. <http://dx.doi.org/10.1093/jme/tjv237>
5. Nofchissey RA, Deardorff ER, Blevins TM, Anishchenko M, Bosco-Lauth A, Berl E, et al. Seroprevalence of Powassan virus in New England deer, 1979–2010. *Am J Trop Med Hyg*. 2013;88:1159–62. <http://dx.doi.org/10.4269/ajtmh.12-0586>
6. Ebel GD. Update on Powassan virus: emergence of a North American tick-borne flavivirus. *Annu Rev Entomol*. 2010;55:95–110. <http://dx.doi.org/10.1146/annurev-ento-112408-085446>
7. Centers for Disease Control and Prevention. Arboviral diseases, neuroinvasive and non-neuroinvasive 2015 case definition [cited 2017 Feb 12]. <https://www.cdc.gov/nndss/conditions/arboviral-diseases-neuroinvasive-and-non-neuroinvasive/case-definition/2015/>
8. El Khoury MY, Hull RC, Bryant PW, Escuyer KL, St George K, Wong SJ, et al. Diagnosis of acute deer tick virus encephalitis. *Clin Infect Dis*. 2013;56:e40–7. <http://dx.doi.org/10.1093/cid/cis938>
9. Thomm A, Schotthoefer A, Kehr S, Kramer L, Frost H, Fritsche T, et al. Development of a serologic test panel for detection of Powassan virus infection. Poster presented at: The 32st Clinical Virology Symposium; May 19–22, 2016; Dayton Beach, FL, USA [cited 2017 Feb 12]. <http://www.abstractsonline.com/pp8/#/14039/presentation/725>
10. Neitzel DF, Lynfield R, Smith K. Powassan virus encephalitis, Minnesota, USA. *Emerg Infect Dis*. 2013;19:686. <http://dx.doi.org/10.3201/eid1904.121651>
11. Sung S, Wurcel AG, Whittier S, Kulas K, Kramer LD, Flam R, et al. Powassan meningoencephalitis, New York, New York, USA. *Emerg Infect Dis*. 2013;19. <http://dx.doi.org/10.3201/eid1909.121846>
12. Venturi G, Martelli P, Mazzolini E, Fiorentini C, Benedetti E, Todone D, et al. Humoral immunity in natural infection by tick-borne encephalitis virus. *J Med Virol*. 2009;81:665–71. <http://dx.doi.org/10.1002/jmv.21431>
13. Ledermann JP, Lorono-Pino MA, Ellis C, Saxton-Shaw KD, Blitvich BJ, Beaty BJ, et al. Evaluation of widely used diagnostic tests to detect West Nile virus infections in horses previously infected with St. Louis encephalitis virus or dengue virus type 2. *Clin Vaccine Immunol*. 2011;18:580–7. <http://dx.doi.org/10.1128/CVI.00201-10>
14. Gustafson R. Epidemiological studies of Lyme borreliosis and tick-borne encephalitis. *Scand J Infect Dis Suppl*. 1994;92:1–63.
15. Davis LE, Beckham JD, Tyler KL. North American encephalitic arboviruses. *Neurol Clin*. 2008;26:727–57. <http://dx.doi.org/10.1016/j.ncl.2008.03.012>

Address for correspondence: Holly M. Frost, Marshfield Clinic and Marshfield Clinic Research Foundation, 9601 Townline Rd, Minocqua, WI 54538, USA; email: frost.holly@marshfieldclinic.org

etymologia Revisited

Originally published in
January 2006

**EMERGING
INFECTIOUS DISEASES**

etymologia

influenza

[inˈflʊ-ɛnˈzə]

Acute viral infection of the respiratory tract. From Latin *influentia*, "to flow into"; in medieval times, intangible fluid given off by stars was believed to affect humans. The Italian *influenza* referred to any disease outbreak thought to be influenced by stars. In 1743, what Italians called an *influenza di catarro* ("epidemic of catarrh") spread across Europe, and the disease came to be known in English as simply "influenza."

Sources: Dorland's illustrated medical dictionary. 30th ed. Philadelphia: Saunders; 2003 and Quinion M. World wide words. 1998 Jan 3 [cited 2005 Dec 5]. Available from <http://www.worldwidewords.org/topicalwords/tw-inf1.htm>

DOI: 10.3201/eid1201.ET1201

https://wwwnc.cdc.gov/eid/article/12/1/et-1201_article

Serologic Evidence of Scrub Typhus in the Peruvian Amazon

Claudine Kocher, Ju Jiang, Amy C. Morrison, Roger Castillo, Mariana Leguia, Steev Loyola, Julia S. Ampuero, Manuel Cespedes, Eric S. Halsey, Daniel G. Bausch, Allen L. Richards

Using a large, passive, febrile surveillance program in Iquitos, Peru, we retrospectively tested human blood specimens for scrub typhus group orientiae by ELISA, immunofluorescence assay, and PCR. Of 1,124 participants, 60 (5.3%) were seropositive, and 1 showed evidence of recent active infection. Our serologic data indicate that scrub typhus is present in the Peruvian Amazon.

Infections with scrub typhus group orientiae (STGO) are a common and widespread cause of fever in Asia, the western Pacific, and northern Australia (the tsutsugamushi triangle). The causative pathogen, *Orientia tsutsugamushi*, is transmitted by the larval stage of trombiculid mites of the genus *Leptobromidium* (chiggers). Clinical manifestations can be mild and nonspecific, but complications include jaundice, meningoencephalitis, myocarditis, and interstitial pneumonia leading to acute respiratory distress syndrome and renal failure (1).

Epidemiologic studies in Southeast Asia have identified rickettsial illness (especially scrub typhus and murine typhus) as leading causes of treatable undifferentiated febrile illness, although they are often misdiagnosed as malaria, dengue, or typhoid fever (2). The causative agent of scrub typhus was not believed to exist outside the tsutsugamushi triangle until *Orientia* spp. were identified by serologic and molecular methods in febrile patients from the Middle East (3) and Chile (4). Recently, more autochthonous cases of scrub typhus were reported from Chiloé Island in southern Chile, suggesting endemicity in the area (5). Therefore, we conducted a study

to obtain serologic evidence of scrub typhus in the Peruvian Amazon.

The Study

This study was conducted in Iquitos, which is located in the Amazon forest in the Department of Loreto in northeastern Peru, where ongoing epidemiologic studies on febrile illness and rickettsial disease (6,7) have been conducted. STGO testing was nested in an ongoing febrile surveillance study (NMRC2010.0010), which was approved by the US Naval Medical Research Unit No. 6 Institutional Review Board (Lima, Peru). The current study protocol was approved by the US Naval Medical Research Unit No. 6 Institutional Review Board in compliance with all applicable federal regulations governing the protection of human subjects.

Febrile surveillance was conducted in 12 health facilities (3 hospitals and 9 outpatient clinics; 2 of the 12 were military facilities) distributed across 4 districts of Iquitos. Febrile patients who fulfilled the inclusion criteria (axillary temperature $\geq 37.5^{\circ}\text{C}$, duration of illness ≤ 5 days, and age ≥ 5 years) were asked to participate in the study. An acute-phase blood sample was collected at the time of enrollment, and a convalescent-phase blood sample was obtained 10–30 days later. These samples had already been used for detection of other pathogens (mainly dengue virus and other arboviruses), and results and testing methods have been reported (8).

We retrospectively screened convalescent-phase blood samples obtained from participants enrolled during 2013 by using an STGO-specific IgG ELISA. We screened convalescent-phase samples for IgG against a mixture of whole-cell antigen preparations from Karp, Kato, and Gilliam strains of *O. tsutsugamushi* in an STGO-specific IgG ELISA as described (9–11). For convalescent-phase samples with net absorbance ≥ 0.500 at a 1:100 serum dilution, we subsequently assessed STGO IgG ELISA titer (range 1:100–1:6,400) with their paired acute-phase samples side-by-side to determine their endpoint titers. We considered samples with a net total absorbance ≥ 1.000 for serum dilutions 1:100, 1:400, 1:1,600, and 1:6,400 titer positive. We classified samples with a seroconversion or a ≥ 4 -fold increase in IgG titer between acute-phase and convalescent-phase blood samples and minimum titer of 1:400 in the convalescent-phase sample as indicative of active rickettsial infection (11).

Author affiliations: Kantonsspital Baden, Baden, Switzerland (C. Kocher); Epidemiology, Biostatistics, and Epidemiology Institute Travel Clinic, Zurich, Switzerland (C. Kocher); US Naval Medical Research Unit No. 6, Lima and Iquitos, Peru (C. Kocher, A.C. Morrison, R. Castillo, M. Leguia, S. Loyola, J.S. Ampuero, E.S. Halsey, D.G. Bausch); US Naval Medical Research Center, Silver Spring, Maryland, USA (J. Jiang, A.L. Richards); National Institute of Health, Lima (M. Cespedes)

DOI: <https://doi.org/10.3201/eid2308.170050>

Samples with evidence of active infection were then confirmed by immunofluorescence assay (IFA) with the *Orientia* MIF IgG Kit (Fuller Laboratories, Fullerton, CA, USA) and Karp, Kato, Gilliam, and Boryong strains of *O. tsutsugamushi* according to the manufacturer's instructions. We further tested acute-phase samples with evidence for active infection by PCR to identify the causative pathogen.

We extracted DNA from whole blood samples by using QIAmp DNA Mini Kits (QIAGEN, Valencia, CA, USA) following the manufacturer's instructions except that a final elution volume of 100 μ L was used. Samples were stored at -80°C . We assessed DNA samples from persons with evidence for recent active disease by using a quantitative PCR specific for the *O. tsutsugamushi* 47-kD antigen gene as reported (12).

During 2013, we enrolled 1,497 participants in the main study. Of these participants, 1,124 had paired serum samples. Results of the STGO-specific IgG were positive for 60 (5.3%) of 1,124 convalescent-phase serum samples with a titer $\geq 1:400$. One participant had a >4 -fold increase in titer (acute-phase sample titer 1:400, convalescent-phase sample titer $\geq 6,400$) and was confirmed by IFA as showing a ≥ 4 -fold increase in titer for 3 of 4 strains of *O. tsutsugamushi* (Karp, Gilliam, and Boryong) and a 2-fold increase in titer for the Kato strain. A test result of the acute-phase sample for *Orientia* sp. DNA was negative. This case-patient was a 22-year-old soldier stationed in a rural military camp at the time of illness. He had fever, chills, malaise, muscle pain, nausea, and vomiting but no rash or jaundice. The patient had not traveled in the 2 weeks before illness and therefore could not have contracted the infection elsewhere.

Conclusions

We performed a retrospective systematic analysis for the presence of scrub typhus in Iquitos, Peru, by testing blood samples collected prospectively during unspecific acute febrile illness. Although definitive molecular evidence of *Orientia* spp. infection was not found, our serologic evidence strongly suggests the presence of this pathogen in tropical areas of Peru.

Seroprevalence among febrile illness patients was low, especially because most patients tested came from urban rather than rural areas. In addition, our study design could further underestimate scrub typhus because we only included patients with fever for <5 days, whereas the mean time to signs of scrub typhus has been reported as 8.2 days (13). Although the 1 patient with ELISA and IFA evidence of seroconversion showed a negative result by PCR, a negative PCR result during the acute phase of scrub typhus is not uncommon, even when testing is performed on whole blood or buffy coat samples (14). In addition, whether the causative agents of scrub typhus in South America are recognized by the primer set used in the quantitative PCR is unknown (4).

Cross-reactivity with other *Rickettsia* spp. does not seem to be a concern. The *Orientia* spp. ELISA using the immunodominant genus-specific, 56-kDa, type-specific antigen (outer membrane protein [Omp]) does not react with antibodies produced during typhus group rickettsiae (TGR) and spotted fever group rickettsiae (SFGR) infections because rickettsiae lack the 56-kDa type-specific antigen. Similarly, antibodies produced against *Orientia* spp. infection do not react against SFGR and TGR ELISA antigens (lipopolysaccharides OmpA and OmpB), because *Orientia* spp. do not contain these antigens (15). As expected, screening results for SFGR and TGR (7) were negative for the case-patient we report.

Dengue virus and other arboviruses were excluded (by PCR or virus isolation) as alternative causes of fever. Furthermore, study participants had probably already received over-the-counter medications, including antimicrobial drugs, which would account for false-negative PCR results. According to the prospectively collected clinical data, a typical rash was not documented for the case-patient we report. However, because this surveillance study was not directed toward scrub typhus features, a small eschar could have been easily missed.

This study raises many new issues, such as possible local reservoirs and vectors. The presence of trombiculid mites in Peru has been reported in other areas (16), but this species has not been studied as a local vector for pathogens. The case-patient we report was in the military and stationed in a rural camp. Therefore, he was regularly exposed to typical vegetation that supports the presence of mites. Our results and those from studies in Chile (4,5) indicate a need for a more expansive survey for evidence of scrub typhus, not only in Peru, but throughout South America.

Acknowledgments

We thank Carolina Guevara and Alfredo Huaman for providing laboratory support.

This study was supported by the Global Emerging Infections Surveillance Section of the Armed Forces Health Surveillance Branch, Work Unit # P0413 and 800000.82000.25GB.B0016.

Dr. Kocher is a physician at the Epidemiology, Biostatistics, and Epidemiology Institute Travel Clinic, Zurich, Switzerland. Her research interests include infectious diseases, travel medicine, arboviruses and other causes of acute febrile illnesses in tropical regions.

References

1. Peter JV, Sudarsan TI, Prakash JA, Varghese GM. Severe scrub typhus infection: clinical features, diagnostic challenges and management. *World J Crit Care Med.* 2015;4:244–50.
2. Mayxay M, Castonguay-Vanier J, Chansamouth V, Dubot-Pérès A, Paris DH, Phetsouvanh R, et al. Causes of non-malarial fever in Laos: a prospective study. *Lancet Glob Health.* 2013;1:e46–54. [http://dx.doi.org/10.1016/S2214-109X\(13\)70008-1](http://dx.doi.org/10.1016/S2214-109X(13)70008-1)

3. Izzard L, Fuller A, Blacksell SD, Paris DH, Richards AL, Aukkanit N, et al. Isolation of a novel *Orientia* species (*O. chuto* sp. nov.) from a patient infected in Dubai. *J Clin Microbiol*. 2010;48:4404–9. <http://dx.doi.org/10.1128/JCM.01526-10>
4. Balcells ME, Rabagliati R, García P, Poggi H, Oddó D, Concha M, et al. Endemic scrub typhus-like illness, Chile. *Emerg Infect Dis*. 2011;17:1659–63. <http://dx.doi.org/10.3201/eid1709.100960>
5. Weitzel T, Dittrich S, López J, Phuklia W, Martínez-Valdebenito C, Velásquez K, et al. Endemic scrub typhus in South America. *N Engl J Med*. 2016;375:954–61. <http://dx.doi.org/10.1056/NEJMoa1603657>
6. Forshey BM, Guevara C, Laguna-Torres VA, Cespedes M, Vargas J, Gianella A, et al.; NMRCDF Febrile Surveillance Working Group. Arboviral etiologies of acute febrile illnesses in western South America, 2000–2007. *PLoS Negl Trop Dis*. 2010;4:e787. <http://dx.doi.org/10.1371/journal.pntd.0000787>
7. Kocher C, Morrison AC, Leguía M, Loyola S, Castillo RM, Galvez HA, et al. Rickettsial disease in the Peruvian Amazon Basin. *PLoS Negl Trop Dis*. 2016;10:e0004843. <http://dx.doi.org/10.1371/journal.pntd.0004843>
8. Halsey ES, Siles C, Guevara C, Vilcarromero S, Jhonston EJ, Ramal C, et al. Mayaro virus infection, Amazon Basin region, Peru, 2010–2013. *Emerg Infect Dis*. 2013;19:1839–42. <http://dx.doi.org/10.3201/eid1911.130777>
9. Richards AL, Soeatmadji DW, Widodo MA, Sardjono TW, Yanuwadi B, Hernowati TE, et al. Seroepidemiologic evidence for murine and scrub typhus in Malang, Indonesia. *Am J Trop Med Hyg*. 1997;57:91–5. <http://dx.doi.org/10.4269/ajtmh.1997.57.91>
10. Maina AN, Farris CM, Odhiambo A, Jiang J, Laktabai J, Armstrong J, et al. Q Fever, Scrub typhus, and rickettsial diseases in children, Kenya, 2011–2012. *Emerg Infect Dis*. 2016;22:883–6. <http://dx.doi.org/10.3201/eid2205.150953>
11. Luce-Fedrow A, Mullins K, Kostik AP, St John HK, Jiang J, Richards AL. Strategies for detecting rickettsiae and diagnosing rickettsial diseases. *Future Microbiol*. 2015;10:537–64. <http://dx.doi.org/10.2217/fmb.14.141>
12. Jiang J, Chan T-C, Temenak JJ, Dasch GA, Ching W-M, Richards AL. Development of a quantitative real-time polymerase chain reaction assay specific for *Orientia tsutsugamushi*. *Am J Trop Med Hyg*. 2004;70:351–6.
13. Abhilash KP, Jeevan JA, Mitra S, Paul N, Murugan TP, Rangaraj A, et al. Acute undifferentiated febrile illness in patients presenting to a tertiary care hospital in south India: clinical spectrum and outcome. *J Glob Infect Dis*. 2016;8:147–54. <http://dx.doi.org/10.4103/0974-777X.192966>
14. Wathanaworawit W, Turner P, Turner C, Tanganuchitcharnchai A, Richards AL, Bourzac KM, et al. A prospective evaluation of real-time PCR assays for the detection of *Orientia tsutsugamushi* and *Rickettsia* spp. for early diagnosis of rickettsial infections during the acute phase of undifferentiated febrile illness. *Am J Trop Med Hyg*. 2013;89:308–10. <http://dx.doi.org/10.4269/ajtmh.12-0600>
15. Land MV, Ching WM, Dasch GA, Zhang Z, Kelly DJ, Graves SR, et al. Evaluation of a commercially available recombinant-protein enzyme-linked immunosorbent assay for detection of antibodies produced in scrub typhus rickettsial infections. *J Clin Microbiol*. 2000;38:2701–5.
16. Gomez-Puerta LA, Olazabal J, Lopez-Urbina MT, Gonzalez AE. Trombiculiasis caused by chigger mites *Eutrombicula* (Acari: Trombiculidae) in Peruvian alpacas. *Vet Parasitol*. 2012;190:294–6. <http://dx.doi.org/10.1016/j.vetpar.2012.06.012>

Address for correspondence: Claudine Kocher, Epidemiology, Biostatistics, and Epidemiology Institute Travel Clinic, Hirschengraben 84, Zurich 8001, Switzerland; email: ckocher@gmx.net

EID SPOTLIGHT TOPIC

Ticks transmit a variety of different pathogens including bacteria, protozoa, and viruses, which can produce serious and even fatal disease in humans and animals. Tens of thousands of cases of tickborne disease are reported each year, including Lyme disease. See the EID Lyme Disease Spotlight. Lyme disease is the most well-known tickborne disease. However, other tickborne illnesses such as Rocky Mountain spotted fever, tularemia, babesiosis, and ehrlichiosis also contribute to severe morbidity and more mortality each year.



Symptoms of tickborne disease are highly variable, but most include sudden onset of fever, headache, malaise, and sometimes rash. If left untreated, some of these diseases can be rapidly fatal.

<https://wwwnc.cdc.gov/eid/page/tick-spotlight>

**EMERGING
INFECTIOUS DISEASES®**

Influenza D Virus in Animal Species in Guangdong Province, Southern China

Shao-Lun Zhai,¹ He Zhang,¹ Sheng-Nan Chen,¹
Xia Zhou, Tao Lin, Runxia Liu, Dian-Hong Lv,
Xiao-Hui Wen, Wen-Kang Wei,¹ Dan Wang, Feng Li

Molecular tests revealed influenza D viruses of D/OK lineage widely circulating in farmed animal species in Guangdong Province, southern China. In particular, we found high levels of influenza D virus infection in goats and pigs. We also detected viral RNA in serum specimens and feces of animals with certain severe diseases.

Four types of influenza viruses (A–D) have been confirmed (<https://www.cdc.gov/flu/about/viruses/types.htm>). The recently discovered influenza D virus is thought to cause respiratory diseases primarily in cattle and to a lesser extent in pigs (1–4). Moreover, serologic evidence for influenza D virus infection in small ruminants and humans has been established (5,6). Since the initial influenza D virus isolation in the United States in 2011 (1), the virus has been reported in China, Mexico, France, Italy, and Japan (7–11). Genetic analysis of the hemagglutinin-esterase-fusion gene demonstrated that these viruses had 2 distinct lineages, represented by D/OK and D/660 (12). Recently, a novel influenza D virus that emerged in Japan has been proposed as the third lineage (11). D/OK lineage-related viruses were previously identified in native Luxi yellow cattle in Shandong Province, northern China (7). Despite good progress in identifying domestic cattle as the primary reservoir of influenza D virus, we know little about prevalence in other animals. We conducted a study to clarify the origin and transmission dynamics of influenza D virus in goats, buffalo, and pigs as well as farmed cattle.

The Study

In 2016, we collected 607 clinical samples from 4 species of animals with different clinical diseases and 250 nasal swab samples from asymptomatic animals (Table) from 16 farms in 4 cities of Guangdong Province: Guangzhou,

Qingyuan, Heyuan, and Jiangmen (Figure 1). In addition, we randomly chose 200 archived Holstein dairy cattle serum samples, 40 per year, from 2011–2015 to investigate possible early RNA distribution of influenza D virus in this region. We used the reverse transcription PCR method and subcloning protocol (online Technical Appendix, <https://wwwnc.cdc.gov/EID/article/23/8/17-0059-Techapp.pdf>). We performed sequence alignment using ClustalW implemented in DNASTar software (DNASTar, Madison, WI, USA), and we conducted phylogenetic analyses based on our obtained sequences and reference truncated sequences (496-bp) of influenza D viruses from GenBank by using MEGA 5.1 software (<http://www.megasoftware.net>; online Technical Appendix Table).

After testing by reverse transcription PCR with further sequencing confirmation, we found influenza D virus–positive rates in 230 total nasal swab samples of 12.8% (20/156) for dairy cattle, 7.3% (4/55) for native yellow cattle, and 36.8% (7/19) for pigs. Rates in 324 total serum samples were 7.8% (15/193) for dairy cattle, 5.9% (3/51) for buffalo, and 33.8% (27/80) for goats. The influenza D virus–positive rate was also high (28.9%, 13/45) in swine lung samples. In contrast, we found no or low prevalence ($\leq 2\%$) in asymptomatic animals tested (Table). Moreover, all of the archived serum samples were found to be influenza D virus negative. Interestingly, 1 of 8 rectal swabs of goats with severe diarrhea tested positive (Table). Samples from animals with reproductive problems had a positive rate of 4.3% (5/116) (Table).

Sequence alignment analysis showed that the nucleotide sequences of influenza D viruses found in this study shared high similarity (99%–100%) with previously described sequences from China (7) and low similarity (93.8%–98.8%) with sequences originating from the United States, France, Italy, Mexico, and Japan (1,8–12). Similarly, phylogenetic analysis revealed that all influenza D virus sequences in this study clustered together with previous sequences from China and belonged to the D/OK lineage (Figure 2).

Conclusions

When first discovered, influenza D virus was reported in diseased pigs in the United States (1). Later, it was

Author affiliations: Guangdong Academy of Agricultural Sciences, Guangzhou, China (S.-L. Zhai, D.-H. Lv, X.-H. Wen, W.-K. Wei); South Dakota State University, Brookings, South Dakota, USA (S.-L. Zhai, S.-N. Chen, T. Lin, R. Liu, D. Wang, F. Li); South China Agricultural University, Guangzhou (H. Zhang, X. Zhou)

DOI: <https://doi.org/10.3201/eid2308.170059>

¹These authors contributed equally to this article.

Table. Animal species, location, sample data, and detection rate of influenza D virus, Guangdong Province, China*

Animal species and farm	Farm type†	Farm location	No. animals	Age range of animals	Sample type	No. positive/no. samples	Detection rate, %
Holstein dairy cattle							
A	Not all-in-all-out	Guangzhou: Tianhe	2,000	3–5 y	Nasal swab	14/86‡	16.3
A	Not all-in-all-out	Guangzhou: Tianhe	2,000	3–5 y	Serum	10/94‡	10.6
B	Not all-in-all-out	Guangzhou: Luogang	800	3–6 y	Nasal swab	6/70‡	8.57
B	Not all-in-all-out	Guangzhou: Luogang	800	3–6 y	Serum	5/99‡	5.05
C	Not all-in-all-out	Guangzhou: Tianhe	175	2–5 y	Nasal swab	1/50§	2
American Landrace pig							
D	Not all-in-all-out	Guangzhou: Huadu	200	10–15 wks	Lung	4/10‡	40
E	All-in-all-out	Heyuan: Yuancheng	1,000	5–5 wks	Nasal swab	4/10‡	40
E	All-in-all-out	Heyuan: Yuancheng	1,000	3–5 wks	Lung	1/8‡	12.5
F	All-in-all-out	Jiangmen: Kaiping	800	8–20 wks	Nasal swab	3/9‡	30
F	All-in-all-out	Jiangmen: Kaiping	800	8–20 wks	Lung	8/27‡	29.6
G	All-in-all-out	Heyuan: Dongyuan	600	9–15 wks	Nasal swab	1/50§	2
Native hybrid white goat							
H	Not all-in-all-out	Guangzhou: Zengcheng	200	0.5–5 y	Serum	7/25‡	28
I	Not all-in-all-out	Guangzhou: Luogang	300	2–4 y	Serum	20/55¶	36.4
Native hybrid black goat							
J	Not all-in-all-out	Qingyuan: Jiangkou	150	1–3 y	Rectal swab	1/8#	12.5
K	Not all-in-all-out	Jiangmen: Enping	500	1–4 y	Nasal swab	0/50§	0
Asian buffalo							
L	Not all-in-all-out	Guangzhou: Nansha	150	3–5 y	Serum	2/26¶	7.7
M	Not all-in-all-out	Guangzhou: Panyu	180	3–6 y	Serum	1/25¶	4
N	Not all-in-all-out	Qingyuan: Yingde	400	1–4 y	Nasal swab	0/50§	0
Native yellow cattle							
O	Not all-in-all-out	Qingyuan: Qingxin	200	2–5 y	Nasal swab	4/55‡	7.3
P	Not all-in-all-out	Qingyuan: Fogang	230	1–3 y	Nasal swab	0/50§	0

*Feeding type of farms A–G was in captivity (poor biosecurity and high density). Feeding type of farms H–K and N–P was free grazing on the hills in the daytime and in captivity (poor biosecurity and high density) in the nighttime. Feeding type of farms L and M was free grazing in wetland in the daytime and in captivity (poor biosecurity and high density) in the nighttime.

†All-in-all-out is a strategy for the control of infectious disease. The barn is emptied of all animals and the accommodation is cleaned and disinfected and then refilled, all on 1 day.

‡These animals had severe respiratory diseases with a 10%–30% mortality rate, mainly characterized by expiratory dyspnea and abdominal respiration.

§These animals were asymptomatic.

¶These animals had severe reproductive disorders with a 60%–70% abortion rate.

#These animals had severe diarrheal disease, characterized by watery diarrhea, limb weakness, and nearly dying.

identified in cattle and swine herds in several other countries, with or without clinical manifestation (7–11). Moreover, antibodies to influenza D virus were detected in goats, sheep, and humans (5–6). Under experimental conditions, influenza D virus replicated and transmitted among ferrets and guinea pigs (13). We confirmed that influenza D virus is widely present in cattle species (dairy cattle, yellow cattle, and buffalo). We also found influenza D virus at a high prevalence (>30%) in pigs and goats (Table), which is in contrast to the low prevalence found in previous investigations (1,5,10). The high prevalence may be caused by poor biosecurity measures and high-density feeding mode practices in China's animal industry as well as possible cross-species transmission (13). Taken together, our findings expand the host range of influenza D virus and further emphasize the health concern this virus poses to multiple animal species.

Previous studies have shown that influenza D viruses are mainly found in respiratory tract samples (1–4,7,9–12) and that they have played an etiologic role in bovine respiratory diseases (2–4). In this study, we found that influenza D virus RNA was present in cattle and goat serum samples; it was also present in goat rectal swabs, accompanied by peste des petits ruminants virus and caprine kobovirus (data not shown). The distribution of influenza D virus in our study is not the same as that described under experimental conditions (3).

Influenza viremia, an indicator of disease severity (14), has been detected in 20.9% of severe cases during the acute phase of infection or before host death. Our detection of influenza D virus genome in serum samples from severely diseased animals (Table) implies that the virus could enter transiently into the animal's circulatory system through capillaries lining the respiratory tract, which



Figure 1. Farm locations for study of influenza D viruses in cattle, goats, buffalo, and pigs, Guangdong Province, China.

further contributes to the possibility of detecting virus in other organs. Similar to previous studies (2,4), we also found that the reverse transcription PCR positive rate was significantly higher (4%–40%) in diseased animals than the rate ($\leq 2\%$) observed in asymptomatic animals ($p < 0.05$), which suggests a potential correlation between the disease severity and presence of influenza D virus. For influenza D virus found in rectal swabs, it might be that animals have swallowed the virus. Another possibility is that, similar to influenza A and B viruses, influenza D virus can replicate within the intestinal tract (15).

We detected influenza D virus in cattle with reproductive disorders. However, we could not determine whether influenza D virus is associated with reproductive problems. Future studies can be designed to investigate these scientific issues.

To date, 2 lineages of influenza D virus (D/OK and D/660) co-circulate in North America and Europe (8–10,12). However, only the D/OK lineage has been found in China, and a potential third lineage was found in Japan (7,11). Our study confirms and further extends the previous observation that D/OK lineage circulates in East Asia. The viral, host, and ecologic factors that shape the observed contrasting phylodynamics of influenza D viruses among different geographic regions warrant further investigation.

In addition, we found different minor genetic variants circulating on the same farm (Figure 2), indicating the ongoing evolution of influenza D viruses in their hosts

(7,8,11). In comparing our sequences to the reference sequences from different animal species, we found 4 frequent nucleotide mutations (at positions 136, 231, 263, and 486) (online Technical Appendix Figure 1), which caused 2 amino acid mutations at positions 77 and 88 (online Technical Appendix Figure 2). Interestingly, among 4 nucleotide mutations, 1 unique nucleotide (T at position 486) was originally from the D/660 lineage. Moreover, we found several consistent sequences co-circulating in multiple animal species (online Technical Appendix Figure 1). Our speculation is that homologous recombination among different influenza D viruses and potential cross-species transmission under field conditions are possible, but further study is needed.

In summary, our study investigating the infection status of influenza D virus in different farmed animal species in Guangdong Province provides novel insights into the epidemiology and evolution of this virus. In particular, we document the molecular evidence for influenza D virus infection in goats and buffalo.

Acknowledgments

We are very grateful to Ben M. Hause, Milton Thomas, and Hunter Nedland for their suggestions and English editing when we revised this manuscript.

This work was supported by Guangdong Provincial Department of Science and Technology (Grant no. 2016A040403083), Guangdong Provincial Agricultural Department (Grant no. 2016LM3177), and Ministry of Science and Technology of the

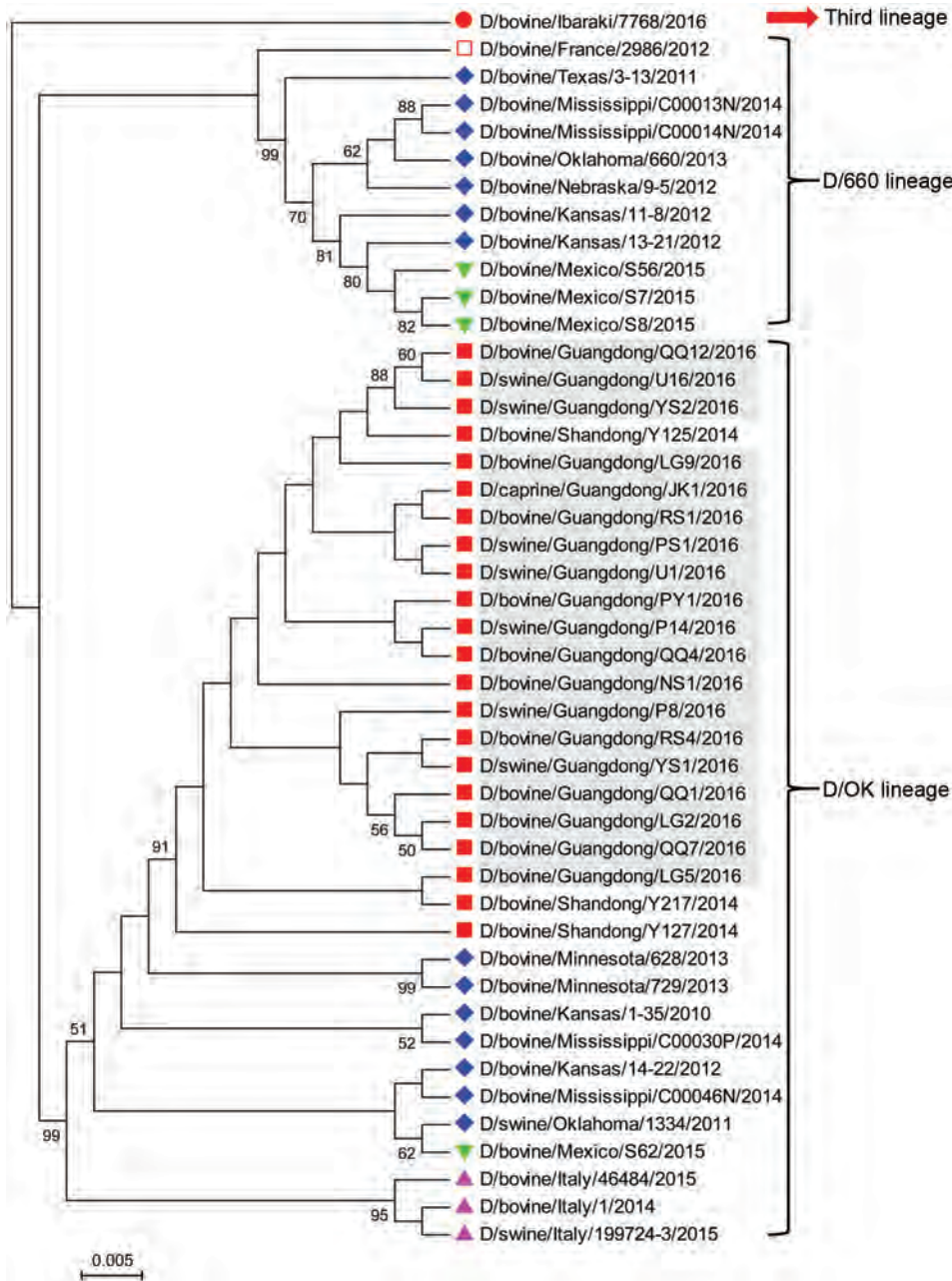


Figure 2. Phylogenetic analysis of viruses from study of influenza D viruses in cattle, goats, buffalo, and pigs in Guangdong Province, China, compared with reference viruses. Partial hemagglutinin-esterase-fusion gene sequences (496 bp) were aligned by using ClustalW implemented in DNASTar software (DNASTar, Madison, WI, USA), and the phylogenetic tree was obtained using neighbor-joining method within MEGA 5.1 software (<http://www.megasoftware.net>). Numbers at nodes are percentages of bootstrap values obtained by repeated analyses (1,000 times) to generate majority consensus tree. Only bootstrap scores of at least 50 were retained. Scale bar indicates 0.5% nucleotide sequence divergence. Gray shading indicates viruses from this study; reference viruses obtained from the United States are marked with ♦; from China, ■; from Italy, ▲; from Mexico, ▼; from France, □; and from Japan ●. Note that D/swine/Guangdong/YS1/2016 and D/swine/Guangdong/YS2/2016 are from the same farm; D/swine/Guangdong/P8/2016 and D/swine/Guangdong/P14/2016 are from the same farm; D/swine/Guangdong/U1/2016 and D/swine/Guangdong/U16/2016 are from the same farm; D/bovine/Guangdong/LG2/2016, D/bovine/Guangdong/LG5/2016 and D/bovine/Guangdong/LG9/2016 are from the same farm; D/bovine/Guangdong/QQ1/2016, D/bovine/Guangdong/QQ4/2016, D/bovine/Guangdong/QQ7/2016 and D/bovine/Guangdong/QQ12/2016 are from the same farm; D/bovine/Guangdong/RS1/2016 and D/bovine/Guangdong/RS4/2016 are from the same farm.

People’s Republic of China (Grant no. 2015GA780010). The work was also supported in part by SDSU AES Fund 3AH-477 to F.L. and D.W. S.-L.Z. is sponsored by Guangdong Academy of Agricultural Sciences, Guangzhou, China.

Dr. Zhai is an associate professor at Animal Disease Diagnostic Center, Institute of Animal Health, Guangdong Academy of Agricultural Sciences. His research interests focus on surveillance and rapid response research of emerging or re-emerging animal pathogens. In 2016–17, he is a visiting scholar at the Department of Biology and Microbiology, South Dakota State University.

References

1. Hause BM, Ducatez M, Collin EA, Ran Z, Liu R, Sheng Z, et al. Isolation of a novel swine influenza virus from Oklahoma in 2011 which is distantly related to human influenza C viruses. *PLoS Pathog.* 2013;9:e1003176. <http://dx.doi.org/10.1371/journal.ppat.1003176>
2. Ng TF, Kondov NO, Deng X, Van Eenennaam A, Neibergs HL, Delwart E. A metagenomics and case-control study to identify viruses associated with bovine respiratory disease. *J Virol.* 2015;89:5340–9. <http://dx.doi.org/10.1128/JVI.00064-15>
3. Ferguson L, Olivier AK, Genova S, Epperson WB, Smith DR, Schneider L, et al. Pathogenesis of influenza D virus in cattle. *J Virol.* 2016;90:5636–42. <http://dx.doi.org/10.1128/JVI.03122-15>

4. Mitra N, Cernicchiaro N, Torres S, Li F, Hause BM. Metagenomic characterization of the virome associated with bovine respiratory disease in feedlot cattle identified novel viruses and suggests an etiologic role for influenza D virus. *J Gen Virol*. 2016;97:1771–84. <http://dx.doi.org/10.1099/jgv.0.000492>
5. Quast M, Sreenivasan C, Sexton G, Nedland H, Singrey A, Fawcett L, et al. Serological evidence for the presence of influenza D virus in small ruminants. *Vet Microbiol*. 2015; 180:281–5. <http://dx.doi.org/10.1016/j.vetmic.2015.09.005>
6. White SK, Ma W, McDaniel CJ, Gray GC, Lednicky JA. Serologic evidence of exposure to influenza D virus among persons with occupational contact with cattle. *J Clin Virol*. 2016;81:31–3. <http://dx.doi.org/10.1016/j.jcv.2016.05.017>
7. Jiang WM, Wang SC, Peng C, Yu JM, Zhuang QY, Hou GY, et al. Identification of a potential novel type of influenza virus in bovine in China. *Virus Genes*. 2014;49:493–6. <http://dx.doi.org/10.1007/s11262-014-1107-3>
8. Ferguson L, Eckard L, Epperson WB, Long LP, Smith D, Huston C, et al. Influenza D virus infection in Mississippi beef cattle. *Virology*. 2015;486:28–34. <http://dx.doi.org/10.1016/j.virol.2015.08.030>
9. Ducatez MF, Pelletier C, Meyer G. Influenza D virus in cattle, France, 2011–2014. *Emerg Infect Dis*. 2015;21:368–71. <http://dx.doi.org/10.3201/eid2102.141449>
10. Chiapponi C, Faccini S, De Mattia A, Baioni L, Barbieri I, Rosignoli C, et al. Detection of influenza D virus among swine and cattle, Italy. *Emerg Infect Dis*. 2016;22:352–4. <http://dx.doi.org/10.3201/eid2202.151439>
11. Murakami S, Endoh M, Kobayashi T, Takenaka-Uema A, Chambers JK, Uchida K, et al. Influenza D virus infection in herd of cattle, Japan. *Emerg Infect Dis*. 2016;22:1517–9. <http://dx.doi.org/10.3201/eid2208.160362>
12. Collin EA, Sheng Z, Lang Y, Ma W, Hause BM, Li F. Cocirculation of two distinct genetic and antigenic lineages of proposed influenza D virus in cattle. *J Virol*. 2015;89:1036–42. <http://dx.doi.org/10.1128/JVI.02718-14>
13. Sreenivasan C, Thomas M, Sheng Z, Hause BM, Collin EA, Knudsen DE, et al. Replication and transmission of the novel bovine influenza D virus in a guinea pig model. *J Virol*. 2015;89:11990–2001. <http://dx.doi.org/10.1128/JVI.01630-15>
14. Tse H, To KK, Wen X, Chen H, Chan KH, Tsoi HW, et al. Clinical and virological factors associated with viremia in pandemic influenza A/H1N1/2009 virus infection. *PLoS One*. 2011;6:e22534. <http://dx.doi.org/10.1371/journal.pone.0022534>
15. Hirose R, Daidoji T, Naito Y, Watanabe Y, Arai Y, Oda T, et al. Long-term detection of seasonal influenza RNA in faeces and intestine. *Clin Microbiol Infect*. 2016;22:813.e1–7. <http://dx.doi.org/10.1016/j.cmi.2016.06.015>

Address for correspondence: Shao-Lun Zhai, Guangdong Key Laboratory of Animal Disease Prevention, Animal Disease Diagnostic Center, Institute of Animal Health, Guangdong Academy of Agricultural Sciences, No. 21 Baishigang St, Tianhe District, Guangzhou, 510640, China; email: zhaishaolun@163.com; Feng Li, Department of Biology and Microbiology & Department of Veterinary and Biomedical Sciences, South Dakota State University, Brookings, SD 57007, USA; email: feng.li@sdstate.edu

EID Podcast: Stained Glass and Flu



The work of art shown here depicts the interrelationship of human, animal, and environmental health.

Stained-glass windows have been appreciated for their utility and splendor for more than 1,000 years, and this engaging work of art by stained glass artist Jenny Hammond reminds us that influenza A viruses—which can be easily spread between animals and humans, use various host species, and exist in many different environments—remain an enduring and global health concern.

Visit our website to listen:

**EMERGING
INFECTIOUS DISEASES**

[https://www2c.cdc.gov/
podcasts/player.
asp?f=8644950](https://www2c.cdc.gov/podcasts/player.asp?f=8644950)

Seroprevalence of *Baylisascaris procyonis* Infection among Humans, Santa Barbara County, California, USA, 2014–2016

Sara B. Weinstein, Camille M. Lake,¹
Holly M. Chastain, David Fisk, Sukwan Handali,
Philip L. Kahn, Susan P. Montgomery,
Patricia P. Wilkins, Armand M. Kuris,
Kevin D. Lafferty

Baylisascaris procyonis (raccoon roundworm) infection is common in raccoons and can cause devastating pathology in other animals, including humans. Limited information is available on the frequency of asymptomatic human infection. We tested 150 adults from California, USA, for *B. procyonis* antibodies; 11 were seropositive, suggesting that subclinical infection does occur.

The raccoon roundworm (*Baylisascaris procyonis*) is a potential health risk to humans. Infected raccoons release eggs in their feces, and these eggs accumulate at communal defecation sites (latrines). When nonraccoon hosts consume eggs, larva migrans can cause blindness and fatal neurologic sequelae (1,2). Less than 5% of migrating larvae reach the brain, and experimental studies suggest that host size, infection site, and inoculating dose drive pathology (1).

Reported human disease cases are rare; however, there is growing evidence for more frequent asymptomatic infections. For example, a recent study showed that 7% of wildlife rehabilitators had *Baylisascaris*-specific antibodies (3). Large and heavily infected raccoon populations probably contaminate many regions with *B. procyonis* eggs (1). These microscopic eggs can survive for years (4), so anyone living in regions with infected raccoons probably has an exposure risk.

Santa Barbara County, California, USA, is a potential high-risk area for exposure to *B. procyonis* eggs. In

Santa Barbara County, a baylisascariasis case was reported in a toddler in 2002 (1,5); raccoon roundworm consistently infects >80% of raccoons (6,7); and latrines are abundant in residential areas (J.F. Mendez, University of California, pers. comm., 2017 Feb 1), potentially exposing residents to roundworms. We describe the use of a parasite-specific antibody assay to detect subclinical *B. procyonis* infections in adult residents of Santa Barbara County. Recruitment, enrollment, and sampling methods were reviewed and approved by the Santa Barbara Cottage Hospital and University of California institutional review boards (14-06u).

The Study

During 2014–2016, we provided public education about raccoon roundworm infection and offered free testing to healthy adults (18–75 years of age) who had lived in Santa Barbara County for ≥ 3 years. We recruited participants by word of mouth and flyers and through presentations at public outreach events and classes at the local university, natural history museum, zoo, and other venues. We also provided information about testing to local wildlife rehabilitators and researchers working with raccoons and *B. procyonis*.

We collected serum samples from a convenience sample of 150 volunteers. This sampling included serum from 5 wildlife rehabilitators and 7 researchers; however, we considered results from these 12 persons separately because their *B. procyonis* roundworm exposure was expected to be higher than that for the general population.

We collected ≈ 5 mL of blood from each volunteer and allowed the samples to clot. We then centrifuged the samples at $1,500 \times g$ for 15 min, separated them, and stored them at -80°C . Participants (149/150) filled out a questionnaire on demographic characteristics and potential risk factors, such as pet ownership, pet and wildlife feeding practices, past contact with raccoons or raccoon feces, and frequency of raccoon observations around their neighborhood and residence (online Technical Appendix, <https://wwwnc.cdc.gov/EID/article/23/8/17-0222-Techapp1.pdf>). We deidentified samples and tested them for *B. procyonis* IgG by using a recombinant *B. procyonis* repeat antigen 1 protein Western blot assay, which has

¹Current affiliation: Uniformed Services University, Bethesda, Maryland, USA.

Author affiliations: University of California, Santa Barbara, California, USA (S.B. Weinstein, C.M. Lake, A.M. Kuris, K.D. Lafferty); IRHC Inc., Atlanta, Georgia, USA (H.M. Chastain); Centers for Disease Control and Prevention, Atlanta, (H.M. Chastain, S. Handali, S.P. Montgomery, P.P. Wilkins); Sansum Clinic, Santa Barbara (D. Fisk); University of California, Berkeley, California, USA (P.L. Kahn); US Geological Survey Western Ecological Research Center, Santa Barbara (K.D. Lafferty)

DOI: <https://doi.org/10.3201/eid2308.170222>

88% sensitivity and 98% specificity (3,8). We generated prevalence estimates by using EpiTools (9), calculating 95% confidence limits (CLs) for an imperfect diagnostic assay (10). We then compared questionnaire responses from seropositive participants with those from seronegative participants by using exact binomial tests in R (11).

The 12 researchers and wildlife rehabilitators tested negative for *B. procyonis* antibodies. Among the remaining 138 volunteers, 11 tested positive (apparent prevalence 8.0%, Wilson CL 4.5%–13.7%; adjusted prevalence 6.9%, accounting for test sensitivity and specificity; Blaker exact CL 2.5%–13.4%). All 11 *B. procyonis*-seropositive participants had seen raccoons in their neighborhood during the past year, and 7 had seen 1 in their yard during the past month. Of the 11 *B. procyonis*-positive study participants, 9 reported no contact with raccoons or their feces; for the 2 who reported contact, the possible exposures occurred 2 and 12 months before testing. Persons with positive serologic test results ranged in age from 20 to 72 years and included an engineer, student, administrator, researcher, social worker, zoo volunteer, and retiree. Some seropositive persons owned dogs, fed animals outside, gardened, and had sandboxes. However, persons with negative serologic test results gave similar responses ($p > 0.15$ for all comparisons), and we found too few infected persons to identify risk factors (Table).

Conclusions

We estimate that $\approx 7\%$ of the sampled persons had antibodies to raccoon roundworm; however, this convenience sample does not represent all county residents. Our recruiting strategy probably introduced income, age, and education biases, and, because we recruited study participants during presentations to groups interested in wildlife

and outdoor activities, we might have selected a sample population with a greater exposure risk. Furthermore, because participants could receive their test results, we expect that persons concerned about past exposure were more likely to participate. Although most baylisascariasis is attributed to *B. procyonis*, cross-reactivity between the *B. procyonis* recombinant antigen assay and other less common *Baylisascaris* spp. is not well characterized and warrants further study. This survey suggests that subclinical *Baylisascaris* infection occurs in the general population; however, additional studies would improve prevalence estimates. These surveys could also include children because most clinical *B. procyonis* infections occur in persons < 2 years of age (1,2) and it is unclear how long antibodies remain after exposure.

Despite frequent contact with raccoons and their feces, no sampled wildlife rehabilitators or researchers tested positive for *B. procyonis* antibodies. Most wildlife rehabilitators and all researchers examined were aware of *B. procyonis* and took precautions when handling raccoons, feces, and parasites. Although the finding of no infection in these high-risk groups could be a reflection of small sample size, it does suggest that preventive measures are effective.

Subclinical human *Baylisascaris* infections might occur wherever humans and infected raccoons overlap. These infections are likely more widespread than previously assumed, and their health risk remains an open question. Subclinical infection might result from lower intensity infection or depend on which tissues are infected (1). Low-intensity infection in organs, such as the brain, could result in subtle clinical manifestations, and clinical and serologic evidence is required to understand the full public health effect of *Baylisascaris* infections.

Table. Questionnaire responses from participants in a study of the seroprevalence of *Baylisascaris procyonis* infection in humans, Santa Barbara County, California, USA, 2014–2016*

Variable	No. (%) seropositive respondents, n = 11	No. (%) seronegative respondents, n = 138
Sex		
M	3 (27)	54 (39)
F	8 (73)	84 (61)
Garden regularly	4 (36)	70 (51)
Sandbox at residence	1 (9)	11 (8)
Own a dog	4 (36)	37 (27)
Feed pets outside	1 (9)	11 (8)
Feed wildlife	1 (9)	18 (13)
Contact with raccoon or their feces	2 (18)	20 (14)
Raccoon seen in neighborhood in past		
Week	3 (27)	23 (17)
Month	4 (36)	45 (33)
Year	4 (36)	48 (35)
>1 y (or never)	0	22 (16)
Raccoon seen in yard in past		
Week	2 (18)	15 (11)
Month	5 (45)	33 (24)
Year	2 (18)	48 (35)
>1 y (or never)	2 (18)	42 (31)

*Responses are from 149/150 participants; 1 seronegative participant did not fill out the questionnaire.

Acknowledgments

We thank all volunteers who provided samples, Pacific Diagnostic Laboratories and Cottage Health for facilitating sampling, Ana Elisa Garcia-Vedrenne for Spanish translations, and everyone who wore the raccoon suit during outreach events.

Financial support was provided by the National Science Foundation Graduate Research Fellowships program (grant no. 1144085 to S.B.W.).

Dr. Weinstein recently completed her PhD dissertation in the Department of Ecology, Evolution and Marine Biology at the University of California, Santa Barbara. Her research interests include parasite ecology and evolution.

References

1. Kazacos KR. *Baylisascaris larva migrans*: US Geological Survey circular 1412. Reston (VA): US Geological Survey; 2016.
2. Graeff-Teixeira C, Morassutti AL, Kazacos KR. Update on baylisascariasis, a highly pathogenic zoonotic infection. *Clin Microbiol Rev*. 2016;29:375–99. <http://dx.doi.org/10.1128/CMR.00044-15>
3. Sapp SGH, Rascoe LN, Wilkins PP, Handali S, Gray EB, Eberhard M, et al. *Baylisascaris procyonis* roundworm seroprevalence among wildlife rehabilitators, United States and Canada, 2012–2015. *Emerg Infect Dis*. 2016;22:2128–31. <http://dx.doi.org/10.3201/eid2212.160467>
4. Shafir SC, Sorvillo FJ, Sorvillo T, Eberhard ML. Viability of *Baylisascaris procyonis* eggs. *Emerg Infect Dis*. 2011;17:1293–5. <http://dx.doi.org/10.3201/eid1707.101774>
5. Schultz T. “Raccoon roundworm” infection confirmed. *Santa Barbara News-Press*. 2002;B1:3.
6. Weinstein SB. *Baylisascaris procyonis* demography and egg production in a California raccoon population. *J Parasitol*. 2016;102:622–8. <http://dx.doi.org/10.1645/15-747>
7. Moore L, Ash L, Sorvillo F, Berlin OGW. *Baylisascaris procyonis* in California. *Emerg Infect Dis*. 2004;10:1693–4. <http://dx.doi.org/10.3201/eid1009.040034>
8. Rascoe LN, Santamaria C, Handali S, Dangoudoubyam S, Kazacos KR, Wilkins PP, et al. Interlaboratory optimization and evaluation of a serological assay for diagnosis of human baylisascariasis. *Clin Vaccine Immunol*. 2013;20:1758–63. <http://dx.doi.org/10.1128/CVI.00387-13>
9. Sergeant ESG. EpiTools epidemiological calculators. Canberra (Australia): Ausvet Pty Ltd; 2016 [cited 2016 Dec 5]. <http://epitools.ausvet.com.au>
10. Reiczigel J, Földi J, Oszvári L. Exact confidence limits for prevalence of a disease with an imperfect diagnostic test. *Epidemiol Infect*. 2010;138:1674–8. <http://dx.doi.org/10.1017/S0950268810000385>
11. R Core Team. R: A language and environment for statistical computing. 3.3.0 ed. Vienna: R Foundation for Statistical Computing; 2016.

Address for correspondence: Sara B. Weinstein, Ecology, Evolution and Marine Biology, University of California, Santa Barbara, CA 93106-9620, USA; email: Batrachoseps@gmail.com

EID Podcast: Deadly Parasite in Raccoons



Infection with *Baylisascaris procyonis* roundworms is rare but often fatal and typically affects children. *B. procyonis*, the common intestinal roundworm of raccoons, has increasingly been recognized as a source of severe, often fatal, neurologic disease in humans, particularly children. Although this devastating disease is rare, lack of effective treatment and the widespread distribution of raccoons in close association with humans make baylisascariasis a disease that seriously affects public health. Raccoons infected with *B. procyonis* roundworms can shed millions of eggs in their feces daily. Given the habit of raccoons to defecate in and around houses, information about optimal methods to inactivate *B. procyonis* eggs is critical for the control of this disease. However, little information is available about survival of eggs and effective disinfection techniques. Additional data provide information on thermal death point and determining the impact of desiccation and freezing on the viability of *B. procyonis* eggs to provide additional information for risk assessments of contamination and guide attempts at environmental decontamination.

Visit our website to listen:

<https://www2c.cdc.gov/podcasts/player.asp?f=8620675>

**EMERGING
INFECTIOUS DISEASES**

Opiate Injection–Associated Skin, Soft Tissue, and Vascular Infections, England, UK, 1997–2016

Dan Lewer, Magdalena Harris, Vivian Hope

In England, UK, hospital admissions caused by bacterial infections associated with opioid use have increased annually since 2012, after 9 years of decline, mirroring trends in overdose deaths. The increase occurred among persons of both sexes and in all age groups and suggests preventive measures need reviewing.

In the United Kingdom, opioid overdose deaths have increased substantially, linked to increasing purity of street heroin and an aging cohort of persons who inject drugs (PWID) (1). PWID also are at risk for skin, soft tissue, and vascular infections (SSTVI), and one third of PWID in the United Kingdom report symptoms of an injection-site infection within the previous year (2). Outbreaks and clusters of bacterial infections among PWID are documented in the United Kingdom (3,4). Most infections are caused by staphylococci and other commensal gram-positive bacteria entering the body at injecting sites. Abscesses and phlebitis are common (5,6) and can lead to invasive infections. Data from a London hospital suggest that such skin and soft tissue infections cause 58% of hospital admissions in PWID, and treatment typically costs several times more than infections in other groups (5). Because little is known about SSTVI trends among PWID over time, we used routine data from all National Health Service hospitals in England to describe hospital admissions for this group.

The Study

We used the Hospital Episode Statistics for England dataset and included all admissions from April 5, 1997, through April 4, 2016, for patients 15–55 years of age. As the most common injecting-related problems (6), we included admissions with a primary (or first-listed) cause of cutaneous abscess (International Classification of Diseases, Tenth Revision, code L02*), cellulitis (L03*), and phlebitis or thrombophlebitis (I80*). We also included admissions where the first-listed cause was endocarditis

(I011, I39*, I330, 1400, I410), septicemia (A40*, A41*), osteomyelitis or septic arthritis (M86*, M00*, M465), or necrotizing fasciitis (M762) and grouped these as invasive infections. Because patients might have multiple episodes of care within 1 admission, we included only first episodes. Age, sex, year of admission, all diagnostic fields, and duration of admission were extracted. Public Health England provided the data.

Hospital Episode Statistics do not report whether a patient injects drugs. Previous studies have identified patients who use drugs as those with a drug-related diagnosis in any diagnostic field (7,8). We identified patients with “injecting-related” infections as those with a relevant infection in the primary diagnostic field and “mental and behavioral disorders due to opioid use” (F11*) in any other diagnostic field, because most PWID in the United Kingdom inject an opioid (9).

We counted injecting-related and non-injecting-related admissions and stratified them by year and patient sex and age group (15–34, 35–44, and 45–55 years). We also tested whether injecting-related infections were associated with longer hospitalization by using a zero-inflated negative binomial model (10) (online Technical Appendix, <https://wwwnc.cdc.gov/EID/article/23/8/17-0439-Techapp1.pdf>).

During 1997–2016, a total of 1,052,444 hospital admissions were caused by SSTVIs, of which 63,671 (6%) were injecting-related. One third (35%) of injecting-related admissions had a primary cause of cutaneous abscess, 32% phlebitis, 23% cellulitis, 4% septicemia, 4% osteomyelitis or septic arthritis, 2% endocarditis, and 0.2% necrotizing fasciitis. Patients with injecting-related infections were younger and more likely to live in deprived neighborhoods, and a minority were female (Table).

The number of injecting-related admissions increased by 33% per year (compound annual growth rate) from 1997–98 through 2003–04 (Figure 1); relative increases were similar in each age group. The total number then decreased each year from 2003–04 through 2012–13; relative changes differed by age group. Admissions reduced by 15% per year for 15–34-year-olds, remained approximately constant for 35–44-year-olds, and increased by 5% per year for 45–55-year-olds. From 2012–13 through 2015–16, the total number of injecting-related admissions increased each year in all age groups. The largest relative increase was for 45–55-year-olds (18% per year). The

Author affiliations: Public Health England, London, UK (D. Lewer); London School of Hygiene and Tropical Medicine, London (M. Harris); Liverpool John Moores University, Liverpool, UK (V. Hope)

DOI: <https://doi.org/10.3201/eid2308.170439>

number of non–injecting-related admissions increased throughout the period; relative increases were similar for each age group and for men and women (online Technical Appendix Figure 1).

As a sensitivity analysis, we excluded admissions within 7 days after discharge, which totaled 4,389 (7%) injecting-related admissions. This exclusion did not change the overall trend (online Technical Appendix).

Injecting-related admissions were longer than non–injecting-related admissions. The difference varied by cause of admission; differences were larger for admissions caused by cutaneous abscess or by invasive infections (Figure 2).

Conclusions

Our analysis of hospital data shows a substantial increase in episodes of serious infection among PWID since 2012. Increases occurred in all age groups and for both men and women. Community surveys have not indicated such a large increase in the prevalence of symptoms of injection-site infections (9), suggesting that the increase might be confined to more severe infections.

The temporal trend found here for bacterial infections mirrors that for opiate overdose–related deaths in England and Wales, which increased sharply from the early 1990s until 2001, decreased gradually until 2012, and then increased again (1). Explanations given for the recent increase in overdoses include an aging cohort of PWID, increasing purity of street heroin, and an increased focus by addiction services on treatment completions, including reducing the number of patients on long-term opioid

Table. Demographic characteristics of patients with skin, soft tissue, and vascular infections, England, UK, April 5, 1997–April 4, 2016*

Characteristic	Patients with injecting-related infections	Patients with non–injecting-related infections
Median age, y (IQR)		
All	34 (29–39)	40 (30–48)
M	34 (30–40)	40 (31–48)
F	32 (27–37)	39 (29–48)
By year		
2000–01	31 (27–36)	39 (30–48)
2005–06	32 (28–37)	39 (30–47)
2010–11	35 (30–41)	40 (30–48)
2015–16	38 (33–43)	41 (30–49)
Female sex, %		
All	28	44
By age group, y		
15–34	32	45
35–44	23	42
45–54	22	43
Neighborhood deprivation quintile, %		
1 (least deprived)	5	21
2	10	21
3	16	20
4	25	20
5 (most deprived)	44	19

*Selected years are shown for brevity. Patients with injecting-related infections were younger for both sexes and in each year ($p < 0.001$, Wilcoxon rank-sum tests). A smaller proportion of patients with injecting-related infections were female for all age groups ($p < 0.001$, χ^2 tests). Age group was associated with sex for both injecting-related and non–injecting-related infections ($p < 0.001$, χ^2 tests). A linear trend described the proportion of injecting-related admissions in each deprivation quintile better than no trend ($p = 0.009$) but not for non–injecting-related admission ($p = 0.504$). Neighborhood deprivation was the UK Department for Community and Local Government’s Index of Multiple Deprivation 2004. IQR, interquartile range.

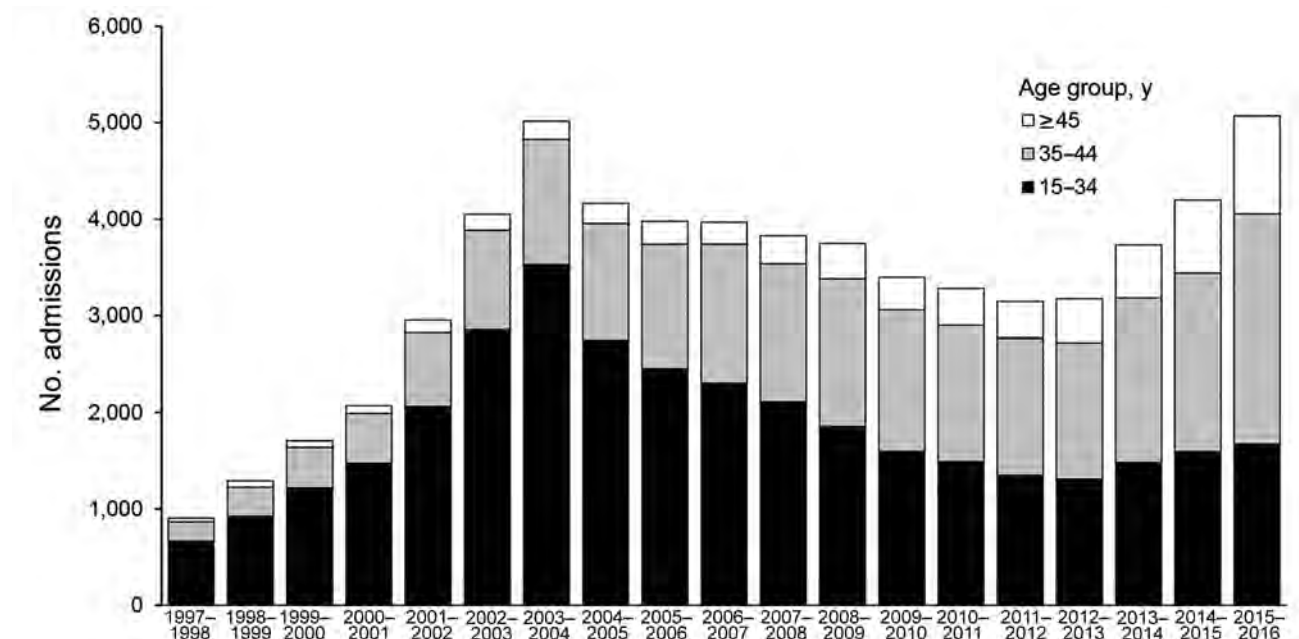


Figure 1. Number of hospital admissions caused by injecting-related bacterial infections, by age group, England, UK, April 5, 1997–April 4, 2016.

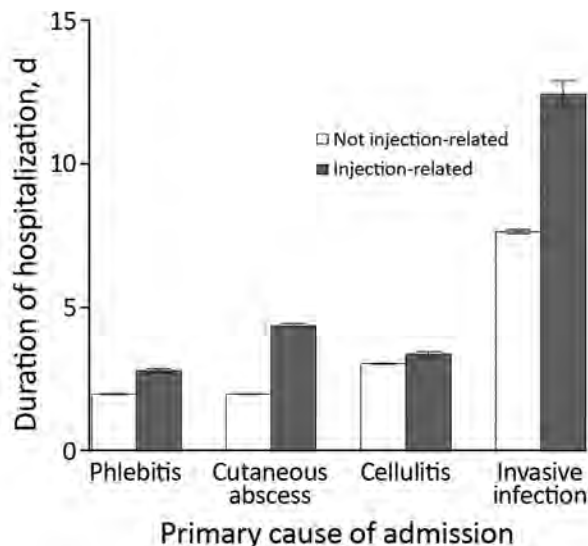


Figure 2. Modeled duration of hospitalization for men 35–44 years of age, by cause of admission, England, UK, April 5, 1997–April 4, 2016. Hospitalization duration was longer for injecting-related admissions for all causes ($p < 0.001$). Error bars indicate 95% CIs.

substitution therapy (1,11). These factors also might contribute to the increase in bacterial infections. Older PWID may lose venous access; miss veins more often when trying to inject (12); and use less accessible and more heavily colonized injection sites, such as the femoral vein (13), leading to more infections. These persons also might have worse immunity and poorer underlying health. An aging cohort of PWID is unlikely to explain the entire increase, however, because increases occurred in all age groups. The role of changes to addiction services and street heroin purity are potential areas for further research.

Additional factors might be contributing to the increase. Opiate users may have started to inject recently emerged psychoactive drugs, which are associated with increased risk for serious bacterial infection (14), although the injection of these drugs remains relatively uncommon in the United Kingdom (9). Primary care services might have become less accessible to PWID, leading to a greater proportion of infections becoming serious and requiring hospitalization. In London, drug preparation using citric acid has been documented to result in highly acidic heroin mixtures (15), potentially precipitating venous damage and infections. Finally, the increase in infections could indicate that the population of PWID has grown since 2012, but little evidence exists with which to test this possibility.

A limitation of our study is that Hospital Episode Statistics do not record whether patients inject drugs, and therefore a proxy was used. The data are likely to underestimate the true number of SSTVI in PWID because hospitals might not always include the opioid-related diagnostic code when PWID are admitted.

Illnesses and deaths from bacterial infections in PWID are more difficult to measure than overdoses because bacterial infections are not specific to drug use. The increasing number of serious infections shown by these data suggests a need for more active surveillance. Preventive measures also need to be considered, including improving access and adherence to wound care and antimicrobial drug regimens, reducing the acidity of heroin preparations, and ensuring accessibility of opioid substitution therapy and sterile injecting equipment.

Mr. Lewer is a specialty registrar in public health, training with the London, Kent, Surrey, and Sussex Deanery, and a member of the South London Health Protection Team at Public Health England. His research interests include the health of marginalized groups and the use of electronic health records for public health research.

References

- Office for National Statistics. Statistical bulletin: deaths related to drug poisoning in England and Wales: 2015 registrations. 2016 [cited 2017 Mar 15]. <https://www.ons.gov.uk/peoplepopulationandcommunity/birthsdeathsandmarriages/deaths/bulletins/deathsrelatedtodrugpoisoninginenglandandwales/2015registrations/pdf>
- Hope V, Kimber J, Vickerman P, Hickman M, Ncube F. Frequency, factors and costs associated with injection site infections: findings from a national multi-site survey of injecting drug users in England. *BMC Infect Dis.* 2008;8:120. <http://dx.doi.org/10.1186/1471-2334-8-120>
- Bundle N, Bubba L, Coelho J, Kwiatkowska R, Cloke R, King S, et al. Ongoing outbreak of invasive and non-invasive disease due to group A streptococcus (GAS) type emm66 among homeless and people who inject drugs in England and Wales, January to December 2016. *Euro Surveill.* 2017;22:30446. <http://dx.doi.org/10.2807/1560-7917.ES.2017.22.3.30446>
- Centers for Disease Control and Prevention. Update: *Clostridium novyi* and unexplained illness among injecting-drug users—Scotland, Ireland, and England, April–June 2000. *MMWR Morb Mortal Wkly Rep.* 2000;49:543–5.
- Marks M, Pollock E, Armstrong M, Morris-Jones S, Kidd M, Gothard P, et al. Needles and the damage done: reasons for admission and financial costs associated with injecting drug use in a central London teaching hospital. *J Infect.* 2013;66:95–102. <http://dx.doi.org/10.1016/j.jinf.2012.10.004>
- Gordon RJ, Lowy FD. Bacterial infections in drug users. *N Engl J Med.* 2005;353:1945–54. <http://dx.doi.org/10.1056/NEJMra042823>
- Irish C, Maxwell R, Dancox M, Brown P, Trotter C, Verne J, et al. Skin and soft tissue infections and vascular disease among drug users, England. *Emerg Infect Dis.* 2007;13:1510–1. <http://dx.doi.org/10.3201/eid1310.061196>
- Ciccarone D, Unick GJ, Cohen JK, Mars SG, Rosenblum D. Nationwide increase in hospitalizations for heroin-related soft tissue infections: associations with structural market conditions. *Drug Alcohol Depend.* 2016;163:126–33. <http://dx.doi.org/10.1016/j.drugalcdep.2016.04.009>
- Public Health England. Shooting up: infections among people who injected drugs in the UK, 2015. An update: November 2016 [cited 2017 Mar 15]. <https://www.gov.uk/government/publications/shooting-up-infections-among-people-who-inject-drugs-in-the-uk>

10. Carter EM, Potts HW. Predicting length of stay from an electronic patient record system: a primary total knee replacement example. *BMC Med Inform Decis Mak*. 2014;14:26. <http://dx.doi.org/10.1186/1472-6947-14-26>

11. Middleton J, McGrail S, Stringer K. Drug related deaths in England and Wales. *BMJ*. 2016;355:i5259. <http://dx.doi.org/10.1136/bmj.i5259>

12. Hope VD, Parry JV, Ncube F, Hickman M. Not in the vein: ‘missed hits’, subcutaneous and intramuscular injections and associated harms among people who inject psychoactive drugs in Bristol, United Kingdom. *Int J Drug Policy*. 2016;28:83–90. <http://dx.doi.org/10.1016/j.drugpo.2015.11.003>

13. Darke S, Ross J, Kaye S. Physical injecting sites among injecting drug users in Sydney, Australia. *Drug Alcohol Depend*. 2001;62:77–82. [http://dx.doi.org/10.1016/S0376-8716\(00\)00161-7](http://dx.doi.org/10.1016/S0376-8716(00)00161-7)

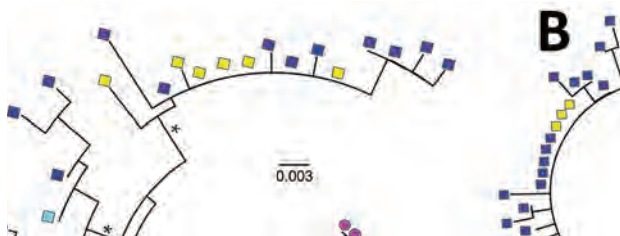
14. Griffith DJ, Mackintosh CL, Inverarity D. *Staphylococcus aureus* bacteraemia associated with injected new psychoactive substances. *Epidemiol Infect*. 2016;144:1257–66. <http://dx.doi.org/10.1017/S095026881500271X>

15. Ciccarone D, Harris M. Fire in the vein: heroin acidity and its proximal effect on users’ health. *Int J Drug Policy*. 2015;26:1103–10. <http://dx.doi.org/10.1016/j.drugpo.2015.04.009>

Address for correspondence: Dan Lewer, South London Health Protection Team, Public Health England, Skipton House, 80 London Rd, London SE1 6LH, UK; email: dan.lewer@phe.gov.uk

April 2017: Emerging Viruses

- Biologic Evidence Required for Zika Disease Enhancements by Dengue Antibodies
- Neurologic Complications of Influenza B Virus Infection in Adults, Romania
- Implementation and Initial Analysis of a Laboratory-Based Weekly Biosurveillance System, Provence-Alpes-Côte d’Azur, France
- Transmission of Hepatitis A Virus through Combined Liver–Small Intestine–Pancreas Transplantation
- Influence of Referral Pathway on Ebola Virus Disease Case-Fatality Rate and Effect of Survival Selection Bias
- *Plasmodium malariae* Prevalence and *csp* Gene Diversity, Kenya, 2014 and 2015



Qinghai H5N8

- Presence and Persistence of Zika Virus RNA in Semen, United Kingdom, 2016
- Three Divergent Subpopulations of the Malaria Parasite *Plasmodium knowlesi*
- Variation in *Aedes aegypti* Mosquito Competence for Zika Virus Transmission
- Outbreaks among Wild Birds and Domestic Poultry Caused by Reassorted Influenza A(H5N8) Clade 2.3.4.4 Viruses, Germany, 2016
- Highly Pathogenic Avian Influenza A(H5N8) Virus in Wild Migratory Birds, Qinghai Lake, China
- Design Strategies for Efficient Arbovirus Surveillance
- Typhus Group Rickettsiosis, Texas, 2003–2013

- Detection and Molecular Characterization of Zoonotic Poxviruses Circulating in the Amazon Region of Colombia, 2014
- Reassortment of Influenza A Viruses in Wild Birds in Alaska before H5 Clade 2.3.4.4 Outbreaks
- Incidence and Characteristics of Scarlet Fever, South Korea, 2008–2015
- Markers of Disease Severity in Patients with Spanish Influenza in the Japanese Armed Forces, 1919–1920
- Molecular Identification of *Spirometra erinaeieuropaei* in Cases of Human Sparganosis, Hong Kong
- Persistent Arthralgia Associated with Chikungunya Virus Outbreak, US Virgin Islands, December 2014–February 2016
- Assessing Sensitivity and Specificity of Surveillance Case Definitions for Zika Virus Disease
- Detection of Zika Virus in Desiccated Mosquitoes by Real-Time Reverse Transcription PCR and Plaque Assay
- Surveillance and Testing for Middle East Respiratory Syndrome Coronavirus, Saudi Arabia, April 2015–February 2016
- Antiviral Drug-Resistant Influenza B Viruses Carrying H134N Substitution in Neuraminidase, Laos, February 2016
- West Nile Virus Seroprevalence, Connecticut, USA, 2000–2014



Risk for Death among Children with Pneumonia, Afghanistan

Rahmani Zabihullah,¹ Bhim G. Dhouhadel,¹
Feroqh A. Rauf, Sahab A. Shafiq, Motoi Suzuki,
Kiawo Watanabe, Lay M. Yoshida, Michio
Yasunami, Salihi Zabihullah, Christopher M.
Parry, Rabi Mirwais, Koya Ariyoshi

In Afghanistan, childhood deaths from pneumonia are high. Among 639 children at 1 hospital, the case-fatality rate was 12.1%, and 46.8% of pneumococcal serotypes detected were covered by the 13-valent vaccine. Most deaths occurred within 2 days of hospitalization; newborns and malnourished children were at risk. Vaccination could reduce pneumonia and deaths.

In Afghanistan, the mortality ratio for children <5 years of age is 90 deaths/1,000 live births, twice the global average; 20% of deaths are from pneumonia (1). Although Afghanistan is considered 1 of the 5 countries with the highest level of childhood deaths from pneumonia, studies of the risk factors for death and etiology of pneumonia among children in Afghanistan are lacking (2). We therefore determined risk factors for death from pneumonia in children <5 years of age in a regional hospital in Afghanistan and the distribution of pneumococcal serotypes carried in the nasopharynx.

The Study

From December 2012 through the second week of March 2013, we conducted a prospective observational study in the Department of Pediatrics in Abu Ali Sina Balkhi Regional Hospital, Mazar-e-Sharif, Afghanistan, a 700-bed regional referral hospital for Balkh Province. This study was conducted before pneumococcal conjugate vaccine 13 (PCV13) had been introduced in Afghanistan. We enrolled children <5 years of age who met the World Health Organization (WHO) criteria for clinical pneumonia at the time of admission (3). We collected data by standardized

questionnaire and determined immunization status by history, immunization report, and bacillus Calmette–Guérin (BCG) scar.

Malnutrition was defined as weight-for-age z score <-2 (WHO Anthro software version 3.2.2, <http://www.who.int/childgrowth/software/en/>). Anemia in children >6 months of age was determined by hemoglobin cutoff values established by WHO (4) and in children ≤6 months by hemoglobin value <2 SDs below the mean for age group (5). Illness severity was classified by WHO criteria (3). Hospital outcomes were classified as discharged (discharged after successful treatment), deceased (died during hospitalization), and unknown (still in hospital at study end). Children with unknown status were excluded from risk factor analysis. Neonates/newborns and infants were defined as children <1 and <12 months of age, respectively.

We collected nasopharyngeal samples according to the WHO protocol by using flocced swabs (Copan Diagnostics, Murietta, CA, USA) that were stored in STGG (skim milk, tryptone, glucose, and glycerine) media at -10°C and transferred within 1 month by airplane with cold ice packs in a thermos to Nagasaki, Japan, where they were stored at -20°C. DNA was extracted by using a QIAamp DNA Blood Mini Kit (QIAGEN, Hilden, Germany). *Streptococcus pneumoniae* was detected by *lytA* real-time PCR (selective for autolysin gene), and serotyping was performed by a nanofluidic real-time PCR that detects 50 serotypes as individual serotype/serogroup including all vaccine serotypes (6).

We considered samples positive by *lytA* PCR but negative for serotypes/serogroups nontypeable and co-colonization with multiple serotypes to be presence of ≥2 serotypes/serogroups in a sample. The percentage of vaccine serotypes was calculated as the proportion of samples that had a vaccine serotype (including minor serotypes in co-colonization) among samples positive by *lytA* PCR.

For analyses we used Epi Info version 7 (Centers for Disease Control and Prevention, Atlanta, GA, USA) and Stata 12 (StataCorp LLP, College Station, TX, USA). In the univariate analysis model, we included risk factors for death from pneumonia at $p < 0.2$, and in the multivariate model we included age, sex, and ethnicity. The study complied with STROBE (https://stroke-statement.org/fileadmin/Strobe/uploads/checklists/STROBE_checklist_

Author affiliations: Nagasaki University, Nagasaki, Japan (R. Zabihullah, B.G. Dhouhadel, M. Suzuki, K. Watanabe, L.M. Yoshida, M. Yasunami, C.M. Parry, K. Ariyoshi); Abu Ali Sina Balkhi Regional Hospital, Mazar-e-Sharif, Afghanistan (F.A. Rauf, S.A. Shafiq, S. Zabihullah); London School of Hygiene and Tropical Medicine, London, UK (C.M. Parry); Public Health Department, Balkh Province, Afghanistan (R. Mirwais)

DOI: <https://doi.org/10.3201/eid2308.151550>

¹These authors contributed equally to this article.

v4_combined.pdf) guidelines and was approved by the Nagasaki University Institutional Review Board, Nagasaki, Japan, and the Balkh Public Health Department, Balkh, Afghanistan. Written informed consent was obtained from the parents of enrolled children.

Parents of 670 children were approached, and 639 children were enrolled (online Technical Appendix Figure 1, <https://wwwnc.cdc.gov/EID/article/23/8/15-1550-Techapp1.pdf>). Median patient age was 5.0 (interquartile range 2.5–9.0) months; 82.5% were infants and 64.3% were male (Table 1). Pneumonia case-fatality ratio (CFR) was 12.1% (75/617; 95% CI 9.6%–14.9%) (online Technical Appendix Table 1). A total of 61 (81.3%) children

Table 1. Characteristics and clinical outcomes for 639 children <5 years of age with pneumonia hospitalized at Ali Sina Balkhi Regional Hospital, Mazar-e-Sharif, Afghanistan, December 2012–March 2013

Characteristics	No. (%)
Sex	
M	411 (64.3)
F	228 (35.7)
Age, mo	
<1 (newborn)	17 (2.7)
1–11	510 (79.8)
≥12	112 (17.5)
Maternal illiteracy	549 (85.9)
Duration of illness >7 d before hospitalization	102 (16.0)
Ethnicity	
Tajik	300 (46.9)
Pashtoon	123 (19.3)
Uzbek	77 (12.0)
Hazara	101 (15.8)
Other	38 (6.0)
Received antimicrobial drugs before hospitalization	
Yes	561 (87.8)
No	65 (10.2)
Unknown	13 (2.0)
Vaccination status, vitamin A intake, and nutritional status	
Bacillus Calmette–Guérin vaccine	545 (85.2)
≥1 dose of pentavalent vaccine, n = 568	436 (76.8)
Measles vaccine, n = 171	107 (62.6)
≥1 dose of vitamin A, n = 345	119 (34.5)
Malnutrition*	
Detected	255 (39.9)
Not detected	381 (59.6)
Not evaluated	3 (0.5)
Anemia†	
Detected	296 (46.3)
Not detected	220 (34.4)
Not evaluated	123 (19.3)
Both malnutrition and anemia, n = 514	126 (24.5)
Very severe pneumonia‡	532 (83.3)
Clinical outcome, n = 617	
Discharged well	542 (87.9)
Death	75 (12.1)

*Defined by weight/age z score <−2, and the z score value was calculated by using World Health Organization Anthro software, version 3.2.2.9 (<http://www.who.int/childgrowth/software/en/>).

†Defined according to the World Health Organization (4) and Janus et al. (5).

‡Severity classified according to World Health Organization (3). Very severe pneumonia is defined as cough or difficulty breathing with 1 of the following: central cyanosis, difficulty feeding, convulsions, lethargy, loss of consciousness, severe respiratory distress.

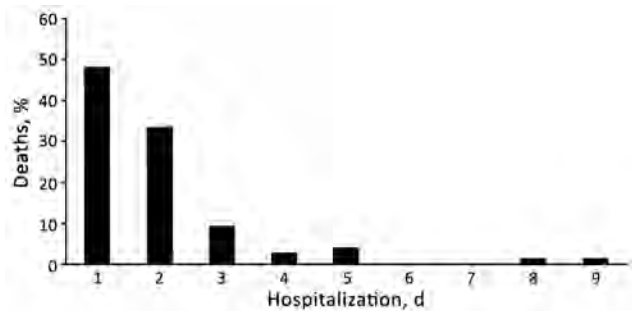


Figure 1. Proportion of deaths and days of hospitalization among children <5 years of age with pneumonia admitted to Abu Ali Sina Balkhi Regional Hospital, Mazar-e-Sharif, Afghanistan, December 2012–March 2013.

died within 2 days of hospitalization (Figure 1), and most were infants (online Technical Appendix Figure 2).

According to univariate analysis, risk for death was increased among newborn (odds ratio [OR] 11.1) and malnourished (OR 2.06) children (Table 2). Protective factors were receipt of BCG vaccine (OR 0.39), ≥1 dose of pentavalent vaccine (OR 0.53), and vitamin A (OR 0.39). Among malnourished children, female sex was associated with death (online Technical Appendix Table 2). We found no significant differences by sex in terms of epidemiologic, clinical, and nutritional status (data not shown). BCG vaccination was independently associated with decreased risk for death among patients with pneumonia (Table 2) and among malnourished children with pneumonia (online Technical Appendix Table 2).

We obtained nasopharyngeal samples from 326 children (online Technical Appendix Figure 1). From half (49.9%) of the children, samples could not be taken because of disease severity; CFR was 18.3% for these children, who were more likely to be malnourished and to have received antimicrobial drugs before hospitalization (online Technical Appendix Table 3). *S. pneumoniae* was detected in 124 (38.0%) of the 326 samples; 24 serotypes/serogroups were identified (Figure 2). Most (87.8%) children had received antimicrobial drugs before admission, which, along with difficulty storing samples at the research site, influenced detection of pneumococci. The proportions of colonization were 35.9% among children who received antimicrobial drugs before hospitalization and 48.8% among children who did not ($p = 0.11$). The proportion of samples that had serotypes covered by 7-, 10-, and 13-valent pneumococcal conjugate vaccines were 39.5%, 39.5% and 46.8%, respectively. Co-colonization with multiple serotypes occurred in 21 (16.9%) of 124 positive samples.

Conclusions

The CFR for children <5 years of age with pneumonia admitted to a regional hospital in Afghanistan was 12.1%,

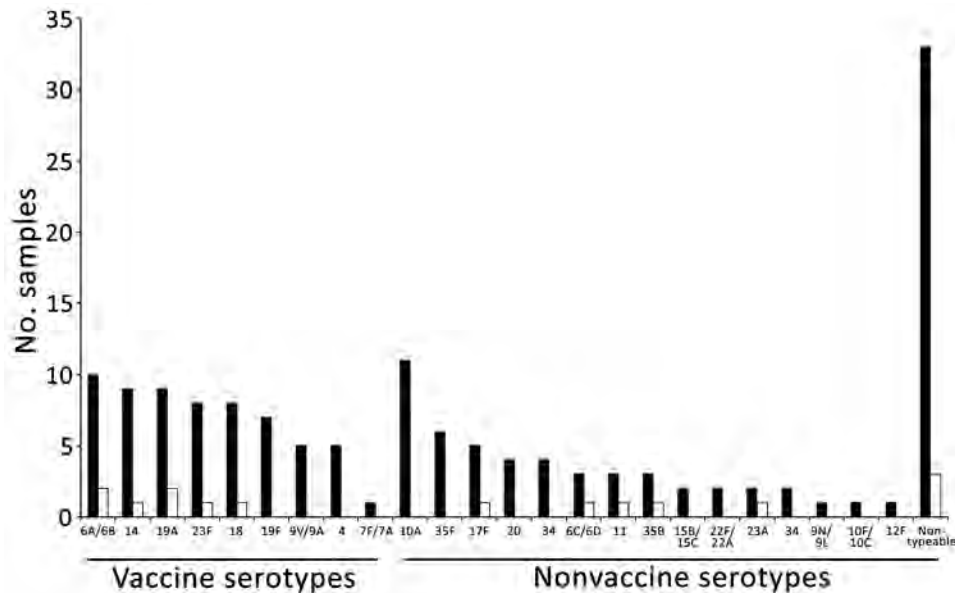


Figure 2. Number of nasopharyngeal samples and pneumococcal serotype/serogroup distribution (including minor serotypes in multiple serotypes) among 110 discharged (black bars) and 11 deceased (white bars) children with pneumonia admitted to Abu Ali Sina Balkhi Regional Hospital, Mazar-e-Sharif, Afghanistan, December 2012–March 2013.

compared with only 7.6% for the full WHO Eastern Mediterranean region (7). Most deaths occurred within 2 days of hospitalization. Factors that may have contributed to the high mortality rate were delays in presentation to health-care facilities, inability to identify severe symptoms in children, and delayed referral from primary care (7). These issues could be addressed by strengthening the Integrated Management of Childhood Illness program of WHO, introduced in Afghanistan in 2004 (8).

Our finding that newborns and children with malnutrition were at increased risk for death is consistent with findings of studies in India and Pakistan (9,10). These risks could be reduced by use of clean delivery kits, clean delivery practices, exclusively breast-feeding, education about complementary feeding, and provision of complementary foods in regions where food is less secure (11,12).

BCG vaccination was protective. Neonatal BCG vaccination is known to be associated with reduced rates of childhood death, respiratory infection, and sepsis, probably by nonspecific immune effects (13); it can also be a proxy for better access to healthcare, immunization, and unmeasured favorable factors.

Female sex was significantly associated with death among malnourished children, which was not explained by association with other variables. A higher incidence of acute lower respiratory infection in male children, particularly in southern Asia, was reported in a recent systematic review, but the pneumonia CFR was higher in girls than in boys <1 year of age (7).

With support from the Global Vaccine Alliance, WHO, and the United Nations Children's Fund, PCV13 was introduced in Afghanistan in January 2014. Our study

detected a wide variety of serotypes, including nonvaccine serotypes. Vaccine coverage was comparable with that found by regional studies (14,15). Serotype data are limited by the short study duration, common use of antimicrobial drugs before hospitalization, and difficult storage of samples.

The high rate of death from pneumonia among children could be reduced by strengthening existing public health programs (e.g., Integrated Management of Childhood Illness, nutrition programs, and immunization programs). Although the proportion of serotypes covered by PCV13 vaccines was 46.8%, PCV13 could still prevent many cases of pneumonia and deaths among children in Afghanistan.

Acknowledgments

We are grateful to the children and their parents who participated in this study. We thank the staff of Abu Ali Sina Balkhi Regional Hospital who helped conduct this research.

The study was funded by the Japan Ministry of Education, Culture, Sports, Science, and Technology. R.Z. and B.G.D. are grateful to the government of Japan, Ministry of Education, Culture, Sports, Science, and Technology for their scholarships.

Dr. Rahmani Zabihullah is a medical doctor from Afghanistan; he performed this work for his Master of Tropical Medicine thesis at Nagasaki University. He works as a health coordinator in Japan International Cooperation Agency, Afghanistan, focusing on improvement of children's health.

References

1. World Health Organization. Afghanistan: health profile. 2014 [cited 2014 May 24]. <http://www.who.int/gho/countries/afg.pdf>

Table 2. Risk factors for death from pneumonia among children <5 years of age hospitalized at Abu Ali Sina Balkhi Regional Hospital, Mazar-e-Sharif, Afghanistan, December 2012–March 2013

Variable	Discharged, no. (%), n = 542	Deceased, no. (%), n = 75	Odds ratio (95% CI)	p value	Adjusted odds ratio (95% CI)*	p value
Sex						
F	186 (34.3)	32 (42.7)	1.42 (0.87–2.32)	0.15	1.61 (0.96–2.71)	0.06
M	356 (65.7)	43 (57.3)	1		1	
Age, mo						
<1 (newborn)	9 (1.7)	8 (10.7)	11.1 (3.36–36.6)	<0.01	13.1 (3.71–46.5)	<0.01
1–11	433 (89.9)	59 (78.6)	1.70 (0.78–3.67)	0.17	1.59 (0.72–3.49)	0.24
≥12	100 (18.4)	8 (10.7)	1			
Maternal illiteracy						
Literate	83 (15.3)	7 (9.3)	0.56 (0.25–1.28)	0.17	0.62 (0.26–1.45)	0.27
Illiterate	459 (84.7)	68 (90.7)	1			
Duration of illness, d						
>7	80 (14.8)	17 (22.7)	1.56 (0.85–2.85)	0.14	1.73 (0.92–3.25)	0.08
≤7	462 (85.2)	58 (77.3)	1			
Ethnicity						
Tajik	252 (46.5)	35 (46.7)	1			
Pashtoon	105 (19.4)	16 (21.3)	1.09 (0.58–2.06)	0.77	0.80 (0.40–1.60)	0.54
Uzbek	62 (11.5)	10 (13.3)	1.16 (0.54–2.47)	0.69	1.04 (0.47–2.31)	0.91
Hazara	89 (16.4)	11 (14.7)	0.88 (0.43–1.82)	0.75	0.81 (0.38–1.72)	0.58
Other	34 (6.3)	3 (4.0)	0.63 (0.18–2.17)	0.47	0.48 (0.13–1.75)	0.27
Received antimicrobial drugs before hospitalization						
Yes	476 (87.8)	65 (86.7)	1.09 (0.47–2.49)	0.83		
No	56 (10.3)	7 (9.3)	1			
Unknown	10 (1.9)	3 (4.0)	2.4 (0.52–10.9)	0.24		
Bacillus Calmette–Guérin vaccine						
Received	474 (87.4)	55 (73.3)	0.39 (0.22–0.69)	<0.01	0.47 (0.25–0.88)	0.02
Not received	68 (12.6)	20 (26.7)	1			
≥1 dose pentavalent vaccine, n = 547†						
Received	380 (79.0)	44 (66.7)	0.53 (0.30–0.92)	0.02		
Not received	101 (21.0)	22 (33.3)	1			
Measles vaccine, n = 165†						
Received	98 (64.9)	6 (42.9)	0.40 (0.13–1.23)	0.11		
Not received	53 (35.1)	8 (57.1)	1			
Vitamin A, n = 336†						
Received	111 (37.1)	7 (18.9)	0.39 (0.16–0.92)	0.03		
Not received	188 (62.9)	30 (81.1)	1			
Malnutrition‡						
Detected	199 (36.7)	41 (54.7)	2.06 (1.26–3.35)	<0.01	2.06 (1.22–3.49)	<0.01
Not detected	340 (62.7)	34 (45.3)	1			
Anemia						
Detected	246 (45.4)	39 (52.0)	1.32 (0.76–2.29)	0.31		
Not detected	192 (35.4)	23 (30.7)	1			
Not evaluated	104 (19.2)	13 (17.3)	1.04 (0.50–2.14)	0.90		

*Age, sex, ethnicities, and variables with $p < 0.2$ in univariate analyses were included in multivariate analysis; blank cells indicate variables without $p < 0.2$ in univariate analysis. Because they had collinearity, bacillus Calmette–Guérin vaccine was included with vaccines and vitamin A was included in multivariate analysis.

†No. children eligible for the vaccines or vitamin A.

‡3 children, whose nutritional status was unknown, were excluded.

- Gilani Z, Kwong YD, Levine OS, Deloria-Knoll M, Scott JA, O'Brien KL, et al. A literature review and survey of childhood pneumonia etiology studies: 2000–2010. *Clin Infect Dis*. 2012;54(Suppl 2):S102–8. <http://dx.doi.org/10.1093/cid/cir1053>
- World Health Organization. Pocket book of hospital care for children: guidelines for the management of common illnesses with limited resources. Geneva: The Organization; 2005.
- World Health Organization. Haemoglobin concentrations for the diagnosis of anaemia and assessment of severity. Vitamin and mineral nutrition information system. WHO/NMH/NHD/MNM/11.1. Geneva: The Organization; 2011.
- Janus J, Moerschel SK. Evaluation of anemia in children. *Am Fam Physician*. 2010;81:1462–71.
- Dhoubhadel BG, Yasunami M, Yoshida LM, Thi HA, Thi TH, Thi TA, et al. A novel high-throughput method for molecular serotyping and serotype-specific quantification of *Streptococcus pneumoniae* using a nanofluidic real-time PCR system. *J Med Microbiol*. 2014;63:528–39. <http://dx.doi.org/10.1099/jmm.0.071464-0>
- Nair H, Simões EA, Rudan I, Gessner BD, Azziz-Baumgartner E, Zhang JS, et al.; Severe Acute Lower Respiratory Infections Working Group. Global and regional burden of hospital admissions for severe acute lower respiratory infections in young children in 2010: a systematic analysis. *Lancet*. 2013; 381:1380–90. [http://dx.doi.org/10.1016/S0140-6736\(12\)61901-1](http://dx.doi.org/10.1016/S0140-6736(12)61901-1)
- Bryce J, Victora CG, Habicht JP, Black RE, Scherpbier RW; MCE-IMCI Technical Advisors. Programmatic pathways to child survival: results of a multi-country evaluation of Integrated Management of Childhood Illness. *Health Policy Plan*. 2005;20(Suppl 1):i5–17. <http://dx.doi.org/10.1093/heapol/czi055>

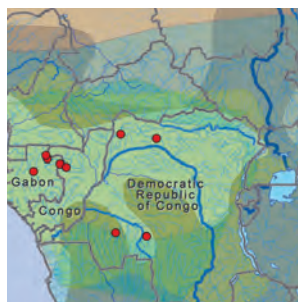
9. The Million Death Study Collaborators. Causes of neonatal and child mortality in India: a nationally representative mortality survey. *Lancet*. 2010;376:1853–60.
10. Mustufa MA, Korejo R, Shahid A, Nasim S. Infection remains a leading cause of neonatal mortality among infants delivered at a tertiary hospital in Karachi, Pakistan. *J Infect Dev Ctries*. 2014;8:1470–5. <http://dx.doi.org/10.3855/jidc.3569>
11. Seward N, Osrin D, Li L, Costello A, Pulkki-Brännström AM, Houweling TA, et al. Association between clean delivery kit use, clean delivery practices, and neonatal survival: pooled analysis of data from three sites in South Asia. *PLoS Med*. 2012;9:e1001180. <http://dx.doi.org/10.1371/journal.pmed.1001180>
12. Lassi ZS, Das JK, Zahid G, Imdad A, Bhutta ZA. Impact of education and provision of complementary feeding on growth and morbidity in children less than 2 years of age in developing countries: a systematic review. *BMC Public Health*. 2013;13(Suppl 3):S13. <http://dx.doi.org/10.1186/1471-2458-13-S3-S13>
13. de Castro MJ, Pardo-Seco J, Martín-Torres F. Nonspecific (heterologous) protection of neonatal BCG vaccination against hospitalization due to respiratory infection and sepsis. *Clin Infect Dis*. 2015;60:1611–9. <http://dx.doi.org/10.1093/cid/civ144>
14. Factor SH, LaClaire L, Bronsdon M, Suleymanova F, Altyntbaeva G, Kadirov BA, et al. *Streptococcus pneumoniae* and *Haemophilus influenzae* type B carriage, central Asia. *Emerg Infect Dis*. 2005;11:1476–9. <http://dx.doi.org/10.3201/eid1109.040798>
15. Sanaei Dashti A, Abdinia B, Karimi A. Nasopharyngeal carrier rate of *Streptococcus pneumoniae* in children: serotype distribution and antimicrobial resistance. *Arch Iran Med*. 2012;15:500–3.

Address for correspondence: Koya Ariyoshi, Department of Clinical Medicine, Institute of Tropical Medicine, Nagasaki University, Sakamoto 3-7-1 Nagasaki 852-8523, Japan; email: kari@nagasaki-u.ac.jp

June 2016: Respiratory Diseases

- Debate Regarding Oseltamivir Use for Seasonal and Pandemic Influenza

- Perspectives on West Africa Ebola Virus Disease Outbreak, 2013–2016



- Human Infection with Influenza A(H7N9) Virus during 3 Major Epidemic Waves, China, 2013–2015

- Integration of Genomic and Other Epidemiologic Data to Investigate and Control a Cross-Institutional Outbreak of *Streptococcus pyogenes*

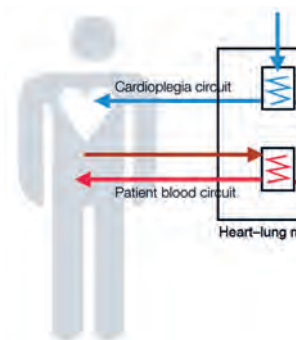
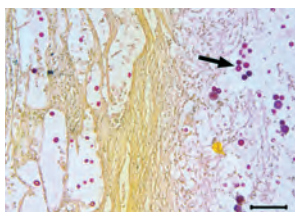
- Infectious Disease Risk Associated with Contaminated Propofol Anesthesia, 1989–2014

- Improved Global Capacity for Influenza Surveillance

- Reemergence of Dengue in Southern Texas, 2013

- Transmission of *Mycobacterium chimaera* from Heater–Cooler Units during Cardiac Surgery despite an Ultraclean Air Ventilation System

- Extended Human-to-Human Transmission during a Monkeypox Outbreak in the Democratic Republic of the Congo



- Use of Population Genetics to Assess the Ecology, Evolution, and Population Structure of *Coccidioides*, Arizona, USA

- Infection, Replication, and Transmission of Middle East Respiratory Syndrome Coronavirus in Alpacas

- Rapid Detection of Polymyxin Resistance in *Enterobacteriaceae*

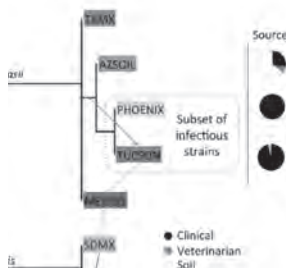
- Human Adenovirus Associated with Severe Respiratory Infection, Oregon, 2013–2014

- Heterogeneous and Dynamic Prevalence of Asymptomatic Influenza Virus Infections

- High MICs for Vancomycin and Daptomycin and Complicated Catheter-Related Bloodstream Infections with Methicillin-Sensitive *Staphylococcus aureus*



- Population-Level Effect of Cholera Vaccine on Displaced Populations, South Sudan, 2014



EMERGING INFECTIOUS DISEASES®

<https://wwwnc.cdc.gov/eid/articles/issue/22/6/table-of-contents>

Detection of *Elizabethkingia* spp. in *Culicoides* Biting Midges, Australia

Peter T. Mee, Stacey E. Lynch, Peter J. Walker, Lorna Melville, Jean-Bernard Duchemin

Author affiliations: The University of Melbourne, Parkville, Victoria, Australia (P.T. Mee); Agriculture Victoria, AgriBio, Bundoora, Victoria, Australia (P.T. Mee, S.E. Lynch); Commonwealth Scientific Industrial Research Organization, Geelong, Victoria, Australia (P.T. Mee, P.J. Walker, J.-B. Duchemin); University of Queensland, St Lucia, Queensland, Australia (P.J. Walker); Department of Primary Industry and Fisheries, Berrimah, Northern Territory, Australia (L. Melville)

DOI: <https://doi.org/10.3201/eid2308.161565>

The bacterial pathogen *Elizabethkingia* is known to exist in certain species of mosquito but was unknown in other arthropods. We report the detection and identification of *Elizabethkingia* in species of *Culicoides* biting midge in Australia, raising the possibility of bacterial transmission via this species.

Bacteria in the genus *Elizabethkingia* (formerly *Chryseobacterium* or *Flavobacterium*) are gram-negative bacilli that occur globally in water sources including rivers, reservoirs, and soils. In recent years, 3 medically important species in this genus, *E. meningoseptica*, *E. anophelis*, and *E. miricola*, have been recognized as the cause of emerging nosocomial infections, neonatal sepsis, and infections in immunocompromised persons. Outbreaks and infections have occurred globally, with cases reported in the Central African Republic; Singapore; Hong Kong, China (1); India; Australia; and the United States. Infection by any of the 3 species can cause septicemia, with a recorded mortality rate of 23.5% (1–3).

Originally, *E. meningoseptica* was thought to be the causative agent of most *Elizabethkingia* infections. However, *E. anophelis* has recently been implicated as the more likely cause and as the primary species associated with bacteremia (1). Isolated from *Anopheles gambiae* mosquitoes in 2011 (4), *E. anophelis* has a relatively high occurrence

(68%) in field-collected mosquitoes (5) and has been identified in *Aedes aegypti* and *An. stephensi* mosquitoes (6,7), with transmission between mosquitoes by vertical, horizontal, and transstadial modes (6,7). Occurrence of *Elizabethkingia* in other arthropods has not been reported.

Culicoides biting midges are classified in the family Ceratopogonidae in the order Diptera. These arthropods are found around the world and are capable of transmitting pathogens (mainly viral or filarial but also bacterial) affecting birds, livestock, and humans. In Australia, there are 78 described and 61 undescribed species of *Culicoides* midges. We investigated the presence of *Elizabethkingia* in *Culicoides* midges in Australia.

In summer 2013, we collected 66 *Culicoides* individuals in Australia from 3 locations (Table) using light traps: 24 *C. victoriana*, 21 *C. multimaculatus*, and 21 *C. brevitarsis*. We examined them for the presence of *Elizabethkingia* using 16S rRNA amplicon sequencing. *Culicoides* were collected from 3 locations (Table) using light traps. The midges were identified to species morphologically from homogenized females at CSIRO, Geelong, Victoria, Australia, before DNA extraction using a QIAGEN blood and tissue kit (QIAGEN, Valencia, California, USA). *Culicoides* species identification was confirmed by sequencing the COI gene (8).

We amplified the hypervariable region V3-V4 of the 16S rRNA (422 bp) using PCR primers (S-D-Bact-0341-b-S-17/S-D-Bact-0785-a-A-21) (9), following a modified 16S MiSeq protocol and barcoded samples before sequencing on a MiSeq (Illumina, Victoria, British Columbia, Canada). Two negative controls were included throughout the sequencing methodology to ensure no contamination. We analyzed data using the Quantitative Insights into Microbial Ecology pipeline (10) with reference to Greengenes database. To confirm *Elizabethkingia* species, we used primers forward 5'-ATCTTCATG-GAAGGAGAGC-3' and reverse 5'-GTACCAACACT-TACCCCTAA-3' to amplify 670 bp of the gene encoding the subunit B protein of the DNA gyrase (*gyrB*). Amplicons were purified and then sequenced using a capillary Sanger method.

Sequencing analysis identified a total of 2,717,401 operational taxonomic units across the 66 samples, after all quality trimming procedures and removal of chimeras. Based on the 16S rRNA (GenBank accession no. KX870017) amplicon sequence (>280 times coverage), we

Table. Collection locations and sequencing results for study of *Elizabethkingia* in *Culicoides* biting midges, Australia*

<i>Culicoides</i> species	Collection location	Collection coordinates	% Infected with <i>Elizabethkingia</i> (no. infected/no. collected)	Average no. <i>Elizabethkingia</i> reads per individual (95% CI)	Average % <i>Elizabethkingia</i> reads to bacterial reads (95% CI)
<i>C. brevitarsis</i>	Beatrice Hill, Northern Territory	12°39'S, 131°19'E	71 (15/21)	1,419 (724–2,113)	0.075 (0.05–0.1)
<i>C. multimaculatus</i>	Lake Wellington, Victoria	38°23'S, 147°21'E	0 (0/21)	NA	NA
<i>C. victoriana</i>	Grampians, Victoria	38°08'S, 142°12'E	0 (0/24)	NA	NA

*NA, not applicable.

determined that *Elizabethkingia* infected only *C. brevitarsis* midges (Table). We did not detect *Elizabethkingia* in negative control samples.

Elizabethkingia sequences had 100% nucleotide identity among the 15 *C. brevitarsis* individuals and high sequence identity to *E. anophelis* (99.05%–99.29%), *E. meningoseptica* (98.34%–100%), and *E. miricola* (99.76%) based on sequences obtained from GenBank. However, we were unable to identify the exact strain based on 16S rRNA alone. We successfully amplified *Elizabethkingia gyrB* (GenBank accession no. KX870018) and concatenated sequences with the 16S rRNA region, forming a 1,072-bp amplicon. The phylogenetic analysis confirmed *E. anophelis* as the closest to the species isolated from *C. brevitarsis*, with 95.8% identity across the 2 amplified gene regions.

The *C. brevitarsis* midge is a known vector of several pathogenic viruses in livestock of Australia. Of the many diverse *Culicoides* midge species, some transmit human pathogens; the close association of some species with humans suggests a need for a more detailed study.

Although we did not detect *Elizabethkingia* in *C. victoriae* or *C. multimaculatus* midges, this finding may be a result of differences in climate or ecosystem. Unlike mosquitoes that breed in water, the *C. brevitarsis* midge uses cow dung, so it is potentially isolated from environmental contamination of *Elizabethkingia*. Because *Culicoides* midges are widespread and can be displaced great distances by wind currents, the potential for them to transport the bacterium warrants further investigation.

The nature of the association between insects and *Elizabethkingia* is unknown. Mosquitoes have been reported to harbor *Elizabethkingia*, but it is unknown if they act as vectors or simply serve as reservoirs, symbionts, or environmental markers. One study investigating the possible role of mosquitoes as vectors of *Elizabethkingia* suggests that they act as reservoirs (3). Nevertheless, while the role of insects as vectors of infection remains unclear, the identification of *Elizabethkingia* in *Culicoides* midges is relevant to public health. The *gyrB* primers developed in this study allow more accurate diagnosis of *Elizabethkingia* species than a single gene classification.

Collection of *C. victoriae* was possible due to the Department of Sustainability and Environment permit number 10006587. Collection of *C. multimaculatus* was possible due to the Department of Health and Human Services–funded Victorian Arbovirus Disease Control Program.

Mr. Mee is a PhD student working on *Culicoides* in collaboration between the University of Melbourne and Commonwealth Scientific Industrial Research Organization Australian Animal Health Laboratory. He has studied insect vectors since 2010, primarily focusing on mosquitoes and biting midges, as well as the bacterial endosymbionts that influence them.

References

1. Lau SKP, Chow W-N, Foo C-H, Curreem SOT, Lo GC-S, Teng JLL, et al. *Elizabethkingia anophelis* bacteremia is associated with clinically significant infections and high mortality. *Sci Rep*. 2016;6:26045. <http://dx.doi.org/10.1038/srep26045>
2. Sarma S, Kumar N, Jha A, Baveja U, Sharma S. *Elizabethkingia meningoseptica*: an emerging cause of septicemia in critically ill patients. *J Lab Physicians*. 2011;3:62–3. <http://dx.doi.org/10.4103/0974-2727.78575>
3. Lau SKP, Wu AKL, Teng JLL, Tse H, Curreem SOT, Tsui SKW, et al. Evidence for *Elizabethkingia anophelis* transmission from mother to infant, Hong Kong. *Emerg Infect Dis*. 2015;21:232–41. <http://dx.doi.org/10.3201/eid2102.140623>
4. Kämpfer P, Matthews H, Glaeser SP, Martin K, Loddens N, Faye I. *Elizabethkingia anophelis* sp. nov., isolated from the midgut of the mosquito *Anopheles gambiae*. *Int J Syst Evol Microbiol*. 2011;61:2670–5. <http://dx.doi.org/10.1099/ijs.0.026393-0>
5. Boissière A, Tchioffo MT, Bachar D, Abate L, Marie A, Nsango SE, et al. Midgut microbiota of the malaria mosquito vector *Anopheles gambiae* and interactions with *Plasmodium falciparum* infection. *PLoS Pathog*. 2012;8:e1002742. <http://dx.doi.org/10.1371/journal.ppat.1002742>
6. Coon KL, Vogel KJ, Brown MR, Strand MR. Mosquitoes rely on their gut microbiota for development. *Mol Ecol*. 2014;23:2727–39. <http://dx.doi.org/10.1111/mec.12771>
7. Ngwa CJ, Glöckner V, Abdelmohsen UR, Scheuermayer M, Fischer R, Hentschel U, et al. 16S rRNA gene-based identification of *Elizabethkingia meningoseptica* (Flavobacteriales: Flavobacteriaceae) as a dominant midgut bacterium of the Asian malaria vector *Anopheles stephensi* (Diptera: Culicidae) with antimicrobial activities. *J Med Entomol*. 2013;50:404–14. <http://dx.doi.org/10.1603/ME12180>
8. Mee PT, Weeks AR, Walker PJ, Hoffmann AA, Duchemin J-B. Detection of low-level *Cardinium* and *Wolbachia* infections in *Culicoides*. *Appl Environ Microbiol*. 2015;81:6177–88. <http://dx.doi.org/10.1128/AEM.01239-15>
9. Klindworth A, Pruesse E, Schweer T, Peplies J, Quast C, Horn M, et al. Evaluation of general 16S ribosomal RNA gene PCR primers for classical and next-generation sequencing-based diversity studies. *Nucleic Acids Res*. 2013;41:e1. <http://dx.doi.org/10.1093/nar/gks808>
10. Caporaso JG, Kuczynski J, Stombaugh J, Bittinger K, Bushman FD, Costello EK, et al. QIIME allows analysis of high-throughput community sequencing data. *Nat Methods*. 2010;7:335–6

Address for correspondence: Peter T. Mee, Agriculture Victoria, AgriBio, Centre for AgriBioscience, Bundoora, Victoria, 3219, Australia; email: peter.mee@ecodev.vic.gov.au

Early Evidence for Zika Virus Circulation among *Aedes aegypti* Mosquitoes, Rio de Janeiro, Brazil

Tania Ayllón, Renata de Mendonça Campos, Patrícia Brasil, Fernanda Cristina Morone, Daniel Cardoso Portela Câmara, Guilherme Louzada Silva Meira, Egbert Tannich, Kristie Aimi Yamamoto, Marília Sá Carvalho, Renata Saraiva Pedro, Jonas Schmidt-Chanasit, Daniel Cadar, Davis Fernandes Ferreira, Nildimar Alves Honório

Author affiliations: Instituto Nacional de Infectologia Evandro Chagas–Fiocruz, Rio de Janeiro, Brazil (T. Ayllón, P. Brasil, R.S. Pedro); Núcleo Operacional Sentinela de Mosquitos Vetores-Nosmove–Fiocruz, Rio de Janeiro (T. Ayllón, F.C. Morone, D.C.P. Câmara, N.A. Honório); Universidade Federal do Rio de Janeiro, Rio de Janeiro (R.M. Campos, G.L.S. Meira, K.A. Yamamoto, D.F. Ferreira); Instituto Oswaldo Cruz–Fiocruz, Rio de Janeiro (D.C.P. Câmara, N.A. Honório); Bernhard Nocht Institute for Tropical Medicine, Hamburg, Germany (E. Tannich, J. Schmidt-Chanasit, D. Cadar); Programa de Computação Científica–Fiocruz, Rio de Janeiro (M.S. Carvalho); German Centre for Infection Research Hamburg-Luebeck-Borstel, Hamburg (J. Schmidt-Chanasit)

DOI: <https://doi.org/10.3201/eid2308.162007>

During 2014–2016, we conducted mosquito-based Zika virus surveillance in Rio de Janeiro, Brazil. Results suggest that Zika virus was probably introduced into the area during May–November 2013 via multiple in-country sources. Furthermore, our results strengthen the hypothesis that Zika virus in the Americas originated in Brazil during October 2012–May 2013.

Zika virus is an emerging arthropod-borne virus that was first isolated from sentinel rhesus macaques in 1947 in Africa. Zika virus caused outbreaks of disease in the Pacific region and emerged in northeastern Brazil in March 2015, followed by Rio de Janeiro in May 2015 (1–3). The *Aedes aegypti* mosquito is considered the main vector of Zika virus in urban and suburban areas throughout the world, including Brazil, where the mosquito has been confirmed, together with *Ae. albopictus* mosquitoes, as a vector for the virus (4). Entomologic surveillance for arboviruses in field-trapped mosquitoes is a critical tool for identifying local natural vectors and key sites for increased transmission risks as well as for predicting arbovirus epidemics (5,6). Therefore, virus surveillance

based on field-trapped mosquitoes is a vital tool for public health authorities.

We conducted a surveillance program for mosquito-borne viruses during February 2014–June 2016 in Manginhos neighborhood in Rio de Janeiro, Brazil. We collected mosquitoes on a weekly basis by using portable backpack aspirators and transported them on dry ice to the Núcleo Operacional Sentinela de Mosquitos Vetores-Nosmove/Fiocruz in Rio de Janeiro, where they were counted and their sex and species level were determined.

The collected mosquitoes included a total of 417 engorged female mosquitoes (406 *Ae. aegypti* and 11 *Ae. albopictus* mosquitoes), which we pooled ($n = 178$) and subjected to Zika virus detection using real-time RT-PCR (7). Two of the pools (C20 and P52) were confirmed positive for Zika virus by conventional PCR (8). Pool C20 comprised 2 *Ae. aegypti* mosquitoes obtained in April 2015 from a household located in the João Goulart Park in Manginhos; sample P52 comprised 1 *Ae. aegypti* mosquito obtained in January 2016 during a mosquito-collecting activity in a junkyard located in the São Pedro slum in Manginhos. Sanger sequencing of the amplified fragments (8) confirmed the presence of Zika virus in pools C20 and P52, and we subjected both pools to deep sequencing to obtain larger fragments of the genome.

We performed phylogenetic and phylogeographic analyses based on the near-complete envelope gene sequences of Zika virus from the 2 positive mosquito pools and on all available sequences for Asian genotype Zika virus strains responsible for outbreaks in the Americas. The analyses revealed that strains from pools C20 and P52 (GenBank accession nos. KY354186 and KY354187, respectively) clustered within the same strongly supported lineage, which included strains detected in Rio de Janeiro and other parts of Brazil in late 2015 and in 2016 (online Technical Appendix Figure, <https://wwwnc.cdc.gov/EID/article/23/8/16-2007-Techapp1.pdf>). The mosquito-derived Zika virus detected in January 2016, strain P52, subsequently formed a subclade with human-derived Zika virus strains from Rio de Janeiro detected during March–April 2016. Furthermore, some previously reported human-derived Zika virus strains from Rio de Janeiro clustered in different lineages (online Technical Appendix Figure). The time-resolved phylogeny including the 2 mosquito strains from this study suggests that Zika virus was probably introduced in Rio de Janeiro during May–November 2013. The time to most recent common ancestor of Zika virus from the Americas is estimated to be October 2012–May 2013. These results further strengthen the hypothesis that Zika virus in the Americas originated in Brazil (9). The different clustering pattern of sequences of the human-derived Zika virus from Rio de Janeiro suggests that multiple Zika virus lineages may be circulating in Rio de Janeiro State.

In this study, we detected Zika virus RNA in 2 pools of engorged *Ae. aegypti* mosquitoes that were collected during a mosquito-borne virus surveillance program in Rio de Janeiro. Information regarding Zika virus infection rates is lacking for female and male mosquitoes trapped in the field. However, experiments performed in the laboratory demonstrated transovarial transmission of Zika virus among *Ae. aegypti* mosquitoes and revealed a minimal filial infection rate of 1:290 (10). Mosquito-borne virus surveillance provides an early warning for arbovirus circulation, points out high-risk areas for virus transmission, and provides data for directing control measures. Furthermore, future surveillance-based studies should further illuminate Zika virus ecology and patterns of spatial dynamics.

In conclusion, we showed the presence of Zika virus in engorged *Ae. aegypti* mosquitoes trapped in Rio de Janeiro before the first case of autochthonous Zika virus disease was diagnosed in the city (3). This finding emphasizes the importance and benefit of routine entomologic surveillance programs to public health in terms of ensuring timely implementation of disease prevention and control measures. Furthermore, considering that the analyzed Zika virus from Rio de Janeiro clustered in different lineages, our phylogenetic analysis suggests multiple introductions of Zika virus from other regions of Brazil, rather than from outside the country, and an early presence (2013) of Zika virus in Rio de Janeiro State.

Acknowledgments

We acknowledge the Sequencing Platform Network, Technological Development Program in Materials for Health—PDTIS (Fiocruz, Brazil), for viral genomic sequencing. We thank Alexandra Bialonski for excellent technical assistance in next-generation sequencing.

This work was supported by grants from the Conselho Nacional de Desenvolvimento Científico e Tecnológico-CNPq, Fundação de Amparo à Pesquisa do Estado do Rio de Janeiro-FAPERJ (grant nos. 401542/2015-7, E-26/102.241/2013, and E-26/010.001610/2016) and Fundação Oswaldo Cruz.

Dr. Ayllón is a postdoctoral researcher in the Instituto Nacional de Infectologia Evandro Chagas—Fiocruz. Her research interests include entomology, virology, and immunology, with special focus on mosquito-borne viruses.

References

- Zammarchi L, Tappe D, Fortuna C, Remoli ME, Günther S, Venturi G, et al. Zika virus infection in a traveller returning to Europe from Brazil, March 2015. *Euro Surveill.* 2015;20:21153. <http://dx.doi.org/10.2807/1560-7917.ES2015.20.23.21153>
- Zanluca C, Melo VC, Mosimann AL, Santos GI, Santos CN, Luz K. First report of autochthonous transmission of Zika virus in Brazil. *Mem Inst Oswaldo Cruz.* 2015;110:569–72. <http://dx.doi.org/10.1590/0074-02760150192>
- Calvet GA, Filippis AM, Mendonça MC, Sequeira PC, Siqueira AM, Veloso VG, et al. First detection of autochthonous Zika virus transmission in a HIV-infected patient in Rio de Janeiro, Brazil. *J Clin Virol.* 2016;74:1–3. <http://dx.doi.org/10.1016/j.jcv.2015.11.014>
- Chouin-Carneiro T, Vega-Rua A, Vazeille M, Yebakima A, Girod R, Goindin D, et al. Differential susceptibilities of *Aedes aegypti* and *Aedes albopictus* from the Americas to Zika virus. *PLoS Negl Trop Dis.* 2016;10:e0004543. <http://dx.doi.org/10.1371/journal.pntd.0004543>
- Jöst H, Bialonski A, Maus D, Sambri V, Eiden M, Groschup MH, et al. Isolation of usutu virus in Germany. *Am J Trop Med Hyg.* 2011;85:551–3. <http://dx.doi.org/10.4269/ajtmh.2011.11-0248>
- dos Reis IC, Honório NA, Codeço CT, Magalhães MA, Lourenço-de-Oliveira R, Barcellos C. Relevance of differentiating between residential and non-residential premises for surveillance and control of *Aedes aegypti* in Rio de Janeiro, Brazil. *Acta Trop.* 2010;114:37–43. <http://dx.doi.org/10.1016/j.actatropica.2010.01.001>
- Lanciotti RS, Kosoy OL, Laven JJ, Velez JO, Lambert AJ, Johnson AJ, et al. Genetic and serologic properties of Zika virus associated with an epidemic, Yap State, Micronesia, 2007. *Emerg Infect Dis.* 2008;14:1232–9. <http://dx.doi.org/10.3201/eid1408.080287>
- Wæhre T, Maagard A, Tappe D, Cadar D, Schmidt-Chanasit J. Zika virus infection after travel to Tahiti, December 2013. *Emerg Infect Dis.* 2014;20:1412–4. <http://dx.doi.org/10.3201/eid2008.140302>
- Naccache SN, Thézé J, Sardi SI, Somasekar S, Greninger AL, Bandeira AC, et al. Distinct Zika virus lineage in Salvador, Bahia, Brazil. *Emerg Infect Dis.* 2016;22:1788–92. <http://dx.doi.org/10.3201/eid2210.160663>
- Thangamani S, Huang J, Hart CE, Guzman H, Tesh RB. Vertical transmission of Zika virus in *Aedes aegypti* mosquitoes. *Am J Trop Med Hyg.* 2016;95:1169–73. <http://dx.doi.org/10.4269/ajtmh.16-0448>

Address for correspondence: Jonas Schmidt-Chanasit, Bernhard Nocht Institute for Tropical Medicine, WHO Collaborating Centre for Arbovirus and Haemorrhagic Fever Reference and Research, Bernhard-Nocht-Strasse 74, 20359 Hamburg, Germany; email: jonassi@gmx.de

Scrub Typhus Outbreak in a Remote Primary School, Bhutan, 2014

Tshokey Tshokey, Stephen Graves, Dorji Tshering, Kelzang Phuntsho, Karchung Tshering, John Stenos

Author affiliations: Jigme Dorji Wangchuck National Referral Hospital, Thimphu, Bhutan (T. Tshokey); University of Newcastle, Australia (T. Tshokey, S. Graves); Australian Rickettsial Reference Laboratory (T. Tshokey, S. Graves, J. Stenos); Bajo Hospital, Wangduephodrang, Bhutan (D. Tshering); Royal Centre for Disease Control, Ministry of Health, Thimphu (K. Phuntsho, K. Tshering)

DOI: <https://doi.org/10.3201/eid2308.162021>

Scrub typhus in Bhutan was first reported in 2009. We investigated an outbreak of scrub typhus in a remote primary school during August–October 2014. Delay in recognition and treatment resulted in 2 deaths from meningoencephalitis. Scrub typhus warrants urgent public health interventions in Bhutan.

Scrub typhus, caused by the intracellular parasite *Orientia tsutsugamushi*, is a miteborne infection that largely occurs in the “tsutsugamushi triangle” (online Technical Appendix Figure 1, <https://wwwnc.cdc.gov/EID/article/23/8/16-2021-Techapp1.pdf>), where Watt et al. estimated ≈1 million cases occurred annually in 2003 (1). Infected persons commonly have fever, headache, conjunctival congestion, myalgia, lymphadenitis, rashes, and eschars with and without complications (2). Among untreated persons, the case-fatality rate is 6%–35% (3). In scrub typhus–endemic areas, central nervous system involvement occurs in ≈25% of patients (4). Consequently, scrub typhus should be considered in the differential diagnosis of aseptic meningitis.

During January–October 2016, Nepal reported scrub typhus in 37 districts, resulting in 8 deaths (5). Himachal Pradesh, India, reported 700 case-patients, 20 of whom died (6). In Bhutan, scrub typhus gained clinical attention after an outbreak in 2009 (7); earlier cases might have been missed because of low awareness.

During August–October 2014, a scrub typhus outbreak occurred in Singye Namgyal Primary School (SNPS), a remote community boarding school in the Wangduephodrang district of Bhutan (online Technical Appendix Figure 2). On August 17, three girls from SNPS reported 5–6 days of fever, headache, cough, and body aches and were treated symptomatically by the visiting health assistant from Kami-chu Basic Health Unit (KBHU). Two of the girls recovered; the third was admitted to the KBHU on August 20 and transferred to Bajo Hospital (BH) the next day. By August 26, she experienced neck stiffness, irritability, and disorientation. Viral encephalitis was suspected, and she was referred to the Jigme Dorji Wangchuck National Referral Hospital (JDWNRH) in Thimphu on August 27. On admission, a

serum sample tested positive for *O. tsutsugamushi* by rapid diagnostic test (RDT); she died the next day.

Another girl and her brother from SNPS were admitted to the Punakha district hospital on September 1 with similar symptoms. The boy was sent home with medications and recovered; his sister had meningeal symptoms and severe thrombocytopenia and was transferred to the JDWNRH on September 2, where she died on September 28. Specimens from both patients were *O. tsutsugamushi*–positive by RDT.

On September 22, a 10-year-old girl from SNPS was referred to JDWNRH with similar symptoms. Her serum specimen was *O. tsutsugamushi* positive, but she recovered with treatment.

After linking the 2 deaths and other cases, an investigation team visited the school during October 2–4. Case-patients were defined as any person from SNPS with fever, headache, and body ache with or without hemorrhagic manifestations currently or in the previous 2 weeks. Forty-one cases related to the outbreak were listed (online Technical Appendix Figure 3); blood samples were drawn from 21 students, 12 of whom were acutely ill, and 10 local residents. Results for all 31 were negative for malaria and dengue; the Widal test of serum samples for enteric fever from 1 student and 2 local residents showed high antibody titers against *Salmonella enterica* serotype Typhi. Serum samples from the 12 acutely ill students were also tested for *O. tsutsugamushi* by RDT (SD Bioline Tsutsugamushi Test; Standard Diagnostics, Yongin, South Korea) in the Bhutan Public Health Laboratory; all were positive. The 12 samples were taken to the JDWNRH for routine blood tests; results showed anemia in 5 patients, thrombocytopenia in 4, neutropenia in 3, lymphocytosis in 2, and neutrophilia in 2 (online Technical Appendix Table). The samples were also sent to the Australian Rickettsial Reference Laboratory (<http://www.rickettsialab.org.au/>), where they were tested for antibodies against *Orientia* by an indirect microimmunofluorescence assay (mIFA) (8). Of the 12 samples, 9 were positive ($\geq 1:512$ for IgM or $\geq 1:256$ for IgG) (Table), including samples from all 6 students who had eschars. All samples from the 12 students were negative for *Orientia* DNA by using quantitative PCR.

Table. Antibody titers by indirect microimmunofluorescence assay of 9 students with diagnosis of scrub typhus, Bhutan, 2014*

Patient ID	Age, y/sex	<i>Orientia tsutsugamushi</i>							
		Gilliam		Karp		Kato		<i>O. chuto</i>	
		IgG	IgM	IgG	IgM	IgG	IgM	IgG	IgM
2	6/M	256	512	256	512	256	128	<128	128
3	9/F	8,192	8,192	8,192	8,192	8,192	8,192	4,096	4,096
4	6/M	512	128	512	256	512	128	128	128
5	10/F	1,024	128	1,024	128	1,024	128	512	128
6	13/M	1,024	256	512	128	256	128	256	128
7	15/M	1,024	128	512	128	512	128	<128	<128
9	7/F	2,048	4,096	2,048	4,096	2,048	2,048	<128	<128
11	10/F	1,024	512	1,024	512	1,024	512	256	256
12	14/F	128	1,024	256	512	128	512	256	256

*ID, identification.

Of the acutely ill patients who had positive mIFA results, 67% had pathognomonic eschars, confirming the clinical diagnostic value in this sign of systemic infection. Thrombocytopenia as a sign of scrub typhus could be useful but is a less specific diagnostic indicator (9). There was only a 75% agreement between the rapid test kit and the precise mIFA, but RDTs were shown to be more useful in early detection (10).

The deaths of 2 children in this outbreak could have been prevented if the public had greater awareness of the signs and symptoms of scrub typhus. Lapses of 7–10 days from symptom onset to initial medical consultation and >1 month until the outbreak was investigated demonstrate the importance of training school health coordinators to identify and report incidences of abnormal medical findings to public health agencies, especially in remote, hard-to-reach areas. Parents delayed seeking medical advice, and in some cases, school staff had to persuade them to take their children for medical evaluation. Rapid medical care during illnesses should be encouraged through better community education.

Despite inadequate identification and reporting, there is increasing evidence of endemic scrub typhus in Bhutan. Outbreaks may be common but unrecognized, and past outbreaks may have been missed. Scrub typhus warrants a dedicated public health program or incorporation into the existing vectorborne disease control program in this country.

Acknowledgments

We thank the Wangduephodrang district health administration, Singye Namgyal Primary School authorities, students and their families, and the local community. We thank Chelsea Nguyen, Mythili Tadepalli, Gemma Vincent, and Hazizul Hussain-Yusef for laboratory support.

Dr. Tshokey is a clinical microbiologist in the Jigme Dorji Wangchuck National Referral Hospital, Thimphu, Bhutan. He is currently pursuing a PhD at the University of Newcastle, Australia, and undertakes academic laboratory work in the Australian Rickettsial Reference Laboratory.

References

1. Watt G, Parola P. Scrub typhus and tropical rickettsioses. *Curr Opin Infect Dis.* 2003;16:429–36. <http://dx.doi.org/10.1097/00001432-200310000-00009>
2. Taylor AJ, Paris DH, Newton PN. A systematic review of mortality from untreated scrub typhus (*Orientia tsutsugamushi*). *PLoS Negl Trop Dis.* 2015;9:e0003971. <http://dx.doi.org/10.1371/journal.pntd.0003971>
3. Mahajan SK. Scrub typhus. *J Assoc Physicians India.* 2005;53:954–8.
4. Abhilash KP, Gunasekaran K, Mitra S, Patole S, Sathyendra S, Jasmine S, et al. Scrub typhus meningitis: An under-recognized cause of aseptic meningitis in India. *Neurol India.* 2015;63:209–14. <http://dx.doi.org/10.4103/0028-3886.156282>
5. 59 new cases of scrub typhus in Chitwan, Nepal. *myRepublica, Nepal.* 2016 [cited 2016 Dec 10]. <http://www.myrepublica.com/news/7173>
6. Dutt A. Scrub typhus outbreak in Himachal affects 700, kills 20. *Hindustan Times.* 2016 Sep 27, 2016 [cited 2016 Dec 10]. <http://www.hindustantimes.com/india-news/scrub-typhus-outbreak-in-himachal-affects-700-kills-20/story-6k5RvlnFLCIdePB-g2cxKAK.html>
7. Tshokey T, Choden T, Sharma R. Scrub typhus in Bhutan: a synthesis of data from 2009 to 2014. *WHO South East Asia J Public Health.* 2016;5:117–122.
8. Graves SR, Dwyer BW, McColl D, McDade JE. Flinders Island spotted fever: a newly recognised endemic focus of tick typhus in Bass Strait. Part 2. Serological investigations. *Med J Aust.* 1991; 154:99–104.
9. Tsay RW, Chang FY. Serious complications in scrub typhus. *J Microbiol Immunol Infect.* 1998;31:240–4.
10. Zhang L, Yu Q, He S, Wang S, Yu H, Li X, Zhang D, Pan L. Comparison of a rapid diagnostic test and microimmunofluorescence assay for detecting antibody to *Orientia tsutsugamushi* in scrub typhus patients in China. *Asian Pac J Trop Med.* 2011;4:666–8.

Address for correspondence: Tshokey Tshokey, Clinical Microbiologist, Department of Laboratory Services, Jigme Dorji Wangchuck National Referral Hospital, Thimphu, Bhutan; email: doc_tshokey@yahoo.com

Scrub Typhus as a Cause of Acute Encephalitis Syndrome, Gorakhpur, Uttar Pradesh, India

Mahima Mittal, Jeromie Wesley Vivian Thangaraj, Winsley Rose, Valsan Philip Verghese, C.P. Girish Kumar, Mahim Mittal, R. Sabarinathan, Vijay Bondre, Nivedita Gupta, Manoj V. Murhekar

Author affiliations: BRD Medical College, Gorakhpur, India (Mahima Mittal, Mahim Mittal); National Institute of Epidemiology, Chennai, India (J.W.V. Thangaraj, C.P. Girish Kumar, R. Sabarinathan, M.V. Murhekar); Christian Medical College, Vellore, India (W. Rose, V.P. Verghese); National Institute of Virology, Gorakhpur (V. Bondre); Indian Council of Medical Research, Delhi, India (N. Gupta)

DOI: <https://doi.org/10.3201/eid2308.170025>

Outbreaks of acute encephalitis syndrome (AES) have been occurring in Gorakhpur Division, Uttar Pradesh, India, for several years. In 2016, we conducted a case–control study. Our findings revealed a high proportion of AES cases with *Orientia tsutsugamushi* IgM and IgG, indicating that scrub typhus is a cause of AES.

Outbreaks of acute encephalitis syndrome (AES) with high case-fatality rates have been occurring in Gorakhpur Division of Uttar Pradesh, India, since 1978 (1). AES predominantly affects children ≤ 15 years of age (2), and its etiology has remained largely unknown (3,4). Studies focusing on AES in the region have documented that cases with unknown etiology accounted for 41.6% of cases in 2011–2012 (5) and 59% in 2013–2014 (6).

Investigations conducted during the 2015 outbreak revealed scrub typhus IgM in $>60\%$ of AES cases (7). The absence of information about IgM positivity from the general population, and the probability of high background antibody levels in areas to which scrub typhus is endemic, led us to conduct an unmatched case-control study in which we compared IgM and IgG seropositivity for *Orientia tsutsugamushi*, the causative agent of scrub typhus, in AES patients and healthy controls.

We conducted the study during August 17–October 16, 2016. Children ≤ 15 years of age with AES admitted to the BRD Medical College in Gorakhpur during the study period were recruited to the study if their parents consented to a blood draw and they had siblings ≤ 15 years of age. We defined a case of AES as an acute onset of fever and change in mental status or new onset seizures, excluding febrile seizures (8), with cerebrospinal fluid pleocytosis (cell counts $>5/\text{mm}^3$). Controls were healthy children ≤ 15 years of age residing in the home (sibling controls) or village (community controls) of AES case-patients. We interviewed mothers and caretakers for information on case-patients and controls.

We collected 2-mL blood samples from case-patients and controls and tested the samples for *O. tsutsugamushi* IgM and IgG using commercial ELISAs (Scrub Typhus Detect; InBios International Inc., Seattle, WA, USA). We considered an optical density value >0.5 to be a positive result (9). We compared IgM and IgG positivity among AES case-patients and their controls by calculating crude and adjusted odds ratios (ORs) with 95% CIs.

We enrolled 46 case-patients and 151 controls (69 sibling and 82 community controls) in the study. The

median age was 5 (interquartile range 3–9) years for patients and 7 (interquartile range 4–10) years for controls. The case-patients and controls did not differ by age group or sex (Table). The mothers of 54 (35.8%) of the control children reported a history of fever in the past 6 months.

Common symptoms among the 46 AES case-patients included seizures (69.6%), altered sensorium (52.2%), and vomiting (37%); physical examinations revealed hepatomegaly (43.4%), cervical or inguinal lymphadenopathy (39.1%), and periorbital edema (54.3%). Cerebrospinal fluid was clear in appearance in 43 of the patients we tested. Cell counts ranged from 5–100/ mm^3 in 41 (95.3%) and were $>100/\text{mm}^3$ in 2 patients. Protein levels in fluid were ≤ 45 mg/dL in 8 patients, 46–100 mg/dL in 15, and >100 mg/dL in 20 patients. All AES case-patients were given intravenous azithromycin; 20 patients also received injected ceftriaxone. Eight patients died.

O. tsutsugamushi IgM was detected in 29 (63%) case-patients and IgG in 38 (82.6%). For controls, IgM was detected in 7 (4.6%) and IgG in 64 (42.4%) children. Of the 8 fatal cases, 6 patients had *O. tsutsugamushi* IgM and all had IgG. The distribution of optical density values for IgM and IgG among cases and controls are shown in the Appendix (online Technical Appendix, <https://wwwnc.cdc.gov/EID/article/23/8/17-0025-Techapp.pdf>). Twenty-eight of the 29 IgM-positive cases and 6 of the 7 controls with IgM seroreactivity were also positive for IgG. Of the 7 controls with IgM seroreactivity, 3 had a history of febrile illness in the past 6 months.

The odds of IgM scrub typhus positivity were 35.1 (95% CI 13.4–92.3) times higher among AES case-patients than among controls; when adjusted for age, the odds were 29.9 (95% CI 9.6–92.9) times higher for case-patients. The odds of IgG positivity were 6.5 (2.8–14.8) times higher among AES case-patients than controls, and when adjusted for age, the odds were 3.8 (95% CI 1.4–10.9) times higher for case-patients. When analyzed separately, AES case-patients had higher odds for IgM positivity compared with

Table. Characteristics of patients with scrub typhus and controls in study of acute encephalitis syndrome, Gorakhpur, Uttar Pradesh, India, 2016

Characteristic	No. (%) patients	No. (%) controls	Odds ratio (95% CI)	p value	Adjusted odds ratio (95% CI)
Age group, y					
≤ 5	24 (52.2)	53 (35.1)	2.0 (0.8–5.2)	0.152	7.4 (1.8–31.0)
6–10	15 (32.6)	67 (44.4)	1.0 (0.4–2.7)	0.987	1.8 (0.5–6.8)
11–15	7 (15.2)	31 (20.5)	1		1
Sex					
M	28 (60.9)	82 (54.3)	1.3 (0.7–2.6)	0.433	
F	18 (39.1)	69 (45.7)	1		
<i>Orientia tsutsugamushi</i> IgM					
Positive	29 (63.0)	7 (4.6)	35.1 (13.4–92.3)	0.000	29.9 (9.6–92.9)
Negative	17 (37.0)	144 (95.4)	1		1
<i>O. tsutsugamushi</i> IgG					
Positive	38 (82.6)	64 (42.4)	6.5 (2.8–14.8)	0.000	3.8 (1.4–10.9)
Negative	8 (17.4)	87 (57.6)	1		1

sibling (OR 25.1, 95% 6.3–99.8) or community (OR 13.2, 95% 2.27–76.7) controls.

Our study had 1 main limitation: patients and controls were selected from the same village and shared the same environmental risk factors. Despite overmatching that underestimates the strength of association, the odds ratios for *O. tsutsugamushi* IgM and IgG positivity were significant. We concluded that the presence of higher levels of *O. tsutsugamushi* IgM and IgG among AES case-patients than among controls indicates a role for scrub typhus in the etiology of AES in Gorakhpur.

Acknowledgments

We thank the members of the expert group on Research-Cum-Intervention project on AES/JE for their inputs on the study findings. We are grateful to Anita Mehta, S.K. Srivastava, and Bhoopendra Sharma for their cooperation. Thanks are also due to Mr. Karunakaran and Mr. Magesh for their technical support.

The study was funded from an extramural grant by the Indian Council of Medical Research, New Delhi.

Dr. Mittal is the head of the Department of Pediatrics at BRD Medical College, Gorakhpur, India. Her research interests include central nervous system infections among children.

References

- Mittal M, Kushwaha KP. AES: Clinical presentation and dilemmas in critical care management. *J Commun Dis* 2014; 46: 50-56
- Ranjan P, Gore M, Selvaraju S, Kushwaha KP, Srivastava DK, Murhekar M. Changes in acute encephalitis syndrome incidence after introduction of Japanese encephalitis vaccine in a region of India. *J Infect*. 2014;69:200–2. <http://dx.doi.org/10.1016/j.jinf.2014.03.013>
- Bhatt GC, Bondre VP, Sapkal GN, Sharma T, Kumar S, Gore MM, et al. Changing clinico-laboratory profile of encephalitis patients in the eastern Uttar Pradesh region of India. *Trop Doct* 2012;42:106e8. <http://journals.sagepub.com/doi/pdf/10.1258/td.2011.110391>
- Joshi R, Kalantri SP, Reingold A, Colford JM Jr. Changing landscape of acute encephalitis syndrome in India: a systematic review. *Natl Med J India*. 2012;25:212–20.
- Jain P, Jain A, Kumar A, Prakash S, Khan DN, Singh KP, et al. Epidemiology and etiology of acute encephalitis syndrome in North India. *Jpn J Infect Dis*. 2014;67:197–203. <http://dx.doi.org/10.7883/yoken.67.197>
- Gupta S, Shahi RK, Nigam P. Clinico-etiological profile and predictors of outcome in acute encephalitis syndrome in adults. *International Journal of Scientific Study*. 2016;3:78–83. http://www.ijss-sn.com/uploads/2/0/1/5/20153321/ijss_feb_oa16_2016.pdf
- Murhekar MV, Mittal M, Prakash JA, Pillai VM, Mittal M, Girish Kumar CP, et al. Acute encephalitis syndrome in Gorakhpur, Uttar Pradesh, India - Role of scrub typhus. *J Infect*. 2016;73:623–6. <http://dx.doi.org/10.1016/j.jinf.2016.08.014>
- World Health Organization. Acute Encephalitis Syndrome. Japanese encephalitis surveillance standards. January 2006. From WHO-recommended standards for surveillance of selected vaccine-preventable diseases. WHO/V&B/03.01 [cited 2016 Oct 14]. http://apps.who.int/iris/bitstream/10665/68334/1/WHO_V-B_03.01_eng.pdf
- Blacksell SD, Tanganuchitcharnchai A, Nawtaisong P, Kantipong P, Laongnualpanich A, Day NP, et al. Diagnostic accuracy of the InBios scrub typhus detect enzyme-linked immunoassay for the detection of IgM antibodies in northern Thailand. *Clin Vaccine Immunol*. 2016;23:148–54. <http://dx.doi.org/10.1128/CVI.00553-15>

Address for correspondence: Manoj V. Murhekar, National Institute of Epidemiology, Indian Council of Medical Research R-127, Tamil Nadu Housing Board, Ayappakkam Chennai 600077, India; email: mmurhekar@nieicmr.org.in

Human Infection with *Burkholderia thailandensis*, China, 2013

Kai Chang, Jie Luo, Huan Xu, Min Li, Fengling Zhang, Jin Li, Dayong Gu, Shaoli Deng, Ming Chen, Weiping Lu

Author affiliations: Third Military Medical University, Chongqing, China (K. Chang, J. Luo, H. Xu, M. Li, F. Zhang, J. Li, S. Deng, M. Chen, W. Lu); Shenzhen Academy of Inspection and Quarantine, Guangdong, China (D. Gu)

DOI: <https://doi.org/10.3201/eid2308.170048>

Burkholderia thailandensis infection in humans is uncommon. We describe a case of *B. thailandensis* infection in a person in China, a location heretofore unknown for *B. thailandensis*. We identified the specific virulence factors of *B. thailandensis*, which may indicate a transition to a new virulent form.

Burkholderia thailandensis is closely related to *B. pseudomallei*, the causative agent of melioidosis (1). *B. thailandensis* shares most virulence factors and extensive genomic similarity with *B. pseudomallei* but can be distinguished by its ability to assimilate arabinose and different rRNA sequences (2,3). Little is known about *B. thailandensis* infection in humans. Two case reports described soft tissue infection and pneumonia with sepsis in Thailand and the United States (4,5). We describe a clinical investigation of human infection with *B. thailandensis* in Chongqing, China.

In October 2013, a 67-year-old man in Chongqing was hospitalized with a 13-day history of fever, productive

cough with white sputum, and shortness of breath. Symptoms had not improved after antimicrobial drug treatment at a local clinic. The patient denied contact with any sick persons and any environmental exposure. Empirical treatment with meropenem was used to prompt resolution of the patient's symptoms before culture results were received. During the 6-day treatment course, the patient was transferred to Chongqing Infectious Disease Hospital for treatment. Subsequently, his general condition worsened, and his family wished to have him close to home. He was discharged and died 2 days later.

Laboratory evaluations of blood samples performed at the time of the patient's admission showed a leukocyte count of 20.72×10^9 cells/L with a markedly elevated 91.5% neutrophils, aspartate aminotransferase level of 75.5 U/L (reference range 15.0–40.0 U/L), alanine aminotransferase level of 85.0 U/L (reference range 9.0–50.0 U/L), interleukin-6 level of 352.1 pg/mL (reference range 0–7 pg/mL), and procalcitonin level of 24.37 ng/mL (reference range 0–0.25 ng/mL). A computed tomography scan of the patient's chest showed a thick-walled cavitory lesion at the posterior segment of the right upper lobe measuring 7.9×6.1 cm and multiple nodules in both lung fields (online

Technical Appendix Figure 1, <https://wwwnc.cdc.gov/EID/article/23/8/17-0048-Techapp1.pdf>).

On day 6 of the patient's hospitalization, we observed via microscopy that the positive blood culture contained many gram-negative rod-shaped bacteria (online Technical Appendix Figure 2, panel A). The colonies were smooth and glossy, with silver pigmentation, on sheep blood agar (online Technical Appendix Figure 2, panel B). The VITEK 2 COMPACT system (bioMérieux, Marcy L'Étoile, France) identified the isolated strain as *B. pseudomallei* (97% probability; bionumber 0003451513500211). The API 20NE system (bioMérieux) also identified the isolated strain as *B. pseudomallei* (50.5% probability; index 1157577). However, the biochemical profiles of the API 20NE system, including arabinose assimilation, identified the isolated strain as *B. thailandensis*, based on the mode of artificial interpretation. We analyzed the 16S rDNA sequence of strain BPM with nucleotide BLAST (<https://blast.ncbi.nlm.nih.gov/Blast.cgi>) and found a 100% similarity with *B. thailandensis* (GenBank accession nos. CP000085.1 and CP000086.1).

These results indicate that commercially available phenotypic assays are not ideal for the identification of

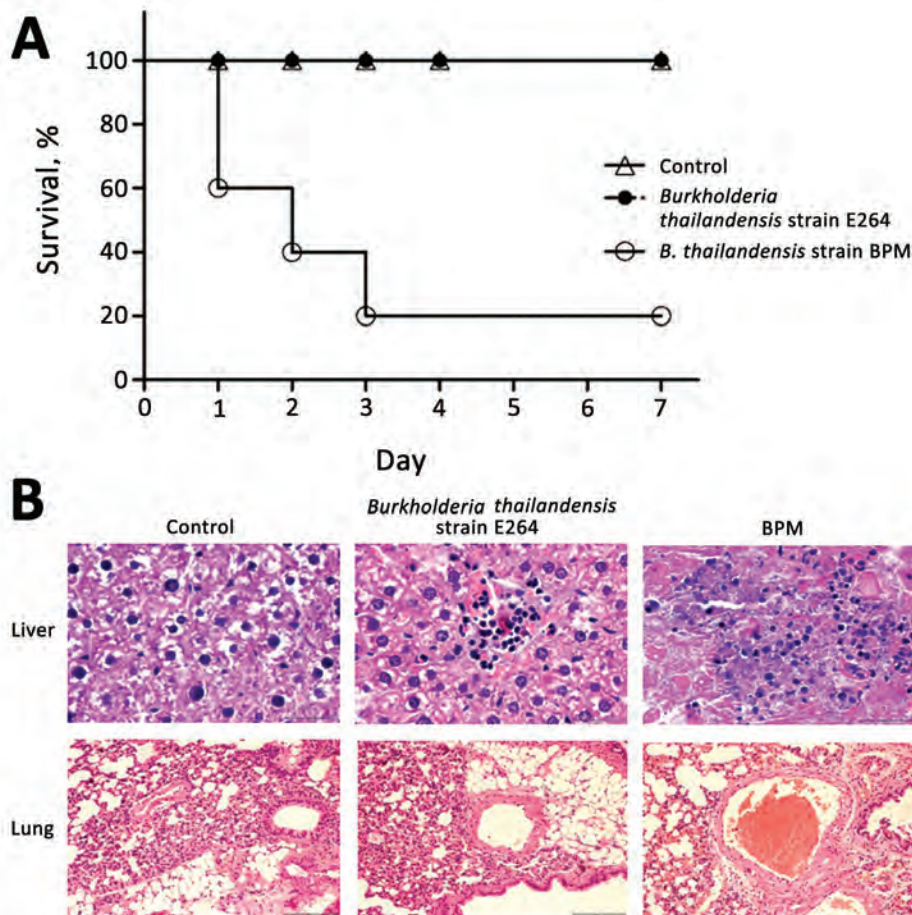


Figure. Virulence comparison of *Burkholderia thailandensis* isolated from a man in Chongqing, China, compared with *B. thailandensis* E264 (strain ATCC 700388). A) Survival pattern of 5 BALB/c mice intraperitoneally challenged with 10^7 CFU and followed up for 7 days after challenge. B) Histopathologic characteristics of *B. thailandensis* intraperitoneal infection in the mice. Sections were stained with hematoxylin and eosin (original magnification $\times 40$).

B. thailandensis, which has not yet been incorporated into the databases of identification systems (6,7). Moreover, the arabinose assimilation proved to be an effective, simple, and accurate method for differentiating *B. thailandensis* from *B. pseudomallei*. When *B. pseudomallei* is presumptively identified, arabinose assimilation should be emphasized in clinical laboratories.

We compared the virulence of the isolated strain with *B. thailandensis* E264 (strain ATCC 700388) in BALB/c mice. *B. thailandensis* E264 is an environmental isolate from northeast Thailand. The clinically isolated *B. thailandensis* from this study was defined as strain BPM. Groups of 5 mice were inoculated with 10^7 CFU of each isolate and observed for a period of 7 days after infection. Four fifths of the mice infected with strain BPM died within 1 week of challenge. *B. thailandensis* could be isolated from the bloodstream of mice at the time of death. In contrast, all mice with *B. thailandensis* E264 infection survived over a 1-week monitoring period (Figure, panel A). The histologic findings were notable for early dissemination to the liver and lung (Figure, panel B). We observed multiple large, necrotizing foci in the livers of mice infected with strain BPM and alveolar-based neutrophilic inflammation in the strain BPM infection group. In addition, the inflammatory infiltrate and lung hyperemia were raised in the BPM-infected mice. This finding is consistent with the clinical case in our study, which appeared as pneumonia and sepsis. Overall, these experiments confirm that strain BPM is a virulent pathogen.

We performed comparative genomics to reveal the pathogenic mechanism of strain BPM. The BPM strain and *B. thailandensis* species share a large proportion of virulence factors. When compared with the reference genome sequences of *B. thailandensis* E264, *B. thailandensis* 2002721723, and *B. thailandensis* E444, the specific virulence factors of VirB/VirD4 type IV secretion system, HSI-I, and WcbR were indicated in strain BPM (online Technical Appendix Table) (8–10). These specific virulence factors may represent a transition toward a new virulent form.

In conclusion, when considering *B. pseudomallei* infection, clinicians should also consider the possibility of *B. thailandensis* infection. *B. thailandensis* is not identified with use of commercially available phenotypic assays and may be mistaken for *B. pseudomallei*. In the future, deep analysis of the complete genome would be helpful in understanding the evolution of *B. thailandensis* and its adaptation to the environment.

This study was supported by the National Natural Sciences Foundation of China (grant nos. 81401751, 81171667),

Shenzhen Science and Technology Research and Development Fund (grant no. CXZZ20150504163004339), and the Guangdong Science and Technology Project (grant no. 20160223).

Dr. Chang is a medical doctor at the Third Military Medical University in Chongqing, China. His main research interests are medical microbiology and molecular diagnostics.

References

1. Ngamdee W, Tandhavanant S, Wikraiphat C, Reamtong O, Wuthiekanun V, Salje J, et al. Competition between *Burkholderia pseudomallei* and *B. thailandensis*. *BMC Microbiol.* 2015;15:56. <http://dx.doi.org/10.1186/s12866-015-0395-7>
2. Yu Y, Kim HS, Chua HH, Lin CH, Sim SH, Lin D, et al. Genomic patterns of pathogen evolution revealed by comparison of *Burkholderia pseudomallei*, the causative agent of melioidosis, to avirulent *Burkholderia thailandensis*. *BMC Microbiol.* 2006;6:46. <http://dx.doi.org/10.1186/1471-2180-6-46>
3. Haraga A, West TE, Brittnacher MJ, Skerrett SJ, Miller SI. *Burkholderia thailandensis* as a model system for the study of the virulence-associated type III secretion system of *Burkholderia pseudomallei*. *Infect Immun.* 2008;76:5402–11. <http://dx.doi.org/10.1128/IAI.00626-08>
4. Lertpatanasuwan N, Sermisri K, Petkaseam A, Trakulsomboon S, Thamlikitkul V, Suputtamongkol Y. Arabinose-positive *Burkholderia pseudomallei* infection in humans: case report. *Clin Infect Dis.* 1999;28:927–8. <http://dx.doi.org/10.1086/517253>
5. Glass MB, Gee JE, Steigerwalt AG, Cavuoti D, Barton T, Hardy RD, et al. Pneumonia and septicemia caused by *Burkholderia thailandensis* in the United States. *J Clin Microbiol.* 2006;44:4601–4. <http://dx.doi.org/10.1128/JCM.01585-06>
6. Amornchai P, Chierakul W, Wuthiekanun V, Mahakhunkijcharoen Y, Phetsouvanh R, Currie BJ, et al. Accuracy of *Burkholderia pseudomallei* identification using the API 20NE system and a latex agglutination test. *J Clin Microbiol.* 2007;45:3774–6. <http://dx.doi.org/10.1128/JCM.00935-07>
7. Zong Z, Wang X, Deng Y, Zhou T. Misidentification of *Burkholderia pseudomallei* as *Burkholderia cepacia* by the VITEK 2 system. *J Med Microbiol.* 2012;61:1483–4. <http://dx.doi.org/10.1099/jmm.0.041525-0>
8. Schröder G, Schuelein R, Quebatte M, Dehio C. Conjugative DNA transfer into human cells by the VirB/VirD4 type IV secretion system of the bacterial pathogen *Bartonella henselae*. *Proc Natl Acad Sci U S A.* 2011;108:14643–8. <http://dx.doi.org/10.1073/pnas.1019074108>
9. Yu Y, Yang H, Li J, Zhang P, Wu B, Zhu B, et al. Putative type VI secretion systems of *Vibrio parahaemolyticus* contribute to adhesion to cultured cell monolayers. *Arch Microbiol.* 2012;194:827–35. <http://dx.doi.org/10.1007/s00203-012-0816-z>
10. Price EP, Sarovich DS, Mayo M, Tuanyok A, Drees KP, Kaestli M, et al. Within-host evolution of *Burkholderia pseudomallei* over a twelve-year chronic carriage infection. *MBio.* 2013;4:e00388-13. <http://dx.doi.org/10.1128/mBio.00388-13>

Address for correspondence: Weiping Lu or Ming Chen, Institute of Surgery Research, Daping Hospital, Third Military Medical University Department of Clinical Laboratory Medicine, 10 Changjiang Branch Road, Yuzhong District, Chongqing 400042, China; email: luweiping19710416@163.com or chming1971@126.com

mcr-1 and *bla*_{KPC-3} in *Escherichia coli* Sequence Type 744 after Meropenem and Colistin Therapy, Portugal

Marta Tacão, Rafael dos Santos Tavares, Pedro Teixeira, Inês Roxo, Elmano Ramalheira, Sónia Ferreira, Isabel Henriques

Author affiliations: University of Aveiro, Aveiro, Portugal (M. Tacão, R. dos Santos Tavares, P. Teixeira, E. Ramalheira, I. Henriques); Centro Hospitalar do Baixo Vouga-EPE, Aveiro (I. Roxo, E. Ramalheira, S. Ferreira); Instituto de Educação e Cidadania, Aveiro (I. Roxo, S. Ferreira)

DOI: <https://doi.org/10.3201/eid2308.170162>

Escherichia coli Ec36 was recovered from a patient in Portugal after treatment with meropenem and colistin. Besides an IncF plasmid with Tn1441d-*bla*_{KPC-3}, already reported in clinical strains in this country, *E. coli* Ec36 co-harbored an IncX4::*mcr-1* gene. Results highlight emerging co-resistance to carbapenems and polymyxins after therapy with drugs from both classes.

The emergence of the *mcr-1* gene (1) and reports on its global dissemination (2) unveiled the danger of plasmid-associated colistin resistance. In July 2016, a 70-year-old woman was admitted to the intensive care unit of Centro Hospitalar do Baixo Vouga-EPE, Aveiro, Portugal, for abdominal pain, ostensibly from an abdominal occlusion. After emergency surgery, the patient received meropenem (20 d), fluconazole, and linezolid (both 10 d) and was transferred to the general medicine ward. After 50 days of antibacterial drug therapy, a urine specimen was positive for *Klebsiella pneumoniae* (Kp81). Further testing showed a multidrug-resistance profile, including resistance to carbapenems, but susceptibility to colistin and tigecycline (Table). The drug regimen was altered to colistin and tigecycline for 6 days, after which urine cultures were negative for *K. pneumoniae*.

Urine culture was performed as a standard procedure after 72 days. *Escherichia coli* (Ec36) was isolated, showing a resistance profile identical to *K. pneumoniae* Kp81 but expressing colistin resistance (Table). PCR screening and amplicon sequencing confirmed the presence of *mcr-1* in Ec36 and *bla*_{KPC-3} in both isolates (1,3). All treatments were discontinued, and the patient was discharged 72 days after admission.

We sequenced the Ec36 whole genome (GenBank accession no. MUGF00000000) by using the Illumina HiSeq

2500 platform (Illumina, San Diego, CA, USA); we assembled it de novo by using CLC Genomics (<https://www.qiagen.com/us/search/clc-genomics-workbench/>) and annotated results by using RAST (<http://rast.nmpdr.org/>). We used tools available at the Center for Genomic Epidemiology (<https://cge.cbs.dtu.dk>) to determine the sequence type, resistome, mobilome, serotype, virulence genes, and pathogenicity potential.

Strain Ec36 was assigned to sequence type 744 (ST-744) and predicted as a human pathogen with serotype O89:H10. Testing detected the virulence gene *gad*, encoding a glutamate decarboxylase involved in acid resistance. Besides *mcr-1* and *bla*_{KPC-3}, Ec36 harbored genes encoding resistance to aminoglycosides (*strA*, *strB*, *aacA4*, *aadA*, *aadA5*), β-lactams (*bla*_{TEM-1B'}, *bla*_{OXA-9}), macrolides (*mph*[A]), chloramphenicol (*catA1*), tetracycline (*tet*[A], *tet*[B]), sulfonamides (*sul1*, *sul2*), and trimethoprim (*dfrA14*, *dfrA17*). We used Plasmidfinder (<https://cge.cbs.dtu.dk/services/PlasmidFinder/>) to identify IncX4 (100%; in the *mcr-1*-encoding contig), IncFIA, IncFII, IncQ1, IncX1, and IncI1. We used pMLST 1.4 (<https://cge.cbs.dtu.dk/services/pMLST/>) to identify IncFIA and IncFII.

*bla*_{KPC-3} was in a 16,455-bp contig, 100% identical to plasmid sequences from clinical *K. pneumoniae* (4). In Portugal, this plasmid was reported in clinical isolates of *K. pneumoniae*, *E. coli*, and *Enterobacter* (5). *bla*_{KPC-3} was part of Tn4401 isoform d (4), flanked by *ISKpn7* and *ISKpn6* and located in a cointegrated FIA and FII plasmid (pEc36-KPC3), co-harboring *bla*_{TEM}, *bla*_{OXA-9}, *aacA4*, and *aadA1*. We analyzed the genetic context of *bla*_{KPC-3} in Kp81 and Ec36 by using a PCR-based protocol (4), which indicated a similar context in both strains within Tn4401d in a FIA-FII plasmid. As highlighted previously (5), results reinforce the role of Tn4401d on the spread of carbapenemase genes among *Enterobacteriaceae* in Portugal.

We identified the *mcr-1* gene in a 9,085-bp contig, which matched *E. coli* SHP45 100% (1). Genetic context analysis identified a 2,600-bp *mcr-1*-containing cassette recognized in different plasmid backbones (6), suggesting its mobilization between different hosts.

The IncX4 plasmid harboring *mcr-1* (pEc36_*mcr-1*) was divided into 2 contigs, which we subsequently cloned by using PCR and sequencing. pEc36_*mcr-1* was 33,140 bp and had no other resistance genes, nor *ISAp11*, found originally associated with *mcr-1* and linked to animal reservoirs (7). Plasmid sequence showed high similarity to pESTMCR (GenBank accession no. KU743383), pMCR1-IncX4 (accession no. KU761327), and pMCR1-NJ-IncX4 (accession no. KX447768).

We performed mating assays by using Ec36 as donor and *E. coli* J53 as recipient. Transconjugants were obtained in Plate-Count-Agar (Merck, Germany) with sodium azide

Table. MICs of antibacterial drugs for *Klebsiella pneumoniae* Kp81, *Escherichia coli* Ec36, transconjugant *E. coli* J53::mcr-1, and recipient strain *E. coli* J53*

Drug	MIC, mg/L (susceptibility)			
	<i>K. pneumoniae</i> Kp81	<i>E. coli</i> Ec 36†	<i>E. coli</i> J53::mcr-1	<i>E. coli</i> J53
Amikacin	≥64 (R)	16 (R)	ND	ND
Aztreonam	≥64 (R)	≥64 (R)	ND	ND
Cefepime	≥64 (R)	2 (I)	ND	ND
Ceftazidime	≥64 (R)	≥64 (R)	ND	ND
Ciprofloxacin	≥4 (R)	≥4 (R)	ND	ND
Colistin	≤0.5 (S)	8 (R)	4 (R)	0.5 (S)
Gentamicin	≥16 (R)	≥16 (R)	ND	ND
Imipenem	≥16 (R)	≥16 (R)	≤0.25 (S)	≤0.25 (S)
Meropenem	≥16 (R)	≥16 (R)	≤0.25 (S)	≤0.25 (S)
Piperacillin	≥128 (R)	≥128 (R)	ND	ND
Piperacillin/tazobactam	≥128 (R)	≥128 (R)	ND	ND
Ticarcillin	≥128 (R)	≥128 (R)	ND	ND
Ticarcillin/clavulanic acid	≥128 (R)	≥128 (R)	ND	ND
Tigecycline	1.5 (S)	1 (S)	0.25 (S)	0.25 (S)
Tobramycin	≥16 (R)	≥16 (R)	ND	ND
Trimethoprim/sulfamethoxazole	≥320 (R)	≥320 (R)	ND	ND

*MICs were determined by using VITEK2 system AST-N222 (bioMérieux, Marcy-l'Étoile, France), except colistin, for which MICRONAUT MIC-strip (BioConnections, Knypersley, UK) was used, and interpreted according to the European Committee on Antimicrobial Susceptibility Testing (<http://www.eucast.org>). Shaded rows indicate antibacterial drugs tested for efficacy against each of the 4 organisms. ND, not determined; R, resistant; S, susceptible.

†Strain isolated from the patient in this study.

(100 mg/L) and colistin (2 mg/L). The MIC of colistin for the transconjugant (4 mg/L) was 8 times higher than that for *E. coli* J53. We detected *mcr-1* by using PCR for the transconjugant, but not *bla*_{KPC-3}.

mcr-1 was previously detected in carbapenem-susceptible *E. coli* ST744 in Denmark (8) and in *E. coli* ST744, co-producing CTX-M-like β -lactamases, in Taiwan (9). Regarding clinical *mcr-1*-positive *E. coli*, >10 STs have been reported, including the high-risk ST-131 (8,9). Therefore, the association of a successful clone to the spread of *mcr-1* is not evident, but apparently, it is associated with successful plasmids (e.g., IncX4).

In Portugal, *mcr-1* has been reported in *Salmonella* and *E. coli* from food products and in clinical *Salmonella* isolates (2,10). Since *bla*_{KPC-3} is increasingly reported in Portugal, its co-occurrence with *mcr-1*-harboring plasmids represents a serious concern.

mcr-1 has been found in isolates that produce carbapenemases KPC, NDM, VIM, and OXA-48 (2,7). Carbapenemase genes usually are associated with mobile elements that encode resistance to several antibacterial drugs, and consequently produce multiresistance traits, as in *E. coli* Ec36. This scenario might predict the emergence of drug-resistant phenotypes, likely jeopardizing treatment.

In summary, we isolated KPC-3-producing and *mcr-1*-harboring *E. coli* Ec36 from a patient after treatment with meropenem, then colistin. Colistin-resistant Ec36 may have been part of the patient's gut microbiome, acquiring the *bla*_{KPC-3}-encoding plasmid from the KP81 strain. Although neutropenic, the patient's samples showed an asymptomatic bacteriuria. Thus, prophylactic administration of antibacterial drugs was likely avoidable.

This work was supported by Fundação para a Ciência e a Tecnologia (FCT) through CESAM (UID/AMB/50017/2013).

I.H. was supported by ESF (EU) and POPH funds (Programa Investigador FCT - IF/00492/2013), and by FCT through SFRH/BPD/81509/2011 (S.F.) and SFRH/BPD/114855/2016 (M.T.).

Ms. Tacão is a research scientist at the University of Aveiro, Aveiro, Portugal. Her primary interest is microbiology, particularly bacterial genetic determinants of antibiotic resistance and their dissemination.

References

- Liu Y-Y, Wang Y, Walsh TR, Yi L-X, Zhang R, Spencer J, et al. Emergence of plasmid-mediated colistin resistance mechanism MCR-1 in animals and human beings in China: a microbiological and molecular biological study. *Lancet Infect Dis*. 2015;3099:1–8.
- Skov RL, Monnet DL. Plasmid-mediated colistin resistance (*mcr-1* gene): three months later, the story unfolds. *Euro Surveill*. 2016;21:30155. <http://dx.doi.org/10.2807/1560-7917.ES.2016.21.9.30155>
- Dallenne C, Da Costa A, Decré D, Favier C, Arlet G. Development of a set of multiplex PCR assays for the detection of genes encoding important beta-lactamases in *Enterobacteriaceae*. *J Antimicrob Chemother*. 2010;65:490–5. <http://dx.doi.org/10.1093/jac/dkp498>
- Chen L, Chavda KD, Melano RG, Hong T, Rojzman AD, Jacobs MR, et al. Molecular survey of the dissemination of two *bla*_{KPC}-harboring IncFIA plasmids in New Jersey and New York hospitals. *Antimicrob Agents Chemother*. 2014;58:2289–94. <http://dx.doi.org/10.1128/AAC.02749-13>
- Rodrigues C, Bavlovič J, Machado E, Amorim J, Peixe L, Novais A. KPC-3-producing *Klebsiella pneumoniae* in Portugal linked to previously circulating non-CG258 lineages and uncommon genetic platforms (Tn4401d-IncFIA and Tn4401d-IncN). *Front Microbiol*. 2016;7:1000. <http://dx.doi.org/10.3389/fmicb.2016.01000>
- Poirer L, Kieffer N, Brink A, Coetze J, Jayol A, Nordmann P. Genetic features of MCR-1-producing colistin-resistant

- Escherichia coli* isolates in South Africa. *Antimicrob Agents Chemother*. 2016;60:4394–7. <http://dx.doi.org/10.1128/AAC.00444-16>
7. Nordmann P, Poirel L. Plasmid-mediated colistin resistance: an additional antibiotic resistance menace. *Clin Microbiol Infect*. 2016;22:398–400. <http://dx.doi.org/10.1016/j.cmi.2016.03.009>
 8. Hasman H, Hammerum AM, Hansen F, Hendriksen RS, Olesen B, Agersø Y, et al. Detection of *mcr-1* encoding plasmid-mediated colistin-resistant *Escherichia coli* isolates from human bloodstream infection and imported chicken meat, Denmark 2015. *Euro Surveill*. 2015;20:30085. <http://dx.doi.org/10.2807/1560-7917.ES.2015.20.49.30085>
 9. Kuo SC, Huang WC, Wang HY, Shiau YR, Cheng MF, Lauderdale TL. Colistin resistance gene *mcr-1* in *Escherichia coli* isolates from humans and retail meats, Taiwan. *J Antimicrob Chemother*. 2016;71:2327–9. <http://dx.doi.org/10.1093/jac/dkw122>
 10. Campos J, Cristiano L, Peixe L, Antunes P. MCR-1 in multidrug-resistant and copper-tolerant clinically relevant *Salmonella* 1,4,[5],12:i:- and S. Rissen clones in Portugal, 2011 to 2015. *Euro Surveill*. 2016;21:30270. <http://dx.doi.org/10.2807/1560-7917.ES.2016.21.26.30270>

Address for correspondence: Marta Tacão, Biology Department, University of Aveiro, Campus Universitário Santiago, 3810-193 Aveiro, Portugal; email: martat@ua.pt

Outcomes for 2 Children after Peripartum Acquisition of Zika Virus Infection, French Polynesia, 2013–2014

Marianne Besnard, Timothée Dub, Patrick Gérardin

Author affiliations: Centre Hospitalier de Polynésie Française, Piraie, Tahiti (M. Besnard); Institut Pasteur, Paris, France (T. Dub); Centre Hospitalier Universitaire, Saint Pierre, Réunion (P. Gérardin)

DOI: <https://doi.org/10.3201/eid2308.170198>

Congenital Zika virus infection is associated with severe brain anomalies and impaired function. To determine outcomes, we followed 2 affected children for ≈30 months. For 1 who was symptomatic at birth, transient hepatitis developed. However, neurodevelopment for both children was age appropriate.

Zika virus, a flavivirus, is a teratogenic and neurotropic infectious pathogen (1). Zika virus infection during pregnancy causes congenital microcephaly and severe brain

anomalies (2). In the newly recognized congenital Zika syndrome, infection is also associated with partially collapsed skull, retinal damage, congenital contractures, early-onset hypertonia, and signs of extrapyramidal involvement; irrespective of a clear pathomechanism, infection is also associated with intrauterine growth restriction and low birth weight (1). Developmental outcomes for children born with congenital Zika virus infection have been reported for infants with severe brain anomalies as consequences of early prenatal exposure (3,4) and include postnatal slowing of head circumference growth and impaired function.

After the first large-scale Zika outbreak in French Polynesia, October 2013–April 2014 (5), 2 cases of peripartum Zika virus infection in full-term neonates were reported (6). We report the follow-up and developmental outcomes through ≈30 months of age for these 2 children. We evaluated cognition by using the Child Development Assessment Scale (CDAS), a screening test suitable for children 0–5 years of age (online Technical Appendix, <https://wwwnc.cdc.gov/EID/article/23/8/17-0198-Techapp1.pdf>).

Case-patient 1 was born at 38 weeks' gestation; his weight, size, and neurologic status were within reference ranges for gestational age. His mother manifested a rash, suggestive of Zika virus infection, on day 2 after delivery. Reverse transcription PCRs for Zika virus were positive in blood and saliva from the mother (day 2) and neonate (day 3) and in breast milk on day 2. The neonate was breastfed for 2 months. He remained asymptomatic, and his neurologic development followed a typical course. At 32 months of age, CDAS scores indicated a need to monitor motor development but overall did not indicate neurocognitive problems.

Case-patient 2 was also born at 38 weeks' gestation but was small for gestational age (weight 1,925 g; height 42 cm; head circumference 32 cm). Signs of Zika virus infection (rash) appeared in the mother on day 3 and in the neonate on day 4. Reverse transcription PCRs for Zika virus of blood and urine were positive for the mother (day 1) and the neonate (days 4 and 7) and in breast milk on day 8. On day 2, laboratory testing of blood from the neonate indicated thrombocytopenia (65.0×10^9 thrombocytes/L), leukopenia (4.6×10^9 cells/L), cytolysis, and cholestasis (Table); the cholestasis resolved 4 months later. Ultrasonograms of the liver were unremarkable, and albumin levels and hemostasis remained within reference ranges. Breastfeeding was maintained for 6 months. At 30 months of age, the child's growth remained within –2 SD for weight (10,725 g) and head circumference (47 cm) and –1.5 SD for height (86 cm). CDAS scores indicated no developmental neurocognitive problems.

Follow-up of these 2 case-patients showed that peripartum Zika virus infection, the exposure situation of mother-

Table. Follow-up of liver function test results associated with perinatal Zika virus infection in case-patient 2, French Polynesia, 2014*

Date (postnatal day)	AST, U/L†	ALT, U/L‡	GGT, U/L§	Bilirubin, total/conjugate, mg/L¶
Feb 4 (2)	84	11	201	158
Feb 6 (4)	38	12	297	145
Feb 10 (8)	52	18	457	128/21
Apr 8 (57)	348	150	281	66/54
Apr 16 (65)	239	139	312	50/42
Apr 30 (79)	117	86	239	10
May 13 (92)	119	104	164	8
Jun 17 (120)	57	51	40	2
Oct 25 (250)	38	47	27	2

*Boldface indicates values out of reference range. ALT, alanine aminotransferase; AST, aspartate aminotransferase; GGT, gamma-glutamyl transferase.

†Reference range 15–40 U/L.

‡Reference range 10–40 U/L.

§Reference range 2–34 U/L.

¶Reference range <14/<3 mg/L.

to-child transmission of Zika virus during gestation (when the mother is viremic during childbirth), was associated with neither marked illness at birth nor neurodevelopmental deficits by 30 months of age. However, assessment of late-onset cognitive or sensory deficits requires longer follow-up. Transmission is assumed unlikely to occur through breastfeeding; Zika virus isolated from milk is not replicative (6). For the 2 case-patients reported here, transmission by contact with the vaginal secretions seems unlikely; viral shedding in these secretions is scarce and weak (7).

Prolonged subclinical hepatitis in case-patient 2, such as that observed with congenital cytomegalovirus infection, resolved after 4 months. To the best of our knowledge, liver pathogenesis in living neonates with Zika virus infection has not been reported but is common with other arboviral (e.g., dengue virus) infections. This milder pattern of peripartum Zika virus infection differs from the usually severe neonatal dengue virus infection (severe thrombocytopenia) and peripartum chikungunya virus infection (postnatal encephalopathy).

Our findings, along with findings of mild brain lesions (e.g., subependymal cysts and lenticulo-striate vasculitis) after late intrauterine exposure to Zika virus (8), need to be replicated on larger populations before it can be suggested that placental and blood–brain barriers may be effective late in gestation, after fetal maturation. Studies on placental barrier function have produced discordant results (9,10). The primary human trophoblast cells of full-term placentae have been shown to be refractory to historic strains of Zika virus from Uganda (MR766) and Cambodia (FSS13025). However, a contemporary strain of Zika virus from Puerto Rico (PRVABC59) was able to infect human placental macrophages and mature primary human trophoblast cells (9). In addition, primary human trophoblast cells in a non-Zika virus–endemic population were permissive to a strain of Zika virus from Colombia (FLR) (10).

Taken together, uncertainty about the mode of transmission and discrepancies in epidemiologic study findings make it imperative to aggregate data to enable comparisons of the risk for transmission as a function of exposure

during gestation. More accurate risk estimates should soon be possible thanks to efforts (meta-analyses of individual participant data of existing cohorts) of the international community, which should enable harmonized follow-up and evaluation of developmental outcomes for children exposed to Zika virus.

Acknowledgment

We thank the nurses and Centre de Liaison sur l'Intervention et la Prévention Psychosociale members for the realization and interpretation of the CDAS.

Dr. Besnard is a pediatrician/neonatologist at the Centre Hospitalier de Polynésie Française. She is involved in prenatal diagnosis and in the description of fetal and child consequences of arboviruses circulating in the Pacific Region.

References

- Moore CA, Staples JE, Dobyns WB, Pessoa A, Ventura CV, Fonseca EB, et al. Characterizing the pattern of anomalies in congenital Zika syndrome for pediatric clinicians. *JAMA Pediatr.* 2017;171:288–95. <http://dx.doi.org/10.1001/jamapediatrics.2016.3982>
- Rasmussen SA, Jamieson DJ, Honein MA, Petersen LR. Zika virus and birth defects—reviewing the evidence for causality. *N Engl J Med.* 2016;374:1981–7. <http://dx.doi.org/10.1056/NEJMsr1604338>
- Moura da Silva AA, Ganz JS, Sousa PD, Doriqui MJ, Ribeiro MR, Branco MD, et al. Early growth and neurologic outcomes of infants with probable congenital Zika virus syndrome. *Emerg Infect Dis.* 2016;22:1953–6. <http://dx.doi.org/10.3201/eid2211.160956>
- van der Linden V, Pessoa A, Dobyns W, Barkovich AJ, Júnior HV, Filho EL, et al. Description of 13 infants born during October 2015–January 2016 with congenital Zika virus infection without microcephaly at birth—Brazil. *MMWR Morb Mortal Wkly Rep.* 2016;65:1343–8. <http://dx.doi.org/10.15585/mmwr.mm6547e2>
- Aubry M, Teissier A, Huart M, Merceron S, Vanhomwegen J, Roche C, et al. Zika virus seroprevalence, French Polynesia, 2014–2015. *Emerg Infect Dis.* 2017;23:669–72. <http://dx.doi.org/10.3201/eid2304.161549>
- Besnard M, Lastère S, Teissier A, Cao-Lormeau V, Musso D. Evidence of perinatal transmission of Zika virus, French Polynesia, December 2013 and February 2014. *Euro Surveill.* 2014;19:20751. <http://dx.doi.org/10.2807/1560-7917.ES2014.19.13.20751>
- Paz-Bailey G, Rosenberg ES, Doyle K, Munoz-Jordan J, Santiago GA, Klein L, et al. Persistence of Zika virus in body fluids. Preliminary report. *N Engl J Med.* 2016 Feb 14 [Epub ahead of print].

8. Soares de Souza A, Moraes Dias C, Braga FD, Terzian AC, Estofolete CF, Oliani AH, et al. Fetal infection by Zika virus in the third trimester. Report of 2 cases. *Clin Infect Dis*. 2016;63:1622–5. <http://dx.doi.org/10.1093/cid/ciw613>
9. Quicke KM, Bowen JR, Johnson EL, McDonald CE, Ma H, O'Neal JT, et al. Zika virus infects human placental macrophages. *Cell Host Microbe*. 2016;20:83–90. <http://dx.doi.org/10.1016/j.chom.2016.05.015>
10. Aagaard KM, Lahon A, Suter MA, Arya RP, Seferovic MD, Vogt MB, et al. Primary human placental trophoblasts are permissive for Zika virus (ZIKV) replication. *Sci Rep*. 2017;7:41389. <http://dx.doi.org/10.1038/srep41389>

Address for correspondence: Marianne Besnard, Centre Hospitalier de Polynésie Française, BP 1640 Papeete Tahiti Papeete 98713, French Polynesia; email: mbesnard@nohao.net

California Serogroup Virus Infection Associated with Encephalitis and Cognitive Decline, Canada, 2015

Duncan Webster, Kristina Dimitrova, Kimberly Holloway, Kai Makowski, David Safronetz, Michael A. Drebot

Author affiliations: Dalhousie University, Saint John, New Brunswick, Canada (D. Webster); Public Health Agency of Canada, Winnipeg, Manitoba, Canada (K. Dimitrova, K. Holloway, K. Makowski, D. Safronetz, M.A. Drebot)

DOI: <https://doi.org/10.3201/eid2308.170239>

California serogroup (CSG) viruses, such as Jamestown Canyon and snowshoe hare viruses, are mosquito-borne pathogens that cause febrile illness and neurologic disease. Human exposures have been described across Canada, but infections are likely underdiagnosed. We describe a case of neuroinvasive illness in a New Brunswick, Canada, patient infected with a CSG virus.

California serogroup (CSG) viruses (family *Bunyaviridae*, genus *Orthobunyavirus*) (1) include the mosquito-borne pathogens Jamestown Canyon virus (JCV), snowshoe hare virus (SSHV), and La Crosse virus. Competent vectors include non-*Culex* mosquitoes (e.g., *Aedes*, *Culiseta*, and *Anopheles* species), all of which circulate in New Brunswick, Canada (2,3). The major reservoir and vertebrate amplifier

of JCV is believed to be the white-tailed deer (4). Squirrels, chipmunks, and hares serve as vertebrate reservoirs for SSHV (5). CSG virus infection is generally asymptomatic; however, after an incubation period of 3–7 days, a febrile illness may develop, and central nervous system involvement may lead to encephalitis or meningoencephalitis (6). No targeted therapies exist; treatment is supportive.

We describe a previously independent 73-year-old man, living on Grand Manan Island, off the Fundy Coast of southern New Brunswick, with a febrile illness that began July 23, 2015. The man was hospitalized, and the next day he exhibited abnormal behaviors (purposeless movements and incoherent speech) and became increasingly confused. The confusion and fever continued to worsen, and headache and neck pain developed. On July 28, he was treated with ceftriaxone and transferred to a tertiary-care hospital (Saint John Regional Hospital, Saint John, New Brunswick), where ampicillin and acyclovir were administered. Cerebral spinal fluid values were as follows: leukocyte count, 1×10^6 cells/L (reference range $0\text{--}5 \times 10^6$ cells/L); glucose, 3.5 mmol/L (reference range 2.2–3.9 mmol/L); and protein concentration, 0.58 g/L (reference range 0.15–0.45 g/L). On July 30, an infectious diseases specialist diagnosed the patient with viral encephalitis, most likely secondary to herpes simplex virus infection; ceftriaxone and ampicillin were discontinued. At a neurology consultation on July 31, the patient was still febrile and confused; brain magnetic resonance imaging revealed no acute pathology.

On August 4, additional information revealed that the patient went on frequent excursions into the woods of Grand Manan Island and had exposures to feral cats. Doxycycline was initiated, and serologic tests were conducted for *Bartonella*, *Borrelia*, *Coxiella*, and *Anaplasma* species and for Powassan virus, JCV, and SSHV; tests were also conducted to rule out paraneoplastic process and autoimmune causes. By August 12, the patient was afebrile but remained confused. On August 18, PCR was negative for herpes simplex virus in CSF, and an electroencephalograph revealed no periodic lateralizing epileptiform discharges; acyclovir was discontinued. Initial serologic test results were negative, and the patient showed no autoimmune or paraneoplastic markers. During a geriatric assessment, the patient showed persistent delirium, scoring 13/30 on a mini-mental state examination.

On August 21, we received the patient's initial CSG serology results and collected follow-up serum samples for standard serologic testing by IgM capture ELISA and plaque-reduction neutralization testing (PRNT) (7,8). The acute-phase serum sample was IgM-negative but positive for CSG virus-specific neutralizing antibodies by PRNT (Table). Serial convalescent-phase serum specimens demonstrated IgM seroconversion several weeks after symptom onset and a ≥ 4 -fold rise in PRNT titers for JCV and SSHV, indicating a diagnostic rise. Because serum neutralization

Table. Serologic test results for a patient with California serogroup virus infection associated with encephalitis and cognitive decline, Canada, 2015*

Virus	July 31	August 10	August 21
Jamestown Canyon virus			
ELISA IgM	Negative	Equivocal	Positive
PRNT titer	1:40	1:160	1:320
Snowshoe hare virus			
ELISA IgM	Negative	Equivocal	Positive
PRNT titer	1:20	1:320	1:320

*PRNT, plaque reduction neutralization test.

titers for both viruses were equivalent or, at most, demonstrated only a 2-fold difference, the specific CSG virus associated with the patient's illness could not be determined. Confirmatory PRNT titers for both viruses and the absence of IgM in the acute-phase serum suggest prior exposure to a CSG virus associated with the etiologic pathogen in this case. Secondary infections with orthobunyaviruses may result in a gradual or delayed rise in IgM, with neutralizing antibodies already detectable early after symptom onset, as documented in other cases involving CSG viruses (9).

Results for all other serologic tests were negative, leading to a modification of the diagnosis to confirmed CSG viral encephalitis. On September 9, the patient was transferred to a nursing home. In January 2016, further assessment revealed a lower mini-mental state examination score of 11/30. The patient, who was totally dependent for personal care and instrumental activities of daily living, was diagnosed with postencephalitic dementia.

Exposures to CSG viruses have been documented in New Brunswick (5; M.A. Drebot, unpub. data), and serologic results described in this report suggest that the patient may have been infected by JCV or SSHV on 2 different occasions. Human seroprevalence of CSG virus, specifically JCV, has been noted to be high in the maritime provinces of Atlantic Canada. A serosurvey in Nova Scotia identified an overall CSG seroprevalence of 21.2% (95% CI 16.1%–27.0%) (10). As such, there is need for increased awareness that these viruses are circulating during the mosquito season and may be associated with human disease.

Although most CSG infections result in mild illness, this case further highlights that these viruses can cause severe and debilitating neuroinvasive disease. Patients who seek medical care for febrile or encephalitic clinical symptoms and who have possible or known exposures to mosquito vectors should be considered for CSG virus testing. JCV and SSHV infection should be considered in the differential diagnosis for such patients during the spring, summer, and fall.

Dr. Webster is an infectious diseases consultant and medical microbiologist at the Saint John Regional Hospital and an associate professor in the Faculty of Medicine at Dalhousie University in Saint John, New Brunswick, Canada. His primary research interests include zoonoses, harm reduction, tuberculosis, and glycosylation.

References

- Bente DA. California encephalitis, hantavirus pulmonary syndrome, and bunyavirus hemorrhagic fevers. In: Bennett JE, Dolin R, Blaser MJ, editors. *Mandell, Douglas, and Bennett's Principles and practice of infectious diseases*, 8th ed. Philadelphia: Elsevier Saunders; 2015. p. 2025–30.
- LeDuc JW. Epidemiology and ecology of the California serogroup viruses. *Am J Trop Med Hyg.* 1987;37(Suppl):60S–8S. <http://dx.doi.org/10.4269/ajtmh.1987.37.60S>
- Webster RP, Giguère M, Maltais P, Roy J, Gallie L, Edsall J. Survey of the mosquitoes of New Brunswick. Government of New Brunswick. January 25, 2004 [cited 2016 Dec 5]. <http://www2.gnb.ca/content/dam/gnb/Departments/h-s/pdf/en/CDC/MosquitoesSurvey.pdf>
- Andreadis TG, Anderson JF, Armstrong PM, Main AJ. Isolations of Jamestown Canyon virus (Bunyaviridae: *Orthobunyavirus*) from field-collected mosquitoes (*Diptera: Culicidae*) in Connecticut, USA: a ten-year analysis, 1997–2006. *Vector Borne Zoonotic Dis.* 2008;8:175–88. <http://dx.doi.org/10.1089/vbz.2007.0169>
- Drebot MA. Emerging mosquito-borne bunyaviruses in Canada. *Can Commun Dis Rep.* 2015;41-06:117–23 [cited 2016 Dec 5]. <http://www.phac-aspc.gc.ca/publicat/ccdr-rmct/15vol41/dr-rm41-06/ar-01-eng.php>
- Artsob H. Arbovirus activity in Canada. In: Calisher CH, editor. *Hemorrhagic fever with renal syndrome, tick- and mosquito-borne viruses.* Archives of Virology Supplementum, vol 1. Vienna: Springer; 1990.
- Martin DA, Muth DA, Brown T, Johnson AJ, Karabatsos N, Roehrig JT. Standardization of immunoglobulin M capture enzyme-linked immunosorbent assays for routine diagnosis of arboviral infections. *J Clin Microbiol.* 2000;38:1823–6.
- Beaty BJ, Calisher CH, Shope RS. Diagnostic procedures for viral, rickettsial and chlamydial infections. In: Schmidt NJ, Emmons RW, editors. 6th ed. *Diagnostic procedures for viral, rickettsial and chlamydial infections.* Washington (DC): American Public Health Association; 1989. p. 797–856.
- Rogstad DK, Schiffman E, Neitzel D, Baddour LM. Severe sepsis caused by California serogroup orthobunyavirus. *Emerg Infect Dis.* 2015;21:1876–7. <http://dx.doi.org/10.3201/eid2110.150394>
- Patriquin G, Schleichauf E, Johnston BL, Dimitrova K, Mask A, Traykova-Andonova M, et al. Seroprevalence of Jamestown Canyon virus in Nova Scotia. *Journal of the Association of Medical Microbiology and Infectious Disease Canada.* 2016;1:18–9 <https://www.ammi.ca/Annual-Conference/2016/Abstracts/2016%20JAMMI%20Abstracts.pdf>.

Address for correspondence: Duncan Webster, Dalhousie University, Faculty of Medicine, Division of Infectious Diseases, Department of Medicine, Saint John Regional Hospital, Saint John, NB E2L 4L2, Canada; email: duncan.webster@horizonNB.ca

Effects of Influenza Strain Label on Worry and Behavioral Intentions

Aaron M. Scherer, Megan Knaus,
Brian J. Zikmund-Fisher, Enny Das,
Angela Fagerlin

Author affiliations: University of Iowa, Iowa City, Iowa, USA (A.M. Scherer); University of Michigan, Ann Arbor, Michigan, USA (M. Knaus, B.J. Zikmund-Fisher); Radboud University Nijmegen, Nijmegen, the Netherlands (E. Das); University of Utah, Salt Lake City, Utah, USA (A. Fagerlin)

DOI: <https://doi.org/10.3201/eid2308.170364>

Persons who read information about a hypothetical influenza strain with scientific (H11N3 influenza) or exotic-sounding (Yarraman flu) name reported higher worry and vaccination intentions than did those who read about strains named after an animal reservoir (horse flu). These findings suggest that terms used for influenza in public communications can influence reactions.

Influenza strains are referred to in several ways by infectious disease experts, public health officials, clinicians, and the media when communicating with the public. These influenza strain labels can focus on where the strain originated (e.g., Spanish flu), the animal reservoir (e.g., avian/bird flu), or the hemagglutinin and neuraminidase surface proteins of the strain (e.g., H1N1 influenza).

Changes in terms used to describe a health risk can shape responses to those risks (1–5). For example, using metaphors to describe influenza (e.g., the flu as an army invading the body) may increase influenza vaccination intentions of the public compared to literal descriptions (e.g., the flu is a virus infecting the body) (1). Labels could affect health behavior by the emotional responses they evoke (e.g., worry about infection) as a result of the terms used (6).

We tested how influenza labels affect vaccination intentions and worry about infection in a number of countries that have different cultures (1), vaccination policies (2), and experience with epidemics (3,7). After receiving exempt status from the University of Michigan Medical School institutional review board, we randomly recruited adults from a panel of internet users identified by using Survey Sampling International (SSI) (<https://www.surveysampling.com/>). Users were from 11 countries, the United States (n = 1,787) and 10 countries in different regions of Europe: northern [Finland (n = 1,554), Sweden (n = 1,539), Norway (n = 764)]; southern [Italy (n = 1,509), Spain (n = 1,604)]; eastern [Hungary (n = 998), Poland (n = 1,509)]; and western [Germany

(n = 1,546), the Netherlands (n = 1,938), the United Kingdom (n = 1,762)]. We established quotas for age and gender to approximate the distribution of these characteristics in each country. Participants received modest compensation.

Respondents read a mock news article, ostensibly from an interview with a national health organization of the participant's country, describing the spread of a pandemic influenza strain within their country (online Technical Appendix, <https://wwwnc.cdc.gov/EID/article/23/8/17-0364-Techapp.pdf>). Each article contained information about the spread, symptoms, and severity of the virus and about the development of a vaccine.

Each version of the article referred to the influenza strain by using 1 of 3 randomized labels: 1) "H11N3 influenza," a surface protein label; 2) "horse flu," an animal reservoir label; or 3) "Yarraman flu," an exotic-sounding label (Yarraman is an Australian aboriginal term for "horse"). We used novel labels to avoid associations with and reactions to established influenza labels. The study included additional factors that were cross-randomized with the label factor and are not discussed here.

After reading the article, participants were asked to imagine that the described scenario was actually occurring and then rate the level of their worry about contracting influenza and plans to receive vaccination once a vaccine for this strain of influenza became available. Responses were on 7-point scales; higher values indicated greater worry or vaccination intentions. We tested for main effects of reactions to labels by using 1-way measured analysis of variance (ANOVA) with Bonferroni-adjusted planned contrasts. We used additional 2-way ANOVA tests to determine whether effects of the label manipulation differed across countries. We used the PROCESS macro for IBM SPSS Statistics 23 (IBM, Armonk, NY, USA) to conduct a mediation analysis and test for the effect of labels on vaccination intentions, controlling for worry.

Of 20,138 participants, 16,510 (82.0%) completed the full survey. The average participant age was 46.8 (range 18–99, SD 16.2) years; 49.8% were female.

Participants reported higher levels of worry about contracting the influenza strain when it was reported as "Yarraman flu" (mean 3.86, SD 1.83) or "H11N3 influenza" (mean 3.83, SD 1.82) compared with "horse flu" (mean 3.74, SD 1.86; F statistic [2–16,339] = 7.73, $p < 0.001$). Participants also reported higher vaccination intentions when the strain was reported as "Yarraman flu" (mean 4.67, 1.99) or "H11N3 influenza" (mean 4.66, SD 2.03) compared with "horse flu" (mean 4.54, SD 2.04, F[10–16,339] 6.48; $p = 0.002$). The effect of the influenza label on vaccination intentions was mediated by worry (Figure). Despite differences in reports of worry (F[10–16,339] = 100.07, $p < 0.001$) and vaccination intentions (F[10–16,384] = 58.27, $p < 0.001$) of participants in the 11 countries, the effects of the influenza label on

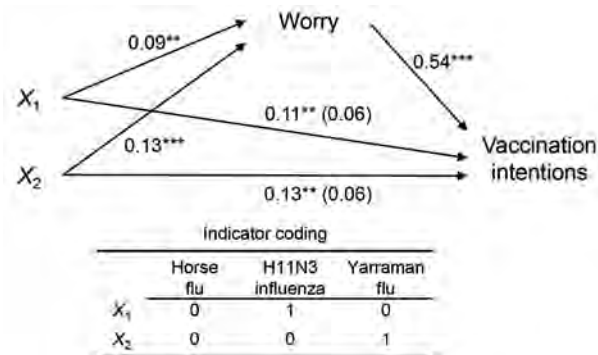


Figure. Regression coefficients for the effect of influenza labels on worry for infection and intentions for vaccination. Label conditions were dummy coded to estimate the effects of “H11N3 influenza” (X_1) and “Yarraman flu” (X_2) labels compared with the “horse flu” label. The effect of influenza labels on vaccination intentions, controlling for worry, is in parentheses. ** $p < 0.01$; *** $p < 0.001$.

worry ($p = 0.281$) and vaccination intentions ($p = 0.467$) did not significantly interact with country status.

Our results indicate that the choice of disease labels for public communications about outbreaks cannot be made by personal preference. In this study, an animal reservoir label evoked weaker responses from participants than other labels. Although these results could be specific to the animal we chose, using an animal reservoir label may produce greater misconceptions (e.g., exposure to the animal necessary for transmission) that undermine suspicions of risk. Further research is needed to determine whether this effect is context-specific or generalizes to other animal reservoir labels for infectious diseases and whether our findings replicate in a nonhypothetical context.

All authors contributed to the intellectual property of this manuscript, including contributing to study design, interpretation of data, and writing of the report. We have no competing interests to declare. All of the authors have had full access to the data, have seen and approved the submission of this version of the manuscript, and take full responsibility for the integrity of the data, the accuracy of the data analysis, and the manuscript.

Funding for this research was provided to A.F. from the European Union’s Seventh Framework Programme for research, technological development and demonstration under grant agreement #278763. The funding agreement assured the authors’ independence in designing the study, in the collection, analysis, and reporting of the data, and in the decision to submit the article for publication.

Dr. Scherer is an Associate of Internal Medicine at the University of Iowa. His research focuses on the psychological mechanisms that shape our responses to health risks in order to better design effective health risk communication.

References

- Scherer AM, Scherer LD, Fagerlin A. Getting ahead of illness: using metaphors to influence medical decision making. *Med Decis Making*. 2015;35:37–45. <http://dx.doi.org/10.1177/0272989X14522547>
- Hauser DJ, Schwarz N. The war on prevention: bellicose cancer metaphors hurt (some) prevention intentions. *Pers Soc Psychol Bull*. 2015;41:66–77. <http://dx.doi.org/10.1177/0146167214557006>
- Scherer LD, Finan C, Simancek D, Finkelstein JI, Tarini BA. Effect of “pink eye” label on parents’ intent to use antibiotics and perceived contagiousness. *Clin Pediatr (Phila)*. 2016;55:543–8. <http://dx.doi.org/10.1177/0009922815601983>
- Scherer LD, Zikmund-Fisher BJ, Fagerlin A, Tarini BA. Influence of “GERD” label on parents’ decision to medicate infants. *Pediatrics*. 2013;131:839–45. <http://dx.doi.org/10.1542/peds.2012-3070>
- Rothman AJ, Bartels RD, Wlaschin J, Salovey P. The strategic use of gain- and loss-framed messages to promote healthy behavior: how theory can inform practice. *J Commun*. 2006;56(s1):S202–20. <http://dx.doi.org/10.1111/j.1460-2466.2006.00290.x>
- Loewenstein GF, Weber EU, Hsee CK, Welch N. Risk as feelings. *Psychol Bull*. 2001;127:267–86. <http://dx.doi.org/10.1037/0033-2909.127.2.267>
- Determann D, de Bekker-Grob EW, French J, Voeten HA, Richardus JH, Das E, et al. Future pandemics and vaccination: Public opinion and attitudes across three European countries. *Vaccine*. 2016;34:803–8. <http://dx.doi.org/10.1016/j.vaccine.2015.12.035>

Address for correspondence: Aaron M. Scherer, Department of Internal Medicine, University of Iowa, 200 Hawkins Dr, Iowa City, IA 52242, USA; email: aaron-scherer@uiowa.edu

Zika Virus Screening among Spanish Team Members After 2016 Rio de Janeiro, Brazil, Olympic Games

Natalia Rodríguez-Valero, Alberto M. Borobia, Mar Lago, Maria Paz Sánchez-Seco, Fernando de Ory, Ana Vázquez, Jose Luis Pérez-Arellano, Cristina Carranza Rodríguez, Miguel J. Martínez, Alicia Capón, Elias Cañas, Joaquin Salas-Coronas, Arkaitz Azcune Galparsoro, Jose Muñoz

Author affiliations: IS Global-Hospital Clínic de Barcelona, Barcelona, Spain (N. Rodríguez-Valero, J. Muñoz); Hospital La Paz-Carlos III, Madrid, Spain (A.M. Borobia, M. Lago); Instituto de Salud Carlos III, Madrid, Madrid, Spain (M.P. Sánchez-Seco, F. de Ory, A. Vázquez); Complejo Hospitalario Universitario

Insular Materno Infantil, Las Palmas de Gran Canaria, Spain (J.L. Pérez-Arellano, C. Carranza Rodríguez); Hospital Clinic de Barcelona, Barcelona, Spain (M.J. Martínez, A. Capón); Hospitales Universitarios Virgen del Rocío, Sevilla, Spain (E. Cañas); Hospital de Poniente, El Ejido, Spain (J. Salas-Coronas); Hospital Universitario de Donostia, Donostia, Spain (A. Azcune Galparsoro)

DOI: <https://doi.org/10.3201/eid2308.170415>

We evaluated the risk for the Spanish Olympic Team acquiring Zika virus in Rio de Janeiro, Brazil, during 2016. We recruited 117 team members, and all tested negative for Zika virus. Lack of cases in this cohort supports the minimum risk estimates made before the Games.

The current Zika virus epidemic became a major concern for national Olympic delegations before they traveled to Rio de Janeiro, Brazil, during summer 2016. Fear about individual consequences of the infection, such as congenital or neurologic disorders, were common among athletes and other participants of the Olympic Games and led some persons not to attend the Games for these reasons. The possibility of the Olympics contributing to a global spread of the Zika virus epidemic also was a concern, initially raised by ≈100 academic researchers, expressed in an open letter addressed to the World Health Organization (WHO) in May 2016 (1,2).

The risk for Zika during the Rio de Janeiro Olympic Games was estimated to be very low in different models published in medical journals (9×10^{-6} to 3×10^{-5}) (3–6). After considering these figures, WHO advised that the Games should not substantially affect the epidemic (7).

To evaluate the risk for the Spanish Olympic Team acquiring Zika virus, our research group from 6 hospitals in Spain invited members of the Spanish delegation to participate in a serologic study of Zika virus 20 and 30 days after returning from Rio de Janeiro. The study was conducted in 6 different recruiting Tropical Medicine Units in cities in Spain (Barcelona, Madrid, Sevilla, San Sebastian, Las Palmas de Gran Canaria, and Almeria).

Athletes and other participants were invited to participate in the study through the Spanish Olympic Committee. A total of 117 Olympics participants accepted and were included in the study during September and October 2016. After providing oral and written information, study participants signed an informed consent form, and demographic and health data were recorded in a medical questionnaire. A total of 10 mL of blood was drawn from each participant, and serologic tests for Zika virus (immunofluorescence antibody assay; EUROIMMUN, Luebeck, Germany), dengue virus (ELISA; Panbio, Kyonggi-do, Republic of Korea), and chikungunya virus (immunofluorescence assay;

EUROIMMUN) were conducted at the Instituto de Salud Carlos III (Spanish National Reference Laboratory, Madrid, Spain). For all samples initially testing positive for Zika virus, we conducted microneutralization testing.

Twenty-one participants had ≥1 signs or symptoms while in Brazil: 18% rash, 23% fever (temperature >38°C), 14% itching, 9% of conjunctival hyperemia, 9% arthralgia, 14% myalgia, 40% malaise, 9% lymphadenopathy, 32% headache, and 19% gastrointestinal symptoms. Ninety-nine percent of participants received Zika virus counseling before they traveled to Rio de Janeiro, including the advice of having protected sex during and after the Games (Table).

For 4 persons, test results for Zika virus IgG was positive; IgM and neutralization testing yielded negative results. The 4 Zika virus IgG-positive participants had received previous yellow fever vaccination and were asymptomatic. One sample showed Zika virus IgM in the absence of specific IgG; the results were confirmed in a follow-up sample. Thus, the sample was classified as false positive.

Table. Demographic and travel-related characteristics of 117 Spanish athletes who attended the Olympic Games, Rio de Janeiro, Brazil, 2016*

Characteristic	Results
Sex	
M	76 (65.0)
F	41 (35.0)
Age, y, median ± SD	35.54 ± 9.46
Athletes	
All athletes	53 (45.3)
Outdoor athletes	35 (66.0)
Spanish nationality	112 (95.7)
Chronic disease	6 (5.1)
Immunosuppression	0
Current pregnancy, own or partner's	9 (7.7)†
Intention to conceive within the following 6 mo	29 (24.8)
Sex	
M	22 (75.9)
F	7 (24.1)
Vaccination and travel advice	
Vaccine	
Yellow fever	23 (19.6)
Japanese encephalitis	0
Tickborne encephalitis	0
Attendance at a travel clinic	115 (98.3)
Zika advice included	116 (99.2)
>1 Visit to a tropical country	74 (63.3)
Previous diagnosis of dengue	0
During the trip	
Length of stay, d, median ± SD	21.35 ± 9.05
Places visited	
Rio de Janeiro	103 (88)
Rio de Janeiro, Deodoro, and Barra	7 (6.0)
Rio de Janeiro and Ilha Grande	4 (3.4)
Rio de Janeiro and Paraty	1 (0.85)
Rio de Janeiro and French Polynesia	1 (0.85)
Use of bed nets or air conditioners	61 (52.6)
Use of repellent	111 (94.9)
Risky sexual behavior	2 (1.7)
Recall ≥1 mosquito bite during stay	56 (47.9)

*All values are no. (%) unless otherwise indicated.

†Male participants' partners who were pregnant before the Games.

Study participants were advised to wait to conceive in accordance with WHO specifications: 6 months for men, 2 months for women. Participants with pregnant partners were advised to use condoms during the entire pregnancy.

A lack of Zika cases in this cohort supports the risk calculations made before the Games and the WHO statement that there were no Zika cases associated with the Olympic Games (8). Although 48% of participants in our study recalled at least 1 mosquito bite during the stay, the overall absence of cases in the Rio de Janeiro population during July and August 2016 (9,10) is believed to be due to the vector-control efforts by Brazilian authorities before the Games and to the winter weather, leading to a low presence of adult mosquitoes and mosquito bites (5,6).

This work was supported by La Caixa Foundation and the Spanish Olympic Committee. The laboratory work was supported by RICET (Network Biomedical Research on Tropical Diseases), RD16CIII/003/003.

Dr. Rodriguez-Valero is an internal medicine specialist working in travel medicine since 2015. Her research interests include new technologies in travel medicine, outbreaks, and emerging infectious diseases.

References

- World Health Organization. Zika virus and the Olympic and Paralympic Games Rio 2016 [cited 2016 Dec 26]. <http://www.who.int/mediacentre/news/statements/2016/zika-olympics/en/>
- Attaran A, Caplan A, Gaffney C, Igel L. Open letter to Dr. Margaret Chan, Director-General, WHO (copied to the International Olympic Committee) [cited 2017 June 9]. <http://www.gannett-cdn.com/usatoday/editorial/sports/olympics/zika-olympics-open-letter.pdf>
- Massad E, Tan S-H, Khan K, Wilder-Smith A. Estimated Zika virus importations to Europe by travellers from Brazil. *Glob Health Action*. 2016;9:31669. <http://dx.doi.org/10.3402/gha.v9.31669>
- Zumla A, McCloskey B, Bin Saeed AA, Dar O, Al Otabi B, Perlmann S, et al. What is the experience from previous mass gathering events? Lessons for Zika virus and the Olympics 2016. *Int J Infect Dis*. 2016;47:1-4. <http://dx.doi.org/10.1016/j.ijid.2016.06.010>
- Codeço C, Villela D, Gomes MF, Bastos L, Cruz O, Struchiner C, et al. Zika is not a reason for missing the Olympic Games in Rio de Janeiro: response to the open letter of Dr Attaran and colleagues to Dr Margaret Chan, Director-General, WHO, on the Zika threat to the Olympic and Paralympic Games. *Mem Inst Oswaldo Cruz*. 2016;111:414-5. <http://dx.doi.org/10.1590/0074-02760160003>
- Grills A, Morrison S, Nelson B, Miniota J, Watts A, Cetron MS. Projected Zika virus importation and subsequent ongoing transmission after travel to the 2016 Olympic and Paralympic Games—country-specific assessment, July 2016. *MMWR Morb Mortal Wkly Rep*. 2016;65:711-5. <http://dx.doi.org/10.15585/mmwr.mm6528e1>
- World Health Organization. Public health advice regarding the Olympics and Zika virus [cited 2016 Dec 26]. <http://www.who.int/mediacentre/news/releases/2016/zika-health-advice-olympics/en/>
- World Health Organization. Fourth meeting of the Emergency Committee under the International Health Regulations (2005) regarding microcephaly, other neurological disorders and Zika virus [cited 2016 Dec 26]. <http://www.who.int/mediacentre/news/statements/2016/zika-fourth-ec/en/>
- Ministerio da Saude. Secretaria de Vigilância em Saúde. Boletim Epidemiológico. Vol 47-nº33.; Brasilia 2016 [cited 2017 June 11]. <http://portalarquivos.saude.gov.br/images/pdf/2016/setembro/16/2016-028---Dengue-SE32.pdf>
- Ministerio da Saude. Secretaria de Vigilância em Saúde. Boletim Epidemiológico. Vol 47-nº34.; Brasilia 2016 [cited 2017 June 11]. <http://portalsauze.saude.gov.br/images/pdf/2016/outubro/18/2016-029-Dengue-publicacao-n-34.pdf>

Address for correspondence: Natalia Rodriguez-Valero and Jose Muñoz, Department of Tropical Medicine and International Health, Hospital Clinic Barcelona. ISGlobal, Barcelona Centre for International Health Research (CRESIB), Hospital Clínic-Universitat de Barcelona C/Rosselló 132 2º2ª, 08036, Barcelona, Spain; email: natalia.rodriguez@isglobal.org and jose.munoz@isglobal.org

***Candidatus* *Dirofilaria hongkongensis* as Causative Agent of Human Ocular Filariasis after Travel to India**

Stefan Winkler, Andreas Pollreis, Michael Georgopoulos, Zsuzsanna Bagò-Horvath, Herbert Auer, Kelvin Kai-Wang To, Jürgen Krücken, Sven Poppert, Julia Walochnik

Author affiliations: Medical University of Vienna, Vienna, Austria (S. Winkler, A. Pollreis, M. Georgopoulos, Z. Bagò-Horvath, H. Auer, J. Walochnik); University of Hong Kong, Pokfulam, Hong Kong, China (K.K.-W. To); Freie Universität Berlin, Germany (J. Krücken); Bernhard Nocht Institute for Tropical Medicine, Hamburg, Germany (S. Poppert); Regio Klinikum, Wedel, Germany (S. Poppert)

DOI: <https://doi.org/10.3201/eid2308.170423>

We report a human case of ocular *Dirofilaria* infection in a traveler returning to Austria from India. Analysis of mitochondrial sequences identified the worm as *Candidatus* *Dirofilaria hongkongensis*, a close relative of *Dirofilaria repens*, which was only recently described in Hong Kong and proposed as a new species.

Dirofilariasis, caused by *Dirofilaria repens* or *D. immitis* nematodes, is a zoonotic filarial infection transmitted through the bite of various mosquitoes. The most frequent

manifestations in humans are subcutaneously migrating worms and formation of nodules in various body parts (1). Increasing numbers of human *D. repens* infections have been reported from Europe, Africa, and Asia (2,3). Austria was considered nonendemic, until the first autochthonous case in a human was reported in 2006 (4) from the most eastern province, the Burgenland, where *D. repens* nematodes

were recently also found for the first time in 2 *Anopheles* mosquito species (5). We describe a case of imported ocular dirofilariasis caused by the recently newly proposed species *Candidatus* *Dirofilaria hongkongensis* (6).

The patient, a 38-year-old woman, had recurrent eyelid swelling in both eyes and conjunctival inflammation with watery discharge beginning in June 2011 (online Technical

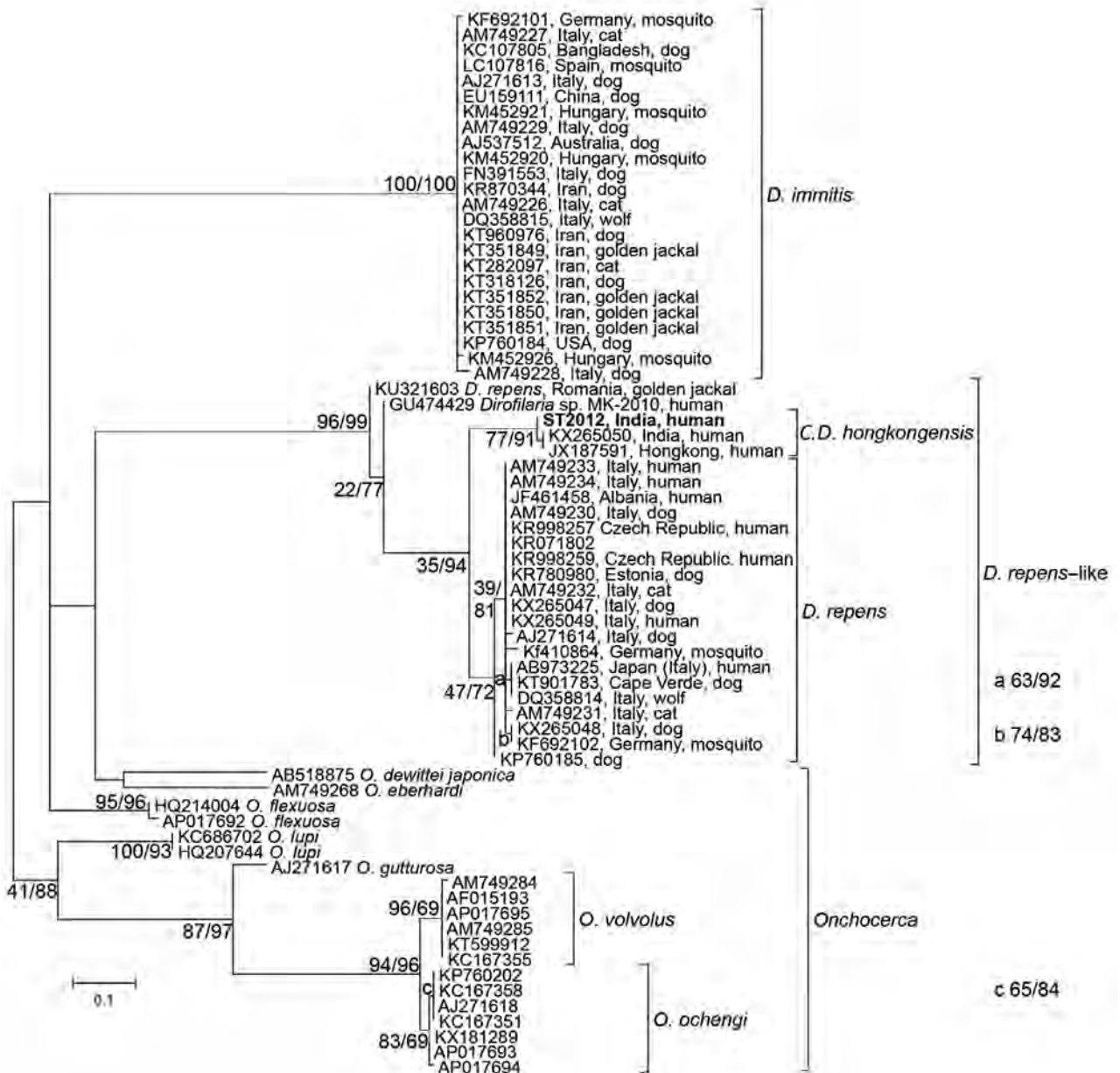


Figure. Phylogenetic analysis of the genus *Dirofilaria* based on cytochrome C oxidase subunit I gene sequences from a worm surgically extracted from the eye of a patient who had returned to Austria after travel to India. Bootstrap values and results of the Shimodaira-Hasegawa test are shown before and after the slash. The sequence from the current patient is shown in bold, and clusters within *Candidatus* *Dirofilaria hongkongensis*, with *Dirofilaria repens* as the sister taxon. Two samples, classified as *Dirofilaria* sp. MK-2010 (GenBank accession no. GU474429) and *D. repens* from Romania (accession no. KU321603), show very high divergence and probably represent different species. The scale bar represents 0.1 substitutions per site. The samples are identified by GenBank accession numbers, country, and host origin, when available. The genera *Dirofilaria* (*D.*) and *Onchocerca* (*O.*) as well as the *Candidatus* status (*C.*) are abbreviated in species names.

Appendix Figure, panel A, <https://wwwnc.cdc.gov/EID/article/23/8/17-0423-Techapp1.pdf>). She visited numerous physicians and, upon various putative diagnoses (ranging from sicca syndrome to burnout syndrome), she received corresponding therapies, including antibiotics, steroids, and acupuncture. From January 2012 on, the eyelid swellings were accompanied by a creeping sensation and occurred more often. In early August 2012, she sought care at the emergency department of a university eye clinic in Vienna, Austria. She had a moving object in her left eye. Slit lamp examination revealed a white slender worm moving sub-conjunctivally in the temporal part of the left eye (online Technical Appendix Figure, panel B). The conjunctiva was opened under topical anesthesia, and a 13-cm worm (online Technical Appendix Figure, panel C) was removed (Video, <https://wwwnc.cdc.gov/EID/article/23/8/17-0423-V1.htm>) and morphologically identified as a non gravid female of *D. repens* (online Technical Appendix Figure, panel D). Results of serologic testing for filariae were negative before and after extraction of the worm, as were results for testing of EDTA blood for microfilariae. Blood test results, including differential blood counts, were within reference ranges throughout the case history. The patient had returned from a 7-week stay in India, including the areas of Goa, Maharashtra, Delhi, and Uttar Pradesh, 3 months before initial onset of symptoms. Her travel history of the preceding 3 years included 4 more trips to India of several weeks each; a 2-week stay in Israel (October 2010); and a 2-week stay in Dubai, United Arab Emirates (July 2009).

For confirmation of the morphologic identification, we isolated DNA from a 1-cm piece of the worm after homogenization by using the QIAamp DNA Mini Kit (QIAGEN, Hilden, Germany). We amplified fragments of the cytochrome C oxidase subunit I (COI) with panfilarial primers COXfw 5'-GCKTTTCCTCGTGTTATGC-3'/COXrev 5'-CCAGCCAAAACAGGAACAG-3' and 12S rRNA with panfilarial primers Panfil-12S-F 5'-GTTC-CAGAATAATCGGCTA-3'/Panfil-12S-R 5'-ATTGAC-GGATGRTTTGTACC-3' (7). We sequenced amplicons and subjected them to phylogenetic analyses (online Technical Appendix). All sequence data were submitted to GenBank (accession nos. KY750548–KY750550).

The 329 bp COI fragment (accession no. KY750548) showed 99%–100% identity to 2 sequences from *Candidatus* *Dirofilaria hongkongensis* (accession nos. KX265050 and JX187591). Identity to *D. repens* sequences was 95%–96%, to *D. immitis* 89%, and to *Onchocerca* spp. up to 92%. The 466 bp mitochondrial 12S rDNA fragment (accession no. KY750549) showed 99% identity to *Candidatus* *Dirofilaria hongkongensis* sequences from case-patients in India (accession no. KX265050) and Hong Kong (accession no. KY750550), the latter derived from original material of the first description of *Candidatus* *Dirofilaria hongkongensis*

(6). Identity to a *Dirofilaria* sp. from a patient returning from India and Sri Lanka and to *Dirofilaria* sp. Thailand II, recently reported among dogs in Thailand (accession nos. KX265092 and KX265093) (8), was also 99%. Phylogenetic analysis using the COI sequence clearly placed the sequence into the *Candidatus* *Dirofilaria hongkongensis* cluster, the sister taxon to *D. repens* (Figure). Although *D. immitis* shows virtually identical COI sequences from 4 continents, genetic variability in *D. repens*-like parasites is obviously much higher, possibly associated with varying zoonotic potentials, reservoirs, and vectors; however, molecular data on *Dirofilaria* are still scarce.

In this case, *Candidatus* *Dirofilaria hongkongensis* was most likely acquired in India. An infection in Austria seems unlikely because, until now, only 1 singular autochthonous *Dirofilaria* infection has been reported, and that case was classic *D. repens* infection (4). Dubai is considered nonendemic for *Dirofilaria* spp. parasites, whereas Israel is known to be endemic for *D. repens* nematodes (1,3), but the patient's trips to these countries were much longer ago than her latest trip to India. Moreover, all cases from India or Sri Lanka analyzed by us so far represented *Candidatus* *Dirofilaria hongkongensis* (8,9; S. Poppert, unpub. data), suggesting that this species is widely distributed on the Indian subcontinent. In fact, whether classical *D. repens* infection occurs in India at all is unclear. Infections with *Candidatus* *Dirofilaria hongkongensis* nematodes might take a similar course as infections with classical *D. repens*; however, a case of meningoencephalitis caused by nematodes of this candidate species also has been described (9). *Dirofilaria* spp. parasites isolated from human case-patients should be investigated by molecular methods to establish an exact species diagnosis, especially if infections were acquired outside Europe.

Acknowledgments

We thank Iveta Häfeli for excellent technical assistance and the Medical University of Vienna for financial support.

Informed written consent was obtained from the patient for publication of this study and any accompanying images and videos. We are very grateful to the patient for kindly providing all the material.

Dr. Winkler is a specialist for infectious diseases and tropical medicine at the General Hospital in Vienna, Austria. He is also professor of internal medicine at the Medical University of Vienna.

References

1. Pampiglione S, Rivasi F. Human dirofilariasis due to *Dirofilaria* (*Nochtiella*) *repens*: an update of world literature from 1995 to 2000. *Parassitologia*. 2000;42:231–54.
2. Pampiglione S, Rivasi F, Angeli G, Boldorini R, Incensati RM, Pastormerlo M, et al. Dirofilariasis due to *Dirofilaria repens* in

- Italy, an emergent zoonosis: report of 60 new cases. *Histopathology*. 2001;38:344–54. <http://dx.doi.org/10.1046/j.1365-2559.2001.01099.x>
3. Genchi C, Kramer LH, Rivasi F. Dirofilarial infections in Europe. *Vector Borne Zoonotic Dis*. 2011;11:1307–17. <http://dx.doi.org/10.1089/vbz.2010.0247>
 4. Auer H, Susani M. The first autochthonous case of subcutaneous dirofilariasis in Austria [in German]. *Wien Klin Wochenschr*. 2008;120(19–20 Suppl 4):104–6. <https://doi.org/10.1007/s00508-008-1031-4>
 5. Silbermayr K, Eigner B, Joachim A, Duscher GG, Seidel B, Allerberger F, et al. Autochthonous *Dirofilaria repens* in Austria. *Parasit Vectors*. 2014;7:226. <http://dx.doi.org/10.1186/1756-3305-7-226>
 6. To KK, Wong SS, Poon RW, Trendell-Smith NJ, Ngan AH, Lam JW, et al. A novel *Dirofilaria* species causing human and canine infections in Hong Kong. *J Clin Microbiol*. 2012;50:3534–41. <http://dx.doi.org/10.1128/JCM.01590-12>
 7. Casiraghi M, Bain O, Guerrero R, Martin C, Pocacqua V, Gardner SL, et al. Mapping the presence of *Wolbachia pipientis* on the phylogeny of filarial nematodes: evidence for symbiont loss during evolution. *Int J Parasitol*. 2004;34:191–203. <http://dx.doi.org/10.1016/j.ijpara.2003.10.004>
 8. Yilmaz E, Fritzenwanker M, Pantchev N, Lendner M, Wongkamchai S, Otranto D, et al. The mitochondrial genomes of the zoonotic canine filarial parasites *Dirofilaria (Nochtiella) repens* and *Candidatus* *Dirofilaria (Nochtiella) hongkongensis* provide evidence for presence of cryptic species. *PLoS Negl Trop Dis*. 2016;10:e0005028. <http://dx.doi.org/10.1371/journal.pntd.0005028>
 9. Poppert S, Hodapp M, Krueger A, Hegasy G, Niesen WD, Kern WV, et al. *Dirofilaria repens* infection and concomitant meningoencephalitis. *Emerg Infect Dis*. 2009;15:1844–6. <http://dx.doi.org/10.3201/eid1511.090936>

Address for correspondence: Julia Walochnik, Medical University of Vienna – Parasitology, Kinderspitalgasse 15, Vienna 1095, Austria; email: julia.walochnik@meduniwien.ac.at

Mucus-Activatable Shiga Toxin Genotype *stx2d* in *Escherichia coli* O157:H7

Sergio Sánchez,¹ María Teresa Llorente, Laura Herrera-León, Raquel Ramiro, Sandra Nebreda, María Antonia Remacha, Silvia Herrera-León¹

Author affiliations: Institute of Health Carlos III, Majadahonda, Spain (S. Sánchez, M.T. Llorente, L. Herrera-León, R. Ramiro, S. Nebreda, S. Herrera-León); León University Hospital, León, Spain (M.A. Remacha)

DOI: <https://doi.org/10.3201/eid2308.170570>

¹These authors contributed equally to this article.

We identified the mucus-activatable Shiga toxin genotype *stx2d* in the most common hemolytic uremic syndrome–associated *Escherichia coli* serotype, O157:H7. *stx2d* was detected in a strain isolated from a 2-year-old boy with bloody diarrhea in Spain, and whole-genome sequencing was used to confirm and fully characterize the strain.

The foodborne zoonotic pathogen Shiga toxin (Stx)–producing *Escherichia coli* (STEC) is responsible for human diseases ranging from uncomplicated diarrhea to the life-threatening hemolytic-uremic syndrome (HUS) (1). Stx production is the most determining virulence factor implicated in HUS, and the intimin, encoded by *eae*, is the most common adherence factor in HUS-associated STEC (1). *Stx2d* is a *Stx2* variant in which cytotoxicity is increased (from 35- to 350-fold) by the action of elastase in intestinal mucus (2). This mucus-enhanced toxicity is termed “activation,” and activatable *Stx2d* proteins are designated *Stx2dact*. *Stx2dact* production and *Stx2dact* genotype (*stx2d*) have been associated primarily with *eae*-negative STEC and considered a predictor for severe clinical outcome in such infections (3).

All STEC strains received or isolated in the Reference and Research Laboratory of Food and Waterborne Bacterial Infections (Majadahonda, Spain) are routinely tested for *stx1* and *stx2* subtypes by a PCR subtyping method (4). For serotyping, O antigen is identified with both commercial antiserum and PCR (5), and H antigen is identified by PCR amplification of the *fliC* gene (6) and further sequencing of the PCR product. During 2012–2016, *stx2d* was identified in 7 (3%) of 236 STEC strains isolated from patients with HUS and/or diarrhea in Spain (193 *eae*-positive and 43 *eae*-negative strains). Six were *eae*-negative non-O157 STEC belonging to serotypes O73:H18 (2 strains), O91:H21, O148:H8, O181:H49, and ONT:H21. Strikingly, the other *stx2d*-positive strain identified (CNM-2140/12) belonged to serotype O157:H7 and contained *stx2d* in combination with *stx2c*, apart from *eae*. The strain had been isolated from a 2-year-old boy with bloody diarrhea July 2012, and it fermented sorbitol after overnight incubation on sorbitol MacConkey agar (Becton Dickinson, Sparks, MD, USA). We confirmed Stx2 production using the enzyme immunoassay kit SHIGA TOXIN QUIK CHEK (TechLab, Blacksburg, VA, USA). The activatable property of the toxin was confirmed by partial sequencing of the *stx2* gene (4), analysis of the resulting nucleotide sequence by comparison with the published *stx2* reference sequences, and comparison of the resulting amino acid sequences. The nucleotide sequence of *stx2d* (GenBank accession no. MF094370) was 100% identical to that of strain 06–5231 (O55:H7, GenBank accession no. EF584538). The sequence was translated to amino acids (online Technical Appendix Figure, <https://wwwnc.cdc.gov/EID/article/23/8/17-0570-Techapp1.pdf>),

Table. Virulence gene profile of the *stx2d*-positive Shiga toxin–producing *Escherichia coli* O157:H7 strain CNM-2140/12*

Virulence factor	Identity	Protein function	GenBank accession no.
<i>ehxA</i>	100.00	Enterohemolysin	AB011549
<i>etpD</i>	100.00	Type II secretion protein	AB011549
<i>nleA</i>	100.00	Non-LEE encoded effector A	AE005174
<i>espP</i>	99.92	Extracellular serine protease plasmid-encoded	AB011549
<i>nleB</i>	99.90	Non-LEE encoded effector B	AE005174
<i>gad</i>	98.50	Glutamate decarboxylase	BA000007
<i>iss</i>	98.30	Increased serum survival	CP001509
<i>eae</i>	100.00	Intimin	AF071034
<i>iha</i>	100.00	Adherence protein	AE005174
<i>tir</i>	100.00	Translocated intimin receptor protein	EU871626
<i>stx2B</i>	100.00	Shiga toxin 2, subunit B, variant c	AB071845
<i>iss</i>	98.54	Increased serum survival	CU928160
<i>astA</i>	100.00	EAST-1 heat-stable toxin	HM099897
<i>astA</i>	91.96	EAST-1 heat-stable toxin	AB042005
<i>nleC</i>	100.00	Non-LEE encoded effector C	AP010960
<i>espA</i>	100.00	Type III secretions system	AE005174
<i>gad</i>	98.50	Glutamate decarboxylase	BA000007
<i>nleB</i>	99.90	Non-LEE encoded effector B	AE005174
<i>espJ</i>	99.85	Prophage-encoded type III secretion system effector	AE005174
<i>katP</i>	100.00	Plasmid-encoded catalase peroxidase	AB011549
<i>espB</i>	100.00	Secreted protein B	AE005174
<i>nleC</i>	100.00	Non-LEE encoded effector C	AE005174
<i>stx2B</i>	100.00	Shiga toxin 2, subunit B, variant d	EF584538

*Determined from raw whole-genome sequence data using VirulenceFinder (<https://cge.cbs.dtu.dk/services/all.php>). A percent identity threshold of 90% between the input and the best matching database gene was selected. Bold indicates the mucus-activatable Shiga toxin genotype. EAST, enteroaggregative *E. coli* heat-stable enterotoxin; LEE, locus of enterocyte effacement.

and the activatable property of Stx2d was confirmed with the combined presence of the “activatable tail,” the last 10 aa in the C-terminal end of the A subunit (KSQSLYTTGE), and the END motif at position 14–16 in the N-terminal end of the B subunit (4). Stx-associated bacteriophage insertion sites genotyping was performed (7). According to the Stx-associated bacteriophage insertion genotype nomenclature proposed by Shringi et al. (8), the strain belonged to the SY2c genotype; both *sbCB* and *yehV* loci were occupied, the former with a Stx2c-associated bacteriophage, plus the additional insertion of the Stx2d-associated bacteriophage within the *yecE* locus, as recently reported for *stx2d*-positive STEC O26:H11 (7).

To confirm the genotypic traits mentioned earlier, we sequenced the strain using an Illumina NextSeq 500 next-generation sequencer system (Illumina, San Diego, CA, USA). We extracted DNA using a QIAamp DNA Mini Kit (QIAGEN, Hilden, Germany) and generated a genomic DNA paired-end library using a Nextera XT DNA Sample Preparation Kit (Illumina). A total of 1,371,617,258 bp were obtained, providing ≈250-fold coverage and 9,083,558 reads. The sequencing reads have been deposited in the SRA-NCBI public sequence repository (accession no. SRP107062). From the raw whole-genome sequence data, we confirmed serotype O157:H7 using SerotypeFinder; investigated the virulence gene profile, including *stx* subtypes, using VirulenceFinder (Table); and identified acquired antimicrobial resistance genes using ResFinder (all publicly available on the Center for Genomic Epidemiology server, <https://cge.cbs.dtu.dk/services/all.php>). In addition, we detected mutations

in the quinolone resistance–determining regions of the *gyrA* and *parC* genes in silico on the whole-genome sequence, and no acquired antimicrobial resistance gene or mutation conferring quinolone resistance were identified.

Despite its usual association with *eae*-negative STEC, we identified the mucus-activatable Stx genotype also in STEC O157:H7, the most common HUS-associated *eae*-positive STEC serotype. This rare virulence gene combination (*stx2d/eae*) was recently described in STEC O26:H11 isolated from several HUS patients (9) and in STEC O80:H2 causing HUS and bacteremia in France (10). Although its clinical implications remain unknown—because the strain in our current study was isolated from a patient with bloody diarrhea but not HUS, whereas those isolated in France originated from patients with HUS—these examples show the potential for acquiring and transferring important STEC virulence factors, which can lead to unusual and potentially more virulent strains. Further studies are needed to better determine whether *stx2d*-positive O157:H7 and other *eae*-positive non-O157 STEC strains carrying this *stx* subtype are statistically significant in humans and to determine their clinical implications.

This work was supported by grants MPY-1042/14 and PI14CIII/00051 from “Fondo de Investigaciones Sanitarias” from the Spanish Ministry of Economy and Competitiveness and S2013/ABI-2747 from the Madrid Regional Government. S.S. performed this work while under a research contract from the Miguel Servet program from “Fondo de Investigaciones Sanitarias” from the Spanish Ministry of Economy and Competitiveness (CP13/00237).

Dr. Sánchez is a researcher at the National Center for Microbiology, Institute of Health Carlos III. His research interests include virulence mechanisms, molecular epidemiology, and antimicrobial drug resistance of diarrheagenic *E. coli*, especially STEC.

References

1. Johnson KE, Thorpe CM, Sears CL. The emerging clinical importance of non-O157 Shiga toxin-producing *Escherichia coli*. *Clin Infect Dis*. 2006;43:1587–95. <http://dx.doi.org/10.1086/509573>
2. Melton-Celsa AR, Darnell SC, O'Brien AD. Activation of Shiga-like toxins by mouse and human intestinal mucus correlates with virulence of enterohemorrhagic *Escherichia coli* O91:H21 isolates in orally infected, streptomycin-treated mice. *Infect Immun*. 1996;64:1569–76.
3. Bielaszewska M, Friedrich AW, Aldick T, Schürk-Bulgrin R, Karch H. Shiga toxin activatable by intestinal mucus in *Escherichia coli* isolated from humans: predictor for a severe clinical outcome. *Clin Infect Dis*. 2006;43:1160–7. <http://dx.doi.org/10.1086/508195>
4. Scheutz F, Teel LD, Beutin L, Piérard D, Buvens G, Karch H, et al. Multicenter evaluation of a sequence-based protocol for subtyping Shiga toxins and standardizing Stx nomenclature. *J Clin Microbiol*. 2012;50:2951–63. <http://dx.doi.org/10.1128/JCM.00860-12>
5. Sánchez S, Llorente MT, Echeita MA, Herrera-León S. Development of three multiplex PCR assays targeting the 21 most clinically relevant serogroups associated with Shiga toxin-producing *E. coli* infection in humans. *PLoS One*. 2015;10:e0117660. <http://dx.doi.org/10.1371/journal.pone.0117660>
6. Machado J, Grimont F, Grimont PA. Identification of *Escherichia coli* flagellar types by restriction of the amplified *fliC* gene. *Res Microbiol*. 2000;151:535–46. [http://dx.doi.org/10.1016/S0923-2508\(00\)00223-0](http://dx.doi.org/10.1016/S0923-2508(00)00223-0)
7. Bonanno L, Loukiadis E, Mariani-Kurkdjian P, Oswald E, Garnier L, Michel V, et al. Diversity of Shiga toxin-producing *Escherichia coli* (STEC) O26:H11 strains examined via *stx* subtypes and insertion sites of Stx and EspK bacteriophages. *Appl Environ Microbiol*. 2015;81:3712–21. <http://dx.doi.org/10.1128/AEM.00077-15>
8. Shringi S, Schmidt C, Katherine K, Brayton KA, Hancock DD, Besser TE. Carriage of *stx2a* differentiates clinical and bovine-biased strains of *Escherichia coli* O157. *PLoS One*. 2012;7:e51572. <http://dx.doi.org/10.1371/journal.pone.0051572>
9. Delannoy S, Mariani-Kurkdjian P, Bonacorsi S, Liguori S, Fach P. Characteristics of emerging human-pathogenic *Escherichia coli* O26:H11 strains isolated in France between 2010 and 2013 and carrying the *stx2d* gene only. *J Clin Microbiol*. 2015;53:486–92. <http://dx.doi.org/10.1128/JCM.02290-14>
10. Mariani-Kurkdjian P, Lemaître C, Bidet P, Perez D, Boggini L, Kwon T, et al. Haemolytic-uraemic syndrome with bacteraemia caused by a new hybrid *Escherichia coli* pathotype. *New Microbes New Infect*. 2014;2:127–31. <http://dx.doi.org/10.1002/nmi2.49>

Address for correspondence: Sergio Sánchez, Reference and Research Laboratory of Food and Waterborne Bacterial Infections, National Center for Microbiology, Institute of Health Carlos III, 28220 Majadahonda, Spain; email: sergio.sanchez@isciii.es



EID
journal

@CDC_EIDjournal

Follow the EID journal on Twitter and get the most current information from Emerging Infectious Diseases.

Acute Encephalitis Syndrome and Scrub Typhus in India

Manoj V. Murhekar

Author affiliation: National Institute of Epidemiology, Chennai, India

DOI: <https://doi.org/10.3201/eid2308.162028>

To the Editor: I read with interest the article by Khan et al. (1). The National Vector-borne Disease Control Program reported >60,000 cases of acute encephalitis syndrome (AES) in India during 2010–2016; 8 states (Assam, Uttar Pradesh, West Bengal, Odisha, Tamil Nadu, Karnataka, Manipur, and Tripura) accounted for most cases (2). In many states, outbreaks of AES occur during the rainy season and are associated with high mortality rates. Following the national surveillance algorithm, AES cases are investigated for IgM against Japanese encephalitis, which accounted for <15% AES cases. Khan et al. reported 20% of AES cases were due to scrub typhus (*Orientia tsutsugamushi* infection) (1). In Gorakhpur, Uttar Pradesh, 62.7% of AES patients had *O. tsutsugamushi* IgM, with a case-fatality rate of 16.2% (3). Studies have reported central nervous system (CNS) involvement among a substantial number of scrub typhus patients from Dehradun, Uttarakhand; Vellore, Tamil Nadu; Puducherry; and Lucknow, Uttar Pradesh (4,5). Given these findings, managers of the national program should consider investigations for scrub typhus as part of the surveillance algorithm for AES cases.

Higher mortality rates among patients with AES could be attributed to delayed care. In Gorakhpur, where outbreaks of AES occur seasonally, the median interval

between fever onset and hospitalization was 7 days (IQR 5–10 days) (3). Although intravenous azithromycin has been recommended for AES patients in Gorakhpur since 2014, fatality rates continue to be high, indicating low response to treatment after CNS involvement. Early treatment of patients with acute febrile illness with antimicrobial drugs such as doxycycline before CNS manifestations is critical. Assessing the contribution of scrub typhus among patients with acute febrile illness, developing algorithms for administering appropriate antimicrobial drugs, and educating healthcare providers about the use of doxycycline are crucial for reducing deaths among patients with AES in scrub typhus–endemic areas.

References

1. Khan SA, Bora T, Laskar B, Khan AM, Dutta P. Scrub typhus leading to acute encephalitis syndrome, Assam, India. *Emerg Infect Dis.* 2017;23:148–50. <http://dx.doi.org/10.3201/eid2301.161038>
2. National Vectorborne Disease Control Program. Ministry of Health and Family Welfare, Government of India. Statewise number of AES/JE cases and deaths from 2010–2017 [cited 2017 May 26]. <http://www.nvbdc.gov.in/Doc/je-aes-cd-April17.pdf>
3. Murhekar MV, Mittal M, Prakash JA, Pillai VM, Mittal M, Girish Kumar CP, et al. Acute encephalitis syndrome in Gorakhpur, Uttar Pradesh, India - Role of scrub typhus. *J Infect.* 2016;73:623–6. <http://dx.doi.org/10.1016/j.jinf.2016.08.014>
4. Peter JV, Sudarsan TI, Prakash JA, Varghese GM. Severe scrub typhus infection: Clinical features, diagnostic challenges and management. *World J Crit Care Med.* 2015;4:244–50.
5. Kumar Bhat N, Dhar M, Mittal G, Shirazi N, Rawat A, Prakash Kalra B, et al. Scrub typhus in children at a tertiary hospital in north India: clinical profile and complications. *Iran J Pediatr.* 2014;24:387–92.

Address for correspondence: Manoj V. Murhekar, National Institute of Epidemiology–ICMR, R-127, Tamil Nadu Housing Board, Chennai, India; email: mmurhekar@nieicmr.org.in

govDELIVERY 

Manage your email alerts so you only receive content of interest to you.

Sign up for an online subscription:
wwwnc.cdc.gov/eid/subscribe.htm

Mosquito: A Discovery Channel Documentary

**Su Rynard, director; Yap Films; first broadcast on
Discovery Channel, July 6, 2017**

Running time: ≈60 minutes

The Discovery Channel documentary *Mosquito*, world-wide premiere scheduled for July 6, 2017, is an excellent film intended to educate those who are unaware of the dangers posed by mosquitoes worldwide. Well, not exactly. Mosquitoes themselves pose no great dangers to humans, livestock, or wildlife. It is the viruses or other potential pathogens that mosquitoes carry and can transmit that are the dangers, and they number in the hundreds, if not thousands. Still, *Mosquito* is rather thorough for a 1-hour film.

Mosquito provides brief background and informative statements by experts including Anthony Fauci, Director, National Institute of Allergy and Infectious Diseases, National Institutes of Health; Thomas Friedan, former director, Centers for Disease Control and Prevention; Bill Gates, co-chair and trustee, Bill and Melinda Gates Foundation; and Bart Knols, entomologist, author, and entrepreneur. The film delves into recent and past viral and parasitic disease transmission and the roles played by mosquitoes with regard to geographic distributions, natural cycles, epidemiologies, and effects on humans. Although the film describes the terrible illnesses caused by Zika, dengue, chikungunya, and West Nile viruses and malarial parasites, it emphasizes the mosquito vectors that transmit them and the environmental changes that are causing transmission rates to increase.

With proper emphasis on *Aedes aegypti*, *Aedes albopictus*, *Anopheles gambiae*, and other principal mosquito vectors of viruses and parasites, *Mosquito* takes us from the essentials of mosquito breeding to the diseases caused by

the agents they carry. The film goes on to show the miserable effects these diseases have on the lives of their victims, along with the economic effects on the victims' families and communities.

Many vectorborne diseases are geographically isolated and simply ignored by persons outside those areas until such time as they burst forth and affect greater and greater numbers of humans, livestock, or wildlife. A recent example is Zika virus. What the film only implies is that those who control the funds that could be used to understand the potential for disease outbreaks and to predict epidemic spread are not those who are on the battlefield asking for such help. To its credit, however, the film highlights use of bed nets, standard and novel vector-control methods, and the need to develop better universal methods for mosquito control.

The photography is brilliant, albeit somewhat repetitive (hospitalized children and their sad parents), and the dialogue is accurate for the most part. However, to say that *Mosquito* is correct in all aspects would be incorrect; its mention of *Culex* species mosquitoes as proven vectors of Zika virus is, if not incorrect, then premature. Bart Knols, an enthusiastic speaker, has a prominent role in this film, explaining complex processes; he is an expert in malaria control and also a fine teacher of virus transmission by mosquitoes.

Charles H. Calisher

Author affiliation: Associate Editor, Emerging Infectious Diseases; Colorado State University, Fort Collins, Colorado, USA

DOI: <https://doi.org/10.3201/eid2308.171064>

Address for correspondence: Charles H. Calisher, Colorado State University—Microbiology, Immunology and Pathology, Delivery Code 1690, Foothills Campus, 3195 Rampart Rd, Fort Collins, CO 80523-1690, USA; email: calisher@cybersafe.net

Correction

Vol. 22 No. 10—October 2016

Streptococcus suis was incorrectly described in the text of *Streptococcus suis* Serotype 2 Capsule In Vivo (Auger J et al.). It is a gram-positive bacterium. The article has been corrected online (https://wwwnc.cdc.gov/eid/article/22/10/15-1640_article).

Correction

Vol. 23 No. 6—June 2017

A subhead was missing and layout was incorrect in the Table for *Brucella neotomae* Infection in Humans, Costa Rica (M. Suárez-Esquivel et al.). The article has been corrected online (https://wwwnc.cdc.gov/eid/article/23/6/16-2018_article).



Alexander Skachkov (b 1973), Varna, Bulgaria. *Old Mosquito*, 2014 (detail). Pencil drawing, continued in Photoshop as grayscale drawing. Colorized with Hard Light, Multiply, Overlay, and Color layer color mode, 36 in × 43.5 in/91.44 cm × 110.48 cm.

Hematophagous Endeavors, Fact and Fancy

Byron Breedlove and Paul M. Arguin

Let's start with some facts. The word "mosquito" is Spanish for "little fly." The single family Culicidae comprises more than 3,500 species of mosquitoes, and these ectoparasites are found in a wide range of environments spanning the globe with the exception of Antarctica. The life span of adult mosquitoes ranges from 2 weeks to 6 months.

Author affiliation: Centers for Disease Control and Prevention, Atlanta, Georgia, USA

DOI: <https://doi.org/10.3201/eid2308.AC2308>

Mosquitoes belonging to about three quarters of recognized species consume blood. Female mosquitoes of those species are equipped with tubular mouthparts that can pierce the skin of their human and animal hosts to consume blood. The blood provides them with protein to produce eggs. When they are not producing eggs, female mosquitoes typically consume the same things that males do, nectar and sap from a variety of plants. Male mosquitoes do not need to feed on blood and consequently have not evolved to have larger mandibles for piercing layers of skin.

Some mosquitoes spread disease-causing agents that have serious and widespread consequences for humans and animals. Mosquitoes transmit the five *Plasmodium* parasite species that cause malaria in humans and the infectious agents that can cause chikungunya disease, dengue hemorrhagic fever, Japanese encephalitis, lymphatic filariasis, Rift Valley fever, West Nile virus infection, and yellow fever. Of those, the illness that sickens and kills most people each year is malaria. For the year 2015, the World Health Organization reported 212 million new cases of malaria and an estimated 429,000 deaths from malaria worldwide.

Mosquitoes are not simply mechanical vectors or mobile fomites. Many pathogens complete stages of their life cycles within the mosquito or may have to move from the mosquito's gut to its salivary glands—which is often why mosquitoes are not immediately infectious after consuming a blood meal from the initial infectious host. This complex relationship helps explain why specific diseases and certain mosquitoes are linked; malaria and *Anopheles* spp., Japanese encephalitis and *Culex* spp., or dengue and *Aedes* spp.

Bill Gates wrote, “When it comes to killing humans, no other animal even comes close.” Science writer Jerry Adler noted in an article, “One species, the *Anopheles gambiae* mosquito, has been called the world's most dangerous animal, although strictly speaking that applies only to the female of the species, which does the bloodsucking and harms only indirectly.”

As we consider the facts, let's shift to fancy for this month's cover art, *Old Mosquito*, by artist, illustrator, and web designer Alexander Skachkov. Much of his art belongs to realms of magic, whimsy, and wonder; his colorful creations often feature a wry sense of humor. He cites as inspiration the contemporary fantasy art created by Scott Gustafson, Paul Bonner, and Jean-Baptiste Monge. Art blogger Lafayette Wattles states that Skachkov “offers a fascinating mix of nature and humanity with neither being quite what we've come to expect in the real world.”

Although Skachkov is not working with bristle brushes and a palette of paints, his approach is nonetheless laborious and deliberate. Skachkov's creations, including this work, typically start with a penciled sketch that forms the basis of the finished image. He scans that drawing into Photoshop, with which he employs a range of tools, filters, layers, and effects to manipulate the textures, tones, and colors.

In this clever image, Skachkov depicts a tired older mosquito heading home after a long night of collecting blood. The bare branches and grayish fog of morning suggest that summer is past and the old mosquito is approaching the end of his days in the end of the year. The bright red blood contained in the mosquito's jug, his red hat and legs, and, of course, his blood-tipped proboscis tinged from its hematophagous endeavors, contrasts with the morning gloom.

Entomologists will be quick to point out that the depiction is scientifically inaccurate because male mosquitoes do not ingest blood. Mosquitoes also do not wear shoes and cute hats (so we hope any entomologists reading this essay will allow the illustrator to exercise artistic license). Skachkov has depicted this recent blood collection not just as the mosquito's prized possession, but also as his burden. The mosquito is bowed with the weight of the bottle strapped on his back. Supported by a cane, he trudges along collecting blood in exchange for an itchy welt or worse—an infectious microorganism that can cause illness, disability, and death for its new host. His resigned expression suggests that our mosquito must be aware of the grim consequences of his actions but has no choice regarding his role in the world. With few friends and not much to smile about, this older mosquito will continue on his appointed rounds for as long as he can bear it.

Bibliography

1. Adler J. Kill all the mosquitoes?! [cited 2017 Jun 14]. <http://www.smithsonianmag.com/innovation/kill-all-mosquitos-180959069/>
2. Centers for Disease Control and Prevention. *Anopheles* mosquitoes [cited 2017 Jun 13]. <https://www.cdc.gov/malaria/about/biology/mosquitoes/>
3. Gates B. The deadliest animal in the world [cited 2017 Jun 13]. <https://www.gatesnotes.com/Health/Most-Lethal-Animal-Mosquito-Week>
4. National Geographic. Mosquitoes [cited 2017 Jun 14]. <http://www.nationalgeographic.com/animals/invertebrates/group/mosquitoes/>
5. Wattles L. Alexander Skachkov [cited 2017 Jun 15]. <http://othercoolbirds.com/other-cool-birds-alexander-skachkov/>
6. World Health Organization. World malaria report 2016. Geneva: World Health Organization; 2016. Licence:CC BY-NC-SA 3.0 IGO [cited 2017 Jun 13]. http://www.who.int/malaria/publications/world_malaria_report/en/

Address for correspondence: Byron Breedlove, EID Journal, Centers for Disease Control and Prevention, 1600 Clifton Rd NE, Mailstop C19, Atlanta, GA 30329-4027, USA; email: wbb1@cdc.gov

EMERGING INFECTIOUS DISEASES®

Upcoming Issue

- Bioinformatic Analyses of Whole-Genome Sequence Data in a Public Health Laboratory
- Real-Time Whole-Genome Sequencing for Surveillance of *Listeria monocytogenes*, France
- Prevalence of *Yersinia enterocolitica* Bioserotype 3/O:3 in Children with Diarrhea, China
- Convergence of Humans, Bats, Trees, and Culture in Nipah Virus Transmission, Bangladesh
- Estimated Annual Numbers of Foodborne Pathogen–Associated Illnesses, Hospitalizations, and Deaths, France, 2008–2013
- Epidemiology of *Salmonella enterica* Serotype Dublin Infections among Humans, United States, 1968–2013
- Phylogeographic Analysis of Rabies Virus Incursions across US/Canada Border
- The Role of Food Insecurity in an Outbreak of Anthrax among Humans and Hippopotamuses Living in a Game Reserve Area, Rural Zambia
- Patterns of Human Plague in Uganda, 2008–2016
- Group A Rotavirus Associated with Encephalitis in Red Fox
- Cost of Nosocomial Outbreak Caused by NDM-1–Containing *Klebsiella pneumoniae* in the Netherlands, 2015–2016
- Imported Infections with *Mansonella perstans* Nematodes, Italy
- Microcephaly Caused by Lymphocytic Choriomeningitis Virus
- Epidemiology of *Neisseria gonorrhoeae* Gyrase A Genotype, Los Angeles, California, USA
- Emergence of Plasmid-Mediated Fosfomycin Resistance Genes among *Escherichia coli* Isolates, France
- Evaluation of 5 Commercially Available Zika Virus Immunoassays
- Identification of Clade E Avipoxvirus, Mozambique, Africa, 2016
- Carbapenemase-Producing *Enterobacteriaceae* and Nonfermentative Bacteria, the Philippines, 2013–2016
- A New Bat-HKU2–like Coronavirus in Swine, China,

Complete list of articles in the September issue at
<http://www.cdc.gov/eid/upcoming.htm>

Upcoming Infectious Disease Activities

October 1–3, 2017

Emerging and Re-emerging Viruses Symposia
 Arlington, VA, USA
<http://cell-symposia.com/emerging-viruses-2017/>

October 3–7, 2017

ID Week
 San Diego, CA, USA
<http://www.idweek.org/>

November 5–9, 2017

ASTMH
 American Society for Tropical Medicine and Hygiene
 66th Annual Meeting
 The Baltimore Convention Center
 Baltimore, MD, USA
<http://www.astmh.org/>

December 5–8, 2017

6th National Congress of Tropical Medicine and International Symposium on HIV/aids Infection
 9th National Congress of Microbiology and Parasitology
 80th Anniversary of the Institute of Tropical Medicine Pedro Kourí
 Havana, Cuba
<http://microbiologia2017.sld.cu/index.php/microbiologia/2017>

Feb. 1–3, 2018

8th Advances in Aspergillosis
 Lisboa Congress Centre
 Lisbon, Portugal
www.AAA2018.org

March 1–4, 2018

18th International Congress on Infectious Diseases (ICID)
 Buenos Aires, Argentina
<http://www.isid.org/icid/>

August 26–28, 2018

ICEID
 International Conference on Emerging Infectious Diseases
 Atlanta, GA, USA

Announcements

To submit an announcement, send an email message to the EID Editor (eideditor@cdc.gov). Include the date of the event, the location, the sponsoring organization(s), and a website that readers may visit or a telephone number or email address that readers may contact for more information.

Announcements may be posted on the journal Web page only, depending on the event date.

Earning CME Credit

To obtain credit, you should first read the journal article. After reading the article, you should be able to answer the following, related, multiple-choice questions. To complete the questions (with a minimum 75% passing score) and earn continuing medical education (CME) credit, please go to <http://www.medscape.org/journal/eid>. Credit cannot be obtained for tests completed on paper, although you may use the worksheet below to keep a record of your answers.

You must be a registered user on <http://www.medscape.org>. If you are not registered on <http://www.medscape.org>, please click on the "Register" link on the right-hand side of the website.

Only one answer is correct for each question. Once you successfully answer all post-test questions, you will be able to view and/or print your certificate. For questions regarding this activity, contact the accredited provider, CME@medscape.net. For technical assistance, contact CME@medscape.net. American Medical Association's Physician's Recognition Award (AMA PRA) credits are accepted in the US as evidence of participation in CME activities. For further information on this award, please go to <https://www.ama-assn.org>. The AMA has determined that physicians not licensed in the US who participate in this CME activity are eligible for AMA PRA Category 1 Credits™. Through agreements that the AMA has made with agencies in some countries, AMA PRA credit may be acceptable as evidence of participation in CME activities. If you are not licensed in the US, please complete the questions online, print the AMA PRA CME credit certificate, and present it to your national medical association for review.

Article Title

***Bartonella quintana*, an Unrecognized Cause of Infective Endocarditis in Children in Ethiopia**

CME Questions

1. You are called to evaluate a 12-year-old boy for suspected endocarditis. Blood cultures are negative after 1 day, and you are concerned regarding the possibility of blood culture–negative endocarditis. Which one of the following statements regarding *Bartonella quintana* is most accurate?

- A. It is historically linked to "trench fever"
- B. Its most significant host is the rat
- C. It is not associated with fever in cases of endocarditis
- D. *Bartonella* spp. usually result in endocarditis of the mitral valve

2. You see that the patient recently emigrated from another country. What was the country of origin of all children in the current case series of endocarditis resulting from *B. quintana*?

- A. Nigeria
- B. Egypt
- C. Jordan
- D. Ethiopia

3. You review the patient's initial history and physical examination. Which one of the following options lists the symptoms most commonly encountered at the children's presentation in the current study?

- A. Orthopnea and weakness
- B. Fever
- C. Pruritus and excoriations
- D. Mental status changes

4. Which one of the following signs was noted among children with *B. quintana* endocarditis in the current study?

- A. Normal erythrocyte sedimentation rate
- B. Markedly elevated C-reactive protein
- C. Infection of the mitral valve
- D. Large valvular vegetations

Earning CME Credit

To obtain credit, you should first read the journal article. After reading the article, you should be able to answer the following, related, multiple-choice questions. To complete the questions (with a minimum 75% passing score) and earn continuing medical education (CME) credit, please go to <http://www.medscape.org/journal/eid>. Credit cannot be obtained for tests completed on paper, although you may use the worksheet below to keep a record of your answers.

You must be a registered user on <http://www.medscape.org>. If you are not registered on <http://www.medscape.org>, please click on the "Register" link on the right-hand side of the website.

Only one answer is correct for each question. Once you successfully answer all post-test questions, you will be able to view and/or print your certificate. For questions regarding this activity, contact the accredited provider, CME@medscape.net. For technical assistance, contact CME@medscape.net. American Medical Association's Physician's Recognition Award (AMA PRA) credits are accepted in the US as evidence of participation in CME activities. For further information on this award, please go to <https://www.ama-assn.org>. The AMA has determined that physicians not licensed in the US who participate in this CME activity are eligible for AMA PRA Category 1 Credits™. Through agreements that the AMA has made with agencies in some countries, AMA PRA credit may be acceptable as evidence of participation in CME activities. If you are not licensed in the US, please complete the questions online, print the AMA PRA CME credit certificate, and present it to your national medical association for review.

Article Title

Human Metapneumovirus and Other Respiratory Viral Infections during Pregnancy and Birth, Nepal

CME Questions

1. You are advising a prenatal clinic in Nepal regarding human metapneumovirus (hMPV) infection during pregnancy. According to the surveillance study in Nepal by Lenahan and colleagues, which one of the following statements about incidence of and risk factors for hMPV infection during pregnancy and up to 6 months postpartum is correct?

- A. Overall incidence of hMPV was 5.4 cases/1000 person-years
- B. Overall incidence of hMPV was half that of respiratory syncytial virus in the same cohort during the same period
- C. Incidence peaked at 71.9 cases/1000 person-years during the hMPV season, from September 2011 through January 2012
- D. Higher median household density was a significant risk factor for hMPV infection

2. According to the surveillance study in Nepal by Lenahan and colleagues, which one of the following statements about clinical presentation and symptoms of hMPV infection among pregnant women with fever testing positive for hMPV is correct?

- A. The most common symptom was cough (67.3%), followed by rhinorrhea/nasal congestion (58.2%) and myalgia (56.4%)
- B. Median duration of symptoms was 2 weeks
- C. Mortality rate was 15%
- D. Viral coinfections were uncommon

3. According to the surveillance study in Nepal by Lenahan and colleagues, which one of the following statements about birth outcomes associated with hMPV infection during pregnancy is correct?

- A. Median gestational age of infants born to mothers with hMPV infection was significantly less than that of those born to mothers without hMPV infection
- B. Among pregnant women with hMPV, 26.3% of their infants with known birthweights were low birthweight vs 24.8% among noninfected women
- C. Among women with hMPV postpartum, 12% had infants who had hMPV within a month of their mother's illness
- D. Preterm births occurred in one quarter of pregnant women infected with hMPV

Emerging Infectious Diseases is a peer-reviewed journal established expressly to promote the recognition of new and reemerging infectious diseases around the world and improve the understanding of factors involved in disease emergence, prevention, and elimination.

The journal is intended for professionals in infectious diseases and related sciences. We welcome contributions from infectious disease specialists in academia, industry, clinical practice, and public health, as well as from specialists in economics, social sciences, and other disciplines. Manuscripts in all categories should explain the contents in public health terms. For information on manuscript categories and suitability of proposed articles, see below and visit <http://wwwnc.cdc.gov/eid/pages/author-resource-center.htm>.

Summary of Authors' Instructions

Author's Instructions. For a complete list of EID's manuscript guidelines, see the author resource page: <http://wwwnc.cdc.gov/eid/page/author-resource-center>.

Manuscript Submission. To submit a manuscript, access Manuscript Central from the Emerging Infectious Diseases web page (www.cdc.gov/eid). Include a cover letter indicating the proposed category of the article (e.g., Research, Dispatch), verifying the word and reference counts, and confirming that the final manuscript has been seen and approved by all authors. Complete provided Authors Checklist.

Manuscript Preparation. For word processing, use MS Word. Set the document to show continuous line numbers. List the following information in this order: title page, article summary line, keywords, abstract, text, acknowledgments, biographical sketch, references, tables, and figure legends. Appendix materials and figures should be in separate files.

Title Page. Give complete information about each author (i.e., full name, graduate degree(s), affiliation, and the name of the institution in which the work was done). Clearly identify the corresponding author and provide that author's mailing address (include phone number, fax number, and email address). Include separate word counts for abstract and text.

Keywords. Use terms as listed in the National Library of Medicine Medical Subject Headings index (www.ncbi.nlm.nih.gov/mesh).

Text. Double-space everything, including the title page, abstract, references, tables, and figure legends. Indent paragraphs; leave no extra space between paragraphs. After a period, leave only one space before beginning the next sentence. Use 12-point Times New Roman font and format with ragged right margins (left align). Italicize (rather than underline) scientific names when needed.

Biographical Sketch. Include a short biographical sketch of the first author—both authors if only two. Include affiliations and the author's primary research interests.

References. Follow Uniform Requirements (www.icmje.org/index.html). Do not use endnotes for references. Place reference numbers in parentheses, not superscripts. Number citations in order of appearance (including in text, figures, and tables). Cite personal communications, unpublished data, and manuscripts in preparation or submitted for publication in parentheses in text. Consult List of Journals Indexed in Index Medicus for accepted journal abbreviations; if a journal is not listed, spell out the journal title. List the first six authors followed by "et al." Do not cite references in the abstract.

Tables. Provide tables within the manuscript file, not as separate files. Use the MS Word table tool, no columns, tabs, spaces, or other programs. Footnote any use of bold-face. Tables should be no wider than 17 cm. Condense or divide larger tables. Extensive tables may be made available online only.

Figures. Submit editable figures as separate files (e.g., Microsoft Excel, PowerPoint). Photographs should be submitted as high-resolution (600 dpi) .tif or .jpeg files. Do not embed figures in the manuscript file. Use Arial 10 pt. or 12 pt. font for lettering so that figures, symbols, lettering, and numbering can remain legible when reduced to print size. Place figure keys within the figure. Figure legends should be placed at the end of the manuscript file.

Videos. Submit as AVI, MOV, MPG, MPEG, or WMV. Videos should not exceed 5 minutes and should include an audio description and complete captioning. If audio is not available, provide a description of the action in the video as a separate Word file. Published or copyrighted material (e.g., music) is discouraged and must be accompanied by written release. If video is part of a manuscript, files must be uploaded with manuscript submission. When uploading, choose "Video" file. Include a brief video legend in the manuscript file.

Types of Articles

Perspectives. Articles should not exceed 3,500 words and 50 references. Use of subheadings in the main body of the text is recommended. Photographs and illustrations are encouraged. Provide a short abstract (150 words), 1-sentence summary, and biographical sketch. Articles should provide insightful analysis and commentary about new and reemerging infectious diseases and related issues. Perspectives may address factors known to influence the emergence of diseases, including microbial adaptation and change, human demographics and behavior, technology and industry, economic development and land use, international travel and commerce, and the breakdown of public health measures.

Synopses. Articles should not exceed 3,500 words in the main body of the text or include more than 50 references. Use of subheadings in the main body of the text is recommended. Photographs and illustrations are encouraged. Provide a short abstract (not to exceed 150 words), a 1-line summary of the conclusions, and a brief

biographical sketch of first author or of both authors if only 2 authors. This section comprises case series papers and concise reviews of infectious diseases or closely related topics. Preference is given to reviews of new and emerging diseases; however, timely updates of other diseases or topics are also welcome. If detailed methods are included, a separate section on experimental procedures should immediately follow the body of the text.

Research. Articles should not exceed 3,500 words and 50 references. Use of subheadings in the main body of the text is recommended. Photographs and illustrations are encouraged. Provide a short abstract (150 words), 1-sentence summary, and biographical sketch. Report laboratory and epidemiologic results within a public health perspective. Explain the value of the research in public health terms and place the findings in a larger perspective (i.e., "Here is what we found, and here is what the findings mean").

Policy and Historical Reviews. Articles should not exceed 3,500 words and 50 references. Use of subheadings in the main body of the text is recommended. Photographs and illustrations are encouraged. Provide a short abstract (150 words), 1-sentence summary, and biographical sketch. Articles in this section include public health policy or historical reports that are based on research and analysis of emerging disease issues.

Dispatches. Articles should be no more than 1,200 words and need not be divided into sections. If subheadings are used, they should be general, e.g., "The Study" and "Conclusions." Provide a brief abstract (50 words); references (not to exceed 15); figures or illustrations (not to exceed 2); tables (not to exceed 2); and biographical sketch. Dispatches are updates on infectious disease trends and research that include descriptions of new methods for detecting, characterizing, or subtyping new or reemerging pathogens. Developments in antimicrobial drugs, vaccines, or infectious disease prevention or elimination programs are appropriate. Case reports are also welcome.

Another Dimension. Thoughtful essays, short stories, or poems on philosophical issues related to science, medical practice, and human health. Topics may include science and the human condition, the unanticipated side of epidemic investigations, or how people perceive and cope with infection and illness. This section is intended to evoke compassion for human suffering and to expand the science reader's literary scope. Manuscripts are selected for publication as much for their content (the experiences they describe) as for their literary merit. Include biographical sketch.

Research Letters Reporting Cases, Outbreaks, or Original Research. EID publishes letters that report cases, outbreaks, or original research as Research Letters. Authors should provide a short abstract (50-word maximum), references (not to exceed 10), and a short biographical sketch. These letters should not exceed 800 words in the main body of the text and may include either 1 figure or 1 table. Do not divide Research Letters into sections.

Letters Commenting on Articles. Letters commenting on articles should contain a maximum of 300 words and 5 references; they are more likely to be published if submitted within 4 weeks of the original article's publication.

Commentaries. Thoughtful discussions (500–1,000 words) of current topics. Commentaries may contain references (not to exceed 15) but no abstract, figures, or tables. Include biographical sketch.

Books, Other Media. Reviews (250–500 words) of new books or other media on emerging disease issues are welcome. Title, author(s), publisher, number of pages, and other pertinent details should be included.

Conference Summaries. Summaries of emerging infectious disease conference activities (500–1,000 words) are published online only. They should be submitted no later than 6 months after the conference and focus on content rather than process. Provide illustrations, references, and links to full reports of conference activities.

Online Reports. Reports on consensus group meetings, workshops, and other activities in which suggestions for diagnostic, treatment, or reporting methods related to infectious disease topics are formulated may be published online only. These should not exceed 3,500 words and should be authored by the group. We do not publish official guidelines or policy recommendations.

Photo Quiz. The photo quiz (1,200 words) highlights a person who made notable contributions to public health and medicine. Provide a photo of the subject, a brief clue to the person's identity, and five possible answers, followed by an essay describing the person's life and his or her significance to public health, science, and infectious disease.

Etymologia. Etymologia (100 words, 5 references). We welcome thoroughly researched derivations of emerging disease terms. Historical and other context could be included.

Announcements. We welcome brief announcements of timely events of interest to our readers. Announcements may be posted online only, depending on the event date. Email to eideditor@cdc.gov.

In This Issue

Synopses

Added Value of Next-Generation Sequencing for Multilocus Sequence Typing Analysis of a <i>Pneumocystis jirovecii</i> Pneumonia Outbreak	1237
<i>Bartonella quintana</i> , an Unrecognized Cause of Infective Endocarditis in Children in Ethiopia	1246
Characteristics of Dysphagia in Infants with Microcephaly Caused by Congenital Zika Virus Infection, Brazil, 2015	1253
Zika Virus Infection in Patient with No Known Risk Factors, Utah, USA, 2016.....	1260
Acute Febrile Illness and Complications Due to Murine Typhus, Texas, USA	1268

Research

High Infection Rates for Adult Macaques after Intravaginal or Intrarectal Inoculation with Zika Virus	1274
Lyme Borreliosis in Finland, 1995–2014	1282
Characterization of Fitzroy River Virus and Serologic Evidence of Human and Animal Infection	1289
Genomic Characterization of Recrudescence <i>Plasmodium malariae</i> after Treatment with Artemether/Lumefantrine	1300
Molecular Characterization of <i>Corynebacterium diphtheriae</i> Outbreak Isolates, South Africa, March–June 2015	1308
Clinical Laboratory Values as Early Indicators of Ebola Virus Infection in Nonhuman Primates.....	1316
Maguari Virus Associated with Human Disease	1325
Human Infection with Highly Pathogenic Avian Influenza A(H7N9) Virus, China	1332
Human Metapneumovirus and Other Respiratory Viral Infections during Pregnancy and Birth, Nepal	1341

Dispatches

Global Spread of Norovirus GII.17 Kawasaki 308, 2014–2016	1350
Preliminary Epidemiology of Human Infections with Highly Pathogenic Avian Influenza A(H7N9) Virus, China, 2017	1355
Real-Time Evolution of Zika Virus Disease Outbreak, Roatán, Honduras	1360
Clonal Expansion of New Penicillin-Resistant Clade of <i>Neisseria meningitidis</i> Serogroup W Clonal Complex 11, Australia.....	1364
Genesis of Influenza A(H5N8) Viruses	1368
West Nile Virus Outbreak in Houston and Harris County, Texas, USA 2014	1372
Density-Dependent Prevalence of <i>Francisella tularensis</i> in Fluctuating Vole Populations, Northwestern Spain	1377
Occupational Exposures to Ebola Virus in Ebola Treatment Center, Conakry, Guinea.....	1380
Serologic Evidence of Powassan Virus Infection in Patients with Suspected Lyme Disease	1384
Serologic Evidence of Scrub Typhus in the Peruvian Amazon	1389
Influenza D Virus in Animal Species in Guangdong Province, Southern China	1392
Seroprevalence of <i>Baylisascaris procyonis</i> Infection among Humans, Santa Barbara County, California, USA, 2014–2016	1397
Opiate Injection–Associated Skin, Soft Tissue, and Vascular Infections, England, UK, 1997–2016.....	1400
Risk for Death among Children with Pneumonia, Afghanistan	1404